frontiers | Research Topics

Anti-inflammatory immunopharmacology in the prevention and treatment of major chronic diseases

Edited by
Shihai Yan, Dongdong Sun, Qiuwang Zhang, Zhirong Geng and Peixiang Zhang

Published in
Frontiers in Pharmacology

ISSN 1664-8714
ISBN 978-2-83251-460-3
DOI 10.3389/978-2-83251-460-3

About Frontiers

Frontiers is more than just an open access publisher of scholarly articles: it is a pioneering approach to the world of academia, radically improving the way scholarly research is managed. The grand vision of Frontiers is a world where all people have an equal opportunity to seek, share and generate knowledge. Frontiers provides immediate and permanent online open access to all its publications, but this alone is not enough to realize our grand goals.

Frontiers journal series

The Frontiers journal series is a multi-tier and interdisciplinary set of open-access, online journals, promising a paradigm shift from the current review, selection and dissemination processes in academic publishing. All Frontiers journals are driven by researchers for researchers; therefore, they constitute a service to the scholarly community. At the same time, the *Frontiers journal series* operates on a revolutionary invention, the tiered publishing system, initially addressing specific communities of scholars, and gradually climbing up to broader public understanding, thus serving the interests of the lay society, too.

Dedication to quality

Each Frontiers article is a landmark of the highest quality, thanks to genuinely collaborative interactions between authors and review editors, who include some of the world's best academicians. Research must be certified by peers before entering a stream of knowledge that may eventually reach the public - and shape society; therefore, Frontiers only applies the most rigorous and unbiased reviews. Frontiers revolutionizes research publishing by freely delivering the most outstanding research, evaluated with no bias from both the academic and social point of view. By applying the most advanced information technologies, Frontiers is catapulting scholarly publishing into a new generation.

What are Frontiers Research Topics?

Frontiers Research Topics are very popular trademarks of the *Frontiers journals series*: they are collections of at least ten articles, all centered on a particular subject. With their unique mix of varied contributions from Original Research to Review Articles, Frontiers Research Topics unify the most influential researchers, the latest key findings and historical advances in a hot research area.

Find out more on how to host your own Frontiers Research Topic or contribute to one as an author by contacting the Frontiers editorial office: frontiersin.org/about/contact

Anti-inflammatory immunopharmacology in the prevention and treatment of major chronic diseases

Topic editors

Shihai Yan — Jiangsu Provincial Hospital of Traditional Chinese Medicine, China
Dongdong Sun — Nanjing University of Chinese Medicine, China
Qiuwang Zhang — Keenan Research Centre for Biomedical Science, St Michael's Hospital, Canada
Zhirong Geng — Nanjing University, China
Peixiang Zhang — University of California, Los Angeles, United States

Citation

Yan, S., Sun, D., Zhang, Q., Geng, Z., Zhang, P., eds. (2023). *Anti-inflammatory immunopharmacology in the prevention and treatment of major chronic diseases*. Lausanne: Frontiers Media SA. doi: 10.3389/978-2-83251-460-3

Table of contents

frontiers | Frontiers in Pharmacology

TYPE Editorial
PUBLISHED 12 January 2023
DOI 10.3389/fphar.2023.1134918

OPEN ACCESS

EDITED AND REVIEWED BY
Paola Patrignani,
University of Studies Gd'Annunzio Chieti and Pescara, Italy

*CORRESPONDENCE
Qiuwang Zhang,
Qiuwang.zhang@unityhealth.to
Shihai Yan,
fsyy00688@njucm.edu.cn

SPECIALTY SECTION
This article was submitted to Inflammation Pharmacology, a section of the journal Frontiers in Pharmacology

RECEIVED 31 December 2022
ACCEPTED 03 January 2023
PUBLISHED 12 January 2023

CITATION
Zhang Q, Yan S, Sun D, Geng Z and Zhang P (2023), Editorial: Anti-inflammatory immunopharmacology in the prevention and treatment of major chronic diseases.
Front. Pharmacol. 14:1134918.
doi: 10.3389/fphar.2023.1134918

Editorial: Anti-inflammatory immunopharmacology in the prevention and treatment of major chronic diseases

Qiuwang Zhang[1]*, Shihai Yan[2]*, Dongdong Sun[3], Zhirong Geng[4] and Peixiang Zhang[5]

[1]Division of Cardiology, Keenan Research Center for Biomedical Science at the Li Ka Shing Knowledge Institute, St. Michael's Hospital, Unity Health Toronto, University of Toronto, Toronto, ON, Canada, [2]Department of Pharmacology, Jiangsu Provincial Hospital of Traditional Chinese Medicine, Nanjing, China, [3]Jiangsu Collaborative Innovation Center of Traditional Chinese Medicine in Prevention and Treatment of Tumor, Nanjing University of Chinese Medicine, Nanjing, China, [4]State Key Laboratory of Coordination Chemistry, School of Chemistry and Chemical Engineering, Nanjing University, Nanjing, China, [5]Department of Human Genetics, University of California, Los Angeles, Los Angeles, CA, United States

KEYWORDS

chronic disease, inflammation, immunopharmacology, precision medicine, biomolecule

Editorial on the Research Topic
Anti-inflammatory Immunopharmacology in the Prevention and Treatment of Major Chronic Diseases

Background

Chronic diseases (CDs) are defined by the World Health Organization (WHO) as non-communicable diseases resulting from combined actions of genetic, environmental and behavioural factors; they are of long duration and generally slow in progression (https://www.who.int/news-room/fact-sheets/detail/noncommunicable-diseases). CDs such as cardiovascular and cerebrovascular diseases, cancer and diabetes are significant contributors to death and disability worldwide. A systematic analysis for the Global Burden of Disease (GBD) Study 2015 revealed that ischemic heart disease, stroke and diabetes were the leading causes for years of life lost (GBD 2015 Mortality and Causes of Death Collaborators, 2016). A more recent study by the GBD 2019 Diseases and Injuries Collaborators, 2020 showed that in 2019, CDs were responsible for significantly increased years lived with disability, and ischemic heart disease and stroke were the top causes of disability-adjusted life-years for individuals aged 50 years and over. Using a dynamic micro-simulation model to analyze the sociodemographic factors, health behaviours, and chronic diseases and geriatric conditions of individuals ≥35 years of age to project multi-morbidity in the older population in the United Kingdom in 2035, Kingston et al., 2018 found that there would be an approximately 200% increase in cancer incidence and a 120% increase in diabetes incidence for the population aged ≥65 years of age in 2035. This data plus the fact that the global population is rapidly aging call for efforts to develop more effective interventions to prevent and treat CDs.

Inflammation has long been recognized as playing a key role in the pathogenesis of CDs (Pawelec et al., 2014; Furman et al., 2019). Inflammation is an evolutionarily conserved self-healing process involving immune and non-immune cells to eliminate pathogens and promote tissue repair

and recovery. Environmental, genetic and lifestyle factors can dysregulate a normal inflammatory response, leading to chronic inflammation and eventually CDs. Despite the recognition of a close link between chronic inflammation and CDs, the mechanisms of CD pathogenesis remain to be fully understood, and more therapeutic approaches are needed.

Against the backdrop described above, this Research Topic aimed to disseminate up-to-date knowledge of anti-inflammatory immunopharmacology in the prevention and treatment of CDs.

Articles published in the Research Topic

A total of 11 articles on basic research, clinical research or review of literature were published in this Research Topic, covering a variety of areas of anti-inflammatory immunopharmacology in the prevention and management of CDs.

Multiple sclerosis (MS), a chronic inflammatory autoimmune disease, is characterized by demyelination and neurodegeneration restricted to the central nervous system. There's currently no cure for MS and treatments focus on controlling the condition and improving the symptoms (Hauser & Cree, 2020). In a search for anti-inflammatory molecules as therapeutic agents, Li et al. developed a recombinant flagellin protein, namely FLaAN/C, from the bacterium *Legionella pneumophila* and tested its therapeutic efficacy in mice with experimental autoimmune encephalomyelitis (EAE). They reported that FLaAN/C reduced EAE severity and repressed inflammatory cell infiltration and demyelination. FLaAN/C administration also inhibited reactive oxygen species production, upregulated anti-inflammatory cytokines, i.e., CD206, IL-10 and Arginase-1 from microglia/macrophages, and reduced levels of serum pro-inflammatory cytokines, e.g., IL-1β and TNF-α in EAE mice. Furthermore, it was demonstrated that FLaAN/C attenuated EAE by blocking NF-kB nuclear translocation and inhibiting NLRP3-mediated neuronal pyroptosis. This study may lead to the development of a novel therapeutic approach for MS.

Herbal medicine using botanical products represents an alternative, effective option for chronic disease care (Kim et al., 2018). Yang et al. explored the therapeutic potential of celastrol, an active compound extracted from *Tripterygium wilfordii,* in a rat model of osteoarthritis (OA). In cultured rat chondrocytes, celastrol was found to inhibit matrix degradation and downregulate IL-1β induced expression of inflammatory mediators, i.e., cyclooxygenase-2, IL-6 and prostaglandin E2. Cartilage tissues from OA patients and OA rats were shown to produce a substantially higher level of toll-like receptor 2 (TLR2), an essential player in inflammation. Celastrol treatment resulted in decreased osteophyte formation and bone resorption, and prevented disease progression in OA rats. Examination of mechanism of action demonstrated that celastrol abolished the up-regulatory effect of IL-1β on TLR2 in cultured chondrocytes and lowered TLR2 levels in OA rats, suggesting celastrol exerts its anti-inflammatory activity by suppressing TLR2. Vaccarin, a flavonoid glycoside extracted from *Vaccariae semen*, possesses endothelial protective activity, with the mechanism not being fully understood. Li et al. reported that vaccarin protected against endothelial inflammatory injury in type 2 diabetes mice by targeting the miR-570-3p/HDAC1 pathway. They discovered that the aorta of diabetic mice had decreased miR-570-3p and elevated HDAC1, both of which were reversed by vaccarin, leading to the alleviation of aortic inflammatory injury.

In a clinical study, Hu et al. looked into cellular heterogeneity and immunogenicity of chondrocytes in OA patients. They performed bioinformatics analysis of single-cell RNA sequencing data established using samples from 10 OA patients, and identified subtypes of chondrocytes. According to the gene expression profiles, chondrocytes from OA patients were divided into 8 subgroups: cartilage progenitor cells, effector chondrocytes (ECs), fibrocartilage chondrocytes (FCs), homeostatic chondrocytes, hypertrophic chondrocytes, prehypertrophic chondrocytes, proliferative chondrocytes and regulatory chondrocytes. Functional analyses revealed that these subtypes of chondrocytes played different roles in OA pathogenesis, with ECs and FCs possessing strong immunogenicity and being associated with disease severity. Furthermore, 6 genes highly expressed in ECs and FCs, i.e., CHRDL2, DSC2, COL1A1, COL14A1, IFI27, and THY1 were found to be valuable biomarkers for early diagnosis of OA. Additionally, findings of this study may help drive more personalized care for patients with OA.

Several review articles were published in this Research Topic. Liu et al. addressed the Research Topic in cancer chemo-immunotherapy. The long-term anticancer immune activity of chemotherapy is often restricted by the immunosuppressive tumor microenvironment. These authors presented the current knowledge of immunogenic regulatory function of chemotherapeutic agents (CTAs) and illustrated the strategies to improve CTA immunomodulatory effect. Finally, the authors suggested more research to better understand the mechanisms underlying the immunomodulatory effects of chemotherapy and identify biomarkers that can be applied to guide immunogenic chemotherapy. In another review paper, Xie et al. summarized the studies of traditional Chinese therapy (TCT) in treating sleep disorders, and concluded that the current literature supported that TCT was effective in relieving anxiety, lowering depression and improving sleep by inhibiting inflammatory reactions. They proposed TCT for the management of sleep disorders caused by COVID-19.

In summary, this Research Topic primarily offers information on mechanisms of CDs that may help improve early diagnosis and promote precision treatment, as well as exploration of biomolecules for disease treatment that could lead to the development of novel therapeutic agents for CDs.

Author contributions

All authors listed have made a substantial, direct, and intellectual contribution to the work and approved it for publication.

Acknowledgments

We would like to thank all authors, reviewers and the staff of the Editorial Offices of Frontiers in Pharmacology for the successful publication of this Research Topic.

Conflict of Interest

The authors declare that the research was conducted in the absence of any commercial or financial relationships that could be construed as a potential conflict of interest.

Publisher's note

References

Furman, D., Campisi, J., Verdin, E., Carrera-Bastos, P., Targ, S., Franceschi, C., et al. (2019). Chronic inflammation in the etiology of disease across the life span. *Nat. Med.* 25, 1822–1832. doi:10.1038/s41591-019-0675-0

GBD 2015 Mortality and Causes of Death Collaborators (2016). Global, regional, and national life expectancy, all-cause mortality, and cause-specific mortality for 249 causes of death. *Lancet* 388, 1459–1544. 1980-2015: a systematic analysis for the Global Burden of Disease Study 2015. doi:10.1016/S0140-6736(16)31012-1

GBD 2019 Diseases and Injuries Collaborators (2020). Global burden of 369 diseases and injuries in 204 countries and territories, 1990-2019: A systematic analysis for the global burden of disease study 2019. *Lancet* 396, 1204–1222. doi:10.1016/S0140-6736(20)30925-9

Hauser, S. L., and Cree, B. A. C. (2020). Treatment of multiple sclerosis: A review. *Am. J. Med.* 133, 1380–1390.e2. doi:10.1016/j.amjmed.2020.05.049

Kim, J. H., Kismali, G., and Gupta, S. C. (2018). Natural products for the prevention and treatment of chronic inflammatory diseases: Integrating traditional medicine into modern chronic diseases care. *Evid. Based Complement. Altern. Med.* 2018, 9837863. doi:10.1155/2018/9837863

Kingston, A., Robinson, L., Booth, H., Knapp, M., and Jagger, C.MODEM project (2018). Projections of multi-morbidity in the older population in england to 2035: Estimates from the population ageing and care simulation (PACSim) model. *Age Ageing* 47, 374–380. doi:10.1093/ageing/afx201

Pawelec, G., Goldeck, D., and Derhovanessian, E. (2014). Inflammation, ageing and chronic disease. *Curr. Opin. Immunol.* 29, 23–28. doi:10.1016/j.coi.2014.03.007

frontiers | Frontiers in Pharmacology

TYPE Original Research
PUBLISHED 10 August 2022
DOI 10.3389/fphar.2022.963506

OPEN ACCESS

EDITED BY
Qiuwang Zhang,
St Michael's Hospital, Canada

REVIEWED BY
Zhen Ouyang,
Jiangsu University, China
Fang Zhou,
China Pharmaceutical University, China

*CORRESPONDENCE
Jian Sun,
Psbyyffs@126.com
Xin Wen,
yaodawenxin@126.com
Lingyun Sun,
lingyunsun@nju.edu.cn

†These authors have contributed equally to this work

SPECIALTY SECTION
This article was submitted to Inflammation Pharmacology, a section of the journal Frontiers in Pharmacology

RECEIVED 07 June 2022
ACCEPTED 11 July 2022
PUBLISHED 10 August 2022

CITATION
Yang G, Wang K, Song H, Zhu R, Ding S, Yang H, Sun J, Wen X and Sun L (2022), Celastrol ameliorates osteoarthritis via regulating TLR2/NF-κB signaling pathway.
Front. Pharmacol. 13:963506.
doi: 10.3389/fphar.2022.963506

Celastrol ameliorates osteoarthritis *via* regulating TLR2/NF-κB signaling pathway

Guangxia Yang[1,2†], Kai Wang[3†], Hua Song[4†], Rujie Zhu[5], Shuai Ding[4], Hui Yang[1], Jian Sun[2*], Xin Wen[4*] and Lingyun Sun[1*]

[1]Nanjing Drum Tower Hospital, Clinical College of Traditional Chinese and Western Medicine, Nanjing University of Chinese Medicine, Nanjing, China, [2]Department of Rheumatology, Affiliated Hospital of Jiangnan University, Wuxi, Jiangsu Province, China, [3]Department of Rheumatology, Affiliated Huai'an No 1 People's Hospital of Nanjing Medical University, Huaian, Jiangsu Province, China, [4]Department of Rheumatology and Immunology, The Affiliated Drum Tower Hospital of Nanjing University Medical School, Nanjing, China, [5]Department of Rheumatology and Immunology, Nanjing Drum Tower Hospital Clinical College of Nanjing Medical University, Nanjing, China

Objectives: Osteoarthritis (OA) is a joint disease characterized by degeneration of joint cartilage and is a significant cause of severe joint pain, physical disability, and impaired quality of life in the aging population. Celastrol, a Chinese herbal medicine, has attracted wide interests because of its anti-inflammatory effects on a variety of diseases. This study aimed to investigate the effect of celastrol on OA as well as the mechanisms *in vivo* and *in vitro*.

Methods: A rat knee OA model was established using "medial collateral ligament transection (MCLT) + partial meniscectomy (pMMT)". Eight weeks after surgery, the OA rats started to receive intra-articular injection of celastrol (1 mg/kg) once a week. Safranin O-fast green (S&F) and hematoxylin and eosin (H&E) staining were used to estimate histopathological changes. Micro-CT was used to evaluate bone volume of the subchondral bone of the knee joint. Chondrocytes were isolated from the knee cartilage of rats and OA patients. Enzyme linked immunosorbent assay (ELISA), Western Blot (WB), Polymerase Chain Reaction (PCR), and Immunohistochemistry (IHC) were used to detect the expression of inflammatory factors and stromal proteins, respectively.

Results: We found that celastrol treatment significantly delayed the progression of cartilage damage with a significant reduction in osteophyte formation and bone resorption in OA rat model. In IL-1β-stimulated rat chondrocytes, celastrol significantly suppressed the production of inflammatory factors such as cyclooxygenase-2 (COX2), interleukin-6 (IL-6), and prostaglandin E2 (PEG2), and reduced IL-1β-induced matrix degradation by down-regulating the expression of matrix metalloproteinase 13 (MMP13). In addition, we found that toll-like receptor 2 (TLR2) was up-regulated in OA patients and rat knee OA models, while celastrol inhibited TLR2 signal and its downstream nuclear factor-kappa B (NF-κB) phosphorylation.

Conclusion: In summary, celastrol may improve OA by inhibiting the TLR2/NF-κB signaling pathway, which provides innovative strategies for the treatment of OA.

KEYWORDS

osteoarthritis, celastrol, innate immunity, TLR2, NF-κB

Introduction

Osteoarthritis (OA) is a chronic joint disorder, which has become a great burden on individuals affected, health care system and broader socio-economic costs (Martel-Pelletier et al., 2016; Hunter and Bierma-Zeinstra, 2019). The main symptoms of OA include joint pain, swelling, deformity and progressive joint activity disorder, which eventually leads to severe limitation of movement and decreased quality of life. Clinically, multiple joints can be involved in OA, especially knee joint, followed by hand and hip (Prieto-Alhambra et al., 2014; Turkiewicz et al., 2014). There are several risk factors that could lead to OA including heredity, environment, dislocation of the knee joint, biomechanical change of joint, overactivity, weight-bearing exercise, metabolic syndrome, and inflammation (Valdes and Spector, 2011; Berenbaum et al., 2018; Bortoluzzi et al., 2018; Cooper et al., 2018; Alberton et al., 2019). Accordingly, the pathogenesis of OA is polyfactorial, with age and obesity being the most influential factors (Hindy et al., 2019; Driban et al., 2020; Hart et al., 2020), both of which are associated with an abnormal inflammatory innate immune response that leads to OA progression (Kalaitzoglou et al., 2017).

Innate immunity participates in the development of OA by inducing a low-grade inflammatory response through damage-associated molecular patterns (DAMPs) and promoting synovitis and cartilage degradation through pattern-acting recognition receptors (Liu-Bryan, 2013). Accordingly, as the core class of pattern recognition receptors (PRRs) in the inflammation scenario, toll-like receptors (TLRs) recognize multiple DAMPs leading to the activation of inflammatory pathways such as nuclear factor-kappa B (NF-κB) and mitogen-activated protein kinase (MAPK) pathways, with subsequent release of cytokines, chemokines, and proteases (Miller et al., 2019). Release of inflammatory mediates, for example interleukin-6 (IL-6), tumor necrosis factor-α (TNF-α) and nitric oxide (NO), as well as chondrocytic mediators, including prostaglandin E2 (PGE2) and matrix metalloproteinases (MMPs), promoted chondrocyte apoptosis and extracellular matrix (ECM) degradation (Goldring and Goldring, 2007; Liu-Bryan and Terkeltaub, 2015). Notably, toll-like receptor 2 (TLR2) is considered necessary in the early stage of inflammation (Abdollahi-Roodsaz et al., 2008). In the progression of OA, DAMPs/TLR2 is a key pathway to the catabolism and anabolism of cartilage ECM(Kim et al., 2006; Hwang et al., 2015; Hwang et al., 2019). Several studies have shown that TLR2-mediated immune responses regulate cytokine gene expression by activating NF-κB, while inhibition of TLR-2/NF-κB signaling reduces the expression of multiple inflammatory cytokines (Arya et al., 2021; Lee et al., 2022). These findings enlighten us to examine whether TLR-2/NF-κB play a role in activation of the innate immune system by mediating cytokine release and ultimately delay OA progression.

The medical treatment of OA has been no substantial progress for a long time with given the major challenges such as repair and regeneration of cartilage or bone loss (Maqbool et al., 2021). Up to date, physical exercise and weight loss remain the cornerstones of OA treatment. In the initial stage of OA, non-steroidal anti-inflammatory drugs (NSAIDs) are widely used to relieve pain. Although symptoms can be alleviated, the progression of OA cannot be delayed. Short-term (6 weeks) treatment with 10 mg prednisolone is effective and safe for patients with sudden onset of hand OA (Kroon et al., 2019). However, long-term usageof glucocorticoids can generate numerous adverse effects. Moreover, oral drugs have non-negligible side effects, such as the potential risk of damaging digestive and cardiovascular system (McAlindon et al., 2014; Bindu et al., 2020).

Celastrol, an active compound extracted from root bark of Tripterygium wilfordii, mainly distributed and cultivated in Asian countries, showssignificant immunosuppressive properties (Zhang et al., 2021). The anti-inflammatory effect of celastrol has been well attested in autoimmune arthritis (An et al., 2020; Cascao et al., 2020). As a valuable inhibitor of NF-κB signaling pathway, celastrol shows anti-inflammatory and bone protective effects in the adjuvant-induced arthritis model (Cascao et al., 2020). Moreover, it has been found that celastrol plays a cardioprotective role in rheumatoid arthritis by inhibiting autophagy mediated by TLR2/HMGB1 signaling pathway (Lu et al., 2021). Compared with autoimmune arthritis, OA is mainly characterized by chronic, relatively low-grade inflammation. To date, few studies have examined the treatment of OA by celastrol comprehensively and thoroughly. Furthermore, whether celastrol can improve low-grade inflammation by inhibiting DAMPs-PRRs signaling has not been studied. Nor has the possible link between celastrol and chronic inflammation been explored in OA treatment.

This study aimed to evaluate the therapeutic effects of celastrol on OA and explore the molecular mechanism of celastrol in the treatment of OA.

Methods

Ethics statement

Human control samples were collected from amputees. Human OA cartilage samples were collected from OA patients during total knee arthroplasty. The protocols for collecting and analyzing human articular cartilage was approved by the Ethical

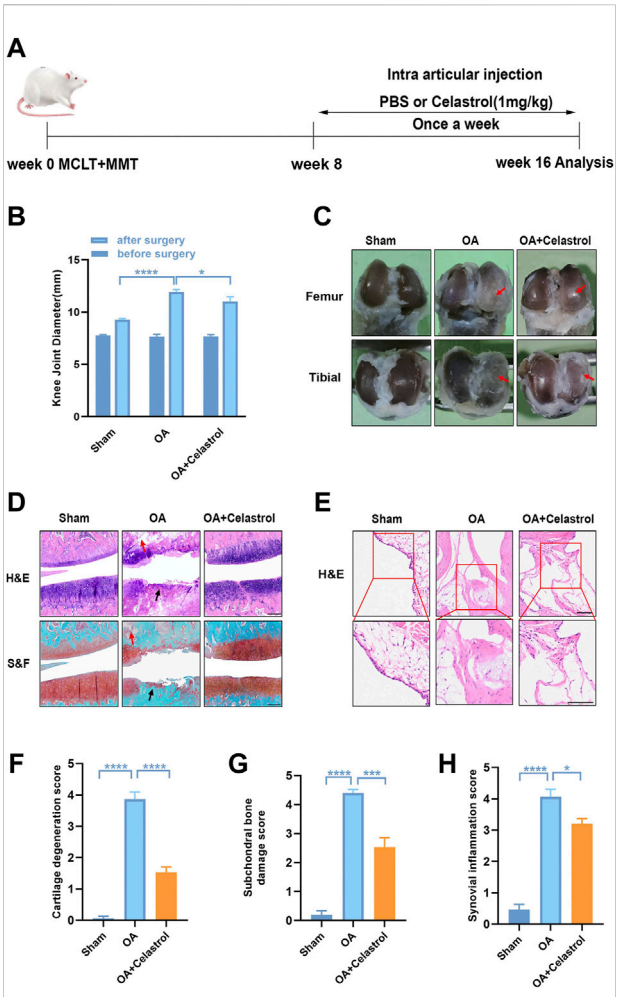

FIGURE 1
Celastrol alleviated the progression of OA in rat model. **(A)** Timeline for depicting overall the design of the study. **(B)** Knee joint diameter of the affected limbs of rats before surgery and 16 weeks after surgery; n = 6. **(C)** Representative macroscopic appearance of femoral condyles and tibial plateau showed joint damage (red arrow). **(D)** H&E and S&F staining of medial compartment cartilage and subchondral bone of knee joints; n = 5 (scale bar: 200 μm). **(E)** H&E staining of synovial membrane of the medial compartment; n = 5 (scale bar: 100 μm). **(F–H)** Quantitative analysis of cartilage degeneration score, subchondral bone damage score and synovitis inflammation score in three groups, n = 5. All data represent mean ± S.E.M.*$p < 0.05$, **$p < 0.01$, ***$p < 0.001$ and ****$p < 0.0001$.

Committee of Nanjing Drum Tower Hospital Clinical College of Traditional Chinese and Western Medicine (2020-156-01). All experimental procedures followed the guidelines of the Declaration of Helsinki (World Medical, 2013). All animal operation, treatment and post-processing were performed in strict accordance with the guidance of the Professional Animal Care and Use Committee of Nanjing Drum Tower Hospital Clinical College of Traditional Chinese and Western Medicine (2020AE02042).

TABLE 1 The primers of genes.

Name	Primer list
rTLR2-F	5′- TCACTGTTCTCCAATCTCACAA -3′
rTLR2-R	5′-CAGCCCAGCAAAATCTATTCTC -3′
rNFKB-F	5′-GTTCGATGCTGATGAAGACTTG -3′
rNFKB-R	5′-AAACTCTGAGTTGTCGACAGAT -3′
rMMP13-F	5′- AGCTCCAAAGGCTACAACTTAT-3′
rMMP13-R	5′- GTCTTCATCTCCTGGACCATAG-3′
rCOX2-F	5′- ATCAGAACCGCATTGCCTCT-3′
rCOX2-R	5′- GCCAGCAATCTGTCTGGTGA-3′
rGAPDH-F	5′- AACTCCCATTCTTCCACCTTTG-3′
rGAPDH-R	5′- CTCTTGCTCTCAGTATCCTTGC-3′
hTLR2-F	5′-CTTCACTCAGGAGCAGCAAGCA-3′
hTLR2-R	5′-ACACCAGTGCTGTCCTGTGACA-3′
hGAPDH-F	5′-TCAGTGGTGGACCTGACCTG-3′
hGAPDH-R	5′-TGCTGTAGCCAAATTCGTTG-3′

Rat model and treatment

The male Sprague-Dawley (SD) rats (6-week-old) were acquired from the Animal Center of Nanjing Medical University (Jiangsu, China). The rats were randomized into three groups (n = 18): sham operation group, OA group, and OA with celastrol treatment group. Rats in OA and celastrol treatment groups received “medial collateral ligament transection (MCLT) + partial meniscectomy (pMMT)” and rats in sham operation group underwent sham surgery. After surgery, OA rats in the celastrol treatment group were injected with 1 mg/kg celastrol (Sigma-Aldrich, Darmstadt, Germany) intra-articularly per week, and rats in the OA group were injected with normal saline. This treatment started 8 weeks after surgery and continued for 8 weeks until the rats were sacrificed (Figure 1A).

OA severity assessment

The maximum length of coronal plane of rat knee joint was taken as the diameter of the knee joint, and measured with vernier caliper (the distance from the medial condyle of the femur to the lateral condyle plus the thickness of swollen joint synovium).

Micro-computed tomography

The knee joints of rat were harvested and fixed in 4% PFA at 8 weeks post-injections. The microstructure of the joints was analyzed by micro-CT scanner (mCT80; Scanco Medical AG). The voltage of the scanner was set as 70 kV, the current was

114 μA, and the resolution was 15.6 μm per pixel. 3D reconstruction images were obtained using Scanco Medical software. Total bone volume (BV), total bone volume/total tissue volume (BV/TV), trabecular number (TB.N), thickness (TB.TH) and separation (TB.SP) were also analyzed. Table 1.

Molecular modeling

All procedures were performed with Maestro (version 9.0.111, Schrödinger, LLC, New York, NY). The structure of celastrol was optimized to predict its protonation state and form stereoisomers. The protein structure of TLR2 was obtained from https://www.rcsb.org/(PDB DOI: 10.2210/pdb 1FYW/pdb). Protein Preparation Wizard was used to remove water molecules and heteroatom groups and add hydrogen. The grid-enclosing box was placed on the celastrol's docking region, and the glide module was used to dock the compounds using the default parameters.

Cell culture

Rat cartilages were isolated from the knee, shoulder, elbow and femur of newborn SD rats (within 24 h). Human cartilages were collected from OA patients (51–64 years old; Kellgren–Lawrence grade IV; n = 4) during total knee replacement surgeries. For primary chondrocyte culture, fresh cartilages were washed with phosphate-buffered saline (PBS) under sterile conditions. Then, the cartilages were cut into 1 mm^3 pieces and digested with 0.2% collagenase II in DMEM/F12 at 37°C overnight. After filtration, the chondrocytes were seeded and cultured in culturing dishes at 37°C and 5% CO_2. Primary chondrocytes were identified by immunofluorescence (Supplementary Figure S1).

Cell viability assay

In order to evaluate the cytotoxicity of celastrol to chondrocytes, the cell counting kit -8 (CCK-8) assay (Dojindo Co., Kumamoto, Japan) was used according to manufacturer's protocol. The same density of rat chondrocytes (rCHs) was seeded in 96-well plate and then treated with celastrol (0.1–2 μM) for 24 h. After washed with PBS, the rCHs in each well were incubated with 10% CCK-8 solution at 37°C for 2 h. The absorbance was measured at 450 nm by a microplate reader (Thermo Scientific, Logan, UT, USA).

Quantitative real-time polymerase chain reaction

Total RNA was extracted from rCHs using TRIzol reagents (Vazyme, China). The HiScript Reverse Transcriptase Kit (Vazyme, China) was used to convert RNA into cDNA. PCR was performed with standard procedure. The primers used are listed in Table 1.

Western blot analysis

RIPA lysis buffer with 1 mM protein phosphatase inhibitor was added into rCHs for protein extraction. The lysate was collected and centrifuged for 10 min at 12,000 r/min at 4°C. A BCA protein assay kit (Thermo Scientific) was used to determine the concentration of protein. The proteins were separated by 10% SDS-polyacrylamide gels, and then transferred onto PVDF membranes (Bio-Rad, Hercules, CA, USA). The block solution was the TBS (Tris-HCL Buffer Solution) containing bovine serum albumin (0.5%) (BSA, Sigma-Aldrich, Darmstadt, Germany) and Tween-20 (0.1%) (Bio Froxx, Guangzhou, China). The membranes were blocked with block solution for 1 h at room temperature, incubated with antibodies against matrix metalloproteinase 13 (MMP13, 1:1000, GTX100665, GeneTex, CA, USA), CollagenII (1:1000, ab34712, Abcam, Cambridge, UK), cyclooxygenase-2 (COX2, 1:1000, #12282, Cell Signaling Technology, Danvers, USA), TLR2 (1:1000, #29071, SAB, Nanjing, China), p-NF-κB (1:1000, #3033T, Cell Signaling Technology, Danvers, USA), NF-κB (1:1000, #8242T, Cell Signaling Technology, Danvers, USA) at 4°C overnight. Next, the TBST was used to wash membranes and the membranes incubated with horseradish peroxidase-conjugated secondary antibodies for 1 h. The ChemiDocXRS + Imaging System (Tanon, Shanghai, China) was used to detect the signals. The protein bands were quantitatively analyzed by ImageJ.

Histopathologic analysis

The affected knee joints were collected after the SD rats were sacrificed. The knee joints were fixed in 4% PFA for 24 h and decalcified with 10% EDTA for 2 months. After decalcification, the knee joints were embedded in paraffin and continuously sectioned at 5 μm. The tissue sections were stained with safranin O-fast green (S&F) and hematoxylin and eosin (H&E). Cartilage degeneration and subchondral bone damage were evaluated according to the international scoring system of the OA Research Association, and the severity of synovitis was graded using a scoring system as previously described (Gerwin et al., 2010).

Enzyme linked immunosorbent assay

Chondrocytes were seeded in 12-well plates, and supernatants were collected after IL-1β treatment with or without celastrol for 24 h. According to the manufacturer's protocol, levels of IL-6 and PGE2 were estimated using

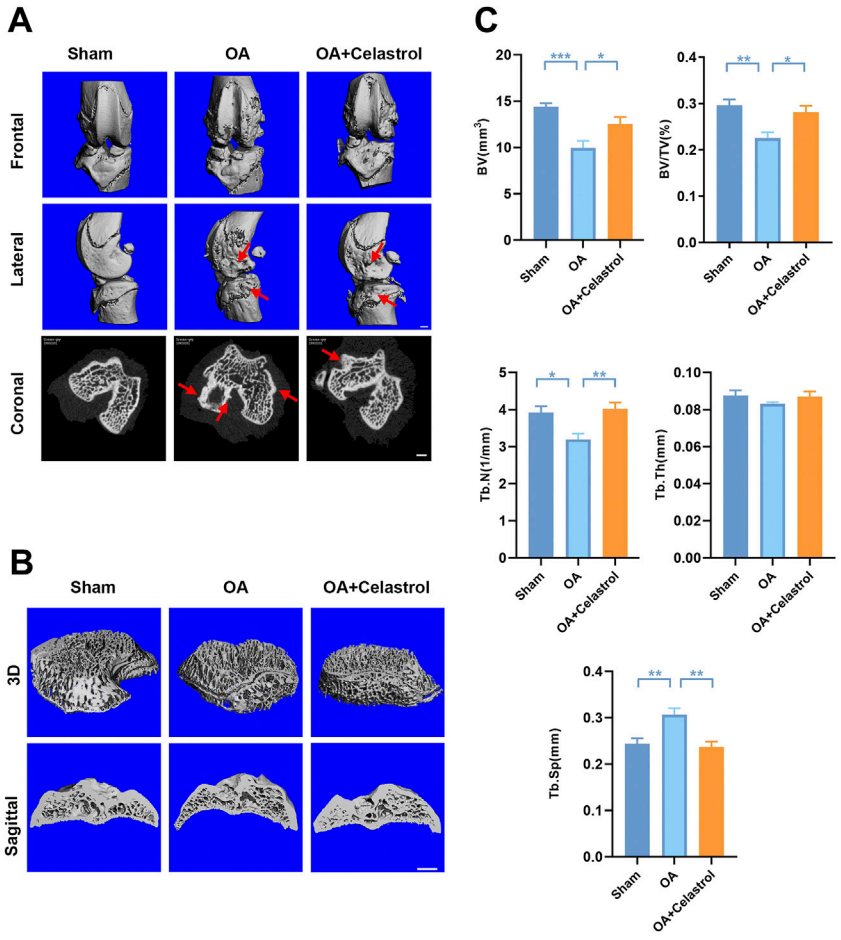

FIGURE 2
Celastrol reduced osteophyte formation and bone resorption induced by MCLT+pMMT *in vivo*. **(A)** Representative μCT images of frontal, lateral and coronal views of the knee joints from different groups (scale bar: 1 mm). **(B)** Representative three-dimensional μCT images of subchondral bone and sagittal views of medial compartment subchondral bone (scale bar: 1 mm). **(C)** Quantitative analysis of BV, BV/TV, Tb.N Tb.Th and Tb. Sp, n = 6. All data represent mean ± S.E.M. $*p < 0.05$, $**p < 0.01$ and $***p < 0.001$.

commercial ELISA kit (Multi Sciences, Hangzhou, China), with OD values measured at 450 and 570 nm.

Immunohistochemical staining

The tissue sections were dewaxed in xylene solution, and then 3% hydrogen peroxide was used to inhibit the activity of endogenous peroxidase. The slices were incubated with 0.4% pepsin (Sigma-Aldrich) in 1 mM hydrochloric acid at 37°C for 1 h for antigen repair. The block solution was the PBS solution containing 5% BSA. After blocking with block solution at 37°C for 30 min, the slices were incubated with the primary antibodies against MMP13 (1:1000, GTX100665, GeneTex, CA, USA), CollagenII (1:1000, ab34712, Abcam, Cambridge, UK), TLR2 (1:1000, #29071, SAB, Nanjing, China) at 4°C overnight, and finally with a HRP-conjugated secondary antibody at room temperature for 1 h. Then, the slices were washed with PBS and developed, and sealed after the re-staining with methyl green (0.2%). The positive cells were counted by ImageJ.

Cell immunofluorescence

The cells were seed in 48-well plates. After IL-1β (10 ng/ml) treatment with or without celastrol (0.025, 0.0.05 and 0.1 μM) for 24 h, the cells were washed with PBS, fixed in 4% PFA for 20 min, and permeabilized with 0.4%Triton-100X for 10 min. The block solution was the PBS solution containing BSA (0.5%) and Tween-20 (0.1%). After blocking with block solution at room temperature for 1 h, the cells were incubated with primary antibody at 4°C overnight and washed with PBS. Then the cells were incubated with FITC-conjugated secondary antibodies at room temperature for 1 h, stained with Hoechst33258 for 10 min, and observed with a microscope. The average fluorescence intensity was measured by ImageJ.

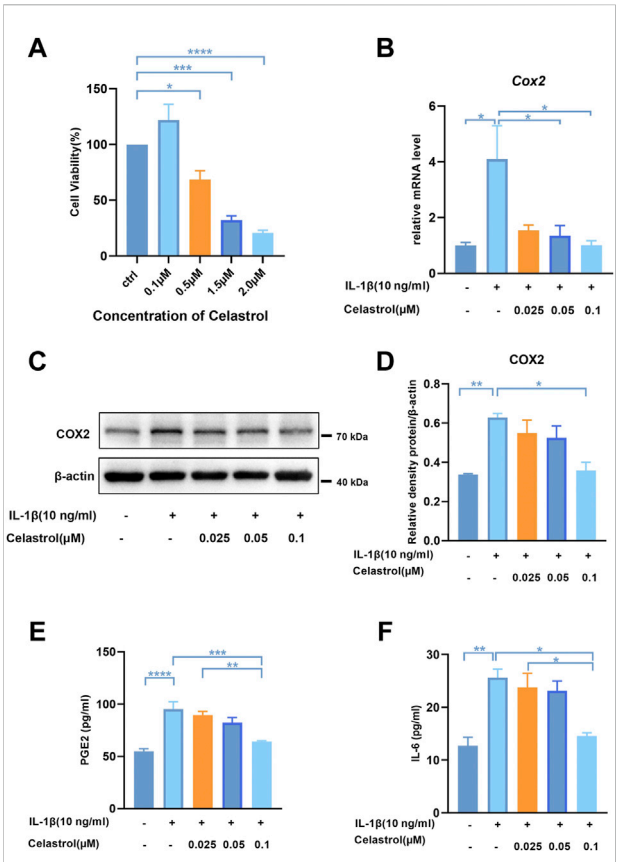

FIGURE 3
Celastrol inhibited IL-1β-induced inflammatory mediators in rat chondrocytes. **(A)** Rat chondrocytes viability for 24 h treated with celastrol at different concentrations examined by CCK-8 kit. **(B)** The mRNA levels of COX2 in rat chondrocytes were assayed by real-time PCR. **(C)** Representative Western blot results for COX2 in rat chondrocytes treated as indicated. **(D)** Quantification of Western blot data from **(C)**. **(E,F)** Levels of PGE2 and IL-6 were assayed by ELISA. All data represent mean ± S.E.M.*$p < 0.05$, **$p < 0.01$, ***$p < 0.001$ and ****$p < 0.0001$. All experiments were repeated 3 times.

Statistical analysis

All data are expressed as the Means ± Sem. Statistical significance between multiple groups was determined by one-way analysis of variance (ANOVA) and Tukey test was conducted post hoc test using GraphPad Prism 8. T-test was used to analyze statistical difference between two independent groups. Differences were considered statistically significant when $p < 0.05$.

Results

Celastrol alleviated the progression of OA in rat model

We performed surgery to remove the medial meniscus from the right knee of 6-week-old rats to induce OA progression. Eight weeks after surgery, the rats received right articular joint injections of saline or 1 mg/kg celastrol once a week for 8 weeks (Figure 1A). We measured the 5-min walking distance and times reared within 5 min at Week 16, and found that celastrol improved the walking ability of rats with OA (Supplementary Figures S2A,B). Then, we observed the lateral view of affected limbs in general, and found that the right knee joint stiffness in full extension was improved in OA group after celastrol treatment (Supplementary Figure S2C). Moreover, we assessed the degree of joint swelling by the maximal coronal diameter of the right knee joint with vernier caliper at week 16, and found that celastrol ameliorated joint swelling compared to OA group (Figure 1B, Supplementary Figure S2D). In addition, celastrol group showed a smooth surface in the posterior portion of the medial tibial plateau and medial femoral condyle, while severe rough surface was observed in OA group (red arrows), suggesting celastrol could alleviate bone wear (Figure 1C). H&E and S&F staining performed in joint section displayed significant damage to the cartilage surfaces, loss of proteoglycans, and thinning articular in OA group, and improved cartilage integrity in celastrol group (Figure 1D). Blinded OARSI scoring was used to measure the severity of OA, and celastrol group had significantly lower cartilage degeneration score and subchondral bone damage score compared to OA group (Figures 1F,G). Moreover, H&E staining and synovial membrane inflammation score indicated the presence of synovial hypercellularity and thickening in the OA group, whereas celastrol treatment alleviated synovitis (Figures 1E,H).

Celastrol reduced osteophyte formation and bone resorption induced by "MCLT+pMMT" *in vivo*

In OA joints, osteophyte formation developed as a characteristic structural change of OA, which was found in micro-computed tomography (μCT) analysis after "MCLT+pMMT" treatment. Remarkably, celastrol group presented less osteophyte (red arrows) formation compared to OA group (Figure 2A). Meanwhile, subchondral bone resorption followed by increased bone remodeling played an important role in the pathogenesis of OA. To investigate the effects of celastrol on the subchondral bone remodeling of OA, we reconstructed the tibian plateau subchondral bone and analyzed the microstructure parameters. "MCLT+pMMT" significantly induced bone resorption, as shown by the increased osteolysis in subchondral bone of the tibia. And celastrol treatment reduced bone loss and increased bone mass in subchondral bone (Figure 2B). BV of tibial plateau subchondral bone was significantly lower in the OA group than the sham and celastrol groups (Figure 2C). In addition, BV/TV and Tb.N were decreased, and Tb. Sp was increased in OA group, which

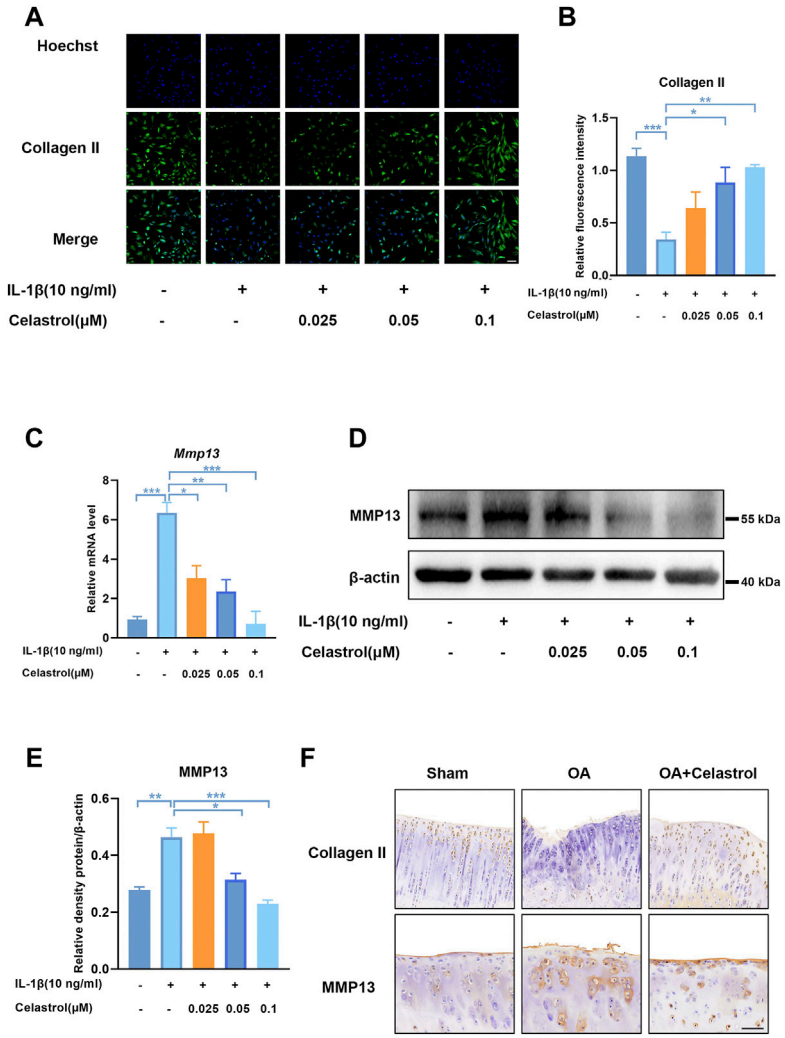

FIGURE 4
Celastrol inhibited matrix degradation in rat chondrocytes. **(A)** Representative immunofluorescence staining for Collagen II in rat chondrocytes (green: Collagen II, blue: DAPI, scale bar:100 μm). **(B)** Quantification of the immunohistochemical staining data from A. **(C)** The mRNA levels of MMP13 in rCHs were assayed by real-time PCR. **(D)** Representative Western blot results for MMP13 in rCHs treated as indicated. **(E)** Quantification of Western blot data from D. **(F)** Immunohistochemical staining for CollagenII and MMP13 in the affected joint cartilage of rats from different groups (scale bar:50 μm). All data represent mean ± S.E.M.*$p < 0.05$, **$p < 0.01$ and ***$p < 0.001$. All experiments were repeated 3 times.

strongly revealed the suppressed bone destruction effect of celastrol.

Celastrol inhibited IL-1β-induced inflammatory mediators in rat chondrocytes

To assess the cytotoxicity of celastrol on chondrocytes, we treated rCHs with different concentrations (0.1–2 μM) of celastrol for 24 h. Celastrol treatment (0.1 μM, 24 h) had no significant cytotoxic effect on rCHs and even slightly promoted the proliferation of rCHs. However, high concentrations (0.5, 1.5 and 2 μM) of celastrol treatment had a dose-dependent cytotoxic effect in terms of cell viability (Figure 3A). Referring to CCK8 analysis, celastrol was divided into low, medium and high dose groups according to different concentrations (0.025, 0.05, 0.1 μM). We examined IL-1β-induced inflammatory cytokines and found that the increased COX2 expression and PGE2 levels were significantly alleviated after celastrol treatment (Figures 3B–E). Besides, elevated IL-6 levels induced by IL-1β were also decreased significantly with the treatment of celastrol (Figure 3F).

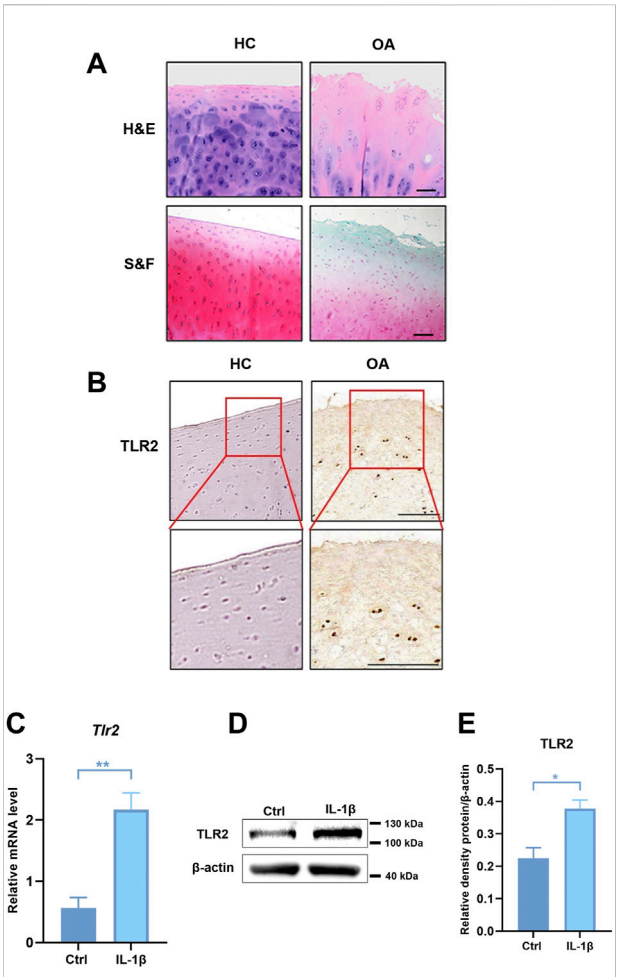

FIGURE 5
The expression of TLR2 was up-regulated in OA patients and in human chondrocytes treated with IL-1β. **(A)** H&E and S&F staining of healthy control and OA patients (scale bar: 200 μm). **(B)** Immunohistochemical staining for TLR2 in healthy control and human OA samples. **(C)** The mRNA levels of TLR2 in hCHs treated with or without IL-1β (10 ng/ml) were assayed by real-time PCR. **(D)** Representative Western blot results for TLR2 in hCHs treated with or without IL-1β (10 ng/ml). **(E)** Quantification of Western blot data from **(D)**. All data represent mean ± S.E.M.*$p < 0.05$, **$p < 0.01$. All experiments were repeated 3 times.

Celastrol inhibited matrix degradation in rat chondrocytes

As Collagen II was the major ECM component, IL-1β inhibited the synthesis of matrix collagen and induced downregulation of COL2A1 in IL-1β group. Fluorescence analysis showed a markedly higher density of Collagen II in rCHs in "IL-1β+celastrol group" than in IL-1β group with a celastrol dose-dependant manner (Figures 4A,B). OA affected joints are mainly characterized by the degradation of cartilage extracellular matrix, and especially matrix metalloproteinase13 (MMP13) is the most effective collagen II degrading enzyme. The Western blot and real-time PCR analysis of rCHs stimulated with IL-1β showed that the expression of MMP13 was significantly decreased by celastrol treatment in a dose-dependent manner (Figures 4C–E). Similar to the results *in vitro*, immunohistochemical staining of rat cartilage with OA showed that the expression of MMP13 was significantly rescued by celastrol treatment. Moreover, the immunohistochemistry revealed the loss of Collagen II was alleviated by celastrol treatment (Figure 4F). Altogether, celastrol promoted ECM anabolism via down-regulating the expression of catabolic factors and affecting Collagen II deposition in pathological chondrocytes.

The expression of TLR2 was up-regulated in OA patients and *in vitro* model of human chondrocytes

As the pathogenesis of OA is associated with abnormal TLRs-mediated innate immune-inflammatory responses, we analyzed the expression of TLRs in degenerative meniscus cells of OA patients (Supplementary Figure S3) (Jiang et al., 2021). Among these, the expression of TLR2 and TLR4 was much higher than the others, especially TLR2. We further collected cartilage from OA patients and healthy cartilage to evaluate cartilage wear and TLR2 expression. H&E and S&F staining showed that the cartilage surface of OA patients was seriously damaged. Chondrocytes were disorderly arranged, and the tide line was distorted (Figure 5A). Compared with healthy control, the expression of TLR2 increased in OA patients (Figure 5B). To further verify these results, we stimulated human chondrocytes (hCHs) with IL-1β to establish a model of OA *in vitro*. We validated that the mRNA level of TLR2 was significantly up-regulated *in vitro* model (Figure 5C). Moreover, we found that the protein level of TLR2 also significantly increased (Figures 5D,E).

Celastrol inhibited TLR2-triggered signals in rat chondrocytes

Docking simulation analysis of celastrol docked to TLR2 by maestro software showed that TLR2 could interact with celastrol (Figures 6A,B). To further investigate the effect of celastrol on TLR2-triggered signals, we first measured the TLR2 expression of rCHs with IL-1β stimulation (Figures 6C–E). As we can see TLR2 expression significantly increased under IL-1β stimulation, and decreased after celastrol treatment. With the activation of the TLR2 signaling pathway, the downstream NF-κB and NF-κB phosphorylation was subsequently induced to activate. Western blot and real-time PCR analysis showed that the IL-1β-stimulated increasement in NF-κB and NF-κB phosphorylation expression was significantly inhibited after celastrol treatment in rCHs (Figures 6F–I). *In vivo*, compared with OA group we also found the decrease in TLR2 expression in

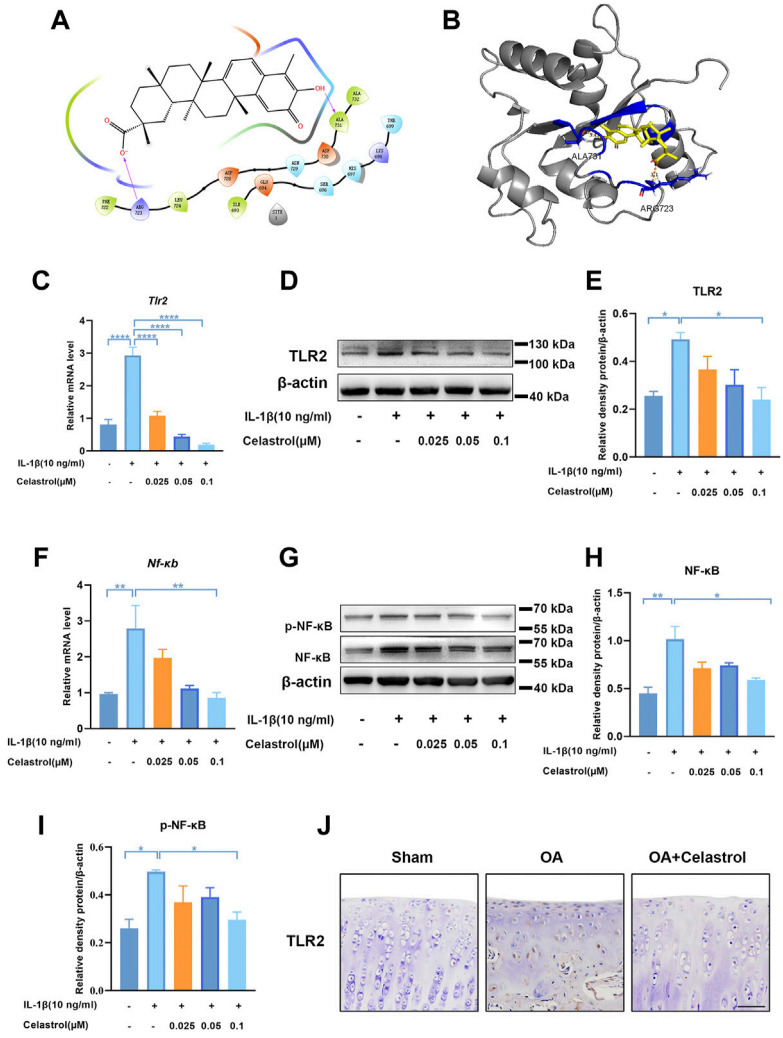

FIGURE 6
Celastrol inhibited TLR2-triggered signals in rat chondrocytes. **(A,B)** Interaction diagrams of celastrol docked to TLR2 using Maestro software. **(C,F)** The mRNA levels of TLR2 and NF-κB in rat chondrocytes were assayed by real-time PCR. **(D,G)** Western blot results for TLR2, p-NF-κB and NF-κB in rat chondrocytes with or without celastrol. **(E,H,I)** Quantification of Western blot data from D and G. **(J)** Immunohistochemical staining for TLR2 in the affected joint cartilage of rats from different groups (scale bar: 50 μm). All data represent mean ± S.E.M. *$p < 0.05$, **$p < 0.01$, ***$p < 0.001$ and ****$p < 0.0001$. All experiments were repeated 3 times.

the "OA+celastrol" group in the cartilage (Figure 6J). Thus, we concluded that celastrol attenuated inflammation and matrix degradation via regulating TLR2-dependent pathway.

Discussion

For a long time, OA was known as a degenerative disease of joints, characterized by articular cartilage degeneration, ECM degradation, bone loss and synovitis. (Bultink and Lems, 2013). Recently, OA has been considered a multifactorial disease rather than a degenerative one, in which low-grade, chronic inflammation plays a crucial role. (Robinson et al., 2016). Previous studies suggested that low-grade inflammation mediated by innate immune system, especially TLRs, contributed to cartilage damage and osteoporosis during OA development (Miller et al., 2019; Saxena et al., 2021). Despite many studies that attempted to delay cartilage degeneration, no effective treatment has yet focused on the roles of innate immunity (Hochberg et al., 2012). Our work demonstrate that celastrol can improve various pathological changes of OA by inhibiting innate immunity and provide an "entry point" for treatment.

Recent studies have revealed that TLRs are closely related to OA. Stimulation of TLRs ultimately activated transcription factors such as NF-κB and activator protein 1 (AP1), leading

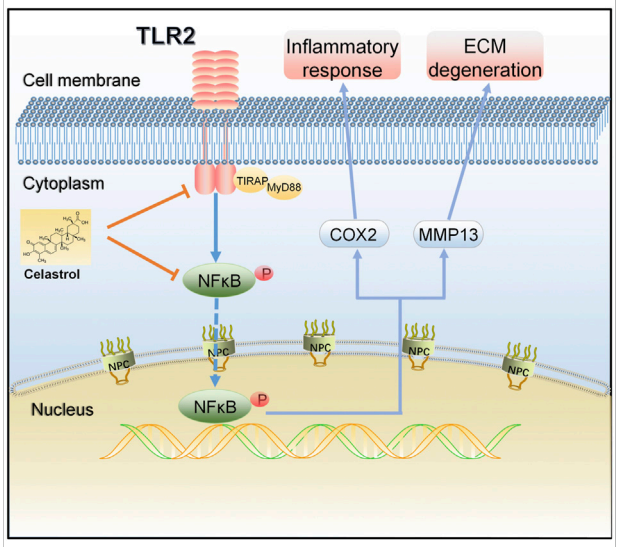

FIGURE 7
A schematic diagram of the proposed mechanism of celastrol on TLR2/NF-κB signals in rat chondrocytes. Celastrol treatment negatively regulated TLR2 activation and NF-κB phosphorylation in IL-1β-induced chondrocytes, thereby inhibiting inflammation and matrix degradation.

to initiate an inflammatory transcription program (Scanzello et al., 2008). Among all the functional TLRs in human, TLR1-TLR7 and TLR9 have been detected in the synovium of OA patients (Scanzello and Goldring, 2012), and the up regulation of TLR2 and TLR4 can be found in human knee lesions (Liu-Bryan, 2013). In the innate immune response, human articular chondrocytes express TLRs. Among all TLRs, TLR2 and TLR4 are the main regulators of innate immunity activated in OA (Barreto et al., 2017; Hamasaki et al., 2020; Korotkyi et al., 2020; Korotkyi et al., 2021). Compared to TLR4, TLR2 plays a crucial role in the early stage of innate immune response, and the effect of controlling the initial inflammatory response in the joint cavity is critical for the prognosis of OA (Abdollahi-Roodsaz et al., 2008; Wojdasiewicz et al., 2014). In this study, we focused on TLR2 and confirmed that the expression of TLR2 was up-regulated in chondrocytes of both OA patients and OA model rats. Our results suggest that cartilage protection can be achieved by inhibiting TLR2. In addition inhibition of TLR2 may suppress osteoclastic bone resorption, thereby improving osteoporosis (Wallimann et al., 2021). NF-κB is a crucial regulator of innate immunity (Chen et al., 2018) and is considered to be an important regulator of TLR induced response (Carmody and Chen, 2007). Aberrant NF-κB regulation is involved in the development of OA and OP(Chen et al., 2020). Therefore, inhibition of the TLR2/NF-κB signaling pathway may be critical to the treatment of OA.

Celastrol is widely used to treat autoimmune and inflammatory diseases such as rheumatoid arthritis (RA), systemic lupus erythematosus, and nephropathy. As a quinone methyl triterpene, celastrol was extracted from the root of Trypterygium wilfordii, which has attracted extensive attention because of its anti-inflammatory and anti-cancer effects (Sethi et al., 2007; Kim et al., 2009). Recent studies validated that Tripterygium wilfordii (TW) and its extracts have regulatory effects on innate immune cells including macrophages and neutrophils, as well as a variety of innate immune molecules including cytokines, adhesion molecules, PRR and complement molecules (Li et al., 2019). A related study found that celastrol could promote autophagy *in vitro* and *in vivo* to protect chondrocyte (Feng et al., 2020). Although celatrol has a powerful anti-inflammatory effect, few studies have examined whether such effects are brought out by inhibiting innate immunity, especially TLR2, which has only been reported in multiple sclerosis and RA (Abdin and Hasby, 2014; Lu et al., 2021). Furthermore, whether celastrol can regulate TLRs-mediated innate immunity in OA has never been investigated to the best of our knowledge. Moreover, a growing number of studies have observed numerous adverse effects associated with oral TW, especially hepatotoxicity, which has hindered its widespread use in clinical practice (Song et al., 2020). As for Tripterygium wilfordii polyglycosides tablet, its efficacy and toxicity are difficult to depict because of its complex components, thus greatly limiting its clinical application. Therefore, in order to reduce drug side effects, we adopted intra-articular injection to observe whether local administration of celastrol could inhibit the innate immunity and delay the progression of OA.

Our results showed that celastrol not only significantly inhibited the expression of inflammatory factors such as COX2, IL-6, and PEG2 but also suppressed the expression of MMP13 and degradation of CollagenII *in vitro*. *In vivo* the results showed that the joint wear and tear was significantly reduced in celastrol treated group compared with OA group. All these results suggest that celastrol has an excellent protective effect on the cartilage of OA in rats. In addition, our study showed the inhibitory effect of celastrol on bone resorption. Knee joints in OA group showed significant bone loss based on a significant decrease in bone volume and BV/TV, a decrease in Tb.N, and an increase in Tb. Sp. Therefore, our therapeutic goal is not simply to relieve pain, but more importantly to inhibit articular cartilage destruction and osteoporosis of subchondral bone. All above results indicate that celastrol can protect cartilage and inhibit OP of subchondral bone, which makes it a potential drug for OA treatment.

IL-1β is a vital pro-inflammatory factor in the development of OA, which can induce chondrocyte inflammation and catabolism independently, and can also act on articular cartilage and other components in combination with other mediators. As a damage factor, IL-1β induces the release of

inflammatory mediators (Kobayashi et al., 2005). These inflammatory mediators aggravate cartilage destruction by activating MMPs and inhibiting the synthesis of collagen and glycoaminoglycan (GAG) (Scanzello et al., 2008; Nair et al., 2012; Gomez et al., 2015). Therefore, IL-1β is often used to establish OA models *in vitro* (Dunn et al., 2014; Wang et al., 2021). We simulated the inflammatory microenvironment of OA *in vitro* and found that IL-1β up-regulated the expression of TLR2 and NF-κB in chondrocytes. Further results showed that celastrol inhibited IL-1β-induced upregulation of TLR2 and NF-κB in chondrocytes to reduce inflammation and extracellular matrix degradation.

In summary, we demonstrated that the TLR2/NF-κB signaling pathway involved in early OA and might be a potential therapeutic target for slowing or altering the progression of OA. Celastrol showed anti-inflammatory and chondroprotective effects both *in vivo* and *in vitro* by down regulating the TLR2/NF-κB pathway, effectively inhibiting the release of inflammatory factors, cartilage degradation and bone loss, indicating that celastrol had a therapeutic effect on OA (Figure 7). Our study provides a new possible therapeutic approach for OA treatment, which could be further verified by future studies.

Data availability statement

The original contributions presented in the study are included in the article/Supplementary Material, further inquiries can be directed to the corresponding authors.

Ethics statement

The studies involving human participants were reviewed and approved by Nanjing Drum Tower Hospital Clinical College of Traditional Chinese and Western Medicine. The patients/participants provided their written informed consent to participate in this study. The animal study was reviewed and approved by Nanjing Drum Tower Hospital Clinical College of Traditional Chinese and Western Medicine.

Author contributions

Conception and design of study: LS, XW, JS, and GY. Acquisition of data: GY, KW, HS, RZ, and HY. Drafting the manuscript: GY and KW. Revising the manuscript critically for important intellectual content: LS, XW, and SD.

Funding

This work was supported by the National Key Research and Development Program of China (2020YFA0710800), the Key Program of National Natural Science Foundation of China (Grant No.81930043), the Major International (Regional) Joint Research Project of China (Grant No. 81720108020), the Jiangsu Provincial Key Research and Development Program (BE2020621).

Conflict of interest

The authors declare that the research was conducted in the absence of any commercial or financial relationships that could be construed as a potential conflict of interest.

Publisher's note

All claims expressed in this article are solely those of the authors and do not necessarily represent those of their affiliated organizations, or those of the publisher, the editors and the reviewers. Any product that may be evaluated in this article, or claim that may be made by its manufacturer, is not guaranteed or endorsed by the publisher.

Supplementary material

The Supplementary Material for this article can be found online at: https://www.frontiersin.org/articles/10.3389/fphar.2022.963506/full#supplementary-material

References

Abdin, A. A., and Hasby, E. A. (2014). Modulatory effect of celastrol on Th1/Th2 cytokines profile, TLR2 and CD3+ T-lymphocyte expression in a relapsing-remitting model of multiple sclerosis in rats. *Eur. J. Pharmacol.* 742, 102–112. doi:10.1016/j.ejphar.2014.09.001

Abdollahi-Roodsaz, S., Joosten, L. A., Helsen, M. M., Walgreen, B., van Lent, P. L., van den Bersselaar, L. A., et al. (2008). Shift from toll-like receptor 2 (TLR-2) toward TLR-4 dependency in the erosive stage of chronic streptococcal cell wall arthritis coincident with TLR-4-mediated interleukin-17 production. *Arthritis Rheum.* 58 (12), 3753–3764. doi:10.1002/art.24127

Alberton, P., Dugonitsch, H. C., Hartmann, B., Li, P., Farkas, Z., Saller, M. M., et al. (2019). Aggrecan hypomorphism compromises articular cartilage biomechanical properties and is associated with increased incidence of spontaneous osteoarthritis. *Int. J. Mol. Sci.* 20 (5), E1008. doi:10.3390/ijms20051008

An, L., Li, Z., Shi, L., Wang, L., Wang, Y., Jin, L., et al. (2020). Inflammation-targeted celastrol nanodrug attenuates collagen-induced arthritis through NF-κB and Notch1 pathways. *Nano Lett.* 20 (10), 7728–7736. doi:10.1021/acs.nanolett.0c03279

Arya, P., Nabi, S., and Bhandari, U. (2021). Modulatory role of atorvastatin against high-fat diet and zymosan-induced activation of TLR2/NF-κB signaling pathway in C57BL/6 mice. *Iran. J. Basic Med. Sci.* 24 (8), 1023–1032. doi:10.22038/ijbms.2021.55460.12409

Barreto, G., Sandelin, J., Salem, A., Nordstorm, D. C., and Waris, E. (2017). Toll-like receptors and their soluble forms differ in the knee and thumb basal osteoarthritic joints. *Acta Orthop.* 88 (3), 326–333. doi:10.1080/17453674.2017.1281058

Berenbaum, F., Wallace, I. J., Lieberman, D. E., and Felson, D. T. (2018). Modern-day environmental factors in the pathogenesis of osteoarthritis. *Nat. Rev. Rheumatol.* 14 (11), 674–681. doi:10.1038/s41584-018-0073-x

Bindu, S., Mazumder, S., and Bandyopadhyay, U. (2020). Non-steroidal anti-inflammatory drugs (NSAIDs) and organ damage: A current perspective. *Biochem. Pharmacol.* 180, 114147. doi:10.1016/j.bcp.2020.114147

Bortoluzzi, A., Furini, F., and Scire, C. A. (2018). Osteoarthritis and its management - epidemiology, nutritional aspects and environmental factors. *Autoimmun. Rev.* 17 (11), 1097–1104. doi:10.1016/j.autrev.2018.06.002

Bultink, I., and Lems, W. (2013). Osteoarthritis and osteoporosis: what is the overlap? *Curr. Rheumatol. Rep.* 15 (5), 328. doi:10.1007/s11926-013-0328-0

Carmody, R., and Chen, Y. (2007). Nuclear factor-kappaB: activation and regulation during toll-like receptor signaling. *Cell. Mol. Immunol.* 4 (1), 31–41.

Cascao, R., Vidal, B., Carvalho, T., Lopes, I. P., Romao, V. C., Goncalves, J., et al. (2020). Celastrol efficacy by oral administration in the adjuvant-induced arthritis model. *Front. Med.* 7, 455. doi:10.3389/fmed.2020.00455

Chen, S., Bonifati, S., Qin, Z., St Gelais, C., Kodigepalli, K., Barrett, B., et al. (2018). SAMHD1 suppresses innate immune responses to viral infections and inflammatory stimuli by inhibiting the NF-κB and interferon pathways. *Proc. Natl. Acad. Sci. U. S. A.* 115 (16), E3798–E3807. doi:10.1073/pnas.1801213115

Chen, Z., Lin, C., Song, B., Li, C., Qiu, J., Li, S., et al. (2020). Spermidine activates RIP1 deubiquitination to inhibit TNF-α-induced NF-κB/p65 signaling pathway in osteoarthritis. *Cell Death Dis.* 11 (7), 503. doi:10.1038/s41419-020-2710-y

Cooper, D. J., Scammell, B. E., Batt, M. E., and Palmer, D. (2018). Factors associated with pain and osteoarthritis at the hip and knee in great britain's olympians: a cross-sectional study. *Br. J. Sports Med.* 52 (17), 1101–1108. doi:10.1136/bjsports-2017-098315

Driban, J. B., Bannuru, R. R., Eaton, C. B., Spector, T. D., Hart, D. J., McAlindon, T. E., et al. (2020). The incidence and characteristics of accelerated knee osteoarthritis among women: the chingford cohort. *BMC Musculoskelet. Disord.* 21 (1), 60. doi:10.1186/s12891-020-3073-3

Dunn, S. L., Wilkinson, J. M., Crawford, A., Le Maitre, C. L., and Bunning, R. A. (2014). Cannabinoid WIN-55, 212-2 mesylate inhibits interleukin-1β induced matrix metalloproteinase and tissue inhibitor of matrix metalloproteinase expression in human chondrocytes. *Osteoarthr. Cartil.* 22 (1), 133–144. doi:10.1016/j.joca.2013.10.016

Feng, K., Chen, H., and Xu, C. (2020). Chondro-protective effects of celastrol on osteoarthritis through autophagy activation and NF-κB signaling pathway inhibition. *Inflamm. Res.* 69 (4), 385–400. doi:10.1007/s00011-020-01327-z

Gerwin, N., Bendele, A. M., Glasson, S., and Carlson, C. S. (2010). The OARSI histopathology initiative - recommendations for histological assessments of osteoarthritis in the rat. *Osteoarthr. Cartil.* 18 (3), S24–S34. doi:10.1016/j.joca.2010.05.030

Goldring, M. B., and Goldring, S. R. (2007). Osteoarthritis. *J. Cell. Physiol.* 213 (3), 626–634. doi:10.1002/jcp.21258

Gomez, R., Villalvilla, A., Largo, R., Gualillo, O., and Herrero-Beaumont, G. (2015). TLR4 signalling in osteoarthritis--finding targets for candidate DMOADs. *Nat. Rev. Rheumatol.* 11 (3), 159–170. doi:10.1038/nrrheum.2014.209

Hamasaki, M., Terkawi, M., Onodera, T., Tian, Y., Ebata, T., Matsumae, G., et al. (2020). Transcriptional profiling of murine macrophages stimulated with cartilage fragments revealed a strategy for treatment of progressive osteoarthritis. *Sci. Rep.* 10 (1), 7558. doi:10.1038/s41598-020-64515-1

Hart, H. F., van Middelkoop, M., Stefanik, J. J., Crossley, K. M., and Bierma-Zeinstra, S. (2020). Obesity is related to incidence of patellofemoral osteoarthritis: the cohort hip and cohort knee (CHECK) study. *Rheumatol. Int.* 40 (2), 227–232. doi:10.1007/s00296-019-04472-9

Hindy, G., Akesson, K. E., Melander, O., Aragam, K. G., Haas, M. E., Nilsson, P. M., et al. (2019). Cardiometabolic polygenic risk scores and osteoarthritis outcomes: A mendelian randomization study using data from the malmo diet and cancer study and the UK biobank. *Arthritis Rheumatol.* 71 (6), 925–934. doi:10.1002/art.40812

Hochberg, M. C., Altman, R. D., April, K. T., Benkhalti, M., Guyatt, G., McGowan, J., et al. (2012). American College of Rheumatology 2012 recommendations for the use of nonpharmacologic and pharmacologic therapies in osteoarthritis of the hand, hip, and knee. *Arthritis Care Res.* 64 (4), 465–474. doi:10.1002/acr.21596

Hunter, D. J., and Bierma-Zeinstra, S. (2019). Osteoarthritis. *Lancet* 393 (10182), 1745–1759. doi:10.1016/S0140-6736(19)30417-9

Hwang, H. S., Lee, M. H., and Kim, H. A. (2019). Fibronectin fragment inhibits xylosyltransferase-1 expression by regulating Sp1/Sp3- dependent transcription in articular chondrocytes. *Osteoarthr. Cartil.* 27 (5), 833–843. doi:10.1016/j.joca.2019.01.006

Hwang, H. S., Park, S. J., Cheon, E. J., Lee, M. H., and Kim, H. A. (2015). Fibronectin fragment-induced expression of matrix metalloproteinases is mediated by MyD88-dependent TLR-2 signaling pathway in human chondrocytes. *Arthritis Res. Ther.* 17, 320. doi:10.1186/s13075-015-0833-9

Jiang, Z., Du, X., Wen, X., Li, H., Zeng, A., Sun, H., et al. (2021). Whole-transcriptome sequence of degenerative meniscus cells unveiling diagnostic markers and therapeutic targets for osteoarthritis. *Front. Genet.* 12, 754421. doi:10.3389/fgene.2021.754421

Kalaitzoglou, E., Griffin, T. M., and Humphrey, M. B. (2017). Innate immune responses and osteoarthritis. *Curr. Rheumatol. Rep.* 19 (8), 45. doi:10.1007/s11926-017-0672-6

Kim, D. H., Shin, E. K., Kim, Y. H., Lee, B. W., Jun, J. G., Park, J. H., et al. (2009). Suppression of inflammatory responses by celastrol, a quinone methide triterpenoid isolated from Celastrus regelii. *Eur. J. Clin. Invest.* 39 (9), 819–827. doi:10.1111/j.1365-2362.2009.02186.x

Kim, H. A., Cho, M. L., Choi, H. Y., Yoon, C. S., Jhun, J. Y., Oh, H. J., et al. (2006). The catabolic pathway mediated by Toll-like receptors in human osteoarthritic chondrocytes. *Arthritis Rheum.* 54 (7), 2152–2163. doi:10.1002/art.21951

Kobayashi, M., Squires, G. R., Mousa, A., Tanzer, M., Zukor, D. J., Antoniou, J., et al. (2005). Role of interleukin-1 and tumor necrosis factor alpha in matrix degradation of human osteoarthritic cartilage. *Arthritis Rheum.* 52 (1), 128–135. doi:10.1002/art.20776

Korotkyi, O., Dvorshchenko, K., Falalyeyeva, T., Sulaieva, O., Kobyliak, N., Abenavoli, L., et al. (2020). Combined effects of probiotic and chondroprotector during osteoarthritis in rats. *Panminerva Med.* 62 (2), 93–101. doi:10.23736/S0031-0808.20.03841-0

Korotkyi, O., Huet, A., Dvorshchenko, K., Kobyliak, N., Falalyeyeva, T., Ostapchenko, L., et al. (2021). Probiotic composition and chondroitin sulfate regulate TLR-2/4-mediated NF-κB inflammatory pathway and cartilage metabolism in experimental osteoarthritis. *Probiotics Antimicrob. Proteins* 13 (4), 1018–1032. doi:10.1007/s12602-020-09735-7

Kroon, F. P. B., Kortekaas, M. C., Boonen, A., Bohringer, S., Reijnierse, M., Rosendaal, F. R., et al. (2019). Results of a 6-week treatment with 10 mg prednisolone in patients with hand osteoarthritis (HOPE): a double-blind, randomised, placebo-controlled trial. *Lancet* 394 (10213), 1993–2001. doi:10.1016/S0140-6736(19)32489-4

Lee, H., Hwang, D., Lee, M., Lee, J., Cho, S., Kim, T. J., et al. (2022). Micro-current stimulation suppresses inflammatory responses in peptidoglycan-treated raw 264.7 macrophages and *Propionibacterium acnes*-induced skin inflammation via TLR2/NF-κB signaling pathway. *Int. J. Mol. Sci.* 23 (5), 2508. doi:10.3390/ijms23052508

Li, J. M., Jiang, Q., Tang, X. P., Yang, H., and Zhou, Z. Q. (2019). Study advances in regulation effect of Tripterygium wilfordii and its extracts on innate immune system in rheumatoid arthritis cases. *Zhongguo Zhong Yao Za Zhi* 44 (16), 3384–3390. doi:10.19540/j.cnki.cjcmm.20190103.001

Liu-Bryan, R. (2013). Synovium and the innate inflammatory network in osteoarthritis progression. *Curr. Rheumatol. Rep.* 15 (5), 323. doi:10.1007/s11926-013-0323-5

Liu-Bryan, R., and Terkeltaub, R. (2015). Emerging regulators of the inflammatory process in osteoarthritis. *Nat. Rev. Rheumatol.* 11 (1), 35–44. doi:10.1038/nrrheum.2014.162

Lu, X., Gong, S., Wang, X., Hu, N., Pu, D., Zhang, J., et al. (2021). Celastrol exerts cardioprotective effect in rheumatoid arthritis by inhibiting TLR2/HMGB1 signaling pathway-mediated autophagy. *Int. Arch. Allergy Immunol.* 182 (12), 1245–1254. doi:10.1159/000517185

Maqbool, M., Fekadu, G., Jiang, X., Bekele, F., Tolossa, T., Turi, E., et al. (2021). An up to date on clinical prospects and management of osteoarthritis. *Ann. Med. Surg.* 72, 103077. doi:10.1016/j.amsu.2021.103077

Martel-Pelletier, J., Barr, A. J., Cicuttini, F. M., Conaghan, P. G., Cooper, C., Goldring, M. B., et al. (2016). Osteoarthritis. *Nat. Rev. Dis. Prim.* 2, 16072. doi:10.1038/nrdp.2016.72

McAlindon, T. E., Bannuru, R. R., Sullivan, M. C., Arden, N. K., Berenbaum, F., Bierma-Zeinstra, S. M., et al. (2014). OARSI guidelines for the non-surgical management of knee osteoarthritis. *Osteoarthr. Cartil.* 22 (3), 363–388. doi:10.1016/j.joca.2014.01.003

Miller, R. E., Scanzello, C. R., and Malfait, A. M. (2019). An emerging role for Toll-like receptors at the neuroimmune interface in osteoarthritis. *Semin. Immunopathol.* 41 (5), 583–594. doi:10.1007/s00281-019-00762-3

Nair, A., Kanda, V., Bush-Joseph, C., Verma, N., Chubinskaya, S., Mikecz, K., et al. (2012). Synovial fluid from patients with early osteoarthritis modulates fibroblast-like synoviocyte responses to toll-like receptor 4 and toll-like receptor 2 ligands via soluble CD14. *Arthritis Rheum.* 64 (7), 2268–2277. doi:10.1002/art.34495

Prieto-Alhambra, D., Judge, A., Javaid, M. K., Cooper, C., Diez-Perez, A., Arden, N. K., et al. (2014). Incidence and risk factors for clinically diagnosed knee, hip and hand osteoarthritis: Influences of age, gender and osteoarthritis affecting other joints. *Ann. Rheum. Dis.* 73 (9), 1659–1664. doi:10.1136/annrheumdis-2013-203355

Robinson, W. H., Lepus, C. M., Wang, Q., Raghu, H., Mao, R., Lindstrom, T. M., et al. (2016). Low-grade inflammation as a key mediator of the pathogenesis of osteoarthritis. *Nat. Rev. Rheumatol.* 12 (10), 580–592. doi:10.1038/nrrheum.2016.136

Saxena, Y., Routh, S., and Mukhopadhaya, A. (2021). Immunoporosis: Role of innate immune cells in osteoporosis. *Front. Immunol.* 12, 687037. doi:10.3389/fimmu.2021.687037

Scanzello, C. R., and Goldring, S. R. (2012). The role of synovitis in osteoarthritis pathogenesis. *Bone* 51 (2), 249–257. doi:10.1016/j.bone.2012.02.012

Scanzello, C. R., Plaas, A., and Crow, M. K. (2008). Innate immune system activation in osteoarthritis: Is osteoarthritis a chronic wound? *Curr. Opin. Rheumatol.* 20 (5), 565–572. doi:10.1097/BOR.0b013e32830aba34

Sethi, G., Ahn, K. S., Pandey, M. K., and Aggarwal, B. B. (2007). Celastrol, a novel triterpene, potentiates TNF-induced apoptosis and suppresses invasion of tumor cells by inhibiting NF-kappaB-regulated gene products and TAK1-mediated NF-kappaB activation. *Blood* 109 (7), 2727–2735. doi:10.1182/blood-2006-10-050807

Song, C., Xu, Y., and Lu, Y. (2020). Use of Tripterygium wilfordii hook F for immune-mediated inflammatory diseases: progress and future prospects. *J. Zhejiang Univ. Sci. B* 21 (4), 280–290. doi:10.1631/jzus.B1900607

Turkiewicz, A., Petersson, I. F., Bjork, J., Hawker, G., Dahlberg, L. E., Lohmander, L. S., et al. (2014). Current and future impact of osteoarthritis on health care: a population-based study with projections to year 2032. *Osteoarthr. Cartil.* 22 (11), 1826–1832. doi:10.1016/j.joca.2014.07.015

Valdes, A. M., and Spector, T. D. (2011). Genetic epidemiology of hip and knee osteoarthritis. *Nat. Rev. Rheumatol.* 7 (1), 23–32. doi:10.1038/nrrheum.2010.191

Wallimann, A., Hildebrand, M., Groeger, D., Stanic, B., Akdis, C., Zeiter, S., et al. (2021). An exopolysaccharide produced by bifidobacterium longum 35624® inhibits osteoclast formation via a TLR2-dependent mechanism. *Calcif. Tissue Int.* 108 (5), 654–666. doi:10.1007/s00223-020-00790-4

Wang, Q., Luo, S., Yang, J., Li, J., Huan, S., She, G., et al. (2021). Circ_0114876 promoted IL-1β-induced chondrocyte injury by targeting miR-671/TRAF2 axis. *Biotechnol. Lett.* 43 (4), 791–802. doi:10.1007/s10529-020-03070-1

Wojdasiewicz, P., Poniatowski, L. A., and Szukiewicz, D. (2014). The role of inflammatory and anti-inflammatory cytokines in the pathogenesis of osteoarthritis. *Mediat. Inflamm.* 2014, 561459. doi:10.1155/2014/561459

World Medical, A. (2013). World medical association declaration of Helsinki: ethical principles for medical research involving human subjects. *JAMA* 310 (20), 2191–2194. doi:10.1001/jama.2013.281053

Zhang, Y., Mao, X., Li, W., Chen, W., Wang, X., Ma, Z., et al. (2021). Tripterygium wilfordii: An inspiring resource for rheumatoid arthritis treatment. *Med. Res. Rev.* 41 (3), 1337–1374. doi:10.1002/med.21762

frontiers | Frontiers in Pharmacology

TYPE Original Research
PUBLISHED 01 September 2022
DOI 10.3389/fphar.2022.956247

OPEN ACCESS

EDITED BY
Dongdong Sun,
Nanjing University of Chinese Medicine, China

REVIEWED BY
Shen Xiang-chun,
Guizhou Medical University, China
Bo Jin,
Zhejiang Chinese Medical University, China

*CORRESPONDENCE
Fei Xu,
feixuhgd@163.com
Liying Qiu,
qiulydoc@sina.com

SPECIALTY SECTION
This article was submitted to Inflammation Pharmacology, a section of the journal Frontiers in Pharmacology

RECEIVED 30 May 2022
ACCEPTED 11 August 2022
PUBLISHED 01 September 2022

CITATION
Li T, Yu X, Zhu X, Wen Y, Zhu M, Cai W, Hou B, Xu F and Qiu L (2022), Vaccarin alleviates endothelial inflammatory injury in diabetes by mediating miR-570-3p/HDAC1 pathway. *Front. Pharmacol.* 13:956247. doi: 10.3389/fphar.2022.956247

Vaccarin alleviates endothelial inflammatory injury in diabetes by mediating miR-570-3p/HDAC1 pathway

Taiyue Li[1], Xiaoyi Yu[1], Xuerui Zhu[2], Yuanyuan Wen[1], Meizhen Zhu[1], Weiwei Cai[1], Bao Hou[1], Fei Xu[1]* and Liying Qiu[1]*

[1]Wuxi Medical School, Jiangnan University, Wuxi, Jiangsu, China, [2]School of Life Science and Health Engineering, Jiangnan University, Wuxi, Jiangsu, China

Vaccarin is a flavonoid glycoside, which has a variety of pharmacological properties and plays a protective role in diabetes and its complications, but its mechanism is unclear. In this study, we aim to investigate whether histone deacetylase 1(HDAC1), a gene that plays a pivotal role in regulating eukaryotic gene expression, is the target of miR-570-3p in diabetic vascular endothelium, and the potential molecular mechanism of vaccarin regulating endothelial inflammatory injury through miR-570-3p/HDAC1 pathway. The HFD and streptozotocin (STZ) induced diabetes mice model, a classical type 2 diabetic model, was established. The aorta of diabetic mice displayed a decrease of miR-570-3p, the elevation of HDAC1, and inflammatory injury, which were alleviated by vaccarin. Next, we employed the role of vaccarin in regulating endothelial cells miR-570-3p and HDAC1 under hyperglycemia conditions *in vitro*. We discovered that overexpression of HDAC1 counteracted the inhibitory effect of vaccarin on inflammatory injury in human umbilical vein endothelial cells (HUVECs). Manipulation of miRNA levels in HUVECs was achieved by transfecting cells with miR-570-3p mimic and inhibitor. Overexpression of miR-570-3p could decrease the expression of downstream components of HDAC1 including TNF-α, IL-1β, and malondialdehyde, while increasing GSH-Px activity in HUVECs under hyperglycemic conditions. Nevertheless, such phenomenon was completely reversed by miR-570-3p inhibitor, and administration of miR-570-3p inhibitor could block the inhibition of vaccarin on HDAC1 and inflammatory injury. Luciferase reporter assay confirmed the 3′- UTR of the HDAC1 gene was a direct target of miR-570-3p. In summary, our findings suggest that vaccarin alleviates endothelial inflammatory injury in diabetes by mediating miR-570-3p/HDAC1 pathway. Our study provides a new pathogenic link between deregulation of miRNA expression in the vascular endothelium of diabetes and inflammatory injury and provides new ideas, insights, and choices for the scope of application and medicinal value of vaccarin and some potential biomarkers or targets in diabetic endothelial dysfunction and vascular complications.

KEYWORDS

vaccarin, microRNA-570-3p, HDAC1, inflammation, diabetes, endothelial dysfunction

Introduction

Diabetes is a metabolic disease characterized by hyperglycemia due to insulin secretion defects and/or insulin dysfunction (American Diabetes 2014). The incidence rate of diabetes worldwide has increased rapidly in recent years, and it can cause a variety of chronic complications, such as cardiovascular, ophthalmic, nephrotic, and nervous system diseases. It seriously threatens diabetic patients' health and quality of life. Among them, diabetic angiopathy is one of the most common and serious complications of diabetes, and it is also the main cause of death in patients with type 2 diabetes mellitus (T2DM) (Kannel and McGee 1979; Ostergard and Nyholm et al., 2006). The initial step that leads to T2DM vascular complications is dysfunction and damage of endothelial cells, including endothelial cell apoptosis, inflammation, or anti-angiogenesis induced by hyperglycemia (Yi and Gao 2019).

Endothelial cells are simple squamous cells arranged on the surface of the vascular lumen. They are the interface between circulating blood and vascular intima. Endothelial cells are very important to maintaining a healthy vascular system and are very sensitive the changes in blood glucose levels (Dhananjayan and Koundinya et al., 2016; Vanhoutte and Shimokawa et al., 2017). Under normal circumstances, endothelial cells remain static and regulate vascular tension. In the development of T2DM, hyperglycemia will lead to endothelial cell dysfunction, resulting in endothelial dysfunction (Roberts and Porter 2013). Endothelial dysfunction is the critical first step to the development of diabetic vascular complications, with increased inflammation as a major manifestation (Wu and Jiang et al., 2018). Thus, targeting inflammation is an effective strategy to attenuate diabetes-induced endothelial injury. To date, a causal relationship between inflammation and diabetic angiopathy has been widely accepted, however, the cellular and molecular mechanisms are still not well defined. Nowadays, several inflammation markers are considered to be associated with diabetes (Tang and Wang et al., 2017), such as interleukin-1β (IL-1β) and tumor necrosis factor-α (TNF-α) (Wu and Jiang et al., 2018). Therefore, it is of interest to identify the new factors that may contribute to the pathogenesis (Tang and Wang et al., 2017) and progression of diabetic angiopathy. There is mounting evidence showing that microRNAs (miRNAs) can potentially play a role as biomarkers or intervention targets for endothelial inflammation.

MiRNA (18–23 nt) is a small endogenous non-coding RNA, which participates in post-transcriptional regulation of gene expression (Cheng and Chen et al., 2019). The complementary sites of mature miRNA in 3′UTR bind to the target mRNA, which will lead to the reduction of target mRNA stability and translation (Booton and Lindsay 2014). The abnormal regulation of miRNAs in T2DM has been well confirmed, but its functional role has been rarely studied. We have previously reported that histone deacetylase 1 (HDAC1) is significantly dysregulated in hyperglycemic mouse models and high glucose (HG)-treated endothelial cells (Sun, Cai et al., 2017; Zhu, Lei et al., 2018; Liu, Sun et al., 2020). Using miRNA target prediction sites TargetScan and Miranda (Betel, Koppal et al., 2010; Xie, Cai et al., 2015), we examined a variety of miRNAs and identified miR-570-3p as a potentially novel candidate that may regulate HDAC1. MiR-570-3p has been previously reported in terms of cell proliferation and inflammation (Baker, Vuppusetty et al., 2018), but has not been studied in the context of HG-induced inflammatory injury in endothelial cells.

Vaccarin (VAC), a flavonoid monomer which contains twelve phenolic hydroxyl groups (Figure 1), is extracted from *Vaccaria segetalis* seeds (Hou et al., 2020; Hou et al., 2020). Vaccarin has a wide range of biological effects, including endothelial cell injury prevention, angiogenesis promotion, wound healing, and liver protection (Sun, Yu et al., 2021). Previous studies have shown that vaccarin can participate in FGF-2 mediated fibroblast growth factor receptor 1 (FGFR-1) induced angiogenesis *in vitro* and *in vivo* (Sun, Cai et al., 2017). In addition, vaccarin can reduce hydrogen peroxide-induced damage to human EA•hy926 endothelial cells by inhibiting the Notch signal (Xie, Cai et al., 2015; Qiu, Du et al., 2016). Recently, it was found that vaccarin can inhibit vascular endothelial dysfunction through ROS/AMPK/miRNA-34a/eNOS signaling pathway through the intervention of the HMEC-1 endothelial dysfunction model induced by HG *in vitro* (Xu, Liu et al., 2019). However, the mechanism of vaccarin on HG-induced inflammatory injury in endothelial cells has not been determined. Therefore, this study reported for the first time that vaccarin inhibited HDAC1 by regulating miR-570-3p to reduce inflammatory injury.

Materials and methods

Cell culture and treatments

Human umbilical vein endothelial cells (HUVECs) were provided by the U533 Institute of the French National Institute of Health Medicine (Paris, French) and were cultured in DMEM (HyClone, St. Louis, MO, United States) containing 5 mM glucose, 10% FBS (Lonsera, Shuangru Biotech, Shanghai, China), and 100 U/L penicillin and 100 μg/ml streptomycin (Gibco, Carlsbad, CA, United States). The cells were cultured at 37°C in a humidified incubator of 5% CO_2 and 95% air. After reaching 70% confluence (Xu, Liu et al., 2019), HUVEC cells were exposed to HG (35 mM) for 24h, then to 5 μM vaccarin or 20 μM metformin (Raj, Natarajan et al., 2021) (Solarbio, Beijing, China) 16 h. Vaccarin was purchased from Shanghai Shifeng Technology (Shanghai, China) (Sun, Yu et al., 2021), purity >98%, the molecular formula is $C_{32}H_{38}O_{19}$, and molecular mass is 726.63 g/mol.

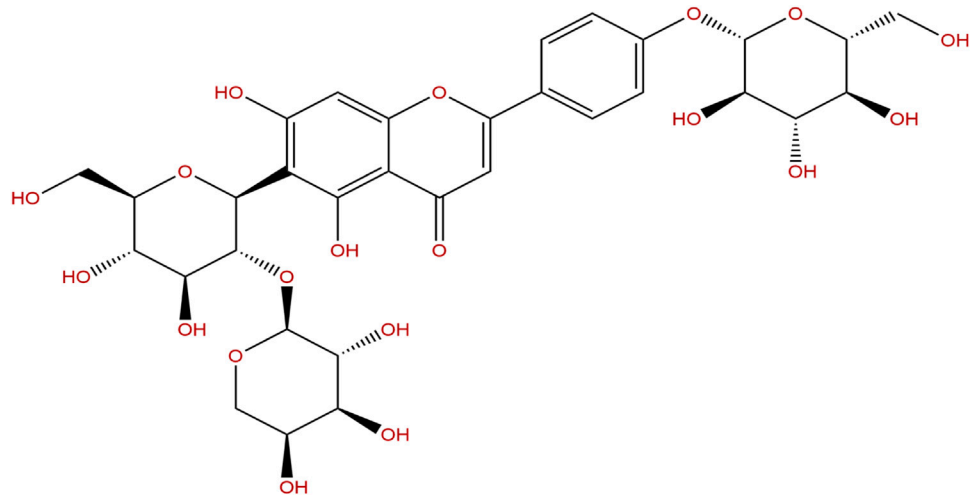

FIGURE 1
Chemical structure of vaccarin.

Transfection of miRNA mimics and inhibitors

The miR-570-3p mimics, miR-570-3p inhibitor, and corresponding negative controls were synthesized by Gene Pharma (Shanghai, China) and transfected by Lipofectamine® 2000 (Invitrogen, Carlsbad, CA) and cells were exposed to HG (35 mM). The final concentration of the mimics and inhibitor was 50 and 100 nM. The primer sequences for miR-570-3p inhibitor: 5′- GCA AAG GUA AUU GCU GUU UUC G-3' (Forward); miR-570-3p mimic: 5′-CGA AAA CAG CAA UUA CCU UUG C-3' (Forward), 5′-AAA GGU AAU UGC UGU UUU CGU U-3' (Reverse); miRNA-NC inhibitor: 5′- CAG UAC UUU UGU GUA CAA -3' (Forward); and miRNA-NC mimic: 5′- UUC UCC GAA CGU GUC ACG UTT -3' (Forward), 5′- ACG UGA CAC GUU CGG AGA ATT -3' (Reverse).

Transfection of small interference RNA (siRNA)

The HDAC1 siRNA and corresponding negative controls were synthesized by Gene Pharma (Shanghai, China) and transfected by Lipofectamine® 2000 (Invitrogen, Carlsbad, CA) and cells were exposed to HG (35 mM). The final concentration was 50 nM. The siRNA sequences that targeted HDAC1 were as follows: 5′- GCC GGU CAU GUC CAA AGU ATT -3' (Forward), 5′- UAC UUU GGA CAU GAC CGG CTT -3' (Reverse); and siRNA-NC: 5′- UUC UCC GAA CGU GUC ACG UTT -3' (Forward), 5′- ACG UGA CAC GUU CGG AGA ATT -3' (Reverse).

Transfection of plasmids

The pcDNA3.1-HDAC1 plasmids and empty vector pcDNA3.1 were synthesized according to the plasmid synthesis method (Wang, Liu et al., 2013). The HUVEC cells were transfected with Lipofectamine® 2000 (Invitrogen, Carlsbad, CA). The cells were subjected to subsequent operations after transfection for 6 h.

Real-time quantitative PCR (RT-qPCR)

Total RNA was extracted using Trizol reagent (Cwbio, Beijing, China). MiRNA was extracted using the miRNA Purification Kit (Cwbio, Beijing, China). RNA (1 μg) and miRNA (1 μg) were used to generate cDNA separately using Hifair® III first Strand cDNA Synthesis SuperMix Kit (YESEN, Shanghai, China) and miRNA cDNA Synthesis Kit (Cwbio, Beijing, China). The RT-qPCR was performed by using Hieff UNICON® qPCR SYBR Green Master Mix (YESEN, Shanghai, China) and miRNA qPCR Assay Kit (Cwbio, Beijing, China). $2^{-\Delta\Delta CT}$ was used to show the fold change.

Western blotting

After cell and tissue lysis, the protein concentration was quantified by using the dioctylic acid (BCA) protein detection kit

(Beyotime, Shanghai, China), then the protein was denatured at 100 °C for 7 min, and finally stored at -80 °C. Protein lysate was resolved on Tris-glycine SDS-PAGE gels, then electrotransferred onto a PVDF membrane. Antibodies against HDAC1 (1:1000, mouse) (Cell Signaling Technology, Beverly, United States), TNF-α (1:1000, rabbit) (ABclonal, Wuhan, China), IL-1β (1:1000, Rabbit) (ABclonal, Wuhan, China), β-actin (1:5000, mouse) (Proteintech, Wuhan, China) were incubated overnight at 4 °C. Secondary antibodies, anti-rabbit (1:2000) and anti-mouse (1:2000) (Cwbio, Beijing, China) were incubated for 1 h at room temperature (Ai, Li et al., 2021). The blots were visualized by a chemiluminescence detection system (Millipore Darmstadt, Burlingtun, MA, United States). ImageJ (National Institutes of Health, Bethesda, MD, United States) and Image Lab (Bio-Rad, Hercules, CA, United States) were used to semi-quantify bands (Xu, Liu et al., 2019).

Luciferase reporter assays

A partial HDAC1 mRNA 3′-UTR containing the miR-570-3p target site was constructed into a pGL-3-promoter vector (Promega, Madison, WI). The reporter was co-transfected with a renilla luciferase plasmid driven by a constitutive promoter reporter into cells. Firefly and renilla luciferase luminescence was measured using a Dual-Luciferase reporter kit (Beyotime, Shanghai, China) as the manufacturer's recommendations. Firefly/renilla ratio was calculated to normalize for variations in transfection efficiencies.

Determination of indicators related to oxidative stress

The content of malondialdehyde (MDA) was detected by the thiobarbituric acid method, and the activity of glutathione peroxidase (GSH-Px) was determined by colorimetry. Kits were purchased from Nanjing jiancheng (Nanjing, China).

Animal models and treatments

Experiments were performed on 6 to 8 weeks-old C57BL/6J mice purchased from the Model Animal Research Center of Nanjing University (Nanjing, China). The mice were housed in a light-dark cycle of 12 h in a temperature and humidity-controlled room and treated with free access to clean food and water. The mice were randomly divided into three groups (n = 10). One group was treated with a normal diet (14.7 kJ/g, 13% of energy as fat) until the experiments finished (Xu, Liu et al., 2019). The other two groups were fed with an HFD (21.8 kJ/kg, 60% energy as fat, D12492, Research Diets, New Brunswick, NJ, United States) for 4 weeks. After 4 weeks of HFD, fasting for 12 h overnight, streptozotocin (STZ) (Sigma, St. Louis, MO, United States) (120 mg/kg, ip) was injected intraperitoneally to form T2DM. After successful modeling, the three groups of mice received intragastric gavage of either vehicle or vaccarin (1 mg/kg, ig) every day for 6 weeks. Terminal experiments were performed after mice were anesthetized (2–5% isoflurane). The entire aorta was isolated and used for immunohistochemistry, RT-qPCR, western blotting, and vascular function. All protocols were approved by the Experimental Animal Care and Use Committee of Jiangnan University (JN. No20210915c0600129 [339]). The experimental procedures were carried out according to the Guide for the Care and Use of Laboratory Animals published by the US National Institute of Health (NIH publication, eighth edition, 2011) (Xu, Liu et al., 2019).

Oral glucose tolerance test (OGTT) and insulin tolerance test (ITT)

Mice were fasted for 12 h, then received glucose (2 g/kg, ig) to examine oral glucose tolerance. And mice were fasted for 6 h, then received insulin (0.75 units/kg, ip) to examine insulin tolerance. Blood glucose was measured in veinal blood at 0, 15, 30, 60, and 90 min using a blood glucometer.

Determination of triglyceride (TG), low-density lipoprotein (LDL), non-esterified fatty acids (NEFA), alanine transaminase (ALT), and aspartate transaminase (AST)

The contents of serum TG, LDL, NEFA, ALT, and AST were detected according to the methods in the corresponding kit (Nanjing Jiancheng).

Histopathological evaluation

Aortic tissue was fixed with 4% paraformaldehyde and embedded in paraffin. The sections were stained with hematoxylin-eosin (H&E) (Solarbio, Beijing, China) (Sun, Yu et al., 2021) and then observed by optical microscope (Nikon, Japan).

Immunohistochemistry

Aortic sections were de-paraffinized with xylene, followed by antigen retrieval by heating in citrate buffer (10 mM). The experiment was performed by SP Rabbit and Mouse HRP Kit

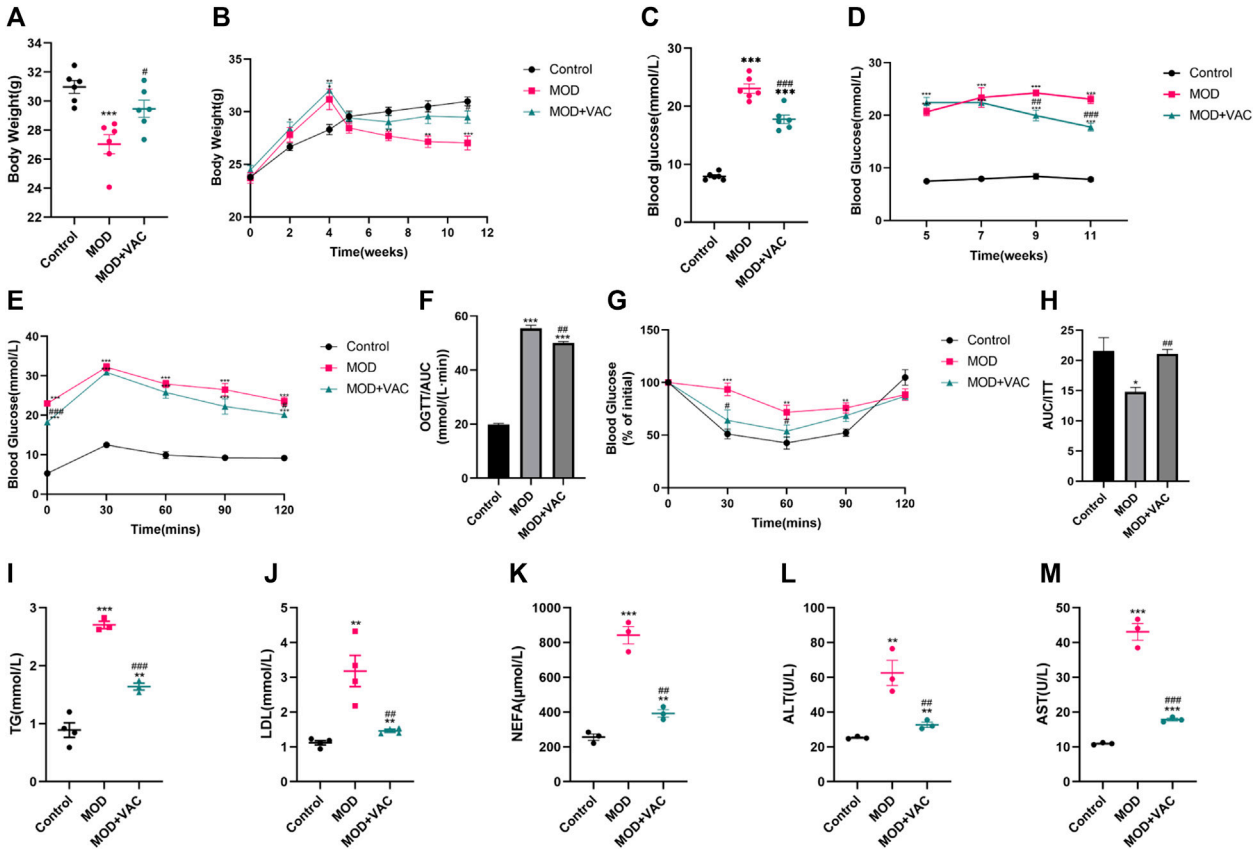

FIGURE 2
Vaccarin can significantly improve the physiological state and blood glucose level of T2DM mice. **(A)**. The weight of the mice at the terminal of the experiment. (The first 5 weeks were the modeling period and the last 6 weeks were the administration period.) **(B)**. Weekly weight changes after the start of the experiment. **(C)**. Fasting blood glucose. After 6 weeks of treatment, fasting blood glucose was tested in the mice. **(D)**. Weekly changes of fasting blood glucose after successful modeling. **(E)**. Oral glucose tolerance test (OGTT). **(F)**. Area under the curve (AUC) level of OGTT. **(G)**. Insulin tolerance test (ITT). **(H)**. Area under the curve (AUC) level of ITT. **(I–M)**. Content of serum TG, LDL, NEFA, ALT and AST. Values are mean ± SEM. n = 3-6 in each group. $^{*}p < 0.05$, $^{**}p < 0.01$, $^{***}p < 0.001$ vs. Control; $^{\#}p < 0.05$, $^{\#\#}p < 0.01$, $^{\#\#\#}p < 0.001$ vs. MOD.

(Cwbio, Beijing, China) (Tan, Jiang et al., 2022). Sections were probed with appropriate primary antibodies. TNF-α antibody (ABclonal, Wuhan, China), and IL-1β antibody (ABclonal, Wuhan, China) were used at a 1:100 dilution followed by a biotinylated secondary antibody, streptavidin peroxidase solution, DAB peroxidase substrate, and hematoxylin counterstain or by an AlexaFluor®647-conjugated anti-mouse IgG (1:500) as the secondary antibody.

Statistical analysis

All results were defined as mean ± SEM from at least three independent experiments. *t*-test was used for the comparisons between the two groups. For multiple group comparisons, statistical analysis was performed by ANOVA followed by Dunnett's test. Differences with p value <0.05 were regarded as significant (Xu, Liu et al., 2019).

Results

Vaccarin can significantly improve the physiological state and blood glucose level of T2DM mice

With the development of T2DM, significantly lower levels of body weight were observed in T2DM mice, but the body weight increased slightly after vaccarin treatment (Figures 2A, B). Fasting blood glucose levels in the vaccarin-treated group decreased steadily and continuously compared with the model group (Figures 2C, D), suggesting that vaccarin partly controlled the elevation of blood glucose in T2DM mice.

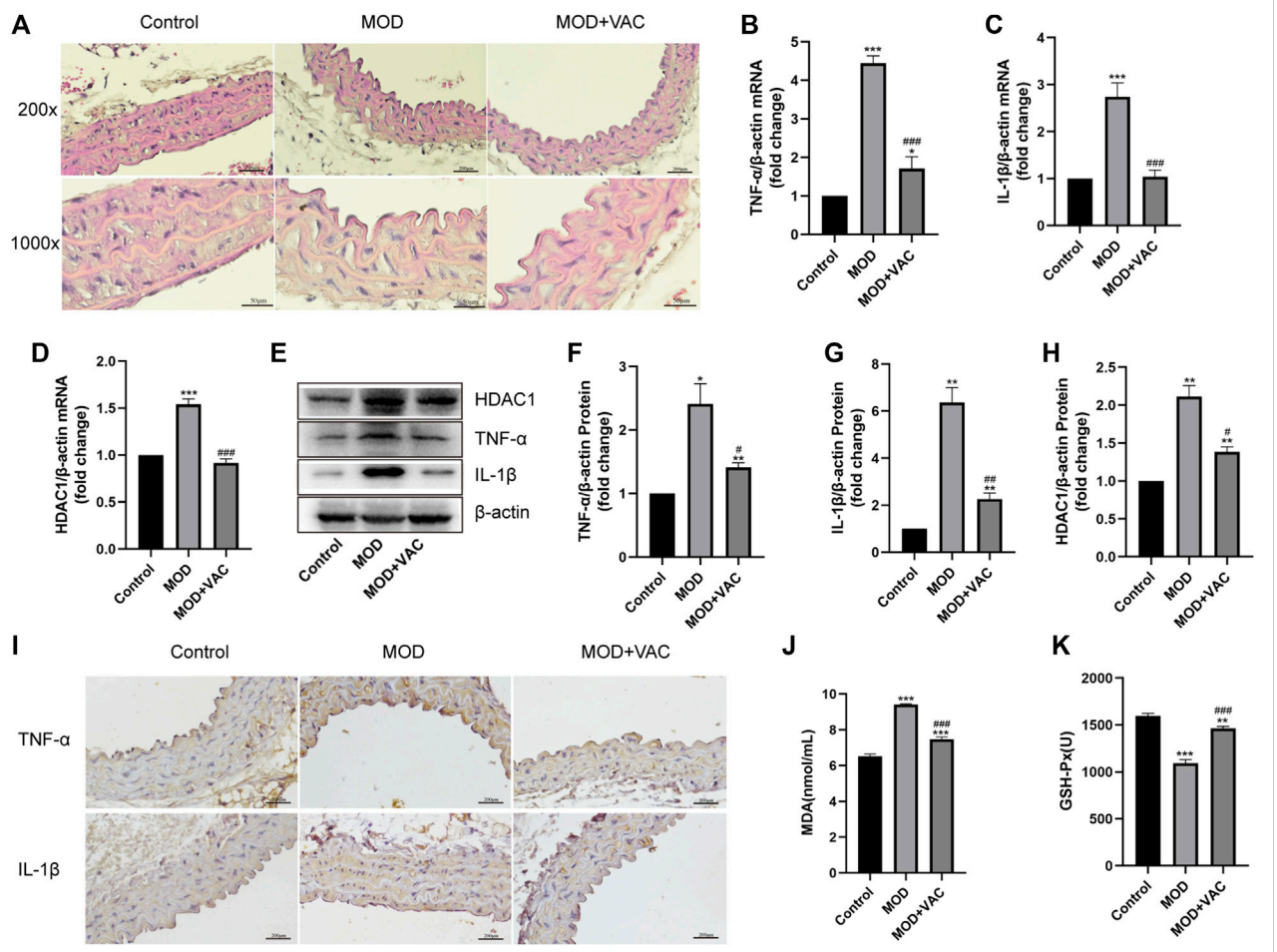

FIGURE 3
Vaccarin improved aortic inflammatory injury in T2DM mice. **(A)**. Representative photomicrographs of aortic tissue with H&E (200X, 1000X). **(B–D)**. The effects of vaccarin on the TNF-α mRNA, IL-1β mRNA, and HDAC1 mRNA expression in aortic tissue in comparison with T2DM mice. **(E–H)**. Western blotting analysis of HDAC1, TNF-α, and IL-1β protein expression levels in aortic tissue. Gray value of western blotting. **(I)**. Representative photomicrographs of aortic tissue with immunohistochemical staining for TNF-α and IL-1β (200X). **(J)**. Content of serum MDA. **(K)**. Activity of serum GSH-Px. Values are mean ± SEM. $n = 3$ in each group. $^{*}p < 0.05$, $^{**}p < 0.01$, $^{***}p < 0.001$ vs. Control; $^{\#}p < 0.05$, $^{\#\#}p < 0.01$, $^{\#\#\#}p < 0.001$ vs. MOD.

The results of the OGTT showed that blood glucose level after oral administration of glucose was significantly lower in the vaccarin intervention group than that of the T2DM mice. The results of the ITT showed that insulin resistance appeared in T2DM mice, which could be alleviated by vaccarin (Figures 2E–H). Both the OGTT and ITT results demonstrated that vaccarin not only improved glucose tolerance but also restored the impaired insulin sensitivity in T2DM mice. Compared with the control group, serum levels of lipid metabolism-related indicators TG, LDL, NEFA, ALT, and AST were increased in T2DM mice, while they had improved significantly upon administering vaccarin (Figures 2I–M). These findings suggested that vaccarin could alleviate glycolipid metabolism disorder to a certain extent in T2DM mice.

Vaccarin improved aortic inflammatory injury in T2DM mice

H&E staining showed that the tunica media of T2DM mice was thickened, which could be alleviated by vaccarin (Figure 3A). The mRNA and protein expressions of TNF-α and IL-1β in the aorta of T2DM mice increased significantly (Figures 3B, C, E–G), suggesting that the aorta of T2DM mice had an inflammatory injury. IHC staining displayed the same results (Figure 3I). Furthermore, the production of MDA increased while the activity of GSH-Px decreased (Figures 3J, K). However, these disorders were alleviated after vaccarin treatment (Figures 3B–K). It indicated that vaccarin had a remarkable effect on aortic inflammatory injury in T2DM

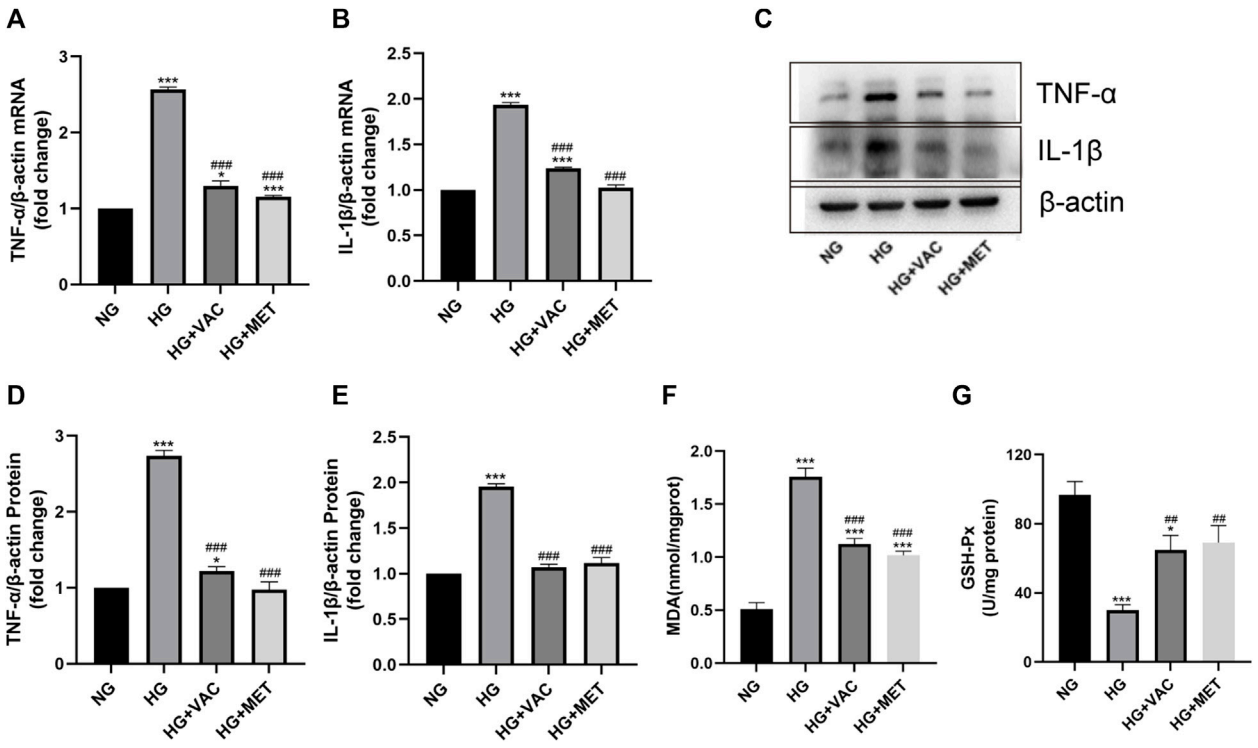

FIGURE 4
Vaccarin attenuated HG-induced inflammatory injury in HUVEC cells. **(A,B)**. The effects of vaccarin or metformin on the TNF-α mRNA and IL-1β mRNA expression in HG-induced HUVEC cells. **(C–E)**. Western blotting analysis of TNF-α and IL-1β protein expression levels in HG-induced HUVEC cells. Gray value of western blotting. **(F)**. Content of MDA. **(G)**. Activity of GSH-Px. Values are mean ± SEM. $n = 3$ in each group. $^{*}p < 0.05$, $^{**}p < 0.01$, $^{***}p < 0.001$ vs. NG; $^{\#}p < 0.05$, $^{\#\#}p < 0.01$, $^{\#\#\#}p < 0.001$ vs. HG.

mice. Beyond that, vaccarin could inhibit the abnormally elevated HDAC1 in the aorta of T2DM mice, which was consistent with the previous research results (Figures 3D, E, H).

Vaccarin attenuated HG-induced inflammatory injury in HUVEC cells

TNF-α, IL-1β mRNA, and protein levels in HUVEC cells induced by HG increased significantly (Figures 4A–E). In addition, it was found that the production of MDA increased and the activity of GSH-Px decreased in HG-induced HUVEC cells, vaccarin treatment could reverse these phenomena (Figures 4F, G), indicating that vaccarin could also play an anti-inflammatory role *in vitro*. Metformin (MET) had been widely proven to relieve inflammatory injury in T2DM(Karam and Radwan 2019; Raj, Natarajan et al., 2021; Wang, Wang et al., 2022). Therefore, we used metformin as a positive control to compare the effects of vaccarin and found that the effect of vaccarin on the inflammatory injury was similar to that of metformin (Figures 4A–G). These phenomena aroused our interest and led us to further study the mechanism of vaccarin reducing HG-induced inflammatory injury.

Vaccarin alleviated HG-induced inflammatory injury in HUVEC cells by inhibiting HDAC1 expression

Consistent with the results of *in vivo* experiments, vaccarin could reverse the increased level of HDAC1 induced by HG *in vitro* (Figures 5A–C). To investigate the role of HDAC1 in HG-induced inflammatory injury, the silence of HDAC1 was made by transfection of HDAC1 siRNA (si-HDAC1). The effect of si-HDAC1 was similar to that of vaccarin, so there was reason to suspect that vaccarin functioned through HDAC1 (Figures 5D–J). Overexpression of HDAC1 was made by transfection of pcDNA3.1-HDAC1 (Figure 5K, L). We found that HDAC1 counteracted the inhibitory effects of vaccarin on TNF-α and IL-1β induced by HG in HUVEC

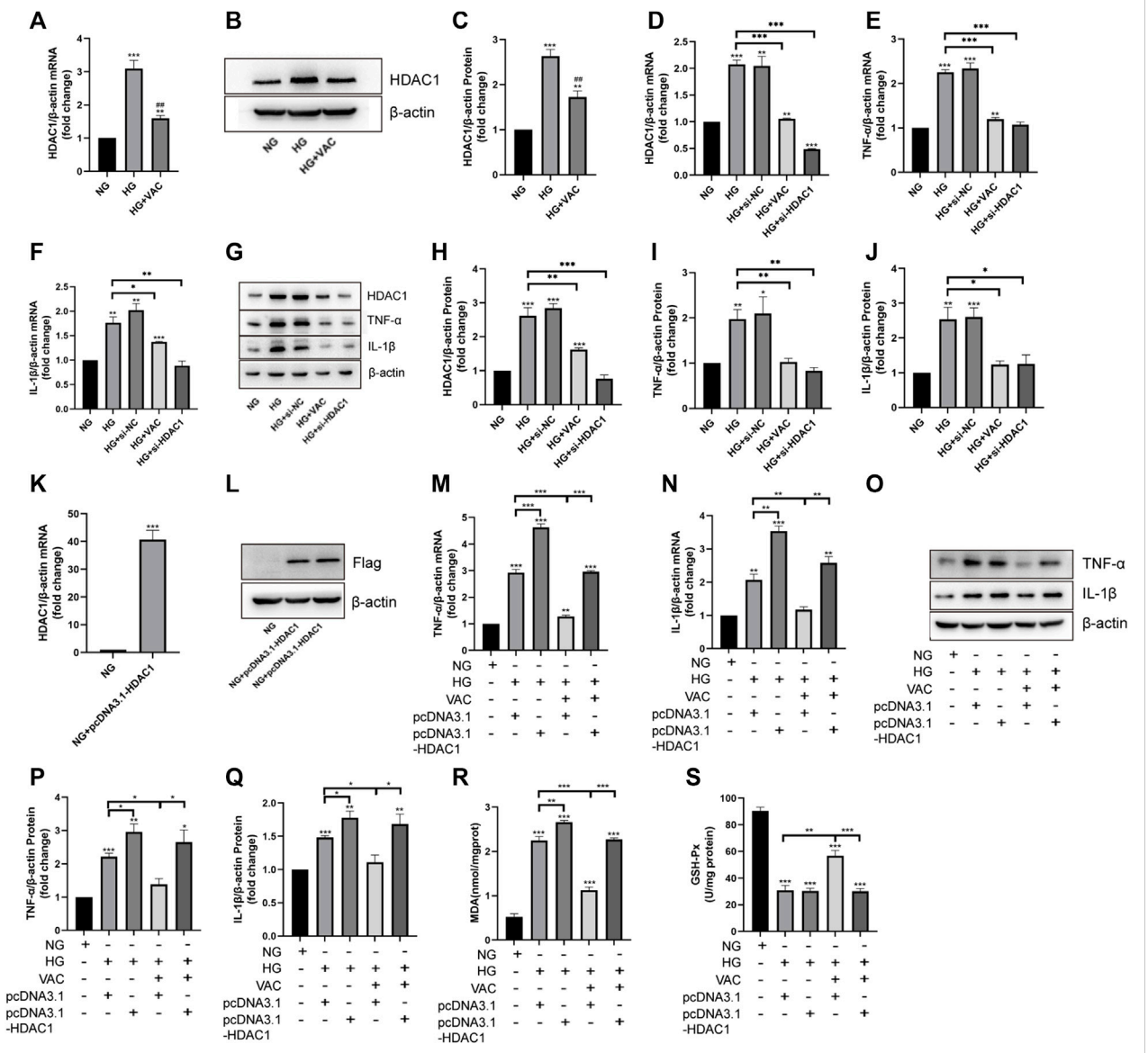

FIGURE 5
Vaccarin alleviated HG-induced inflammatory injury in HUVEC cells by inhibiting HDAC1 expression. **(A)**. The effects of vaccarin on HDAC1 mRNA expression in HG-induced HUVEC cells. **(B,C)**. Western blotting analysis of HDAC1 protein expression levels in HG-induced HUVEC cells. Gray value of western blotting. **(D–F)**. The expression of HDAC1 mRNA, TNF-α mRNA, and IL-1β mRNA in HUVEC cells transfected with siRNA NC or HDAC1 siRNA. **(G–J)**. Western blotting analysis of HDAC1, TNF-α, and IL-1β protein expression levels in HUVEC cells transfected with siRNA NC or HDAC1 siRNA. Gray value of western blotting. **(K)**. The expression of HDAC1 mRNA in HUVEC cells transfected with pcDNA3.1-HDAC1. **(L)**. Western blotting analysis of Flag protein expression levels in HUVEC cells transfected with pcDNA3.1-HDAC1. **(M,N)**. The effects of vaccarin on TNF-α mRNA and IL-1β mRNA expression in HUVEC cells transfected with pcDNA3.1 or pcDNA3.1-HDAC1. **(O–Q)**. Western blotting analysis of TNF-α and IL-1β protein expression levels in HUVEC cells transfected with pcDNA3.1 or pcDNA3.1-HDAC1. Gray value of western blotting. **(R)**. Content of MDA. **(S)**. Activity of GSH-Px. Values are mean ± SEM. n = 3 in each group. $^{*}p < 0.05$, $^{**}p < 0.01$, $^{***}p < 0.001$ vs. NG; $^{\#}p < 0.05$, $^{\#\#}p < 0.01$, $^{\#\#\#}p < 0.001$ vs. HG.

cells (Figure 5M–Q). Meanwhile, the overexpression of HDAC1 also reversed the effects of vaccarin on mitigating MDA production and GSH-Px activity (Figure 5R, S). These results demonstrated that vaccarin alleviates the HG-induced inflammatory injury by decreasing the expression of HDAC1.

Vaccarin inhibited the HG-induced decrease of miR-570-3p *in vitro*

Then we focused on miRNA to further inquire about the upstream regulatory of HDAC1 (Figure 6A). The results of RT-

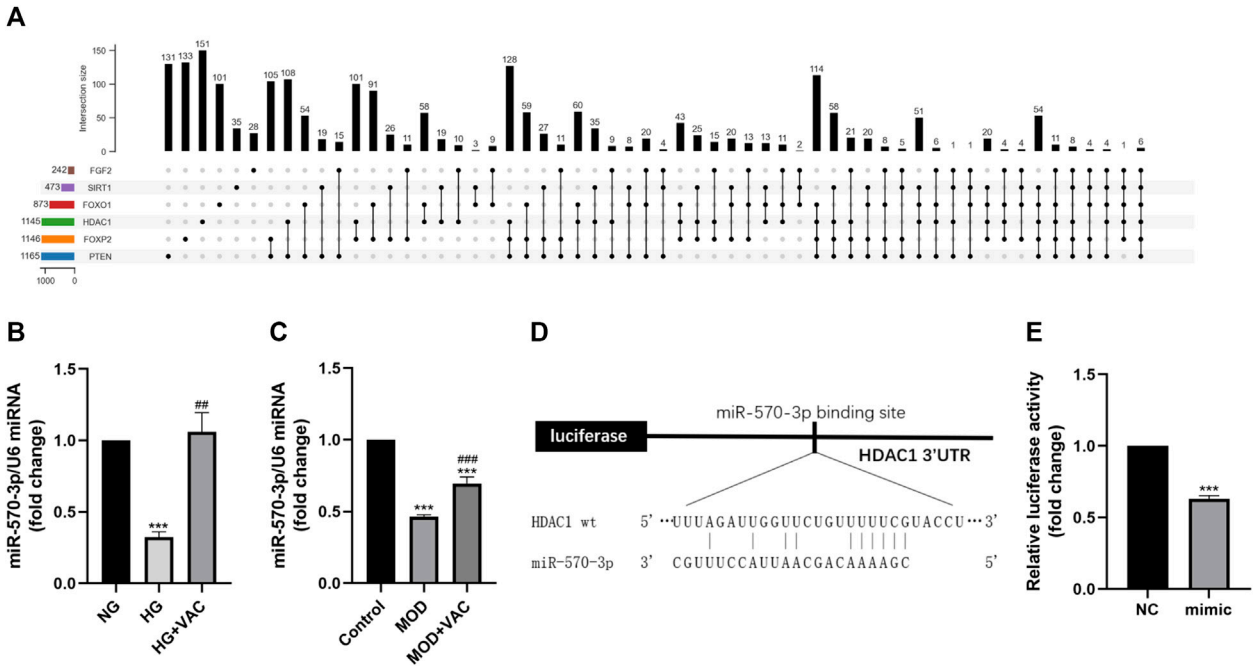

FIGURE 6
Vaccarin inhibited the HG-induced decrease of miR-570-3p *in vitro*. **(A)**. Upset graph is used to represent overlapping sets of elements for miRNAs. **(B–C)**. The effects of vaccarin on the expression of miR-570-3p miRNA in HG-induced HUVEC cells and aortic tissue. **(D)**. Complementary bases between miR-570-3p and the 3′ UTR of HDAC1. **(E)**. Luciferase activity was detected in the HUVEC cells. Values are mean ± SEM. n = 3 in each group. $^{*}p < 0.05$, $^{**}p < 0.01$, $^{***}p < 0.001$ vs. NG or Control; $^{\#}p < 0.05$, $^{\#\#}p < 0.01$, $^{\#\#\#}p < 0.001$ vs. HG or MOD.

qPCR further confirmed that the level of miR-570-3p in HUVEC cells was suppressed in the HG group, while increasing after vaccarin treatment (Figure 6B). This trend was also proved in the aorta of T2DM mice (Figure 6C). The binding sites of HDAC1 and miR-570-3p were predicted by TargetScan (Figure 6D). The dual-luciferase reporter system was used to confirm the binding of miR-570-3p with the HDAC1 mRNA. Luciferase reporter vectors carrying the wild-type 3′-UTR of HDAC1 were transfected into HUVEC cells. It was observed that miR-570-3p mimic significantly suppressed the luciferase activity in the cells transfected with the luciferase vectors carrying the wild-type 3′-UTR of HDAC1, indicating that HDAC1 is a potential target of miR-570-3p (Figure 6E).

Overexpression of miR-570-3p inhibited HDAC1 expression and inflammatory injury in HUVEC cells

We further investigated the potential role of miR-570-3p in inflammatory injury. Through the application of miR-570-3p mimics, the expression of miR-570-3p in HUVEC cells was significantly increased (Figure 7A). The overexpression of miR-570-3p led to the inhibition of HDAC1 at the mRNA and protein levels (Figures 7B, E, F). Simultaneously, the application of miR-570-3p mimics also inhibited TNF-α and IL-1β, decreased MDA production, and increased GSH-Px activity (Figures 7C–E, G, J), thus alleviating the degree of inflammatory injury. From these phenomena, the overexpression of miR-570-3p had similar anti-inflammatory effects as vaccarin. Hence, we have reason to suspect that vaccarin plays an anti-inflammatory role through miR-570-3p.

Vaccarin inhibited the expression of HDAC1 and inflammatory injury by up-regulating miR-570-3p

To determine whether vaccarin exerts anti-inflammatory effects through miR-570-3p, we transfected HUVEC cells with miR-570-3p inhibitor. The expression of miR-570-3p in HUVEC cells was significantly reduced after transfection, and the up-regulation of miR-570-3p by vaccarin was also observably offset (Figure 8A). In the meantime, the inhibition of vaccarin on HDAC1, TNF-α, and IL-1β was counteracted because of the application of miR-570-3p inhibitor (Figures 8B–H). It played a similar role in MDA production and GSH-Px activity (Figures 8I, J). It indicated that vaccarin will not play the role of anti-inflammatory in the absence of

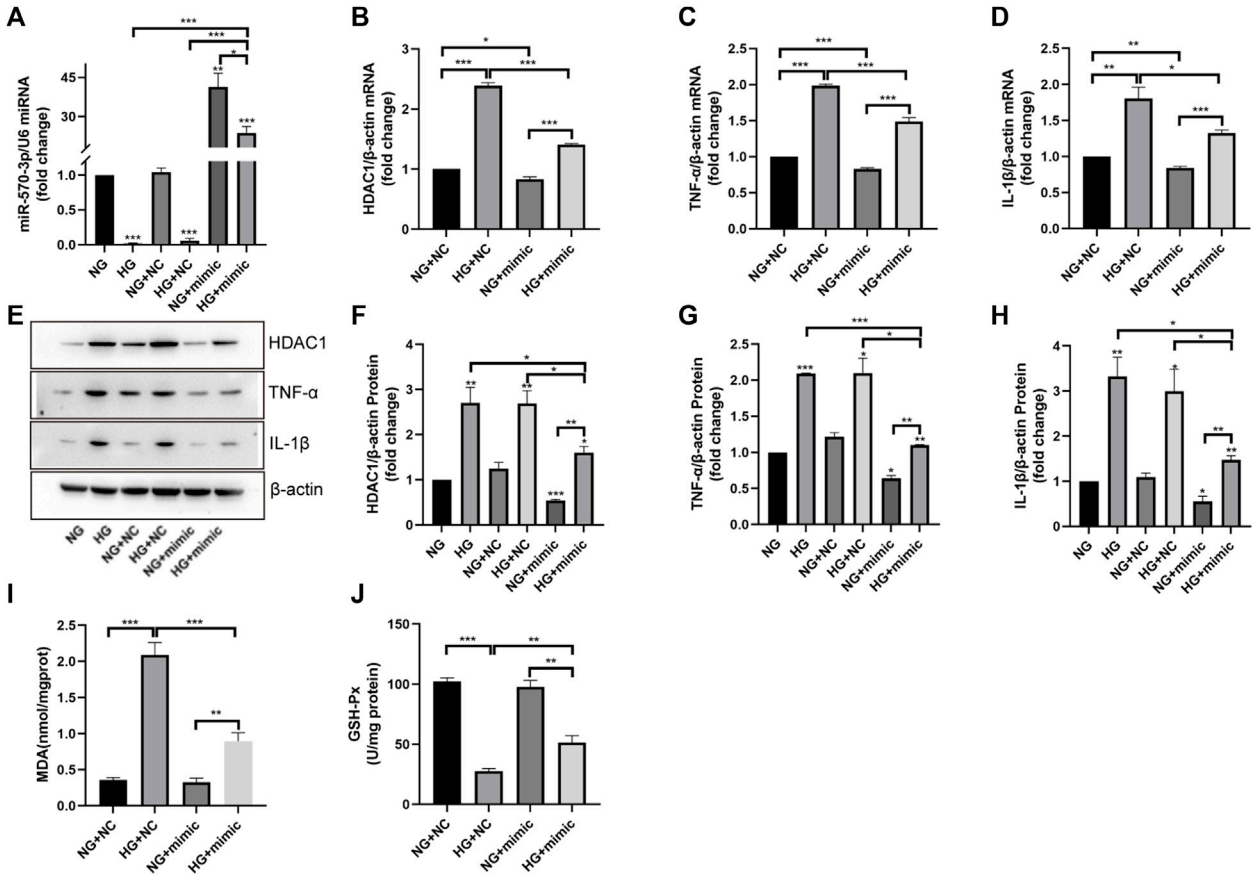

FIGURE 7
Overexpression of miR-570-3p inhibited HDAC1 expression and inflammatory injury in HUVEC cells. **(A)**. The expression of miR-570-3p miRNA in HUVEC cells transfected with miR-570-3p NC or miR-570-3p mimics. **(B–D)**. The expression of HDAC1 mRNA, TNF-α mRNA, and IL-1β mRNA in HUVEC cells transfected with miR-570-3p NC or miR-570-3p mimics. **(E–H)**. Western blotting analysis of HDAC1, TNF-α, and IL-1β protein expression levels in HUVEC cells transfected with miR-570-3p NC or miR-570-3p mimics. Gray value of western blotting. **(I)**. Content of MDA. **(J)**. Activity of GSH-Px. Values are mean ± SEM. n = 3 in each group. $*p < 0.05$, $**p < 0.01$, $***p < 0.001$.

miR-570-3p, and proved that vaccarin can inhibit the expression of HDAC1 and inflammatory injury by upregulating miR-570-3p.

Effect of vaccarin on the inflammatory injury when co-transfected with miR-570-3p mimics and pcDNA3.1-HDAC1

Finally, we studied the effects of vaccarin on inflammatory injury in HUVEC cells co-transfected with miR-570-3p mimics and pcDNA3.1-HDAC1. After co-transfection, the anti-inflammatory effects of vaccarin were inhibited, reversing the effect of vaccarin after transfection of miR-570-3p mimics alone. In contrast, the remission effect of vaccarin on inflammatory injury increased after co-transfection compared with pcDNA3.1-HDAC1 alone (Figures 9A–G).

Discussion

Diabetic angiopathy develops in over half of diabetic patients, which is a severe threat to public health. Endothelial dysfunction is a critical early event in the pathogenesis of diabetic vascular complications (Jiang, Wu et al., 2020). Therefore, the improvement and treatment of endothelial dysfunction are of great significance for the prevention of vascular complications in patients with diabetes. Evidence has shown that hyperglycemia promotes inflammation and oxidative stress owing to endothelial dysfunction (Basta, Lazzerini et al., 2005; Hulsmans and Holvoet 2010; Mittal, Siddiqui et al., 2014; Sharma, Rizky et al., 2017). Thus, the improvement of anti-inflammation function may be beneficial to endothelial dysfunction. Recently, mounting attention has been paid to traditional Chinese medicines due to their therapeutic effects on diabetes and its

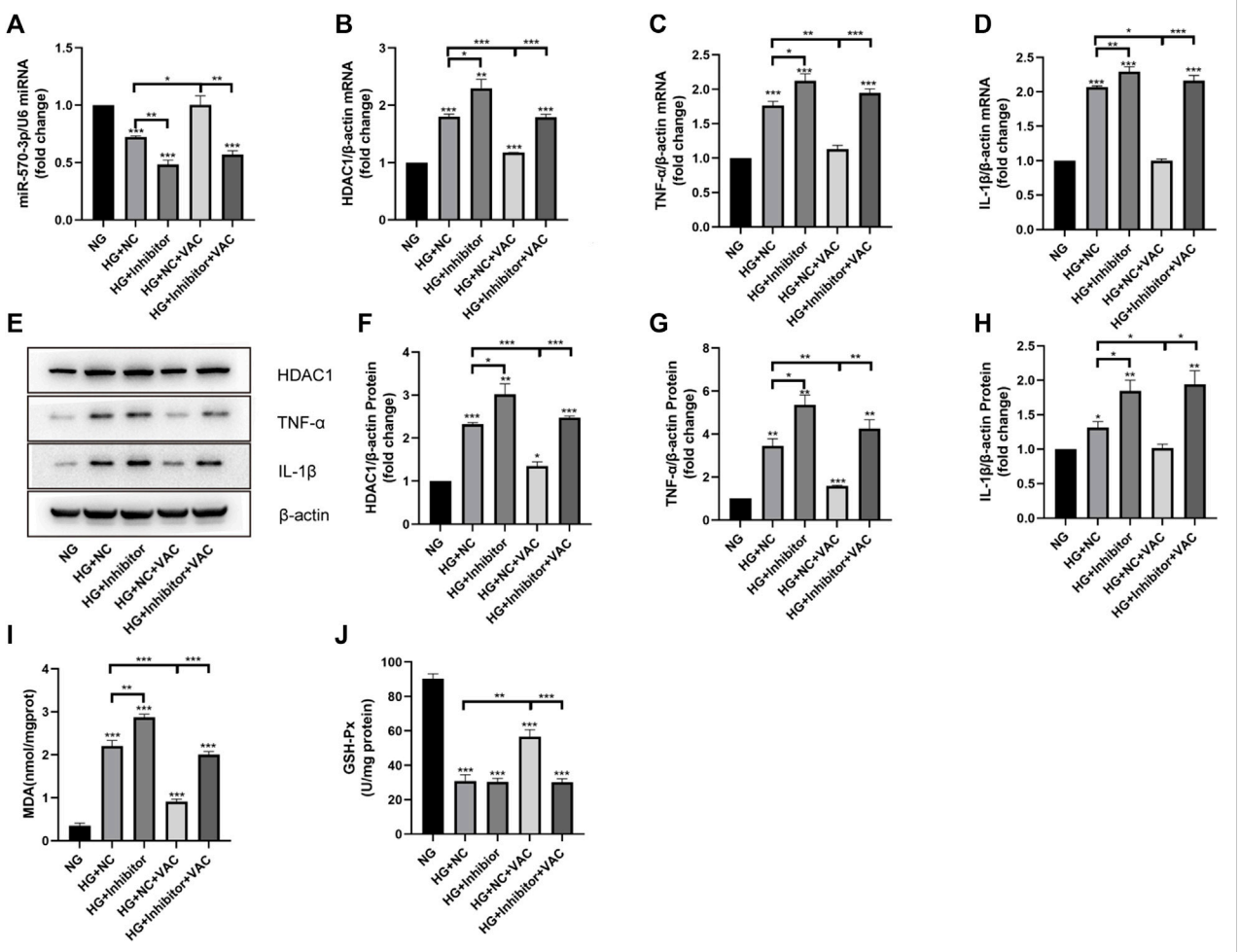

FIGURE 8
Vaccarin inhibited the expression of HDAC1 and inflammatory injury by up-regulating miR-570-3p. **(A)**. The effects of vaccarin on the expression of miR-570-3p miRNA in HUVEC cells transfected with miR-570-3p NC or miR-570-3p inhibitor. **(B–D)**. The effects of vaccarin on the expression of HDAC1 mRNA, TNF-α mRNA, and IL-1β mRNA in HUVEC cells transfected with miR-570-3p NC or miR-570-3p inhibitor. **(E–H)**. Western blotting analysis of HDAC1, TNF-α, and IL-1β protein expression levels in HUVEC cells transfected with miR-570-3p NC or miR-570-3p inhibitor. Gray value of western blotting. **(I)**. Content of MDA. **(J)**. Activity of GSH-Px. Values are mean ± SEM. $n = 3$ in each group. $^{*}p < 0.05$, $^{**}p < 0.01$, $^{***}p < 0.001$.

complications such as macrovascular disease (Zhang, Xu et al., 2020). Vaccarin is an active monomer of saponaria vaccaria, an ancient Chinese medicine. Previous studies have proved that vaccarin shows the potential function in a variety of complications caused by diabetes, including macrovascular disease (Xie, Cai et al., 2015; Qiu, Du et al., 2016; Sun, Cai et al., 2017; Zhu, Lei et al., 2018; Lei, Gong et al., 2019; Xu, Liu et al., 2019; Hou, Cai et al., 2020; Hou, Qi et al., 2020; Liu, Sun et al., 2020; Sun, Yu et al., 2021). However, the effect of vaccarin on alleviating endothelial inflammatory injury in T2DM and the molecular mechanism has not been elucidated. In this study, we aim to further investigate the effect of vaccarin on vascular disease in T2DM and to further clarify its pharmacological effects.

First of all, vaccarin effectively reduced the blood glucose of T2DM mice (Figures 2C, D), improved glucose tolerance (Figures 2E, F), insulin tolerance (Figures 2G, H), a disorder of glucose and lipid metabolism, and physiological conditions of T2DM mice (Figures 2I–M), and also had a good effect on alleviating the inflammatory injury in the aorta of T2DM mice (Figures 3B–K). In the HG-induced HUVEC cells, vaccarin had a similar effect *in vitro* (Figures 4A–G).

Histone deacetylases (HDACs) remove histone acetylation marks, resulting in compaction of chromatin structure and transcriptional repression. HDACs operate by direct association with DNA binding factors, and by incorporation into large multifunctional repressor complexes. HDACs form a large family, of which Class I HDACs(LeBoeuf, Terrell et al., 2010),

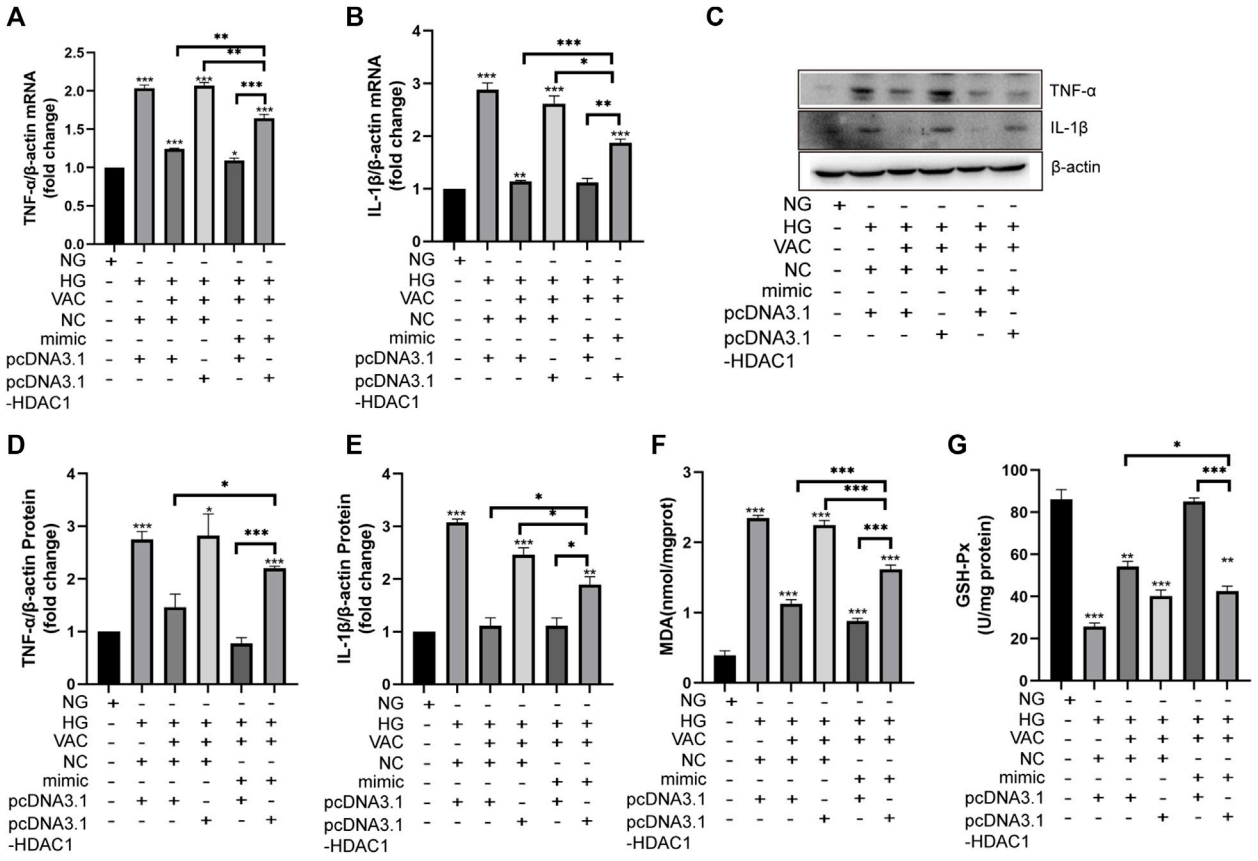

FIGURE 9
Effect of vaccarin on the inflammatory injury when co-transfected with miR-570-3p mimic and pcDNA3.1-HDAC1. **(A,B)**. The effects of vaccarin on the expression of TNF-α mRNA and IL-1β mRNA in HUVEC cells transfected with miR-570-3p NC or miR-570-3p mimics or pcDNA3.1 or pcDNA3.1-HDAC1. **(C,E)**. Western blotting analysis of TNF-α and IL-1β protein expression levels in HUVEC cells transfected with miR-570-3p NC or miR-570-3p mimics or pcDNA3.1 or pcDNA3.1-HDAC1. Gray value of western blotting. **(F)**. Content of MDA. **(G)**. Activity of GSH-Px. Values are mean ± SEM. n = 3 in each group. $*p < 0.05$, $**p < 0.01$, $***p < 0.001$.

including HDAC1, show the strongest histone deacetylase activity (Haberland, Montgomery et al., 2009; LeBoeuf, Terrell et al., 2010). There are relevant studies on the relationship between HDAC1 and inflammation. For example, down-regulation of HDAC1 can restore myocardial injury in septic mice to a certain extent (Nong, Qin et al., 2022), and ellagic acid can alleviate rheumatoid arthritis in rats by inhibiting HDAC1 (Song, Wu et al., 2021), and HDAC1 can control the metabolism of intestinal epithelial cells by regulating the supply of acetyl groups, resulting in impaired response to oxidative stress, AMPK kinase activation and mitochondrial biogenesis (Gonneaud, Turgeon et al., 2015). Our study found that the expression of HDAC1 was significantly increased in the aorta of T2DM mice as well as HG-induced HUVEC cells (Figures 3D, E, H, Figures 5A–C). Supplementary vaccarin or HDAC1 siRNA inhibited the expression of HDAC1 and alleviated inflammatory injury (Figures 5A–J). Overexpression of HDAC1 had offset the inhibitory effects of vaccarin on inflammatory injury in HG-induced HUVEC cells (Figure 5M–S). These results indicated that vaccarin suppressed inflammatory injury by inhibiting HDAC1.

In recent years, the role of miRNA in biological physiological, and pathological processes has gradually become clear, especially in the field of chronic diseases such as diabetes. Studies have found that miRNA-34a, miRNA-24, miRNA-181c, miRNA-29b, miRNA-200a, miRNA-383, and other miRNAs play a role in inflammation (Li, Kim et al., 2016; Lo, Yang et al., 2018; Shen, Li et al., 2018; Cheng, Chen et al., 2019; Zhang, Cai et al., 2019; Hu, Gong et al., 2020), thus participating in the occurrence of endothelial dysfunction in diabetes. To study the exact mechanism of vaccarin in regulating HDAC1, databases were used to screen the possible miRNA targets (Figure 6A). We found that the 3′ UTR of HDAC1's mRNA was a potential target of miR-570-3p which declined in the aorta of T2DM mice and HG-induced HUVEC cells, while increased with supplementary vaccarin (Figures 6B, C). The binding of miR-570-3p with the 3′ UTR of HDAC1's mRNA was confirmed by

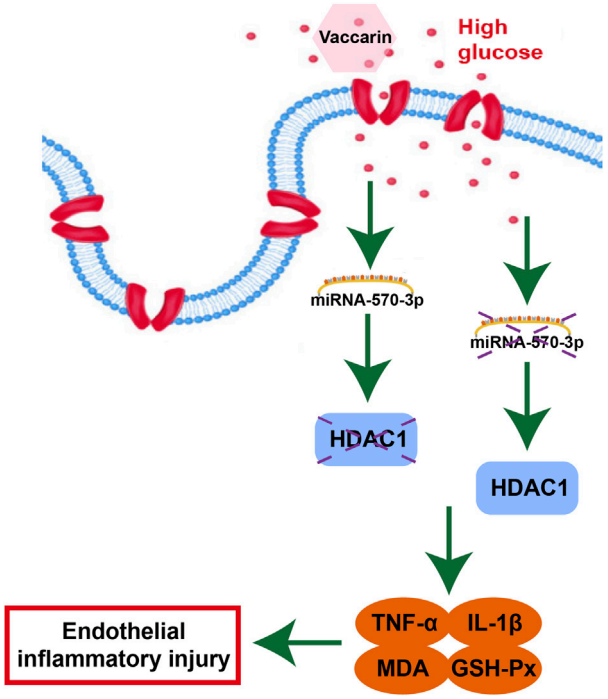

FIGURE 10
Protective mechanisms of vaccarin against HG-induced endothelial inflammatory injury.

the dual-luciferase reporter system (Figures 6D, E). From a phenomenal point of view, miR-570-3p mimic and vaccarin had similar effects on inflammatory injury (Figures 7A–J). Giving miR-570-3p inhibitor offset the inhibition of vaccarin on HDAC1 and inflammatory injury in HUVEC cells (Figures 8A–J). Finally, we co-transfected miR-570-3p mimic and pcDNA3.1-HDAC1 to study the role of vaccarin in this case (Figures 9A–G). These results indicated that vaccarin alleviates diabetic inflammatory injury by mediating the miR-570-3p/HDAC1 pathway.

In brief, vaccarin alleviates inflammatory injury by restoring miR-570-3p/HDAC1 in HUVEC cells stimulated by HG. Based on these results, we propose a novel mechanism by which vaccarin protects endothelial function, which may provide a novel treatment strategy for vascular complications in T2DM. Our findings provide new insights into the protective role of vaccarin in diabetic endothelial dysfunction, suggesting that miR-570-3p and HDAC1 may serve as biomarkers of vascular endothelial inflammatory injury and potential therapeutic targets. We provide evidence that under diabetic conditions, overexpression of miR-570-3p alleviates endothelial dysfunction by reducing HDAC1 expression and endothelial inflammatory injury, thereby reducing endothelial dysfunction. In conclusion, our outcomes show that vaccarin can reduce inflammatory injury by upregulating miR-570-3p thus inhibiting the increase of HDAC1 in the aorta of T2DM mice and HG-treated HUVEC cells (Figure 10), which provides new ideas, insights, and choices for the scope of application and medicinal value of vaccarin and some potential biomarkers or targets in diabetic endothelial dysfunction and vascular complications. Of course, this experiment also has shortcomings. We need to achieve the inhibition and overexpression of miR-570-3p and HDAC1 *in vivo* in order to further verify these conclusions.

Data availability statement

The original contributions presented in the study are included in the article/supplementary material further inquiries can be directed to the corresponding authors.

Ethics statement

The animal study was reviewed and approved by the Experimental Animal Care and Use Committee of Jiangnan University (JN. No20210915c0600129[339]).

Author contributions

Conceptualization, FX and TL; methodology, TL; software, TL; validation, XY; formal analysis, TL, XY, XZ, YW, and MZ; investigation, TL; resources, WC, BH, FX, and LQ; data curation, TL and XY; writing—original draft preparation, TL; writing—review and editing, FX and LQ; visualization, TL and XZ; supervision, LQ; project administration, TL; funding acquisition, LQ and FX.

Funding

This work was supported by the Chinese Postdoctoral Science Fund (Grant no. 2019M661729) and the Natural Science Foundation of Jiangsu Province (Grant no. BK20190597).

Acknowledgments

We thank the general support of the experimental public platform, Wuxi School of Medicine, Jiangnan University.

Conflict of interest

The authors declare that the research was conducted in the absence of any commercial or financial relationships that could be construed as a potential conflict of interest.

Publisher's note

References

Ai, M., Li, S. S., Chen, H., Wang, X. T., Sun, J. N., Hou, B., et al. (2021). 1, 25(OH) 2 D3 attenuates sleep disturbance in mouse models of Lewis lung cancer, *in silico* and *in vivo*. *J. Cell. Physiol.* 236 (11), 7473–7490. doi:10.1002/jcp.30458

Baker, J. R., Vuppusetty, C., Colley, T., Hassibi, S., Fenwick, P. S., Donnelly, L. E., et al. (2018). MicroRNA-570 is a novel regulator of cellular senescence and inflammaging. *FASEB J.* 33 (2), 1605–1616. doi:10.1096/fj.201800965R

Basta, G., Lazzerini, G., Del Turco, S., Ratto, G. M., Schmidt, A. M., and De Caterina, R. (2005). At least 2 distinct pathways generating reactive oxygen species mediate vascular cell adhesion molecule-1 induction by advanced glycation end products. *Arterioscler. Thromb. Vasc. Biol.* 25 (7), 1401–1407. doi:10.1161/01.ATV.0000167522.48370.5e

Betel, D., Koppal, A., Agius, P., Sander, C., and Leslie, C. (2010). Comprehensive modeling of microRNA targets predicts functional non-conserved and non-canonical sites. *Genome Biol.* 11 (8), R90. doi:10.1186/gb-2010-11-8-r90

Booton, R., and Lindsay, M. A. (2014). Emerging role of MicroRNAs and long noncoding RNAs in respiratory disease. *Chest* 146 (1), 193–204. doi:10.1378/chest.13-2736

Cheng, X. W., Chen, Z. F., Wan, Y. F., Zhou, Q., Wang, H., and Zhu, H. Q. (2019). Long non-coding RNA H19 suppression protects the endothelium against hyperglycemic-induced inflammation via inhibiting expression of miR-29b target gene vascular endothelial growth factor a through activation of the protein kinase B/endothelial nitric oxide synthase pathway. *Front. Cell Dev. Biol.* 7, 263. doi:10.3389/fcell.2019.00263

Dhananjayan, R., Koundinya, K. S., Malati, T., and Kutala, V. K. (2016). Endothelial dysfunction in type 2 diabetes mellitus. *Indian J. Clin. biochem.* 31 (4), 372–379. doi:10.1007/s12291-015-0516-y

2014). Diagnosis and classification of diabetes mellitus. *Diabetes Care* 37 (1), S81–S90. doi:10.2337/dc14-s081

Gonneaud, A., Turgeon, N., Boisvert, F. M., Boudreau, F., and Asselin, C. (2015). Loss of histone deacetylase Hdac1 disrupts metabolic processes in intestinal epithelial cells. *FEBS Lett.* 589 (19), 2776–2783. doi:10.1016/j.febslet.2015.08.009

Haberland, M., Montgomery, R. L., and Olson, E. N. (2009). The many roles of histone deacetylases in development and physiology: Implications for disease and therapy. *Nat. Rev. Genet.* 10 (1), 32–42. doi:10.1038/nrg2485

Hou, B., Cai, W., Chen, T., Zhang, Z., Gong, H., Yang, W., et al. (2020). Vaccarin hastens wound healing by promoting angiogenesis via activation of MAPK/ERK and PI3K/AKT signaling pathways *in vivo*. *Acta Cir. Bras.* 34 (12), e201901202. doi:10.1590/s0102-865020190120000002

Hou, B., Qi, M., Sun, J., Ai, M., Ma, X., Cai, W., et al. (2020). Preparation, characterization and wound healing effect of vaccarin-chitosan nanoparticles. *Int. J. Biol. Macromol.* 165, 3169–3179. doi:10.1016/j.ijbiomac.2020.10.182

Hu, B., Gong, Z., and Bi, Z. (2020). Inhibition of miR-383 suppresses oxidative stress and improves endothelial function by increasing sirtuin 1. *Braz J. Med. Biol. Res.* 53 (2), e8616. doi:10.1590/1414-431X20198616

Hulsmans, M., and Holvoet, P. (2010). The vicious circle between oxidative stress and inflammation in atherosclerosis. *J. Cell. Mol. Med.* 14 (1-2), 70–78. doi:10.1111/j.1582-4934.2009.00978.x

Jiang, Z., Wu, J., Ma, F., Jiang, J., Xu, L., Du, L., et al. (2020). MicroRNA-200a improves diabetic endothelial dysfunction by targeting KEAP1/NRF2. *J. Endocrinol.* 245 (1), 129–140. doi:10.1530/JOE-19-0414

Kannel, W. B., and McGee, D. L. (1979). Diabetes and cardiovascular disease. The Framingham study. *JAMA* 241 (19), 2035–2038. doi:10.1001/jama.241.19.2035

Karam, H. M., and Radwan, R. R. (2019). Metformin modulates cardiac endothelial dysfunction, oxidative stress and inflammation in irradiated rats: A new perspective of an antidiabetic drug. *Clin. Exp. Pharmacol. Physiol.* 46 (12), 1124–1132. doi:10.1111/1440-1681.13148

LeBoeuf, M., Terrell, A., Trivedi, S., Sinha, S., Epstein, J. A., Olson, E. N., et al. (2010). Hdac1 and Hdac2 act redundantly to control p63 and p53 functions in epidermal progenitor cells. *Dev. Cell* 19 (6), 807–818. doi:10.1016/j.devcel.2010.10.015

Lei, Y., Gong, L., Tan, F., Liu, Y., Li, S., Shen, H., et al. (2019). Vaccarin ameliorates insulin resistance and steatosis by activating the AMPK signaling pathway. *Eur. J. Pharmacol.* 851, 13–24. doi:10.1016/j.ejphar.2019.02.029

Li, Q., Kim, Y. R., Vikram, A., Kumar, S., Kassan, M., Gabani, M., et al. (2016). P66Shc-Induced MicroRNA-34a causes diabetic endothelial dysfunction by downregulating Sirtuin1. *Arterioscler. Thromb. Vasc. Biol.* 36 (12), 2394–2403. doi:10.1161/ATVBAHA.116.308321

Liu, Y., Sun, J., Ma, X., Li, S., Ai, M., Xu, F., et al. (2020). Vaccarin regulates diabetic chronic wound healing through FOXP2/AGGF1 pathways. *Int. J. Mol. Sci.* 21 (6), E1966. doi:10.3390/ijms21061966

Lo, W. Y., Yang, W. K., Peng, C. T., Pai, W. Y., and Wang, H. J. (2018). MicroRNA-200a/200b modulate high glucose-induced endothelial inflammation by targeting O-linked N-acetylglucosamine transferase expression. *Front. Physiol.* 9, 355. doi:10.3389/fphys.2018.00355

Mittal, M., Siddiqui, M. R., Tran, K., Reddy, S. P., and Malik, A. B. (2014). Reactive oxygen species in inflammation and tissue injury. *Antioxid. Redox Signal.* 20 (7), 1126–1167. doi:10.1089/ars.2012.5149

Nong, R., Qin, C., Lin, Q., Lu, Y., and Li, J. (2022). Down-regulated HDAC1 and up-regulated microRNA-124-5p recover myocardial damage of septic mice. *Bioengineered* 13 (3), 7168–7180. doi:10.1080/21655979.2022.2034583

Ostergard, T., Nyholm, B., Hansen, T. K., Rasmussen, L. M., Ingerslev, J., Sorensen, K. E., et al. (2006). Endothelial function and biochemical vascular markers in first-degree relatives of type 2 diabetic patients: The effect of exercise training. *Metabolism.* 55 (11), 1508–1515. doi:10.1016/j.metabol.2006.06.024

Qiu, Y., Du, B., Xie, F., Cai, W., Liu, Y., Li, Y., et al. (2016). Vaccarin attenuates high glucose-induced human EA*hy926 endothelial cell injury through inhibition of Notch signaling. *Mol. Med. Rep.* 13 (3), 2143–2150. doi:10.3892/mmr.2016.4801

Raj, V., Natarajan, S., Chatterjee, S., Ramasamy, M., Ramanujam, G. M., Arasu, M. V., et al. (2021). Cholecalciferol and metformin protect against lipopolysaccharide-induced endothelial dysfunction and senescence by modulating sirtuin-1 and protein arginine methyltransferase-1. *Eur. J. Pharmacol.* 912, 174531. doi:10.1016/j.ejphar.2021.174531

Roberts, A. C., and Porter, K. E. (2013). Cellular and molecular mechanisms of endothelial dysfunction in diabetes. *Diab. Vasc. Dis. Res.* 10 (6), 472–482. doi:10.1177/1479164113500680

Sharma, A., Rizky, L., Stefanovic, N., Tate, M., Ritchie, R. H., Ward, K. W., et al. (2017). The nuclear factor (erythroid-derived 2)-like 2 (Nrf2) activator dh404 protects against diabetes-induced endothelial dysfunction and senescence by modulating sirtuin-1 and protein arginine methyltransferase-1. *Eur. J. Pharmacol.* 912, 174531. doi:10.1016/j.ejphar.2021.174531

Roberts, A. C., and Porter, K. E. (2013). Cellular and molecular mechanisms of endothelial dysfunction in diabetes. *Diab. Vasc. Dis. Res.* 10 (6), 472–482. doi:10.1177/1479164113500680

Sharma, A., Rizky, L., Stefanovic, N., Tate, M., Ritchie, R. H., Ward, K. W., et al. (2017). The nuclear factor (erythroid-derived 2)-like 2 (Nrf2) activator dh404 protects against diabetes-induced endothelial dysfunction. *Cardiovasc. Diabetol.* 16 (1), 33. doi:10.1186/s12933-017-0513-y

Shen, X., Li, Y., Sun, G., Guo, D., and Bai, X. (2018). miR-181c-3p and -5p promotes high-glucose-induced dysfunction in human umbilical vein endothelial cells by regulating leukemia inhibitory factor. *Int. J. Biol. Macromol.* 115, 509–517. doi:10.1016/j.ijbiomac.2018.03.173

Song, H., Wu, H., Dong, J., Huang, S., Ye, J., and Liu, R. (2021). Ellagic acid alleviates rheumatoid arthritis in rats through inhibiting MTA1/HDAC1-mediated Nur77 deacetylation. *Mediat. Inflamm.* 2021, 6359652. doi:10.1155/2021/6359652

Sun, H. J., Cai, W. W., Gong, L. L., Wang, X., Zhu, X. X., Wan, M. Y., et al. (2017). FGF-2-mediated FGFR1 signaling in human microvascular endothelial cells is activated by vaccarin to promote angiogenesis. *Biomed. Pharmacother.* 95, 144–152. doi:10.1016/j.biopha.2017.08.059

Sun, J. N., Yu, X. Y., Hou, B., Ai, M., Qi, M. T., Ma, X. Y., et al. (2021). Vaccarin enhances intestinal barrier function in type 2 diabetic mice. *Eur. J. Pharmacol.* 908, 174375. doi:10.1016/j.ejphar.2021.174375

Tan, Y., Jiang, C., Jia, Q., Wang, J., Huang, G., and Tang, F. (2022). A novel oncogenic seRNA promotes nasopharyngeal carcinoma metastasis. *Cell Death Dis.* 13 (4), 401. doi:10.1038/s41419-022-04846-1

Tang, S.-t., Wang, F., Shao, M., Wang, Y., and Zhu, H.-q. (2017). MicroRNA-126 suppresses inflammation in endothelial cells under hyperglycemic condition by targeting HMGB1. *Vasc. Pharmacol.* 88, 48–55. doi:10.1016/j.vph.2016.12.002

Vanhoutte, P. M., Shimokawa, H., Feletou, M., and Tang, E. H. (2017). Endothelial dysfunction and vascular disease - a 30th anniversary update. *Acta Physiol.* 219 (1), 22–96. doi:10.1111/apha.12646

Wang, G., Wang, Y., Yang, Q., Xu, C., Zheng, Y., Wang, L., et al. (2022). Metformin prevents methylglyoxal-induced apoptosis by suppressing oxidative stress *in vitro* and *in vivo*. *Cell Death Dis.* 13 (1), 29. doi:10.1038/s41419-021-04478-x

Wang, J., Liu, D., Liang, X., Gao, L., Yue, X., Yang, Y., et al. (2013). Construction of a recombinant eukaryotic human ZHX1 gene expression plasmid and the role of ZHX1 in hepatocellular carcinoma. *Mol. Med. Rep.* 8 (5), 1531–1536. doi:10.3892/mmr.2013.1700

Wu, J., Jiang, Z., Zhang, H., Liang, W., Huang, W., Zhang, H., et al. (2018). Sodium butyrate attenuates diabetes-induced aortic endothelial dysfunction via P300-mediated transcriptional activation of Nrf2. *Free Radic. Biol. Med.* 124, 454–465. doi:10.1016/j.freeradbiomed.2018.06.034

Xie, F., Cai, W., Liu, Y., Li, Y., Du, B., Feng, L., et al. (2015). Vaccarin attenuates the human EA.hy926 endothelial cell oxidative stress injury through inhibition of Notch signaling. *Int. J. Mol. Med.* 35 (1), 135–142. doi:10.3892/ijmm.2014.1977

Xu, F., Liu, Y., Zhu, X., Li, S., Shi, X., Li, Z., et al. (2019). Protective effects and mechanisms of vaccarin on vascular endothelial dysfunction in diabetic angiopathy. *Int. J. Mol. Sci.* 20 (18), E4587. doi:10.3390/ijms20184587

Yi, J., and Gao, Z. F. (2019). MicroRNA-9-5p promotes angiogenesis but inhibits apoptosis and inflammation of high glucose-induced injury in human umbilical vascular endothelial cells by targeting CXCR4. *Int. J. Biol. Macromol.* 130, 1–9. doi:10.1016/j.ijbiomac.2019.02.003

Zhang, J., Cai, W., Fan, Z., Yang, C., Wang, W., Xiong, M., et al. (2019). MicroRNA-24 inhibits the oxidative stress induced by vascular injury by activating the Nrf2/Ho-1 signaling pathway. *Atherosclerosis* 290, 9–18. doi:10.1016/j.atherosclerosis.2019.08.023

Zhang, S., Xu, L., Liang, R., Yang, C., and Wang, P. (2020). Baicalin suppresses renal fibrosis through microRNA-124/TLR4/NF-κB axis in streptozotocin-induced diabetic nephropathy mice and high glucose-treated human proximal tubule epithelial cells. *J. Physiol. Biochem.* 76 (3), 407–416. doi:10.1007/s13105-020-00747-z

Zhu, X., Lei, Y., Tan, F., Gong, L., Gong, H., Yang, W., et al. (2018). Vaccarin protects human microvascular endothelial cells from apoptosis via attenuation of HDAC1 and oxidative stress. *Eur. J. Pharmacol.* 818, 371–380. doi:10.1016/j.ejphar.2017.09.052

frontiers | Frontiers in Pharmacology

TYPE Review
PUBLISHED 05 September 2022
DOI 10.3389/fphar.2022.975784

OPEN ACCESS

EDITED BY
Dongdong Sun,
Nanjing University of Chinese Medicine, China

REVIEWED BY
Dayun Sui,
Department of Pharmacology, Jilin University, China
Changgang Sun,
Affiliated Hospital of Weifang Medical University, China

*CORRESPONDENCE
Qibiao Wu,
qbwu@must.edu.mo
Xiangyan Li,
xiangyan_li1981@163.com
Tan Wang,
wangtanccutcm@outlook.com

†These authors have contributed equally to this work

SPECIALTY SECTION
This article was submitted to Inflammation Pharmacology, a section of the journal Frontiers in Pharmacology

RECEIVED 22 June 2022
ACCEPTED 14 July 2022
PUBLISHED 05 September 2022

CITATION
Wang J, Zeng L, Zhang Y, Qi W, Wang Z, Tian L, Zhao D, Wu Q, Li X and Wang T (2022), Pharmacological properties, molecular mechanisms and therapeutic potential of ginsenoside Rg3 as an antioxidant and anti-inflammatory agent.
Front. Pharmacol. 13:975784.
doi: 10.3389/fphar.2022.975784

Pharmacological properties, molecular mechanisms and therapeutic potential of ginsenoside Rg3 as an antioxidant and anti-inflammatory agent

Jing Wang[1,2†], Li Zeng[2†], Ying Zhang[1], Wenxiu Qi[3], Ziyuan Wang[1], Lin Tian[1], Daqing Zhao[3], Qibiao Wu[2,4]*, Xiangyan Li[3]* and Tan Wang[1]*

[1]Department of Respiratory, The Affiliated Hospital to Changchun University of Chinese Medicine, Changchun, China, [2]State Key Laboratory of Quality Research in Chinese Medicines, Faculty of Chinese Medicine, Macau University of Science and Technology, Macau, China, [3]Jilin Ginseng Academy, Changchun University of Chinese Medicine, Changchun, China, [4]Guangdong-Hong Kong-Macao Joint Laboratory for Contaminants Exposure and Health, Guangzhou, China

Inflammation and oxidative stress lead to various acute or chronic diseases, including pneumonia, liver and kidney injury, cardiovascular and cerebrovascular diseases, metabolic diseases, and cancer. Ginseng is a well-known and widely used ethnic medicine in Asian countries, and ginsenoside Rg3 is a saponin isolated from *Panax ginseng C. A. Meyer, Panax notoginseng,* or *Panax quinquefolius L.* This compound has a wide range of pharmacological properties, including antioxidant and anti-inflammatory activities, which have been evaluated in disease models of inflammation and oxidative stress. Rg3 can attenuate lung inflammation, prevent liver and kidney function damage, mitigate neuroinflammation, prevent cerebral and myocardial ischemia–reperfusion injury, and improve hypertension and diabetes symptoms. The multitarget, multipathway mechanisms of action of Rg3 have been gradually deciphered. This review summarizes the existing knowledge on the anti-inflammatory and antioxidant effects and underlying molecular mechanisms of ginsenoside Rg3, suggesting that ginsenoside Rg3 may be a promising candidate drug for the treatment of diseases with inflammatory and oxidative stress conditions.

KEYWORDS

ginsenoside Rg3, oxidative stress, inflammation, molecular mechanism, therapeutic effect

1 Introduction

Ginseng, the root of *Panax ginseng C.A. Meyer*, has been used for 2000 years in ethnomedicine in Asia to treat various diseases (Lee et al., 2020a). The roots, leaves, and fruits of ginseng plants have been extensively used as herbal medicines. The antioxidant activity of ginseng is exploited to treat cardiovascular diseases (Hyun et al., 2022). Interestingly, red ginseng has better antioxidant activity and is used to treat neurodegenerative diseases, gastroenteritis, liver damage, diabetes, and aging (Lee et al., 2017a). The Rg3 content of fresh ginseng is relatively low, and the content in ginseng after processing or enzymatic transformation accounts for 0.37–1.13% of the total saponins (Chang et al., 2009; Kim et al., 2013). Red ginseng has undergone steaming treatment. During this process, some ginsenosides with lower polarity are produced. The Rg3 content increases with increasing steaming batches. After nine steam cycles, the Rg3 content in the total saponins was 15–18% (Lee et al., 2012a; Jeong et al., 2017). According to the same process used to make red ginseng roots, Chen *et al.* steamed ginseng leaves, and Rg3 increased 8.6-fold (Chen et al., 2020). These findings suggest that Rg3 is one of the primary ginsenosides in red ginseng.

This work aimed to understand how Rg3 regulates oxidative stress and inflammation to elicit pharmacological effects and to review the literature on the therapeutic use of Rg3 based on antioxidant and anti-inflammatory effects. We briefly introduced the biological functions of Rg3 in response to inflammation and oxidative stress. We then summarized the effects of Rg3 on neurological disorders, cardiovascular diseases, cancer, lung diseases, diabetes, and digestive system diseases (Figure 1).

2 Methodology

A literature search was performed in PubMed from August 1998 to January 2022, and the last search date was 30 April 2022. The search term was "Ginsenoside Rg3". A secondary search was conducted by screening the list of articles that met the inclusion criteria. The keywords were inflammation, oxidative stress, antioxidant, and anti-inflammatory. The obtained articles were screened, irrelevant studies were excluded, and eligible articles were sorted and classified. Finally, we organized the tables, wrote the text, and made figures to summarize the application of Rg3 antioxidant and anti-inflammatory effects.

3 Overview of oxidative stress and inflammation

Reactive oxygen species (ROS), including superoxide, hydroxyl radicals, and hydrogen peroxide (H_2O_2), are necessary for cell growth, differentiation, responses to external stimuli, and other processes. ROS are primarily produced in the mitochondria through the respiratory chain and the nicotinamide adenine dinucleotide phosphate (NADPH) oxidase system. In addition to mitochondria, cytochrome P450 2E1 (CYP2E1), cyclooxygenase-2 (COX-2), and

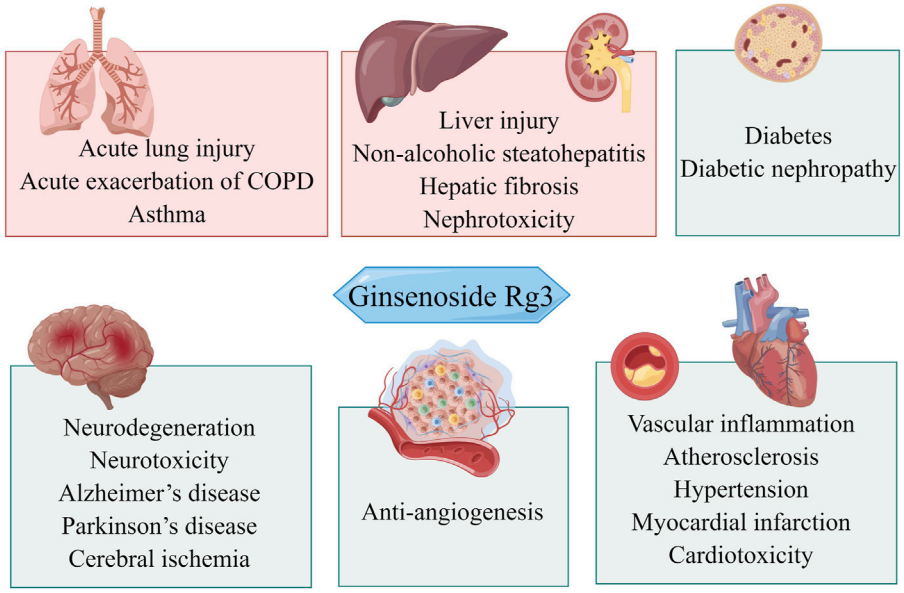

FIGURE 1
Overview of the potential therapeutic effects of Rg3 on different organ systems.

lipoxygenases in the plasma membrane and cytosol produce ROS. ROS are subsequently eliminated by superoxide dismutase (SOD), catalase (CAT), glutathione peroxidase (GSH-px), and nonenzymatic scavenging factors, such as glutathione (GSH) and vitamin C, to maintain redox homeostasis (Ramos-Tovar and Muriel, 2020). In response to ROS accumulation, peroxidase production activates the NF-E2-related factor 2 (Nrf2)/heme oxygenase 1 (HO-1) pathway (Kobayashi and Yamamoto, 2005). Lipid oxidation produces toxic metabolic compounds, hydroperoxides, and hydroxides; they aggravate the formation of atherosclerosis and liver injury. Malondialdehyde (MDA) is an end product of lipid oxidation used as a biomarker for assessing oxidative damage (Ayala et al., 2014; Silva et al., 2022). Nitric oxide synthase (NOS) catalyzes the production of nitric oxide (NO) and citrulline using oxygen and L-arginine as substrates. There are three isoforms of NOS. Endothelial NOS (eNOS) and neuronal NOS (nNOS) are expressed in the normal state. NO produced by eNOS is critical for maintaining vascular homeostasis (Balligand et al., 2009). Inducible NOS (iNOS) is induced after injury (Brown, 2007). iNOS-derived NO reacts with superoxide anions to form peroxynitrite, leading to oxidative stress related to inflammatory neurodegeneration, endothelial dysfunction, and liver and kidney injury (Jaeschke et al., 2002; Landmesser et al., 2003; Heemskerk et al., 2009; Incalza et al., 2018).

Oxidative stress and inflammation occur concomitantly. The accumulation of ROS can induce inflammation. In turn, the inflammatory response triggers oxidative stress. In the inflammatory response, inflammatory factors activate Toll-like receptor (TLR) signaling receptors in neutrophils and macrophages, and inflammatory mediators are released in large quantities. This process leads to oxygen consumption, which is produced through the NADPH pathway, and the accumulation of oxygen free radicals causes oxidative stress (Furman et al., 2019). When cells are damaged by oxidative stress, ROS accumulate in large quantities and activate TLR receptors in Kupffer cells and macrophages, thus increasing proinflammatory mediators such as the release of interleukin-1β (IL-1β) and IL-6 (Yoon et al., 2015; Ramos-Tovar and Muriel, 2020).

4 Antioxidant and anti-inflammatory effects and molecular mechanisms of Rg3

In response to oxidative stress, Rg3 inhibits ROS accumulation and MDA content, improves mitochondrial function, and increases the activity of antioxidant enzymes, including SOD, GSH, GSH-px, and CAT, to promote oxygen free radical metabolism. Rg3 responds to oxidative stress by regulating Nrf2/HO-1 and sirtuin 1 (SIRT1) (Xing et al., 2017; Kee and Hong, 2019; Ren et al., 2021). Rg3 inhibits iNOS and NO release to reduce peroxynitrite formation; interestingly, it promotes eNOS-derived NO to protect vascular endothelial cells (Singh et al., 2018).

In lipopolysaccharide (LPS)-mediated inflammation models, Rg3 decreased the expression of COX-2 and prostaglandin E2 (PGE2) and the secretion of tumor necrosis factor-α (TNF-α), IL-1β, and IL-6 (Shin et al., 2013; Lee et al., 2017b; Kee and Hong, 2019). Inhibitory NLRP3 inflammasome activation and NLRP3-apoptosis-associated speck-like protein (ASC) interaction were observed in an LPS-induced mouse model after treatment with Rg3 (Kang et al., 2018; Shi et al., 2020). The mechanisms of response to inflammation relate to inhibition of the nuclear factor-κB (NF-κB) pathway, including upstream TLR4/myeloid differentiation primary response 88 (MyD88) and downstream COX-2 expression (Kang et al., 2018; Candelario-Jalil et al., 2022). Rg3 upregulates SIRT1 to inhibit the NF-κB pathway, contributing to anti-inflammatory activity (Ren et al., 2021). Downregulation of the phosphatidylinositol-3-kinase (PI3K)/Akt and p38 mitogen-activated protein kinase (MAPK) pathways by Rg3 suppressed inflammation directly or by crosstalk with the NF-κB pathway (Hou et al., 2017; Yang et al., 2018; Kee and Hong, 2019).

4.1 Pulmonary diseases

Inflammation is present in various pulmonary diseases. Persistent inflammation in the airway and lung tissue is involved in the pathogenesis of chronic lung diseases such as chronic obstructive pulmonary disease (COPD), asthma, and pulmonary fibrosis (Racanelli et al., 2018). Acute lung disease is often accompanied by acute inflammation, including acute lung injury (ALI), pneumonia, and acute exacerbation of COPD (AECOPD) (Robb et al., 2016). Inflammation promotes the accumulation of oxidative stress products. These findings suggest that anti-inflammation is a critical step in pulmonary disease treatment (Domej et al., 2014). In animal models of chemical-induced ALI, Rg3 inhibited cytokines and increased the content of antioxidant enzymes (SOD, CAT, and GSH) to reduce pulmonary inflammation and neutrophil infiltration (Wang et al., 2016; Yang et al., 2018). The anti-inflammatory effect of Rg3 was also observed in the AECOPD mouse model, and these effects were related to the inhibition of the PI3K/Akt pathway (Yang et al., 2018; Guan et al., 2020). In an airway inflammation model stimulated by Asian sand dust, upregulation of mucin (MUC)5AC and MUC5B stimulates mucus secretion; significantly, mucus cross-linking exacerbates pulmonary disease (Dunican et al., 2021). Rg3 decreased mucin gene expression through the NF-κB pathway (Shin et al., 2021). Regarding asthma, Rg3 inhibited p65 phosphorylation, and COX-2 inhibited the secretion of chemokine ligands, ILs, and TNF-α. Rg3 exerts its antioxidant effect through the Nrf2/HO-1 pathway to decrease ROS generation. Anti-inflammatory and

TABLE 1 Summary of Rg3 in pulmonary diseases.

Diseases	Model	Treatment	Outcome	Mechanism	Ref
ALI	Male SD rats injected subcutaneously with 60 mg/kg omethoate	5, 10, and 20 mg/kg Rg3 via tail vein	MDA↓, SOD↑, CAT↑, GSH↑, MPO↓, TNF-α↓	Improved lung inflammation and neutrophil infiltration by antioxidant function	Wang et al. (2016)
ALI	RAW264.7 cells stimulated with 2 μg/mL LPS	25, 50, or 100 μg/mL Rg3	MPO↓, TNF-α↓, IL-1β↓, IL-6↓, IL-10↑, TGF-β↓, PI3K/Akt/mTOR↓, p-MerTK↑	Decreased MerTK to mediated activation of PI3K/Akt/mTOR pathway	Yang et al. (2018)
	C57BL/6 mice and MerTK$^{-/-}$ C57BL/6 mice with 10 μg LPS intranasally	10, 20, and 30 mg/kg Rg3 intraperitoneally			
AECOPD	BEAS–2B cells with cigarette smoke	10, 20 and 40 μM 20 (S)-Rg3	Neutrophil migration↓, IL-6↓, p-PI3K↓, p-Akt↓	Reduced the migration of neutrophils through downregulation of PI3K/Akt pathway	Guan et al. (2020)
	BALB/c mice exposured to cigarette smoke for 14 weeks then infected with non–typeable *Haemophilus* inflenza	10, 20, 40 mg/kg 20 (S)-Rg3 intragastrically			
Airway inflammatory disease	BEAS-2B cells stimulated with 50 or 100 μg/mL of Asian sand dust for 48 h	50 μg/mL Rg3	MUC5AC↓, MUC5B↓, NF-κB↓	Inhibited mucin gene expression and protein through NF-κB pathway	Shin et al. (2021)
Asthma	10 ng/mL IL-1β induced A549 cells	900 nM Rg3	COX-2↓, IL-4↓, TNF-α↓, eotaxin↓, p-p65↓	Inhibited NF-κB p65 activity for anti-inflammatory effect	Lee et al. (2016)
	Human asthmatic airway epithelial tissues	50 μM Rg3			
Asthma	BEAS-2B cells with 10 ng/mL IL-4/TNF-α	3, 10 and 30 μM Rg3	Eotaxin↓, Eotaxin-2↓, TNF-α↓, IL-5↓, IL-4↓, IL-13↓, IL-6↓, and IFN-γ↑, COX-2↓, ICAM-1↓, Nrf2↑, HO-1↑, MDA↓, GSH↑, ROS↓	Inhibited the oxidative stress and inflammation via Nrf2/HO-1 pathway	Huang et al. (2021)
	Female BALB/c mice with intraperitoneal injection of 50 μg ovalbumin	Intraperitoneal injection of 10 mg/kg Rg3			

ALI, acute lung injury; SD, rat, Sprague–Dawley rat; MerTK, mer tyrosine kinase; LPS, lipopolysaccharide; MDA, malondialdehyde; SOD, superoxide dismutase; CAT, catalase; GSH, glutathione; MPO, myeloperoxidase; TNF-α, tumor necrosis factor-α; IL, interleukin; TGF-β, transforming growth factor-β; PI3K/Akt/mTOR, phosphatidylinositol-3-kinase/Akt/mammalian target of rapamycin; AECOPD, acute exacerbation chronic obstructive pulmonary disease; MUC, mucin; NF-κB, nuclear factor-κB; COX-2, cyclooxygenase-2; IFN-γ, interferon-γ; ICAM-1, intercellular adhesion molecule-1; Nrf2, NF-E2-related factor 2; HO-1, heme oxygenase 1; ROS, reactive oxygen species.

antioxidant effects have been used to treat asthma models *in vitro* and *in vivo* (Lee et al., 2016; Huang et al., 2021). In summary, Rg3 exerts anti-inflammatory effects to alleviate lung damage (Table 1).

4.2 Liver and kidney injury

Several studies have demonstrated that Rg3 downregulates abnormally elevated alanine aminotransferase (ALT) and aspartate aminotransferase (AST) to improve liver function in models of drug-induced or inflammation-mediated liver injury (Kang et al., 2007; Zhou et al., 2018). In addition, Rg3 alleviated acetaminophen-mediated liver tissue apoptosis by activating the PI3K/Akt pathway (Zhou et al., 2018). In a mouse model of acetaminophen-mediated/induced liver injury, Rg3 reduced GSH consumption and inhibited CYP2E1 overexpression to combat oxidative stress and hepatotoxicity (Zhou et al., 2018; Gao et al., 2021). Rg3 decreased thiobarbituric acid (TBA) and iNOS to mitigate oxidative damage in the livers and kidneys of LPS-treated rats (Kang et al., 2007). Rg3 also protected against acute liver and kidney function injury caused by chemotherapeutic agents. Chemotherapy containing cis-platinum (DDP) causes liver and kidney damage, and several studies found that Rg3 treatment significantly protected against hepatotoxicity and nephrotoxicity. ALT, AST, blood urea nitrogen (BUN), and creatinine (CRE), which represent liver and kidney function, decreased after treatment with Rg3 in a DDP-induced mouse model (Lee et al., 2012b). Upregulation of GSH, GSH-Px, and SOD enhanced antioxidant capacity and reduced ROS generation and MDA content (Lee et al., 2012b; Zhang et al., 2021). Rg3 downregulates p53 and caspase-3 to inhibit apoptosis of kidney cells (Park et al., 2015; Zhang et al., 2021). For liver fibrosis, Rg3 decreased NF-κB to inhibit hepatic inflammation and fibrosis distribution in a nonalcoholic steatohepatitis mouse model (Lee et al., 2020b). In a thioacetamide (TAA)-induced hepatic fibrosis mouse model, Rg3 reduced inflammation-mediated autophagy and increased SOD, CAT, and GSH levels to improve liver function and attenuate fibrosis (Liu et al., 2020) (Table 2).

4.3 Neurological disorders

When neurons suffer oxidative stress, ROS cooperate with mitochondrial Ca^{2+} to increase the permeability of the

TABLE 2 Summary of Rg3 on liver and kidney injury.

Diseases	Model	Treatment	Outcome	Mechanism	Ref
Liver injury	Male ICR mice with injection of 250 mg/kg acetaminophen	10 and 20 mg/kg 20(R)-Rg3 for 7 days orally	ALT↓, AST↓, TNF-α↓, IL-1β↓, GSH↑, MDA↓, CYP2E1↓, 4-hydroxynonenal↓, Bax↓, Bcl-2↑, PI3K/Akt↑, IKKα↓, IKKβ↓, NF-κB↓	Inhibited the overexpression of CYP2E1 against oxidative stress, inhibited NF-κB to reduce inflammatory infiltration	Zhou et al. (2018)
Liver injury	C57BL/6J mice with intragastric 350 mg/kg acetaminophen	Oral 5, 10, and 20 mg/kg Rg3	ALT↓, AST↓, LDH↓, alkaline phosphatase↓, GSH↑, GSH-px↑, MDA↓, IL-1α↓, IL-1β↓, IL-5↓, IL-6↓, CCL3↓, CCL5↓, CCL11↓, TNF-α↓, caspase-1↓, NLRP3↓	Inhibited oxidative stress, inflammatory reaction and apoptosis through NLRP3	Gao et al. (2021)
Liver and kidney injury	Male Wistar rats with 5 mg/kg LPS	5 or 10 mg/kg 20(S)-Rg3 for 15 days orally	AST↓, ALT↓, CRE↓, NO_2^-/NO_3^-↓, TBA↓, NF-κB↓, COX-2↓, iNOS↓, HO-1↑	Inhibited NF-κB p65 to mitigate liver and kidney injury	Kang et al. (2007)
Colon cancer and DDP-induced hepatotoxicity and nephrotoxicity	LLC-RK1 cells, NCTC1469 cells and CT-26 cells	10–50 μM Rg3	BUN↓, CRE↓, ALT↓, AST↓, MDA↓, GSH↑, GSH-Px↑, SOD↑, ROS↓, Nrf2↓, HO-1↓	Enhanced the sensitivity of cisplatin, and ameliorate the kidney and liver damage against oxidative stress	Lee et al. (2012b)
	CT26 cells tumor-bearing nude mice	5 or 10 mg/kg Rg3			
DDP-induced nephrotoxicity	LLC-PK1 cells with 25 μM DDP	50, 100 and 250 μM Rg3	JNK↓, p53↓, caspase-3↓	Inhibited inflammation and apoptosis through downregulation of JNK and p53	Park et al. (2015)
DDP-induced nephrotoxicity	HK-2 and HepG2 cells with 4 μM DDP	1, 2 and 4 μM 20(R)-Rg3	BUN↓, CRE↓, MDA↓, CAT↑, SOD↑, GSH↑, ROS↓, iNOS↓, COX-2↓, p53↓, NF-κB↓	Downregulated NF-κB to improve oxidative stress against kidney damage	Zhang et al. (2021)
	ICR mice with 20 mg/kg DDP	10 and 20 mg/kg 20(R)-Rg3			
Nonalcoholic steatohepatitis	THP-1, HepG2, stellate cells, and hepatic LX2 cells with TGF-β, LPS or palmitate	0.01, 0.1, 1 and 10 μg/mL Rg3	α-SMA↓, collagen1↓, IL-1β↓, TNF-α↓, p-NF-κB↓	Decreased NF-κB for distribution of hepatic inflammation and fibrosis	Lee et al. (2020b)
	C57BL/6J mice with a methionine- and choline-deficient L-amino acid diet for 6 weeks	Oral 15 and 30 mg/kg Rg3			
Hepatic fibrosis	HSC-T6 and L02 cells with LPS	16 μM Rg3	ALT↓, AST↓, SOD↑, CAT↑, GSH↑, MDA↓, TGF-β1↓, α-SMA↓, p62↓, ATG5↓, ATG7↓, LC3b/LC3a↓, PI3K/Akt/mTOR↑	Reduced inflammation-mediated autophagy via upregulation of PI3K/Akt/mTOR	Liu et al. (2020)
	ICR mice with intraperitoneal injection TAA 150 mg/kg 4 weeks or 50 mg/kg TAA for 10 weeks	5 and 10 mg/kg Rg3 orally			

ICR, institute of cancer research; ALT, alanine aminotransferase; AST, aspartate aminotransferase; TNF-α, tumor necrosis factor-α; IL, interleukin; GSH, glutathione; MDA, malondialdehyde; CYP2E1, cytochrome P450 2E1; Bax, Bcl-2-associated X; Bcl-2, B-cell lymphoma-2; PI3K, phosphatidylinositol-3-kinase; IKK, inhibitory kappa kinase; NF-κB, nuclear factor-κB; LDH, lactate dehydrogenase; GSH-px, glutathione peroxidase; CCL, chemokine (C-C motif) ligand; LPS, lipopolysaccharide; NO, nitric oxide; CRE, creatinine; TBA, thiobarbituric acid; COX-2, cyclooxygenase-2; iNOS, inducible nitric oxide synthase; HO-1, heme oxygenase 1; DDP, cis-platinum; BUN, blood urea nitrogen; SOD, superoxide dismutase; ROS, reactive oxygen species; Nrf2, NF-E2-related factor 2; JNK, c-Jun N-terminal kinases; CAT, catalase; α-SMA, α-smooth muscle actin; TGF-β, transforming growth factor-β; TAA, thioacetamide; ATG, autophagy-related; LC3, light chain 3; mTOR, mammalian.

mitochondrial transition pore (MPTP), resulting in mitochondrial swelling. This process leads to cellular inflammation, senescence, and apoptosis (Zhao et al., 2022). In an H_2O_2-induced mitochondrial suspension from the rat forebrain, 20(S)-Rg3 provided neuroprotection and inhibited mitochondrial swelling through suppression of ROS (Tian et al., 2009). Rg3 inhibited IL-6, IL-8, and monocyte chemotactic protein 1 (MCP-1) and ameliorated cellular senescence via inactivation of NF-κB and p38 in H_2O_2-treated human astrocyte CRT cells (Hou et al., 2017). The antioxidant effect of Rg3 mitigated neurotoxic effects associated with the prevention and treatment of neurodegeneration. Rg3 protected cortical cells from glutamate-induced nerve damage by enhancing SOD and GSH-px (Kim et al., 1998). Trimethyltin chloride-induced neurotoxicity of ICR mice promoted oxidative stress, inflammation, hippocampal neuron loss, and astrocytic activation in the mouse brain, which generates a clinical syndrome characterized by amnesia and complex seizures. Rg3 and Rh2 improved neurotoxicity via upregulation of PI3K/Akt and suppression of extracellular signal-regulated kinase (ERK) (Hou et al., 2018). In a mouse model of systemic inflammation mediated by LPS, 20(S)-Rg3 suppressed iNOS and COX-2 to attenuate inflammatory activation of the brain (Park et al., 2012).

Cognitive and memory impairments are closely associated with Alzheimer's disease (AD). Chronic neuroinflammation of

the entorhinal cortex and hippocampus leads to memory impairments (Lukiw and Bazan, 2000). The inhibition of COX-2 caused by Rg3 ameliorated LPS-induced learning and memory impairments in rats (Lee et al., 2013). Pathologically, the accumulation of abnormally folded amyloid-β (Aβ) and neuronal fiber aggregation lead to early cognitive impairment in AD. Rg3 reduced the neurotoxicity of Aβ42-treated BV-2 microglial cells. The mechanism suggested that Rg3 inhibited NF-κB p65 nuclear translocation to reduce the release of inflammatory factors and upregulated scavenger receptor type A (SRA) (Joo et al., 2008); this membrane protein recognizes pathological products and activates microglia to clear necrotic neurons (Bairamian et al., 2022). Bairamian *et al.* reported that Rg3 reduced ROS and Aβ deposition in a *Caenorhabditis elegans* model of AD (Tangrodchanapong et al., 2020). In addition, an *in vitro* study confirmed that regulation of inflammatory factors by Rg3 restored M2 activation and promoted Aβ uptake in microglia and neuronal cells (Ahn et al., 2021). In summary, Rg3 increases Aβ uptake to improve memory and cognitive function, which is associated with the inhibition of inflammatory factors through NF-κB and COX-2.

Parkinson's disease (PD) is a neurodegenerative disorder with a decreased number of nigrostriatal neurons. Loss of nigrostriatal dopamine and α-synuclein aggregation correlates with the severity of PD. In a transgenic *Caenorhabditis elegans* model of PD, Rg3 suppressed apoptosis and enhanced antioxidant enzymes to prolong lifespan (Chalorak et al., 2021). Another study reported that Rg3 prolonged the latency of rotenone-induced PD mice through evaluation of pole, rotarod, and open field tests. The mice showed improved motor function and dopamine content in the striatum, suggesting that Rg3 enhances the expression of glutamate cysteine ligase (GCL) (Han et al., 2021), which catalyzes GSH synthesis to prevent oxidative damage and ROS generation (Forman et al., 2009). To sum up, Rg3 increases peroxidase activity to promote dopamine secretion and slow PD progression.

Cerebral ischemia is a common disease with severe consequences. The excessive accumulation of cytokines increases the adhesion of leukocytes to blood vessels, leading to endothelial damage and aggravating cerebral ischemia–reperfusion (I/R) injury (Candelario-Jalil et al., 2022). Rg3 attenuated IL-1β, IL-6, TNF-α, and ROS generation in a middle cerebral artery occlusion (MCAO) rat model. The mechanism suggests that Rg3 inhibits TLR4/MyD88 and SIRT1 to protect the brain from ischemic injury (Cheng et al., 2019).

Accelerated chronic inflammation and aging of nucleus pulposus cells (NPCs) lead to intervertebral disk degeneration (IDD) (Heathfield et al., 2008; Li et al., 2017). In TNF-α-treated NPCs, Rg3 improved oxidative stress status and extracellular matrix (ECM) metabolism by inhibiting NF-κB p65 activation in a dose-dependent manner (Chen et al., 2019). Spinal cord injury is a destructive spinal cord lesion that is more severe than IDD. 20(*S*)-Rg3 promoted the recovery of motor function and attenuated iNOS and COX-2 in a spinal cord injury rat model. (Kim et al., 2017).

In conclusion, Rg3 has a strong neuroprotective effect. When neurons are stimulated by peroxide, Rg3 scavenges free radicals, protects mitochondrial function, inhibits inflammatory factors, suppresses cell senescence. When neurons are exposed to toxic substances, Rg3 increases peroxidase activity to detoxify and activate PI3K/Akt to prevent apoptosis. The development of neurodegenerative and chronic diseases, including AD, PD, and stroke, is often accompanied by oxidative stress and inflammation (Zhao et al., 2022). These studies suggest that Rg3 inhibits cytokines, COX-2, ROS generation, and mitochondrial dysfunction and enhances peroxidase activity and microglial polarization to exert therapeutic effects on neurological disorders (Table 3).

4.4 Cardiovascular diseases

In the early pathological processes of hypertension and atherosclerosis, chronic vascular inflammation and toxic metabolic compounds of lipid oxidation lead to vascular endothelial dysfunction and lipid deposition (Dasagrandhi et al., 2022). This process is accompanied by upregulation of vascular cell adhesion molecule-1 (VCAM-1) and intercellular adhesion molecule-1 (ICAM-1), and oxidized lipids and adhesion molecules mutually promote the plaque formation process of atherosclerosis (Blankenberg et al., 2003; Malekmohammad et al., 2019). In the presence of various inducers (e.g., LPS, NOD1 agonist, or ox-LDL), Rg3 downregulates ICAM-1 and VCAM-1 to inhibit endothelial dysfunction, which is related to anti-inflammatory action by the NF-κB pathway (Cho et al., 2014; Lee et al., 2020c; Geng et al., 2020). Rg3 inhibited THP-1-cell adhesion into human umbilical vein endothelial cells (HUVECs) by suppressing the NF-κB pathway *in vitro* (Cho et al., 2014). Oral Rg3 restrained the formation of atherosclerosis and inflammation in $ApoE^{-/-}$ mice via the regulation of peroxisome proliferator-activated receptor γ (PPARγ)/focal adhesion kinase (FAK) (Geng et al., 2020).

NO is a significant factor in maintaining vascular homeostasis. Rg3 promoted NO release to increase thoracic aortic relaxation in rats, which had a therapeutic effect on hypertension (Kim et al., 1999; Nagar et al., 2016). The mechanism is related to the activation of eNOS or iNOS. Kim *et al.* suggested that iNOS was upregulated by NF-κB activation. Low-dose Rg3 promoted macrophage proinflammatory responses, including upregulation of IL-1 and TNF and NO release (Kim et al., 2003). Another study found that the activation and phosphorylation of eNOS mediated Rg3 treatment of hypertension. Rg3 activated estrogen receptor (ER)-dependent

TABLE 3 Summary of Rg3 in neurological disorders.

Diseases	Model	Treatment	Outcome	Mechanism	Ref
Neurodegeneration	Mixed cortical cells exposed to 50 μM glutamate for15 min, which were from old fetal SD rats	0.1 and 1 μM Rg3	LDH↓, SOD↑, H_2O_2↓, GSH-px↑, MDA↓, Nitrite↓, Ca^{2+} influx↓	Antioxidation on suppression of extensive neuronal death	Kim et al. (1998)
Neuroprotection	50 μM $CaCl_2$ or 3 mM H_2O_2 induced mitochondrial suspension from rat forebrain	2–16 μM 20(S)-Rg3	Mitochondria swelling↓, ROS↓	Inhibited the opening of MPTP by free radical scavenging action	Tian et al. (2009)
Brain aging	35 μM H_2O_2 induced human astrocytic CRT cells; 150 μM H_2O_2 induced primary rat astrocytes	5 and 10 μg/mL Rg3	P53↓, P21↓, IL-6↓, IL-8↓, MCP-1↓, NF-κB↓, p38↓	Decreased senescence by suppressing NF-κB and p38 activation	Hou et al. (2017)
Neuroinflammation	C57BL/6 mice intraperitoneally injected with LPS (3 mg/kg)	20, and 30 mg/kg 20(S)-Rg3 orally	TNF-α↓, IL-1β↓, IL-6↓, iNOS↓, COX-2↓	Suppressed iNOS and COX-2 to attenuate microglia inflammation activation	Park et al. (2012)
Neurotoxicity	Primary rat astrocytes cultured with 1 μmol/L trimethyltin chloride	5 μg/mL Rg3	SOD↑, GSH-px↑, MDA↓, IL-1α/β↓, IL-6↓, TNF-α↓, Akt↑, ERK↓, cleaved caspase-3↓	Improved the oxidative stress and neuroinflammation through upregulation of PI3K/Akt and suppression of ERK	Hou et al. (2018)
	ICR mice intraperitoneal injection of 2 mg/kg trimethyltin chloride	20 mg/kg/day Rg3 injected intraperitoneally for 28 days			
Learning and memory impairments	Adult male SD rats with microinjection of 50 μg LPS into the lateral ventricles	10, 20 and 50 mg/kg Rg3 intraperitoneally for 21 days	Memory impairment↓ TNF-α↓, IL-1β↓, COX-2↓	Decreased inflammatory mediators and COX-2 to repair the memory impairment	Lee et al. (2013)
Neurodegeneration	5 μg/mL Aβ42 induced BV-2 microglial cells	10 μg/mL Rg3	IL-1β↓, IL-6↓, MCP-1↓, MIP-1↓, TNF-α↓, iNOS↓, NF-κB p65↓, SRA↑	Attenuated the inflammatory of microglia and neuroblastoma through suppression of NF-κB p65 nuclear translocation	Joo et al. (2008)
	50 ng/mL induced TNF-α Neuro-2a neuroblastoma cells	20 μg/mL Rg3			
AD	Transgenic *Caenditis elegans* model of AD	50 μM Rg3	Aβ deposit↓, ROS↓	-	Tangrodchanapong et al. (2020)
AD	20 ng/mL IFN-γ induced Neuro-2a murine neuroblastoma and HMO6 human microglial cells	5 μg/mL Rg3	IL-6↓, TNF-α↓, iNOS↓, Arg1↑, IL-10↑, SRA↑	Enhanced Aβ uptake through M2 microglial activation	Ahn et al. (2021)
PD	6-hydroxydopamine induced transgenic *Caenorhabditis elegans* model of PD	0.5, 1, 5, and 10 μM Rg3	Dopaminergic neurons↑, α-Synuclein↓, caspase-9↓, *Cat-2*↑, *Sod-3*↑	Suppressed apoptosis and enhanced antioxidant enzymes	Chalorak et al. (2021)
PD	C57BL/6J male mice intragastric administration with 30 mg/kg rotenone for 6 weeks	5, 10, or 20 mg/kg Rg3 intragastrically for 6 weeks	Dopamine↑, ROS↓, GCL↑	Improved motor function of PD mice through GCL	Han et al. (2021)
Cerebral ischemia	1 mmol/L $CoCl_2$ induced PC12 cells	20 μg/mL Rg3	ROS↓, mitochondrial membrane↑, IL-1β↓, TNF-α↓, IL-6↓, TLR4/MyD88↓, NF-κB p65↓, SIRT1↑	Inhibited TLR4/MyD88 and activited SIRT1 to protected the brain from ischemic injury	Cheng et al. (2019)
	MCAO rat model	10 mg/kg Rg3 injected from the tail vein			
IDD	10 ng/mL TNF-α induced NPCs cells	25, 50 and 100 μg/mL Rg3	ROS↓, MDA↓, SOD↑, GSH↑, ECM metabolism↑ (MMP3↑, ADAMTS5↑, Aggrecan↓ and COL2A1↓), NF-κB p65↓	Improved oxidative stress, ECM metabolism and cell cycle through inhibiting NF-κB p65	Chen et al. (2019)
Spinal cord injury	Rats underwent laminectomy with spinal cord compression injury	Orally 10 or 30 mg/kg/day 20(*S*)-Rg3 for 14 days	Bax↓, Bcl-2↓, iNOS↓, COX-2↓, TNF-α, IL-1β, IL-6↓, Iba1↓	Promoted the recovery of motor function, reduced neuronal apoptosis and the activation of microglia via Iba1	Kim et al. (2017)

SD, rat, Sprague–Dawley rat; LDH, lactate dehydrogenase; SOD, superoxide dismutase; GSH-px, glutathione peroxidase; MDA, malondialdehyde; ROS, reactive oxygen species; MPTP, mitochondrial transition pore; IL, interleukin; MCP-1, monocyte chemotactic protein 1; NF-κB, nuclear factor-κB; LPS, lipopolysaccharide; TNF-α, tumor necrosis factor-α; iNOS, inducible nitric oxide synthase; COX-2, cyclooxygenase-2; ICR, institute of cancer research; ERK, extracellular signal-regulated kinase; MIP-1, macrophage inflammatory protein-1; SRA, scavenger receptor type A; AD, Alzheimer's disease; IFN-γ, interferon-γ; Arg1, PD, Parkinson's disease; GCL, glutamate cysteine ligase; MCAO, middle cerebral artery occlusion; TLR4/MyD88, Toll-like receptor 4/myeloid differentiation primary response 88; SIRT1, sirtuin 1; IDD, intervertebral disk degeneration; ECM, extracellular matrix; MMP, matrix metalloproteinases.

PI3K and AMP-activated protein kinase (AMPK) pathways to upregulate eNOS in endothelial cells (Hien et al., 2010). These studies suggest that Rg3 regulates vasodilatation by increasing the release of NO in hypertension.

Ginseng invigorates vitality in ethnic medicine, which is related to the regulation of heart function. Rg3 improved cardiac function and myocardial damage in rats with myocardial I/R surgery (Wang et al., 2015a; Zhang et al., 2016). In the treatment of myocardial injury, Rg3 reduced the secretion of IL-6, IL-1β, and TNF-α, inhibited lactic acid accumulation, improved the oxidative stress state, including upregulation of SOD content and downregulation of ROS accumulation, indicating that Rg3 is a SIRT1 agonist that downregulates the NF-κB pathway (Li et al., 2020a; Tu et al., 2020). Li *et al.* developed Rg3-loaded ROS-responsive polymeric nanoparticles, which have a lower therapeutic dose (Li et al., 2020a). In addition, Rg3 enhanced B-cell lymphoma-2 (Bcl-2) and inhibited p53, Bcl-2-associated X (Bax) and caspase-3 to resist apoptosis of cardiomyocytes *in vitro* and in SD rats with myocardial I/R surgery *in vivo* (Wang et al., 2015a; Zhang et al., 2016; Li et al., 2020a). Upregulation of Akt/eNOS for NO release by Rg3 protected against myocardial injury (Wang et al., 2015a). For hypertrophic cardiomyopathy, Rg3 alleviated oxidative stress, inflammation, and fibrosis via SIRT1/NF-κB in rats undergoing transverse aortic coarctation (TAC) surgery (Ren et al., 2021). Rg3 improved heart function and aortic ring endothelial function in adriamycin (ADM)-treated rats. The mechanism involved the activation of Nrf2/HO-1 to reduce ROS and increase eNOS levels (Wang et al., 2015b). The beneficial effects of Rg3 on cardiovascular disease are summarized in Table 4.

4.5 Diabetes and diabetic complications

Diabetes is a metabolic disease with increasing incidence worldwide. Oxidative stress promotes metabolic dysfunction and complications in diabetes (Bhatti et al., 2022). Rg3 exerts its therapeutic effect in the treatment of diabetes, diabetic nephropathy (DN), and dyslipidemia. In streptozotocin (STZ)-induced diabetes models, Rg3 reduced fasting blood glucose (FBG) and glycosylated protein (Kang et al., 2008; Li et al., 2021). iNOS, COX-2, and NF-κB p65 were decreased after Rg3 intervention (Kang et al., 2008; Kim et al., 2014). iNOS-derived overproduction of NO leads to the development of diabetes (Bahadoran et al., 2020). The NF-κB signaling cascade is the initial event in response to oxidative stress in diabetes (Archuleta et al., 2009). A study showed that Rg3 decreased urine protein associated with DN in a rat model via inhibition of NF-κB p65 (Zhou et al., 2020). Another study found that 20(S)-Rg3 ameliorated renal histopathological injury and dyslipidemia through the MAPK and NF-κB pathways in C57BL/6 mice with an intraperitoneal injection of STZ and a high-fat diet (HFD). At the same time, 20(S)-Rg3 improved oxidative stress status by diminishing the overproduction of MDA and enhancing serum SOD (Zhou et al., 2020). Guo *et al.* found that 20(S)-Rg3 skewed macrophages to the M2 phenotype and decreased the expression of TNF-α, IL-6, IL-10, and transforming growth factor-β (TGF-β) to mitigate atherosclerosis in diabetic apoE$^{-/-}$ mice (Guo et al., 2018). For diabetic complications, inhibition of the apoptotic signaling pathway can protect renal tissue in DN. Rg3 protected renal tubular epithelial cells from apoptosis *in vitro* (Zhou et al., 2020). Li *et al.* suggested that Rg3 reduced Bax and cleaved caspase3 and enhanced the expression of Bcl-2 and Bcl-XL to inhibit apoptosis in the kidneys of DN mice (Li et al., 2021). In addition, Rg3 improved erectile function by upregulating SOD and protected nerve fibers from apoptosis in diabetic rats (Liu et al., 2015). These studies suggest that Rg3 is useful in treating diabetes and complications, attributable to its antioxidant, anti-inflammatory and anti-apoptosis effects (Table 5).

4.6 Cancer

Rg3-rich extracts of ginseng upregulated NO production to activate an immune response in LPS-treated Raw 264.7 cells and inhibited the proliferation of HUVECs (Lee et al., 2009). Interestingly, Kim *et al.* observed that Rg3 inhibited the differentiation and migration of endothelial progenitor cells through suppression of vascular endothelial growth factor (VEGF)/Akt/eNOS signaling, suggesting an antiangiogenic effect (Kim et al., 2012). However, the study did not detect the release of NO. In addition, a red ginseng preparation with Rg3-fortified facilitated NO release for the proliferation of splenocytes and inhibition of tumor growth in lung cancer tumor-bearing mice (Park et al., 2011). These findings suggest that the promotion of NO release by Rg3 inhibits angiogenesis and tumor proliferation; however, the synthesis pathway of NO production requires further study.

Oxidative stress status and tumor therapy need to be analysed from two aspects. ROS accumulation in tumor tissue induces tumor cell apoptosis (e.g., ferroptosis) (Liang et al., 2019). On the other hand, free radicals derived from tumor cells promote DNA damage and mutation to cause tumorigenesis and tumor metastasis (Prasad et al., 2017). Graphene oxide nanoparticle-loaded Rg3 promoted apoptosis and enhanced ROS generation to enhance photodynamic therapy of osteosarcoma (Lu et al., 2021). Rg3 nanoparticles (Rg3-NPs) promoted apoptosis and improved oxidative stress states against Ehrlich solid tumor growth in mice (El-Banna et al., 2022). Regarding tumorigenesis, abnormal expression of COX-2 and proinflammatory cytokines is associated with skin carcinogenesis (Moon et al., 2020). The topical application of Rg3 inhibited COX-2 and decreased skin

TABLE 4 Summary of Rg3 on cardiovascular diseases.

Diseases	Model	Treatment	Outcome	Mechanism	Ref
Vascular inflammation	HUVECs cells with the NOD1 agonist	10 μg/mL Rg3	NOD1↓, miR-139–5p↑, fibronectin↓, N-cadherin↓, VE-cadherin↓, smooth muscle-22α↓, NF-κB↓, IκBα↑, p65 (nucleus)↓	Inhibited inflammation and epithelial-mesenchymal transition through miR-139/NF-κB axis	Lee et al. (2020c)
Vascular inflammation	HUVECs with 1 μg/mL LPS stimulation and THP-1 macrophage cells	1, 10, 20 and 50 μM of Rg3	ICAM–1↓, VCAM–1↓, IκBα↑	Inhibited leukocyte adhesion into vascular wall and NF-κB pathway	Cho et al. (2014)
	Male C57BL/6 mice with 20 mg/kg LPS	20 mg/mL Rg3			
Atherosclerosis	200 μg/mL ox-LDL stimulated HUVECs, THP-1 cells	15 and 30 μM Rg3	VCAM-1↓, ICAM-1↓, MMP-2↓, MMP-9↓, NF-κB↓, MCP-1↓, IL-6↓, α-SMA↑, CD68↓, PPARγ↑, FAK↓	Upregulated PPARγ to repress FAK and inflammation	Geng et al. (2020)
	$ApoE^{-/-}$ mice fed a high-fat diets	15 and 30 mg/kg Rg3 orally			
Hypertension	Thoracic aortas isolated from male SD rats	0.1 μg/mL Rg3	NO↑, cGMP↑, K^+ channels↑	Increased endothelium derived NO production for relaxation of aortic rings	Kim et al. (1999)
Hypertension	Thoracic aortas of SD rats	100 mg/kg Rg3 orally for 5 days	iNOS↑, NO↑, NF-κB↑, IκBα↓, p-IκBα↑, p65 (nucleus)↑, IL-1↑, TNF-α↑	Activated NF-κB pathway to release iNOS for vasodilation	Kim et al. (2003)
	Raw264.7 cells	10 μg/mL Rg3			
Hypertension	ECV 304 cells	1, 3 and 10 μg/mL Rg3	NO↑, eNOS↑, p-eNOS↑, Akt↑, JNK↑, p38↑, AMPK↑, calmodulin-dependent protein kinase II↑	Activated eNOS through PI3K and AMPK pathway	Hien et al. (2010)
	Endothelium-intact aortic rings from thoracic aortas of SD rats	10 μg/mL Rg3			
Myocardial I/R injury	SD rats with myocardial I/R surgery	Intraperitoneal injection 60 mg/kg Rg3	LDH/CK↓, SOD↑, caspase-3↓, caspase-9↓, Bcl-2/Bax↑, p-eNOS↑, NO↑, p-Akt↑	Upregulated Akt/eNOS to reduced rat myocardial injury; Upregulated Bcl-2/Bax ratio to resist apoptosis	Wang et al. (2015a)
	1 mM $CaCl_2$ induced primary neonatal rat cardiomyocytes	10 μM Rg3			
Myocardial I/R injury	Male SD rats with myocardial I/R surgery	5 or 20 mg/kg Rg3 intragastrically	Caspase-3↓, P53↓, Bax↓, Bcl-2↑, TNF-α↓, IL-1β↓	Ameliorated cardiac function through antioxidant and anti-apoptosis	Zhang et al. (2016)
Myocardial I/R injury	Male SD rats with myocardial I/R surgery	2.5 mg/kg Rg3-NPs injected into the heart	CK↓, CK-MB↓, LDH↓, FOXO3a↑, SIRT1↑, PPARγ; Antioxidant: ROS↓, SOD↑, MDA↓, Nrf1↑, Nrf2↑, HO-1↑, SOD1↑; Anti-inflammatory: C-reactive protein↓, IL-6↓, IL-1β↓, TNF-α1↑, p65 NFκ, p-IKBα↓	Increased FOXO3a/SIRT1 pathway to response to myocardial I/R injury	Li et al. (2020a)
	H9C2 cells	10 nM Rg3-NPs	Anti-fibrosis: TGF-β↓, p-Smad2/Smad2↓, MMP2↓, MMP9↓		
Myocardial I/R injury	Male SD rats with myocardial I/R surgery	30 mg/kg Rg3 intragastrically for 7 days	LDH↓, CK-MB↓, cardiac troponin I↓, TNF-α↓, IL-1β↓, IL-6↓, IL-10↑, SIRT1↑, p-p65/p65↓	Activated SIRT1 to inhibit the inflammatory response of myocardial infarction rats	Tu et al. (2020)
Myocardial hypertrophy	SD rats with transverse aortic coarctation surgery	30 mg/kg/day, intragastrically Rg3 for 14 days	Anti-fibrosis: myosin heavy chain↓, collagen I↓, TGF-β1↓ Inflammasome: NLRP3↓, ASC↓, caspase-1↓	Alleviate oxidative stress, inflammation and fibrosis via SIRT1/NF-κB pathway	Ren et al. (2021)
	Human cardiomyocytes AC16 and HCM cells cultured with 200 nM Angiotensin II	10, 20 and 40 μM Rg3	Antioxidant: MDA↓, SOD↑, HO-1↑, Nrf2↑ SIRT1↑, NF-κB↓		
ADM induced cardiotoxicity	SD rats intraperitoneal injection of 15 mg/kg ADM	Rg3 intraperitoneal injection 10, 20, 40 mg/kg	ICAM-1↓, TGF-β↓, TIMP-1↓, VEGF↓, LDH↓, ROS↓, MDA↓, eNOS↑, endothelin-1↓, SOD↑, Nrf2↑, HO-1↑, Keap1↓	Activated Nrf2/HO-1 to improve cardiac function and aortic ring endothelial function	Wang et al. (2015b)
	CMEC cells isolated from neonatal rats with 1 μM ADM	Rg3 10 μM			

NOD1,nucleotide-binding oligomerization domain 1; NF-κB, nuclear factor-κB; IκB, inhibitor of NF-κB; LPS, lipopolysaccharide; ICAM–1, intercellular adhesion molecule-1; VCAM–1, vascular cell adhesion molecule-1; MMP, matrix metalloproteinases; MCP-1, monocyte chemotactic protein 1; IL, interleukin; α-SMA, α-smooth muscle actin; PPARγ, peroxisome proliferator-activated receptor-γ; FAK, focal adhesion kinase; SD, rat, Sprague–Dawley rat; NO, nitric oxide; cGMP′ 3′,5′-cyclic guanosine monophosphate; iNOS, inducible nitric oxide synthase; eNOS, endothelial nitric oxide synthase; TNF-α, tumor necrosis factor-α; JNK, c-Jun N-terminal kinases; AMPK, AMP-activated protein kinase; I/R, ischemia–reperfusion; LDH, lactate dehydrogenase; CK, creatine kinase; SOD, superoxide dismutase; Bcl-2, B-cell lymphoma-2; Bax, Bcl-2-associated X; NP, nucleus pulposus; ROS, reactive oxygen species; MDA, malondialdehyde; FOXO3a, Forkhead box O 3a; SIRT1, sirtuin 1; Nrf2, NF-E2-related factor 2; HO-1, heme oxygenase 1; TGF-β, transforming growth factor-β; ASC, apoptosis-associated speck-like protein; ADM, adriamycin; TIMP-1, tissue inhibitor of metalloproteinases 1; VEGF, vascular endothelial growth factor; Keap1, Kelch-like ECH-associated protein 1.

TABLE 5 Summary of Rg3 on diabetes and diabetic complications.

Diseases	Model	Treatment	Outcome	Mechanism	Ref
Diabetes	Islets isolated from BALB/c mice pancreas with high glucose concentration (16.7 mmol/L)	4 mmol/L Rg3 for 24, 48, and 72 h	NO↓, iNOS↓, PARP↓	Enhanced islet cell function and attenuated apoptosis through inhibiting iNOS and PARP	Kim et al. (2014)
DN	C57BL/6 mice with intraperitoneal injection of 100 mg/kg STZ and combined HFD	10 and 20 mg/kg 20(R)- Rg3 for 8 weeks orally	FBG↓, blood lipids↓, SOD↑, MDA↓, HO-1↑, TNF-α↓, IL-1β↑, p-JNK↓, p-ERK↓, p-p38↓, p-p65↓, cleaved caspase-3, 8↓, Bcl-2↑, Bcl-XL↑	Inhibited MAPK and NF-κB pathways to prevent DN	Li et al. (2021)
Diabetes and DN	Wistar rats with 50 mg/kg STZ injected intraperitoneally	Orally 5, 10, and 20 mg/kg/day 20(S)-Rg3	Serum glucose↓, TBA↓, glycosylated protein↓, NF-κB p65↓, COX-2↓, iNOS↓, 3-nitrotyrosine protein↓, N-methyl-D-aspartate↓	Improved the renal nitrosative stress of diabetes rats through NF-κB pathway	Kang et al. (2008)
DN	NRK-52E cells with palmitic acid	25 and 50 μM 20(S)-Rg3	Urine protein↓, TGF-β1↓, NF-κB p65↓, TNF-α↓	Inhibited NF-κB p65 to protect the renal tubular epithelial cell from apoptosis	Zhou et al. (2020)
	SD rats with intraperitoneal injection of 60 mg/kg STZ injected and combined HFD	10 mg/kg/day 20(S)-Rg3 for 12 weeks			
Progress of atherosclerosis in diabetes	THP-1 cells with 100 ng/mL phorbol-12-myristate-13 acetate and the bone marrow cells isolated from mice with 20 ng/mL macrophage colony-stimulating factor	25 μM 20(S)-Rg3	Blood glucose↓, blood lipids↓, TNF-α↓, IL-6↓, IL-10↑, TGF-β↑, PPARγ↓, iNOS↓, arginase-1↑, CD86↓, CD206↑	Skewed macrophages to the M2 phenotype to mitigate atherosclerosis in diabetic $ApoE^{-/-}$ mice	Guo et al. (2018)
	$ApoE^{-/-}$ mice 50 mg/kg STZ injected intraperitoneally	Intragastric 10 mg/kg 20(S)-Rg3			
Diabetes and erectile function	SD rats 60 mg/kg STZ injected intraperitoneally	Intragastric 10 and 100 mg/kg Rg3 for 3 months	Cleaved caspase-3↓, Bcl-2↑, Bcl-xl↑, PECAM-1↑, α-SMA↑, SOD↑, MDA↓	Improved erectile function through antioxidant effect	Liu et al. (2015)

NO, nitric oxide; iNOS, inducible nitric oxide synthase; PARP, poly (ADP-ribose) polymerase; DN, diabetic nephropathy; STZ, streptozotocin; HFD, high-fat diet; FBG, fasting blood glucose; SOD, superoxide dismutase; MDA, malondialdehyde; HO-1, heme oxygenase 1; TNF-α, tumor necrosis factor-α; IL, interleukin; JNK, c-Jun N-terminal kinases; ERK, extracellular signal-regulated kinase; Bcl-2, B-cell lymphoma-2; MAPK, mitogen-activated protein kinase; NF-κB, nuclear factor-κB; TBA, thiobarbituric acid; COX-2, cyclooxygenase-2; SD, rat, Sprague–Dawley rat; TGF-β, transforming growth factor-β; PPARγ, peroxisome proliferator-activated receptor-γ; α-SMA, α-smooth muscle actin.

carcinogenesis through the downregulation of the transcription factors NF-κB and activator protein-1 (AP-1) (Keum et al., 2003).

4.7 Other oxidative stress-related diseases

The aging process is accompanied by impairment of free radical scavenging and oxidative stress damage (Papaconstantinou, 2019). Rg3 increases mitochondrial biogenesis and enhances antioxidation to reduce ROS against cell senescence (Hong et al., 2020). Reduction of ROS by Rg3 protected keratinocytes from ultraviolet irradiation (Lim et al., 2014). In a D-galactose-induced aging mouse model, Rg3 inhibited CYP2E1 and MDA to protect against aging-related hepatic and renal dysfunction (Li et al., 2020b). Rg3 protected the gastric mucosa and inhibited gastric ulcer formation. Rg3 reduced iNOS-reducing NO release and the accumulation of free radicals in gastric mucosa mediated by alcohol; Rg3 also promoted the expression of epidermal growth factor (EGF) for epithelial proliferation and tissue repair (Zhang et al., 2019). Nanoparticles loaded with Rg3 could increase gastric ulcer treatment efficacy (Cao et al., 2022). Rg3 improved mitochondrial biogenesis and downregulated ROS by activating SIRT1 in TNF-α-treated chondrocytes, which could serve as an adjunct therapy for arthritis (Ma et al., 2021). Rg3 attenuated aluminum-induced osteoporosis by enhancing GSH and SOD activity (Song et al., 2020). Cyclophosphamide is an alkylating agent used to treat hematologic malignancies; however, it is associated with bone marrow toxicity. Rg3 inhibited CP-induced DNA damage by improving oxidative stress states *in vivo* (Zhang et al., 2008). In TNF-α-treated human chondrocytes, Rg3 inhibited mitochondrial ROS production and enhanced ATP content, which has potential as a therapeutic remedy for muscle weakness and atrophy (Lee et al., 2019). Several studies found that Rg3 inhibited the release of inflammatory factors and downregulated VEGF expression during wound healing, which is a potential treatment for hypertrophic scars (Cheng et al., 2013; Cheng et al., 2014; Ma et al., 2020).

5 Overview of the therapeutic potential of ginsenoside Rg3

Rg3 has potent antioxidant and anti-inflammatory effects, indicating that it might have a potential therapeutic role in acute

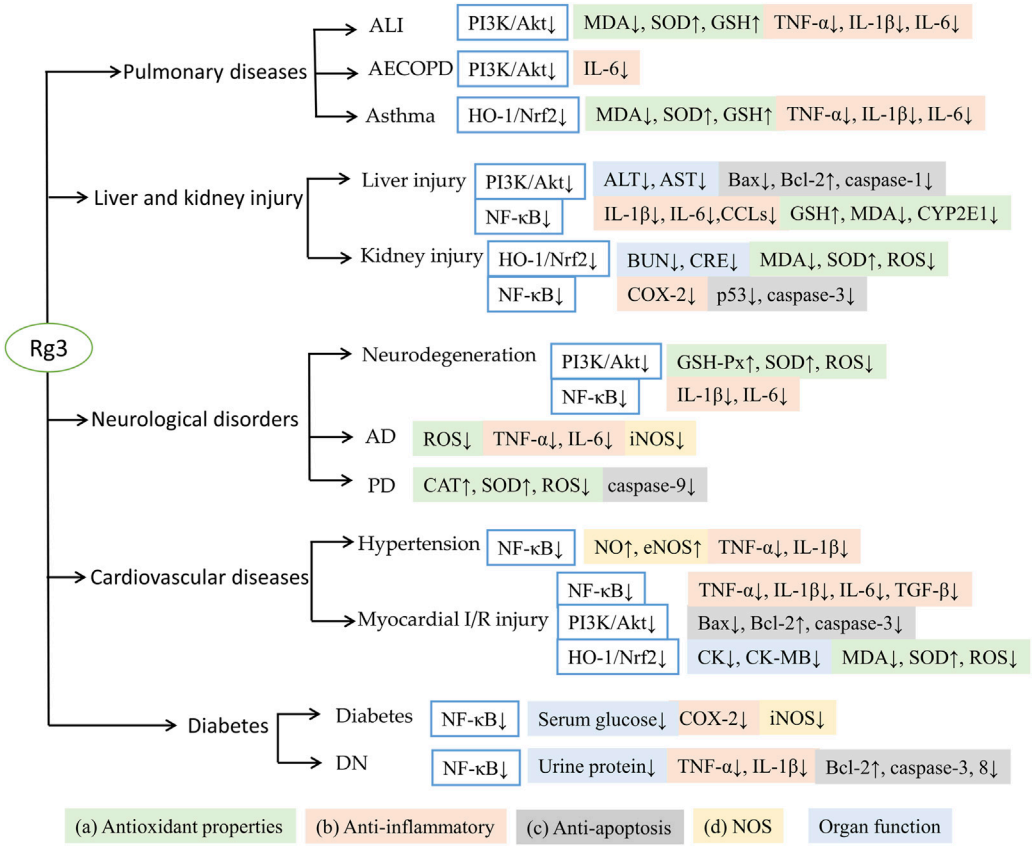

FIGURE 2
Summary of Rg3 against different diseases with antioxidant and anti-inflammatory effects.

organ injuries such as acute lung injury, acute liver and kidney injury, etc. Rg3 alleviates inflammatory infiltration of lung tissue and inhibits IL release in lung tissue in mouse and rat models of ALI (Yang et al., 2018). In an OVA-induced asthma mouse model, Rg3 ameliorates goblet cell hyperplasia and eosinophil infiltration (Huang et al., 2021). For liver and kidney injury caused by external factors, Rg3 significantly improves liver function, mainly by inhibiting the abnormal elevation of aminotransferases and overexpression of CYP2E1; meanwhile, Rg3 improves acetaminophen-induced focal centrilobular necrosis and pericentral venous degeneration of liver tissue (Zhou et al., 2018; Gao et al., 2021). In addition, Rg3 inhibits the expression of α-SMA and collagen I during the fibrosis process of nonalcoholic steatohepatitis and hepatic fibrosis (Lee et al., 2020b; Liu et al., 2020). In DDP-mediated nephrotoxicity, Rg3 increases kidney tissue GSH expression, inhibits MDA levels, and downregulates serum BUN and CRE to protect renal function (Lee et al., 2012b; Zhang et al., 2021).

Rg3 can improve cardiac function, reduce markers of cardiac damage, suppress neurocyte aging, and reduce memory impairment in rats (Lee et al., 2013; Hou et al., 2017), indicating that Rg3 might also have the potential to become a promising therapeutic agent for chronic diseases, including cardiovascular diseases, cerebrovascular diseases, diabetes and cancers, etc. Rg3 enhanced Aβ uptake through M2 microglial activation in AD (Ahn et al., 2021). Rg3 prolonged the latency of rotenone-induced PD mice through evaluation of pole, rotarod, and open field tests (Han et al., 2021). The above effects can improve neurological damage, memory deterioration and cognitive impairment, which alleviates the progression of neurodegenerative diseases. In cardiovascular diseases, vascular inflammation and lipid accumulation are reduced after Rg3 intervention (Lee et al., 2020c; Geng et al., 2020). Several studies concluded that Rg3 activated eNOS for vasodilation in the treatment of hypertension (Kim et al., 2003; Hien et al., 2010). Rg3 enhanced left ventricular ejection fraction (EF%) to improve cardiac function in rats with myocardial I/R surgery. Rg3 ameliorated myocardial infarction-related serum markers, including creatine kinase (CK), CK-MB, and lactate dehydrogenase (LDH) (Wang et al., 2015a; Zhang et al., 2016). In metabolic diseases, Rg3 reduces FBG, glycosylated protein and blood lipids in diabetic rats (Kang

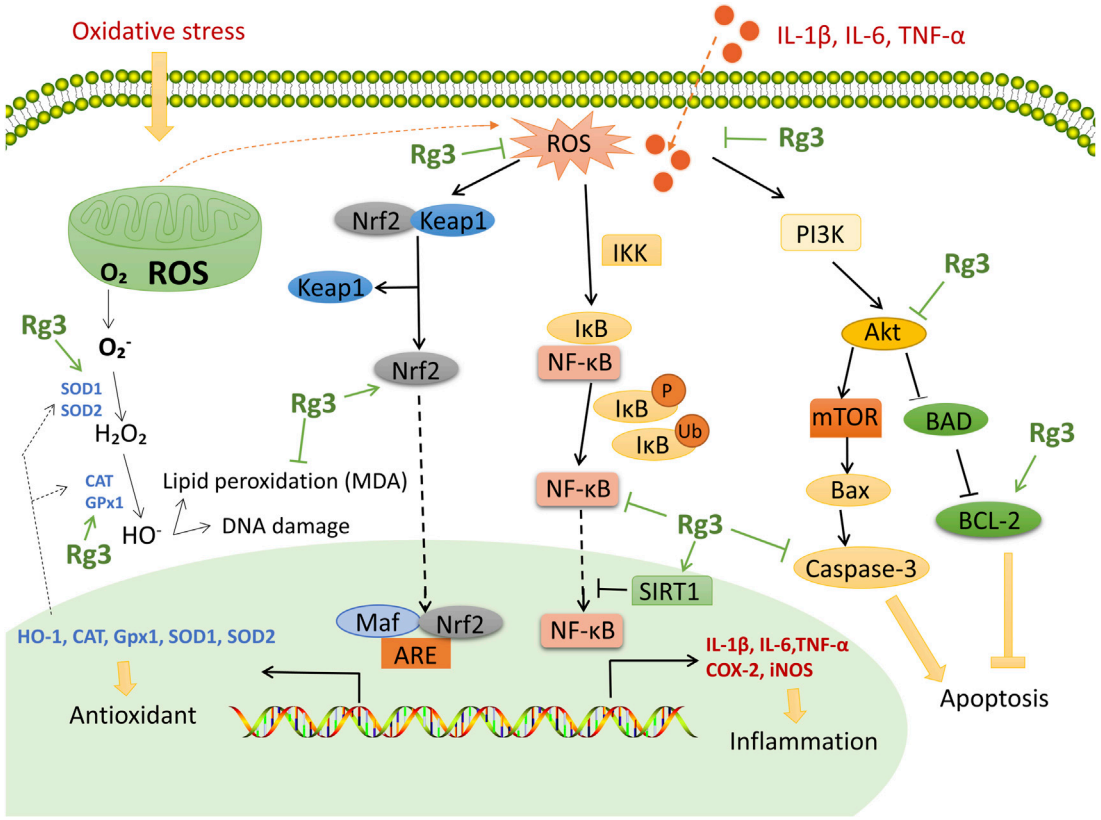

FIGURE 3
Functional mechanisms and targets of Rg3 on antioxidant and anti-inflammatory effects. Rg3 upregulates Nrf2 to enhance antioxidase activity. Rg3 inhibits the NF-κB pathway and downstream COX-2 to ameliorate inflammation and oxidative stress. Rg3 activates SIRT1 to inhibit the NF-κB pathway. Rg3 protects tissue from apoptosis through the PI3K/Akt pathway.

et al., 2008; Li et al., 2021). Rg3 improves CRE and urine protein elevation in DN mice by increasing antioxidant activity and reducing renal inflammation (Zhou et al., 2020; Li et al., 2021). Rg3 inhibited the proliferation and metastasis of various cancer cells, such as liver cancer cells, intestinal cancer cells, osteosarcoma cells, etc. (Sun et al., 2017). Either Rg3 alone or Rg3 in combination with DDP suppressed the growth of colon tumor in nude mice (Lee et al., 2012b). Treatment with Rg3 decreased the tumor size of Ehrlich solid tumor in mice (El-Banna et al., 2022).

In summary, increasing evidence has shown that Rg3 has therapeutic potential for the treatment of acute organ injuries and chronic diseases, which is worthy of further research.

6 Discussion

The antioxidant and anti-inflammatory effects of Rg3 have been attributed to 1) antioxidant properties, including inhibition of ROS accumulation, promotion of peroxidase activity, and reduction of MDA content; 2) anti-inflammatory properties, inhibition of TNF-α, interleukins, chemokine ligands, suppression of NLRP3 formation and COX-2 expression; 3) regulation of apoptosis: downregulating the expression of p53, caspases and Bax/Bcl-2 ratio to protect tissue injury and apoptosis; and 4) regulation of NOS, inhibition of iNOS to reduce oxidative stress and upregulation of eNOS to protect vascular endothelial function. These antioxidant and anti-inflammatory activities of Rg3 help to maintain or improve organ functions, such as reducing neuroinflammation, attenuating neurotoxicity, protecting myocardial, hepatic and renal functions (Figure 2).

These effects are related to several potential mechanisms of action: (Lee et al., 2020a): inhibition of the NF-κB pathway decreases downstream COX-2 to ameliorate inflammation and oxidative stress; (Hyun et al., 2022); the PI3K/Akt pathway regulates the process of inflammation and apoptosis; and (Lee et al., 2017a) upregulation of the Nrf2/HO-1 pathway is an important pathway to reduce oxidative stress. Therefore, the key mechanism of action of Rg3 is shown in Figure 3. However, the content of these studies tends to be homogeneous, and there is a lack of Rg3 target screening based on high-throughput methods. In the future, we look forward to clinical research to explore the antioxidant activity of Rg3 and in-depth research into

the critical targets of Rg3 antioxidant and anti-inflammatory activity.

7 Conclusion

Increasing evidence supports that ginsenoside Rg3 has remarkable anti-inflammatory and antioxidant effects on animal and cell models with various diseases, such as pulmonary, neurological, cardiovascular, metabolic diseases, cancer, and liver and kidney injury, and the multitarget and multipathway molecular mechanisms of action of Rg3 have been gradually deciphered. Rg3 may be a promising candidate drug for the treatment of diseases with inflammatory and oxidative stress conditions and is worthy of further research and development.

Author contributions

JW, QW, and TW designed the work. JW, YZ, WQ, ZW, and LT collected and reviewed the references. JW wrote the first draft. JW, LZ, DZ, XL and TW wrote and reviewed the final version of the manuscript. All authors discussed and contributed to the manuscript.

Funding

This study was supported by the National Natural Science Foundation of China (U19A2013), the Education Department of Jilin Province (JJKH20210964KJ), the Science and Technology Development Plan Project of Jilin Province (202002053JC), the Science and Technology Development Fund, Macau SAR (file No.: 0098/2021/A2, 130/2017/A3, and 0099/2018/A3), and the Science and Technology Planning Project of Guangdong Province (2020B1212030008).

Acknowledgments

Figure 1 of the article was drawn by Figdraw (www.figdraw.com).

Conflict of interest

The authors declare that the research was conducted in the absence of any commercial or financial relationships that could be construed as a potential conflict of interest.

Publisher's note

References

Ahn, J. W., Jang, S. K., Jo, B. R., Kim, H. S., Park, J. Y., Park, H. Y., et al. (2021). A therapeutic intervention for alzheimer's disease using ginsenoside Rg3: Its role in M2 microglial activation and non-amyloidogenesis. *J. Physiol. Pharmacol.* 72 (2). Epub 2021/08/11PubMed PMID: 34374655. doi:10.26402/jpp.2021.2.04

Archuleta, T. L., Lemieux, A. M., Saengsirisuwan, V., Teachey, M. K., Lindborg, K. A., Kim, J. S., et al. (2009). Oxidant stress-induced loss of IRS-1 and IRS-2 proteins in rat skeletal muscle: Role of p38 MAPK. *Free Radic. Biol. Med.* 47 (10), 1486–1493. Epub 2009/08/26PubMed PMID: 19703555; PubMed Central PMCID: PMCPMC2767452. doi:10.1016/j.freeradbiomed.2009.08.014

Ayala, A., Muñoz, M. F., and Argüelles, S. (2014). Lipid peroxidation: Production, metabolism, and signaling mechanisms of malondialdehyde and 4-hydroxy-2-nonenal. *Oxidative Med. Cell. Longev.* 2014, 360438. Epub 2014/07/08PubMed PMID: 24999379; PubMed Central PMCID: PMCPMC4066722. doi:10.1155/2014/360438

Bahadoran, Z., Mirmiran, P., and Ghasemi, A. (2020). Role of nitric oxide in insulin secretion and glucose metabolism. *Trends Endocrinol. Metab.* 31 (2), 118–130. Epub 2019/11/07PubMed PMID: 31690508. doi:10.1016/j.tem.2019.10.001

Bairamian, D., Sha, S., Rolhion, N., Sokol, H., Dorothée, G., Lemere, C. A., et al. (2022). Microbiota in neuroinflammation and synaptic dysfunction: A focus on alzheimer's disease. *Mol. Neurodegener.* 17 (1), 19. Epub 2022/03/07PubMed PMID: 35248147; PubMed Central PMCID: PMCPMC8898063. doi:10.1186/s13024-022-00522-2

Balligand, J. L., Feron, O., and Dessy, C. (2009). eNOS activation by physical forces: from short-term regulation of contraction to chronic remodeling of cardiovascular tissues. *Physiol. Rev.* 89 (2), 481–534. Epub 2009/04/04PubMed PMID: 19342613. doi:10.1152/physrev.00042.2007

Bhatti, J. S., Sehrawat, A., Mishra, J., Sidhu, I. S., Navik, U., Khullar, N., et al. (2022). Oxidative stress in the pathophysiology of type 2 diabetes and related complications: Current therapeutics strategies and future perspectives. *Free Radic. Biol. Med.* 184, 114–134. Epub 2022/04/11PubMed PMID: 35398495. doi:10.1016/j.freeradbiomed.2022.03.019

Blankenberg, S., Barbaux, S., and Tiret, L. (2003). Adhesion molecules and atherosclerosis. *Atherosclerosis* 170 (2), 191–203. Epub 2003/11/13PubMed PMID: 14612198. doi:10.1016/s0021-9150(03)00097-2

Brown, G. C. (2007). Mechanisms of inflammatory neurodegeneration: iNOS and NADPH oxidase. *Biochem. Soc. Trans.* 35 (5), 1119–1121. Epub 2007/10/25PubMed PMID: 17956292. doi:10.1042/bst0351119

Candelario-Jalil, E., Dijkhuizen, R. M., and Magnus, T. (2022). Neuroinflammation, stroke, blood-brain barrier dysfunction, and imaging modalities. *Stroke* 53 (5), 1473–1486. Epub 2022/04/08PubMed PMID: 35387495; PubMed Central PMCID: PMCPMC9038693. doi:10.1161/strokeaha.122.036946

Cao, L., Wang, S., Zhang, L., and Li, J. (2022). mPEG-b-P(Glu-co-Phe) nanoparticles increase gastric retention time and gastric ulcer treatment efficacy of 20(S)-ginsenoside Rg3. *Biomed. Pharmacother. = Biomedecine Pharmacother.* 146, 112608. Epub 2022/01/23PubMed PMID: 35062071. doi:10.1016/j.biopha.2021.112608

Chalorak, P., Sanguanphun, T., Limboonreung, T., and Meemon, K. (2021). Neurorescue effects of frondoside A and ginsenoside Rg3 in *C. elegans* model of Parkinson's disease. *Mol. (Basel, Switz.* 26 (16), 4843. Epub 2021/08/28PubMed PMID: 34443430; PubMed Central PMCID: PMCPMC8402114. doi:10.3390/molecules26164843

Chang, K. H., Jee, H. S., Lee, N. K., Park, S. H., Lee, N. W., Paik, H. D., et al. (2009). Optimization of the enzymatic production of 20(S)-ginsenoside Rg(3) from white ginseng extract using response surface methodology. *N. Biotechnol.* 26 (3-4), 181–186. Epub 2009/09/09PubMed PMID: 19735748. doi:10.1016/j.nbt.2009.08.011

Chen, J., Liu, G. Z., Sun, Q., Zhang, F., Liu, C. Y., Yuan, L., et al. (2019). Protective effects of ginsenoside Rg3 on TNF-α-induced human nucleus pulposus cells through inhibiting NF-κB signaling pathway. *Life Sci.* 216, 1–9. Epub 2018/11/15PubMed PMID: 30428306. doi:10.1016/j.lfs.2018.11.022

Chen, W., Balan, P., and Popovich, D. G. (2020). Changes of ginsenoside composition in the creation of black ginseng leaf. *Mol. (Basel, Switz.* 25 (12), E2809. Epub 2020/06/24PubMed PMID: 32570758; PubMed Central PMCID: PMCPMC7355439. doi:10.3390/molecules25122809

Cheng, L., Sun, X., Hu, C., Jin, R., Sun, B., Shi, Y., et al. (2014). *In vivo* early intervention and the therapeutic effects of 20(s)-ginsenoside rg3 on hypertrophic scar formation. *PloS one* 9 (12), e113640. Epub 2014/12/17PubMed PMID: 25502572; PubMed Central PMCID: PMCPMC4264739. doi:10.1371/journal.pone.0113640

Cheng, L., Sun, X., Hu, C., Jin, R., Sun, B., Shi, Y., et al. (2013). *In vivo* inhibition of hypertrophic scars by implantable ginsenoside-Rg3-loaded electrospun fibrous membranes. *Acta Biomater.* 9 (12), 9461–9473. Epub 2013/08/14PubMed PMID: 23938200. doi:10.1016/j.actbio.2013.07.040

Cheng, Z., Zhang, M., Ling, C., Zhu, Y., Ren, H., Hong, C., et al. (2019). Neuroprotective effects of ginsenosides against cerebral ischemia. *Mol. (Basel, Switz.* 24 (6), E1102. Epub 2019/03/23PubMed PMID: 30897756; PubMed Central PMCID: PMCPMC6471240. doi:10.3390/molecules24061102

Cho, Y. S., Kim, C. H., Kim, H. N., Ha, T. S., and Ahn, H. Y. (2014). Ginsenoside Rg3 inhibits lipopolysaccharide-induced adhesion molecule expression in human umbilical vein endothelial cell and C57BL/6 mice. *Pharmazie* 69 (11), 818–822. Epub 2015/05/20. PubMed PMID: 25985577.

Dasagrandhi, D., Muthuswamy, A., and Swaminathan, J. K. (2022). Atherosclerosis: Nexus of vascular dynamics and cellular cross talks. *Mol. Cell. Biochem.* 477 (2), 571–584. Epub 2021/12/01PubMed PMID: 34845570. doi:10.1007/s11010-021-04307-x

Domej, W., Oettl, K., and Renner, W. (2014). Oxidative stress and free radicals in COPD--implications and relevance for treatment. *Int. J. Chron. Obstruct. Pulmon. Dis.* 9, 1207–1224. Epub 2014/11/08PubMed PMID: 25378921; PubMed Central PMCID: PMCPMC4207545. doi:10.2147/copd.S51226

Dunican, E. M., Elicker, B. M., Henry, T., Gierada, D. S., Schiebler, M. L., Anderson, W., et al. (2021). Mucus plugs and emphysema in the pathophysiology of airflow obstruction and hypoxemia in smokers. *Am. J. Respir. Crit. Care Med.* 203 (8), 957–968. Epub 2020/11/13PubMed PMID: 33180550; PubMed Central PMCID: PMCPMC8048745. doi:10.1164/rccm.202006-2248OC

El-Banna, M. A., Hendawy, O. M., El-Nekeety, A. A., and Abdel-Wahhab, M. A. (2022). Efficacy of ginsenoside Rg3 nanoparticles against Ehrlich solid tumor growth in mice. *Environ. Sci. Pollut. Res. Int.* 29, 43814–43825. Epub 2022/02/05PubMed PMID: 35118592. doi:10.1007/s11356-022-19019-y

Forman, H. J., Zhang, H., and Rinna, A. (2009). Glutathione: Overview of its protective roles, measurement, and biosynthesis. *Mol. Asp. Med.* 30 (1-2), 1–12. Epub 2008/09/18PubMed PMID: 18796312; PubMed Central PMCID: PMCPMC2696075. doi:10.1016/j.mam.2008.08.006

Furman, D., Campisi, J., Verdin, E., Carrera-Bastos, P., Targ, S., Franceschi, C., et al. (2019). Chronic inflammation in the etiology of disease across the life span. *Nat. Med.* 25 (12), 1822–1832. Epub 2019/12/07PubMed PMID: 31806905; PubMed Central PMCID: PMCPMC7147972. doi:10.1038/s41591-019-0675-0

Gao, Y., Yan, J., Li, J., Li, X., Yang, S., Chen, N., et al. (2021). Ginsenoside Rg3 ameliorates acetaminophen-induced hepatotoxicity by suppressing inflammation and oxidative stress. *J. Pharm. Pharmacol.* 73 (3), 322–331. Epub 2021/04/02PubMed PMID: 33793882. doi:10.1093/jpp/rgaa069

Geng, J., Fu, W., Yu, X., Lu, Z., Liu, Y., Sun, M., et al. (2020). Ginsenoside Rg3 alleviates ox-LDL induced endothelial dysfunction and prevents atherosclerosis in ApoE(-/-) mice by regulating PPARγ/FAK signaling pathway. *Front. Pharmacol.* 11, 500. Epub 2020/05/12PubMed PMID: 32390845; PubMed Central PMCID: PMCPMC7188907. doi:10.3389/fphar.2020.00500

Guan, X., Yuan, Y., Wang, G., Zheng, R., Zhang, J., Dong, B., et al. (2020). Ginsenoside Rg3 ameliorates acute exacerbation of COPD by suppressing neutrophil migration. *Int. Immunopharmacol.* 83, 106449. Epub 2020/04/12PubMed PMID: 32278128. doi:10.1016/j.intimp.2020.106449

Guo, M., Xiao, J., Sheng, X., Zhang, X., Tie, Y., Wang, L., et al. (2018). Ginsenoside Rg3 mitigates atherosclerosis progression in diabetic apoE-/- mice by skewing macrophages to the M2 phenotype. *Front. Pharmacol.* 9, 464. Epub 2018/06/06PubMed PMID: 29867472; PubMed Central PMCID: PMCPMC5954105. doi:10.3389/fphar.2018.00464

Han, Y., Wang, T., Li, C., Wang, Z., Zhao, Y., He, J., et al. (2021). Ginsenoside Rg3 exerts a neuroprotective effect in rotenone-induced Parkinson's disease mice via its anti-oxidative properties. *Eur. J. Pharmacol.* 909, 174413. Epub 2021/08/16PubMed PMID: 34391769. doi:10.1016/j.ejphar.2021.174413

Heathfield, S. K., Le Maitre, C. L., and Hoyland, J. A. (2008). Caveolin-1 expression and stress-induced premature senescence in human intervertebral disc degeneration. *Arthritis Res. Ther.* 10 (4), R87. Epub 2008/08/07PubMed PMID: 18681962; PubMed Central PMCID: PMCPMC2575636. doi:10.1186/ar2468

Heemskerk, S., Masereeuw, R., Russel, F. G., and Pickkers, P. (2009). Selective iNOS inhibition for the treatment of sepsis-induced acute kidney injury. *Nat. Rev. Nephrol.* 5 (11), 629–640. Epub 2009/09/30PubMed PMID: 19786992. doi:10.1038/nrneph.2009.155

Hien, T. T., Kim, N. D., Pokharel, Y. R., Oh, S. J., Lee, M. Y., Kang, K. W., et al. (2010). Ginsenoside Rg3 increases nitric oxide production via increases in phosphorylation and expression of endothelial nitric oxide synthase: Essential roles of estrogen receptor-dependent PI3-kinase and AMP-activated protein kinase. *Toxicol. Appl. Pharmacol.* 246 (3), 171–183. Epub 2010/06/16PubMed PMID: 20546771. doi:10.1016/j.taap.2010.05.008

Hong, T., Kim, M. Y., Da Ly, D., Park, S. J., Eom, Y. W., Park, K. S., et al. (2020). Ca(2+)-activated mitochondrial biogenesis and functions improve stem cell fate in Rg3-treated human mesenchymal stem cells. *Stem Cell Res. Ther.* 11 (1), 467. Epub 2020/11/06PubMed PMID: 33148318; PubMed Central PMCID: PMCPMC7640456. doi:10.1186/s13287-020-01974-3

Hou, J., Kim, S., Sung, C., and Choi, C. (2017). Ginsenoside Rg3 prevents oxidative stress-induced astrocytic senescence and ameliorates senescence paracrine effects on glioblastoma. *Mol. (Basel, Switz.* 22 (9), E1516. Epub 2017/09/12PubMed PMID: 28891967; PubMed Central PMCID: PMCPMC6151485. doi:10.3390/molecules22091516

Hou, J., Xue, J., Wang, Z., and Li, W. (2018). Ginsenoside Rg3 and Rh2 protect trimethyltin-induced neurotoxicity via prevention on neuronal apoptosis and neuroinflammation. *Phytother. Res.* 32 (12), 2531–2540. Epub 2018/10/03PubMed PMID: 30277284. doi:10.1002/ptr.6193

Huang, W. C., Huang, T. H., Yeh, K. W., Chen, Y. L., Shen, S. C., Liou, C. J., et al. (2021). Ginsenoside Rg3 ameliorates allergic airway inflammation and oxidative stress in mice. *J. Ginseng Res.* 45 (6), 654–664. Epub 2021/11/13PubMed PMID: 34764720; PubMed Central PMCID: PMCPMC8569325. doi:10.1016/j.jgr.2021.03.002

Hyun, S. H., Bhilare, K. D., Park, C. K., and Kim, J. H. (2022). Effects of Panax ginseng and ginsenosides on oxidative stress and cardiovascular diseases: Pharmacological and therapeutic roles. *J. Ginseng Res.* 46 (1), 33–38. Epub 2022/01/22PubMed PMID: 35058725; PubMed Central PMCID: PMCPMC8753520. doi:10.1016/j.jgr.2021.07.007

Incalza, M. A., D'Oria, R., Natalicchio, A., Perrini, S., Laviola, L., Giorgino, F., et al. (2018). Oxidative stress and reactive oxygen species in endothelial dysfunction associated with cardiovascular and metabolic diseases. *Vasc. Pharmacol.* 100, 1–19. Epub 2017/06/06PubMed PMID: 28579545. doi:10.1016/j.vph.2017.05.005

Jaeschke, H., Gores, G. J., Cederbaum, A. I., Hinson, J. A., Pessayre, D., Lemasters, J. J., et al. (2002). Mechanisms of hepatotoxicity. *Toxicol. Sci.* 65 (2), 166–176. Epub 2002/01/29PubMed PMID: 11812920. doi:10.1093/toxsci/65.2.166

Jeong, D., Irfan, M., Kim, S. D., Kim, S., Oh, J. H., Park, C. K., et al. (2017). Ginsenoside Rg3-enriched red ginseng extract inhibits platelet activation and *in vivo* thrombus formation. *J. Ginseng Res.* 41 (4), 548–555. Epub 2017/10/13PubMed PMID: 29021703; PubMed Central PMCID: PMCPMC5628340. doi:10.1016/j.jgr.2016.11.003

Joo, S. S., Yoo, Y. M., Ahn, B. W., Nam, S. Y., Kim, Y. B., Hwang, K. W., et al. (2008). Prevention of inflammation-mediated neurotoxicity by Rg3 and its role in microglial activation. *Biol. Pharm. Bull.* 31 (7), 1392–1396. Epub 2008/07/02PubMed PMID: 18591781. doi:10.1248/bpb.31.1392

Kang, K. S., Kim, H. Y., Yamabe, N., Park, J. H., and Yokozawa, T. (2007). Preventive effect of 20(S)-ginsenoside Rg3 against lipopolysaccharide-induced hepatic and renal injury in rats. *Free Radic. Res.* 41 (10), 1181–1188. Epub 2007/09/22PubMed PMID: 17886040. doi:10.1080/10715760701581740

Kang, K. S., Yamabe, N., Kim, H. Y., Park, J. H., and Yokozawa, T. (2008). Therapeutic potential of 20(S)-ginsenoside Rg(3) against streptozotocin-induced diabetic renal damage in rats. *Eur. J. Pharmacol.* 591 (1-3), 266–272. Epub 2008/07/10PubMed PMID: 18611400. doi:10.1016/j.ejphar.2008.06.077

Kang, S., Park, S. J., Lee, A. Y., Huang, J., Chung, H. Y., Im, D. S., et al. (2018). Ginsenoside Rg(3) promotes inflammation resolution through M2 macrophage polarization. *J. Ginseng Res.* 42 (1), 68–74. Epub 2018/01/20PubMed PMID: 29348724; PubMed Central PMCID: PMCPMC5766702. doi:10.1016/j.jgr.2016.12.012

Kee, J. Y., and Hong, S. H. (2019). Ginsenoside Rg3 suppresses mast cell-mediated allergic inflammation via mitogen-activated protein kinase signaling pathway. *J. Ginseng Res.* 43 (2), 282–290. Epub 2019/04/13PubMed PMID: 30976166; PubMed Central PMCID: PMCPMC6437450. doi:10.1016/j.jgr.2018.02.008

Keum, Y. S., Han, S. S., Chun, K. S., Park, K. K., Park, J. H., Lee, S. K., et al. (2003). Inhibitory effects of the ginsenoside Rg3 on phorbol ester-induced cyclooxygenase-2 expression, NF-kappaB activation and tumor promotion. *Mutat. Res.* 523-524, 52375–52485. Epub 2003/03/12PubMed PMID: 12628505. doi:10.1016/s0027-5107(02)00323-8

Kim, D. K., Kweon, K. J., Kim, P., Kim, H. J., Kim, S. S., Sohn, N. W., et al. (2017). Ginsenoside Rg3 improves recovery from spinal cord injury in rats via suppression

of neuronal apoptosis, pro-inflammatory mediators, and microglial activation. *Mol. (Basel, Switz.* 22 (1), E122. Epub 2017/01/14PubMed PMID: 28085110; PubMed Central PMCID: PMCPMC6155773. doi:10.3390/molecules22010122

Kim, J. W., Jung, S. Y., Kwon, Y. H., Lee, S. H., Lee, J. H., Lee, B. Y., et al. (2012). Ginsenoside Rg3 inhibits endothelial progenitor cell differentiation through attenuation of VEGF-dependent Akt/eNOS signaling. *Phytother. Res.* 26 (9), 1286–1293. Epub 2012/01/19PubMed PMID: 22253055. doi:10.1002/ptr.3722

Kim, N. D., Kang, S. Y., Park, J. H., and Schini-Kerth, V. B. (1999). Ginsenoside Rg3 mediates endothelium-dependent relaxation in response to ginsenosides in rat aorta: Role of K+ channels. *Eur. J. Pharmacol.* 367 (1), 41–49. Epub 1999/03/19PubMed PMID: 10082263. doi:10.1016/s0014-2999(98)00898-x

Kim, N. D., Kim, E. M., Kang, K. W., Cho, M. K., Choi, S. Y., Kim, S. G., et al. (2003). Ginsenoside Rg3 inhibits phenylephrine-induced vascular contraction through induction of nitric oxide synthase. *Br. J. Pharmacol.* 140 (4), 661–670. Epub 2003/10/10PubMed PMID: 14534150; PubMed Central PMCID: PMCPMC1574077. doi:10.1038/sj.bjp.0705490

Kim, S. J., Kim, J. D., and Ko, S. K. (2013). Changes in ginsenoside composition of ginseng berry extracts after a microwave and vinegar process. *J. Ginseng Res.* 37 (3), 269–272. Epub 2013/11/08PubMed PMID: 24198651; PubMed Central PMCID: PMCPMC3818952. doi:10.5142/jgr.2013.37.269

Kim, S. S., Jang, H. J., Oh, M. Y., Eom, D. W., Kang, K. S., Kim, Y. J., et al. (2014). Ginsenoside Rg3 enhances islet cell function and attenuates apoptosis in mouse islets. *Transpl. Proc.* 46 (4), 1150–1155. Epub 2014/05/13PubMed PMID: 24815149. doi:10.1016/j.transproceed.2013.12.028

Kim, Y. C., Kim, S. R., Markelonis, G. J., and Oh, T. H. (1998). Ginsenosides Rb1 and Rg3 protect cultured rat cortical cells from glutamate-induced neurodegeneration. *J. Neurosci. Res.* 53 (4), 426–432. Epub 1998/08/26PubMed PMID: 9710262. doi:10.1002/(sici)1097-4547(19980815)53:4<426::Aid-jnr4>3.0.Co;2-8

Kobayashi, M., and Yamamoto, M. (2005). Molecular mechanisms activating the Nrf2-Keap1 pathway of antioxidant gene regulation. *Antioxid. Redox Signal.* 7 (3-4), 385–394. Epub 2005/02/12PubMed PMID: 15706085. doi:10.1089/ars.2005.7.385

Landmesser, U., Dikalov, S., Price, S. R., McCann, L., Fukai, T., Holland, S. M., et al. (2003). Oxidation of tetrahydrobiopterin leads to uncoupling of endothelial cell nitric oxide synthase in hypertension. *J. Clin. Invest.* 111 (8), 1201–1209. Epub 2003/04/17PubMed PMID: 12697739; PubMed Central PMCID: PMCPMC152929. doi:10.1172/jci14172

Lee, A., Yun, E., Chang, W., and Kim, J. (2020). Ginsenoside Rg3 protects against iE-DAP-induced endothelial-to-mesenchymal transition by regulating the miR-139-5p-NF-κB axis. *J. Ginseng Res.* 44 (2), 300–307. Epub 2020/03/10PubMed PMID: 32148412; PubMed Central PMCID: PMCPMC7031736. doi:10.1016/j.jgr.2019.01.003

Lee, B., Sur, B., Park, J., Kim, S. H., Kwon, S., Yeom, M., et al. (2013). Ginsenoside rg3 alleviates lipopolysaccharide-induced learning and memory impairments by anti-inflammatory activity in rats. *Biomol. Ther.* 21 (5), 381–390. Epub 2013/11/19PubMed PMID: 24244826; PubMed Central PMCID: PMCPMC3825202. doi:10.4062/biomolther.2013.053

Lee, C. K., Park, K. K., Chung, A. S., and Chung, W. Y. (2012). Ginsenoside Rg3 enhances the chemosensitivity of tumors to cisplatin by reducing the basal level of nuclear factor erythroid 2-related factor 2-mediated heme oxygenase-1/NAD(P)H quinone oxidoreductase-1 and prevents normal tissue damage by scavenging cisplatin-induced intracellular reactive oxygen species. *Food Chem. Toxicol.* 50 (7), 2565–2574. Epub 2012/01/24PubMed PMID: 22266358. doi:10.1016/j.fct.2012.01.005

Lee, H., Kong, G., Tran, Q., Kim, C., Park, J., Park, J., et al. (2020). Relationship between ginsenoside Rg3 and metabolic syndrome. *Front. Pharmacol.* 11, 130. Epub 2020/03/13PubMed PMID: 32161549; PubMed Central PMCID: PMCPMC7052819. doi:10.3389/fphar.2020.00130

Lee, I. S., Uh, I., Kim, K. S., Kim, K. H., Park, J., Kim, Y., et al. (2016). Anti-inflammatory effects of ginsenoside Rg3 via NF-κB pathway in A549 cells and human asthmatic lung tissue. *J. Immunol. Res.* 2016, 7521601. Epub 2017/01/25PubMed PMID: 28116321; PubMed Central PMCID: PMCPMC5223042 of this paper. doi:10.1155/2016/7521601

Lee, J. H., Oh, J. Y., Kim, S. H., Oh, I. J., Lee, Y. H., Lee, K. W., et al. (2020). Pharmaceutical efficacy of gypenoside LXXV on non-alcoholic steatohepatitis (NASH). *Biomolecules* 10 (10), E1426. Epub 2020/10/15PubMed PMID: 33050067; PubMed Central PMCID: PMCPMC7599508. doi:10.3390/biom10101426

Lee, J. J., Kwon, H. K., Jung, I. H., Cho, Y. B., Kim, K. J., Kim, J. L., et al. (2009). Anti-cancer activities of ginseng extract fermented with phellinus linteus. *Mycobiology* 37 (1), 21–27. Epub 2009/03/01PubMed PMID: 23983502; PubMed Central PMCID: PMCPMC3749450. doi:10.4489/myco.2009.37.1.021

Lee, J. W., Choi, Y. R., Mok, H. J., Seong, H. A., Lee, D. Y., Kim, G. S., et al. (2017). Characterization of the changes in eicosanoid profiles of activated macrophages treated with 20(S)-ginsenoside Rg3. *J. Chromatogr. B Anal. Technol. Biomed. Life Sci.* 1065-1066, 106514–110669. Epub 2017/09/25PubMed PMID: 28938131. doi:10.1016/j.jchromb.2017.09.002

Lee, S. A., Jo, H. K., Im, B. O., Kim, S., Whang, W. K., Ko, S. K., et al. (2012). Changes in the contents of prosapogenin in the red ginseng (Panax ginseng) depending on steaming batches. *J. Ginseng Res.* 36 (1), 102–106. Epub 2012/01/01PubMed PMID: 23717110; PubMed Central PMCID: PMCPMC3659570. doi:10.5142/jgr.2012.36.1.102

Lee, S. J., Bae, J. H., Lee, H., Lee, H., Park, J., Kang, J. S., et al. (2019). Ginsenoside Rg3 upregulates myotube formation and mitochondrial function, thereby protecting myotube atrophy induced by tumor necrosis factor-alpha. *J. Ethnopharmacol.* 242, 112054. Epub 2019/07/05PubMed PMID: 31271820. doi:10.1016/j.jep.2019.112054

Lee, Y. M., Yoon, H., Park, H. M., Song, B. C., and Yeum, K. J. (2017). Implications of red Panax ginseng in oxidative stress associated chronic diseases. *J. Ginseng Res.* 41 (2), 113–119. Epub 2017/04/18PubMed PMID: 28413314; PubMed Central PMCID: PMCPMC5386131. doi:10.1016/j.jgr.2016.03.003

Li, L., Wang, Y., Guo, R., Li, S., Ni, J., Gao, S., et al. (2020). Ginsenoside Rg3-loaded, reactive oxygen species-responsive polymeric nanoparticles for alleviating myocardial ischemia-reperfusion injury. *J. Control. Release* 317, 259–272. Epub 2019/11/30PubMed PMID: 31783047; PubMed Central PMCID: PMCPMC7384207. doi:10.1016/j.jconrel.2019.11.032

Li, P., Gan, Y., Xu, Y., Wang, L., Ouyang, B., Zhang, C., et al. (2017). 17beta-estradiol attenuates TNF-α-Induced premature senescence of nucleus pulposus cells through regulating the ROS/NF-κB pathway. *Int. J. Biol. Sci.* 13 (2), 145–156. Epub 2017/03/04PubMed PMID: 28255267; PubMed Central PMCID: PMCPMC5332869. doi:10.7150/ijbs.16770

Li, W., Wang, J. Q., Zhou, Y. D., Hou, J. G., Liu, Y., Wang, Y. P., et al. (2020). Rare ginsenoside 20(R)-Rg3 inhibits D-galactose-induced liver and kidney injury by regulating oxidative stress-induced apoptosis. *Am. J. Chin. Med.* 48 (5), 1141–1157. Epub 2020/07/17PubMed PMID: 32668974. doi:10.1142/s0192415x20500561

Li, Y., Hou, J. G., Liu, Z., Gong, X. J., Hu, J. N., Wang, Y. P., et al. (2021). Alleviative effects of 20(R)-Rg3 on HFD/STZ-induced diabetic nephropathy via MAPK/NF-κB signaling pathways in C57BL/6 mice. *J. Ethnopharmacol.* 267, 113500. Epub 2020/10/23PubMed PMID: 33091499. doi:10.1016/j.jep.2020.113500

Liang, C., Zhang, X., Yang, M., and Dong, X. (2019). Recent progress in ferroptosis inducers for cancer therapy. *Adv. Mat.* 31 (51), e1904197. Epub 2019/10/09PubMed PMID: 31595562. doi:10.1002/adma.201904197

Lim, C. J., Choi, W. Y., and Jung, H. J. (2014). Stereoselective skin anti-photoaging properties of ginsenoside Rg3 in UV-B-irradiated keratinocytes. *Biol. Pharm. Bull.* 37 (10), 1583–1590. Epub 2014/07/25PubMed PMID: 25056231. doi:10.1248/bpb.b14-00167

Liu, T., Peng, Y. F., Jia, C., Yang, B. H., Tao, X., Li, J., et al. (2015). Ginsenoside Rg3 improves erectile function in streptozotocin-induced diabetic rats. *J. Sex. Med.* 12 (3), 611–620. Epub 2014/12/03PubMed PMID: 25442300. doi:10.1111/jsm.12779

Liu, X., Mi, X., Wang, Z., Zhang, M., Hou, J., Jiang, S., et al. (2020). Ginsenoside Rg3 promotes regression from hepatic fibrosis through reducing inflammation-mediated autophagy signaling pathway. *Cell Death Dis.* 11 (6), 454. Epub 2020/06/14PubMed PMID: 32532964; PubMed Central PMCID: PMCPMC7293224. doi:10.1038/s41419-020-2597-7

Lu, S. L., Wang, Y. H., Liu, G. F., Wang, L., Li, Y., Guo, Z. Y., et al. (2021). Graphene oxide nanoparticle-loaded ginsenoside Rg3 improves photodynamic therapy in inhibiting malignant progression and stemness of osteosarcoma. *Front. Mol. Biosci.* 8, 663089. Epub 2021/05/11PubMed PMID: 33968991; PubMed Central PMCID: PMCPMC8100436. doi:10.3389/fmolb.2021.663089

Lukiw, W. J., and Bazan, N. G. (2000). Neuroinflammatory signaling upregulation in Alzheimer's disease. *Neurochem. Res.* 25 (9-10), 1173–1184. Epub 2000/11/04PubMed PMID: 11059791. doi:10.1023/a:1007627725251

Ma, C. H., Chou, W. C., Wu, C. H., Jou, I. M., Tu, Y. K., Hsieh, P. L., et al. (2021). Ginsenoside Rg3 attenuates TNF-α-induced damage in chondrocytes through regulating SIRT1-mediated anti-apoptotic and anti-inflammatory mechanisms. *Antioxidants (Basel, Switz.* 10 (12), 1972. Epub 2021/12/25PubMed PMID: 34943075; PubMed Central PMCID: PMCPMC8750552. doi:10.3390/antiox10121972

Ma, L., Li, L. Y., and Zhao, T. L. (2020). Anti-inflammatory effects of ginsenoside Rg3 on the hypertrophic scar formation via the NF-κB/IκB signaling pathway in rabbit ears. *Pharmazie* 75 (2), 102–106. Epub 2020/03/28PubMed PMID: 32213242. doi:10.1691/ph.2020.9852

Malekmohammad, K., Sewell, R. D. E., and Rafieian-Kopaei, M. (2019). Antioxidants and atherosclerosis: Mechanistic aspects. *Biomolecules* 9 (8), E301. Epub 2019/07/28PubMed PMID: 31349600; PubMed Central PMCID: PMCPMC6722928. doi:10.3390/biom9080301

Moon, H., White, A. C., and Borowsky, A. D. (2020). New insights into the functions of Cox-2 in skin and esophageal malignancies. *Exp. Mol. Med.* 52 (4), 538–547. Epub 2020/04/03PubMed PMID: 32235869; PubMed Central PMCID: PMCPMC7210257. doi:10.1038/s12276-020-0412-2

Nagar, H., Choi, S., Jung, S. B., Jeon, B. H., and Kim, C. S. (2016). Rg3-enriched Korean Red Ginseng enhances blood pressure stability in spontaneously hypertensive rats. *Integr. Med. Res.* 5 (3), 223–229. Epub 2017/05/04PubMed

PMID: 28462122; PubMed Central PMCID: PMCPMC5390432. doi:10.1016/j.imr.2016.05.006

Papaconstantinou, J. (2019). The role of signaling pathways of inflammation and oxidative stress in development of senescence and aging phenotypes in cardiovascular disease. *Cells* 8 (11), E1383. Epub 2019/11/07PubMed PMID: 31689891; PubMed Central PMCID: PMCPMC6912541. doi:10.3390/cells8111383

Park, D., Bae, D. K., Jeon, J. H., Lee, J., Oh, N., Yang, G., et al. (2011). Immunopotentiation and antitumor effects of a ginsenoside Rg3-fortified red ginseng preparation in mice bearing H460 lung cancer cells. *Environ. Toxicol. Pharmacol.* 31 (3), 397–405. Epub 2011/07/27PubMed PMID: 21787710. doi:10.1016/j.etap.2011.01.008

Park, J. Y., Choi, P., Kim, T., Ko, H., Kim, H. K., Kang, K. S., et al. (2015). Protective effects of processed ginseng and its active ginsenosides on cisplatin-induced nephrotoxicity: *In vitro* and *in vivo* studies. *J. Agric. Food Chem.* 63 (25), 5964–5969. Epub 2015/06/09PubMed PMID: 26050847. doi:10.1021/acs.jafc.5b00782

Park, S. M., Choi, M. S., Sohn, N. W., and Shin, J. W. (2012). Ginsenoside Rg3 attenuates microglia activation following systemic lipopolysaccharide treatment in mice. *Biol. Pharm. Bull.* 35 (9), 1546–1552. Epub 2012/09/15PubMed PMID: 22975507. doi:10.1248/bpb.b12-00393

Prasad, S., Gupta, S. C., and Tyagi, A. K. (2017). Reactive oxygen species (ROS) and cancer: Role of antioxidative nutraceuticals. *Cancer Lett.* 387, 95–105. Epub 2016/04/03PubMed PMID: 27037062. doi:10.1016/j.canlet.2016.03.042

Racanelli, A. C., Kikkers, S. A., Choi, A. M. K., and Cloonan, S. M. (2018). Autophagy and inflammation in chronic respiratory disease. *Autophagy* 14 (2), 221–232. Epub 2017/11/14PubMed PMID: 29130366; PubMed Central PMCID: PMCPMC5902194. doi:10.1080/15548627.2017.1389823

Ramos-Tovar, E., and Muriel, P. (2020). Molecular mechanisms that link oxidative stress, inflammation, and fibrosis in the liver. *Antioxidants (Basel, Switz.* 9 (12), E1279. Epub 2020/12/19PubMed PMID: 33333846; PubMed Central PMCID: PMCPMC7765317. doi:10.3390/antiox9121279

Ren, B., Feng, J., Yang, N., Guo, Y., Chen, C., Qin, Q., et al. (2021). Ginsenoside Rg3 attenuates angiotensin II-induced myocardial hypertrophy through repressing NLRP3 inflammasome and oxidative stress via modulating SIRT1/NF-κB pathway. *Int. Immunopharmacol.* 98, 107841. Epub 2021/06/22PubMed PMID: 34153662. doi:10.1016/j.intimp.2021.107841

Robb, C. T., Regan, K. H., Dorward, D. A., and Rossi, A. G. (2016). Key mechanisms governing resolution of lung inflammation. *Semin. Immunopathol.* 38 (4), 425–448. Epub 2016/04/28PubMed PMID: 27116944; PubMed Central PMCID: PMCPMC4896979. doi:10.1007/s00281-016-0560-6

Shi, Y., Wang, H., Zheng, M., Xu, W., Yang, Y., Shi, F., et al. (2020). Ginsenoside Rg3 suppresses the NLRP3 inflammasome activation through inhibition of its assembly. *FASEB J. official Publ. Fed. Am. Soc. Exp. Biol.* 34 (1), 208–221. Epub 2020/01/10PubMed PMID: 31914640. doi:10.1096/fj.201901537R

Shin, S. H., Ye, M. K., Lee, D. W., Kang, B. J., and Chae, M. H. (2021). Effect of Korean red ginseng and Rg3 on asian sand dust-induced MUC5AC, MUC5B, and MUC8 expression in bronchial epithelial cells. *Mol. (Basel, Switz.* 26 (7), 2002. Epub 2021/05/01PubMed PMID: 33916022; PubMed Central PMCID: PMCPMC8037637. doi:10.3390/molecules26072002

Shin, Y. M., Jung, H. J., Choi, W. Y., and Lim, C. J. (2013). Antioxidative, anti-inflammatory, and matrix metalloproteinase inhibitory activities of 20(S)-ginsenoside Rg3 in cultured mammalian cell lines. *Mol. Biol. Rep.* 40 (1), 269–279. Epub 2012/10/12PubMed PMID: 23054007. doi:10.1007/s11033-012-2058-1

Silva, D., Baião, D. D. S., Ferreira, V. F., and Paschoalin, V. M. F. (2022). Betanin as a multipath oxidative stress and inflammation modulator: A beetroot pigment with protective effects on cardiovascular disease pathogenesis. *Crit. Rev. Food Sci. Nutr.* 62 (2), 539–554. Epub 2020/10/01PubMed PMID: 32997545. doi:10.1080/10408398.2020.1822277

Singh, H., Du, J., Singh, P., Mavlonov, G. T., and Yi, T. H. (2018). Development of superparamagnetic iron oxide nanoparticles via direct conjugation with ginsenosides and its *in-vitro* study. *J. Photochem. Photobiol. B* 185, 100–110. Epub 2018/06/10PubMed PMID: 29885646. doi:10.1016/j.jphotobiol.2018.05.030

Song, M., Jia, F., Cao, Z., Zhang, H., Liu, M., Gao, L., et al. (2020). Ginsenoside Rg3 attenuates aluminum-induced osteoporosis through regulation of oxidative stress and bone metabolism in rats. *Biol. Trace Elem. Res.* 198 (2), 557–566. Epub 2020/03/17PubMed PMID: 32173789. doi:10.1007/s12011-020-02089-9

Sun, M., Ye, Y., Xiao, L., Duan, X., Zhang, Y., Zhang, H., et al. (2017). Anticancer effects of ginsenoside Rg3 (review). *Int. J. Mol. Med.* 39 (3), 507–518. Epub 2017/01/19PubMed PMID: 28098857. doi:10.3892/ijmm.2017.2857

Tangrodchanapong, T., Sobhon, P., and Meemon, K. (2020). Frondoside A attenuates amyloid-β proteotoxicity in transgenic *Caenorhabditis elegans* by suppressing its formation. *Front. Pharmacol.* 11, 553579. Epub 2020/10/06PubMed PMID: 33013392; PubMed Central PMCID: PMCPMC7513805. doi:10.3389/fphar.2020.553579

Tian, J., Zhang, S., Li, G., Liu, Z., and Xu, B. (2009). 20(S)-ginsenoside Rg3, a neuroprotective agent, inhibits mitochondrial permeability transition pores in rat brain. *Phytother. Res.* 23 (4), 486–491. Epub 2008/11/13PubMed PMID: 19003949. doi:10.1002/ptr.2653

Tu, C., Wan, B., and Zeng, Y. (2020). Ginsenoside Rg3 alleviates inflammation in a rat model of myocardial infarction via the SIRT1/NF-κB pathway. *Exp. Ther. Med.* 20 (6), 238. Epub 2020/11/17PubMed PMID: 33193843; PubMed Central PMCID: PMCPMC7646702. doi:10.3892/etm.2020.9368

Wang, J., Yu, X. F., Zhao, J. J., Shi, S. M., Fu, L., Sui, D. Y., et al. (2016). Ginsenoside Rg3 attenuated omethoate-induced lung injury in rats. *Hum. Exp. Toxicol.* 35 (6), 677–684. Epub 2015/08/05PubMed PMID: 26240163. doi:10.1177/0960327115597984

Wang, X., Chen, L., Wang, T., Jiang, X., Zhang, H., Li, P., et al. (2015). Ginsenoside Rg3 antagonizes adriamycin-induced cardiotoxicity by improving endothelial dysfunction from oxidative stress via upregulating the Nrf2-ARE pathway through the activation of akt. *Phytomedicine* 22 (10), 875–884. Epub 2015/09/01PubMed PMID: 26321736. doi:10.1016/j.phymed.2015.06.010

Wang, Y., Hu, Z., Sun, B., Xu, J., Jiang, J., Luo, M., et al. (2015). Ginsenoside Rg3 attenuates myocardial ischemia/reperfusion injury via Akt/endothelial nitric oxide synthase signaling and the Bcell lymphoma/Bcell lymphomaassociated X protein pathway. *Mol. Med. Rep.* 11 (6), 4518–4524. Epub 2015/02/13PubMed PMID: 25672441. doi:10.3892/mmr.2015.3336

Xing, W., Yang, L., Peng, Y., Wang, Q., Gao, M., Yang, M., et al. (2017). Ginsenoside Rg3 attenuates sepsis-induced injury and mitochondrial dysfunction in liver via AMPK-mediated autophagy flux. *Biosci. Rep.* 37 (4), BSR20170934. Epub 2017/08/06PubMed PMID: 28779013; PubMed Central PMCID: PMCPMC5577177. doi:10.1042/bsr20170934

Yang, J., Li, S., Wang, L., Du, F., Zhou, X., Song, Q., et al. (2018). Ginsenoside Rg3 attenuates lipopolysaccharide-induced acute lung injury via MerTK-dependent activation of the PI3K/AKT/mTOR pathway. *Front. Pharmacol.* 9, 850. Epub 2018/08/18PubMed PMID: 30116194; PubMed Central PMCID: PMCPMC6082957. doi:10.3389/fphar.2018.00850

Yoon, S. J., Park, J. Y., Choi, S., Lee, J. B., Jung, H., Kim, T. D., et al. (2015). Ginsenoside Rg3 regulates S-nitrosylation of the NLRP3 inflammasome via suppression of iNOS. *Biochem. Biophys. Res. Commun.* 463 (4), 1184–1189. Epub 2015/06/19PubMed PMID: 26086107. doi:10.1016/j.bbrc.2015.06.080

Zhang, J. J., Zhou, Y. D., Liu, Y. B., Wang, J. Q., Li, K. K., Gong, X. J., et al. (2021). Protective effect of 20(R)-Ginsenoside Rg3 against cisplatin-induced renal toxicity via PI3K/AKT and NF-[Formula: See text]B signaling pathways based on the premise of ensuring anticancer effect. *Am. J. Chin. Med.* 49 (7), 1739–1756. Epub 2021/09/01PubMed PMID: 34461812. doi:10.1142/s0192415x21500828

Zhang, K., Liu, Y., Wang, C., Li, J., Xiong, L., Wang, Z., et al. (2019). Evaluation of the gastroprotective effects of 20 (S)-ginsenoside Rg3 on gastric ulcer models in mice. *J. Ginseng Res.* 43 (4), 550–561. Epub 2019/11/07PubMed PMID: 31695563; PubMed Central PMCID: PMCPMC6823781. doi:10.1016/j.jgr.2018.04.001

Zhang, L. P., Jiang, Y. C., Yu, X. F., Xu, H. L., Li, M., Zhao, X. Z., et al. (2016). Ginsenoside Rg3 improves cardiac function after myocardial ischemia/reperfusion via attenuating apoptosis and inflammation. *Evidence-based complementary Altern. Med.* 2016, 6967853. Epub 2017/01/21PubMed PMID: 28105061; PubMed Central PMCID: PMCPMC5220470. doi:10.1155/2016/6967853

Zhang, Q. H., Wu, C. F., Duan, L., and Yang, J. Y. (2008). Protective effects of ginsenoside Rg(3) against cyclophosphamide-induced DNA damage and cell apoptosis in mice. *Arch. Toxicol.* 82 (2), 117–123. Epub 2007/06/29PubMed PMID: 17598087. doi:10.1007/s00204-007-0224-3

Zhao, M., Zhang, B., and Deng, L. (2022). The mechanism of acrylamide-induced neurotoxicity: Current status and future perspectives. *Front. Nutr.* 9, 859189. PubMed PMID: 35399689. doi:10.3389/fnut.2022.859189

Zhou, T., Sun, L., Yang, S., Lv, Y., Cao, Y., Gang, X., et al. (2020). 20(S)-Ginsenoside Rg3 protects kidney from diabetic kidney disease via renal inflammation depression in diabetic rats. *J. Diabetes Res.* 2020, 7152176. Epub 2020/04/08PubMed PMID: 32258169; PubMed Central PMCID: PMCPMC7106937 of this article. doi:10.1155/2020/7152176

Zhou, Y. D., Hou, J. G., Liu, W., Ren, S., Wang, Y. P., Zhang, R., et al. (2018). 20(R)-ginsenoside Rg3, a rare saponin from red ginseng, ameliorates acetaminophen-induced hepatotoxicity by suppressing PI3K/AKT pathway-mediated inflammation and apoptosis. *Int. Immunopharmacol.* 59, 21–30. Epub 2018/04/06PubMed PMID: 29621733. doi:10.1016/j.intimp.2018.03.030

frontiers | Frontiers in Pharmacology

TYPE Original Research
PUBLISHED 29 September 2022
DOI 10.3389/fphar.2022.1004766

OPEN ACCESS

EDITED BY
Dongdong Sun,
Nanjing University of Chinese Medicine, China

REVIEWED BY
Shuai Wang,
University of Pittsburgh Medical Center, United States
Yaying Sun,
Fudan University, China

*CORRESPONDENCE
Jun Lu,
junlusuper@163.com

SPECIALTY SECTION
This article was submitted to Inflammation Pharmacology, a section of the journal Frontiers in Pharmacology

RECEIVED 27 July 2022
ACCEPTED 17 August 2022
PUBLISHED 29 September 2022

CITATION
Hu X, Li Z, Ji M, Lin Y, Chen Y and Lu J (2022), Identification of cellular heterogeneity and immunogenicity of chondrocytes via single-cell RNA sequencing technique in human osteoarthritis.
Front. Pharmacol. 13:1004766.
doi: 10.3389/fphar.2022.1004766

Identification of cellular heterogeneity and immunogenicity of chondrocytes *via* single-cell RNA sequencing technique in human osteoarthritis

Xinyue Hu[1], Zhuang Li[1], Mingliang Ji[2], Yucheng Lin[2], Yuzhi Chen[1] and Jun Lu[2]*

[1]School of Medicine, Southeast University, Nanjing, Jiangsu, China, [2]Department of Orthopaedic Surgery, Zhongda Hospital, School of Medicine, Southeast University, Nanjing, Jiangsu, China

Background: Osteoarthritis (OA) has placed a heavy burden to the economy and humanistics. To explore the biological functions and markers of chondrocytes contributes significantly to the accurate diagnosis and targeted treatment of OA.

Methods: We systematically analyzed the immunogenicity and biological function of varied chondrocytes at single cell resolution, and identified the chondrocyte subtypes and biomarkers involved in the development of OA, which are verified in the bulk sequencing cohort.

Results: Based on previous study, we defined eight subtypes of chondrocytes with different biological functions, finding out that effector chondrocytes (ECs) and fibrocartilage chondrocytes (FCs) may promote the development of OA. Compared with other chondrocytes, ECs and FCs show stronger immunogenicity. FCs mainly affects the degeneration of cartilage caused by fibrous degeneration, while ECs mainly exerts immune function and causes tissues inflammation. In addition, the canonical gene markers of EC and FC assist with the prediction of OA, which has been verified in Bulk RNA sequencing data from two GEO datasets.

Conclusion: In summary, this study provides a new perspective for the exploration of cellular heterogeneity and pathophysiology in OA and will make contribution to the accurate diagnosis and targeted treatment of OA.

KEYWORDS

single-cell RNA sequencing (scRNA-seq), osteoarthritis, heterogeneity, immunogenicity, bulk RNA sequencing

Introduction

Osteoarthritis (OA) is one of the most prevalent chronic joint diseases and a leading cause of progressive joint dysfunction (Edwards et al., 2015). On a global scale, OA has placed a heavy burden to the economy and humanistics and is expected to become the major cause of disability in patients aged over 40 years by 2040 (Thomas et al., 2014; Xie et al., 2016). The primary feature of OA is the impairment of articular cartilage homeostasis, which is followed by cartilage degradation and synovitis (Goldring and Otero, 2011; Jin et al., 2015; Wang and Chen, 2016). The articular cartilage is a physiologically non-self-renewing seavascular tissue composed of chondrocytes (Jiang and Tuan, 2015). Current evidence strongly supports that chondrocytes are involved in the pathology of OA owing to its specific phenotypes (Jiang and Tuan, 2015). However, there remains no chondrocytes-targeting prediction and treatment strategies for OA by now. In this context, it is essential to research the role of chondrocytes in immunoregulation and their pathophysiological changes during the progression of OA. Most of the existing studies were concentrating on the repair of cartilage tissues through stem cell transplantation (Johnson et al., 2012; Trounson and McDonald, 2015). Nevertheless, the results are limited due to the largely unknown information including the detailed subtypes of chondrocytes and their effects on OA, and the lack of biomarkers available to predict OA progression.

Chondrocytes are derived from the differentiation of condensed mesenchymal stem cells (MSCs) and then form articular cartilage, whose fibrocartilage matrix is composed of proteoglycan and collagen that are produced by chondrocytes (Chaly et al., 2015; Baboolal et al., 2016). In previous research, chondrocytes were subclassified by their developmental origin, site, morphology and molecular function according to experience. The first three subtypes are proliferative chondrocytes (ProCs), prehypertrophic chondrocytes (preHTCs) and hypertrophic chondrocytes (HTCs) (St-Jacques et al., 1999; Saito et al., 2010; Prein et al., 2016). ProCs are cells located to the proliferative zone; preHTCs can induce cell differentiation toward hypertrophy; and HTCs are capable of regulating the mineralization of cartilage matrix. Recently, two new subtypes of chondrocytes have been identified: senescent cells (SNCs) and cartilage progenitor cells (CPCs) (Koelling et al., 2009; Jiang and Tuan, 2015; Worthley et al., 2015; Childs et al., 2017; Jeon et al., 2017). SNCs feature senescence-associated secretory phenotype (SASP), which is beneficial for the development of OA (Jeon et al., 2017); CPCs express stem cell surface markers and can differentiate along multiple lineages, with the self-renewal capacity to maintain the repair of cartilage tissues (Koelling et al., 2009; Jiang and Tuan, 2015). While in most cases, such experience-based classification is not accurate, and there are limited markers which are available to recognize and differentiate these subtypes. As a consequence, it is difficult to carry out relevant studies. By the march of high-throughput sequencing technique, tissue heterogeneity has been studied at the molecular level and the sub-classification of chondrocytes in Human OA holds enormous promise for research.

The traditional Bulk RNA-sequencing technique determines the average expression of a gene in each cell at the tissue level, which fails to help study the cartilage tissue heterogeneity at the cellular level. The emergence of single-cell RNA sequencing (scRNA-seq) technique has compensated for the deficiency as it can provide transcriptome data of single cells. Ji et al. (2019) preliminarily made a profile showing the heterogeneity of chondrocytes in OA based on the scRNA-seq technique. Based on their research, we identified the sutypes of chondrocytes involved in OA progression and explored their immunogenicity via further bioinformatics analysis. In the meantime, we integrated the scRNA-seq data and the Bulk RNA-seq data from GEO to validate the performance of different cell subtypes and gene markers in diagnosis of OA. Findings of our study further reveal the biological properties of chondrocytes in OA and provide new ideas for the precision diagnosis and targeted therapy of OA.

Materials and methods

Data source

scRNA-seq matrix was obtained from the GSE104782 dataset uploaded by Ji et al. (2019) and the detailed information could be found in their study. Patient information was obtained from their Supplementary Material, including 1,600 chondrocytes samples from 10 OA patients. Severity score of each cell was calculated as described in their study (a lower severity score indicates a higher degree of disease severity).

Bulk RNA-seq data from two GEO datasets, GSE51588 (Chou et al., 2013) (GPL13497; OA, n = 40; Normal, n = 10) and GSE114007 (Fisch et al., 2018) (GPL18573; OA, n = 18; Normal, n = 18), were downloaded as validation data.

Quality control, clustering analysis and sub-classification

The scRNA-seq data were processed for quality control, clustering and identification of marker genes using the R package Seurat (Version 3.0.1) (Butler et al., 2018). The PercentageFeatureSet function was used to examine mitochondrial genes, and cells with mitochondrial gene >5% and gene number >5,000 or <500 were excluded. Normalization was fulfilled using the NormalizeData and ScaleData functions of Seurat. PCA was performed to identify the main cell clusters with the appropriate PC number using the FindClusters function, which were visualized by 2D UMAP. Eventually, 1,343 cells were included for further analysis.

The FindAllMarkers function was applied to identify marker genes of each cell cluster with the "biomed" (Likelihood-ratio test), following logFC >0.25 and expression >25%. Chondrocyte type was identified according to the markers described by Ji et al. (2019) GO analysis (Chen et al., 2009) was performed using the ToppGene, and the GO terms with $p < 0.05$ were displayed. DO analysis (Yu et al., 2012) was conducted using the package "Clusterprofiler" with the significance threshold set as $p < 0.05$. Single-cell trajectory analysis was performed using the package "monocle" in marker genes (Trapnell et al., 2014) and the results were visualized in a 2D diagram.

Copy number variation estimation

R package "inferCNV" was applied to estimate the copy number variation (CNV) of each cell type (Patel et al., 2014). We used all cell types as the reference background and set "denoised". Finally, we use a threshold of 0.1 to detect CNV. For more details, please refer to the original article (Patel et al., 2014).

Cell-cell communication analysis

Python package "CellphoneDB" (Vento-Tormo et al., 2018) was used to recognize the ligand-receptor interactions between cell clusters with a value of $p < 0.01$ set at significance. R package "Cellchat" was applied to infer the biological pathways involved in the cell-cell interactions (Jin et al., 2021).

Functional enrichment analysis

ssGSEA was used to estimate the immune pathway activity of chondrocytes, with the background gene set obtained from the previous literature (Liang et al., 2020).

GSVA and GSEA were performed using the KEGG gene set downloaded from the MSigDB database (http://www.gsea-msigdb.org/gsea/msigdb/). The differential gene sets between cell clusters were explored using the R package "GSVA" with the default parameters.

GSEA was performed to analyze the enrichment of the gene sets with a value of $p < 0.05$ for cut-off.

Bulk RNA-seq data validation

ssGSEA was performed to estimate the abundance of chondrocytes in the two independent datasets with Bulk RNA-seq data based on corresponding gene markers. PCA was conducted to evaluate the ability of cell clusters to differentiate OA tissues from normal tissues. ROC curve was generated to explore the diagnostic performance of the gene markers.

TF-mRNA-miRNA regulatory network establishment

Upstream TF and miRNA of gene markers were predicted through the Enrichr (https://maayanlab.cloud/Enrichr/) database ($p < 0.05$). mRNA-TF pairs were predicted via TRANSFAC and JASPAR algorithms (Kuleshov et al., 2016), and miRNA-mRNA pairs were predicted through the mirTarBase of Enrichr. Following intersection, a TF-mRNA-miRNA regulatory network was established and visualized by Cytoscape. Python package "scenic" was used to identify specific TF of each cell cluster to validate the network. We generated transcription factor activities using default parameters and identified possible TF by a threshold of 10.

Statistical analysis

Between-group comparison was performed using the Wilcoxon test. Correlation analysis was completed with the Spearman method and the result was displayed in a network. Without special statement, $p < 0.05$ was considered as statistically significant.

Results

scRNA-seq profile of chondrocytes in human osteoarthritis

scRNA-seq was performed in the GSE104782 dataset. Following quality control for the transcriptome data of the total 1,600 chondrocytes (500<=gene number<=5,000), 1,343 chondrocytes were obtained for further analysis (Supplementary Figure S1A). Uniform manifold approximation and projection (UMAP) was used to cluster the 1,343 chondrocytes into 8 clusters of known cell lineages, with 10 set as the appropriate number of principal components (PCs). According to the canonical gene markers, the 8 cell clusters were annotated as: cartilage progenitor cells (CPCs), effector chondrocytes (ECs), fibrocartilage chondrocytes (FCs), homeostatic chondrocytes (HomCs), hypertrophic chondrocytes (HTCs), prehypertrophic chondrocytes (preHTCs), proliferative chondrocytes (ProCs) and regulatory chondrocytes (RegCs) (Figures 1A,B, Supplementary Table S1). Further functional annotation for the gene markers revealed that ECs were actively secreted and associated with cell activation and lymphocyte activation (Supplementary Table S2); FCs were involved in angiogenesis and blood vessel development (Figure 1C) and highly expressed fibroblast markers COL1A1 and COL14A1 (Figure 1B). Additionally, canonical gene markers of the 8 clusters were processed for Disease Ontology (DO) analysis, and most of them were in relation to bone diseases and inflammation (Supplementary Figure S2; Supplementary

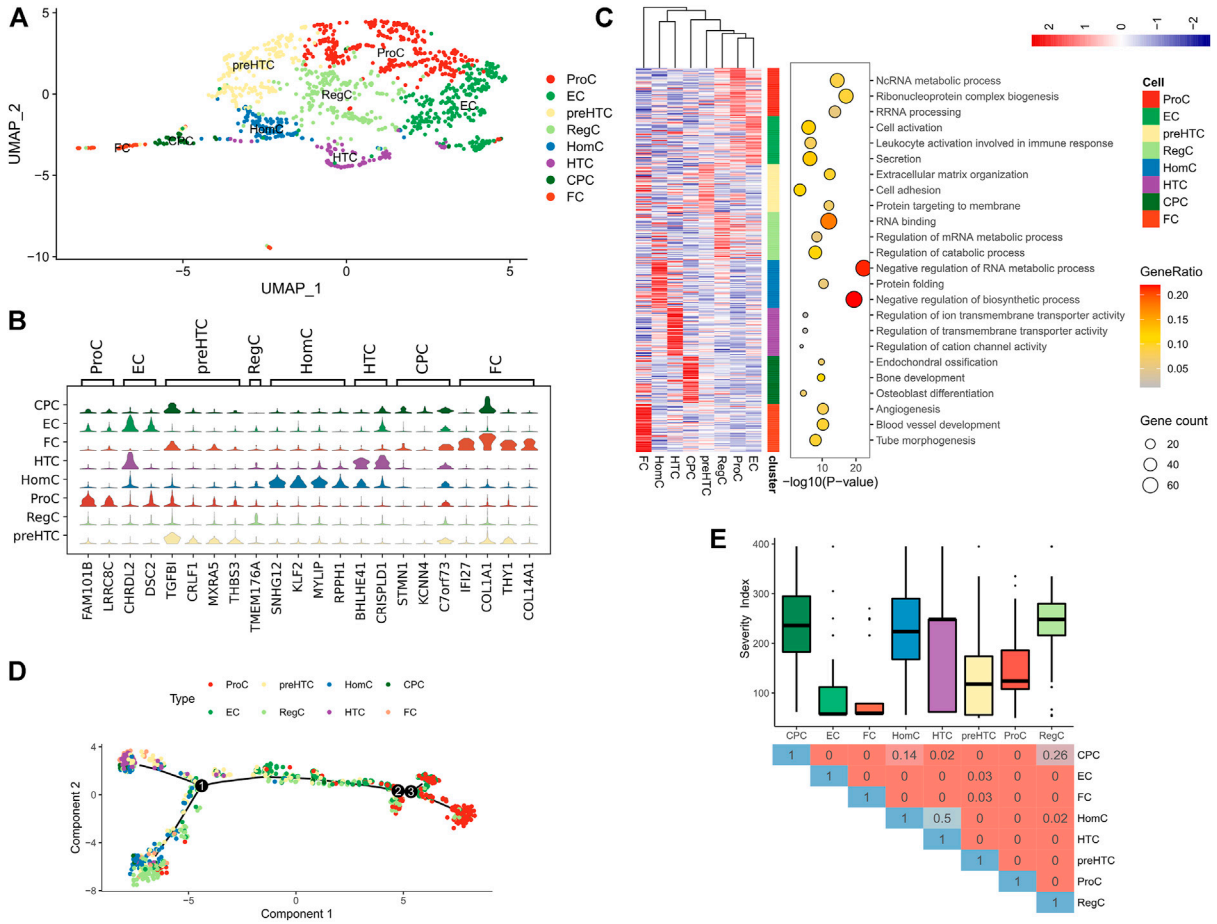

FIGURE 1
Sub-classification of chondrocytes in OA tissues. **(A)** UMAP plot of all chondrocytes, which are distinguished by color; **(B)** Violin plots showing the expression of canonical marker genes of each chondrocyte type; **(C)** The Heatmap (left) of the expression of the top 50 differential genes in each cell cluster (Z-score normalized) and the representative GO terms (right); **(D)** Differentiation trajectory of each cell cluster (distinguished by color) in OA tissue; **(E)** The Box plots showing the Severity score of the 8 cell clusters (upper) and the Heatmap showing the difference represented by p value in Wilcoxon test (below).

Table S3). Moreover, the pseudotime analysis as implemented by R package "monocle" revealed that FCs, HTCs and preHTCs were mainly located at the start point of the trajectory, while ProCs were majorly present at the end point. RegCs and ECs were distributed along the trajectory (Figure 1D). The results indicated that the 8 cell clusters were functionally different. FCs may participate in the initial fiber degeneration, while RegCs and ECs may play a regulatory role during the whole process of arthritis. Further analysis into the clinical significance of the 8 cell clusters was conducted with the Hospital for Special Surgery (HSS) scoring system and OA grading, the results of which demonstrated that ECs and FCs were associated with a higher disease severity than other cell clusters, suggesting their potential role in promoting progression of OA (Figure 1E). Therefore, we focused on ECs and FCs in subsequent analysis.

Copy number variation in each cell cluster

CNV was analyzed in individual cell clusters using the package "inferCNV" and was found much more prevalent in ECs than in FCs (Figure 2).

Effector chondrocytes and fibrocartilage chondrocytes exhibit strong immunogenicity

Single sample GSEA (GSEA) algorithm was adopted to assess immune activity in each cell clusters, and the enrichment of 13 immune-related pathways was displayed in a Heatmap (Figure 3A). It was found that ECs and FCs, especially ECs, had higher enrichment scores of the HLA and MHC

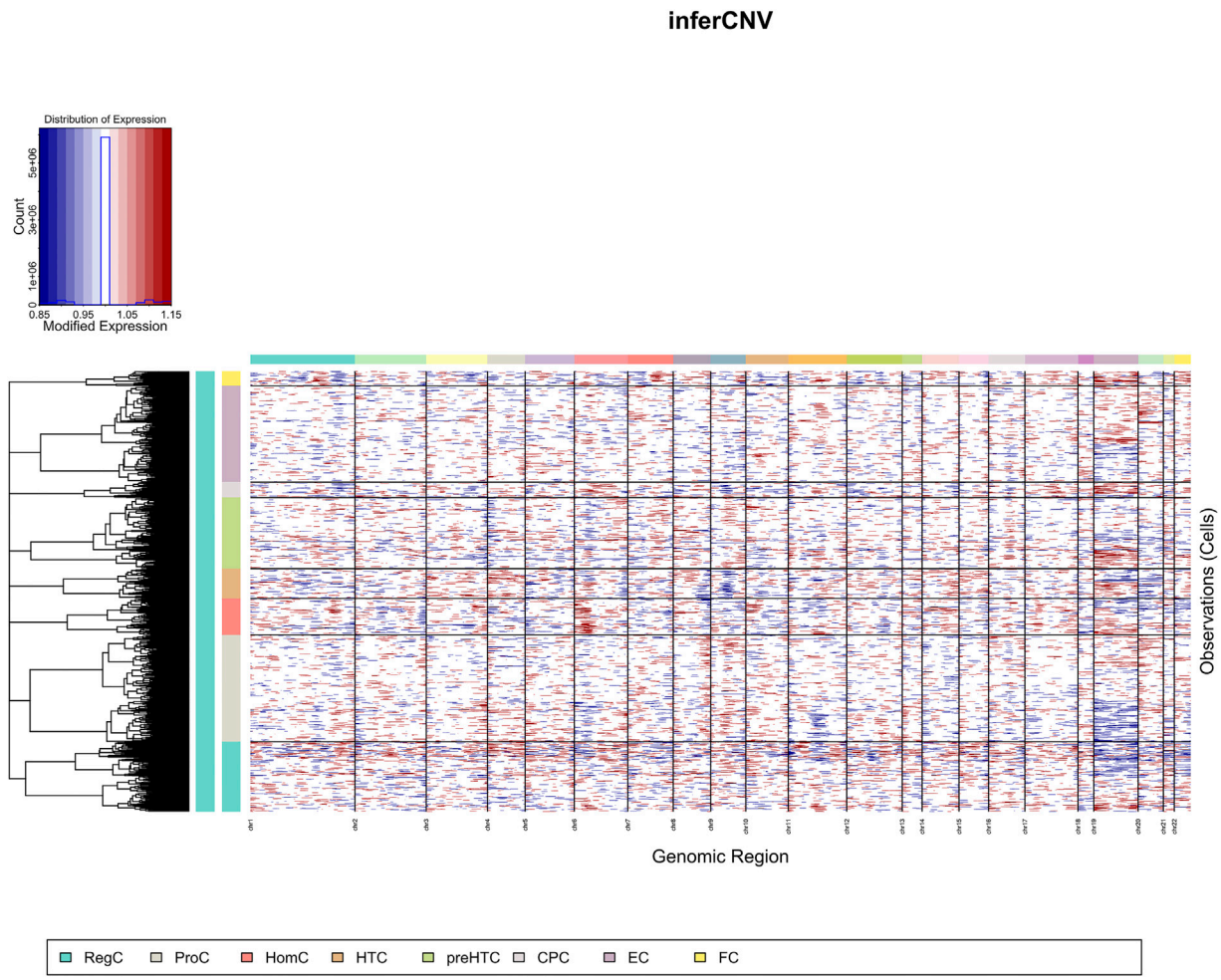

FIGURE 2
CNV landscape (the X-axis represents chromosome, and the Y-axis represents cell cluster).

class1 pathways than other cell clusters, demonstrating that ECs and FCs possessed stronger immunogenicity (Figures 3B,C). Moreover, the expression of MHC genes was examined. The result revealed that CD74, CD80, CD86, HLA-DPA1 and HLA-DRA exhibited high expression in a small number of ECs and FCs (Figure 3D). These findings indicated that ECs and FCs may have some functions as immune cells during the progression of OA.

Interactions of effector chondrocytes and fibrocartilage chondrocytes with other cell clusters

Ligand-receptor interactions among the 8 cell clusters were explored using the CellPhoneDB. Extensive cell-cell communications were demonstrated among the 8 cell clusters (Figure 4A) and the detailed ligand-receptor interactions were revealed in Supplementary Table S4. We noted that ProCs had the most extensive interactions with other cell groups, followed by ECs (Figure 4B). Further analysis found that ECs and FCs highly expressed HLA-C and communicated with other cell groups via receptor FAM3C (Figure 4C). The result implied that ECs and FCs exhibited much stronger immunogenicity than other cell groups and they were involved in the immunoregulation. Notably, ECs also highly expressed CD55 and chemokine CCL3 while less TNF, and corresponding receptors were widely present in each cell groups. Therefore, ECs may play a more vital role in the immunoregulation. In addition, FCs mainly expressed COL1A1, COL6A3, FGF1 and FGF2 and communicated with other cell types via corresponding receptors, suggesting their role in fibrillogenesis and protein secretion (Figure 4C). This is in agreement with our previous finding. Subsequently, the specific

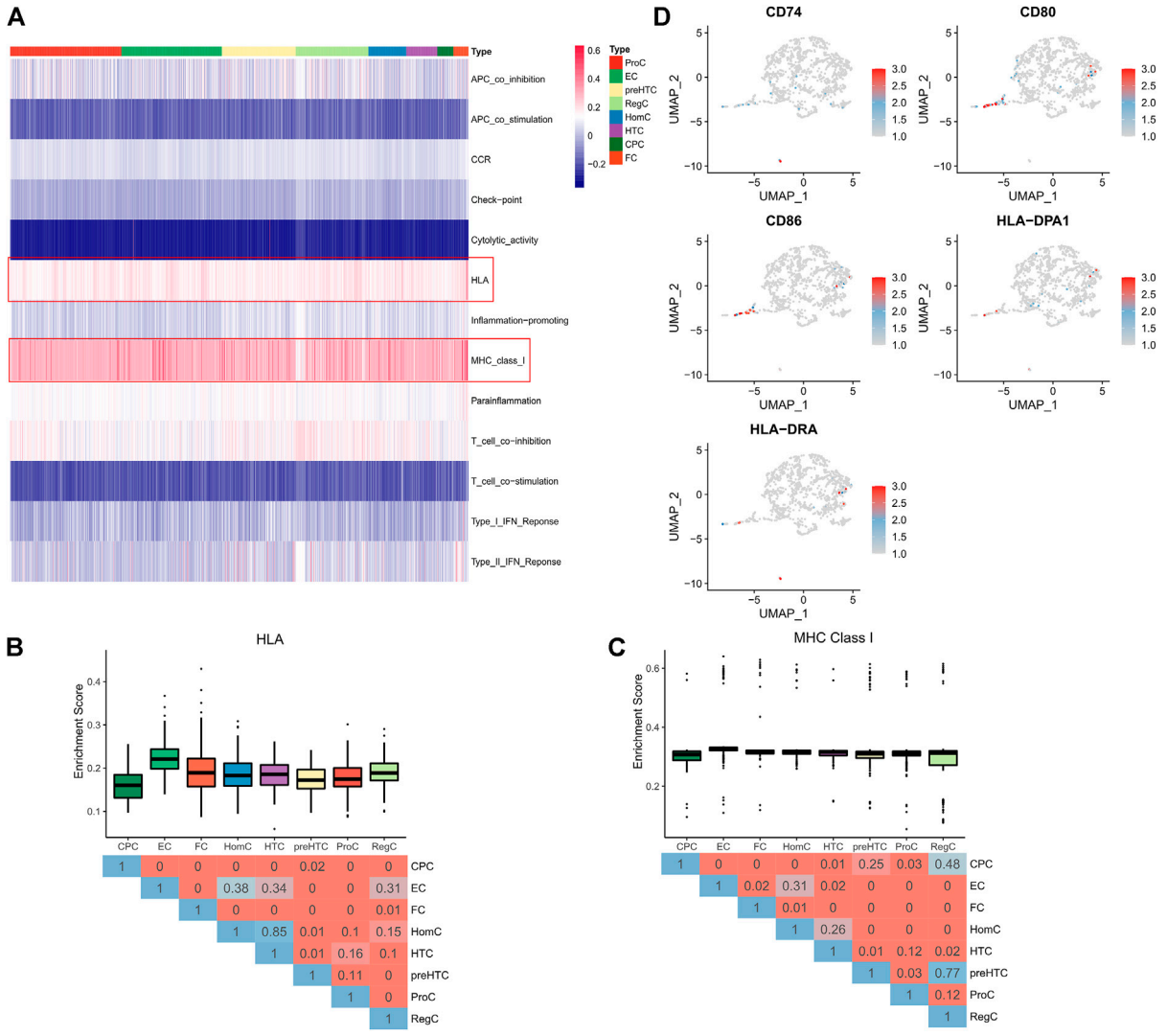

FIGURE 3
Immunogenicity of each cell cluster. **(A)** The Heatmap showing the activity of 13 immune pathways in cell clusters (pathways of interest are highlighted by red frames); **(B)** The Box plots showing the activity of the HLA pathway in 8 cell clusters (upper) and the Heatmap showing the difference represented by p value in Wilcoxon test (below); **(C)** The Box plots showing the activity of the MHC ClassIpathway in 8 cell clusters (upper) and the Heatmap showing the difference represented by p value in Wilcoxon test (below); **(D)** UMAP plots of each cell clusters colored by expression of marker genes.

pathways involved in the cell-cell communications were explored (Figure 4D). It was found that ECs communicated with preHTCs and FCs mainly via the CCL signaling pathway (Figure 4E). Additionally, ECs could also communicate with CPCs, HTCs and ProCs through the CXCL signaling pathway (Figure 4F). FCs communicated with HTCs predominantly through the EGF signaling pathway (Figure 4G) and with ProCs, RegCs and ECs *via* the VEGF signaling pathway (Figure 4H). In all, the results collectively indicated that ECs mainly play an immunoregulatory role in the cartilage microenvironment while FCs are the main participants in fibrillogenesis.

Fibrocartilage chondrocytes have stronger immunogenicity and effector chondrocytes have higher metabolic activity

In the context of the difference in immunocompetence between FCs and ECs, the functional difference between the two cell groups was further investigated via GSVA and KEGG analyses. The enriched KEGG pathways of the two cell groups were displayed in the Heatmap (Figure 5A). It was found that ECs had higher activity in regulating chemokine signal

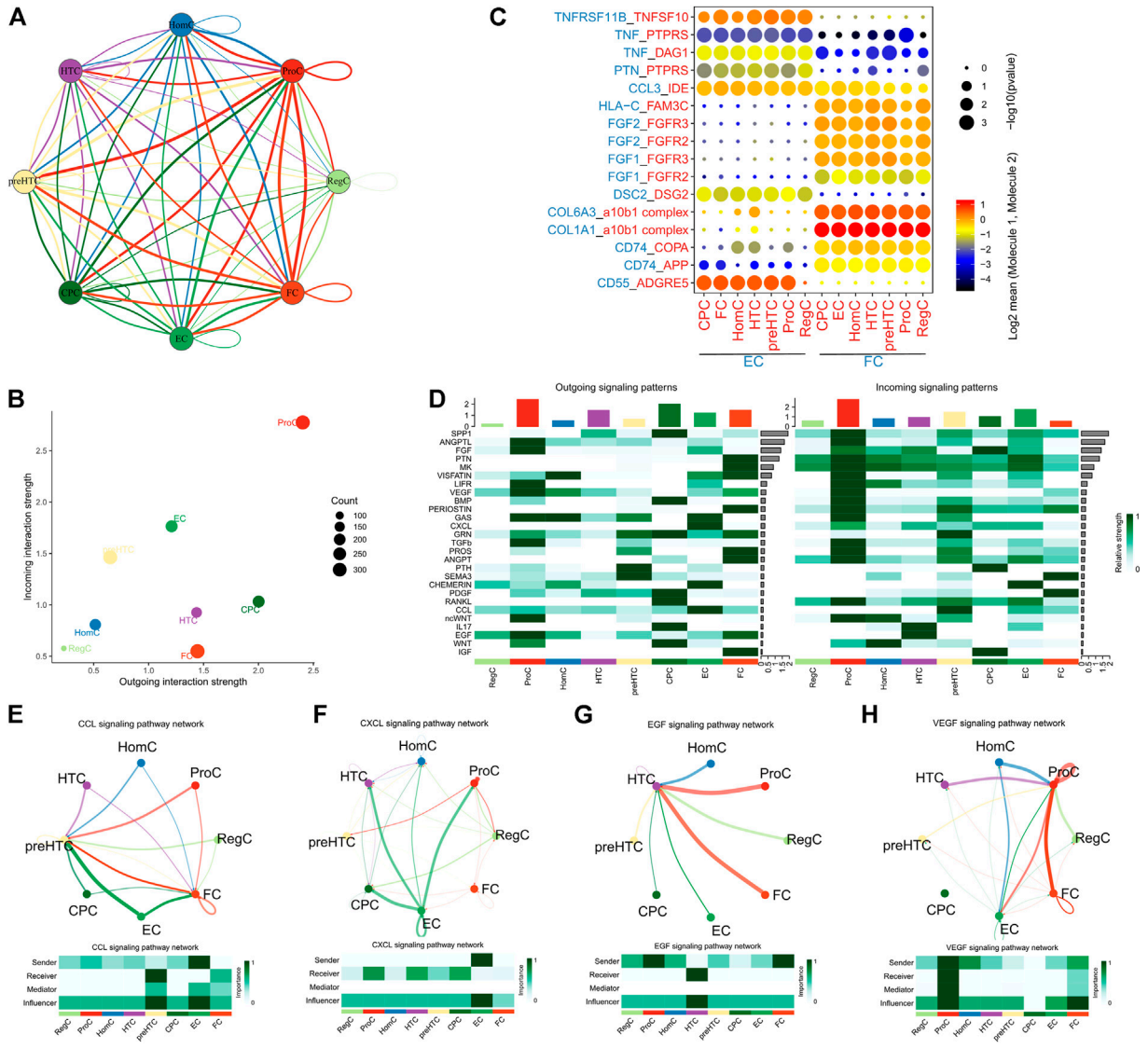

FIGURE 4
Cell-cell interactions. **(A)** The network showing the overall interactions between the 8 cell clusters (the thickness of the lines represents the number of receptor-ligand pairs); **(B)** The Scatter plot showing the number of interactions between the 8 cell clusters (the X-axis represents the number of outgoing interactions and the Y-axis represents the number of incoming interactions); **(C)** The point diagram showing the specific receptor-ligand interactions between ECs/FCs and other cell clusters (p value is represented by the circle size, and the mean expression of genes in ECs and FCs are represented by color); **(D)** The Heatmap showing the activity of signaling pathways involved in the interactions between the 8 cell clusters (left, outgoing signals; right, incoming signals); **(E)** ECs communicate with preHTCs and FCs through the CCL signaling pathway; **(F)** ECs communicate with CPCs, HTCs, HomCs and ProCs through the CXCL signaling pathway; **(G)** FCs communicate with HTCs through the EGF signaling pathway; **(H)** FCs communicate with ProCs through the VEGF signaling pathway.

transduction, Toll-like receptor and other signaling pathways, while FCs exhibited stronger metabolic activity involved in amino acid, ribose and glucose metabolisms (Figure 5B). GSEA revealed enhanced activity of Toll-like receptor, JAK/STAT and chemokine signaling pathways in ECs (Figure 5C) while augumented amino acid, ribose and glucose metabolisms in FCs, together with active glycolysis and gluconeogenesis (Figure 5D). The detailed results were shown in Supplementary Table S5. The above results illustrated that ECs have stronger immunogenicity than FCs and they participate in immunoregulation via regulating multiple signaling pathways. In the meantime, FCs show stronger catabolic function and have higher levels of amino acid metabolism and protein transportation involved in glycolysis and gluconeogenesis. All these findings are consistent with the previous report.

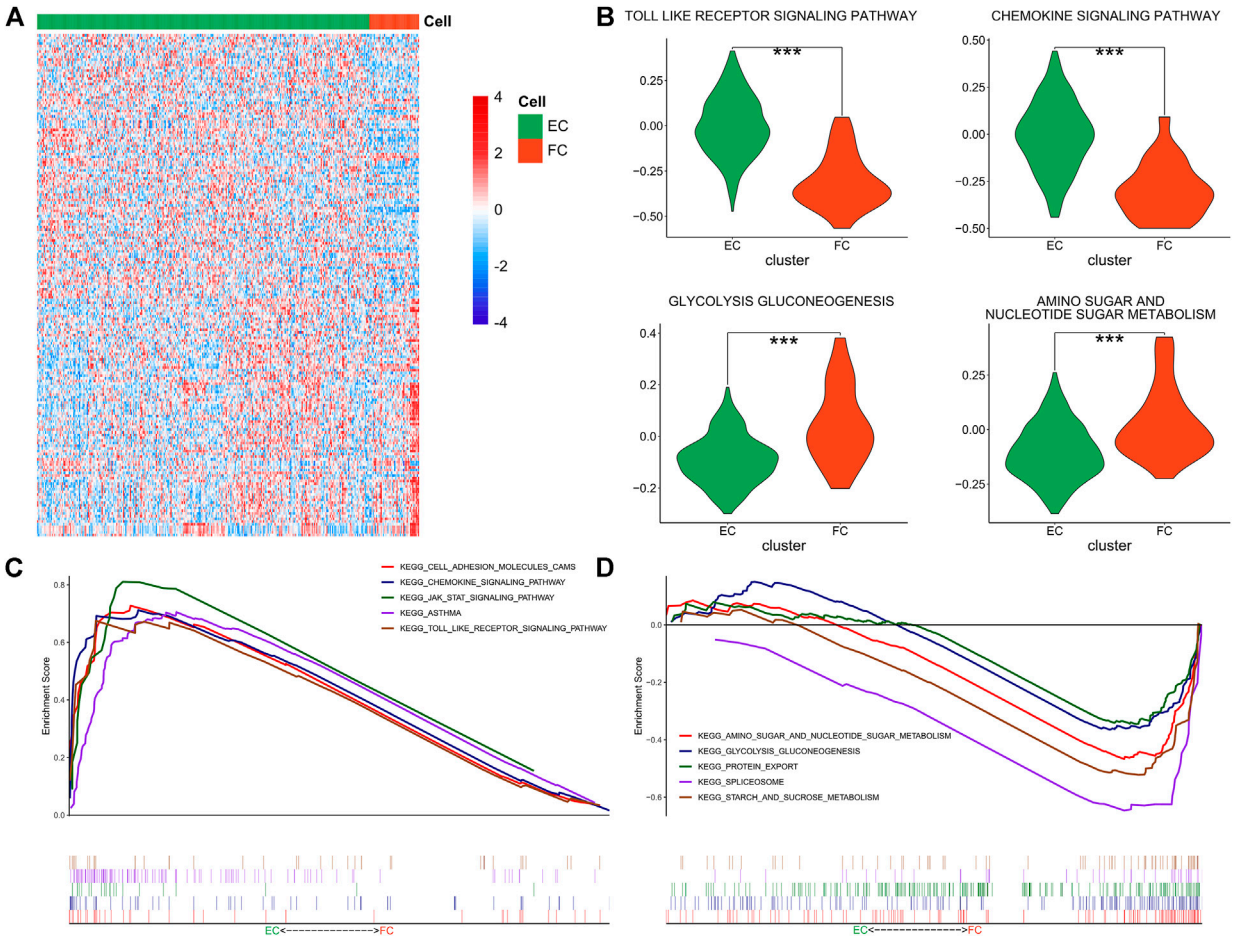

FIGURE 5
Functional enrichment of ECs and FCs. **(A)** The Heatmap showing the GSVA enrichment scores of KEGG pathways in ECs and FCs; **(B)** The Violin plots showing the specific GSVA results in ECs and FCs (***$p < 0.001$); **(C)** GSEA results in ECs; **(D)** GSEA results in FCs.

Canonical gene markers of effector chondrocytes and fibrocartilage chondrocytes are predictors for the severity of Osteoarthritis

We had proved that ECs and FCs actively participated in the development of OA. Then, the clinical significance of their canonical gene markers (ECs: CHRDL2, DSC2; FCs: COL1A1, COL14A1, IFI27, THY1) was explored. PCA was firstly performed to confirm the strong correlation of ECs and FCs with their canonical gene markers. The results showed that the 8 cell clusters were distributed along PC1 (Figure 6A), and consistently, expression of the canonical gene markers of ECs and FCs also changed along PC1 (Figure 6B). Following exclusion of the samples not expressing the canonical markers, samples were sub-classified into the high- and low-expression groups according to the median expression of marker genes. We found that samples expressing more marker genes had a higher degree of disease severity (Figure 6C), suggesting that these marker genes of ECs and FCs may accurately predict the disease status of OA.

Bulk RNA-seq analysis

Bulk RNA-seq data from two independent datasets, GSE51588 and GSE114007, were used to validate the role of ECs and FCs in OA development. ssGSEA algorithm was firstly applied to estimate the enrichment score of each cell cluster in samples based on the gene markers (Figures 7A,E). Then, correlation analysis was conducted and showed that FCs were positively associated with CPCs and preHTCs, while ECs showed weak correlations with other cell clusters (Figures 7B,F). It is noteworthy that FCs were significantly associated with most cell groups in both

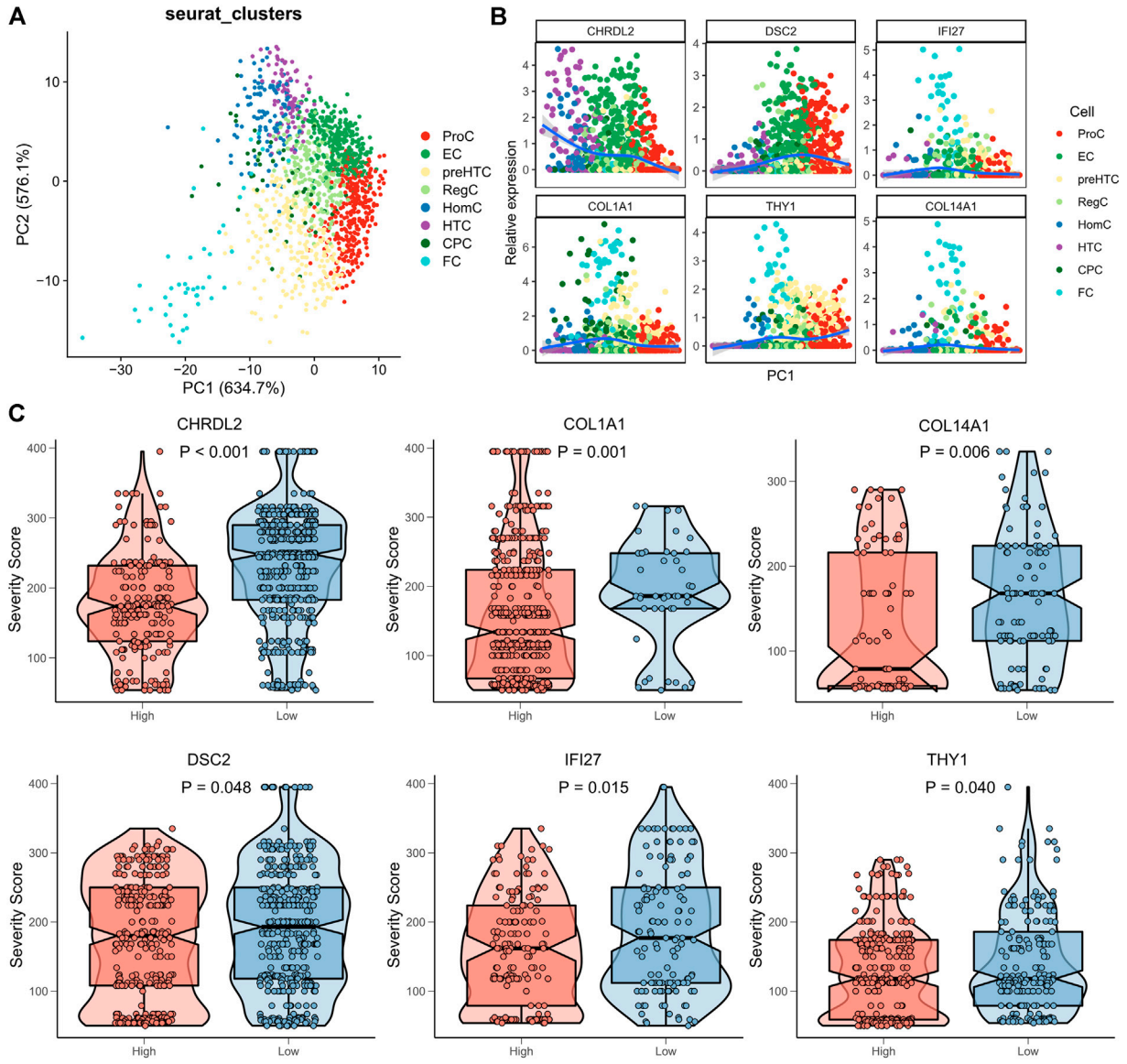

FIGURE 6
Clinical significance of marker genes of ECs and FCs. **(A)** PCA plots showing the distribution of the 8 cell clusters based on their marker genes; **(B)** Expression pattern of canonical marker genes along PC1; **(C)** The box plots showing the association between the Severity score and expression of gene markers (red for high expression and blue for low expression).

GSE51588 and GSE114007, suggesting that FCs more actively communicate with other cells than ECs. Moreover, PCA demonstrated that the enrichment score of each cell cluster could well differentiate OA samples from healthy samples (Figures 7C,G). ECs and FCs had remarkably increased enrichment scores in OA samples than healthy samples (Figures 7D,H). All these results showed that the ECs and FCs may promote the development of OA and could be used as predictors for OA disease severity with high accuracy.

Validation of the diagnostic performance of gene markers of effector chondrocytes and fibrocartilage chondrocytes in osteoarthritis

The diagnostic performance of the gene markers of ECs and FCs (CHRDL2, DSC2, COL1A1, COL14A1, IFI27, THY1) in OA was further analyzed in the GSE51588 and GSE114007. Significantly up-regulated expression of the gene markers was found in OA samples (Figures 8A,C). In addition, ROC curves showed that all the 6 gene

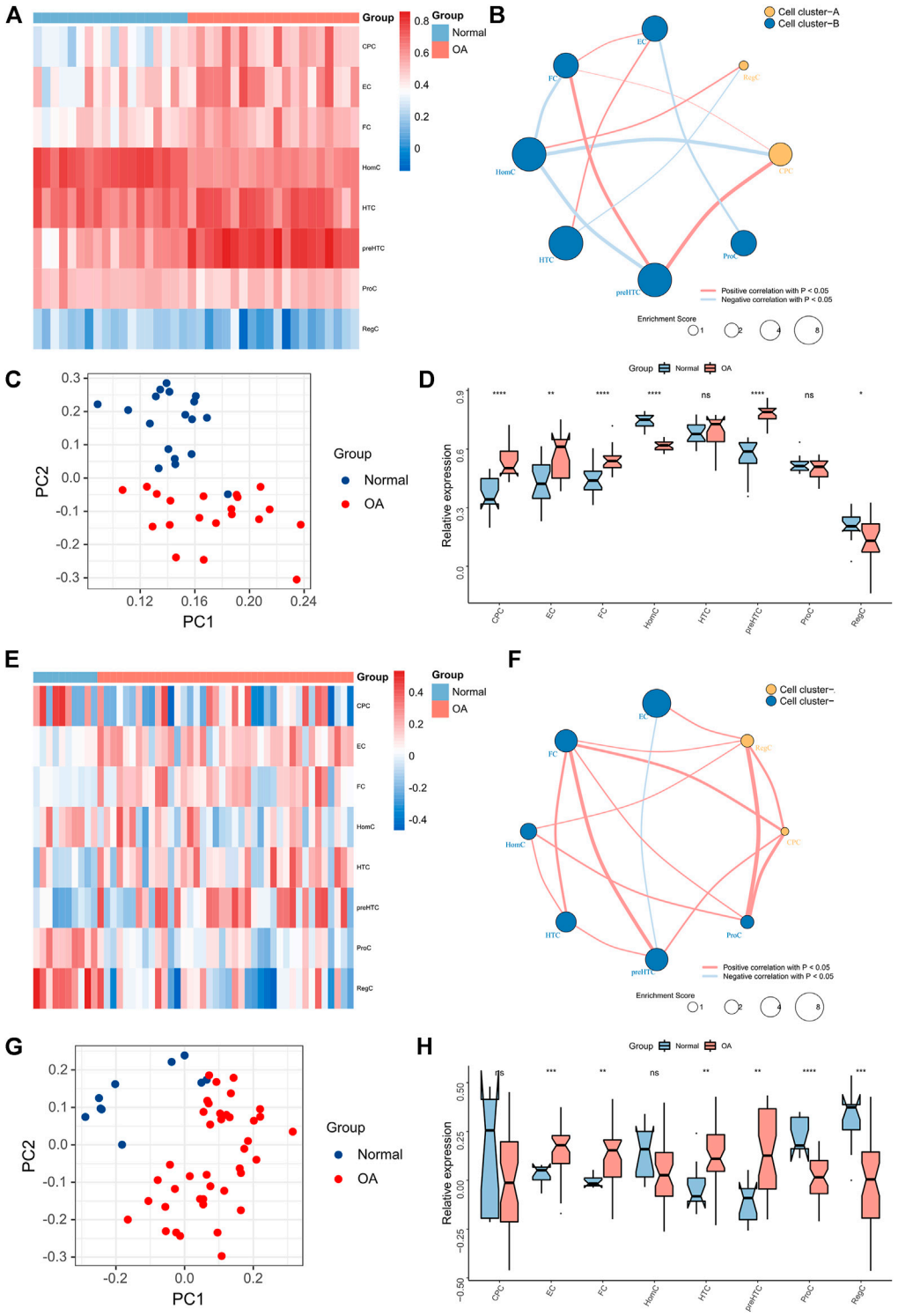

FIGURE 7
Chondrocytes profile in Bulk-seq data. **(A)** The Heatmap showing the relative abundance of the 8 cell clusters between OA and normal tissues in the GSE51588 dataset; **(B)** The network showing the significant associations between the 8 cell clusters in the GSE51588 dataset (the dot size represents the total enrichment score of chondrocytes and the clusters are distinguished by color; **(C)** PCA plot of chondrocytes based on enrichment scores in the GSE51588 dataset; **(D)** The box plots showing the relative abundance of the 8 cell clusters in OA and normal tissues in the GSE51588 dataset (*$p < 0.05$, **$p < 0.01$, ***$p < 0.001$; ns, not significant); **(E)** The Heatmap showing the relative abundance of the 8 cell clusters between OA and normal tissues in the GSE114007 dataset; **(F)** The network showing the significant associations between the 8 cell clusters in the
(*Continued*)

FIGURE 7 (Continued)
GSE114007 dataset (the dot size represents the total enrichment score of chondrocytes and the clusters are distinguished by color; (G) PCA plot of chondrocytes based on enrichment scores in the GSE114007 dataset; **(H)** The box plots showing the relative abundance of the 8 cell clusters in OA and normal tissues in the GSE114007 dataset (*p < 0.05, **p < 0.01, ***p < 0.001; ns, not significant).

markers could well predict OA in the GSE51588 and GSE114007 (all AUC>0.6) (Figures 8B,D).

Transcription factor (FC) -mRNA-miRNA regulatory network

A TF-mRNA-miRNA regulatory network of the gene markers of ECs and FCs (CHRDL2, DSC2, COL1A1, COL14A1, IFI27, THY1) was constructed to reveal the underlying mechanism by which the gene markers regulate OA progression. Upstream miRNA and TF of the gene markers were searched from the Enrichr database. Combining the miRNA-mRNA and TF-mRNA pairs, a TF-mRNA-miRNA regulatory network was correspondingly established, including 4 TFs, 87 miRNAs and 6 mRNAs (Figure 9A). Most of the gene markers were found to be regulated by both IRF8 and TFAP2A. Subsequently, TFs specific to ECs and FCs were inferred using the Scenic. IRF8 was specific to

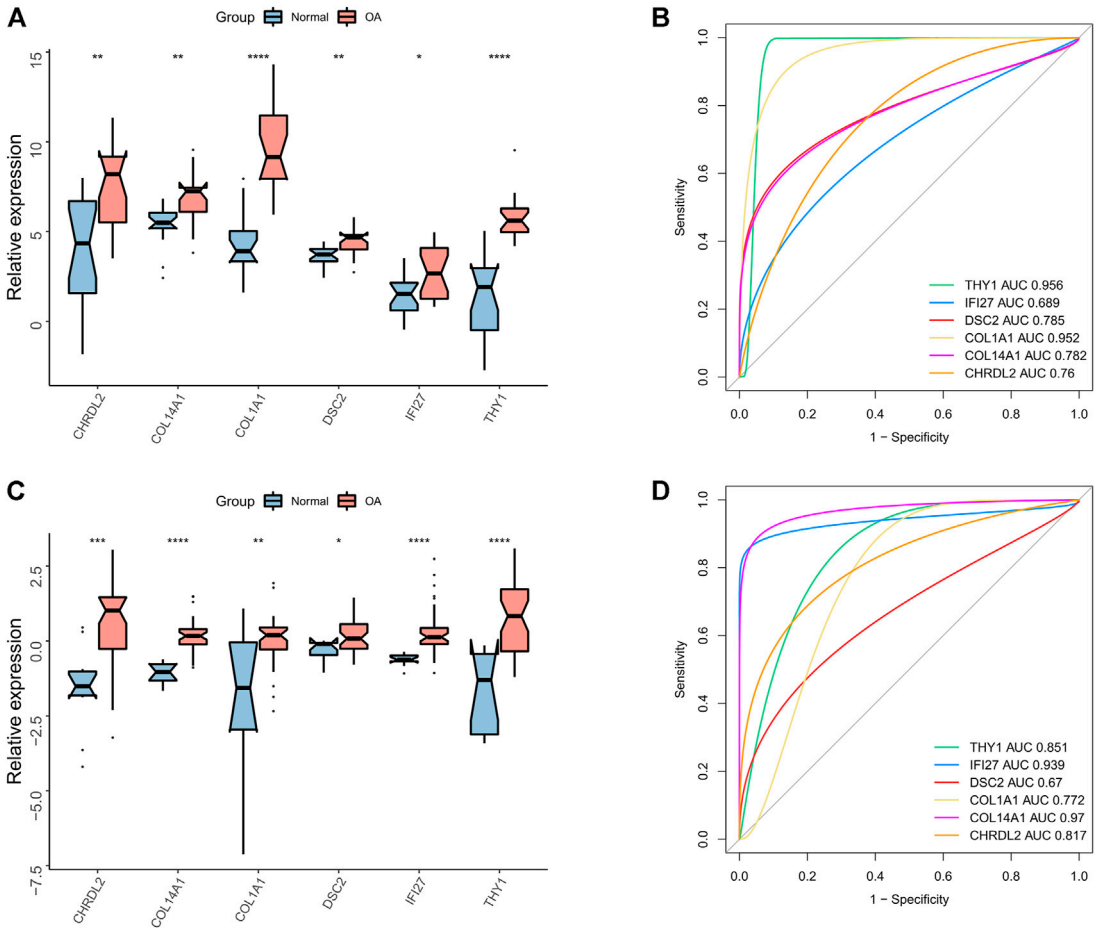

FIGURE 8
Diagnostic performance of canonical gene markers. **(A)** The box plots showing the expression difference between OA and normal tissues in expression of canonical gene markers in the GSE51888 dataset (*p < 0.05, **p < 0.01, ***p < 0.001; ns, not significant); **(B)** ROC curve of the gene markers in the GSE51888 dataset; **(C)** The box plots showing the expression difference between OA and normal tissues in expression of canonical gene markers in the GSE114007 dataset (*p < 0.05, **p < 0.01, ***p < 0.001; ns, not significant); **(D)** ROC curve of the gene markers in the GSE114007 dataset.

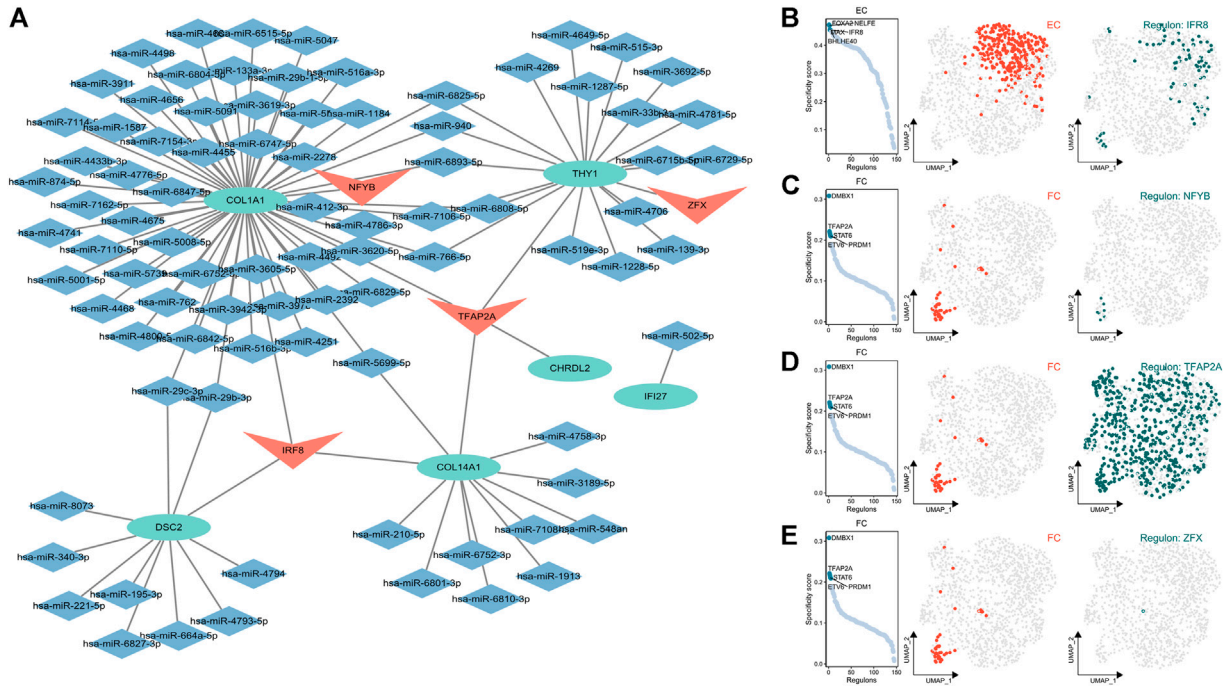

FIGURE 9
Establishment of TF-mRNA-miRNA regulatory network. **(A)** The TF-mRNA-miRNA regulatory network (TF, v-shaped frame; mRNA, oval shape; miRNA, rhombus); **(B)** Activity of TFs specific to ECs (from left to right: TF rank based on the regulon score, UMAP plot of the regulon activity, TF IFR8 regulon activity); **(C–E)** Activity of TFs specific to FCs (from left to right: TF rank based on the regulon score, UMAP plot of the regulon activity, TF **(C)** NFY8, (TFAP2A), and (ZFX) regulon activity).

ECs and had higher transcriptional activity in ECs and FCs than in other cell clusters (Figure 9B). We also found that NFYB, TFAP2A and ZFX were specific to FCs and also exhibited stronger transcriptional activity in FCs than ECs (Figures 9C–E). Notably, TFAP2A had high transcriptional activity in almost all cell clusters (Figure 9D), suggesting its potential role in OA development.

Conclusion

This study identified two subtypes of chondrocytes that advance the progression of OA, including ECs and FCs, with the former mainly responsible for cartilage degradation via affecting fiber degeneration while the latter for tissue inflammation via functions as immune cells. This finding provides new insight into the cellular heterogeneity and pathophysiology of OA. Moreover, their canonical gene markers, including CHRDL2, DSC2, COL1A1, COL14A1, IFI27, and THY1, can help for early diagnosis and precision treatment of OA.

Discussion

OA is the most common age-associated chronic degenerative disease of articular cartilage and regarded as the leading cause of disability (Abusarah et al., 2017). Currently, arthroplasty is used as an effective approach to treat symptomatic end-stage OA, but it is limited in clinical application due to the dissatisfied outcome, limited longevity of prosthesis, and high economic burden (Glyn-Jones et al., 2015). Under the background of aging population and increasing economic burden, more attention has been paid to the early detection and treatment of OA (Schnitzer et al., 2015; Pan et al., 2016). The emergence of biomarkers helps for diagnosis of OA and formulation of new treatment strategies. However, markers specific to chondrocytes are limited given the heterogeneity of chondrocytes, which prompts us to identify the role of chondrocytes in pathogenesis of OA. In the present study, we used scRNA-seq technique to study the heterogeneity of chondrocytes in OA and revealed their immunogenicity and interactions among different cell types. In addition, we identified new biomarkers available to predict OA and validated their performance using the Bulk RNA-seq technique. Our findings are conducive to further studying the heterogeneity and biological functions of chondrocytes in OA and provide new targets for early diagnosis and treatment of OA.

Due to the highly complicated heterogeneity of chondrocytes in OA, we focused on the subtypes of chondrocytes that potentiate OA development. We found that ECs and FCs had a significant effect in promoting OA development. Functional analysis revealed that ECs exhibited stronger immunocompetence and secretion activity, while FCs had higher property of fibroblasts. All these

results suggested that ECs may participate in the activation of immune cells and the synthesis of proteoglycan during OA progression, and FCs may be involved in fiber degeneration. Research found that CNV was abundant in MHC and TCR genes, which potentiated the ability of the immune system to recognize genetic variants, indicating that CNV might be an important mechanism that boosts immune diversity (Bailey et al., 2002; Nguyen et al., 2006; Olsson and Holmdahl, 2012). Similarly, our study found that ECs had a higher prevalence of CNV than FCs, suggesting their higher immune diversity and stronger chromosomal heterogeneity.

In general cases, OA is considered non-inflammatory but can manifest inflammatory phenotypes. Increasing studies has also noted that chronic low-grade inflammation can result in symptoms and disease progression (Sokolove and Lepus, 2013; Rhoads et al., 2017). Our study revealed that ECs and FCs had the highest activity of MHC and HLA pathways than other cell groups and highly expressed MHC genes. In the meantime, ECs and FCs actively communicated with other cell groups. These results demonstrated that FCs and ECs had stronger immunogenicity as compared to other cell types (Blais et al., 2011; Calis et al., 2013; Rossjohn et al., 2015). Interestingly, we found that ECs communicated with other cells mainly *via* CD55, which indicated that ECs potentiated OA development mainly through regulating the complement system of innate immunity (Hamann et al., 1999; Manferdini et al., 2016). Additionally, ECs had higher levels of CCL3 and TNF, showing their active participation in antigen-presentation and chemokine signaling pathway (Kalliolias and Ivashkiv, 2016; Jordan et al., 2018). Moreover, further analysis showed that ECs communicated with other cell types mainly via CCL and CXCL, which also indicated that ECs mediated the inflammation and immune cell recruitment in OA (Raghu et al., 2017; Ding et al., 2020). Furthermore, ECs exhibited stronger activity in regulating multiple signaling pathways including Toll-like receptor, JAK/STAT and chemokine signaling pathways. All these results implied that ECs are more potent in immunoregulation and advance inflammation and disease progression in OA, consistent with the previous report (Ji et al., 2019).

It is a fact that metabolic activities, including catabolism and anabolism, are essential to maintain the optimal cartilage function and promote cartilage tissue self-repair (Zhang et al., 2015). During the development of OA, glycolysis gradually becomes the main approach of metabolism, causing damages to the normal anabolic process of extracellular matrix (ECM) (Suurmond et al., 2015; Zhang et al., 2015; Hui et al., 2016). In the present study, FCs, compared to ECs, exhibited stronger metabolic activity in amino acid, ribose and glucose metabolisms and had active glycolysis and gluconeogenesis. In the meantime, they were found to actively communicate with other chondrocytes *via* the FGF family members, COL1A1 and COL6A3, showing a strong capability to secret fibers and their participation in cartilage tissue repair (Katoh, 2016; Xie et al., 2020). Moreover, the role of FCs in regulating fibrillogenesis was also proved by the participation of EGF and VEGF pathways in their interactions with other cell types (Schultz et al., 1991; Apte et al., 2019). It has been established that active glycolysis and gluconeogenesis may result in synthesis of abnormal proteoglycan, which then impedes the self-repair of cartilage tissue.

Collectively, our study demonstrated that ECs and FCs are important players during the progression of OA. More specifically, FCs mainly affect fiber degeneration and cartilage tissue repair to induce cartilage degradation, while ECs mainly play a role as immune cells via regulating inflammation and multiple signaling pathways, leading to joint tissue inflammation. In further steps, we also used Bulk RNA-seq data to validate the performance of ECs and FCs in predicting OA severity as well as the performance of their gene markers including CHRDL2, DSC2, COL1A1, COL14A1, IFI27, and THY1, which showed high expression in OA samples. Since the gene markers studied here are specific to OA, they can be used as flow cytometry markers with higher effectiveness than traditional markers and thus are highly valuable in early diagnosis and precision treatment of OA.

One of the limitations is the retrospective design of the study, and the sub-classification of chondrocytes requires further validation through *in vivo* and *ex vivo* experiments. In addition, the biological functions of ECs and FCs deserve further exploration. Furthermore, a larger-scale clinical cohort study is also on demand to investigate the performance of ECs, FCs and their canonical gene markers in early diagnosis of OA.

Data availability statement

The datasets presented in this study can be found in online repositories. The names of the repository/repositories and accession number(s) can be found in the article/Supplementary Material.

Author contributions

XH and JL were responsible for the conception, design. XH, MJ, and YL were responsible for the development of methodology and analysis. XH and ZL performed the bioinformatics analysis. XH, ZL, and YC wrote and revised the draft. JL final approval of the submitted version. All authors read and approved the final manuscript.

Funding

This work was supported by The National Natural Science Foundation of China (Grant numbers 81672159, 81972105 and 82072427).

Acknowledgments

We thank all the participants who supported our study. In particular, thanks to the GEO database for the analytical data.

Conflict of interest

The authors declare that the research was conducted in the absence of any commercial or financial relationships that could be construed as a potential conflict of interest.

Publisher's note

All claims expressed in this article are solely those of the authors and do not necessarily represent those of their affiliated organizations, or those of the publisher, the editors and the reviewers. Any product that may be evaluated in this article, or claim that may be made by its manufacturer, is not guaranteed or endorsed by the publisher.

Supplementary material

The Supplementary Material for this article can be found online at: https://www.frontiersin.org/articles/10.3389/fphar.2022.1004766/full#supplementary-material

References

Abusarah, J., Benabdoune, H., Shi, Q., Lussier, B., Martel-Pelletier, J., Malo, M., et al. (2017). Elucidating the role of protandim and 6-gingerol in protection against osteoarthritis. *J. Cell. Biochem.* 118 (5), 1003–1013. doi:10.1002/jcb.25659

Apte, R. S., Chen, D. S., and Ferrara, N. (2019). VEGF in signaling and disease: Beyond discovery and development. *Cell.* 176 (6), 1248–1264. doi:10.1016/j.cell.2019.01.021

Baboolal, T. G., Mastbergen, S. C., Jones, E., Calder, S. J., Lafeber, F. P., and McGonagle, D. (2016). Synovial fluid hyaluronan mediates MSC attachment to cartilage, a potential novel mechanism contributing to cartilage repair in osteoarthritis using knee joint distraction. *Ann. Rheum. Dis.* 75 (5), 908–915. doi:10.1136/annrheumdis-2014-206847

Bailey, J. A., Gu, Z., Clark, R. A., Reinert, K., Samonte, R. V., Schwartz, S., et al. (2002). Recent segmental duplications in the human genome. *Sci. (New York, NY)* 297 (5583), 1003–1007. doi:10.1126/science.1072047

Blais, M. E., Dong, T., and Rowland-Jones, S. (2011). HLA-C as a mediator of natural killer and T-cell activation: Spectator or key player? *Immunology* 133 (1), 1–7. doi:10.1111/j.1365-2567.2011.03422.x

Butler, A., Hoffman, P., Smibert, P., Papalexi, E., and Satija, R. (2018). Integrating single-cell transcriptomic data across different conditions, technologies, and species. *Nat. Biotechnol.* 36 (5), 411–420. doi:10.1038/nbt.4096

Calis, J. J., Maybeno, M., Greenbaum, J. A., Weiskopf, D., De Silva, A. D., Sette, A., et al. (2013). Properties of MHC class I presented peptides that enhance immunogenicity. *PLoS Comput. Biol.* 9 (10), e1003266. doi:10.1371/journal.pcbi.1003266

Chaly, Y., Blair, H. C., Smith, S. M., Bushnell, D. S., Marinov, A. D., Campfield, B. T., et al. (2015). Follistatin-like protein 1 regulates chondrocyte proliferation and chondrogenic differentiation of mesenchymal stem cells. *Ann. Rheum. Dis.* 74 (7), 1467–1473. doi:10.1136/annrheumdis-2013-204822

Chen, J., Bardes, E. E., Aronow, B. J., and Jegga, A. G. (2009). ToppGene Suite for gene list enrichment analysis and candidate gene prioritization. *Nucleic Acids Res.* 37, W305–W311. doi:10.1093/nar/gkp427

Childs, B. G., Gluscevic, M., Baker, D. J., Laberge, R. M., Marquess, D., Dananberg, J., et al. (2017). Senescent cells: An emerging target for diseases of ageing. *Nat. Rev. Drug Discov.* 16 (10), 718–735. doi:10.1038/nrd.2017.116

Chou, C. H., Wu, C. C., Song, I. W., Chuang, H. P., Lu, L. S., Chang, J. H., et al. (2013). Genome-wide expression profiles of subchondral bone in osteoarthritis. *Arthritis Res. Ther.* 15 (6), R190. doi:10.1186/ar4380

Ding, C., Song, Z., Shen, A., Chen, T., and Zhang, A. (2020). Small molecules targeting the innate immune cGAS–STING–TBK1 signaling pathway. *Acta Pharm. Sin. B* 10 (12), 2272–2298. doi:10.1016/j.apsb.2020.03.001

Edwards, J. J., Khanna, M., Jordan, K. P., Jordan, J. L., Bedson, J., and Dziedzic, K. S. (2015). Quality indicators for the primary care of osteoarthritis: A systematic review. *Ann. Rheum. Dis.* 74 (3), 490–498. doi:10.1136/annrheumdis-2013-203913

Fisch, K. M., Gamini, R., Alvarez-Garcia, O., Akagi, R., Saito, M., Muramatsu, Y., et al. (2018). Identification of transcription factors responsible for dysregulated networks in human osteoarthritis cartilage by global gene expression analysis. *Osteoarthr. Cartil.* 26 (11), 1531–1538. doi:10.1016/j.joca.2018.07.012

Glyn-Jones, S., Palmer, A. J., Agricola, R., Price, A. J., Vincent, T. L., Weinans, H., et al. (2015). *Lancet* 386 (9991), 376–387. doi:10.1016/s0140-6736(14)60802-3

Goldring, M. B., and Otero, M. (2011). Inflammation in osteoarthritis. *Curr. Opin. Rheumatol.* 23 (5), 471–478. doi:10.1097/BOR.0b013e328349c2b1

Hamann, J., Wishaupt, J. O., van Lier, R. A., Smeets, T. J., Breedveld, F. C., and Tak, P. P. (1999). Expression of the activation antigen CD97 and its ligand CD55 in rheumatoid synovial tissue. *Arthritis Rheum.* 42 (4), 650–658. doi:10.1002/1529-0131(199904)42:4<650::Aid-anr7>3.0.Co;2-s

Hui, W., Young, D. A., Rowan, A. D., Xu, X., Cawston, T. E., and Proctor, C. J. (2016). Oxidative changes and signalling pathways are pivotal in initiating age-related changes in articular cartilage. *Ann. Rheum. Dis.* 75 (2), 449–458. doi:10.1136/annrheumdis-2014-206295

Jeon, O. H., Kim, C., Laberge, R. M., Demaria, M., Rathod, S., Vasserot, A. P., et al. (2017). Local clearance of senescent cells attenuates the development of post-traumatic osteoarthritis and creates a pro-regenerative environment. *Nat. Med.* 23 (6), 775–781. doi:10.1038/nm.4324

Ji, Q., Zheng, Y., Zhang, G., Hu, Y., Fan, X., Hou, Y., et al. (2019). Single-cell RNA-seq analysis reveals the progression of human osteoarthritis. *Ann. Rheum. Dis.* 78 (1), 100–110. doi:10.1136/annrheumdis-2017-212863

Jiang, Y., and Tuan, R. S. (2015). Origin and function of cartilage stem/progenitor cells in osteoarthritis. *Nat. Rev. Rheumatol.* 11 (4), 206–212. doi:10.1038/nrrheum.2014.200

Jin, S., Guerrero-Juarez, C. F., Zhang, L., Chang, I., Ramos, R., Kuan, C. H., et al. (2021). Inference and analysis of cell-cell communication using CellChat. *Nat. Commun.* 12 (1), 1088. doi:10.1038/s41467-021-21246-9

Jin, X., Beguerie, J. R., Zhang, W., Blizzard, L., Otahal, P., Jones, G., et al. (2015). Circulating C reactive protein in osteoarthritis: A systematic review and meta-analysis. *Ann. Rheum. Dis.* 74 (4), 703–710. doi:10.1136/annrheumdis-2013-204494

Johnson, K., Zhu, S., Tremblay, M. S., Payette, J. N., Wang, J., Bouchez, L. C., et al. (2012). A stem cell-based approach to cartilage repair. *Sci. (New York, NY)* 336 (6082), 717–721. doi:10.1126/science.1215157

Jordan, L. A., Erlandsson, M. C., Fenner, B. F., Davies, R., Harvey, A. K., Choy, E. H., et al. (2018). Inhibition of CCL3 abrogated precursor cell fusion and bone erosions in human osteoclast cultures and murine collagen-induced arthritis. *Rheumatol. Oxf. Engl.* 57 (11), 2042–2052. doi:10.1093/rheumatology/key196

Kalliolias, G. D., and Ivashkiv, L. B. (2016). TNF biology, pathogenic mechanisms and emerging therapeutic strategies. *Nat. Rev. Rheumatol.* 12 (1), 49–62. doi:10.1038/nrrheum.2015.169

Katoh, M. (2016). Therapeutics targeting FGF signaling network in human diseases. *Trends Pharmacol. Sci.* 37 (12), 1081–1096. doi:10.1016/j.tips.2016.10.003

Koelling, S., Kruegel, J., Irmer, M., Path, J. R., Sadowski, B., Miro, X., et al. (2009). Migratory chondrogenic progenitor cells from repair tissue during the later stages of human osteoarthritis. *Cell. stem Cell.* 4 (4), 324–335. doi:10.1016/j.stem.2009.01.015

Kuleshov, M. V., Jones, M. R., Rouillard, A. D., Fernandez, N. F., Duan, Q., Wang, Z., et al. (2016). Enrichr: A comprehensive gene set enrichment analysis web server 2016 update. *Nucleic Acids Res.* 44 (W1), W90–W97. doi:10.1093/nar/gkw377

Liang, J. Y., Wang, D. S., Lin, H. C., Chen, X. X., Yang, H., Zheng, Y., et al. (2020). A novel ferroptosis-related gene signature for overall survival prediction in patients with hepatocellular carcinoma. *Int. J. Biol. Sci.* 16 (13), 2430–2441. doi:10.7150/ijbs.45050

Manferdini, C., Paolella, F., Gabusi, E., Silvestri, Y., Gambari, L., Cattini, L., et al. (2016). From osteoarthritic synovium to synovial-derived cells characterization: Synovial macrophages are key effector cells. *Arthritis Res. Ther.* 18, 83. doi:10.1186/s13075-016-0983-4

Nguyen, D. Q., Webber, C., and Ponting, C. P. (2006). Bias of selection on human copy-number variants. *PLoS Genet.* 2 (2), e20. doi:10.1371/journal.pgen.0020020

Olsson, L. M., and Holmdahl, R. (2012). Copy number variation in autoimmunity--importance hidden in complexity? *Eur. J. Immunol.* 42 (8), 1969–1976. doi:10.1002/eji.201242601

Pan, F., Ding, C., Winzenberg, T., Khan, H., Martel-Pelletier, J., Pelletier, J. P., et al. (2016). The offspring of people with a total knee replacement for severe primary knee osteoarthritis have a higher risk of worsening knee pain over 8 years. *Ann. Rheum. Dis.* 75 (2), 368–373. doi:10.1136/annrheumdis-2014-206005

Patel, A. P., Tirosh, I., Trombetta, J. J., Shalek, A. K., Gillespie, S. M., Wakimoto, H., et al. (2014). Single-cell RNA-seq highlights intratumoral heterogeneity in primary glioblastoma. *Sci. (New York, NY)* 344 (6190), 1396–1401. doi:10.1126/science.1254257

Prein, C., Warmbold, N., Farkas, Z., Schieker, M., Aszodi, A., and Clausen-Schaumann, H. (2016). Structural and mechanical properties of the proliferative zone of the developing murine growth plate cartilage assessed by atomic force microscopy. *Matrix Biol.* 50, 1–15. doi:10.1016/j.matbio.2015.10.001

Raghu, H., Lepus, C. M., Wang, Q., Wong, H. H., Lingampalli, N., Oliviero, F., et al. (2017). CCL2/CCR2, but not CCL5/CCR5, mediates monocyte recruitment, inflammation and cartilage destruction in osteoarthritis. *Ann. Rheum. Dis.* 76 (5), 914–922. doi:10.1136/annrheumdis-2016-210426

Rhoads, J. P., Major, A. S., and Rathmell, J. C. (2017). Fine tuning of immunometabolism for the treatment of rheumatic diseases. *Nat. Rev. Rheumatol.* 13 (5), 313–320. doi:10.1038/nrrheum.2017.54

Rossjohn, J., Gras, S., Miles, J. J., Turner, S. J., Godfrey, D. I., and McCluskey, J. (2015). T cell antigen receptor recognition of antigen-presenting molecules. *Annu. Rev. Immunol.* 33, 169–200. doi:10.1146/annurev-immunol-032414-112334

Saito, T., Fukai, A., Mabuchi, A., Ikeda, T., Yano, F., Ohba, S., et al. (2010). Transcriptional regulation of endochondral ossification by HIF-2alpha during skeletal growth and osteoarthritis development. *Nat. Med.* 16 (6), 678–686. doi:10.1038/nm.2146

Schnitzer, T. J., Ekman, E. F., Spierings, E. L., Greenberg, H. S., Smith, M. D., Brown, M. T., et al. (2015). Efficacy and safety of tanezumab monotherapy or combined with non-steroidal anti-inflammatory drugs in the treatment of knee or hip osteoarthritis pain. *Ann. Rheum. Dis.* 74 (6), 1202–1211. doi:10.1136/annrheumdis-2013-204905

Schultz, G., Rotatori, D. S., and Clark, W. (1991). EGF and TGF-alpha in wound healing and repair. *J. Cell. Biochem.* 45 (4), 346–352. doi:10.1002/jcb.240450407

Sokolove, J., and Lepus, C. M. (2013). Role of inflammation in the pathogenesis of osteoarthritis: Latest findings and interpretations. *Ther. Adv. Musculoskelet. Dis.* 5 (2), 77–94. doi:10.1177/1759720x12467868

St-Jacques, B., Hammerschmidt, M., and McMahon, A. P. (1999). Indian hedgehog signaling regulates proliferation and differentiation of chondrocytes and is essential for bone formation. *Genes. Dev.* 13 (16), 2072–2086. doi:10.1101/gad.13.16.2072

Suurmond, J., Rivellese, F., Dorjée, A. L., Bakker, A. M., Rombouts, Y. J., Rispens, T., et al. (2015). Toll-like receptor triggering augments activation of human mast cells by anti-citrullinated protein antibodies. *Ann. Rheum. Dis.* 74 (10), 1915–1923. doi:10.1136/annrheumdis-2014-205562

Thomas, E., Peat, G., and Croft, P. (2014). Defining and mapping the person with osteoarthritis for population studies and public health. *Rheumatol. Oxf. Engl.* 53 (2), 338–345. doi:10.1093/rheumatology/ket346

Trapnell, C., Cacchiarelli, D., Grimsby, J., Pokharel, P., Li, S., Morse, M., et al. (2014). The dynamics and regulators of cell fate decisions are revealed by pseudotemporal ordering of single cells. *Nat. Biotechnol.* 32 (4), 381–386. doi:10.1038/nbt.2859

Trounson, A., and McDonald, C. (2015). Stem cell therapies in clinical trials: Progress and challenges. *Cell. stem Cell.* 17 (1), 11–22. doi:10.1016/j.stem.2015.06.007

Vento-Tormo, R., Efremova, M., Botting, R. A., Turco, M. Y., Vento-Tormo, M., Meyer, K. B., et al. (2018). Single-cell reconstruction of the early maternal-fetal interface in humans. *Nature* 563 (7731), 347–353. doi:10.1038/s41586-018-0698-6

Wang, T. Y., and Chen, D. (2016). Differential roles of TGF-β signalling in joint tissues during osteoarthritis development. *Ann. Rheum. Dis.* 75 (11), e72. doi:10.1136/annrheumdis-2016-210312

Worthley, D. L., Churchill, M., Compton, J. T., Tailor, Y., Rao, M., Si, Y., et al. (2015). Gremlin 1 identifies a skeletal stem cell with bone, cartilage, and reticular stromal potential. *Cell.* 160 (1-2), 269–284. doi:10.1016/j.cell.2014.11.042

Xie, F., Kovic, B., Jin, X., He, X., Wang, M., and Silvestre, C. (2016). Economic and humanistic burden of osteoarthritis: A systematic review of large sample studies. *PharmacoEconomics* 34 (11), 1087–1100. doi:10.1007/s40273-016-0424-x

Xie, Y., Zinkle, A., Chen, L., and Mohammadi, M. (2020). Fibroblast growth factor signalling in osteoarthritis and cartilage repair. *Nat. Rev. Rheumatol.* 16 (10), 547–564. doi:10.1038/s41584-020-0469-2

Yu, G., Wang, L. G., Han, Y., and He, Q. Y. (2012). clusterProfiler: an R package for comparing biological themes among gene clusters. *Omics a J. Integr. Biol.* 16 (5), 284–287. doi:10.1089/omi.2011.0118

Zhang, Y., Vasheghani, F., Li, Y. H., Blati, M., Simeone, K., Fahmi, H., et al. (2015). Cartilage-specific deletion of mTOR upregulates autophagy and protects mice from osteoarthritis. *Ann. Rheum. Dis.* 74 (7), 1432–1440. doi:10.1136/annrheumdis-2013-204599

frontiers | Frontiers in Pharmacology

TYPE Review
PUBLISHED 10 October 2022
DOI 10.3389/fphar.2022.1009527

OPEN ACCESS

EDITED BY
Dongdong Sun,
Nanjing University of Chinese Medicine, China

REVIEWED BY
Alina Gonzalez-Quevedo,
Instituto de Neurología y Neurocirugía, Cuba
Tsvetelina Velikova,
Lozenetz Hospital, Bulgaria

*CORRESPONDENCE
Zhijun Liu,
zhijun_liu@xjtufh.edu.cn

†These authors share first authorship

SPECIALTY SECTION
This article was submitted to Inflammation Pharmacology, a section of the journal Frontiers in Pharmacology

RECEIVED 02 August 2022
ACCEPTED 23 September 2022
PUBLISHED 10 October 2022

CITATION
Xie X, Zhang N, Fu J, Wang Z, Ye Z and Liu Z (2022), The potential for traditional Chinese therapy in treating sleep disorders caused by COVID-19 through the cholinergic anti-inflammatory pathway.
Front. Pharmacol. 13:1009527.
doi: 10.3389/fphar.2022.1009527

The potential for traditional Chinese therapy in treating sleep disorders caused by COVID-19 through the cholinergic anti-inflammatory pathway

Xiaoxia Xie[1,2†], Nana Zhang[1,3,4†], Jingya Fu[1,2], Zhenzhi Wang[1,2], Zirun Ye[1,3,4] and Zhijun Liu[1,3,4*]

[1]Institute of Regenerative and Reconstructive Medicine, Med-X Institute, First Affiliated Hospital of Xi'an Jiaotong University, Xi'an, China, [2]Shaanxi University of Chinese Medicine, Xian yang, China, [3]National Local Joint Engineering Research Center for Precision Surgery & Regenerative Medicine, First Affiliated Hospital of Xi'an Jiaotong University, Xi'an, China, [4]Shaanxi Provincial Center for Regenerative Medicine and Surgical Engineering, First Affiliated Hospital of Xi'an Jiaotong University, Xi'an, China

Since the outbreak of Coronavirus disease (COVID-19) in 2019, it has spread rapidly across the globe. Sleep disorders caused by COVID-19 have become a major concern for COVID-19 patients and recovered patients. So far, there's no effective therapy on this. Traditional Chinese therapy (TCT) has a great effect on sleep disorders, with rare side effects and no obvious withdrawal symptoms. The cholinergic anti-inflammatory pathway, a neuroregulatory pathway in the central nervous system that uses cholinergic neurons and neurotransmitters to suppress inflammatory responses, has been reported to be associated with sleep disorders and psychiatric symptoms. Many studies have shown that TCT activates the cholinergic anti-inflammatory pathway (CAP), inhibits inflammation, and relieves associated symptoms. Therefore, we believe that TCT may be a potential therapeutic strategy to alleviate sleep disorders induced by COVID-19 through CAP. In this review, we analyzed the relationship between cytokine storm induced by Coronavirus and sleep disorders, explained the influence of CAP on sleep disorders, discussed the TCT's effect on CAP, and summarized the treatment effect of TCT on sleep disorders. Based on these practical researches and theoretical basis, we propose potential strategies to effectively improve the sleep disorders caused by COVID-19.

Abbreviations: ACh, acetylcholine; ARDS, acute respiratory distress syndrome; AD: Alzheimer's disease; α7nAChR, α 7 nicotinic acetylcholine receptor; CAP, cholinergic anti-inflammatory pathway; COVID-19, coronavirus disease 2019; CRP, C-reactive protein; EA, electroacupuncture; EAED, ethyl acetate extract of dandelion; ICU, intensive care unit; IL, interleukin; LPS, lipopolysaccharide; NHD, hypnotic decoction; NREM, non-rapid eye movements; PCPA, para-chlorophenylalanine; PPT, pedunculopontine tegmental; PSQI, pittsburgh sleep quality index; PTSD, post-traumatic stress disorder; SARS, severe acute respiratory syndrome; taVNS, transcutaneous auricular vagal nerve stimulation; TCT, traditional Chinese therapy; TMPRSS2, recombinant transmembrane protease, serine 2; TNF, tumor necrosis factor

KEYWORDS

traditional Chinese therapy, cholinergic anti-inflammatory pathway, sleep disorders, coronavirus disease 2019, cytokine storms

1 Introduction

An outbreak of pneumonia was caused by a novel coronavirus in Wuhan, Hubei Province province, China, at the end of 2019. Since then, the novel coronavirus has spread rapidly to different countries and regions and has evolved into a major international public health emergency. Clinically, the symptoms of the Coronavirus disease (COVID-19) in 2019 range from asymptomatic to mild symptoms such as fever, fatigue, and cough to severe acute respiratory distress syndrome (ARDS) (Chen et al., 2020; Kwenandar et al., 2020; Zhou et al., 2021). In addition, the COVID-19 pandemic has led to an epidemic of mental illnesses, such as insomnia, depression and anxiety, and symptoms of post-traumatic stress (Guo et al., 2020; Akıncı and Melek Başar, 2021; Huang et al., 2021). Recently, a systematic review of 10 studies using the Pittsburgh Sleep Quality Index (PSQI) questionnaire to assess sleep quality found that about a quarter of COVID-19 survivors was diagnosed with sleep disorders (Cheng et al., 2021a). Sleep disorders were the most common neuropsychiatric symptoms in patients 14–182 days after recovery from COVID-19 (Ding and Yao, 2020). The severity of COVID-19 was closely related to the intensity of the virus and the body's inflammatory responses (Mehta et al., 2020). In severe cases, an excessive inflammatory response, known as namely, the "cytokine storm," occurs due to the release of high levels of proinflammatory cytokines and chemokines produced by inflammatory cells. Cytokine storms can lead to multiple organ failures and even death (Channappanavar and Perlman, 2017). While many drugs are effective in relieving symptoms associated with COVID-19 (Polack et al., 2020; Doroftei et al., 2021), there have been relatively rare evidence-based assessments and interventions for mental health disorders (Lai et al., 2020).

Traditional Chinese therapy has been used in epidemic treatment for thousands of years. From smallpox and ancient plagues to avian influenza, Middle East Respiratory Syndrome (MERS), and Severe Acute Respiratory Syndrome (SARS), Chinese have extensive experience in treating infections with Traditional Chinese therapy (TCT) (Chen and Nakamura, 2004; Hsu et al., 2006; Lin et al., 2017). Traditional Chinese therapy includes acupuncture, massage, Chinese herbal medicine, ear acupuncture, moxibustion and so on. The common treatment options of TCT including acupuncture, Chinese herbal medicine and taVNS have been summarized in this paper to reveal the most promising three treatment methods. Acupuncture, Chinese herbal medicine, and transcutaneous auricular vagal nerve stimulation (taTNS) have also been explored as complementary treatments for sleep disorders, and with great effect (Lu et al., 2022; Luan et al., 2022). As a result, TCT has the potential to treat sleep disorders and psychiatric symptoms caused by COVID-19.

The cholinergic anti-inflammatory pathway (CAP) represents a neurological mechanism that suppresses inflammatory responses and was first discovered by Tracey KJ in 2000. They found that parasympathetic nervous system activity affects circulating tumor necrosis factor (TNF) concentrations and shock response to endotoxemia, a so-called "cholinergic anti-inflammatory pathway" (Qin et al., 2017). Activation of CAP is also considered a therapeutic strategy for respiratory diseases (Lv et al., 2022) and has the potential to be a promising therapeutic intervention for COVID-19 infection. The active ingredient in Chinese herbal medicine has been reported to inhibit proinflammatory cytokines and prevent cytokine storms (Dai et al., 2021; Yang et al., 2022). In addition, The World Health Organization (WHO) recommends acupuncture for 16 inflammatory diseases, and some clinical practice guidelines recommend acupuncture for multiple inflammatory diseases (Yang et al., 2016a; Wang et al., 2018a). TaVNS, derived from Chinese ear acupuncture, stimulate the auricle branch of the vagus nerve to activate CAP, which helps reduce inflammation. Several clinical and laboratory studies have also found that taVNS significantly improve and relieve inflammatory reactions (Baptista et al., 2020; Go et al., 2022a). Therefore, TCT has a high potential for treating inflammatory response symptoms caused by the novel coronavirus. In this review, we aim to analyze and summarize if TCT will be a promising strategy for the treatment of treating sleep disorders caused by COVID-19.

2 Methodology

The keywords "sleep disorders" was searched in PubMed and web of science from 1986 to 2022. A secondary search was conducted by screening the list of articles that met the inclusion criteria. The keywords were COVID-19, cholinergic anti-inflammatory pathway, acupuncture, taVNS and Chinese herbal medicine. The obtained articles were screened, and irrelevant title or abstract was excluded. Finally, we organized the tables, drew the figures and wrote the text to summarize the traditional Chinese therapy in treating sleep disorders caused by COVID-19 through the cholinergic anti-inflammatory pathway.

TABLE 1 Summary of the different neurological symptoms induced by the COVID-19.

Authors and publication year	Country	Sample size	Follow-up time	Experienced neurological symptoms
Jing Guo, 2020 (Guo et al., 2020)	China	2993	NA	Insomnia, depression, post-Traumatic stress symptoms, mental Health Problems
Chaolin Huang, 2020 (Huang et al., 2021)	China	1733	6 months	Sleep difficulties, anxiety and depression
Tuba Akıncı, 2020 (Akıncı and Melek Başar, 2021)	Beylikduzu	189	NA	Insomnia, anxiety and depression
Zijun Xu, 2021 (Xu et al., 2021)	China	1456	2 months	Post-traumatic stress disorder, sleep disorders, anxiety and depressive symptoms
Philip Cheng, 2021 (Cheng et al., 2021b)	America	208	1 year	Anxiety and depressive symptoms
Wenning Fu, 2020 (Fu et al., 2020)	China	1242	NA	Stress disorder, sleep disorders
Xiushi Ding, 2020 (Ding and Yao, 2020)	China	150	2 months	Anxiety, depressive symptoms
Kai Liu, 2020 (Liu et al., 2020a)	China	51	5 days	Anxiety and sleep disorders
Luisa Weiner, 2020 (Weiner et al., 2020)	China	120	6 months	Sleep disorders and depressive symptoms
Greg J Elder, 2020 (Elder et al., 2020)	England	60	8 months	Anxiety, sleep disorders, and depressive symptoms
Lígia Passos, 2020 (Passos et al., 2020)	Portugal and Brazil	550	NA	Anxiety and depressive symptoms
Lorenzo Tarsitani, 2021 (Tarsitani et al., 2021)	Italian	115	3 months	Post-traumatic stress disorder
David T Arnold, 2021 (Arnold et al., 2021)	England	110	4 weeks	Insomnia

COVID-19, coronavirus disease 2019.

3 The relationship between cytokines storm and sleep disorders caused by COVID-19

Cytokines storm is essentially an immune system overreaction to infection. As the novel coronavirus enters the lungs, its S-protein specifically recognizes the host angiotensin-converting enzyme 2 receptor in alveolar epithelial type II cells. Upon binding, the host serine protease TMPRSS2 breaks down the S protein, allowing the virus to fuse with the cell membrane, and then the novel coronavirus enters the host cell (Wan et al., 2020). The host activates an immune response to clear the virus. In the early stages, virus infection causes the absorption and activation of various inflammatory cells in the lungs, releasing large amounts of cytokines and inflammatory chemokines. The TNF-α and IL-1β and other early active cytokines are rapidly secreted and peak within a few hours. Subsequently, anti-inflammatory cytokines are secreted to regulate the inflammatory response, allowing the body to eliminate harmful stimuli while maintaining cellular homeostasis. However, when the pro-inflammatory balance is disrupted, early reactive cytokines can further trigger the activation and release of a range of cytokines such as IL-2, IL-6, IL-8, IL-12, and inflammatory chemokines, leading to "cascading" effects and the uncontrolled inflammatory responses (Mehta et al., 2020). A retrospective multicenter study involving 150 COVID-19 patients suggests that virus-activated "cytokines storm syndrome" may be associated with COVID-19 mortality (Koralnik and Tyler, 2020). Meanwhile, elevated levels of serum IL-2, TNF-α, IL-7, granulocyte colony-stimulating factor, and interferon-gamma-induced protein 10 were correlated with the severity of COVID-19 (Mehta et al., 2020). Plasma levels of IL-2, IL-7, TNF-α, and other pro-inflammatory cytokines were elevated in COVID-19 patients, and levels of various inflammatory cytokines were higher in (ICU) patients than in non-ICU patients (Huang et al., 2020). Clinical studies have found that severe COVID-19 patients often experience this cytokine storm. Not only can it lead to acute lung injury, but it can also progress to multiple organs, including the central nervous system and peripheral nervous system organs (Gimeno et al., 2009; Koralnik and Tyler, 2020). Table 1 summarized the different neurological symptoms induced by COVID-19. COVID-19 patients experienced many different neurological symptoms during their illness, such as headaches, post-traumatic stress disorder (PTSD), sleep disorders, and depressive symptoms (Arnold et al., 2021; Xu et al., 2021). A previous study found that blocking the biological effects of the cytokines IL-1 and TNF can reduce the amount of non-REM sleep or NREM sleep rebound after sleep deprivation. On the other hand, increasing the supply of these cytokines promoted and inhibits NREM sleep volume and intensity. These findings suggested that both IL-1 and TNF are involved in the homeostatic regulation of sleep (Krueger and Majde, 1995; Zhang et al., 2020). In addition, anti-inflammatory cytokines IL-4, IL-10, and IL-13 were reported to reduce NREM sleep amount in rabbits (Kushikata et al., 1999; Kubota et al., 2000; Opp, 2005), while anti-inflammatory cytokines IFN-γ, IL-2, IL-6, and IL-15 promoted NREM sleep in animal models (Kubota

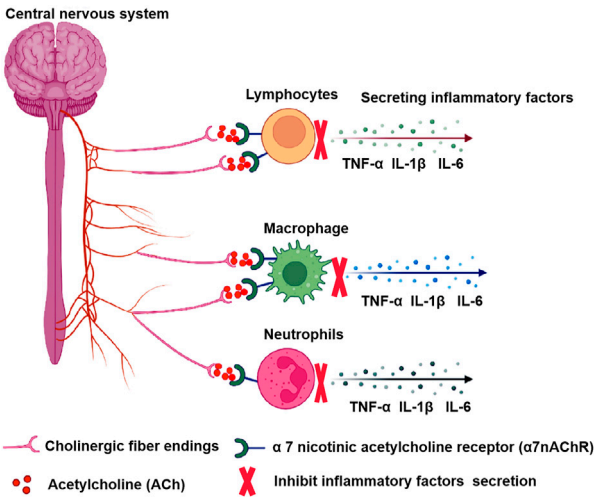

FIGURE 1
The molecular mechanisms of the CAP. The central nervous system releases ACh through efferent vagal endings and binds to α7nAChR on various inflammatory cells, inhibiting the release of pro-inflammatory factors.

et al., 2001a; Kubota et al., 2001b; Hogan et al., 2003). A clinical study found circulating levels of IL-1, TNF, and IL-6 peak during sleep or early morning (Lange et al., 2010; Chavan et al., 2017). Studies have shown that injecting healthy volunteers with IL-6 prolongs the NREM phase, leading to subjective fatigue and elevated CRP levels (Ranjbaran et al., 2007). In summary, high levels of inflammatory cytokines could lead to sleep disorders during COVID-19.

4 The anti-inflammatory mechanism of the cholinergic anti-inflammatory pathway

CAP is a neuroregulatory pathway in the central nervous system that uses cholinergic neurons and neurotransmitters to suppress systemic inflammatory responses. It releases acetylcholine through the vented ending of efferent vagal endings and binds to α7 nicotinic acetylcholine receptor (α7nAChR) on macrophages and other immune cells, inhibiting macrophage activation and inhibiting the release of pro-inflammatory factors such as TNF-α, IL-1β, IL-6 (Pavlov et al., 2003; Pavlov and Tracey, 2015). The α7nAChR plays a key role in regulating immune responses and oxidative stress in the central and peripheral nervous systems (Ren et al., 2017), participating in processes of learning, memory consolidation, movement, and attention (Fucile et al., 2003; Park et al., 2007). α7nAChR agonist PHA-543613 reduces inflammatory damage and enhances anti-inflammatory factors and antioxidant enzymes (Xue et al., 2019). Furthermore, when the vagus nerve is electrically stimulated, the axon terminals secrete large amounts of ACh, further activating anti-inflammatory pathways in various inflammatory cells (Go et al., 2022b). Experimental results show that stimulation of the distal vagus nerve transection can prevent the elevation of liver and blood TNF caused by septic shock (Song et al., 2008). In addition, an animal model found that electrical stimulation of the vagus nerve and administration of cholinergic neurotransmitter acetylcholine inhibited levels of pro-inflammatory factor TNF-α and reduced inflammatory responses, which were exacerbated by vagotomy (Bonaz et al., 2016). Vagus nerve stimulation (VNS) also significantly reduced levels of pro-inflammatory cytokines IL-6 and IL-1β, as well as the proportion of microglia and macrophages in mice stimulated by lipopolysaccharides (Meneses et al., 2016). In summary, stimulating the vagus nerve or activating α7nAChR effectively inhibits the development of inflammation, and Figure 1 depicted the molecular mechanisms by which CAP attenuates inflammation.

Recently, activation of CAP has also been considered a strategy for the treatment of respiratory diseases (Yamada and Ichinose, 2018). The α7nAChR has been shown to activate lung resident immune cells such as alveolar macrophages, epithelial cells, and activated neutrophils, as well as slow local inflammatory responses and reduce lung injury. In the mice model of acute lung injury, VNS prevents lung injury by lung injury autonomic nervous system imbalance and activating α7nAChR through CAP (dos Santos et al., 2011; Yang et al., 2014; Liu et al., 2017a). A cohort clinical study reported the role of α7nAChR in regulating inflammatory response and oxidative stress in the chronic sleep deprivation model. Stimulation of α7nAChR contributes to adverse reactions caused by sleep deprivation. α7nAChR as a biomarker of hippocampal inflammation and oxidative stress after chronic sleep deprivation (Xue et al., 2019). Therefore, targeting CAP with VNS may be a promising treatment for lung injury and sleep disorders caused by COVID-19.

5 The effect of cholinergic anti-inflammatory pathway on sleep disorders

The CAP pathway is an important component of the cholinergic system that connects the nervous system to the immune system and acts as an anti-inflammatory agent through the ACh and vagus nerve (Liu et al., 2015). The cholinergic system has been reported to regulate sleep cycles (Jasper and Tessier, 1971). Studies have shown that acetylcholine plays an important role in wakefulness and breathing in people with sleep apnea (Otuyama et al., 2013). Meng et al. (2021) also found that daytime sleepiness and high blood pressure are associated with sympathetic-vagus nerve imbalance, which may be associated with decreased plasma ACh level. A clinical trial found that short sleepers responded significantly less to ACh forearm blood flow response than normal sleepers (Stockelman et al., 2021). Another study showed that ozone-induced abnormal

TABLE 2 Summary of TCT's effect on CAP and their advantages and limitations.

Types of TCT	Operational principle	Representative method	The effect on CAP[ref]	Strengths	Limitations
Acupuncture	Stimulate the specific position of the human body	Zusanli (ST36); Hegu (LI4); Shenting (GV24); Baihui (GV20)	Stimulating vagus nerve of auricle or cutaneous branch inhibits inflammatory mediators produced by macrophages (da Silva and Dorsher, 2014)	Easy; safe; less toxic; side effects	Improper operation is easy to cause infection
TaVNS	Stimulate the auricular branch of vagus nerve	Non-invasive taVNS	TaVNS can increase efferent vagus nerve excitability by stimulating auricular points in the conchal region and increase the ACh release and activate CAP (Andersson and Tracey, 2012; Pavlov and Tracey, 2012; Kaczmarczyk et al., 2017)	Convenient; easy; non-traumatic	Need professional guide
Chinese herbal medicine	Oral administration (Chinese medicine Formula and Chinese patent medicine)	Berberine; Dandelion; Chinese medicine Formula (albizzia bark, nocturnal vine, lily, and Lanzhi); Chinese patent medicine (Coptis Chinensis and cinnamon)	Inhibiting the activity of acetylcholinesterase and increasing the level of ACh and the expression of α7nAChR, thus regulating CAP and inhibiting inflammation (Li et al., 2016; Wang et al., 2018b; Wang et al., 2019; Zhao et al., 2020; Yang et al., 2021)	Efficient; multitarget; safe	Need the guidance of a professional doctor; there is a high demand for the purity of the medicine

TaVNS, transcutaneous auricular vagal stimulation; ACh, acetylcholine; CAP, cholinergic anti-inflammatory pathway.

sleep loss is associated with decreased ACh levels in the medial preoptic region rats (Alfaro-Rodríguez and González-Piña, 2005). Dexzopicclone is one of the most commonly used sleeping drugs in the clinic. It has a sedative, hypnotic effect and partially suppresses pedunculopontine tegmental (PPT) neurons by enhancing gamma-aminobutyric acid. One study reported inhibition of dextran, which reduced the release of the PPT-neuron terminals ACh in the pontine reticular formation and promoted sleep (Hambrecht-Wiedbusch et al., 2010). Cao Q Neurotransmitter test showed that saponins promoted sleep by increasing levels of acetylcholine, acetylcholine laterodorsal tegmental, and acetylcholine in PPT in mice (Cao et al., 2016). Studies have shown that cholinergic neuronal antagonists can block the activation of α7nAChR and increase the wakefulness-associated state induced by cholinergic stimulation (Zant et al., 2016). Nyctinastic herbs decoction (NHD) can prolong para-chlorophenylalanine (PCPA)-induced insomnia in mice, sleep duration, sleep quality, and depressive state was improved, and the mechanism was that the level of ACh attenuated the insomnia effect of PCPA (Yang et al., 2021). These results suggest that ACH levels play a significant role in sleep disturbance.

6 The effect of traditional Chinese therapy on cholinergic anti-inflammatory pathway

Some studies have found that α7nAChR plays a key role in the pathophysiology of sleep disorders and may represent a target for the treatment and control of sleep disorders (Saint-Mleux et al., 2004; Xue et al., 2019). TCT has been used in China for more than 2000 years to treat insomnia, such as acupuncture, taVNS, and Chinese herbal medicine (Sarris, 2012). However, the underlying biological mechanisms are largely unknown. Some studies have shown that they can affect CAP, suppress inflammation, and may have sleep relief (Liu et al., 2020b; Liu et al., 2021). Table 2 summarized the impact of the three most common TCT effects on CAP and their advantages and disadvantages.

6.1 Acupuncture

Acupuncture is one of the most popular complementary and alternative therapies. The efficacy of acupuncture in the treatment of inflammatory diseases has been widely reported (Li et al., 2007; Liu et al., 2022). Its anti-inflammatory effect is mainly achieved by activating the vagus nerve (Liu et al., 2013; Yu, 2022). It is performed by anatomically stimulating acupuncture points near the vagus nerve or its cutaneous branches in the ear, mastoid, and occipital regions (da Silva and Dorsher, 2014) and can be operated by manual or electrical stimulation (electroacupuncture) at different acupoints. In recent years, acupuncture has been widely recognized worldwide for its anti-inflammatory effects mediated by CAP. Acupuncture of the ear branch, which is mainly located in the stud and dorsal part of ear branch the ear, has been proven to directly affect vagus nerve activity or regulate the parasympathetic nerve (Nosadini et al., 1986; Gao et al., 2008; Imai et al., 2008; Imai et al., 2009; La Marca et al., 2010). Previous studies have found that the protective effects of electroacupuncture on the intestinal barrier are primarily associated

with CAP and the reduction of inflammatory cytokines (Borovikova et al., 2000; Baek et al., 2005). In addition, acupuncture has a neuroregulatory effect on the plant nervous system and can play a role in regulating the balance of the autonomic nervous system clinically. In a mouse model of endotoxemia, Borovikova et al. found that stimulation of the vagus nerve by electroacupuncture inhibits inflammatory mediators produced by macrophages in a concentration-dependent manner (Li et al., 2015). In animal models of arthritis, electroacupuncture inhibits the production of inflammatory cytokines such as IL-1, IL-6, IL-8, and TNF through choline and reduces inflammatory pain (Cai et al., 2019; Zhou et al., 2019). Auricular acupuncture and electroacupuncture "Zusanli" (ST36) inhibited the expression of the pro-inflammatory factors TNF-α and IL-6 in rat models of endotoxemia through the cholinergic anti-inflammatory pathway (Zhao et al., 2012). In addition, electroacupuncture ST36 increased local acetylcholine transferase, promotes ACh transcription and synthesis, inhibits NF-κB expression in lung tissue, and stimulates local CAP in the lung. In another study of LPS-induced systemic infections in animals, ST36 electroacupuncture activated the vagus nerve pathway that connects the spleen, reducing the production of TNF in the spleen (Lim et al., 2016). Low-intensity electroacupuncture at ST36 acupoint in the hindlimb can effectively reduce persistent systemic inflammation (Liu et al., 2020c). Studies have also shown that electroacupuncture "Hegu" (LI4) activates muscarinic acetylcholine receptor signals in the brain through somatic afferent, and then activates the efferent vagus nerve and splenic nerve, exerting an anti-inflammatory effect, reducing TNF, IL-1β, and IL-6 levels and improving survival rate in endotoxemia model rats (Song et al., 2012). In ischemic stroke, seven consecutive days of electroacupuncture on GV20 and GV24 also increase the expression of α7nAChR in hippocampal neurons and decreased the levels of proinflammatory cytokines TNF-α and IL-1β, leading to impaired learning and memory impairment (Liu et al., 2017b). These results suggested that acupuncture's CAP-mediated anti-inflammatory effects may improve neurological symptoms and may be an effective treatment for sleep disorders caused by COVID-19.

It is worth noting that the anti-inflammatory effect of electroacupuncture is related to acupoint selection, stimulation intensity, body condition, etc. To optimize the stimulation parameters and improve the efficacy and safety of acupuncture therapy, it is worth clinical research to investigate the stimulation intensity of electroacupuncture in driving different autonomic nerve pathways.

6.2 Transcutaneous auricular vagal stimulation

TaVNS comes from ear acupuncture. The ear is thought to be directly or indirectly connected to 12 meridians (six yang and six yin) (Round et al., 2013). Neuroanatomical evidence confirmed that the outer ear is the only region of the body where the vagus nerve sensory endings are located (Peuker and Filler, 2002). Recent clinical and animal experiments have shown that percutaneous auricular point vagus nerve stimulation can increase the excitability of efferent vagus nerve excitability, and increase the ACh release and CAP activation by stimulating the cochlea region. ACh binding to α7nAChR resulted in reduced secretion of inflammatory cytokines TNF, IL-1β, and IL-6 (Andersson and Tracey, 2012; Pavlov and Tracey, 2012; Kaczmarczyk et al., 2017). One study found that taVNS inhibited the expression of TNF-α, IL-1β, IL-6, and NF-kB p65 in endotoxemia rat serum through α7nAChR-mediated CAP (Jiang et al., 2018). The results implied that taVNS are a novel neurostimulation therapy with immunomodulatory and anti-inflammatory effects that may be beneficial for sleep disorders caused by inflammation caused by COVID-19.

6.3 Chinese herbal medicine

A large number of Chinese herbal medicine preparations for the treatment of lung diseases have an excellent effect. Activation of CAP is a theoretical basis for traditional Chinese treatment of COVID-19 infection. Berberine is an acetylcholinesterase inhibitor whose main active ingredient is derived from the Chinese herbal medicine Coptis Chinensis (Cho et al., 2006). Berberine has a neuroprotective effect by inhibiting acetylcholinesterase activity, increasing ACh levels and a7nAChR expression, thus regulating CAP, suppressing inflammation, and improving abnormal oxidative stress and cholinergic function (Li et al., 2016; Wang et al., 2019).

Jiao-Tai-Wan contains two kinds of Chinese herbal medicine: Coptis Chinensis and cinnamon. The Coptis Chinensis alkaloid is the most important component in Coptis Chinensis, possessing a variety of medicinal values. Studies have shown that berberine has antibacterial, antioxidant, cardiac, neuroprotective, and spasmodic effects (Ji and Shen, 2011; Park et al., 2012; Li et al., 2019). Cinnamon's main active ingredient is cinnamon, which has anti-inflammatory, antioxidant, and neuroprotective effects (Yang et al., 2016b). Another study has found that Jiao-Tai-Wan activates the cholinergic pathway and improves cognitive function by reducing acetylcholinesterase activity and increasing acetylcholinesterase content (Wang et al., 2018b).

Pharmacological studies have shown that dandelions have antimicrobial, antiviral, anticancer, antioxidant, anti-inflammatory, and anti-allergic effects (He et al., 2011; Ovadje et al., 2011; Ovadje et al., 2012; Qian et al., 2014; Wang, 2014; Ma et al., 2015; Ovadje et al., 2016; Jedrejek et al., 2017; Rehman et al., 2017; Ding and Wen,

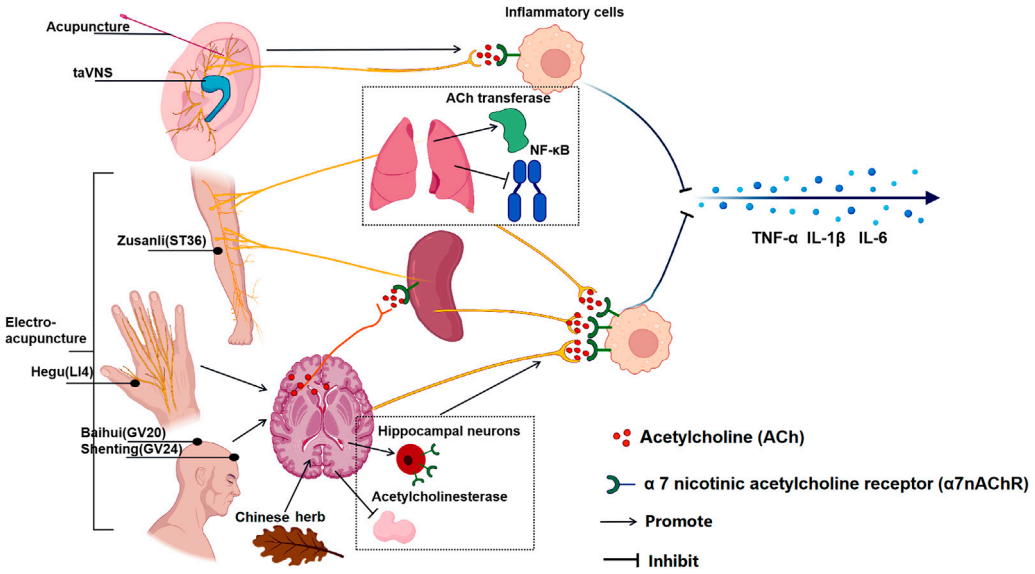

FIGURE 2
The effect of multiple TCT on CAP. Acupuncture and taVNS stimulating in ear branch can activate CAP and the reduce inflammatory cytokines; Auricular acupuncture and electroacupuncture "Zusanli" (ST36) increased the activity of local acetylcholine transferase, promoted the transcription and synthesis of ACh, inhibiting the expression of NF-κB in lung tissue and stimulating the CAP in the lung; Moreover, electroacupuncture ST36 activated the vagus nerve pathway connected to the spleen and reduced the production of TNF in the spleen; Electroacupuncture "Hegu" (LI4) activates muscarinic acetylcholine receptor signals in the brain, and then activates the efferent vagus nerve and splenic nerve to activate CAP; Electroacupuncture at "Baihui" (GV20) and "Shenting" (GV24) increase the expression of α7nAChR in hippocampal neurons; The chinese medcine Jiao-Tai-Wan reduced the activity of acetylcholinesterase (AChE) and increase the content of ACh. The ultimate effect of TCT is to activate CAP to reduce the production of inflammatory factors in effector organs to inhibit inflammation.

2018; Liu et al., 2018; Rahmat and Damon, 2018). Extract from Dandelion: ethyl acetate extract (EAED). Experimental results of precontraction of the tracheal ring in mice induced by high K + and ACH stimulation showed that EAED could inhibit the high concentration of Ca2+ caused by high potassium and acetylcholine. Improve airway hyperresponsiveness and reduce airway inflammation (Zhao et al., 2020). In addition, in an *in vivo* study, EAED effectively reduced ACh-induced respiratory resistance in healthy and asthmatic mice.

NHD is a traditional Chinese medicine prescription composed of albizzia bark, nocturnal vine, lily, and Lanzhi. A study of insomnia rodents induced by PCPA found that NHD has a good sedative effect in reducing exercise distance, prolonging sleep time, improving sleep quality, and improving depression, as. NHD effectively inhibits CNS excitability and relieves PCPA-induced insomnia by reducing dopamine, noradrenaline, and ACh levels (Yang et al., 2021). Figure 2 summarized the effect of multiple TCT on CAP.

7 The effect of traditional chinese therapy on sleep disorders

For patients with sleep disorders of different severity, the best treatment is individualized therapy tailored to each patient's symptoms which could implement appropriate physical therapy or external treatment. TCT may be an alternative treatment for this problem. A large meta-analysis on the effects of TCT concluded that acupuncture and taVNS therapy could relieve anxiety and alleviate sleep disturbance, and even lower depression level (Wang et al., 2022). Acupuncture and Chinese herbal medicine are most commonly used in the treatment of depression-related insomnia. Studies have verified their efficacy and safety in treating insomnia (Wang et al., 2006; Song, 2007; Liu and Wan, 2010; Huo et al., 2013). Two systematic studies showed that TCT had fewer adverse reactions to insomnia than Western medicine (Yang et al., 2019; Lin et al., 2021). However, there are still some limitations in the studies related to poor methodology in Chinese herbal medicine, such as complex chemical compositions and unclear efficacy that might be the result of the comprehensive action of all drug ingredients, which to some extent restrict clear conclusions. In addition, many other TCT treatments have also improved sleep disorders (Cho et al., 2013; Bergdahl et al., 2017; Karadag et al., 2017; Li et al., 2018; Meng et al., 2018; Jiao et al., 2020; Hu et al., 2021; Jiang et al., 2021; Jiang et al., 2022a; Jiang et al., 2022b). Table 3 summarizes the effects of most TCT treatments on sleep disorders under different conditions. These studies showed that TCT

TABLE 3 Summary for the effect of TCT on the sleep disorders.

Species and disease model	Symptoms	TCT methods	Follow-up time	Impact on sleep disorders[ref]
Human, patients In intensive care unit	Depression, anxiety, relaxation and disorders related with sleep and stress	Lavender essential oil	15 days	Alleviated patients' stress and improved their sleep quality (Karadag et al., 2017)
Huamn, sleep disorders	Insomnia	Thermosensitive moxibustion	15 days	Improved their sleep quality (Li et al., 2018)
Mice, chronic sleep deprivation	Sleep or wakefulness disorder	Traitional medicinal herb (Dendrobium nobile Lindl extract)	2 weeks	Might be used to prevent and treat sleep or wakefulness disorder (Jiang et al., 2022a)
Human, insomnia	Insomnia	Acupuncture	12 weeks	Might adjust the emotional brain regions in adult insomnia patients, resulting in an improvement in sleep (Jiang et al., 2022b)
Human, cancer	Cancer-related fatigue, anxiety, and poor sleep quality	Traditional Chinese medicine exercise therapy (Tai Chi, Ba Duan Jin, the classics of tendon changing, Six Healing Sounds, and Wu Qin Xi)	NA	Strengthened the body and relaxed the mind, which is of significance in promoting sleep disorders (Jiang et al., 2021)
Human, insomnia	Insomnia, anxiety, depression	Chinese patent medicine (Xiao Yao San)	NA	Beneficial for improving sleep quality and relieving anxiety (Hu et al., 2021)
Human, perimenopausal insomnia	Insomnia	Auricular intradermal needling combined with erjian (HX 6,7i) bloodletting	4 weeks	Improved the sleep quality of patients with perimenopausal sleep disorders (Meng et al., 2018)
Human, insomnia	Insomnia	Auricular Acupuncture	NA	Appeared to be effective for treating insomnia (Bergdahl et al., 2017)
Human, nursing home residents with sleep disorders and psychological distress	Poor sleep quality and psychological distress	Acupressure	1 month	Improved sleep quality, reduces psychological distress (Cho et al., 2013)
Human, insomnia	Insomnia	Transcutaneous Vagus Nerve Stimulation at Auricular Concha	4 weeks	TaVNS relieved insomnia, alleviated fatigue as well as other concomitant symptoms such as depression and anxiety (Jiao et al., 2020)

possesses a great effect on sleep disorders treatment, so it should be extremely informative for sleep disorders induced by COVID-19 in the future.

In summary, high-quality sleep contributes to a strong immune system, so it is possible to resist virus invasion and kill the invaded viruses and promote the recovery of physical function. Therefore, it is worth discussing whether TCT is necessary for the treatment of the patient sleep distress. Our review firstly analyzes the reasons for the sleep disorders caused by the novel coronavirus and found that inflammation was the main reason leading to sleep distress in patients. And we reviewed the mechanisms of three common traditional Chinese in inhibiting inflammation through CAP and relieving the sleep or symptoms. We, therefore, propose that TCT may be a potential strategy to take for the treatment of sleep problems due to inflammation caused by COVID-19.

Author contributions

XX and NZ conceived the idea, participated in its design and coordination, and drafted the manuscript. JF, ZW, and ZY searched all relevant references and collected the related information. ZL critically revised the manuscript. All authors read and approved the final manuscript.

Funding

This study was funded by the Institutional Foundation of Xi'an Jiaotong University No. xzy012022100, and Institutional Foundation of The First Affiliated Hospital of Xi'an Jiaotong University No. 2021QN-23.

Acknowledgments

We would like to thank the website of https://www.biorender.com for providing icons and cell morphological elements that used to complete our Figures 1, 2.

Conflict of interest

The authors declare that the research was conducted in the absence of any commercial or financial relationships that could be construed as a potential conflict of interest.

Publisher's note

References

Akıncı, T., and Melek Başar, H. (2021). Relationship between sleep quality and the psychological status of patients hospitalised with COVID-19. *Sleep. Med.* 80, 167–170. doi:10.1016/j.sleep.2021.01.034

Alfaro-Rodríguez, A., and González-Piña, R. (2005). Ozone-induced paradoxical sleep decrease is related to diminished acetylcholine levels in the medial preoptic area in rats. *Chem. Biol. Interact.* 151, 151–158. doi:10.1016/j.cbi.2004.10.001

Andersson, U., and Tracey, K. J. (2012). Reflex principles of immunological homeostasis. *Annu. Rev. Immunol.* 30, 313–335. doi:10.1146/annurev-immunol-020711-075015

Arnold, D. T., Milne, A., Samms, E., Stadon, L., Maskell, N. A., and Hamilton, F. W. (2021). Symptoms after COVID-19 vaccination in patients with persistent symptoms after acute infection: A case series. *Ann. Intern. Med.* 174, 1334–1336. doi:10.7326/M21-1976

Baek, Y. H., Choi, D. Y., Yang, H. I., and Park, D. S. (2005). Analgesic effect of electroacupuncture on inflammatory pain in the rat model of collagen-induced arthritis: mediation by cholinergic and serotonergic receptors. *Brain Res.* 1057, 181–185. doi:10.1016/j.brainres.2005.07.014

Baptista, A. F., Baltar, A., Okano, A. H., Moreira, A., Campos, A., Fernandes, A. M., et al. (2020). Applications of non-invasive neuromodulation for the management of disorders related to COVID-19. *Front. Neurol.* 11, 573718. doi:10.3389/fneur.2020.573718

Bergdahl, L., Broman, J. E., Berman, A. H., Haglund, K., von Knorring, L., and Markström, A. (2017). Sleep patterns in a randomized controlled trial of auricular acupuncture and cognitive behavioral therapy for insomnia. *Complement. Ther. Clin. Pract.* 28, 220–226. doi:10.1016/j.ctcp.2017.06.006

Bonaz, B., Sinniger, V., and Pellissier, S. (2016). Anti-inflammatory properties of the vagus nerve: potential therapeutic implications of vagus nerve stimulation. *J. Physiol.* 594, 5781–5790. doi:10.1113/JP271539

Borovikova, L. V., Ivanova, S., Zhang, M., Yang, H., Botchkina, G. I., Watkins, L. R., et al. (2000). Vagus nerve stimulation attenuates the systemic inflammatory response to endotoxin. *Nature* 405, 458–462. doi:10.1038/35013070

Cai, L., Lu, K., Chen, X., Huang, J. Y., Zhang, B. P., and Zhang, H. (2019). Auricular vagus nerve stimulation protects against postoperative cognitive dysfunction by attenuating neuroinflammation and neurodegeneration in aged rats. *Neurosci. Lett.* 703, 104–110. doi:10.1016/j.neulet.2019.03.034

Cao, Q., Jiang, Y., Cui, S. Y., Tu, P. F., Chen, Y. M., Ma, X. L., et al. (2016). Tenuifolin, a saponin derived from Radix Polygalae, exhibits sleep-enhancing effects in mice. *Phytomedicine* 23, 1797–1805. doi:10.1016/j.phymed.2016.10.015

Channappanavar, R., and Perlman, S. (2017). Pathogenic human coronavirus infections: Causes and consequences of cytokine storm and immunopathology. *Semin. Immunopathol.* 39, 529–539. doi:10.1007/s00281-017-0629-x

Chavan, S. S., Pavlov, V. A., and Tracey, K. J. (2017). Mechanisms and therapeutic relevance of neuroimmune communication. *Immunity* 46, 927–942. doi:10.1016/j.immuni.2017.06.008

Chen, Z., and Nakamura, T. (2004). Statistical evidence for the usefulness of Chinese medicine in the treatment of SARS. *Phytother. Res.* 18, 592–594. doi:10.1002/ptr.1485

Chen, N., Zhou, M., Dong, X., Qu, J., Gong, F., Han, Y., et al. (2020). Epidemiological and clinical characteristics of 99 cases of 2019 novel coronavirus pneumonia in wuhan, China: a descriptive study. *Lancet* 395, 507–513. doi:10.1016/S0140-6736(20)30211-7

Cheng, P., Casement, M. D., Kalmbach, D. A., Castelan, A. C., and Drake, C. L. (2021). Digital cognitive behavioral therapy for insomnia promotes later health resilience during the coronavirus disease 19 (COVID-19) pandemic. *Sleep* 44 (4), zsaa258. doi:10.1093/sleep/zsaa258

Cheng, P., Casement, M. D., Kalmbach, D. A., Castelan, A. C., and Drake, C. L. (2021). Digital cognitive behavioral therapy for insomnia promotes later health resilience during the coronavirus disease 19 (COVID-19) pandemic. *Sleep* 44, zsaa258. doi:10.1093/sleep/zsaa258

Cho, K. M., Yoo, I. D., and Kim, W. G. (2006). 8-hydroxydihydrochelerythrine and 8-hydroxydihydrosanguinarine with a potent acetylcholinesterase inhibitory activity from Chelidonium majus L. *Biol. Pharm. Bull.* 29, 2317–2320. doi:10.1248/bpb.29.2317

Cho, M. Y., Min, E. S., Hur, M. H., and Lee, M. S. (2013). Effects of aromatherapy on the anxiety, vital signs, and sleep quality of percutaneous coronary intervention patients in intensive care units. *Evid. Based. Complement. Altern. Med.* 2013, 381381. doi:10.1155/2013/381381

da Silva, M. A., and Dorsher, P. T. (2014). Neuroanatomic and clinical correspondences: acupuncture and vagus nerve stimulation. *J. Altern. Complement. Med.* 20, 233–240. doi:10.1089/acm.2012.1022

Dai, Y., Qiang, W., Gui, Y., Tan, X., Pei, T., Lin, K., et al. (2021). A large-scale transcriptional study reveals inhibition of COVID-19 related cytokine storm by traditional Chinese medicines. *Sci. Bull.* 66, 884–888. doi:10.1016/j.scib.2021.01.005

Ding, A., and Wen, X. (2018). Dandelion root extract protects NCM460 colonic cells and relieves experimental mouse colitis. *J. Nat. Med.* 72, 857–866. doi:10.1007/s11418-018-1217-7

Ding, X., and Yao, J. (2020). Peer education intervention on adolescents' anxiety, depression, and sleep disorder during the COVID-19 pandemic. *Psychiatr. Danub.* 32 (3-4), 527–535. doi:10.24869/psyd.2020.527

Doroftei, B., Ciobica, A., Ilie, O. D., Maftei, R., and Ilea, C. (2021). Mini-review discussing the reliability and efficiency of COVID-19 vaccines. *Diagnostics* 11, 579. doi:10.3390/diagnostics11040579

dos Santos, C. C., Shan, Y., Akram, A., Slutsky, A. S., and Haitsma, J. J. (2011). Neuroimmune regulation of ventilator-induced lung injury. *Am. J. Respir. Crit. Care Med.* 183, 471–482. doi:10.1164/rccm.201002-0314OC

Elder, G. J., Alfonso-Miller, P., Atkinson, W., Santhi, N., and Ellis, J. G. (2020). Testing an early online intervention for the treatment of disturbed sleep during the COVID-19 pandemic (sleep COVID-19): structured summary of a study protocol for a randomised controlled trial. *Trials* 21, 704. doi:10.1186/s13063-020-04644-0

Fu, W., Wang, C., Zou, L., Guo, Y., Lu, Z., Yan, S., et al. (2020). Psychological health, sleep quality, and coping styles to stress facing the COVID-19 in Wuhan, China. *Transl. Psychiatry* 10, 225. doi:10.1038/s41398-020-00913-3

Fucile, S., Renzi, M., Lax, P., and Eusebi, F. (2003). Fractional Ca(2+) current through human neuronal alpha7 nicotinic acetylcholine receptors. *Cell Calcium* 34, 205–209. doi:10.1016/s0143-4160(03)00071-x

Gao, X. Y., Zhang, S. P., Zhu, B., and Zhang, H. Q. (2008). Investigation of specificity of auricular acupuncture points in regulation of autonomic function in anesthetized rats. *Auton. Neurosci.* 138, 50–56. doi:10.1016/j.autneu.2007.10.003

Gimeno, D., Kivimäki, M., Brunner, E. J., Elovainio, M., De Vogli, R., Steptoe, A., et al. (2009). Associations of C-reactive protein and interleukin-6 with cognitive symptoms of depression: 12-year follow-up of the whitehall II study. *Psychol. Med.* 39, 413–423. doi:10.1017/S0033291708003723

Go, Y. Y., Ju, W. M., Lee, C. M., Chae, S. W., and Song, J. J. (2022). Different transcutaneous auricular vagus nerve stimulation parameters modulate the anti-inflammatory effects on lipopolysaccharide-induced acute inflammation in mice. *Biomedicines* 10, 247. doi:10.3390/biomedicines10020247

Go, Y. Y., Ju, W. M., Lee, C. M., Chae, S. W., and Song, J. J. (2022). Different transcutaneous auricular vagus nerve stimulation parameters modulate the anti-inflammatory effects on lipopolysaccharide-induced acute inflammation in mice. *Biomedicines* 10, 247. doi:10.3390/biomedicines10020247

Guo, J., Feng, X. L., Wang, X. H., and van Ijzendoorn, M. H. (2020). Coping with COVID-19:exposure to COVID-19 and negative impact on livelihood predict elevated mental health problems in Chinese adults. *Int. J. Environ. Res. Public Health* 17, 3857. doi:10.3390/ijerph17113857

Hambrecht-Wiedbusch, V. S., Gauthier, E. A., Baghdoyan, H. A., and Lydic, R. (2010). Benzodiazepine receptor agonists cause drug-specific and state-specific alterations in EEG power and acetylcholine release in rat pontine reticular formation. *Sleep* 33, 909–918. doi:10.1093/sleep/33.7.909

He, W., Han, H., Wang, W., and Gao, B. (2011). Anti-influenza virus effect of aqueous extracts from dandelion. *Virol. J.* 8, 538. doi:10.1186/1743-422X-8-538

Hogan, D., Morrow, J. D., Smith, E. M., and Opp, M. R. (2003). Interleukin-6 alters sleep of rats. *J. Neuroimmunol.* 137, 59–66. doi:10.1016/s0165-5728(03)00038-9

Hsu, C. H., Hwang, K. C., Chao, C. L., Chang, S. G., Ho, M. S., and Chou, P. (2006). Can herbal medicine assist against avian flu? Learning from the experience of using supplementary treatment with Chinese medicine on SARS or SARS-like infectious disease in 2003. *J. Altern. Complement. Med.* 12, 505–506. doi:10.1089/acm.2006.12.505

Hu, J., Teng, J., Wang, W., Yang, N., Tian, H., Zhang, W., et al. (2021). Clinical efficacy and safety of traditional Chinese medicine Xiao Yao San in insomnia combined with anxiety. *Med. Baltim.* 100, e27608. doi:10.1097/MD.0000000000027608

Huang, C., Wang, Y., Li, X., Ren, L., Zhao, J., Hu, Y., et al. (2020). Clinical features of patients infected with 2019 novel coronavirus in Wuhan, China. *Lancet* 395, 497–506. doi:10.1016/S0140-6736(20)30183-5

Huang, C., Huang, L., Wang, Y., Li, X., Ren, L., Gu, X., et al. (2021). 6-month consequences of COVID-19 in patients discharged from hospital: a cohort study. *Lancet* 397, 220–232. doi:10.1016/S0140-6736(20)32656-8

Huo, Z. J., Guo, J., and Li, D. (2013). Effects of acupuncture with meridian acupoints and three Anmian acupoints on insomnia and related depression and anxiety state. *Chin. J. Integr. Med.* 19, 187–191. doi:10.1007/s11655-012-1240-6

Imai, K., Ariga, H., Chen, C., Mantyh, C., Pappas, T. N., and Takahashi, T. (2008). Effects of electroacupuncture on gastric motility and heart rate variability in conscious rats. *Auton. Neurosci.* 138, 91–98. doi:10.1016/j.autneu.2007.11.003

Imai, K., Ariga, H., and Takahashi, T. (2009). Electroacupuncture improves imbalance of autonomic function under restraint stress in conscious rats. *Am. J. Chin. Med.* 37, 45–55. doi:10.1142/S0192415X0900662X

Jasper, H. H., and Tessier, J. (1971). Acetylcholine liberation from cerebral cortex during paradoxical (REM) sleep. *Science* 172, 601–602. doi:10.1126/science.172.3983.601

Jedrejek, D., Kontek, B., Lis, B., Stochmal, A., and Olas, B. (2017). Evaluation of anti-oxidant activity of phenolic fractions from the leaves and petals of dandelion in human plasma treated with H2O2 and H2O2/Fe. *Chem. Biol. Interact.* 262, 29–37. doi:10.1016/j.cbi.2016.12.003

Ji, H. F., and Shen, L. (2011). Berberine: a potential multipotent natural product to combat alzheimer's disease. *Mol. (Basel, Switz.* 16, 6732–6740. doi:10.3390/molecules16086732

Jiang, Y., Cao, Z., Ma, H., Wang, G., Wang, X., Wang, Z., et al. (2018). Auricular vagus nerve stimulation exerts antiinflammatory effects and immune regulatory function in a 6-OHDA model of Parkinson's disease. *Neurochem. Res.* 43, 2155–2164. doi:10.1007/s11064-018-2639-z

Jiang, L., Ouyang, J., and Du, X. (2021). Effects of traditional Chinese medicine exercise therapy on cancer-related fatigue, anxiety and sleep quality in cancer patients: A protocol for systematic review and network meta-analysis. *Med. Baltim.* 100, e27681. doi:10.1097/MD.0000000000027681

Jiang, N., Li, Y. J., Wang, M. D., Huang, H., Chen, S., Liu, X., et al. (2022). The cognitive-enhancing effects of dendrobium nobile lindl extract in sleep deprivation-induced amnesic mice. *Front. Psychiatry* 12, 596017. doi:10.3389/fpsyt.2021.596017

Jiang, T., Zhang, Q., Yuan, F., Zhang, F., and Guo, J. (2022). Efficacy of acupuncture and its influence on the emotional network in adult insomnia patients: protocol for a randomized controlled clinical trial. *Trials* 23, 11. doi:10.1186/s13063-021-05913-2

Jiao, Y., Guo, X., Luo, M., Li, S., Liu, A., Zhao, Y., et al. (2020). Effect of transcutaneous vagus nerve stimulation at auricular concha for insomnia: A randomized clinical trial. *Evid. Based. Complement. Altern. Med.* 2020, 6049891. doi:10.1155/2020/6049891

Kaczmarczyk, R., Tejera, D., Simon, B. J., and Heneka, M. T. (2017). Microglia modulation through external vagus nerve stimulation in a murine model of Alzheimer's disease. *J. Neurochem.* 146, 76–85. doi:10.1111/jnc.14284

Karadag, E., Samancioglu, S., Ozden, D., and Bakir, E. (2017). Effects of aromatherapy on sleep quality and anxiety of patients. *Nurs. Crit. Care* 22, 105–112. doi:10.1111/nicc.12198

Koralnik, I. J., and Tyler, K. L. (2020). COVID-19: a global threat to the nervous system. *Ann. Neurol.* 88, 1–11. doi:10.1002/ana.25807

Krueger, J. M., and Majde, J. A. (1995). Cytokines and sleep. *Int. Arch. Allergy Immunol.* 106, 97–100. doi:10.1159/000236827

Kubota, T., Fang, J., Kushikata, T., and Krueger, J. M. (2000). Interleukin-13 and transforming growth factor-beta1 inhibit spontaneous sleep in rabbits. *Am. J. Physiol. Regul. Integr. Comp. Physiol.* 279, R786–R792. doi:10.1152/ajpregu.2000.279.3.R786

Kubota, T., Brown, R. A., Fang, J., and Krueger, J. M. (2001). Interleukin-15 and interleukin-2 enhance non-REM sleep in rabbits. *Am. J. Physiol. Regul. Integr. Comp. Physiol.* 281, R1004–R1012. doi:10.1152/ajpregu.2001.281.3.R1004

Kubota, T., Majde, J. A., Brown, R. A., and Krueger, J. M. (2001). Tumor necrosis factor receptor fragment attenuates interferon-γ-induced non-REM sleep in rabbits. *J. Neuroimmunol.* 119, 192–198. doi:10.1016/s0165-5728(01)00382-4

Kushikata, T., Fang, J., and Krueger, J. M. (1999). Interleukin-10 inhibits spontaneous sleep in rabbits. *J. Interferon Cytokine Res.* 19, 1025–1030. doi:10.1089/107999099313244

Kwenandar, F., Japar, K. V., Damay, V., Hariyanto, T. I., Tanaka, M., Lugito, N. P. H., et al. (2020). Coronavirus disease 2019 and cardiovascular system: A narrative review. *Int. J. Cardiol. Heart Vasc.* 29, 100557. doi:10.1016/j.ijcha.2020.100557

La Marca, R., Nedeljkovic, M., Yuan, L., Maercker, A., and Ehlert, U. (2010). Effects of auricular electrical stimulation on vagal activity in healthy men: evidence from a three-armed randomized trial. *Clin. Sci.* 118, 537–546. doi:10.1042/CS20090264

Lai, J., Ma, S., Wang, Y., Cai, Z., Hu, J., Wei, N., et al. (2020). Factors associated with mental health outcomes among health care workers exposed to coronavirus disease 2019. *JAMA Netw. Open* 3, e203976. doi:10.1001/jamanetworkopen.2020.3976

Lange, T., Dimitrov, S., and Born, J. (2010). Effects of sleep and circadian rhythm on the human immune system. *Ann. N. Y. Acad. Sci.* 1193, 48–59. doi:10.1111/j.1749-6632.2009.05300.x

Li, Y. Q., Zhu, B., Rong, P. J., Ben, H., and Li, Y. H. (2007). Neural mechanism of acupuncture-modulated gastric motility. *World J. Gastroenterol.* 13, 709–716. doi:10.3748/wjg.v13.i5.709

Li, J., Li, J., Chen, R., and Cai, G. (2015). Targeting NF-κB and TNF-α activation by electroacupuncture to suppress collagen-induced rheumatoid arthritis in model rats. *Altern. Ther. Health Med.* 21, 26–34.

Li, F., Zhao, Y. B., Wang, D. K., Zou, X., Fang, K., and Wang, K. F. (2016). Berberine relieves insulin resistance via the cholinergic anti-inflammatory pathway in HepG2 cells. *J. Huazhong Univ. Sci. Technol. Med. Sci.* 36, 64–69. doi:10.1007/s11596-016-1543-5

Li, L. C., Xing, H. J., Liang, Y., Hu, Y. H., An, X., He, X. X., et al. (2018). Comparison of therapeutic effects between thermosensitive moxibustion and medication in the treatment of insomnia of liver-qi stagnation pattern. *Acupunct. Res.* 43, 573–575. doi:10.13702/j.1000-0607.170765

Li, W., Yin, N., Tao, W., Wang, Q., Fan, H., and Wang, Z. (2019). Berberine suppresses IL-33-induced inflammatory responses in mast cells by inactivating NF-κB and p38 signaling. *Int. Immunopharmacol.* 66, 82–90. doi:10.1016/j.intimp.2018.11.009

Lim, H. D., Kim, M. H., Lee, C. Y., and Namgung, U. (2016). Anti-inflammatory effects of acupuncture stimulation via the vagus nerve. *Plos One* 11, e0151882. doi:10.1371/journal.pone.0151882

Lin, S. C., Ho, C. T., Chuo, W. H., Li, S., Wang, T. T., and Lin, C. C. (2017). Effective inhibition of MERS-CoV infection by resveratrol. *BMC Infect. Dis.* 17, 144. doi:10.1186/s12879-017-2253-8

Lin, Y. H., Chen, C., Zhao, X., Mao, Y. F., Xiang, G. X., Yang, M. Q., et al. (2021). Efficacy and safety of banxia formulae for insomnia: A systematic review and meta-analysis of high-quality randomized controlled trials. *Evid. Based. Complement. Altern. Med.* 2021, 8833168. doi:10.1155/2021/8833168

Liu, Q. X., and Wan, H. (2010). Treatment of 60 cases of insomnia with depression by the combination of Wu Ling Capsule and acupuncture. *JGMCM* 25, 2269–2270.

Liu, R. P., Fang, J. L., Rong, P. J., Zhao, Y., Meng, H., Ben, H., et al. (2013). Effects of electroacupuncture at auricular concha region on the depressive status of unpredictable chronic mild stress rat models. *Evid. Based. Complement. Altern. Med.* 2013, 789674. doi:10.1155/2013/789674

Liu, F., Li, Y., Jiang, R., Nie, C., Zeng, Z., Zhao, N., et al. (2015). miR-132 inhibits lipopolysaccharide-induced inflammation in alveolar macrophages by the cholinergic anti-inflammatory pathway. *Exp. Lung Res.* 41, 261–269. doi:10.3109/01902148.2015.1004206

Liu, Y., Tao, T., Li, W., and Bo, Y. (2017). Regulating autonomic nervous system homeostasis improves pulmonary function in rabbits with acute lung injury. *BMC Pulm. Med.* 17, 98. doi:10.1186/s12890-017-0436-0

Liu, J., Li, C., Peng, H., Yu, K., Tao, J., Lin, R., et al. (2017). Electroacupuncture attenuates learning and memory impairment via activation of α7nAChR-mediated anti-inflammatory activity in focal cerebral ischemia/reperfusion injured rats. *Exp. Ther. Med.* 14, 939–946. doi:10.3892/etm.2017.4622

Liu, Q., Zhao, H., Gao, Y., Meng, Y., Zhao, X. X., and Pan, S. N. (2018). Effects of dandelion extract on the proliferation of rat skeletal muscle cells and the inhibition

of a lipopolysaccharide-induced inflammatory reaction. *Chin. Med. J.* 131, 1724–1731. doi:10.4103/0366-6999.235878

Liu, K., Zhang, W., Yang, Y., Zhang, J., Li, Y., and Chen, Y. (2020). Respiratory rehabilitation in elderly patients with COVID-19: A randomized controlled study. *Complement. Ther. Clin. Pract.* 39, 101166. doi:10.1016/j.ctcp.2020.101166

Liu, Z., Qin, G., Mana, L., Dong, Y., Huang, S., Wang, Y., et al. (2020). GAPT regulates cholinergic dysfunction and oxidative stress in the brains of learning and memory impairment mice induced by scopolamine. *Brain Behav.* 10, e01602. doi:10.1002/brb3.1602

Liu, S., Wang, Z. F., Su, Y. S., Ray, R. S., Jing, X. H., Wang, Y. Q., et al. (2020). Somatotopic organization and intensity dependence in driving distinct NPY-expressing sympathetic pathways by electroacupuncture. *Neuron* 108, 436–450. doi:10.1016/j.neuron.2020.07.015

Liu, S., Wang, Z., Su, Y., Qi, L., Yang, W., Fu, M., et al. (2021). A neuroanatomical basis for electroacupuncture to drive the vagal-adrenal axis. *Nature* 598, 641–645. doi:10.1038/s41586-021-04001-4

Liu, S., Wang, Z., Su, Y., Qi, L., Yang, W., Fu, M., et al. (2022). Author correction: a neuroanatomical basis for electroacupuncture to drive the vagal-adrenal axis. *Nature* 601, E9. doi:10.1038/s41586-021-04290-9

Lu, Y., Zhu, H., Wang, Q., Tian, C., Lai, H., Hou, L., et al. (2022). Comparative effectiveness of multiple acupuncture therapies for primary insomnia: a systematic review and network meta-analysis of randomized trial. *Sleep. Med.* 93, 39–48. doi:10.1016/j.sleep.2022.03.012

Luan, X., Zhang, X., and Zhou, Y. (2022). The role and clinical observation of traditional Chinese medicine in relieving senile insomnia: A systematic review and meta-analysis. *Biomed. Res. Int.* 2022, 9484095. doi:10.1155/2022/9484095

Lv, Z. Y., Shi, Y. L., Bassi, G. S., Chen, Y. J., Yin, L. M., Wang, Y., et al. (2022). Electroacupuncture at ST36 (zusanli) prevents T-cell lymphopenia and improves survival in septic mice. *J. Inflamm. Res.* 15, 2819–2833. doi:10.2147/JIR.S361466

Ma, C., Zhu, L., Wang, J., He, H., Chang, X., Gao, J., et al. (2015). Anti-inflammatory effects of water extract of Taraxacum mongolicum hand-Mazz on lipopolysaccharide-induced inflammation in acute lung injury by suppressing PI3K/Akt/mTOR signaling pathway. *J. Ethnopharmacol.* 168, 349–355. doi:10.1016/j.jep.2015.03.068

Mehta, P., McAuley, D. F., Brown, M., Sanchez, E., Tattersall, R. S., Manson, J. J., et al. (2020). COVID-19: consider cytokine storm syndromes and immunosuppression. *LANCET* 395, 1033–1034. doi:10.1016/S0140-6736(20)30628-0

Meneses, G., Bautista, M., Florentino, A., Diaz, G., Acero, G., Besedovsky, H., et al. (2016). Electric stimulation of the vagus nerve reduced mouse neuroinflammation induced by lipopolysaccharide. *J. Inflamm.* 13, 33. doi:10.1186/s12950-016-0140-5

Meng, F., Gong, W. J., Liao, Y. X., Xu, H. W., and Wang, X. (2018). Effect of auricular intradermal needling combined with erjian (HX6, 7i) bloodletting on sleep quality and neuroendocrine level in patients with perimenopausal insomnia. *Chin. Acupunct. Moxibust* 38, 575–579. doi:10.13703/j.0255-2930.2018.06.002

Meng, Z., Sun, B., Chen, W., Zhang, X., Huang, M., and Xu, J. (2021). Depression of non-neuronal cholinergic system may play a role in Co-occurrence of subjective daytime sleepiness and hypertension in patients with obstructive sleep apnea syndrome. *Nat. Sci. Sleep.* 13, 2153–2163. doi:10.2147/NSS.S339038

Nosadini, A., Costantini, M., Ambrosio, F., Zaninotto, G., Ruol, A., Tremolada, C., et al. (1986). Lower esophageal sphincter and acupuncture: electromanometric evaluation in esophageal achalasia. *Dig. Surg.* 3, 243–245. doi:10.1159/000171737

Opp, M. R. (2005). Cytokines and sleep. *Sleep. Med. Rev.* 9, 355–364. doi:10.1016/j.smrv.2005.01.002

Otuyama, L. J., Rizzi, C. F., Piovezan, R. D., Werli, K. S., Brasil, E. L., Sukys-Claudino, L., et al. (2013). The cholinergic system may play a role in the pathophysiology of residual excessive sleepiness in patients with obstructive sleep apnea. *Med. Hypotheses* 81, 509–511. doi:10.1016/j.mehy.2013.06.024

Ovadje, P., Chatterjee, S., Griffin, C., Tran, C., Hamm, C., and Pandey, S. (2011). Selective induction of apoptosis through activation of caspase-8 in human leukemia cells (Jurkat) by dandelion root extract. *J. Ethnopharmacol.* 133, 86–91. doi:10.1016/j.jep.2010.09.005

Ovadje, P., Chochkeh, M., Akbari-Asl, P., Hamm, C., and Pandey, S. (2012). Selective induction of apoptosis and autophagy through treatment with dandelion root extract in human pancreatic cancer cells. *Pancreas* 41, 1039–1047. doi:10.1097/MPA.0b013e31824b22a2

Ovadje, P., Ammar, S., Guerrero, J. A., Arnason, J. T., and Pandey, S. (2016). Dandelion root extract affects colorectal cancer proliferation and survival through the activation of multiple death signalling pathways. *Oncotarget* 7, 73080–73100. doi:10.18632/oncotarget.11485

Park, H. J., Lee, P. H., Ahn, Y. W., Choi, Y. J., Lee, G., Lee, D. Y., et al. (2007). Neuroprotective effect of nicotine on dopaminergic neurons by anti-inflammatory action. *Eur. J. Neurosci.* 26, 79–89. doi:10.1111/j.1460-9568.2007.05636.x

Park, D., Lee, H. J., Joo, S. S., Bae, D. K., Yang, G., Yang, Y. H., et al. (2012). Human neural stem cells over-expressing choline acetyltransferase restore cognition in rat model of cognitive dysfunction. *Exp. Neurol.* 234, 521–526. doi:10.1016/j.expneurol.2011.12.040

Passos, L., Prazeres, F., Teixeira, A., and Martins, C. (2020). Impact on mental health due to COVID-19 pandemic: Cross-sectional study in Portugal and Brazil. *Int. J. Environ. Res. Public Health* 17, E6794. doi:10.3390/ijerph17186794

Pavlov, V. A., and Tracey, K. J. (2012). The vagus nerve and the inflammatory reflex--linking immunity and metabolism. *Nat. Rev. Endocrinol.* 8, 743–754. doi:10.1038/nrendo.2012.189

Pavlov, V. A., and Tracey, K. J. (2015). Neural circuitry and immunity. *Immunol. Res.* 63, 38–57. doi:10.1007/s12026-015-8718-1

Pavlov, V. A., Wang, H., Czura, C. J., Friedman, S. G., and Tracey, K. J. (2003). The cholinergic anti-inflammatory pathway: a missing link in neuroimmunomodulation. *Mol. Med.* 9, 125–134. doi:10.1007/bf03402177

Peuker, E. T., and Filler, T. J. (2002). The nerve supply of the human auricle. *Clin. Anat.* 15, 35–37. doi:10.1002/ca.1089

Polack, F. P., Thomas, S. J., Kitchin, N., Absalon, J., Gurtman, A., Lockhart, S., et al. (2020). Safety and efficacy of the BNT162b2 mRNA Covid-19 vaccine. *N. Engl. J. Med.* 383, 2603–2615. doi:10.1056/NEJMoa2034577

Qian, L., Zhou, Y., Teng, Z., Du, C. L., and Tian, C. (2014). Preparation and antibacterial activity of oligosaccharides derived from dandelion. *Int. J. Biol. Macromol.* 64, 392–394. doi:10.1016/j.ijbiomac.2013.12.031

Qin, Z., Wan, J. J., Sun, Y., Wu, T., Wang, P. Y., Du, P., et al. (2017). Nicotine protects against DSS colitis through regulating microRNA-124 and STAT3. *J. Mol. Med.* 95 (2), 221–233. doi:10.1007/s00109-016-1473-5

Rahmat, L. T., and Damon, L. E. (2018). The use of natural health products especially papaya leaf extract and dandelion root extract in previously untreated chronic myelomonocytic leukemia. *Case Rep. Hematol.* 2018, 7267920. doi:10.1155/2018/7267920

Ranjbaran, Z., Keefer, L., Stepanski, E., Farhadi, A., and Keshavarzian, A. (2007). The relevance of sleep abnormalities to chronic inflammatory conditions. *Inflamm. Res.* 56, 51–57. doi:10.1007/s00011-006-6067-1

Rehman, G., Hamayun, M., Iqbal, A., Khan, S. A., Khan, H., Shehzad, A., et al. (2017). Effect of methanolic extract of dandelion roots on cancer cell lines and AMP-activated protein kinase pathway. *Front. Pharmacol.* 8, 875. doi:10.3389/fphar.2017.00875

Ren, C., Tong, Y. L., Li, J. C., Lu, Z. Q., and Yao, Y. M. (2017). The protective effect of alpha 7 nicotinic acetylcholine receptor activation on critical illness and its mechanism. *Int. J. Biol. Sci.* 13, 46–56. doi:10.7150/ijbs.16404

Round, R., Litscher, G., and Bahr, F. (2013). Auricular acupuncture with laser. *Evid. Based Complement. Altern. Med.* 2013, 984763. doi:10.1155/2013/984763

Saint-Mleux, B., Eggermann, E., Bisetti, A., Bayer, L., Machard, D., Jones, B. E., et al. (2004). Nicotinic enhancement of the noradrenergic inhibition of sleep-promoting neurons in the ventrolateral preoptic area. *J. Neurosci.* 24, 63–67. doi:10.1523/JNEUROSCI.0232-03.2004

Sarris, J. (2012). Chinese herbal medicine for sleep disorders: poor methodology restricts any clear conclusion. *Sleep. Med. Rev.* 16, 493–495. doi:10.1016/j.smrv.2012.06.004

Song, X. M., Li, J. G., Wang, Y. L., Hu, Z. F., Zhou, Q., Du, Z. H., et al. (2008). The protective effect of the cholinergic anti-inflammatory pathway against septic shock in rats. *Shock* 30, 468–472. doi:10.1097/SHK.0b013e31816d5e49

Song, J. G., Li, H. H., Cao, Y. F., Lv, X., Zhang, P., Li, Y. S., et al. (2012). Electroacupuncture improves survival in rats with lethal endotoxemia via the autonomic nervous system. *Anesthesiology* 116, 406–414. doi:10.1097/ALN.0b013e3182426ebd

Song, Q. (2007). 56 cases of correlation between acupuncture baihui EX-HN1 treatment of depression insomnia. *Cap. Med.* 48, 48–49.

Stockelman, K. A., Bain, A. R., Dow, C. A., Diehl, K. J., Greiner, J. J., Stauffer, B. L., et al. (2021). Regular aerobic exercise counteracts endothelial vasomotor dysfunction associated with insufficient sleep. *Am. J. Physiol. Heart Circ. Physiol.* 320, H1080–H1088. doi:10.1152/ajpheart.00615.2020

Tarsitani, L., Vassalini, P., Koukopoulos, A., Borrazzo, C., Alessi, F., Di Nicolantonio, C., et al. (2021). Post-traumatic stress disorder among COVID-19 survivors at 3-month follow-up after hospital discharge. *J. Gen. Intern. Med.* 36, 1702–1707. doi:10.1007/s11606-021-06731-7

Wan, Y., Shang, J., Graham, R., Baric, R. S., and Li, F. (2020). Receptor recognition by the novel coronavirus from wuhan: an analysis based on decade-long structural studies of SARS coronavirus. *J. Virol.* 94, 001277-20. doi:10.1128/JVI.00127-20

Wang, J., Jiang, J. F., and Wang, L. L. (2006). Clinical observation on governor vessel Daoqi method for treatment of dyssomnia in the patient of depression. *Chin. Acupuncture&Moxibusion.* 26, 328–330.

Wang, H., Yang, G., Wang, S., Zheng, X., Zhang, W., and Li, Y. (2018). The most commonly treated acupuncture indications in the United States: A cross-sectional study. *Am. J. Chin. Med.* 46, 1387–1419. doi:10.1142/S0192415X18500738

Wang, X. C., Xu, Y. M., Li, H. Y., Wu, C. Y., Xu, T. T., Luo, N. C., et al. (2018). Jiao-tai-wan improves cognitive dysfunctions through cholinergic pathway in scopolamine-treated mice. *Biomed. Res. Int.* 2018, 3538763. doi:10.1155/2018/3538763

Wang, K., Chen, Q., Wu, N., Li, Y., Zhang, R., Wang, J., et al. (2019). Berberine ameliorates spatial learning memory impairment and modulates cholinergic anti-inflammatory pathway in diabetic rats. *Front. Pharmacol.* 10, 1003. doi:10.3389/fphar.2019.01003

Wang, J., Chen, Y., Zhai, X., Chu, Y., Liu, X., and Ma, X. (2022). Visualizing research trends and identifying hotspots of traditional Chinese medicine (TCM) nursing technology for insomnia: A 18-years bibliometric analysis of web of science core collection. *Front. Neurol.* 13, 816031. doi:10.3389/fneur.2022.816031

Wang, H. B. (2014). Cellulase-assisted extraction and antibacterial activity of polysaccharides from the dandelion *Taraxacum officinale*. *Carbohydr. Polym.* 103, 140–142. doi:10.1016/j.carbpol.2013.12.029

Weiner, L., Berna, F., Nourry, N., Severac, F., Vidailhet, P., and Mengin, A. C. (2020). Efficacy of an online cognitive behavioral therapy program developed for healthcare workers during the COVID-19 pandemic: the REduction of STress (REST) study protocol for a randomized controlled trial. *Trials* 21, 870. doi:10.1186/s13063-020-04772-7

Xu, Z., Zhang, D., Xu, D., Li, X., Xie, Y. J., Sun, W., et al. (2021). Loneliness, depression, anxiety, and post-traumatic stress disorder among Chinese adults during COVID-19: A cross-sectional online survey. *Plos one* 16, e0259012. doi:10.1371/journal.pone.0259012

Xue, R., Wan, Y., Sun, X., Zhang, X., Gao, W., and Wu, W. (2019). Nicotinic mitigation of neuroinflammation and oxidative stress after chronic sleep deprivation. *Front. Immunol.* 10, 2546. doi:10.3389/fimmu.2019.02546

Yamada, M., and Ichinose, M. (2018). The cholinergic anti-inflammatory pathway:an innovative treatment strategy for respiratory diseases and their comorbidities. *Curr. Opin. Pharmacol.* 40, 18–25. doi:10.1016/j.coph.2017.12.003

Yang, X., Zhao, C., Gao, Z., and Su, X. (2014). A novel regulator of lung inflammation and immunity: pulmonary parasympathetic inflammatory reflex. *QJM* 107, 789–792. doi:10.1093/qjmed/hcu005

Yang, G., Hu, R. Y., Deng, A. J., Huang, Y., and Li, J. (2016). Effects of electro-acupuncture at zusanli, guanyuan for sepsis patients and its mechanism through immune regulation. *Chin. J. Integr. Med.* 22, 219–224. doi:10.1007/s11655-016-2462-9

Yang, D., Liang, X. C., Shi, Y., Sun, Q., Liu, D., Liu, W., et al. (2016). Anti-oxidative and anti-inflammatory effects of cinnamaldehyde on protecting high glucose-induced damage in cultured dorsal root ganglion neurons of rats. *Chin. J. Integr. Med.* 22, 19–27. doi:10.1007/s11655-015-2103-8

Yang, X. Q., Liu, L., Ming, S. P., Fang, J., and Wu, D. N. (2019). Tian Wang bu xin dan for insomnia: A systematic review of efficacy and safety. *Evid. Based. Complement. Altern. Med.* 2019, 4260801. doi:10.1155/2019/4260801

Yang, Y., Wu, Y., Xu, P., Guo, F., Guo, F., and Yang, B. (2021). Nyctinastic herbs decoction improves para-chlorophenylalanine-induced insomnia by regulating the expression level of neurotransmitters. *Ann. Transl. Med.* 9, 1524. doi:10.21037/atm-21-4462

Yang, Z., Liu, Y., Wang, L., Lin, S., Dai, X., Yan, H., et al. (2022). Traditional Chinese medicine against COVID-19: Role of the gut microbiota. *Biomed. Pharmacother.* 149, 112787. doi:10.1016/j.biopha.2022.112787

Yu, X. (2022). Potential value of electroacupuncture in the treatment of gastrointestinal symptoms of COVID-19. *Inflamm. Bowel Dis.* 28, e21. doi:10.1093/ibd/izab223

Zant, J. C., Kim, T., Prokai, L., Szarka, S., McNally, J., McKenna, J. T., et al. (2016). Cholinergic neurons in the basal forebrain promote wakefulness by actions on neighboring non-cholinergic neurons:An opto-dialysis study. *J. Neurosci.* 36, 2057–2067. doi:10.1523/JNEUROSCI.3318-15.2016

Zhang, J., Lu, H., Zeng, H., Zhang, S., Du, Q., Jiang, T., et al. (2020). The differential psychological distress of populations affected by the COVID-19 pandemic. *Brain Behav. Immun.* 87, 49–50. doi:10.1016/j.bbi.2020.04.031

Zhao, Y. X., He, W., Jing, X. H., Liu, J. L., Rong, P. J., Ben, H., et al. (2012). Transcutaneous auricular vagus nerve stimulation protects endotoxemic rat from lipopolysaccharide-induced inflammation. *Evid. Based Complement. Altern. Med.* 2012, 627023. doi:10.1155/2012/627023

Zhao, P., Liu, J., Ming, Q., Tian, D., He, J., Yang, Z., et al. (2020). Dandelion extract relaxes mouse airway smooth muscle by blocking VDLCC and NSCC channels. *Cell Biosci.* 10, 125. doi:10.1186/s13578-020-00470-8

Zhou, L., Filiberti, A., Humphrey, M. B., Fleming, C. D., Scherlag, B. J., Po, S. S., et al. (2019). Low-level transcutaneous vagus nerve stimulation attenuates cardiac remodelling in a rat model of heart failure with preserved ejection fraction. *Exp. Physiol.* 104, 28–38. doi:10.1113/EP087351

Zhou, Y., Chi, J., Lv, W., and Wang, Y. (2021). Obesity and diabetes as high-risk factors for severe coronavirus disease 2019 (Covid -19). *Diabetes. Metab. Res. Rev.Covid-19)* 37 (2), e3377. doi:10.1002/dmrr.3377

frontiers | Frontiers in Pharmacology

TYPE Review
PUBLISHED 11 October 2022
DOI 10.3389/fphar.2022.1035954

OPEN ACCESS

EDITED BY
Dongdong Sun,
Nanjing University of Chinese Medicine, China

REVIEWED BY
Xiaohong Zhao,
Moffitt Cancer Center, United States
Yu Cai,
Jinan University, China

*CORRESPONDENCE
Qiming Zhang,
zhang_917@126.com
Changgang Sun,
scgdoctor@126.com

†These authors have contributed equally to this work and share first authorship

SPECIALTY SECTION
This article was submitted to Inflammation Pharmacology, a section of the journal Frontiers in Pharmacology

RECEIVED 03 September 2022
ACCEPTED 29 September 2022
PUBLISHED 11 October 2022

CITATION
Liu J, Yu Y, Liu C, Gao C, Zhuang J, Liu L, Wu Q, Ma W, Zhang Q and Sun C (2022), Combinatorial regimens of chemotherapeutic agents: A new perspective on raising the heat of the tumor immune microenvironment. *Front. Pharmacol.* 13:1035954. doi: 10.3389/fphar.2022.1035954

Combinatorial regimens of chemotherapeutic agents: A new perspective on raising the heat of the tumor immune microenvironment

Jingyang Liu[1†], Yang Yu[2†], Cun Liu[3], Chundi Gao[1], Jing Zhuang[4], Lijuan Liu[4,5], Qibiao Wu[6], Wenzhe Ma[7], Qiming Zhang[1,8*] and Changgang Sun[3,4*]

[1]College of First Clinical Medicine, Shandong University of Traditional Chinese Medicine, Jinan, China, [2]College of Traditional Chinese Medicine, Shandong University of Traditional Chinese Medicine, Jinan, China, [3]College of Traditional Chinese Medicine, Weifang Medical University, Weifang, China, [4]Department of Oncology, Weifang Traditional Chinese Hospital, Weifang, China, [5]Department of Special Medicine, School of Basic Medicine, Qingdao University, Qingdao, China, [6]Faculty of Chinese Medicine, Macau University of Science and Technology, Macau, Macau SAR, China, [7]State Key Laboratory of Quality Research in Chinese Medicine, Macau University of Science and Technology, Macau, Macau SAR, China, [8]Department of Experimental Research Center, China Academy of Chinese Medical Sciences, Beijing, China

Harnessing the broad immunostimulatory capabilities of chemotherapy in combination with immune checkpoint inhibitors has improved immunotherapy outcomes in patients with cancer. Certain chemotherapeutic agents can extensively modify the tumor microenvironment (TME), resulting in the reprogramming of local immune responses. Although chemotherapeutic agents with an enhanced generation of potent anti-tumor immune responses have been tested in preclinical animal models and clinical trials, this strategy has not yet shown substantial therapeutic efficacy in selected difficult-to-treat cancer types. In addition, the efficacy of chemotherapeutic agent-based monotherapy in eliciting a long-term anti-tumor immune response is restricted by the immunosuppressive TME. To enhance the immunomodulatory effect of chemotherapy, researchers have made many attempts, mainly focusing on improving the targeted distribution of chemotherapeutic agents and designing combination therapies. Here, we focused on the mechanisms of the anti-tumor immune response to chemotherapeutic agents and enumerated the attempts to advance the use

Abbreviations: ADC, antibody-drug conjugate; ADCs, Antibody-drug conjugates; APC, antigen-presenting cell; BCMA, B-cell maturation antigen; CTL, cytotoxic T lymphocyte; CTX, cyclophosphamide; DAMP, damage-associated molecular pattern; DC, dendritic cell; ER, endoplasmic reticulum; eIF2α, eukaryotic translation initiation factor 2 alpha; GSH, glutathione; ICD, immunogenic cell death; ISR, integrated stress response; MMAE, monomethyl auristatin E; MMAF, monomethyl auristatin F; MDSCs, myeloid-derived suppressor cells; MHC, major histocompatibility complex; MMP, matrix metalloproteinases; NOX2, NADPH oxidase 2; OXA, Oxaliplatin; OVs, oncolytic viruses; ROS, reactive oxygen species; TAA, tumor-associated antigen; TAMs, tumor-associated macrophages; TEMs, Tie2-expressing macrophages; Tregs, regulatory T cells; TME, tumor microenvironment; UPR, unfolded protein response.

of chemo-immunotherapy. Furthermore, we have listed the important considerations in designing combinations of these drugs to maximize efficacy and improve treatment response rates in patients with cancer.

KEYWORDS

chemotherapeutic agents, combinatorial regimens, immunogenic cell death, tumor immune microenvironment, cancer therapy

Introduction

After years of intensive research to utilize the power of cytotoxic responses to fight cancer, we are witnessing a revolution in cancer therapy that harnesses the tumor recognition and destruction capabilities of the immune system (Principe et al., 2022). Conventional chemotherapy works by blocking the cell cycle and inducing apoptosis, which led to the development of multiple cytotoxic agents with non-specific targets, such as the synthesis of nucleic acids or proteins (Zitvogel et al., 2008). The effects of chemotherapeutic agents on the immune system have been neglected because of the use of cell culture and immune-deficient animal models (Galluzzi et al., 2020a). Recently, an abundance of preclinical literature has demonstrated that the immunomodulatory efficacy of conventional chemotherapeutic agents, including platinum-based drugs, anthracyclines, mitoxantrone, and taxanes, was much higher in immunocompetent mouse models than in their immunodeficient counterparts (Zitvogel et al., 2016). Further studies found that the activation of the immune system by chemotherapeutic agents leads to a two-pronged tumor eradication process: first, chemotherapeutic agents rely on cytotoxicity to directly destroy tumor cells (Casares et al., 2005); and second, the anti-tumor immune response produced by effector lymphocytes, such as cytotoxic T lymphocytes (CTLs), by secreting cytotoxic molecules and expressing ligands (Fas/TRAIL) that can bind to cell death receptors (Minute et al., 2020). This provides a partial understanding of the use of chemotherapeutic agents to potentiate therapeutic responses to immunotherapy and reprogram the tumor immune microenvironment.

The rise of immunotherapy has shifted public attention to a new field of immunomodulatory anti-tumor therapy. The improved clinical benefits brought by chemo-immunotherapy have further changed the long-held belief that chemotherapeutic agents are immunosuppressive (Galluzzi et al., 2020b). Hence, it is vital to identify the biological mechanisms underlying chemotherapy-induced immune stimulation and the key factors that can improve the efficacy of immunotherapy. There is increasing evidence that both dose and treatment interval are indispensable variables for the effective immunomodulatory effects of chemotherapeutic agents (Wu and Waxman, 2018; Fares et al., 2020; Lai et al., 2021). However, further preclinical research on chemotherapeutic agents at appropriate doses and treatment intervals has resulted in moderate anti-tumor immune responses and unsatisfactory results. Most drugs have difficulty producing durable immune efficacy because of their poor stability and off-target distribution *in vivo* and because of tumor heterogeneity and the persistently immunosuppressive microenvironment. To overcome these restrictive factors and improve overall anti-tumor efficacy, combinatorial regimens of chemotherapeutic agents, including immunotherapy agents, have been tested in clinical trials (Pfirschke et al., 2016). The intersection between chemotherapy and immunotherapy has been under evaluation for a long time, and several FDA-approved chemo-immunotherapy regimens have demonstrated significant advantages in real-world clinical applications. Therapies to obtain selective chemotherapy mediated by nanoformulations (e.g., nab-paclitaxel) or antibody-drug conjugates (ADCs; e.g., TDM-1, brentuximab vedotin) have been recently designed to achieve targeted distribution and local accumulation of anti-tumor drugs, showing significant alterations in the immunogenicity of the tumor microenvironment (TME) (Goldberg, 2015; Gu and Mooney, 2016; Coats et al., 2019).

In this review, we first summarized the immunomodulatory effects of chemotherapeutic agents, with a particular emphasis on immunogenicity and immuno-adjuvant effects. Additionally, we described the main factors affecting the immunomodulatory effects of chemotherapeutic agents and how the drugs can be used in new combinations to maximize treatment outcomes and improve response rates. Finally, we outlined some key considerations in the design of combinatorial regimens of chemotherapeutic agents to increase the application of chemo-immunotherapy in the future.

Multiple immunoregulatory mechanisms of chemotherapeutic agents

The ability of chemotherapeutic agents to drive adaptive immunity depends on three main parameters: immunogenicity, adjuvanticity, and microenvironmental conditions, all of which dramatically influence neoplastic cells to develop potentially immunogenic mutations or immune susceptibility, ultimately blocking both the priming and effector phases of the immunological response (Figure 1).

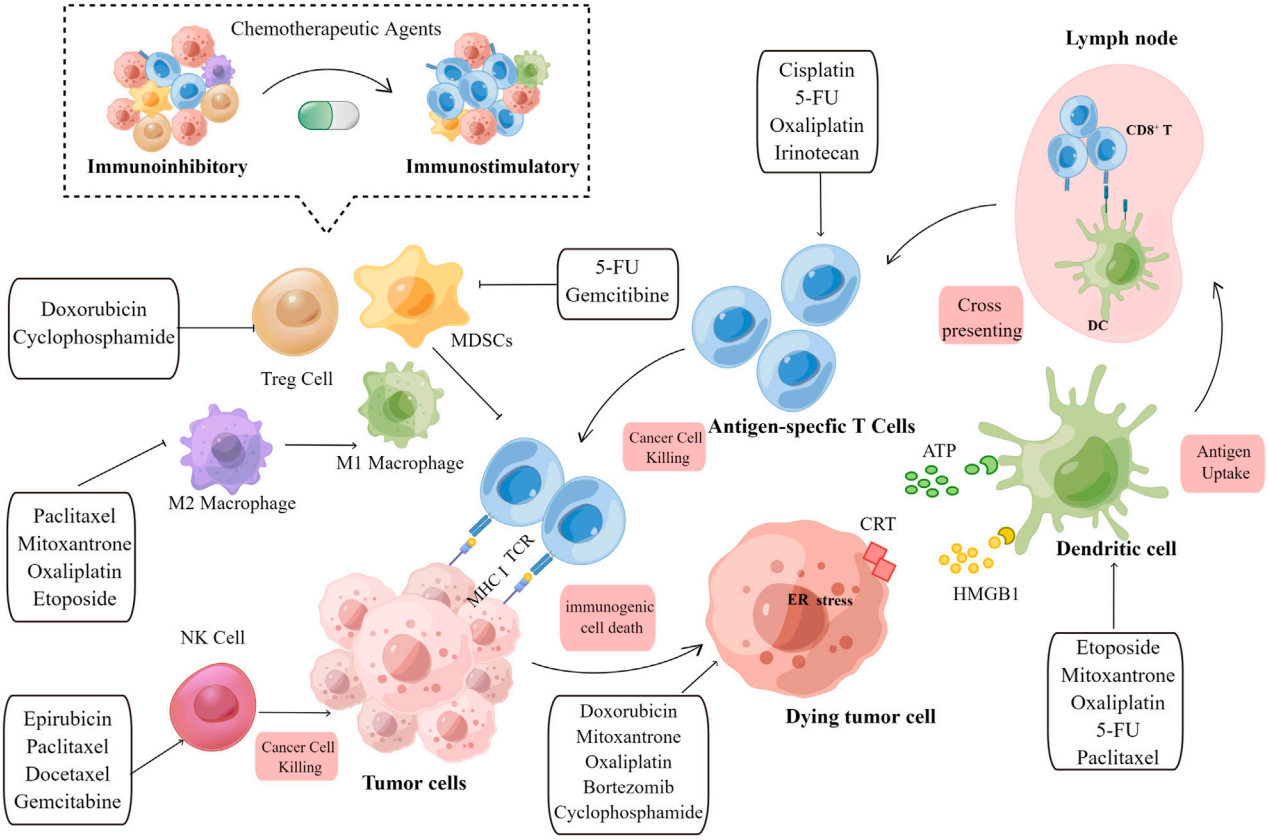

FIGURE 1
Overview of the immunostimulatory properties of chemotherapeutic agents. Immunogenic effects: When tumor cells are exposed to chemotherapeutic agents, TAA, TSA, and DAMPs released by dying tumor cells are engulfed by immature DCs, which promote APC maturation. Archived antigen-bearing APCs then migrate to the tumor-draining lymph node, where they cross-prime to T cells. Subsequently, antigen-specific T cells undergo clonal expansion. Activated T cells then recognize tumor cells and mediate the cytotoxic killing of tumor cells. Immuno-adjuvant effects: Chemotherapeutic agents can activate immune effector cells, including natural killer (NK) cells and dendritic cells (DCs), and promote the infiltration of cytotoxic T cells. The immunoinhibitory microenvironment is then transformed into an immunostimulatory microenvironment upon the depletion of immunosuppressive cells, including Treg cells, M2 macrophages, and MDSCs. Chemotherapeutic agents and their corresponding immunomodulatory effects are shown in the text boxes with arrows. TAA, tumor-associated antigen; TSA, tumor specific antigen; DAMP, damage-associated molecular pattern; DC, dendritic cell; APC, antigen-presenting cell; NK, natural killer cell; MDSC, myeloid-derived suppressor cells; Treg, regulatory T cell; MHC, major histocompatibility complex; TCR, T cell receptor; CRT,calreticulin; HMGB1, high-mobility group box 1.

Immunogenic regulation of chemotherapeutic agents

Eliciting immunogenic cell death

Various cytotoxic chemotherapy agents, such as anthracyclines, platinum-based drugs, mitoxantrone, oxaliplatin, and taxanes, that block cell cycle progression and induce apoptosis have been demonstrated to potentiate immunogenic cell death (ICD) (Casares et al., 2005; Kopecka et al., 2018; Li C et al., 2020; Tesniere et al., 2010; Fucikova et al., 2022). As a form of regulated cell death, ICD is amenable to activating the cellular stress response that promotes the spatiotemporally coordinated production and localization of damage-associated molecular patterns (DAMPs) from dying cells in immunocompetent hosts (Kroemer et al., 2022). DAMPs can be recognized by inherent pattern recognition receptors, such as Toll-like receptors and Nod-like receptors, on dendritic cells (DCs), which attract these cells to the tumor cells and ultimately promote tumor-associated antigen (TAA) presentation. Subsequently, antigen-presenting cells (APCs) represented by DCs, could migrate to the draining lymph nodes and present antigens to CTLs, killing tumor cells presenting the major histocompatibility complex (MHC). This event then triggers immune memory in a favorable environment with high levels of co-stimulatory signals and cytokines.

Howener, the release of DAMPs from dying cancer cells occurs during a failed intracellular stress response, and the kinetics and intensity of DAMP release can be determined

through the cellular response driven by the initiating stressor (Clement et al., 2021). An increasing amount of research has confirmed that cells succumbing to intracellular stress can initiate an adaptive immune response associated with immunological memory. In contrast to chemotherapeutic agents that do not elicit ICD, most ICD inducers efficiently stimulate integrated stress responses (ISRs) (Costa-Mattioli and Walter, 2020). As a result, defects in various mechanisms associated with maintaining cellular homeostasis could influence the strength of the immune response.

ISR, a multi-pronged molecular mechanism for maintaining cellular homeostasis, is an adaptive signaling pathway activated by various forms of cellular stress, such as endoplasmic reticulum (ER) stress and the unfolded protein response (UPR) (Hetz et al., 2020; Kohli et al., 2021). One of the core molecules modulating ISR is eukaryotic translation initiation factor 2 alpha (eIF2α), whose phosphorylation is regulated by eIF2α kinase (EIF2AK1-4) (Bezu et al., 2018). Cisplatin was previously defined as incapable of triggering ICD because it does not promote the kinase-dependent phosphorylation of eIF2α or exposure of ER chaperones on the cell surface (Tesniere et al., 2010). This can be corrected by administering drugs, such as digoxin, tetracycline, that stimulate the ER stress response (Michaud et al., 2014; Xiang et al., 2020). In addition, non-phosphorylated eIF2α (eIF2αS51A) has been shown to inhibit the activation of anthracycline-driven autophagy, further demonstrating the central role of ISR in chemotherapy-induced ICD (Martins et al., 2011). This implies that one of the mechanisms underlying chemotherapeutic agent-induced ICD is ISR associated with cellular stress.

Enhancing the antigenicity of cancer cells

While there is ample evidence that chemotherapy increases the immunogenicity of cancer cells via ICD, little is known about the chemotherapy-induced enhancement of antigenicity. In contrast to ICD, the phenotypic changes in tumor cells upon exposure to non-lethal/sublethal doses of chemotherapeutic agents are mainly manifested into enhanced antigenicity, making tumors more sensitive to CTL-mediated killing (Hodge et al., 2013). The chemotherapy-induced enhancement of tumor antigenicity is mainly associated with the upregulation of major histocompatibility complex (MHC) expression and the emergence of tumor neoantigens or TAA. Many commonly used cytotoxic agents, such as topotecan, mitoxantrone, gemcitabine, and cisplatin, have been found to upregulate the expression of antigen-presenting machinery (Grabosch et al., 2019; Li et al., 2021; Zhou et al., 2021). In addition, some chemotherapy drugs, such as docetaxel, cisplatin and 5-fluorouracil, can also promote the expression of TAA and tumor-specific antigen (TSA) and enhance antigenicity (Coral et al., 2002; Correale et al., 2003; Spehner et al., 2020). Furthermore, immune responses of $CD4^+$ T cells against tumor-associated antigens were observed following oxaliplatin treatment in chemotherapy-naïve patients with mCRC (colorectal cancer) (Galaine et al., 2019). Therefore, anti-tumor T-cell responses stand out as key elements for the long-term efficacy of chemotherapy upon treatment discontinuation.

Immuno-adjuvant effects of chemotherapeutic agents

The immune microenvironment in which cancer cells reside is a major determinant of their ability to trigger adaptive immune responses, even in the presence of sufficient antigenicity and immunogenicity (Belli et al., 2018). The immuno-adjuvant effects of the chemotherapeutic agents discussed in this review may principally rely on the recruitment and activation of immunologic effector cells to reverse the effect of an immunosuppressive microenvironment.

Promoting dendritic cell-mediated antigen presentation

DCs have become the core initiator and regulator cells associated with anti-cancer immunity, owing to their highly complex antigen presentation mechanism. However, the abnormal evolution of tumors interferes with the mechanism of DC maturation and antigen processing in tumors, resulting in immunosuppressive effects (Murphy and Murphy, 2022). An increasing amount of evidence supports the role of chemotherapeutic agents in modulating DCs at low doses, particularly in promoting their maturation (Pfannenstiel et al., 2010; Wanderley et al., 2018) and antigen presentation capability (Shurin et al., 2009; Zhang et al., 2021). Antigen cross-presentation is a prerequisite for the induction of an effective anti-tumor immune response, and its immunomodulatory potency can be improved by apoptosis-inducing chemotherapy. McDonnell AM et al. demonstrates that gemcitabine-induced tumor cell apoptosis can increase the incidence of nuclear antigen cross-presentation *in vivo*, which is associated with an increased proportion of CTLs (McDonnell et al., 2015a; McDonnell et al., 2015b). Other drugs such as cyclophosphamide (CTX) act by altering DC biology, especially by changing DC subsets (Nakahara et al., 2010; Fumet et al., 2020).

Trafficking and infiltration of immune effector cells

In addition, one potentially important biological response to chemotherapy is the ability to initiate T cell influx into the

TME. Activated immune cells could enter the bloodstream and initiate T cell influx into the TME. *In vivo* treatment of tumor-bearing mice showed that doxorubicin, paclitaxel significantly increased the number of $CD4^+$ and $CD8^+$ T cells, which may be related to the expression of IFN-γ and granase B (Tsuda et al., 2007; Alizadeh et al., 2014; Heeren et al., 2019). Recent studies have shown that cisplatin can promote the production of the chemokine CCL20 and the pro-inflammatory cytokine IL-1β in tumor sites, leading to the synthesis and activation of ILC3 (Bruchard et al., 2022). ILC3 promotes the production of chemokine CXCL10 in tumors, which is associated with the generation of $CD4^+$ and $CD8^+$ T lymphocytes (Goc et al., 2021). It has been observed that partial chemotherapeutic agents activate NK cell-mediated anti-tumor immune responses, depending on the release of cytokines (Markasz et al., 2007; Garofalo et al., 2021). Chemotherapeutic agents also affect the composition of tumor-infiltrating lymphocytes (TILs), and it has been proven that the composition ratio between TILs and infiltrating cells is related to the efficacy of immunotherapy (Farhood et al., 2019; Saleh and Elkord, 2019). In metastatic colon cancer, multi-drug chemotherapy regimens, including FOLFOX (5-FU, folinic acid, and oxaliplatin) and FOLFIRI (5-FU, folinic acid, and irinotecan), significantly altered the composition ratio of peripheral blood lymphocytes (Maeda et al., 2011; Che et al., 2021). This change is mainly manifested by an increase in the CD8/Foxp3 TIL ratio, which can effectively predict and improve the recurrence-free and overall survival of patients. These data suggest that the immune adjuvant effect of chemotherapeutic agents runs through all stages of the cancer immune cycle and plays a role in continuous anti-tumor immune regulation.

Depletion of immunosuppressive cells

Immunosuppressive cells, represented by myeloid-derived suppressor cells (MDSCs), regulatory T cells (Tregs), and tumor-associated macrophages (TAMs), are key influencing factors of immune escape and immunotherapy resistance and play a major role in the anti-tumor immune response (Tie et al., 2022). Interestingly, some chemotherapeutic agents have been shown to deplete immunosuppressive cell populations, thus remodeling the immune cell landscape to mount an efficient anti-tumor immune response.

The absolute or relative depletion of Treg cells, especially during tumor infiltration, is associated with the (re)induction of protective anti-cancer immunity, indicating a shift from silent or ineffective immune responses to open or effective ones (Ikegawa and Matsuoka, 2021; Nishikawa and Koyama, 2021). Previous studies on CTX-induced Treg cell depletion have obtained favorable results, confirming that CTX can mediate multiple mechanisms to selectively deplete Treg cells and further improve the effectiveness of immunotherapy by increasing the activation of autoreactive T cells (Laheurte et al., 2020). Cytokines such as IFN, IL-6, and CXCL10 play a role in CTX-mediated restoration of Treg homeostasis. CTX-induced Treg depletion and the expression of related cytokines have been shown to be directly or indirectly regulated by IFN regulatory factor (IRF)-1 (Buccione et al., 2018). In addition to CTX, many other chemotherapeutic agents selectively target Tregs. For example, patients with NSCLC who received four cycles of docetaxel chemotherapy presented fewer peripheral Tregs than at baseline, similar to that observed with cisplatin and vinorelbine (Roselli et al., 2013; Li et al., 2014).

Recent studies have shown that several aspects of macrophage biology are affected by chemotherapy. Some chemotherapeutic agents, such as CTX and doxorubicin, can activate macrophages by enhancing the secretion of GM-CSF to generate anti-tumor immune responses in mouse models of breast cancer or further potentiating Th1 responses that can enhance the tumoricidal effects of macrophages (Machiels et al., 2001; Li T et al., 2020). In addition to promoting macrophage activation, chemotherapeutic drugs can also induce macrophage polarization. For example, paclitaxel promoted the repolarization of TAMs from an M2-like to an M1-like phenotype (Wanderley et al., 2018). However, studies have similarly shown that a taxane-based chemotherapy regimen can enhance the recruitment of Tie2-expressing macrophages (TEMs) in breast cancer, promote tumor cell entry into circulation, and lead to metastasis (Karagiannis et al., 2017). Thus, the mechanism underlying the impact of chemotherapeutic agents on macrophage biology is still unclear but is most likely dependent on microenvironmental factors.

The same phenomenon can be observed with cytotoxic agents against MDSCs since many chemotherapeutic agents can selectively inhibit MDSC differentiation. Cisplatin has been shown to inhibit the conversion of monocyte precursors to inhibitory M-MDSCs through the regulation of the STAT3-COX-2 signaling axis, overcoming M-MDSC-mediated immunosuppression and improving the overall response rate to cancer immunotherapy (Van Wigcheren et al., 2021). Oxaliplatin is also known to selectively deplete MDSCs, especially Mo-MDSCs, by decreasing the expression of the immunosuppressive functional mediators argininase 1 (ARG1) and NADPH oxidase 2 (NOX2) (Kim and Kim, 2019). However, it appears that different drug combinations affect the immunomodulatory effects of chemotherapeutic drugs. Both 5-FU and gemcitabine are anti-metabolic chemotherapeutic agents that inhibit the proliferation of MDSCs by inhibiting thymidylate synthase and cytidine deaminase (Vincent et al., 2010). Interestingly, this effect was only maintained with oxaliplatin alone, and the blocking effect of MDSCs was discontinued when 5-FU was combined with irinotecan (Kanterman et al., 2014; Li et al., 2022). Given the complex regulatory effects of

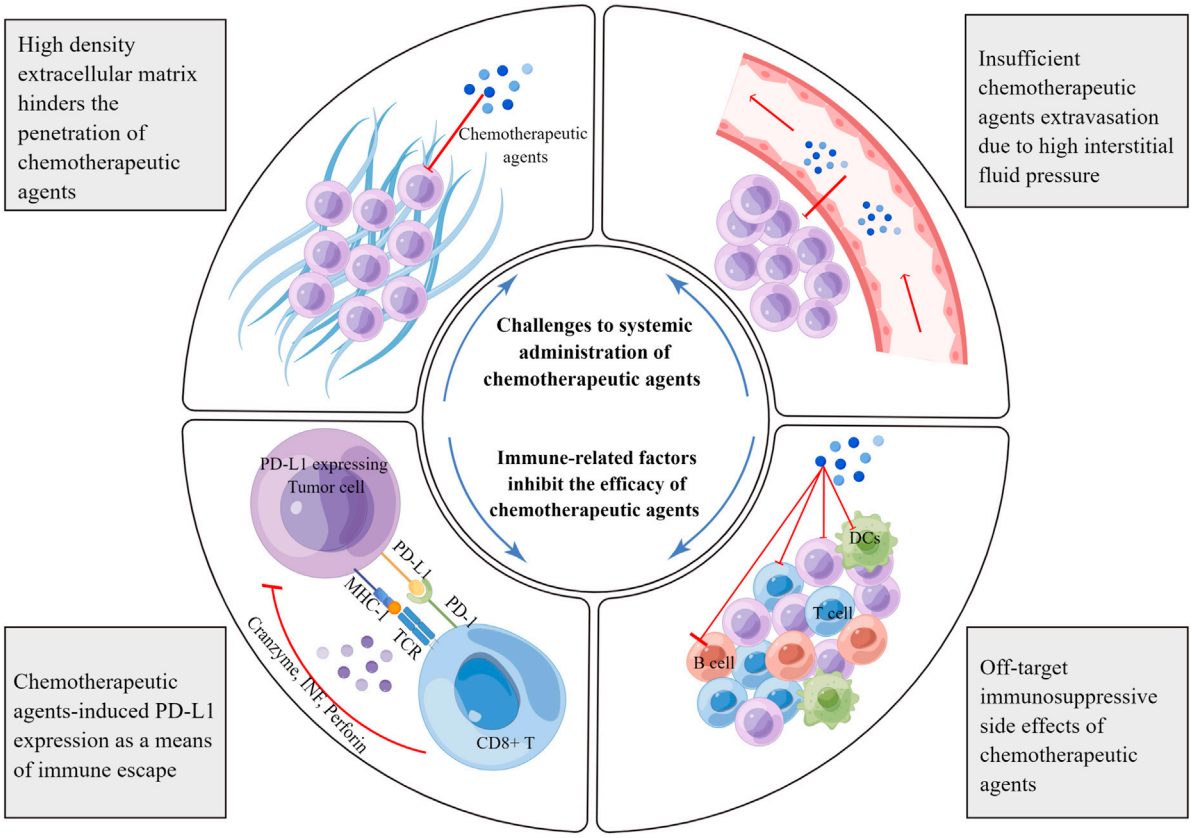

FIGURE 2
Limiting factors affecting the immunoregulatory effects of chemotherapeutic agents. Chemotherapeutic agents can induce the expression of negative immune checkpoints, especially PD-L1. PD-L1 associates with the PD-1 receptor on effector T cells, blunting anti-tumor immune responses and facilitating immune escape. Furthermore, chemotherapeutic agents target rapidly proliferating immune cells, resulting in off-target side effects. The dense network of the extracellular matrix hinders the spread of chemotherapeutic agents in tumors. In addition, there is high interstitial fluid pressure in tumor tissues, which prevents the extravasation of chemotherapeutic agents from the blood vessels. MHC, major histocompatibility complex; TCR, T cell receptor; TNF, tumor necrosis factor; DC, dendritic cell.

chemotherapeutic agents on MDSCs, this is an important area worthy of further research.

Challenges with immunoregulatory chemotherapeutic agents to be as successful as monotherapies

As mentioned above, various chemotherapeutic agents can alter the crosstalk between cancer and the immune system at multiple levels. This alteration may inhibit or kill cancer cells in an immunogenic or immuno-adjuvant-modulated manner, affect different leukocyte populations, or affect systemic physiological responses. However, it is often difficult to overcome the complexity and compensatory evolution of tumors, resulting in limited anti-tumor immune effects. Through a review of relevant studies, we have listed several key factors affecting the clinical application of chemotherapy in the following sections (Figure 2).

Substantial barriers that hinder the penetration of chemotherapeutic agents

Emerging evidence suggests that the TME imposes biological barriers that hinder effective cancer therapy (Binnewies et al., 2018). The structures of these biological barriers are highly irregular and are mainly characterized by a highly disordered vascular network, the absence of a lymphatic network, and high interstitial fluid pressure (Heldin et al., 2004; Jain et al., 2007). In addition, the abundant expression of extracellular matrix proteins and the proliferation of interstitial tissue in the TME constitute the mechanical barrier in cancer, resulting in insufficient tumor infiltration and obstructed blood circulation after the intravenous injection of chemotherapeutic agents (Casazza et al., 2014). Previous experiments have shown that gaps between vascular endothelial cells rarely occur in tumors in mouse models and in tumors from patients with cancer; this phenomenon is always associated with the insufficient extravasation of chemotherapeutic agents (Golombek et al.,

2018). This observation suggests that trans-endothelial pathways play an integral role in the precise infiltration of chemotherapeutic agents into tumors (Sindhwani et al., 2020). To promote more efficient cancer chemotherapy in the clinic, various nanoscale drug delivery systems have been explored to achieve tumor-targeted delivery of chemotherapeutic agents. These drug delivery systems can be used to enhance the tissue-specific distribution of chemotherapeutic agents, activate immune cells, and amplify anti-tumor immune responses (Saeed et al., 2019; Wang W. et al., 2020). However, the improvement effect of traditional nanomedicine is still limited owing to the metabolic environment in tumor tissue, such as hypoxia and inflammation, which negatively affect the intratumoral immune activation effect of chemotherapeutic agents.

Immune resistance to chemotherapeutic agents

During tumor-host co-evolution, robust immunosuppressive circuits established in the TME hamper the ability of chemotherapeutics to drive anti-tumor immunomodulatory effects. Consequently, it is crucial to maintain the function of chemotherapeutic agents within the immunosuppressive TME. Although cisplatin, paclitaxel, and 5-fluorouracil promoted the clonal expansion of tumor-specific $CD8^+$ T cells, an inadequate magnitude of an immune response was eventually manifested, owing to the increased expression of microenvironment-related IDO (Munn and Mellor, 2016). Additionally, oxaliplatin has been shown to suppress T-cell responses by promoting PD-L1 expression on DCs and reducing the expression of the co-stimulatory molecules CD80/CD86 (Tel et al., 2012). Subsequent trials have also revealed that the combination of 5-FU and oxaliplatin decreased the expression of immune checkpoints PD-L1 and PD-L2 on the surface of DCs, promoting DC maturation in tumor-bearing mice (Hong et al., 2018). Notably, the perturbation of multiple factors in the immune system drives the expression of these negative regulatory pathways, making chemotherapy monotherapy insufficient to reverse the effects of an immunosuppressive microenvironment. In addition to the influence of immunosuppressive microenvironment-related factors, the activation of unknown immune-related signaling pathways during treatment is also a key factor that inhibits the anti-tumor efficacy of chemotherapeutic drugs. Recent studies have shown that cessation of immunogenic chemotherapy may provoke the restoration of the immunosuppressive microenvironment and the immune escape of tumor cells, which could accelerate the malignant progression of tumors. Gemcitabine, a standard chemotherapy regimen for advanced pancreatic ductal carcinoma, induces the infiltration of pro-inflammatory macrophages into the liver and activates cytotoxic T cells. However, Bellomo et al. experimentally observed that after cessation of the standard chemotherapy regimen, tumor cells recruited growth- and arrest-specific 6 (Gas6)-expressing neutrophils to the liver through the secretion of CXCL1 and CXCL2, resulting in liver metastases (Bellomo et al., 2022).

Off-target immunosuppressive side effects of chemotherapeutics

Many chemotherapeutic agents have notable immunosuppressive side effects. These effects occur either directly by inhibiting or killing effector cells, characterized by rapid proliferation, or indirectly by inducing anergy or immune paralysis (Zitvogel et al., 2008). The off-target effects of chemotherapeutic agents on the immune system are extensive and could affect their therapeutic efficacy (Medzhitov and Janeway, 2002). This applies to CTX, which primarily impairs the proliferation of peripheral T cells and hinders their effector functions. In addition, post-transplant CTX alters immune signatures and leads to impaired T cell reconstitution in allogeneic hematopoietic stem cell transplant by increasing Treg while reducing naïve T cells (Zhao et al., 2022). Current research suggests that the number and function of immune-infiltrating effector cells are closely related to the efficacy and prognosis (Denkert et al., 2018; Paijens et al., 2021); similarly, the depletion of non-targeted immune cells affects the anti-tumor effect of chemotherapy. Clinically, owing to myelosuppression and its related immunosuppressive adverse effects, the maximum tolerated dose of chemotherapeutic agents is rarely used for the routine treatment of patients with cancer. However, it has also been suggested that the recovery phase from chemotherapy-induced lymphopenia can serve as an important window to enhance the anti-tumor immune response, providing a reasonable and feasible theoretical support for the application of chemotherapy followed by immunotherapy (Williams et al., 2007; Moschella et al., 2011). Hence, the role of transient immunosuppression in long-term immune responses and immune memory needs to be further demonstrated.

To generate a strong and durable anti-tumor immune response, it is necessary to modify the chemotherapeutic agents themselves or design a more efficient combination regimen. This can be done by changing the distribution of the chemotherapeutic drug in the body or using a combination of drugs that can better target the tumors of interest, activating the anti-tumor immune response, improving the immune response rate, and reducing the incidence of non-target immune-related side effects.

Attempts to improve the immunomodulatory effect of chemotherapeutic agents

Antibody-drug conjugates

ADCs were originally designed to exploit the exquisite specificity of antibodies to deliver targeted and potent

chemotherapeutics. ADCs undergo a complex sequence of drug internalization procedures that often require intracellular processing and eventual payload release (Drago et al., 2021). Emerging evidence suggests that the payloads act as the workhorse of ADCs, exerting tumor-killing effects through complex interactions between ADCs and various components of the tumor immune microenvironment. A variety of cytotoxic drugs and their derivatives were used in the design of ADC drugs, which are mainly divided into the following categories: microtubule inhibitors/stability disruptors, such as auristatin derivatives (monomethyl auristatin F [MMAF] or monomethyl auristatin E [MMAE]); Mayden derivatives (DM1/DM4); and calicheamicin and its derivatives that act on DNA grooves or breaks in the double helix. Some ADC payloads, such as MMAF/MMAE, auristatins, pyrrolobenzodiazepines, and anthracycline T-PNU, have been identified as potent substances that could promote DC maturation and activate antigenic responses (Muller et al., 2014a; D'Amico et al., 2019). Additional studies have shown that cytotoxic chemotherapeutics, such as dolastatin, MMAE, and maytansinoid, are commonly used as ADC payloads to stimulate $CD8^+$ effector cell migration to experimental tumors grown in mice (Muller et al., 2014b).

Several experiments have confirmed the immunomodulatory effects of the payload-based ADCs. For example, brentuximab vedotin (SGN-35) comprises an anti-CD30 antibody conjugated to vcMMAE via a protease-cleavable linker. Immunohistochemical analysis of Hodgkin's lymphoma tumor samples from patients treated with SGN-35 revealed significant changes in the number of intra-tumoral $CD8^+$ effector T cells (Theurich et al., 2013). Furthermore, when used alone or in combination with an anti-PD-L1 antibody, ADCs that target EphA2 molecules in combination with a tubulin payload could induce ICD, showing a strong ability to induce $CD8^+$ T-cell infiltration (Muller et al., 2015; Agostinetto et al., 2022). These studies provide evidence that ADC-destabilizing drugs stimulate the cancer immunity cycle. Recently, the FDA-approved drug belantamab mafodotin (GSK2857916), an ADC that targets B-cell maturation antigen (BCMA) in multiple myeloma cells using MMAF as a payload, induced ICD in BCMA-expressing cancer cells and promoted DC activation *in vivo* (Yu et al., 2020). In a syngeneic mouse model, GSK2857916 was shown to induce ICD, promoting the intratumoral enrichment of TILs and T cell-dependent anti-tumor activity (Montes de Oca et al., 2021). To further optimize the targeted immunomodulatory effects of ADCs, researchers have screened potential targets of ADCs that are not just limited to malignant cells. Based on this, a CD25-targeted pyrrolobenzodiazepine dimer-based ADC was investigated for its ability to deplete Tregs and eradicate established tumors (Zammarchi et al., 2020).

In addition to ADC monotherapy, numerous ongoing or completed clinical trials have demonstrated the clinical efficacy of ADC combined with chemotherapy (Table 1), which showed good efficacy and safety in hematologic tumors and breast cancer. However, there are many challenges in the development of this type of drug. For example, the selection of potential targets, improvement of potential toxicity caused by off-target effects, and development of cytotoxic drugs with other mechanisms of action require numerous experiments to verify.

Nanosized drug delivery systems based on the tumor microenvironment

Owing to the negative role of the TME in compromising the therapeutic response of various cancer therapies, therapeutic modalities targeting the TME appear to enhance the overall response rate of patients to cancer treatment (Tang et al., 2021). Nano-drug delivery systems, which provide a prerequisite for the TME-targeted delivery of chemotherapeutic agents, are a promising strategy to address these challenges, because of their adequate circulation time, increased intratumoral accumulation and retention, efficient uptake by tumor cells, and precise release at tumor tissues (Weber and Mule, 2015; Abdou et al., 2020). Depending on the particular metabolic characteristics of the TME, such as hypoxia, acidic pH, overexpressed enzymes (e.g., matrix metalloproteinases 2 and 9 [MMP-2 and-9], hyaluronidase, legumain, or cathepsin B), reactive oxygen species (ROS), or glutathione (GSH), different responsive nanomaterials have been developed. These nanomaterials were initially applied to load chemotherapeutic agents and achieve intratumoral local delivery. Generally, these nanoparticles remain intact in the blood circulation to protect their payloads from degradation or leakage until they are activated by the TME (Zhou et al., 2020). The loaded chemotherapeutic agents are subsequently released into local tumor tissues, focusing on the modulation of immune-related molecules that normalize immune responses and induce ICD to restore the ability of CTLs to eradicate tumor cells.

Wang et al. developed an ROS-responsive hydrogel loaded with gemcitabine that showed significant therapeutic efficacy against both primary tumors and distant metastases. In response to ROS signaling in the TME, the released gemcitabine reduced the percentage of immunosuppressive cells, including MDSCs and M2 macrophages, while increasing PD-L1 expression in cancer cells, T cells, macrophages, and DCs. In turn, this increased PD-L1 expression synergizes with the effect of anti-PD-L1 antibodies to improve immunotherapy effect (Wang et al., 2018). A pH-responsive nanoparticle co-loaded with the ICD inducer doxorubicin was designed to induce potent ICD in cancer cells while synergistically limiting the production of immunosuppressive kynurenine by binding to alkylated NLG919 (an inhibitor of indoleamine 2,3-dioxygenase 1). Moreover, the introduction of pH-responsive nanoparticles could enable deep intratumoral penetration of therapeutic

TABLE 1 Clinical trials on combination regimens of ADC and chemotherapy in cancers.

Drugs	Comibinations	Phase	Status	Cancer	References
Gemtuzumab Ozogamicin	Mitoxantrone + Etoposide	II	Recruiting	Acute Myeloid Leukemia	NCT03839446
	CPX-351(Liposome-encapsulated Daunorubicin-Cytarabine)	I	Recruiting	Acute Myeloid Leukemia	NCT03904251
	Tretinoin + Arsenic Trioxide	II	Recruiting	Acute Promyelocytic Leukemia	NCT01409161
	Fludarabine + high-dose cytarabine + filgrastim-sndz + idarubicin	II	Recruiting	Acute Myeloid Leukemia/High-Risk Myelodysplastic Syndrome	NCT00801489
Brentuximab vedotin	Bendamustine	II	Recruiting	Follicular Lymphoma	NCT04587687
	CHEP (Cyclophosphamide + Doxorubicin + Etoposide + Prednisone tablet)	II	Recruiting	Peripheral T-cell Lymphomas	NCT05006664
	CHP (Cyclophosphamide + Doxorubicin + Prednisone tablet)	II	Recruiting	Peripheral T-cell Lymphoma	NCT04569032
	Lenalidomide + rituximab	III	Recruiting	Diffuse Large B-cell Lymphoma	NCT04404283
	Doxorubicin + vinblastine + dacarbazine	III	Not yet recruiting	Hodgkin Lymphoma	NCT04685616
	Pralatrexate + cyclophosphamide + Doxorubicin + Prednisone	I	Recruiting	NK T-cell Leukemia/Lymphoma	NCT03719105
Ado-trastuzumabemtansine (T-DM1)	Atezolizumab + paclitaxel + trastuzumab + docetaxel	II	Recruiting	Neoplasm Metastasis	NCT00781612
	Methotrexate + hydrocortisone + cytarabine	II	Recruiting	Acute Lymphoblastic Leukemia	NCT03913559
Inotuzumab ozogamicin	mBFM (Cyclophosphamide + cytarabine + mercaptopurine + leucovorin calcium + vincristine)	II	Recruiting	B-Lymphoblastic Lymphoma or Relapsed or Refractory CD22 Positive B Acute Lymphoblastic Leukemia	NCT02981628
	Etoposide + Doxorubicin + Vincristine + Prednisoneand Cyclophosphamide	I	Recruiting	B-cell Acute Lymphoblastic Leukemia	NCT03991884
Polatuzumab Vedotin	Rituximab + Ifosfamide + Carboplatin + Etoposide (PolaR-ICE)	II	Recruiting	Diffuse Large B-Cell Lymphoma	NCT04665765
Sacituzumab govitecanhziy	Pembrolizumab + Carboplatin/Cisplatin	II	Recruiting	Non-small Cell Lung Cancer	NCT05186974
	Cyclophosphamide + N-803+PD-L1 t-haNK	I/II	Recruiting	Advanced Triple Negative Breast Cancer	NCT04927884

This table is according to https://clinicaltrials.gov/

agents and effectively neutralize low pH levels, reversing the immunosuppressive effect of the TME (Zhu et al., 2020). Furthermore, Koo AN et al. developed GSH-responsive core-shell nanoparticles carrying docetaxel for selective delivery in tumor-bearing mice. These self-assembled nanoscale coordination polymer core-shell nanoparticles are cleaved by GSH in tumor cells, releasing docetaxel, and leading to T-cell priming and anti-tumor effects (Koo et al., 2012). However, complex nanosystems face hinderance such as possible interactions between different components and overall stability, which may also limit the immunomodulatory effects of chemotherapeutic drugs. Therefore, it is necessary to determine the best combination scheme to ensure that the targeted effects of chemotherapy drugs are maintained.

Chemotherapy combined with PD-L1/PD-1 inhibitors

Since the early 2010s, many immunotherapies based on immune checkpoint inhibition have been developed, especially antibodies targeting the PD-1/PD-L1 pathway, thereby changing the status quo of cancer treatment. Tumors respond poorly to immunotherapy despite their revolutionary efficacy, which can be explained by exhibiting a loss of lymphocyte infiltration (NK, CD8, Th1), the so-called "cold tumors."(Fumet et al., 2020) As an immune adjuvant, chemotherapy can increase the number of TILs, reverse the cold immune environment, and reduce the enrichment of immunosuppressive cells, significantly improving the response rate to immune checkpoint inhibitors (Park et al., 2020). Moreover, several chemotherapeutic agents, such as cisplatin, oxaliplatin, doxorubicin, and paclitaxel, can also enhance the expression of immune checkpoints, mostly PD-L1 (Ng et al., 2018). In this context, the expression of PD-L1 on cancer cells can associate with the PD-1 receptor on effector T cells, reducing anti-tumor immune responses and facilitating immune escape (Li et al., 2021).

Harnessing the broad immunostimulatory capabilities of chemotherapeutic agents in combination with immune checkpoint inhibitors has shown great promise with improved clinical outcomes. The FDA has already approved combinations of chemotherapy and PD-L1/PD-1 therapy (Gandhi et al., 2018;

TABLE 2 Clinical trials on neoadjuvant immuno-chemotherapy in cancer.

Drugs	Neoadjuvant chemotherapy	Phase	Status	Cancer	References
Pembrolizumab	Paclitaxel + Cisplatin	II	Not yet recruiting	Esophageal Squamous Cell Carcinoma	NCT05281003
	Cisplatin+5-FU	II	Recruiting	EGJ Adenocarcinoma	NCT04813523
	Gemcitabine + Cisplatin	III	Recruiting	Cisplatin-eligible Muscle-invasive Bladder Cancer (MIBC)	NCT03924856
	Folfirinox (Oxaliplatin + Leucovorin + Irinotecan+5-Fluorouracil)	II	Not yet recruiting	Pancreatic Ductal Adenocarcinoma	NCT05132504
	Nab-paclitaxel + doxorubicin + Cyclophosphamide + Carboplatin + Paclitaxel	I	Completed	Triple Negative Breast Cancer	NCT02622074
	Decitabine + dose-dense AC + paclitaxel (or paclitaxel plus carboplatin)	II	Recruiting	Locally Advanced HER2- Breast Cancer	NCT02957968
	mFOLFOX6	II	Recruiting	Gastroesophageal Junction (GEJ) and Stomach Adenocarcinoma	NCT03488667
Atezolizumab	paclitaxel + carboplatin	I/II	Completed	Advanced-Stage Ovarian Cancer	NCT03394885
	cisplatin + gemcitabine	II	Not yet recruiting	Bladder Cancer	NCT04630730
	Carboplatin + Etoposide	II	Not yet recruiting	Limited-Stage Small Cell Lung Cancer	NCT04696939
	cisplatin/carboplatin + pemetrexed (for non-squamous only)				
	cisplatin/carboplatin + gemcitabine (for squamous only)				
	carboplatin + paclitaxel	II	Recruiting	Previously Untreated Locally Advanced Resectable Stage II, IIIA, or Select IIIB Non-Small Cell Lung Cancer	NCT04832854
Nivolumab	paclitaxel + carboplatin ± cabiralizumab	I/II	Recruiting	Triple Negative Breast Cancer	NCT04331067
	cisplatin/carboplatin + pemetrexed (for non-squamous only)				
	cisplatin/carboplatin + gemcitabine (for squamous only)				
	carboplatin + paclitaxel	III	Recruiting	Surgically Removable Early Stage Non-small Cell Lung Cancer	NCT04025879
	paclitaxel + carboplatin	II	Recruiting	Non Small Cell Lung Cancer	NCT03838159
	Paclitaxel + Doxorubicin + Cyclophosphamide + Paclitaxel/Docetaxel	II	Completed	Inflammatory Breast Cancer (IBC)	NCT03742986
	pemetrexed + cisplatin/carboplatin	I	Recruiting	Mesothelioma	NCT04162015
Durvalumab	Paclitaxel + Carboplatin	II	Recruiting	Ovarian Cancer	NCT03899610
	Gemcitabine + Cisplatin				
	Gemcitabine + Carboplatin	II	Recruiting	Urothelial Carcinoma	
				Cancer	NCT04617756
	paclitaxel + epirubicin + cyclophosphamide	I/II	Recruiting	Luminal B HER2(-) or Triple Negative Breast Cancers	NCT03356860
	Gemcitabine + Cisplatin	II	Recruiting	Biliary Tract Neoplasms	
				Gallbladder Cancer	
				Cholangiocarcinoma	NCT04308174
	Carboplatin + nab-paclitaxel + anlotinib	II	Recruiting	Stage III Non-Small-Cell Lung Cancer	NCT04762030
	Docetaxel + oxaliplatin + S-1	II	Recruiting	Gastric or Gastroesophageal Junction Adenocarcinoma	NCT04221555
	FLOT (flurouroacil + leucovorin + oxaliplatin + docetaxel)	III	Recruiting	Gastric and Gastroesophageal Junction Cancer	NCT04592913
	carboplatin + paclitaxel				
	cisplatin + gemcitabine				
	pemetrexed + cisplatin				
	pemetrexed + carboplatin	III	Recruiting	Non-small Cell Lung Cance	NCT03800134

This table is according to https://clinicaltrials.gov/

Horn et al., 2018; Schmid et al., 2018). Numerous phase III trials are currently underway for various cancer types that will alter the face of oncology for multiple indications. Our review has focused on the administration sequence and dosing schedule of combined immunochemotherapy.

Immunochemotherapy combinations currently comprise adjuvant standard-of-care chemotherapy regimens being added to immunotherapy, but the elements in this combination have not been optimized. With the deepening of the clinical application of chemotherapy combined with Immune checkpoint inhibitors, more studies began to focus on practical clinical issues such as the schedule, interval, and cycle of the combination therapy to obtain better clinical benefits (Principe et al., 2022; Leonetti et al., 2019). Studies have shown that neoadjuvant chemotherapy plays an important role in cancer treatment, and a large number of clinical trials are currently underway to evaluate the mechanism of action of immunochemotherapy regimens in neoadjuvant therapy (Table 2). In addition, increasing attention has been given to the sequence of administering anti-PD-1 antibodies and chemotherapeutic agents. A recent phase II study demonstrated that chemotherapy prior to anti-PD-L1 treatment could exert a better immunomodulatory effect in the neoadjuvant treatment of locally advanced esophageal squamous cell carcinoma (Fukuoka et al., 2019). Although this study is still ongoing, the current results suggest that delaying toripalimab administration to day 3 in immuno-chemotherapy may achieve higher pCR rates than administering both agents on the same day. This conclusion requires further large-sample clinical trials for verification.

With these general considerations related to drug scheduling, researchers should further investigate the different doses and lengths of drug-free periods required for various drugs and cancer types to improve the efficacy of immunogenic chemotherapy. This would further standardize the combination dynamics of different chemotherapy and immunotherapy drugs for different cancer types.

Chemotherapy combined with oncolytic virus therapy

Oncolytic viruses (OVs) comprise a novel immune anti-tumor therapy that can target tumor cells and replicate within them, thereby killing tumor cells (Martin and Bell, 2018). OVs, including adenovirus, parvovirus, reovirus, coxsackie virus, and HSV, can promote the expression of DAMPs to induce ICD. The synergistic combination of OVs and chemotherapeutic agents can compensate for the current situation wherein the inability of chemotherapeutic agents to induce ICD is the limiting factor. This combination has a significantly improved efficacy in enhancing the stimulation of an anti-tumor immune response compared with single-drug treatment (Habiba et al., 2020). For example, the combination of ONYX-015 and cisplatin significantly improved OS in a tumor xenograft model, showing superior efficacy to cisplatin monotherapy (Khuri et al., 2000). In addition, combination therapy with the oncolytic HSV-1 and mitoxantrone increased the accumulation of antigen-specific $CD8^+$ T cells in the tumor (Workenhe et al., 2013). Several clinical trials employing OVs in association with chemotherapeutic agents in various tumor types have been performed or are ongoing (Table 3). In a phase I/II trial of intravenous carboplatin/paclitaxel plus reovirus showed good objective responses and inhibition of tumor progression in cancer of the head and neck (Karapanagiotou et al., 2012). ONCOS-102 (previously known as CGTG-102) is an adenovirus equipped with GM-CSF. In a phase I trial, the safety and recommended dose of the oncolytic adenovirus ONCOS-102 combined with low-dose oral CTX for advanced cancer was investigated (Ranki et al., 2016). In a subsequent next phase I/II clinical trial, the safety and clinical efficacy of chemotherapy combined with ONCOS-102 in the treatment of malignant pleural mesothelioma were further evaluated (Kuryk et al., 2016). Therefore, chemotherapy combined with OV seems to provide a new therapeutic strategy for targeting the immune microenvironment since combining the two can better exert anti-tumor immune regulation.

Chemotherapy combined with cellular stress inducers

The mechanisms through which chemotherapeutic agents induce ICD are complex, diverse, and mainly related to cellular stress responses, manifested through ER stress, induction of autophagy, and ATP release (Zhou et al., 2021; Radogna and Diederich, 2018). Owing to tumor heterogeneity and the influence of the physicochemical properties of chemotherapeutic drugs, the restricted adjuvanticity of chemotherapy compromises the ability of dying cells to activate anti-tumor adaptive immunity. Recently, several cellular stress inducers have been discovered and used synergistically with chemotherapeutic agents to improve the overall response rate of ICD. As a representative cardiac glycoside, digoxin can potentially induce characteristic biomarkers of ICD, such as CRT exposure, ATP secretion, and HMGB1 release (Menger et al., 2012). When combined with cisplatin, a significant percentage of tumor-free mice were revaccinated with live tumor cells in mouse models (Xiang et al., 2020). This experimental result was confirmed to depend on the activation of anti-tumor immune responses. Likewise, statins have great potential to promote calreticulin exposure on the tumor cell surface and enhance cellular signaling associated with ER stress. In addition, statins can promote the activation and recruitment of APCs and tumor-

TABLE 3 Clinical trials on combination regimens of OVs and chemotherapy in cancer.

Drugs	Comibinations	Phase	Status	Cancer	References
TG6002	5-flucytosine	I/II	Recruiting	Glioblastoma	NCT03294486
				Brain Cancer	
LOAd703	gemcitabine/nab-paclitaxel/atezolizumab	I/II	Recruiting	Pancreatic Cancer	NCT02705196
Enadenotucirev	Capecitabine + Radiotherapy	I	Recruiting	Locally Advanced Rectal Cancer	NCT03916510
TBI-1401(HF10)	Gemcitabine + Nab-paclitaxel or TS-1	I	Active, not recruiting	Pancreatic Cancer Stage III/IV	NCT03252808
rQNestin34.5v.2	Cyclophosphamide	I	Recruiting	Brain Tumor	NCT03152318
Talimogene laherparepvec	Paclitaxel	I/II	Active, not recruiting	Breast Cancer	NCT02779855
OH2 oncolytic virus	LP002 + Cisplatin + Fluorouracil	I	Recruiting	Digestive System Neoplasms	NCT04755543
olvimulogene nanivacirepvec(Olvi-Vec)	Platinum chemotherapy: carboplatin (preferred) or cisplatin	III	Not yet recruiting	Ovarian Cancer	NCT05281471
Pelareorep	paclitaxel + avelumab	II	Recruiting	Breast Cancer Metastatic	NCT04215146
JX-594 (Pexa-Vec)	Irinotecan	I/II	Completed	Colorectal Carcinoma	NCT01394939
Reovirus Serotype 3—Dearing Strain (REOLYSIN®)	chemotherapy(Gemcitabine/Irinotecan/ Leucovorin+5-fluorouracil)+pembrolizumab	I	Completed	Pancreatic Adenocarcinoma	NCT02620423
Reovirus Serotype 3—Dearing Strain (REOLYSIN®)	Carboplatin + Paclitaxel	II	Completed	Carcinoma, Non-small Cell Lung	NCT00861627
Reovirus Serotype 3—Dearing Strain (REOLYSIN®)	Irinotecan/Fluorouracil/Leucovorin (FOLFIRI)+bevacizumab	I	Completed	KRAS Mutant Metastatic Colorectal Cancer	NCT01274624
oncolytic measles virus encoding thyroidal sodium iodide symporter (MV-NIS)	pegylated liposomal doxorubicin/gemcitabine/ topotecan/paclitaxel + bevacizumab	II	Recruiting	Ovarian Carcinoma	NCT02364713
DNX2401	Temozolomide	I	Completed	Glioblastoma Multiforme	
				Recurrent Tumor	NCT01956734
Oncolytic Reovirus (Reolysin NSC # 729,968)	Paclitaxel	II	Completed	ovarian epithelial, fallopian tube, or primary peritoneal cancer	NCT01199263
CGTG-102	low-dose metronomic cyclophosphamide	I	Completed	Malignant Solid Tumour	NCT01598129
CGTG-102	Pemetrexed/cisplatin (carboplatin)/ Cyclophosphamide	I/II	Active, not recruiting	Unresectable Malignant Pleural Mesothelioma	NCT02879669

This table is according to https://clinicaltrials.gov/

specific $CD8^+$ T cells in tumor tissues and draining lymph nodes, further enhancing the sensitivity of immune effector cells to ICD-related markers (Kwon et al., 2021). This effect was shown to be significantly improved after combined treatment with cisplatin. Moreover, chemotherapy-induced autophagy is required for the trafficking of T lymphocytes and dendritic cells. Oxaliplatin (OXA) has been experimentally shown to activate immunomodulatory responses by activating autophagy-dependent ATP release (Martins et al., 2012). On this basis, Wang et al. used the autophagy inducer Thiostrepton in combination with OXA and observed the shrinkage of TC1 NSCLC and MCA205 fibrosarcoma cells in an immunoactive C57BL/6 mouse model, which was dependent on the activation of T lymphocytes (Wang Y. et al., 2020). However, further preclinical studies focusing on the complete and dynamic biological mechanisms that account for cellular stress inducers are needed to facilitate the development of additional cell stress inducers. This would enable clinicians to strategically combine chemotherapy to induce immunogenic cellular stress.

Conclusion

As traditional anti-cancer agents, chemotherapeutic agents have exhibited significant benefits to patients with cancer. Although long considered immunosuppressive, there is mounting evidence to support the selection of chemotherapeutic agents with immunostimulatory properties as effective anti-cancer therapies. However, despite multiple mechanisms, the critical role of chemotherapeutics in determining the overall efficacy of cancer treatment remains unclear. With an improved understanding of the association of immunology and tumor biology at the molecular level, immunogenic cell death emerges as one of several crucial mechanisms by which chemotherapeutics elicit tumor-targeted

immune responses. Prospective preclinical results and preliminary clinical findings suggest that the integrated stress response induced by chemotherapeutic agents may be key to their long-term immunomodulatory effects. Further research and exploration of the mechanisms underlying the immunomodulatory effects of chemotherapy are required.

Accumulating clinical data indicate the potency of chemotherapeutics in combination with other anti-cancer drugs, particularly immunotherapy. When combining chemotherapeutic agents with immunotherapies or designing suitable delivery systems for chemotherapeutic drugs, such as nano-targeted delivery and ADCs, one should consider the relative merits of the constituent drugs in terms of their targets, pharmacokinetics, and safety. In addition, we also need to consider the administration sequence, time interval, and dose of the combination therapy. Lastly, biomarkers that can identify responses to combinatorial regimens of chemotherapeutic agents remain unknown. Recently, liquid biopsy, owing to its ability to monitor the immune landscape of the TME dynamically, appears to be useful for guiding immunogenic chemotherapy and providing a real-time biomarker screening approach. Overall, combinatorial regimens of chemotherapeutic agents are promising therapeutic platforms for optimizing combinatorial cancer treatments.

Author contributions

JL wrote the manuscript, searched the literature and prepared the figures and tables. YY was involved in the design of the study, and revised the manuscript. CL and CG provided article ideas, modified the tables and revised the manuscript. JZ, LL, QW, and WM performed literature research and collected relevant articles. QZ and CS participated in and helped draft the manuscript. All authors read and approved the final manuscript.

Funding

This work was supported by the National Natural Science Foundation of China (grant number 82174222 and 81973677).

Acknowledgments

Figures were created by Figdraw (www.figdraw.com).

Conflict of Interest

The authors declare that the research was conducted in the absence of any commercial or financial relationships that could be construed as a potential conflict of interest.

Publisher's note

References

Abdou, P., Wang, Z., Chen, Q., Chan, A., Zhou, D. R., Gunadhi, V., et al. (2020). Advances in engineering local drug delivery systems for cancer immunotherapy. *Wiley Interdiscip. Rev. Nanomed. Nanobiotechnol.* 12, e1632. doi:10.1002/wnan.1632

Agostinetto, E., Montemurro, F., Puglisi, F., Criscitiello, C., Bianchini, G., Del Mastro, L., et al. (2022). Immunotherapy for HER2-positive breast cancer: Clinical evidence and future perspectives. *Cancers (Basel)* 14, 2136. doi:10.3390/cancers14092136

Alizadeh, D., Trad, M., Hanke, N. T., Larmonier, C. B., Janikashvili, N., Bonnotte, B., et al. (2014). Doxorubicin eliminates myeloid-derived suppressor cells and enhances the efficacy of adoptive T-cell transfer in breast cancer. *Cancer Res.* 74, 104–118. doi:10.1158/0008-5472.CAN-13-1545

Belli, C., Trapani, D., Viale, G., D'Amico, P., Duso, B. A., Della Vigna, P., et al. (2018). Targeting the microenvironment in solid tumors. *Cancer Treat. Rev.* 65, 22–32. doi:10.1016/j.ctrv.2018.02.004

Bellomo, G., Rainer, C., Quaranta, V., Astuti, Y., Raymant, M., Boyd, E., et al. (2022). Chemotherapy-induced infiltration of neutrophils promotes pancreatic cancer metastasis via Gas6/AXL signalling axis. *Gut*, 325272. doi:10.1136/gutjnl-2021-325272

Bezu, L., Sauvat, A., Humeau, J., Gomes-da-Silva, L. C., Iribarren, K., Forveille, S., et al. (2018). eIF2α phosphorylation is pathognomonic for immunogenic cell death. *Cell Death Differ.* 25, 1375–1393. doi:10.1038/s41418-017-0044-9

Binnewies, M., Roberts, E. W., Kersten, K., Chan, V., Fearon, D. F., Merad, M., et al. (2018). Understanding the tumor immune microenvironment (TIME) for effective therapy. *Nat. Med.* 24, 541–550. doi:10.1038/s41591-018-0014-x

Bruchard, M., Geindreau, M., Perrichet, A., Truntzer, C., Ballot, E., Boidot, R., et al. (2022). Recruitment and activation of type 3 innate lymphoid cells promote antitumor immune responses. *Nat. Immunol.* 23, 262–274. doi:10.1038/s41590-021-01120-y

Buccione, C., Fragale, A., Polverino, F., Zicchedda, G., Arico, E., Belardelli, F., et al. (2018). Role of interferon regulatory factor 1 in governing Treg depletion, Th1 polarization, inflammasome activation and antitumor efficacy of cyclophosphamide. *Int. J. Cancer* 142, 976–987. doi:10.1002/ijc.31083

Casares, N., Pequignot, M. O., Tesniere, A., Ghiringhelli, F., Roux, S., Chaput, N., et al. (2005). Caspase-dependent immunogenicity of doxorubicin-induced tumor cell death. *J. Exp. Med.* 202, 1691–1701. doi:10.1084/jem.20050915

Casazza, A., Di Conza, G., Wenes, M., Finisguerra, V., Deschoemaeker, S., and Mazzone, M. (2014). Tumor stroma: A complexity dictated by the hypoxic tumor microenvironment. *Oncogene* 33, 1743–1754. doi:10.1038/onc.2013.121

Che, L. H., Liu, J. W., Huo, J. P., Luo, R., Xu, R. M., He, C., et al. (2021). A single-cell atlas of liver metastases of colorectal cancer reveals reprogramming of the tumor microenvironment in response to preoperative chemotherapy. *Cell Discov.* 7, 80. doi:10.1038/s41421-021-00312-y

Clement, C. C., Nanaware, P. P., Yamazaki, T., Negroni, M. P., Ramesh, K., Morozova, K., et al. (2021). Pleiotropic consequences of metabolic stress for the major histocompatibility complex class II molecule antigen processing and presentation machinery. *Immunity* 54, 721–736.e10. doi:10.1016/j.immuni.2021.02.019

Coats, S., Williams, M., Kebble, B., Dixit, R., Tseng, L., Yao, N. S., et al. (2019). Antibody-drug conjugates: Future directions in clinical and translational strategies to improve the therapeutic index. *Clin. Cancer Res.* 25, 5441–5448. doi:10.1158/1078-0432.CCR-19-0272

Coral, S., Sigalotti, L., Altomonte, M., Engelsberg, A., Colizzi, F., Cattarossi, I., et al. (2002). 5-aza-2'-deoxycytidine-induced expression of functional cancer testis antigens in human renal cell carcinoma: Immunotherapeutic implications. *Clin. Cancer Res.* 8, 2690–2695.

Correale, P., Aquino, A., Giuliani, A., Pellegrini, M., Micheli, L., Cusi, M. G., et al. (2003). Treatment of colon and breast carcinoma cells with 5-fluorouracil enhances expression of carcinoembryonic antigen and susceptibility to HLA-A(*) 02.01 restricted, CEA-peptide-specific cytotoxic T cells *in vitro*. *Int. J. Cancer* 104, 437–445. doi:10.1002/ijc.10969

Costa-Mattioli, M., and Walter, P. (2020). The integrated stress response: From mechanism to disease. *Science* 368, eaat5314. doi:10.1126/science.aat5314

D'Amico, L., Menzel, U., Prummer, M., Muller, P., Buchi, M., Kashyap, A., et al. (2019). A novel anti-HER2 anthracycline-based antibody-drug conjugate induces adaptive anti-tumor immunity and potentiates PD-1 blockade in breast cancer. *J. Immunother. Cancer* 7, 16. doi:10.1186/s40425-018-0464-1

Denkert, C., von Minckwitz, G., Darb-Esfahani, S., Lederer, B., Heppner, B. I., Weber, K. E., et al. (2018). Tumour-infiltrating lymphocytes and prognosis in different subtypes of breast cancer: A pooled analysis of 3771 patients treated with neoadjuvant therapy. *Lancet. Oncol.* 19, 40–50. doi:10.1016/S1470-2045(17)30904-X

Drago, J. Z., Modi, S., and Chandarlapaty, S. (2021). Unlocking the potential of antibody-drug conjugates for cancer therapy. *Nat. Rev. Clin. Oncol.* 18, 327–344. doi:10.1038/s41571-021-00470-8

Fares, J. E., El Tomb, P., Khalil, L. E., Atwani, R. W., Moukadem, H. A., Awada, A., et al. (2020). Metronomic chemotherapy for patients with metastatic breast cancer: Review of effectiveness and potential use during pandemics. *Cancer Treat. Rev.* 89, 102066. doi:10.1016/j.ctrv.2020.102066

Farhood, B., Najafi, M., and Mortezaee, K. (2019). CD8(+) cytotoxic T lymphocytes in cancer immunotherapy: A review. *J. Cell. Physiol.* 234, 8509–8521. doi:10.1002/jcp.27782

Fucikova, J., Palova-Jelinkova, L., Klapp, V., Holicek, P., Lanickova, T., Kasikova, L., et al. (2022). Immunological control of ovarian carcinoma by chemotherapy and targeted anticancer agents. *Trends Cancer* 8, 426–444. doi:10.1016/j.trecan.2022.01.010

Fukuoka, E., Yamashita, K., Tanaka, T., Sawada, R., Sugita, Y., Arimoto, A., et al. (2019). Neoadjuvant chemotherapy increases PD-L1 expression and CD8(+) tumor-infiltrating lymphocytes in esophageal squamous cell carcinoma. *Anticancer Res.* 39, 4539–4548. doi:10.21873/anticanres.13631

Fumet, J. D., Limagne, E., Thibaudin, M., and Ghiringhelli, F. (2020). Immunogenic cell death and elimination of immunosuppressive cells: A double-edged sword of chemotherapy. *Cancers (Basel)* 12, E2637. doi:10.3390/cancers12092637

Galaine, J., Turco, C., Vauchy, C., Royer, B., Mercier-Letondal, P., Queiroz, L., et al. (2019). CD4 T cells target colorectal cancer antigens upregulated by oxaliplatin. *Int. J. Cancer* 145, 3112–3125. doi:10.1002/ijc.32620

Galluzzi, L., Humeau, J., Buque, A., Zitvogel, L., and Kroemer, G. (2020b). Immunostimulation with chemotherapy in the era of immune checkpoint inhibitors. *Nat. Rev. Clin. Oncol.* 17, 725–741. doi:10.1038/s41571-020-0413-z

Galluzzi, L., Vitale, I., Warren, S., Adjemian, S., Agostinis, P., Martinez, A. B., et al. (2020a). Consensus guidelines for the definition, detection and interpretation of immunogenic cell death. *J. Immunother. Cancer* 8, e000337. doi:10.1136/jitc-2019-000337

Gandhi, L., Rodriguez-Abreu, D., Gadgeel, S., Esteban, E., Felip, E., De Angelis, F., et al. (2018). Pembrolizumab plus chemotherapy in metastatic non-small-cell lung cancer. *N. Engl. J. Med.* 378, 2078–2092. doi:10.1056/NEJMoa1801005

Garofalo, C., De Marco, C., and Cristiani, C. M. (2021). NK cells in the tumor microenvironment as new potential players mediating chemotherapy effects in metastatic melanoma. *Front. Oncol.* 11, 754541. doi:10.3389/fonc.2021.754541

Goc, J., Lv, M., Bessman, N. J., Flamar, A. L., Sahota, S., Suzuki, H., et al. (2021). Dysregulation of ILC3s unleashes progression and immunotherapy resistance in colon cancer. *Cell* 184, 5015–5030.e16. doi:10.1016/j.cell.2021.07.029

Goldberg, M. S. (2015). Immunoengineering: How nanotechnology can enhance cancer immunotherapy. *Cell* 161, 201–204. doi:10.1016/j.cell.2015.03.037

Golombek, S. K., May, J. N., Theek, B., Appold, L., Drude, N., Kiessling, F., et al. (2018). Tumor targeting via EPR: Strategies to enhance patient responses. *Adv. Drug Deliv. Rev.* 130, 17–38. doi:10.1016/j.addr.2018.07.007

Grabosch, S., Bulatovic, M., Zeng, F., Ma, T., Zhang, L., Ross, M., et al. (2019). Cisplatin-induced immune modulation in ovarian cancer mouse models with distinct inflammation profiles. *Oncogene* 38, 2380–2393. doi:10.1038/s41388-018-0581-9

Gu, L., and Mooney, D. J. (2016). Biomaterials and emerging anticancer therapeutics: Engineering the microenvironment. *Nat. Rev. Cancer* 16, 56–66. doi:10.1038/nrc.2015.3

Habiba, U., Hossain, E., Yanagawa-Matsuda, A., Chowdhury, A., Tsuda, M., Zaman, A. U., et al. (2020). Cisplatin relocalizes RNA binding protein HuR and enhances the oncolytic activity of E4orf6 deleted adenovirus. *Cancers (Basel)* 12, E809. doi:10.3390/cancers12040809

Heeren, A. M., van Luijk, I. F., Lakeman, J., Pocorni, N., Kole, J., de Menezes, R. X., et al. (2019). Neoadjuvant cisplatin and paclitaxel modulate tumor-infiltrating T cells in patients with cervical cancer. *Cancer Immunol. Immunother.* 68, 1759–1767. doi:10.1007/s00262-019-02412-x

Heldin, C. H., Rubin, K., Pietras, K., and Ostman, A. (2004). High interstitial fluid pressure - an obstacle in cancer therapy. *Nat. Rev. Cancer* 4, 806–813. doi:10.1038/nrc1456

Hetz, C., Zhang, K., and Kaufman, R. J. (2020). Mechanisms, regulation and functions of the unfolded protein response. *Nat. Rev. Mol. Cell Biol.* 21, 421–438. doi:10.1038/s41580-020-0250-z

Hodge, J. W., Garnett, C. T., Farsaci, B., Palena, C., Tsang, K. Y., Ferrone, S., et al. (2013). Chemotherapy-induced immunogenic modulation of tumor cells enhances killing by cytotoxic T lymphocytes and is distinct from immunogenic cell death. *Int. J. Cancer* 133, 624–636. doi:10.1002/ijc.28070

Hong, X., Dong, T., Yi, T., Hu, J., Zhang, Z., Lin, S., et al. (2018). Impact of 5-Fu/oxaliplatin on mouse dendritic cells and synergetic effect with a colon cancer vaccine. *Chin. J. Cancer Res.* 30, 197–208. doi:10.21147/j.issn.1000-9604.2018.02.03

Horn, L., Mansfield, A. S., Szczesna, A., Havel, L., Krzakowski, M., Hochmair, M. J., et al. (2018). First-line atezolizumab plus chemotherapy in extensive-stage small-cell lung cancer. *N. Engl. J. Med.* 379, 2220–2229. doi:10.1056/NEJMoa1809064

Ikegawa, S., and Matsuoka, K. I. (2021). Harnessing Treg homeostasis to optimize posttransplant immunity: Current concepts and future perspectives. *Front. Immunol.* 12, 713358. doi:10.3389/fimmu.2021.713358

Jain, R. K., Tong, R. T., and Munn, L. L. (2007). Effect of vascular normalization by antiangiogenic therapy on interstitial hypertension, peritumor edema, and lymphatic metastasis: Insights from a mathematical model. *Cancer Res.* 67, 2729–2735. doi:10.1158/0008-5472.CAN-06-4102

Kanterman, J., Sade-Feldman, M., Biton, M., Ish-Shalom, E., Lasry, A., Goldshtein, A., et al. (2014). Adverse immunoregulatory effects of 5FU and CPT11 chemotherapy on myeloid-derived suppressor cells and colorectal cancer outcomes. *Cancer Res.* 74, 6022–6035. doi:10.1158/0008-5472.CAN-14-0657

Karagiannis, G. S., Pastoriza, J. M., Wang, Y., Harney, A. S., Entenberg, D., Pignatelli, J., et al. (2017). Neoadjuvant chemotherapy induces breast cancer metastasis through a TMEM-mediated mechanism. *Sci. Transl. Med.* 9, eaan0026. doi:10.1126/scitranslmed.aan0026

Karapanagiotou, E. M., Roulstone, V., Twigger, K., Ball, M., Tanay, M., Nutting, C., et al. (2012). Phase I/II trial of carboplatin and paclitaxel chemotherapy in combination with intravenous oncolytic reovirus in patients with advanced malignancies. *Clin. Cancer Res.* 18, 2080–2089. doi:10.1158/1078-0432.CCR-11-2181

Khuri, F. R., Nemunaitis, J., Ganly, I., Arseneau, J., Tannock, I. F., Romel, L., et al. (2000). A controlled trial of intratumoral ONYX-015, a selectively-replicating adenovirus, in combination with cisplatin and 5-fluorouracil in patients with recurrent head and neck cancer. *Nat. Med.* 6, 879–885. doi:10.1038/78638

Kim, N. R., and Kim, Y. J. (2019). Oxaliplatin regulates myeloid-derived suppressor cell-mediated immunosuppression via downregulation of nuclear factor-κB signaling. *Cancer Med.* 8, 276–288. doi:10.1002/cam4.1878

Kohli, E., Causse, S., Baverel, V., Dubrez, L., Borges-Bonan, N., Demidov, O., et al. (2021). Endoplasmic reticulum chaperones in viral infection: Therapeutic perspectives. *Microbiol. Mol. Biol. Rev.* 85, e0003521. doi:10.1128/MMBR.00035-21

Koo, A. N., Min, K. H., Lee, H. J., Lee, S. U., Kim, K., Kwon, I. C., et al. (2012). Tumor accumulation and antitumor efficacy of docetaxel-loaded core-shell-corona micelles with shell-specific redox-responsive cross-links. *Biomaterials* 33, 1489–1499. doi:10.1016/j.biomaterials.2011.11.013

Kopecka, J., Salaroglio, I. C., Righi, L., Libener, R., Orecchia, S., Grosso, F., et al. (2018). Loss of C/EBP-beta LIP drives cisplatin resistance in malignant pleural mesothelioma. *Lung Cancer* 120, 34–45. doi:10.1016/j.lungcan.2018.03.022

Kroemer, G., Galassi, C., Zitvogel, L., and Galluzzi, L. (2022). Immunogenic cell stress and death. *Nat. Immunol.* 23, 487–500. doi:10.1038/s41590-022-01132-2

Kuryk, L., Haavisto, E., Garofalo, M., Capasso, C., Hirvinen, M., Pesonen, S., et al. (2016). Synergistic anti-tumor efficacy of immunogenic adenovirus ONCOS-102

(Ad5/3-D24-GM-CSF) and standard of care chemotherapy in preclinical mesothelioma model. *Int. J. Cancer* 139, 1883–1893. doi:10.1002/ijc.30228

Kwon, M., Nam, G. H., Jung, H., Kim, S. A., Kim, S., Choi, Y., et al. (2021). Statin in combination with cisplatin makes favorable tumor-immune microenvironment for immunotherapy of head and neck squamous cell carcinoma. *Cancer Lett.* 522, 198–210. doi:10.1016/j.canlet.2021.09.029

Laheurte, C., Thiery-Vuillemin, A., Calcagno, F., Legros, A., Simonin, H., Boullerot, L., et al. (2020). Metronomic cyclophosphamide induces regulatory T cells depletion and PSA-specific T cells reactivation in patients with biochemical recurrent prostate cancer. *Int. J. Cancer* 147, 1199–1205. doi:10.1002/ijc.32803

Lai, V., Neshat, S. Y., Rakoski, A., Pitingolo, J., and Doloff, J. C. (2021). Drug delivery strategies in maximizing anti-angiogenesis and anti-tumor immunity. *Adv. Drug Deliv. Rev.* 179, 113920. doi:10.1016/j.addr.2021.113920

Leonetti, A., Wever, B., Mazzaschi, G., Assaraf, Y. G., Rolfo, C., Quaini, F., et al. (2019). Molecular basis and rationale for combining immune checkpoint inhibitors with chemotherapy in non-small cell lung cancer. *Drug resist. updat.* 46, 100644. doi:10.1016/j.drup.2019.100644

Li, C., Sun, H., Wei, W., Liu, Q., Wang, Y., Zhang, Y., et al. (2020). Mitoxantrone triggers immunogenic prostate cancer cell death via p53-dependent PERK expression. *Cell. Oncol.* 43, 1099–1116. doi:10.1007/s13402-020-00544-2

Li, D., Schaub, N., Guerin, T. M., Bapiro, T. E., Richards, F. M., Chen, V., et al. (2021). T cell-mediated antitumor immunity cooperatively induced by TGFβR1 antagonism and gemcitabine counteracts reformation of the stromal barrier in pancreatic cancer. *Mol. Cancer Ther.* 20, 1926–1940. doi:10.1158/1535-7163.MCT-20-0620

Li, J. Y., Duan, X. F., Wang, L. P., Xu, Y. J., Huang, L., Zhang, T. F., et al. (2014). Selective depletion of regulatory T cell subsets by docetaxel treatment in patients with nonsmall cell lung cancer. *J. Immunol. Res.* 2014, 286170. doi:10.1155/2014/286170

Li, R., Mukherjee, M. B., and Lin, J. (2022). *Coordinated Regulation of Myeloid-Derived Suppressor Cells by Cytokines and Chemokines*, 14. doi:10.3390/cancers14051236*Cancers (Basel)*

Li, T., Wu, B., Yang, T., Zhang, L., and Jin, K. (2020). The outstanding antitumor capacity of CD4(+) T helper lymphocytes. *Biochim. Biophys. Acta. Rev. Cancer* 1874, 188439. doi:10.1016/j.bbcan.2020.188439

Machiels, J. P., Reilly, R. T., Emens, L. A., Ercolini, A. M., Lei, R. Y., Weintraub, D., et al. (2001). Cyclophosphamide, doxorubicin, and paclitaxel enhance the antitumor immune response of granulocyte/macrophage-colony stimulating factor-secreting whole-cell vaccines in HER-2/neu tolerized mice. *Cancer Res.* 61, 3689–3697.

Maeda, K., Hazama, S., Tokuno, K., Kan, S., Maeda, Y., Watanabe, Y., et al. (2011). Impact of chemotherapy for colorectal cancer on regulatory T-cells and tumor immunity. *Anticancer Res.* 31, 4569–4574.

Markasz, L., Stuber, G., Vanherberghen, B., Flaberg, E., Olah, E., Carbone, E., et al. (2007). Effect of frequently used chemotherapeutic drugs on the cytotoxic activity of human natural killer cells. *Mol. Cancer Ther.* 6, 644–654. doi:10.1158/1535-7163.MCT-06-0358

Martin, N. T., and Bell, J. C. (2018). Oncolytic virus combination therapy: Killing one bird with two stones. *Mol. Ther.* 26, 1414–1422. doi:10.1016/j.ymthe.2018.04.001

Martins, I., Kepp, O., Schlemmer, F., Adjemian, S., Tailler, M., Shen, S., et al. (2011). Restoration of the immunogenicity of cisplatin-induced cancer cell death by endoplasmic reticulum stress. *Oncogene* 30, 1147–1158. doi:10.1038/onc.2010.500

Martins, I., Michaud, M., Sukkurwala, A. Q., Adjemian, S., Ma, Y., Shen, S., et al. (2012). Premortem autophagy determines the immunogenicity of chemotherapy-induced cancer cell death. *Autophagy* 8, 413–415. doi:10.4161/auto.19009

McDonnell, A. M., Joost Lesterhuis, W., Khong, A., Nowak, A. K., Lake, R. A., Currie, A. J., et al. (2015a). Restoration of defective cross-presentation in tumors by gemcitabine. *Oncoimmunology* 4, e1005501. doi:10.1080/2162402X.2015.1005501

McDonnell, A. M., Lesterhuis, W. J., Khong, A., Nowak, A. K., Lake, R. A., Currie, A. J., et al. (2015b). Tumor-infiltrating dendritic cells exhibit defective cross-presentation of tumor antigens, but is reversed by chemotherapy. *Eur. J. Immunol.* 45, 49–59. doi:10.1002/eji.201444722

Medzhitov, R., and Janeway, C. A., Jr. (2002). Decoding the patterns of self and nonself by the innate immune system. *Science* 296, 298–300. doi:10.1126/science.1068883

Menger, L., Vacchelli, E., Adjemian, S., Martins, I., Ma, Y., Shen, S., et al. (2012). Cardiac glycosides exert anticancer effects by inducing immunogenic cell death. *Sci. Transl. Med.* 4, 143ra99. doi:10.1126/scitranslmed.3003807

Michaud, M., Sukkurwala, A. Q., Di Sano, F., Zitvogel, L., Kepp, O., and Kroemer, G. (2014). Synthetic induction of immunogenic cell death by genetic stimulation of endoplasmic reticulum stress. *Oncoimmunology* 3, e28276. doi:10.4161/onci.28276

Minute, L., Teijeira, A., Sanchez-Paulete, A. R., Ochoa, M. C., Alvarez, M., Otano, I., et al. (2020). Cellular cytotoxicity is a form of immunogenic cell death. *J. Immunother. Cancer* 8, e000325. doi:10.1136/jitc-2019-000325

Montes de Oca, R., Alavi, A. S., Vitali, N., Bhattacharya, S., Blackwell, C., Patel, K., et al. (2021). Belantamab mafodotin (GSK2857916) drives immunogenic cell death and immune-mediated antitumor responses *in vivo*. *Mol. Cancer Ther.* 20, 1941–1955. doi:10.1158/1535-7163.MCT-21-0035

Moschella, F., Valentini, M., Arico, E., Macchia, I., Sestili, P., D'Urso, M. T., et al. (2011). Unraveling cancer chemoimmunotherapy mechanisms by gene and protein expression profiling of responses to cyclophosphamide. *Cancer Res.* 71, 3528–3539. doi:10.1158/0008-5472.CAN-10-4523

Muller, P., Kreuzaler, M., Khan, T., Thommen, D. S., Martin, K., Glatz, K., et al. (2015). Trastuzumab emtansine (T-DM1) renders HER2+ breast cancer highly susceptible to CTLA-4/PD-1 blockade. *Sci. Transl. Med.* 7, 315ra188. doi:10.1126/scitranslmed.aac4925

Muller, P., Martin, K., Theurich, S., Schreiner, J., Savic, S., Terszowski, G., et al. (2014a). Microtubule-depolymerizing agents used in antibody-drug conjugates induce antitumor immunity by stimulation of dendritic cells. *Cancer Immunol. Res.* 2, 741–755. doi:10.1158/2326-6066.CIR-13-0198

Muller, P., Martin, K., Theurich, S., von Bergwelt-Baildon, M., and Zippelius, A. (2014b). Cancer chemotherapy agents target intratumoral dendritic cells to potentiate antitumor immunity. *Oncoimmunology* 3, e954460. doi:10.4161/21624011.2014.954460

Munn, D. H., and Mellor, A. L. (2016). Ido in the tumor microenvironment: Inflammation, counter-regulation, and tolerance. *Trends Immunol.* 37, 193–207. doi:10.1016/j.it.2016.01.002

Murphy, T. L., and Murphy, K. M. (2022). Dendritic cells in cancer immunology. *Cell. Mol. Immunol.* 19, 3–13. doi:10.1038/s41423-021-00741-5

Nakahara, T., Uchi, H., Lesokhin, A. M., Avogadri, F., Rizzuto, G. A., Hirschhorn-Cymerman, D., et al. (2010). Cyclophosphamide enhances immunity by modulating the balance of dendritic cell subsets in lymphoid organs. *Blood* 115, 4384–4392. doi:10.1182/blood-2009-11-251231

Ng, H. Y., Li, J., Tao, L., Lam, A. K., Chan, K. W., Ko, J. M. Y., et al. (2018). Chemotherapeutic treatments increase PD-L1 expression in esophageal squamous cell carcinoma through EGFR/ERK activation. *Transl. Oncol.* 11, 1323–1333. doi:10.1016/j.tranon.2018.08.005

Nishikawa, H., and Koyama, S. (2021). Mechanisms of regulatory T cell infiltration in tumors: Implications for innovative immune precision therapies. *J. Immunother. Cancer* 9, e002591. doi:10.1136/jitc-2021-002591

Paijens, S. T., Vledder, A., de Bruyn, M., and Nijman, H. W. (2021). Tumor-infiltrating lymphocytes in the immunotherapy era. *Cell. Mol. Immunol.* 18, 842–859. doi:10.1038/s41423-020-00565-9

Park, Y. H., Lal, S., Lee, J. E., Choi, Y. L., Wen, J., Ram, S., et al. (2020). Chemotherapy induces dynamic immune responses in breast cancers that impact treatment outcome. *Nat. Commun.* 11, 6175. doi:10.1038/s41467-020-19933-0

Pfannenstiel, L. W., Lam, S. S., Emens, L. A., Jaffee, E. M., and Armstrong, T. D. (2010). Paclitaxel enhances early dendritic cell maturation and function through TLR4 signaling in mice. *Cell. Immunol.* 263, 79–87. doi:10.1016/j.cellimm.2010.03.001

Pfirschke, C., Engblom, C., Rickelt, S., Cortez-Retamozo, V., Garris, C., Pucci, F., et al. (2016). Immunogenic chemotherapy sensitizes tumors to checkpoint blockade therapy. *Immunity* 44, 343–354. doi:10.1016/j.immuni.2015.11.024

Principe, D. R., Kamath, S. D., Korc, M., and Munshi, H. G. (2022). The immune modifying effects of chemotherapy and advances in chemo-immunotherapy. *Pharmacol. Ther.* 236, 108111. doi:10.1016/j.pharmthera.2022.108111

Radogna, F., and Diederich, M. (2018). Stress-induced cellular responses in immunogenic cell death: Implications for cancer immunotherapy. *Biochem. Pharmacol.* 153, 12–23. doi:10.1016/j.bcp.2018.02.006

Ranki, T., Pesonen, S., Hemminki, A., Partanen, K., Kairemo, K., Alanko, T., et al. (2016). Phase I study with ONCOS-102 for the treatment of solid tumors - an evaluation of clinical response and exploratory analyses of immune markers. *J. Immunother. Cancer* 4, 17. doi:10.1186/s40425-016-0121-5

Roselli, M., Cereda, V., di Bari, M. G., Formica, V., Spila, A., Jochems, C., et al. (2013). Effects of conventional therapeutic interventions on the number and function of regulatory T cells. *Oncoimmunology* 2, e27025. doi:10.4161/onci.27025

Saeed, M., Gao, J., Shi, Y., Lammers, T., and Yu, H. (2019). Engineering nanoparticles to reprogram the tumor immune microenvironment for improved cancer immunotherapy. *Theranostics* 9, 7981–8000. doi:10.7150/thno.37568

Saleh, R., and Elkord, E. (2019). Treg-mediated acquired resistance to immune checkpoint inhibitors. *Cancer Lett.* 457, 168–179. doi:10.1016/j.canlet.2019.05.003

Schmid, P., Adams, S., Rugo, H. S., Schneeweiss, A., Barrios, C. H., Iwata, H., et al. (2018). Atezolizumab and nab-paclitaxel in advanced triple-negative breast cancer. *N. Engl. J. Med.* 379, 2108–2121. doi:10.1056/NEJMoa1809615

Shurin, G. V., Tourkova, I. L., Kaneno, R., and Shurin, M. R. (2009). Chemotherapeutic agents in noncytotoxic concentrations increase antigen presentation by dendritic cells via an IL-12-dependent mechanism. *J. Immunol.* 183, 137–144. doi:10.4049/jimmunol.0900734

Sindhwani, S., Syed, A. M., Ngai, J., Kingston, B. R., Maiorino, L., Rothschild, J., et al. (2020). The entry of nanoparticles into solid tumours. *Nat. Mat.* 19, 566–575. doi:10.1038/s41563-019-0566-2

Spehner, L., Kim, S., Vienot, A., Francois, E., Buecher, B., Adotevi, O., et al. (2020). Anti-telomerase CD4(+) Th1 immunity and monocytic-myeloid-derived-suppressor cells are associated with long-term efficacy achieved by docetaxel, cisplatin, and 5-fluorouracil (DCF) in advanced anal squamous cell carcinoma: Translational study of epitopes-HPV01 and 02 trials. *Int. J. Mol. Sci.* 21, E6838. doi:10.3390/ijms21186838

Tang, T., Huang, X., Zhang, G., Hong, Z., Bai, X., and Liang, T. (2021). Advantages of targeting the tumor immune microenvironment over blocking immune checkpoint in cancer immunotherapy. *Signal Transduct. Target. Ther.* 6, 72. doi:10.1038/s41392-020-00449-4

Tel, J., Hato, S. V., Torensma, R., Buschow, S. I., Figdor, C. G., Lesterhuis, W. J., et al. (2012). The chemotherapeutic drug oxaliplatin differentially affects blood DC function dependent on environmental cues. *Cancer Immunol. Immunother.* 61, 1101–1111. doi:10.1007/s00262-011-1189-x

Tesniere, A., Schlemmer, F., Boige, V., Kepp, O., Martins, I., Ghiringhelli, F., et al. (2010). Immunogenic death of colon cancer cells treated with oxaliplatin. *Oncogene* 29, 482–491. doi:10.1038/onc.2009.356

Theurich, S., Malcher, J., Wennhold, K., Shimabukuro-Vornhagen, A., Chemnitz, J., Holtick, U., et al. (2013). Brentuximab vedotin combined with donor lymphocyte infusions for early relapse of Hodgkin lymphoma after allogeneic stem-cell transplantation induces tumor-specific immunity and sustained clinical remission. *J. Clin. Oncol.* 31, e59–e63. doi:10.1200/JCO.2012.43.6832

Tie, Y., Tang, F., Wei, Y. Q., and Wei, X. W. (2022). Immunosuppressive cells in cancer: Mechanisms and potential therapeutic targets. *J. Hematol. Oncol.* 15, 61. doi:10.1186/s13045-022-01282-8

Tsuda, N., Chang, D. Z., Mine, T., Efferson, C., Garcia-Sastre, A., Wang, X., et al. (2007). Taxol increases the amount and T cell activating ability of self-immune stimulatory multimolecular complexes found in ovarian cancer cells. *Cancer Res.* 67, 8378–8387. doi:10.1158/0008-5472.CAN-07-0327

Van Wigcheren, G. F., De Haas, N., Mulder, T. A., Horrevorts, S. K., Bloemendal, M., Hins-Debree, S., et al. (2021). Cisplatin inhibits frequency and suppressive activity of monocytic myeloid-derived suppressor cells in cancer patients. *Oncoimmunology* 10, 1935557. doi:10.1080/2162402X.2021.1935557

Vincent, J., Mignot, G., Chalmin, F., Ladoire, S., Bruchard, M., Chevriaux, A., et al. (2010). 5-Fluorouracil selectively kills tumor-associated myeloid-derived suppressor cells resulting in enhanced T cell-dependent antitumor immunity. *Cancer Res.* 70, 3052–3061. doi:10.1158/0008-5472.CAN-09-3690

Wanderley, C. W., Colon, D. F., Luiz, J. P. M., Oliveira, F. F., Viacava, P. R., Leite, C. A., et al. (2018). Paclitaxel reduces tumor growth by reprogramming tumor-associated macrophages to an M1 profile in a TLR4-dependent manner. *Cancer Res.* 78, 5891–5900. doi:10.1158/0008-5472.CAN-17-3480

Wang, C., Wang, J., Zhang, X., Yu, S., Wen, D., Hu, Q., et al. (2018). *In situ* formed reactive oxygen species-responsive scaffold with gemcitabine and checkpoint inhibitor for combination therapy. *Sci. Transl. Med.* 10, eaan3682. doi:10.1126/scitranslmed.aan3682

Wang, W., Jin, Y., Xu, Z., Liu, X., Bajwa, S. Z., Khan, W. S., et al. (2020a). Stimuli-activatable nanomedicines for chemodynamic therapy of cancer. *Wiley Interdiscip. Rev. Nanomed. Nanobiotechnol.* 12, e1614. doi:10.1002/wnan.1614

Wang, Y., Xie, W., Humeau, J., Chen, G., Liu, P., Pol, J., et al. (2020b). Autophagy induction by thiostrepton improves the efficacy of immunogenic chemotherapy. *J. Immunother. Cancer* 8, e000462. doi:10.1136/jitc-2019-000462

Weber, J. S., and Mule, J. J. (2015). Cancer immunotherapy meets biomaterials. *Nat. Biotechnol.* 33, 44–45. doi:10.1038/nbt.3119

Williams, K. M., Hakim, F. T., and Gress, R. E. (2007). T cell immune reconstitution following lymphodepletion. *Semin. Immunol.* 19, 318–330. doi:10.1016/j.smim.2007.10.004

Workenhe, S. T., Pol, J. G., Lichty, B. D., Cummings, D. T., and Mossman, K. L. (2013). Combining oncolytic HSV-1 with immunogenic cell death-inducing drug mitoxantrone breaks cancer immune tolerance and improves therapeutic efficacy. *Cancer Immunol. Res.* 1, 309–319. doi:10.1158/2326-6066.CIR-13-0059-T

Wu, J., and Waxman, D. J. (2018). Immunogenic chemotherapy: Dose and schedule dependence and combination with immunotherapy. *Cancer Lett.* 419, 210–221. doi:10.1016/j.canlet.2018.01.050

Xiang, Y., Chen, L., Li, L., and Huang, Y. (2020). Restoration and enhancement of immunogenic cell death of cisplatin by coadministration with digoxin and conjugation to HPMA copolymer. *ACS Appl. Mat. Interfaces* 12, 1606–1616. doi:10.1021/acsami.9b19323

Yu, B., Jiang, T., and Liu, D. (2020). BCMA-targeted immunotherapy for multiple myeloma. *J. Hematol. Oncol.* 13, 125. doi:10.1186/s13045-020-00962-7

Zammarchi, F., Havenith, K., Bertelli, F., Vijayakrishnan, B., Chivers, S., and van Berkel, P. H. (2020). CD25-targeted antibody-drug conjugate depletes regulatory T cells and eliminates established syngeneic tumors via antitumor immunity. *J. Immunother. Cancer* 8, e000860. doi:10.1136/jitc-2020-000860

Zhang, J., Pan, S., Jian, C., Hao, L., Dong, J., Sun, Q., et al. (2021). Immunostimulatory properties of chemotherapy in breast cancer: From immunogenic modulation mechanisms to clinical practice. *Front. Immunol.* 12, 819405. doi:10.3389/fimmu.2021.819405

Zhao, C., Bartock, M., Jia, B., Shah, N., Claxton, D. F., Wirk, B., et al. (2022). Post-transplant cyclophosphamide alters immune signatures and leads to impaired T cell reconstitution in allogeneic hematopoietic stem cell transplant. *J. Hematol. Oncol.* 15, 64. doi:10.1186/s13045-022-01287-3

Zhou, L., Zhang, P., Wang, H., Wang, D., and Li, Y. (2020). Smart nanosized drug delivery systems inducing immunogenic cell death for combination with cancer immunotherapy. *Acc. Chem. Res.* 53, 1761–1772. doi:10.1021/acs.accounts.0c00254

Zhou, Y., Bastian, I. N., Long, M. D., Dow, M., Li, W., Liu, T., et al. (2021). Activation of NF-κB and p300/CBP potentiates cancer chemoimmunotherapy through induction of MHC-I antigen presentation. *Proc. Natl. Acad. Sci. U. S. A.* 118, e2025840118. doi:10.1073/pnas.2025840118

Zhu, Y., Yang, Z., Dong, Z., Gong, Y., Hao, Y., Tian, L., et al. (2020). CaCO3-Assisted preparation of pH-responsive immune-modulating nanoparticles for augmented chemo-immunotherapy. *Nanomicro. Lett.* 13, 29. doi:10.1007/s40820-020-00549-4

Zitvogel, L., Apetoh, L., Ghiringhelli, F., and Kroemer, G. (2008). Immunological aspects of cancer chemotherapy. *Nat. Rev. Immunol.* 8, 59–73. doi:10.1038/nri2216

Zitvogel, L., Pitt, J. M., Daillere, R., Smyth, M. J., and Kroemer, G. (2016). Mouse models in oncoimmunology. *Nat. Rev. Cancer* 16, 759–773. doi:10.1038/nrc.2016.91

frontiers | Frontiers in Pharmacology

TYPE Original Research
PUBLISHED 14 October 2022
DOI 10.3389/fphar.2022.978421

OPEN ACCESS

EDITED BY
Dongdong Sun,
Nanjing University of Chinese Medicine, China

REVIEWED BY
Jing Zhao,
University of Macau, China
Jing Guo,
Stanford University, United States

*CORRESPONDENCE
Ji Wang,
doctorwang2009@126.com
Qi Wang,
wangqi710@126.com

SPECIALTY SECTION
This article was submitted to Inflammation Pharmacology, a section of the journal Frontiers in Pharmacology

RECEIVED 26 June 2022
ACCEPTED 14 September 2022
PUBLISHED 14 October 2022

CITATION
Zhou Y, Hu L, Zhang H, Zhang H, Liu J, Zhao X, Wang J and Wang Q (2022), Guominkang formula alleviate inflammation in eosinophilic asthma by regulating immune balance of Th1/2 and Treg/Th17 cells.
Front. Pharmacol. 13:978421.
doi: 10.3389/fphar.2022.978421

Guominkang formula alleviate inflammation in eosinophilic asthma by regulating immune balance of Th1/2 and Treg/Th17 cells

Yumei Zhou[1], Linhan Hu[1], Honglei Zhang[1], Haiyun Zhang[1], Juntong Liu[1], Xiaoshan Zhao[2], Ji Wang[1]* and Qi Wang[1]*

[1]School of Chinese Medicine, National Institute of TCM Body Constitution and Preventive Medicine, Beijing University of Chinese Medicine, Beijing, China, [2]School of Traditional Chinese Medicine, Southern Medical University, Guangzhou, Guangdong, China

The number of patients with allergic asthma is rising yearly, and hormonal drugs, such as dexamethasone, have unique advantages and certain limitations. In the treatment of allergic diseases especially allergic asthma, increasing the percentage or the function of immunosuppressive cells, such as Treg cells, may achieve a good effect. On the basis of good clinical results, we found that Guominkang (GMK) especially high-concentration GMK can achieve a similar effect with dexamethasone in controlling the symptoms of allergic asthma and inhibiting inflammation of allergic asthma. In our study, GMK can inhibit the recruitment of inflammatory cells, decrease mucus production, and reduce airway resistance. Besides, GMK can reconstruct the cellular immune balance of Th1/2 and Treg/Th17 cells. Metabolome results show that DL-glutamine, L-pyroglutamic acid, prostaglandin b1, prostaglandin e2, and 3,4-dihydroxyhydrocinnamic acid are the metabolic biomarkers and are associated with Th1/2 and Treg/Th17 cell balance. GMK can also change the gut microbiota in the allergic asthma mouse model. The genus_*Muriculum*, genus_*(Clostridium) GCA900066575*, genus_*klebsiella*, *genus_Desulfovibrio*, genus_Rikenellaceae *RC9 gut group*, family_Chitinophagaceae, family_Nocardioidaceae, and genus_*Corynebacterium* are gut microbiota biomarkers treated by GMK. Among these biomarkers, genus_*Muriculum* is the gut microbiota biomarker associated with Th1/2 and Treg/Th17 cell balance. Interestingly, we first found that DL-glutamine, L-pyroglutamic acid, prostaglandin b1, prostaglandin e2, and 3,4-dihydroxyhydrocinnamic acid are all associated with genus_*Muriculum*. GMK will be a new strategy for the treatment of eosinophilic asthma, and biomarkers will also be a new research direction.

KEYWORDS

GMK, Th1/Th2, Treg/Th17, cellular immune balance, eosinophilic asthma

Introduction

Asthma is a chronic inflammatory disease with high incidence rate, which can cause more than 250000 deaths every year (Fahy, 2015). Epidemiological studies showed that environmental risk factors (such as respiratory viral infections (Busse et al., 2010) and air pollutants (Peden, 2005)) and increasing urbanized lifestyles (including reduced exposure to microbes or their products (Braun-Fahrländer et al., 2002)) are factors inducing allergic asthma. Among the various forms of asthma (e.g., caused by allergens, air pollution, exercise, aspirin, and cold), allergic asthma is the most prevalent and can be induced by allergens, such as peanut, house dust mite (HDM), pollen, and animal dander. Inhaled corticosteroids (ICS) and long acting β Agonists are the basic treatment of asthma, which can effectively control the symptoms of allergic asthma. However, these therapies are not suitable for all patients with allergic asthma because some patients develop severe asthma. Severe asthma is characterized as difficulty in drug control, recurrent attacks, and chronic airflow obstruction (Lloyd and Hawrylowicz, 2009). Acute exacerbation of allergic asthma has a huge impact on both adults and children. At the same time, it brings a huge economic burden to patients with allergic asthma and endangers public health. According to the regularly revised global Asthma Initiative, few drugs are suitable for new biological agents or treatment schemes such as allergen specific immunotherapy (Duan et al., 2004; Sakaguchi et al., 2008).

Allergic asthma is predominantly divided into two inflammatory subtypes caused by T helper (Th) cells, i.e., Th2-high and Th2-low. The Th2-high subtype are associated with Th2 subtype cytokines such as IL (interleukin)-4, IL-5, and IL-13, and are characterized by airway eosinophilic infiltration. In allergic asthma, airway eosinophilia and goblet cell metaplasia are predominantly induced by IL-5 and IL-13, respectively (Finkelman et al., 2010; Chung, 2015). IL-4 has a certain correlation with sensitization and IgE production. IL-5 participates in eosinophil survival, and IL-13 affects the development and reorganization of airway hyperresponsiveness (AHR) (Sun et al., 2020). Studies have shown that the pathogenesis of airway inflammation in allergic asthma is related to the imbalance of Th1/Th2 cells, and the main reason for the excessive differentiation of Th2 cells is the insufficient differentiation of Th1 cells. An important strategy for the treatment of allergic asthma is to induce allergen immune tolerance (Heffler et al., 2019).

Current treatments based on glucocorticoid inhalation can only control Th2-driven eosinophil inflammation but cannot induce immune tolerance (Dhami et al., 2017). Foxp3+ Treg cells are critical for maintaining immune homeostasis in allergic asthma, and can inhibit inflammatory response (Joetham et al., 2007). Treg cells are a type of $CD4^+$ T cell subpopulation, and the transcription factor Forkhead Box 3 (FOXP3), as a specific Treg cell maker, is essential to their function (Bullens et al., 2006; Finkelman et al., 2010). FOXP3 is the key to the differentiation of Treg cells. If FOXP3 gene is mutated, abnormal Treg cells will be produced. They lack regulatory function (Berker et al., 2017; Asayama et al., 2020). For patients with allergic asthma, the imbalance of Treg and Th cells in the process of allergic reaction has a certain impact on the development of asthma (Lee et al., 2009). IL-10 and TGF-β play an irreplaceable role in the regulation of allergic asthma. TGF-β can induce Foxp3 expression and Treg cell differentiation. IL-10 is also critical for the effective suppression of allergic reactions in the lung (Kudo et al., 2012). Recent studies showed that the IL-17A produced by Th17 cells promotes allergen-induced AHR through direct effects on airway smooth muscle (Gavin et al., 2007). The elevated levels of IL-17A are found in serum, sputum, and bronchoalveolar lavage (BAL) of patients with allergic asthma, and the concentrations of IL-17A are positively correlated with asthma severity at these sites (Baatjes et al., 2015; Zhao and Wang, 2018). Recent studies have shown that both Treg and Th17 cells have the ability to redifferentiate and belong to an unstable population (Tortola et al., 2019). Some treatment schemes are aimed at improving the symptoms of allergy and asthma. They all start from stimulating the proliferation of Treg cells to increase the number of Treg cells or restore the function of Treg cells (Hori et al., 2003). Therefore, increasing studies focused on stimulating Treg cell proliferation or inhibiting Th17 cell redifferentiation and changing the differentiation level of Treg or Th17 cells to rebuild the balance of Th17/Treg cells, which is correlated with asthma severity (Fontenot et al., 2003; Lin et al., 2007).

In the past few years, the combination of hormone therapy, such as ICS, with other medications, including a long-acting β2-agonist or a leukotriene modifier, is the first choice to treat allergic asthma, but not all patients achieve asthma control (Durrant and Metzger, 2010). A new drug that can induce immune tolerance and is expected to inhibit the recurrence of asthma is urgently needed. GMK is a drug prescribed by academician Qi Wang after many years of clinical experience and has achieved good clinical effect in treating allergic disease. In this study, we try to clarify the mechanism of GMK in treating eosinophilic asthma.

Materials and methods

Mice

Female BALB/c mice (age: 6–8 weeks old) were obtained from Beijing Vital River Laboratory Animal Technology Co. Ltd., Beijing, China. These mice were housed in pathogen-free conditions. All animal procedures were approved by Beijing University of Chinese Medicine Animal Care and Use Committee and conducted in accordance with AAALAC and IACUC guidelines.

Preparation of GMK

The four components of GMK used in our experiment are: Wu-Mei (Mume Fructus) 20 g, Chan-Tui (Cicadae Periostracum) 10 g,

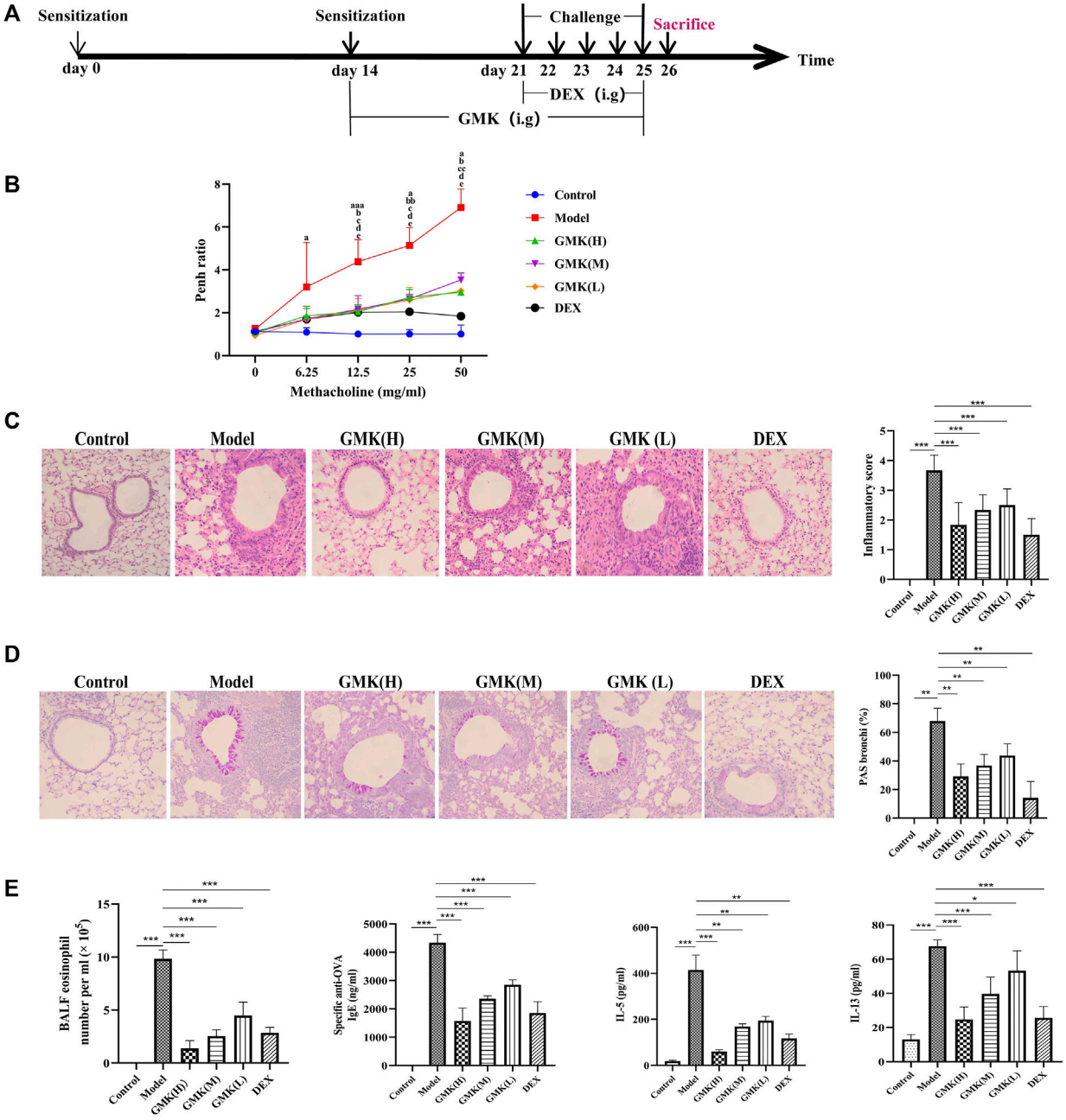

FIGURE 1
GMK can alleviate inflammation of eosinophilic asthma in BALB/c mice model. **(A)** Flow chart of eosinophilic asthma model construction in BALB/c mice. **(B)** Allergens airway hyperresponsiveness assessment by non-invasive methods. Mice (n = 4–5/group) were sensitized and challenged with OVA. a, $p < 0.05$ vs. Control; aa, $p < 0.01$ vs. Control; aaa, $p \leq 0.001$ vs. Control. b, $p < 0.05$ vs. GMK(H); bb, $p < 0.01$ vs. GMK(H); bbb, $p \leq 0.001$ vs. GMK(H). c, $p < 0.05$ vs. GMK(M); cc, $p < 0.01$ vs. GMK(M); ccc, $p \leq 0.001$ vs. GMK(M). d, $p < 0.05$ vs. GMK (L); dd, $p < 0.01$ vs. GMK(L); ddd, $p \leq 0.001$ vs. GMK(L); e, $p < 0.05$ vs. DEX; ee, $p < 0.01$ vs. DEX; eee, $p \leq 0.001$ vs. DEX. **(C)** HE staining and inflammation score of lung tissue. **(D)** Typical PAS staining and the related corresponding score of lung tissue. **(E)** Specific OVA-IgE antibody detection in serum, eosinophil count in bronchoalveolar lavage fluid (BALF), IL-5 and IL-13 cytokines detection in BALF (n = 5–6/group). The experiments repeated 2–3 times in this study. *$p < 0.05$, **$p < 0.01$, ***$p \leq 0.001$.

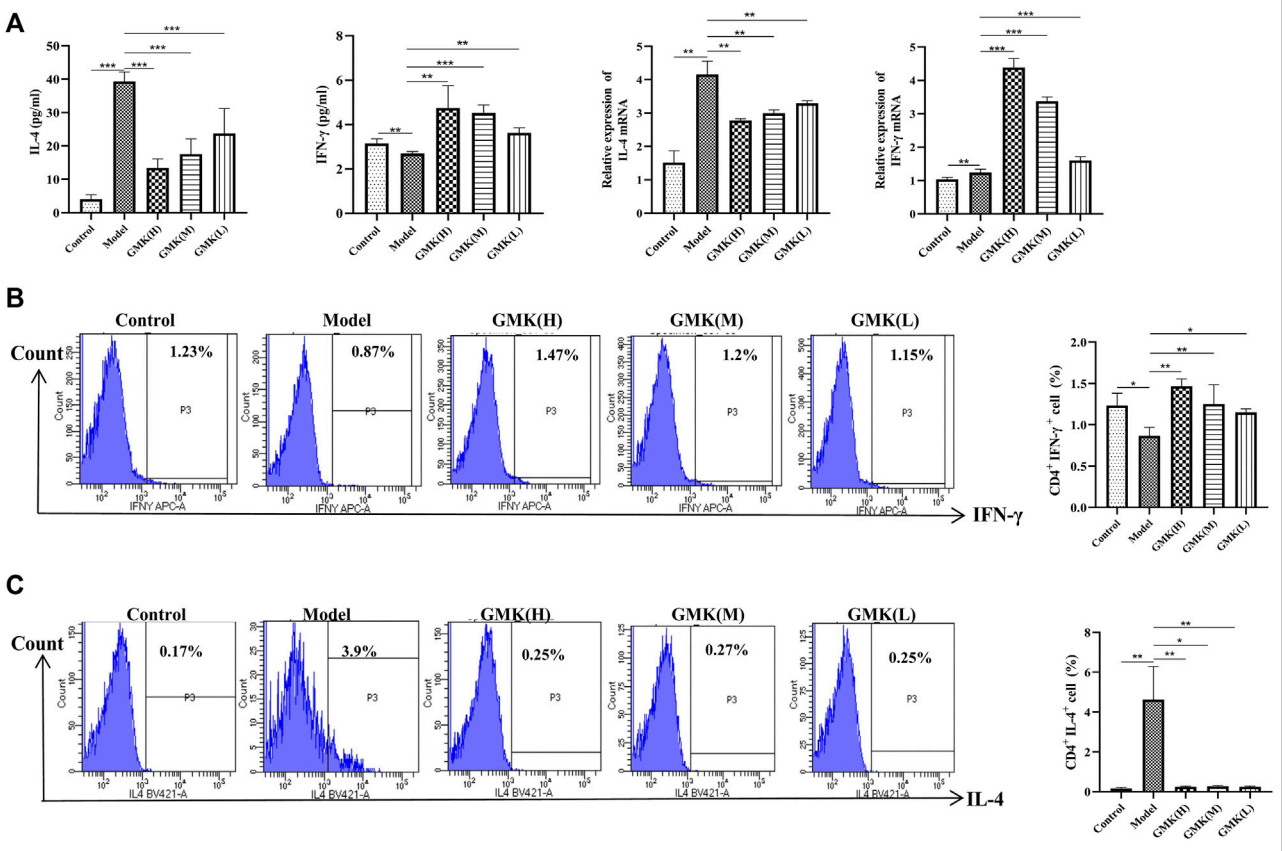

FIGURE 2
Th1, Th2 cells and their related cytokines and gene detection. **(A)** Th1 and Th2 cells related cytokines detection in BALF and the IL-4 and IFN-γ mRNA expression in lung tissue analyzed by real-time RT-PCR. **(B,C)** Flow cytometry detection of Th1 and Th2 cells in spleen tissue, results was all represent as mean±SEM (n = 5–6/group). $CD3^+CD4^+$ cells were gated, then IFN-γ+ cells were gated for Th1 cells. $CD3^+CD4^+$ cells were gated, then $IL\text{-}4^+$ cells were gated for Th2 cells. The experiments repeated 3 times in this study. *$p < 0.05$, **$p < 0.01$, ***$p \leq 0.001$.

Fang-feng (Saposhnikoviae radix) 10 g, Ling-zhi (Ganoderma) 10 g, Shou-Wuteng (Caulis Polygoni Multiflori) 15 g, Tian-ma (Gastrodia elata Blume) 10g, they were named by Pharmacopoeia of China (2020). After soaked in deionized water for 30 min. The final concentration of the drug were GMK(H) group:19.5 g/kg/d, GMK(M) group: 9.75 g/kg/d, GMK(L) group:4.875 g/kg/d. More details can be found in references (Wu et al., 2019). DEX (Dexamethasone) was given 1 mg/kg/d, and it was dissolved in saline solution. The drug of GMK and DEX were given according to Figure 1A, GMK were given from day 14 to day 25, DEX was given from day 21 to day 25, they were all given once a day.

Construction of eosinophilic asthma mouse model, administration of GMK, and detection of airway resistance

The eosinophilic asthma mouse model was induced by ovalbumin (OVA). Mice were sensitized on days 0 and 14 by intraperitoneal injection with 2 mg OVA (Sigma-Aldrich, Cat#A5503) and 2 mg Alum Adjuvant (Invitrogen, Cat#77161) dissolved in PBS. Mice inhaled 1%ova for 30 min from day 21 to day 25. BAL fluid (BALF) was collected 24 h after the last challenge.

On day 26, after challenge for 5 days, 0, 6.25, 12.5, 25, and 50 mg/ml methacholine (Sigma, Cat#A2251) was used to detect the enhanced pause (Penh) value. The airway resistance experiment was carried through the noninvasive measurement of airway hyperresponsiveness by whole-body plethysmography (WBP-4MR, TOW, China) as described previously (Li et al., 2009). The Penh ratio was used to represent the Penh measured (using methacholine divided by the mean Penh over a 5-min interval using PBS).

Hematoxylin and eosin and periodic acid–schiff staining of lung tissue

Lung tissues were fixed in 4% paraformaldehyde, embedded into paraffin, and cut into 4 μm prepared

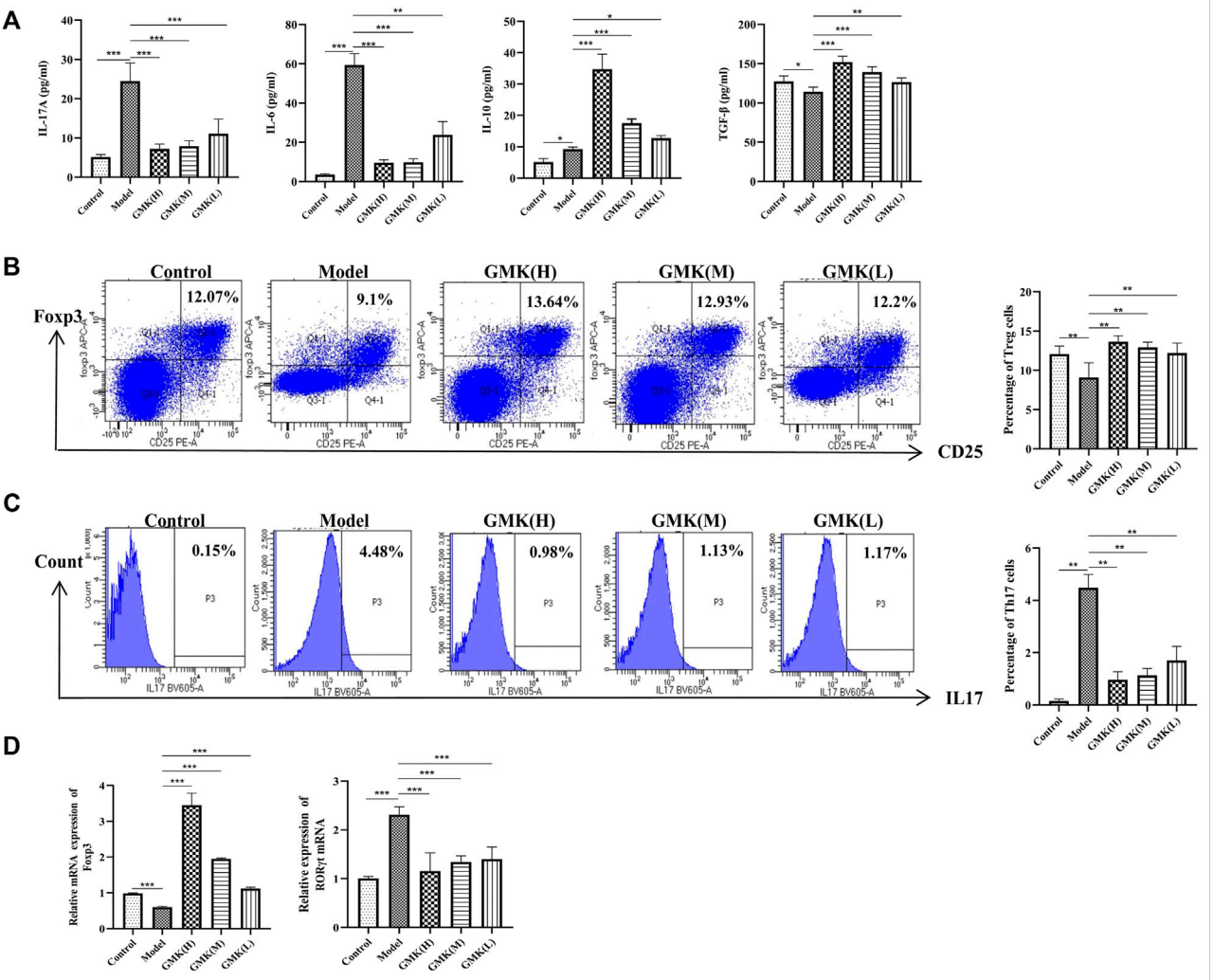

FIGURE 3
Treg, Th17 cells and their related cytokines and mRNA detection. **(A)** Treg and Th17 cells related cytokines detection in BALF. **(B,C)** Percentage detection of Treg and Th17 cells in spleen tissue. **(D)** The Foxp3 and RORγt mRNA relative expression in the lung tissue analyzed by real-time RT-PCR, results was represent as mean±SEM (n = 5–6/group). $CD3^+CD4^+$ cells were gated, then $CD25^+Foxp3^+$ cells were gated for Treg cells. $CD3^+CD4^+$ cells were gated, then IL-17^+ cells were gated for Th17 cells. The experiments repeated 3 times in this study.*$p < 0.05$, **$p < 0.01$, ***$p \leq 0.001$.

sections. Lung tissues were stained by HE staining for cell infiltration detection or PAS for mucus production. As mentioned earlier, inflammatory cells and goblet cells were scored in at least three different areas of each lung section (Buzney et al., 2016).

Percentage of Th1, Th2, Treg and Th17 cells and cytokines in BALF and specific OVA–IgE detection in Serum

Collecting spleen tissue and prepareing it into single cell suspension. Pay attention to the aseptic operation. For flow cytometry, cells were stimulated in complete RPMI containing 2 μl cocktail A (BD, Cat#550583) for 4 Construction of eosinophilic asthma mouse h, after blocked by Fc-receptor blocker (BD, Cat#513141) in 37°C for 40Construction of eosinophilic asthma mouse min, washed, and resuspended in 1 × PBS, and stained with FVS780 (BD, Cat#565388) to discriminate viable cells. The eBioscience Fix/Perm (Cat#00-5523-00) and BD Fix/Perm (Cat#554714) buffer kits were used to fix and permeabilize the cells. The intracellular staining Foxp3 (eBioscience, Cat#17-5773-82), IFN-γ (BD, Cat#557735), IL-4 (BD, Cat# 562915), or IL-17A (BD, Cat#564169) were used. Finally, we analyzed the data by the LSR Fortessa cell analyzer and Diva software (BD).

Multi-cytokine detection containing IL-4, IFN-γ, IL-5, IL-13, TGF-β, IL-6, IL-10, and IL17A was performed in accordance

with the premixed AimPlex™ multiplex-assay kits (Cat#T2C0710709 and Cat#B111206). OVA-specific IgE in the serum was detected in accordance with the protocol (Cayman, Cat#500840).

Detection of IFN-γ, IL-4, Foxp3, and RORγt mRNA levels by real-time PCR

\The transcription factors of IFN-γ, IL-4, FOXP3, and RORγt in lung tissue were detected, and the total RNA from the tissues was extracted by TRIzol (Invitrogen) in accordance with the manufacturer's instructions. cDNA was synthesized by reverse transcription by using the first-strand cDNA synthesis kit (Servicebio, G3330) in accordance with the manufacturer's instructions and used for real-time PCR assay performed in 1× SYBR green qPCR master mix (Servicebio, G3320) together with 0.2 mM forward and reverse primers. The amount of mRNA of the indicated genes after normalization of β-actin mRNA. The primers of GAPDH, Foxp3, RORγt, IFN-γ and IL-4 genes were as described as in a previous study (Zhou et al., 2022).

Untargeted plasma metabolomics detection and analysis

In this study, UHPLC (1290 Infinity LC, Agilent Technologies) and quadrupole time-of-flight (AB Sciex TripleTOF 6,600) in Shanghai Applied Protein Technology Co., Ltd. were used to perform LC-MS/MS analysis. The orthogonal partial least-squares discriminant analysis was used to perform multivariate data analysis, and VIP >1 and p value <0.05 were used to screen metabolites' significant changes. The Pearson correlation analysis with R package was used to determine the correlation between variables.

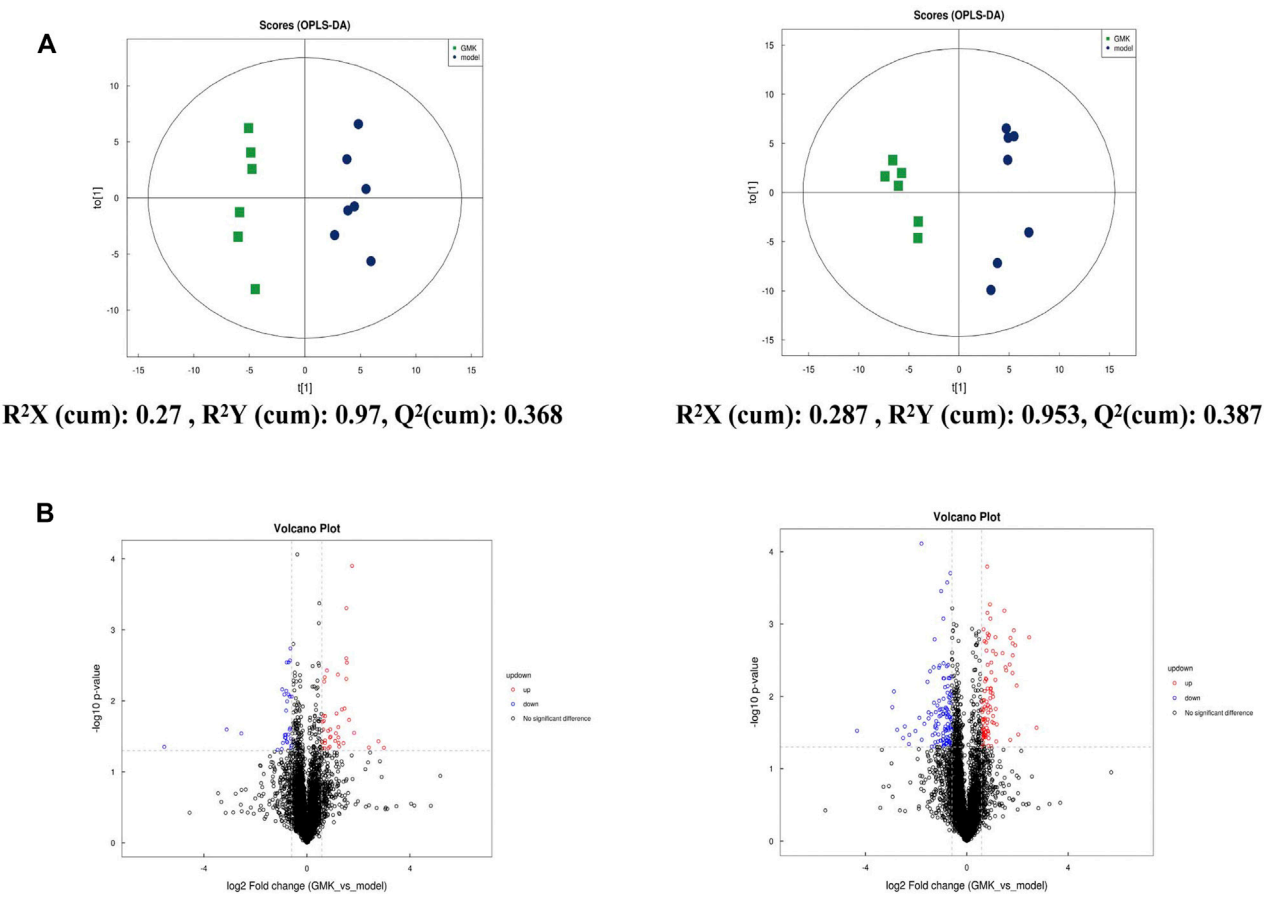

FIGURE 4
(Continued).

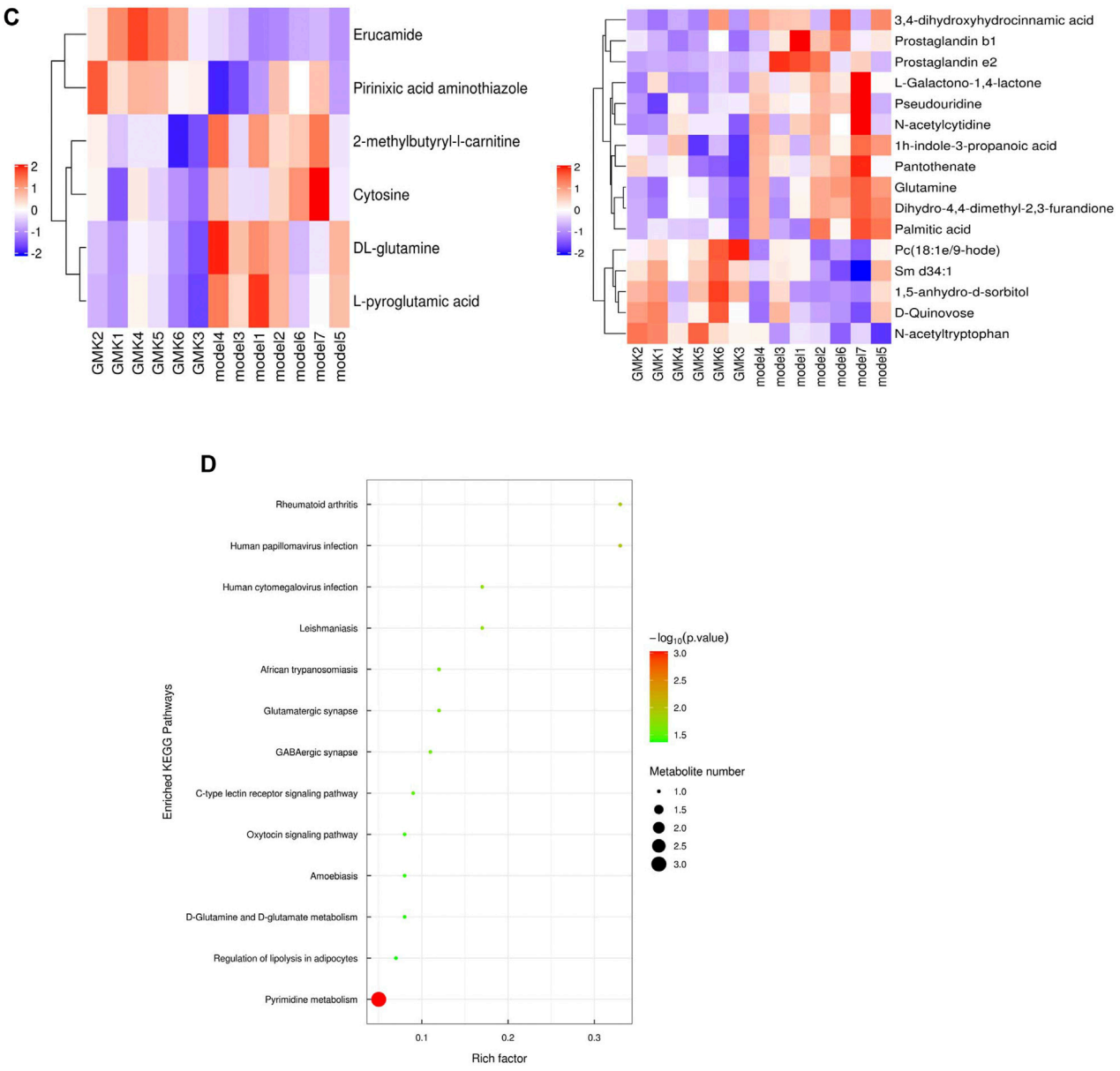

FIGURE 4
(Continued). Untargeted metabolomics of plasma detection treated by GMK. **(A)** OPLS-DA score plots derived from UPLC-Q-TOF/MS in positive and negative ionization modes. **(B)** Volcano map in positive mode and negative mode. **(C)** The hierarchical cluster analysis of different metabolites between GMK and model group under positive and negative modes. **(D)** Enriched KEGG pathways based on significant different metabolites between GMK(H) and model group (*n* = 7/group).

Gut microbiota detection and analysis

The 16S rDNA amplicon sequencing was used to detect gut microbiota after extracting the total genome DNA by the CTAB/SDS method (Bansal et al., 2018). Sequencing libraries were generated using the NEB Next®Ultra™DNA Library Prep Kit for Illumina (NEB, United States) following the manufacturer's recommendations, and index codes were added. The library was sequenced on the Illumina Miseq/HiSeq2500 platform. STAMP software was used to confirm the difference in abundance value, and LEfSe was used to conduct quantitative analysis of biomarkers in different groups.

TABLE 1 Differentiated plasma metabolites between model and GMK groups.

Name	ESI	VIP	Fold Change	*p* value
Erucamide	+	10.05189	3.374263664	0.000125
L-pyroglutamic acid	+	3.846949	0.830618952	0.004358
DL-glutamine	+	2.412555	0.832989231	0.005224
2-methylbutyryl-L-carnitine	+	1.272464	0.799934156	0.011032
Pirinixic acid aminothiazole	+	1.030683	1.77173329	0.02643
Cytosine	+	1.239749	0.849232667	0.03137
N-acetyltryptophan	–	1.779763	1.402748814	0.001626
Glutamine	–	3.114074	0.760124438	0.004224
1,5-anhydro-d-sorbitol	–	2.085506	1.391837849	0.006918
Dihydro-4,4-dimethyl-2,3-furandione	–	1.167511	0.78160733	0.007372
L-Galactono-1,4-lactone	–	1.725859	0.684250598	0.013781
Pc(18:1e/9-hode)	–	2.2884	1.885403306	0.013944
Prostaglandin e2	–	3.424605	0.130341353	0.014098
Prostaglandin b1	–	1.169405	0.514396644	0.014977
Pantothenate	–	1.852229	0.745324355	0.017882
1h-indole-3-propanoic acid	–	1.479907	0.595061082	0.01828
Pseudouridine	–	1.240415	0.78508799	0.030125
Sm d34:1	–	2.112093	1.383823251	0.031022
3,4-dihydroxyhydrocinnamic acid	–	1.449743	0.689174528	0.036569
D-Quinovose	–	1.304085	1.279815081	0.039916
N-acetylcytidine	–	1.363898	0.736552224	0.047463
Palmitic acid	–	15.57049	0.78886185	0.049912

Correlation analysis of differential plasma metabolites and differential gut microbiota with Th1, Th2, Treg and Th17 cells in eosinophilic asthma

The Pearson correlation analysis with R package was performed to determine the correlation of variables, such as differential plasma metabolites; differential gut microbiota; Th1, Th2, Treg and Th17 cell percentages; specific OVA–IgE antibody; Penh value (Methacholine: 12.5, 25, and 50 mg/ml); and eosinophilic number in BALF.

Statistical analysis

Use SPSS 20.0 software for statistical analysis of data. Data are presented as means ± SEM. Analysis of variance (ANOVA) with the Bonferroni correction for post hoc comparisons was used to test group differences, and the rank sum test was used for percentage analysis. $p < 0.05$ was considered statistically significant. The Pearson correlation analysis was used to analyze the correlation of differential metabolites and differential gut microbiota with Th1/2 and Treg/Th17 cells.

Results

GMK plays a certain role in relieving allergic inflammation in eosinophilic asthmatic mouse model

The allergic asthma model in BALB/c mice with eosinophil infiltration was constructed as shown in Figure 1A. The Penh value, which reflected airway resistance, indicated that GMK could significantly decrease the Penh value. The high-concentration GMK, GMK(H) had good effect, whereas the positive drug group, i.e., Dexamethasone (DEX) group, had the best effect (Figure 1B). The same effect could be seen in Figures 1C,D. GMK especially the (GMK(H)) group could achieve improved effect, whereas DEX had the best effect in inhibiting allergic inflammation, such as inflammatory cell infiltration (Figure 1C) and mucus production (Figure 1D). Interestingly, in the detection of specific OVA–IgE, IL-5, and IL-13 antibodies and eosinophilic number (Figure 1E), DEX had the best effect, and compared with the middle- and low-concentration GMK, GMK(H) had the best effect.

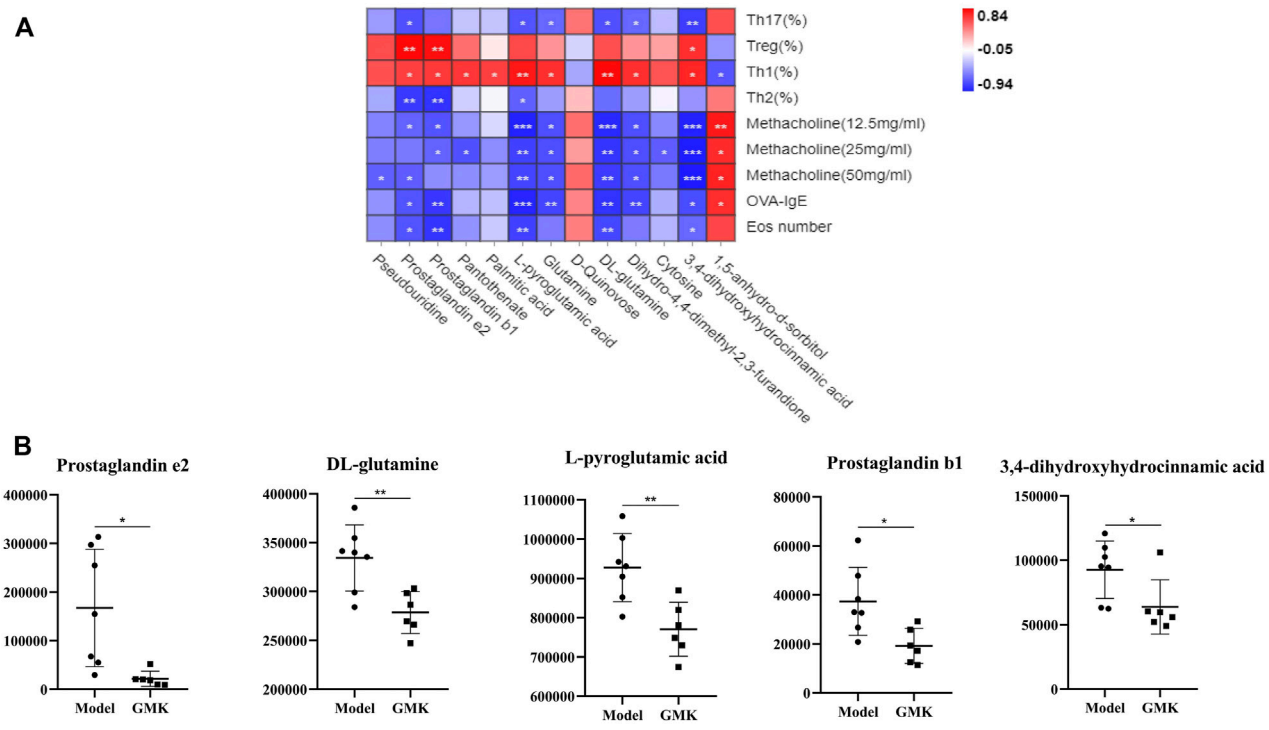

FIGURE 5
Correlation analysis between differential metabolites and Th1/2, Treg/Th17 cells balance treated by GMK in eosinophilic asthma. **(A)** Pearson correlation analysis between differential metabolites and Th1/2, Treg/Th17 immune balance, Penh value, OVA-IgE antibody and eosinophil number in BALF compared between GMK(H) and model group. **(B)** Metabolic biomarkers closely related to Th1/2 and Treg/Th17 cell balance in eosinophilic asthma (n = 7/group). *p < 0.05, **p < 0.01, ***$p \leq 0.001$.

GMK can reconstruct Th1/2 cellular balance in eosinophilic asthma

The Th1/2 cell balance was destroyed in the eosinophilic asthma model but reconstructed after GMK treatment especially in the GMK(H) group (Figures 2B,C). The cytokines of IL-4 and IFN-γ in serum and the mRNA expression levels of IL-4 and IFN-γ in lung tissue had the same effect (Figure 2A). Surprisingly, DEX did not have the same effect and could decrease Th2 cell percentage and related cytokines, such as IL-4 and IFN-γ mRNA expression, but can not increase Th1 cell percentage and the related cytokine and mRNA expression, such as IFN-γ.

Treg/Th17 cellular immune balance is reconstructed after GMK treatment

The allergic asthma model group showed a significant decrease in the percentage of Treg cells. In contrast, the percentage of Treg cells increased significantly in the GMK groups, especially in the GMK (H) group (Figures 3B,C). Interestingly, GMK groups especially the GMK(H) group had decreased Th17 cell detection. The mRNA expression of Foxp3 and RORγt in lung tissue is consistent with the detection results of Treg and Th17 cells in Figure 3D. The cytokine detection result showed that GMK treatment decreased IL-17A and IL-6 levels and increased IL-10 and TGF-β levels (Figure 3A). DEX also achieved the same effect as GMK(H) in the detection.

Plasma metabolites were changed after GMK treatment

We studied the plasma metabolism after GMK treatment to explore the mechanism of GMK on immune balance reconstruction in eosinophilic asthma. As shown in Figure 4A, metabolites were detected in the positive (POS) and negative (NEG) modes (i.e., $0.3 < Q^2 = 0.368 < 0.5$ in POS

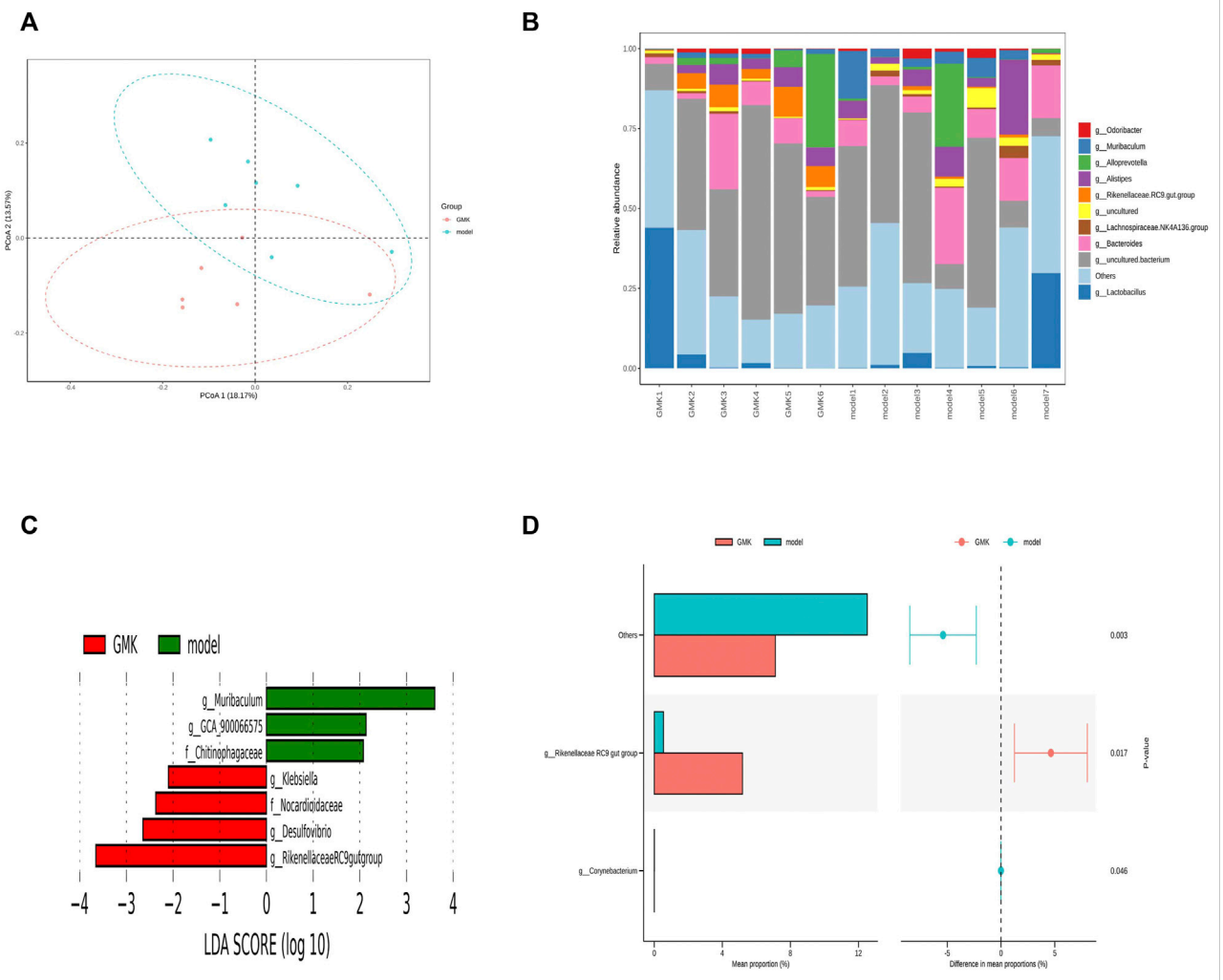

FIGURE 6
Gut microbiota Biomarker detection after GMK treated. **(A)** Principal coordinate analysis (PCoA) of gut microbiota in GMK treated group and eosinophilic asthma model group; **(B)** The top 10 gut microbiota at genus level between GMK treated group and model group; **(C)** Lefse analysis of differential gut microbiota between GMK treated group and model group (LDA >2 was used); **(D)** STAMP analysis of differential gut microbiota between GMK(H) treated group and model group ($p < 0.05$ was used), $n = 7$/group.

mode and $0.3 < Q^2 = 0.387 < 0.5$ in NEG mode), which indicated that the model was stable. A total of 5,058 and 4,387 metabolites in the POS and NEG modes, respectively, were detected. Six of these metabolites were significantly expressed in POS mode and 16 were significantly expressed in NEG mode (Table 1). Differential metabolites with FC > 1.5 or FC < 0.67 and p value <0.05 were visualized using a volcano graph in Figure 4B. The results of the hierarchical clustering analysis of differential metabolites, 6 and 16 metabolites in POS and NEG modes respectively are shown in Figure 4C. In the KEGG pathway analysis, most differential metabolites were enriched to pyrimidine metabolism and D-glutamine and D-glutamate metabolism pathway (Figure 4D).

Biomarkers associated with Th1/2 cell or Treg/Th17 cellular immune balance at the metabolic and gut microbiota levels

The Pearson correlation analysis was used to analyze the correlation and further explore the immune mechanism of GMK in treating eosinophilic asthma at the metabolic level (Figures 5A,B). The plasma metabolites in the GMK(H) and eosinophilic asthma mice model groups were detected. Among the differential metabolites, DL-glutamine, L-pyroglutamic acid, prostaglandin b1, prostaglandin e2 and 3,4-dihydroxyhydrocinnamic acid were the metabolic biomarkers, they were all connected to OVA-IgE, Penh value (Mch:12.5,25,50 mg/ml), Eos number, Th1/2 and Treg/Th17 cell balance.

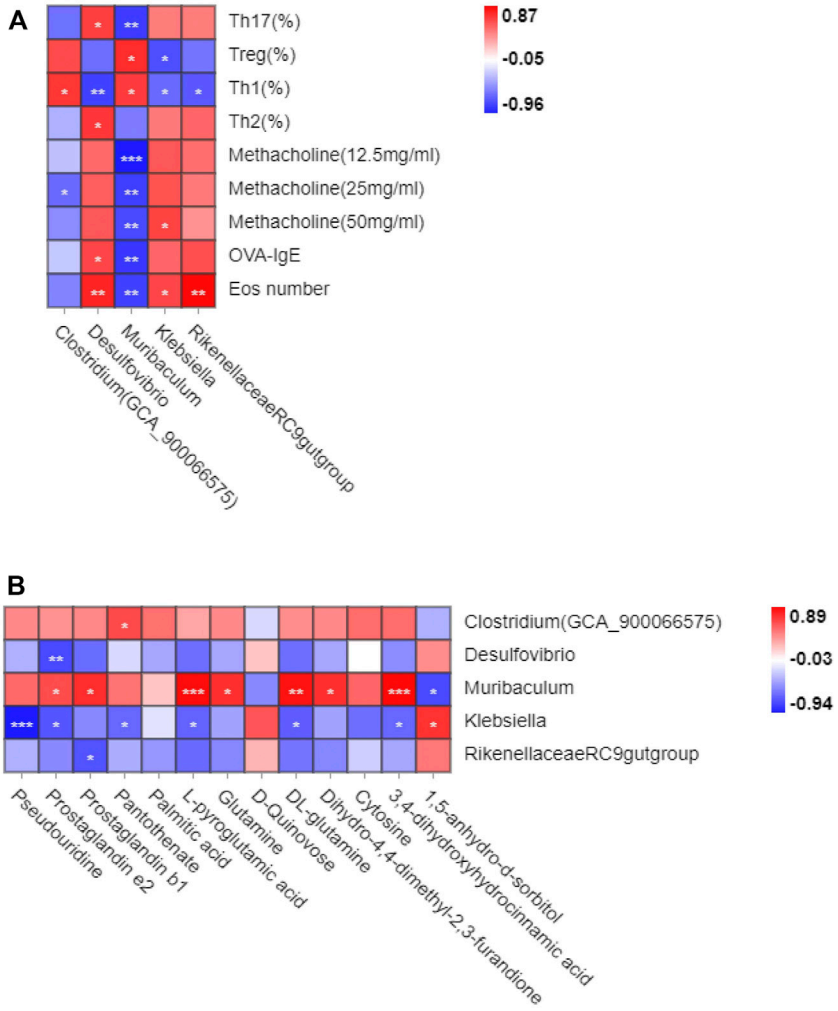

FIGURE 7
Correlation analysis between gut microbiota and Th1/2, Treg/Th17 cell balance in eosinophilic asthma. **(A)** Correlation analysis between differential microbiota and Th1,Th2, Treg and Th17 cell percentage, Penh value, OVA-IgE antibody and eosinophil number in BALF. **(B)** Correlation analysis of diffenential metabolites and gut microbiota biomarker treated by GMK (n = 5–6/group).

GMK was treated by intragastric administration to further investigate whether GMK could change gut microbiota, and 16S rDNA amplicon sequencing analysis was performed in the study. The gut microbiota was separated significantly (Figure 6A) and the top 10 relative abundance at genus level (Figure 6B). The LDA Effect Size (LEfSe) and STAMP analyses were used to examine the differential gut microbiota between GMKand model groups. LDA value >2 was used in the LEfSe analysis, and p value <0.05 was used in STAMP analysis. Genus_*Muriculum*, genus_*(Clostridium) GCA900066575*, genus_*klebsiella*, genus_*Desulfovibrio*, genus_Rikenellaceae *RC9 gut group*, family_Chitinophagaceae, family_Nocardioidaceae, and genus_ *Corynebacterium* were gut microbiota biomarkers after GMK treatment as shown in Figures 6C,D.

The Pearson correlation analysis was used in this study to investigate whether gut microbiota changes were related to the reconstruction of immune balance. The genus_ (*Clostridium*) *GCA900066575*, genus_*Desulfovibrio*, genus_*Muriculum*, and genus_ Rikenellaceae *RC9 gut group* were all associated with Th1 cells, and genus_*Desulfovibrio* was associated with Th2 cells. These cells were important in the Th1/2 cell balance. Genus_*Muriculum* and genus_*klebsiella* were associated with Treg cells, and genus_*Desulfovibrio* and genus_*Muriculum* related to Th17 cells. These cells were essential in the Treg/Th17 immune balance. Among them, genus_*Muriculum* is the biomarker based on the OVA-IgE, Penh value (Mch:12.5, 25, 50 mg/ml), Eos number, Th1, Th2, Treg and Th17 cell percentage, which indicated that genus_*Muriculum* is the gut microbiota biomarker interrelated to Th1/2 and Treg/Th17 cell balance (Figure 7A).

Gut microbiota and plasma metabolites play essential roles in GMK treatment. Genus_(*Clostridium*)*GCA900066575* was associated with pantothenate, genus_ *Desulfovibrio* was associated with prostaglandin e2, and genus_*Muriculum* was associated with prostaglandin e2, prostaglandin b1, L-pyroglutamic acid, glutamine, DL-glutamine, dihydro-4,4-dimethyl-2,3-furandione, 3,4-dihydroxyhydrocinnamic acid, and 1,5-anhydro-d-sorbitol. Genus_*klebsiella* was associated with pseudouridine, prostaglandin e2, pantothenate, L-pyroglutamic acid, DL-glutamine, 3,4-dihydroxyhydrocinnamic acid, and 1,5-anhydro-d-sorbitol. Genus_Rikenellaceae *RC9 gut group* was associated with prostaglandin b1 (Figure 7B). Very interesting, the metabolites biomarker of prostaglandin e2, prostaglandin b1, L-pyroglutamic acid, DL-glutamine, 3,4-dihydroxyhydrocinnamic acid are all associated with genus_*Muriculum*.

Discussion

Many studies have proved that the inflammation induced by a variety of Th cells, including Th1, Th2, Th9, Th17 and Th22 cells and their specific cytokines, has a certain correlation with the onset and development of allergic asthma. Th2 cells should not be neglected in the pathogenesis of allergic inflammation due to an imbalance of Th1/Th2 response (Hartl et al., 2007). More and more studies have shown that the root causes of Th2 response enhancement and allergic asthma are insufficient differentiation and functional defects of Treg cells. One study (Hanania, 2008) reported that patients with allergic asthma have fewer Treg cells in the peripheral blood than nonasthma normal ones. Another study proved that young patients with asthma and ICS treatment have fewer Treg cells in the lungs than normal ones, but this treatment fails to suppress pulmonary Th2 responses (Sun et al., 2021). Treg cells have an immuno suppressive function and are predominantly adjusted to the Foxp3 gene (Kim et al., 2022). Th17 cells have a certain correlation with the pathogenesis of asthma. This cell regulates eosinophil and neutrophil inflammation. (Maggi et al., 2021). Therefore, Th1, Th2, Treg, and Th17 cells play critical roles in maintaining immune homeostasis. Reducing immune response caused by Th2 or Th17 cells, promoting differentiation of Treg cells, or increasing the numbers of Th1 and Treg cells to rebuild the immune balance of Th1/2 or Treg/Th17 cells are new strategies to treat allergic asthma.

GMK, which regulates body constitution, is a classic prescription in the field of allergy field for academician Qi Wang. Regulating body constitution in allergic asthma disease means regulating immune homeostasis in patients with allergic asthma. GMK plays a role in reducing Ag-specific IgE, Ag-induced T-cell proliferation, and mast cell histamine release in treating allergic rhinitis (Zhou et al., 2018). Eosinophilia is a hallmark of allergic airway inflammation, and eosinophils can participate in many immune processes, such as Ag presentation and release of stored proinflammatory mediators (e.g., cytokines, chemokines, reactive oxygen species, lipid mediators, and granule proteins) (Heul et al., 2019). In the present study, an allergic asthma mouse model predominantly infiltrated by eosinophils with OVA and aluminum hydroxide is successfully constructed. GMK has a critical role in inhibiting eosinophil infiltration by reducing the eosinophil number and inhibiting related cytokines, such as IL-5 and IL-13. Imbalances in Th1/2 and Treg/Th17 cells exist in the allergic asthma model. The role of GMK in regulating immune balance is first evaluated. GMK can inhibit eosinophilic asthma by decreasing eosinophil number, decreasing inflammation index, and reducing airway resistance. GMK can also make the immune balance of Th1/2 and Treg/Th17 cells normal. GMK has the same function of DEX in suppressing allergic asthma and has unique advantages in immune balance reconstruction especially in increasing the percentage of Th1 cells. This result may be related to the way the model is constructed and needs to be validated in combination with clinical practice.

In the plasma metabolism detection, DL-glutamine, L-pyroglutamic acid, prostaglandin b1, and 3,4-dihydroxyhydrocinnamic acid are initially identified as biomarkers associated with Th1/2 and Treg/Th17 immune balance on the basis of reducing eosinophil number, inhibiting Ag-specific IgE antibody, and reducing inflammation induction. Glutamine can suppress allergic airway inflammation through the upregulation of MAPK phosphatase-1, which is consistent with our results (Kim et al., 2022). ILC2s predominantly participate in the physiopathology of allergic diseases especially eosinophilic asthma (Maggi et al., 2021). Prostaglandin E2 can inhibit the production of IL-5 and IL-13 and the amplification of ILC2 *in vitro* (Zhou et al., 2018). At present, there is no report that prostaglandin b1 and 3,4-dihydroxyhydrocinnamic acid are involved in the treatment of allergic asthma. They may be a new strategy for the treatment of allergic asthma. While until now, there are few study focus on the relationship between gut microbiota and plasma metabolites, and the relationship between gut microbiota, plasma metabolites and the function of T cells, they will be a new research direction for us.

Intestinal microbiota can affect the immune response and physiology of allergic asthma, and also affect the activity and number of T cell subsets including Th1, Th2, Th17 and effector/memory T lymphocytes (Heul et al., 2019). Study shows *Klebsiella*/*Bifidobacterium* in early life is correlate with later development in paediatric allergy (Low et al., 2017). Genus_ *Corynebacterium* in the nasopharynx (NP) impacts severity of lower respiratory infection and risk of asthma development (Teo et al., 2015). T lymphocyte activation is dependent on glutamine, which is essential nutrient in the

activation of naive T cells (Carr et al., 2010). Prostaglandin e2 (PGE2) can regulate immune response, such as it can modulate local attraction and degranulation of mast cells (Hu et al., 1995; Weller et al., 2007), it plays essential role in activation and migration of DC cells (Kalinski et al., 1998), it can also inhibit activation and expansion of naive T cells (Muthuswamy et al., 2010). Moreover, PGE2 can influence Th1 and Th2 response (Betz and Fox, 1991; Kapsenberg et al., 1999), differentiation of Treg and Th17 cells (Muthuswamy et al., 2008; Boniface et al., 2009), which is important in allergic asthma. All these results is consistent with our results and can support our preliminary conclusions, while it still need further experimental verification in the future study.

The oral administration of *Clostridium* can reduce OVA-induced allergic airway inflammation in a mouse model, whereas it is only associated with airway resistance and Th1 cells in our study (Juan et al., 2017). At present, we focus our research on the biomarkers of genus_*Muriculum*, genus_*klebsiella*, and genus_*Desulfovibrio*. Genus_*Desulfovibrio* may influence Treg/Th17 balance in ulcerative colitis (Cui et al., 2018). Interestingly, DL-glutamine, L-pyroglutamic acid, prostaglandin b1, prostaglandin e2, and 3,4-dihydroxyhydrocinnamic acid are associated with genus_*Muriculum*; prostaglandin e2 is associated with genus_*Desulfovibrio*; and DL-glutamine, L-pyroglutamic acid, prostaglandin b1, prostaglandin e2, and 3,4-dihydroxyhydrocinnamic acid are associated with genus_*klebsiella*. The above results are studied, and they may be a new strategy to treat allergic asthma. While, until now there are none research about the DL-glutamine, L-pyroglutamic acid, prostaglandin b1, prostaglandin e2, and 3,4-dihydroxyhydrocinnamic acid associated with genus_*Muriculum*. 1,5-anhydro-d-sorbitol is associated with Treg/Th17 cell balance in allergic asthma mouse model (Zhou et al., 2022). There are none research based on the penh value associated them. Our future research will be conducted on the above basis. Given the limitations, in the future study, it should be combined with clinical results. Besides that, the research will also focus on other allergic asthma model like neutrophilic asthma induce by HDM or other inducer.

Data availability statement

The datasets presented in this study can be found in online repositories. The names of the repository/repositories and accession number(s) can be found in the article/supplementary material.

Ethics statement

The animal study was reviewed and approved by the Beijing university of chinese medicine.

Author contributions

YZ performed the experiment, analysed and wrote the manuscript. XZ, JW, and QW contributed significantly to analysed the manuscript. LH, HZ, HZ, and JL participated in the data analysis.

Funding

This work was supported by the General program of National Natural Science Foundation of China (Nos. 82174243, 81973715), the National Natural Science Foundation of China, (82204948), the General project of Beijing Natural Science Foundation (No.7202110), the Innovation Team and Talents Cultivation Program of National Administration of Traditional Chinese Medicine (No. ZYYCXTD-C-202001) and the National Key R&D Program of China (2020YFC2003100, 2020YFC2003101).

Conflict of interest

The authors declare that the research was conducted in the absence of any commercial or financial relationships that could be construed as a potential conflict of interest.

Publisher's note

Supplementary material

The Supplementary Material for this article can be found online at: https://www.frontiersin.org/articles/10.3389/fphar.2022.978421/full#supplementary-material

References

Asayama, K., Kobayashi, T., D'Alessandro-Gabazza, C. N., Toda, M., Yasuma, T., Fujimoto, H., et al. (2020). Protein S protects against allergic bronchial asthma by modulating Th1/Th2 balance. *Allergy* 75 (9), 2267–2278. doi:10.1111/all.14261

Baatjes, A. J., Smith, S. G., Watson, R., Howie, K., Murphy, D., Larché, M., et al. (2015). T regulatory cell phenotypes in peripheral blood and bronchoalveolar lavage from non-asthmatic and asthmatic subjects. *Clin. Exp. Allergy* 45 (11), 1654–1662. doi:10.1111/cea.12594

Bansal, S., Thakur, S., Mangal, M., Mangal, A. K., and Gupta, R. K. (2018). DNA barcoding for specific and sensitive detection of Cuminum cyminum adulteration in Bunium persicum. *Phytomedicine* 50, 178–183. doi:10.1016/j.phymed.2018.04.023

Berker, M., Frank, L. J., Geßner, A. L., Grassl, N., Holtermann, A. V., Höppner, S., et al. (2017). Allergies - a T cells perspective in the era beyond the TH1/TH2 paradigm. *Clin. Immunol.* 174, 73–83. doi:10.1016/j.clim.2016.11.001

Betz, M., and Fox, B. S. (1991). Prostaglandin E2 inhibits production of Th1 lymphokines but not of Th2 lymphokines. *J. Immunol.* 146, 108–113.

Boniface, K., Bak-Jensen, K. S., Li, Y., Blumenschein, W. M., McGeachy, M. J., McClanahan, T. K., et al. (2009). Prostaglandin E2 regulates Th17 cell differentiation and function through cyclic AMP and EP2/EP4 receptor signaling. *J. Exp. Med.* 206, 535–548. doi:10.1084/jem.20082293

Braun-Fahrländer, C., Riedler, J., Herz, U., Eder, W., Waser, M., Grize, L., et al. (2002). Environmental exposure to endotoxin and its relation to asthma in school-age children. *N. Engl. J. Med.* 347 (12), 869–877. doi:10.1056/NEJMoa020057

Bullens, D. M. A., Truyen, E., Coteur, L., Dilissen, E., Hellings, P. W., Dupont, L. J., et al. (2006). IL-17 mRNA in sputum of asthmatic patients: linking T cell driven inflammation and granulocytic influx? *Respir. Res.* 7, 135. doi:10.1186/1465-9921-7-135

Busse, W. W., Lemanske, R. F., and Gern, J. E. (2010). Role of viral respiratory infections in asthma and asthma exacerbations. *Lancet* 376 (9743), 826–834. doi:10.1016/S0140-6736(10)61380-3

Buzney, C. D., Gottlieb, A. B., and Rosmarin, D. (2016). Asthma and atopic dermatitis: A review of targeted inhibition of interleukin-4 and interleukin-13 as therapy for atopic disease. *J. Drugs Dermatol.* 15 (2), 165–171.

Carr, E. L., Kelman, A., Wu, G. S., Gopaul, R., Senkevitch, E., Aghvanyan, A., et al. (2010). Glutamine uptake and metabolism are coordinately regulated by ERK/MAPK during T lymphocyte activation. *J. Immunol.* 185 (2), 1037–1044. doi:10.4049/jimmunol.0903586

Chung, K. F. (2015). Targeting the interleukin pathway in the treatment of asthma. *Lancet* 386 (9998), 1086–1096. doi:10.1016/S0140-6736(15)00157-9

Cui, H., Cai, Y., Wang, L., Jia, B., Li, J., Zhao, S., et al. (2018). Berberine regulates Treg/Th17 balance to treat ulcerative colitis through modulating the gut microbiota in the colon. *Front. Pharmacol.* 9, 571. doi:10.3389/fphar.2018.00571

Dhami, S., Kakourou, A., Asamoah, F., Agache, I., Lau, S., Jutel, M., et al. (2017). Allergen immunotherapy for allergic asthma: A systematic review and meta-analysis. *Allergy* 72 (12), 1825–1848. doi:10.1111/all.13208

Duan, W., Chan, J., Wong, C., Leung, B., and Wong, W. (2004). Anti-inflammatory effects of mitogen-activated protein kinase kinase inhibitor U0126 in an asthma mouse model. *J. Immunol.* 172 (11), 7053–7059. doi:10.4049/jimmunol.172.11.7053

Durrant, D. M., and Metzger, D. W. (2010). Emerging roles of T helper subsets in the pathogenesis of asthma. *Immunol. Invest.* 39 (4-5), 526–549. doi:10.3109/08820131003615498

Fahy, J. V. (2015). Type 2 inflammation in asthma--present in most, absent in many. *Nat. Rev. Immunol.* 15 (1), 57–65. doi:10.1038/nri3786

Finkelman, F., Hogan, S., Hershey, G., Rothenberg, M., and Wills-Karp, M. (2010). Importance of cytokines in murine allergic airway disease and human asthma. *J. Immunol.* 184 (4), 1663–1674. doi:10.4049/jimmunol.0902185

Fontenot, J. D., Gavin, M. A., and Rudensky, A. Y. (2003). Foxp3 programs the development and function of CD4+CD25+ regulatory T cells. *Nat. Immunol.* 4 (4), 330–336. doi:10.1038/ni904

Gavin, M. A., Rasmussen, J. P., Fontenot, J. D., Vasta, V., Manganiello, V. C., Beavo, J. A., et al. (2007). Foxp3-dependent programme of regulatory T-cell differentiation. *Nature* 445 (7129), 771–775. doi:10.1038/nature05543

Hanania, N. A. (2008). Targeting airway inflammation in asthma: Current and future therapies. *Chest* 133 (4), 989–998. doi:10.1378/chest.07-0829

Hartl, D., Koller, B., Mehlhorn, A. T., Reinhardt, D., Nicolai, T., Schendel, D. J., et al. (2007). Quantitative and functional impairment of pulmonary CD4+CD25hi regulatory T cells in pediatric asthma. *J. Allergy Clin. Immunol.* 119 (5), 1258–1266. doi:10.1016/j.jaci.2007.02.023

Heffler, E., Paoletti, G., Giorgis, V., Puggioni, F., Racca, F., Del Giacco, S., et al. (2019). Real-life studies of biologics used in asthma patients: Key differences and similarities to trials. *Expert Rev. Clin. Immunol.* 15 (9), 951–958. doi:10.1080/1744666X.2019.1653758

Heul, A., Planer, J., and Kau, A. (2019). The human microbiota and asthma. *Clin. Rev. Allergy Immunol.* 57 (3), 350–363. doi:10.1007/s12016-018-8719-7

Hori, S., Nomura, T., and Sakaguchi, S. (2003). Control of regulatory T cell development by the transcription factor Foxp3. *Science* 299 (5609), 1057–1061. doi:10.1126/science.1079490

Hu, Z. Q., Asano, K., Seki, H., and Shimamura, T. (1995). An essential role of prostaglandin E on mouse mast cell induction. *J. Immunol.* 155, 2134–2142.

Joetham, A., Takeda, K., Takada, K., Taube, C., Miyahara, N., Matsubara, S., et al. (2007). Naturally occurring lung CD4(+)CD25(+) T cell regulation of airway allergic responses depends on IL-10 induction of TGF-beta. *J. Immunol.* 178 (3), 1433–1442. doi:10.4049/jimmunol.178.3.1433

Juan, Z., Zhao-Ling, S., Ming-Hua, Z., Chun, W., Hai-Xia, W., Meng-Yun, L., et al. (2017). Oral administration of Clostridium butyricum CGMCC0313-1 reduces ovalbumin-induced allergic airway inflammation in mice. *Respirology* 22 (5), 898–904. doi:10.1111/resp.12985

Kalinski, P., Schuitemaker, J. H., Hilkens, C. M., and Kapsenberg, M. L. (1998). Prostaglandin E2 induces the final maturation of IL-12-deficient CD1a+CD83+ dendritic cells: The levels of IL-12 are determined during the final dendritic cell maturation and are resistant to further modulation. *J. Immunol.* 161, 2804–2809.

Kapsenberg, M. L., Hilkens, C. M., Wierenga, E. A., and Kalinski, P. (1999). The paradigm of type 1 and type 2 antigen-presenting cells. Implications for atopic allergy. *Clin. Exp. Allergy* 29 (2), 33–36. doi:10.1046/j.1365-2222.1999.00006.x-i2

Kim, J-M., Im, Y. N., Chung, Y-J., Youm, J-H., Im, S. Y., Han, M. K., et al. (2022). Glutamine deficiency shifts the asthmatic state toward neutrophilic airway inflammation. *Allergy* 77 (4), 1180–1191. doi:10.1111/all.15121

Kudo, M., Melton, A. C., Chen, C., Engler, M. B., Huang, K. E., Ren, X., et al. (2012). IL-17A produced by αβ T cells drives airway hyper-responsiveness in mice and enhances mouse and human airway smooth muscle contraction. *Nat. Med.* 18 (4), 547–554. doi:10.1038/nm.2684

Lee, Y. K., Turner, H., Maynard, C. L., Oliver, J. R., Chen, D., Elson, C. O., et al. (2009). Late developmental plasticity in the T helper 17 lineage. *Immunity* 30 (1), 92–107. doi:10.1016/j.immuni.2008.11.005

Li, X-M., Wang, Q-F., Schofield, B., Lin, J., Huang, S-K., and Wang, Q. (2009). Modulation of antigen-induced anaphylaxis in mice by a traditional Chinese medicine formula, Guo Min Kang. *Am. J. Chin. Med.* 37 (1), 113–125. doi:10.1142/S0192415X09006710

Lin, W., Haribhai, D., Relland, L. M., Truong, N., Carlson, M. R., Williams, C. B., et al. (2007). Regulatory T cell development in the absence of functional Foxp3. *Nat. Immunol.* 8 (4), 359–368. doi:10.1038/ni1445

Lloyd, C. M., and Hawrylowicz, C. M. (2009). Regulatory T cells in asthma. *Immunity* 31 (3), 438–449. doi:10.1016/j.immuni.2009.08.007

Low, J. S. Y., Soh, S. E., Lee, Y. K., Kwek, K. Y. C., Holbrook, J. D., Van der Beek, E. M., et al. (2017). Ratio of Klebsiella/Bifidobacterium in early life correlates with later development of paediatric allergy. *Benef. Microbes* 8 (5), 681–695. doi:10.3920/BM2017.0020

Maggi, L., Mazzoni, A., Capone, M., Liotta, F., Annunziato, F., and Cosmi, L. (2021). The dual function of ILC2: From host protection to pathogenic players in type 2 asthma. *Mol. Asp. Med.* 80, 100981. doi:10.1016/j.mam.2021.100981

Muthuswamy, R., Mueller-Berghaus, J., Haberkorn, U., Reinhart, T. A., Schadendorf, D., and Kalinski, P. (2010). PGE(2) transiently enhances DC expression of CCR7 but inhibits the ability of DCs to produce CCL19 and attract naive T cells. *Blood* 116, 1454–1459. doi:10.1182/blood-2009-12-258038

Muthuswamy, R., Urban, J., Lee, J. J., Reinhart, T. A., Bartlett, D., and Kalinski, P. (2008). Ability of mature dendritic cells to interact with regulatory T cells is imprinted during maturation. *Cancer Res.* 68, 5972–5978. doi:10.1158/0008-5472.CAN-07-6818

Peden, D. B. (2005). The epidemiology and genetics of asthma risk associated with air pollution. *J. Allergy Clin. Immunol.* 115 (2), 213–219. quiz 220. doi:10.1016/j.jaci.2004.12.003

Sakaguchi, S., Yamaguchi, T., Nomura, T., and Ono, M. (2008). Regulatory T cells and immune tolerance. *Cell* 133 (5), 775–787. doi:10.1016/j.cell.2008.05.009

Sun, L., Fan, M., Huang, D., Li, B., Xu, R., Gao, F., et al. (2021). Clodronate-loaded liposomal and fibroblast-derived exosomal hybrid system for enhanced drug delivery to pulmonary fibrosis. *Biomaterials* 271, 120761. doi:10.1016/j.biomaterials.2021.120761

Sun, L., Fu, J., Lin, S-H., Sun, J-L., Xia, L., Lin, C-H., et al. (2020). Particulate matter of 2.5 μm or less in diameter disturbs the balance of TH17/regulatory T cells by targeting glutamate oxaloacetate transaminase 1 and hypoxia-inducible factor 1α in an asthma model. *J. Allergy Clin. Immunol.* 145 (1), 402–414. doi:10.1016/j.jaci.2019.10.008

Teo, S. M., Mok, D., Pham, K., Kusel, M., Serralha, M., Troy, N., et al. (2015). The infant nasopharyngeal microbiome impacts severity of lower respiratory infection and risk of asthma development. *Cell Host Microbe* 17 (5), 704–715. doi:10.1016/j.chom.2015.03.008

Tortola, L., Pawelski, H., Sonar, S. S., Ampenberger, F., Kurrer, M., and Kopf, M. (2019). IL-21 promotes allergic airway inflammation by driving apoptosis of FoxP3+ regulatory T cells. *J. Allergy Clin. Immunol.* 143 (6), 2178–2189. e5. doi:10.1016/j.jaci.2018.11.047

Weller, C. L., Collington, S. J., Hartnell, A., Conroy, D. M., Kaise, T., Barker, J. E., et al. (2007). Chemotactic action of prostaglandin E2 on mouse mast cells acting via the PGE2 receptor 3. *Proc. Natl. Acad. Sci. U. S. A.* 104, 11712–11717. doi:10.1073/pnas.0701700104

Wu, Z. S., Shi, H. F., Zeng, J. Q., Zhang, J., Liao, Y., Huang, X. G., et al. (2019). Study on famous prescription of prestigious traditional Chinese medicine based on QbD concept: Optimization of extraction process and granule forming process of tuomin dingchuan prescription. *Zhongguo Zhong Yao Za Zhi* 44 (20), 4322–4328. doi:10.19540/j.cnki.cjcmm.20190629.308

Zhao, S-T., and Wang, C-Z. (2018). Regulatory T cells and asthma. *J. Zhejiang Univ. Sci. B* 19 (9), 663–673. doi:10.1631/jzus.B1700346

Zhou, Y., Wang, T., Zhao, X., Wang, J., and Wang, Q. (2022). Plasma metabolites and gut microbiota are associated with T cell imbalance in BALB/c model of eosinophilic asthma. *Front. Pharmacol.* 13, 819747. doi:10.3389/fphar.2022.819747

Zhou, Y., Wang, W., Zhao, C., Wang, Y., Wu, H., Sun, X., et al. (2018). Prostaglandin E2 inhibits group 2 innate lymphoid cell activation and allergic airway inflammation through E-prostanoid 4-cyclic adenosine monophosphate signaling. *Front. Immunol.* 9, 501. doi:10.3389/fimmu.2018.00501

frontiers | Frontiers in Pharmacology

TYPE Systematic Review
PUBLISHED 09 November 2022
DOI 10.3389/fphar.2022.1059737

OPEN ACCESS

EDITED BY
Zhirong Geng,
Nanjing University, China

REVIEWED BY
Fang Li,
China Pharmaceutical University, China
Fengmei Wang,
Zhejiang University, China
Zhengtang Liu,
Xiyuan Hospital, China Academy of Chinese Medical Sciences, China

*CORRESPONDENCE
Fuming Liu,
doctor.liufuming@outlook.com

†These authors have contributed equally to this work

SPECIALTY SECTION
This article was submitted to Inflammation Pharmacology, a section of the journal Frontiers in Pharmacology

RECEIVED 02 October 2022
ACCEPTED 21 October 2022
PUBLISHED 09 November 2022

CITATION
Li J, Du Y, Cai C and Liu F (2022), Effectiveness and safety of treating carotid atherosclerotic plaques with the method of nourishing qi, promoting blood circulation and expelling phlegm: A systematic review and meta-analysis. *Front. Pharmacol.* 13:1059737. doi: 10.3389/fphar.2022.1059737

Effectiveness and safety of treating carotid atherosclerotic plaques with the method of nourishing qi, promoting blood circulation and expelling phlegm: A systematic review and meta-analysis

Jia Li†, Yuying Du†, Chao Cai and Fuming Liu*

Affiliated Hospital of Nanjing University of Chinese Medicine, Jiangsu Province Hospital of Chinese Medicine, Nanjing, China

Objectives: This meta-analysis aimed at evaluating the effectiveness and safety of Chinese medicine (TCM), which nourished qi, promoted blood circulation, and expelled phlegm (YQHXZT), in treating carotid atherosclerosis (CAS) from an immunological perspective.

Background: The incidence of CAS has been increasing and tends to be younger. Although western medicine is effective, there are some limitations. TCM has certain advantages over the multichannel and multitarget treatment strategies in slowing down the process of CAS. However, there is no comprehensive review in this field.

Methods: Nine databases were searched from January, 2012, to September, 2022. After applying the inclusion and exclusion criteria to the RCTs, research quality evaluation and data extraction were conducted, and a meta-analysis of the articles was performed. The GRADE was used to assess the quality of the evidence.

Results: Fourteen RCTs involving 1,191 patients were identified. The results indicated that the experimental group was more effective in improving carotid intima-media thickness (CIMT)[SMD = −0.97, 95%CI(−.30,−0.65), $p < 0.00001$], reducing carotid plaque area [SMD = −1.98, 95%CI(−3.06,−0.89), $p = 0.0003$], lowering hs-CRP [SMD = −1.33, 95%CI(−1.59,-1.06), $p < 0.00001$] and LDL-C levels [SMD = −0.60, 95%CI(−0.83,-0.38), $p < 0.00001$]. Moreover, the experimental group was superior to peak systolic blood flow velocity (PSV) [SMD = −0.37, 95%CI(−0.59,−0.16), $p = 0.0007$], clinical efficacy [RR = 1.64, 95% CI (1.39, 1.94), $p < 0.00001$] and plaque area efficacy [RR = 1.36, 95% CI (1.22,

Abbreviations: YQHXZT, nourishing qi, promoting blood circulation, and expelling phlegm; CAS, carotid arteriosclerosis; AS, arteriosclerosis; RCTs, Randomized controlled trials; TCM, Traditional Chinese medicine.

1.52), $p < 0.0001$]. The adverse reactions were not statistically significant in the two groups [RD = -0.01, 95% CI (-0.04.0.01), $p = 0.17$]. The results of grade evaluation suggested that the outcome indicators LDL-C, hs-CRP, plaque area efficacy, PSV, and adverse events were moderate. CIMT, plaque reduction area, and TCM clinical efficacy were low-quality.

Conclusion: The combination of YQHXZT can alleviate the process of CAS by inhibiting the thickening of CIMT, reducing plaque area and lowering hs-CRP and LDL-C levels. The mechanism may possibly be related to reducing lipid deposition and inhibiting the inflammatory response. Besides, the combination did not increase the risk of adverse effects. However, more well-designed RCTs are needed in the future.

Systematic review registration: CRD42022360529, https://www.crd.york.ac.uk/prospero/

KEYWORDS

carotid atherosclerosis, Chinese medicine, inflammation, meta-analysis, grade evaluation

1 Introduction

Atherosclerosis-related diseases such as ischemic heart diseases and strokes have a high morbidity and mortality rate as well as a poor prognosis (Libby, 2021), putting a heavy physical and financial burden on patients (Humphries et al., 2018). Atherosclerosis (AS), as a high-risk factor and a major pathological basis for cardiovascular and cerebrovascular events (Prandoni et al., 2017), has become more prominent in modern decades as people's living standards have enhanced, and the prevalence is expected to rise by 18% by 2030 (Valanti et al., 2021). AS is commonly classified as Carotid atherosclerosis sclerosis (CAS), Coronary atherosclerosis, lower limb atherosclerosis, and so on, depending on the location of the lesion. The carotid artery is one of the most commonly involved sites of systemic AS and is frequently used as a window into and assessment of the body's large middle arteries, which can provide a general picture of systemic AS. According to studies, AS in the extracranial segment of the carotid artery is associated with the onset of cerebral infarction in 20%–25% of patients (Chen et al., 2019). Previous investigation (Karataş et al., 2016) has confirmed that the occurrence of AS is closely related to the inflammatory response mediated by inflammatory factors in the body, suggesting that the occurrence and progression of cerebral infarction may be related to the overexpression of inflammatory factors, dyslipidemia, and other factors. There is a critical need to address CAS prevention and treatment strategies.

In recent decades, both domestic and international researchers have identified AS a chronic inflammatory disease (Zhu et al., 2018). There is widespread agreement that inflammation plays a role in the development of AS (Geovanini and Libby, 2018). A growing number of clinical studies have attempted new anti-AS treatments based on anti-inflammation and immune regulation. Western medicine has had some success with lipid regulation, anti-inflammation, and anti-platelet aggregation. Nevertheless, there are some drawbacks to clinical application (Pang et al., 2017), such as muscle aches and pains, liver and kidney toxicity, increased transaminases (Backes et al., 2017), high drug production costs, the single target of the action, and so on (Li et al., 2020). As a result, research into CAS treatment is still a long way off. Traditional Chinese medicine (TCM) has been actively participating in the treatment of CAS in Asia and has demonstrated a definite curative effect with fewer side effects (Sun et al., 2021). TCM can affect multiple aspects of the occurrence and development of diseases from a holistic standpoint. TCM's prevention and treatment of AS *via* immune inflammation-related pathways is a hot topic in current research. Extensive studies have discovered that qi deficiency and phlegm stasis are the most common types of evidence in CAS patients. The treatment of CAS primarily focuses on activating blood, resolving stasis, expelling phlegm, and benefiting qi (Wu et al., 2017), which shares similarities with western medicine in terms of lipid regulation and anti-inflammation. Randomized controlled trials (RCTs) on the clinical efficacy of AS have confirmed that Chinese medicines can reduce the size of CAS plaques and slow down the progression of CAS. However, few writers have drawn on any systematic study. The majority of RCTs were restricted to individual clinical observation and examination of a specific prescription. Most of the recommendations were self-recommended and based on empirical evidence, which was relatively weak. The safety and efficacy of these medications were not yet supported by scientific evidence due to the wide variety of Chinese medications, inconsistent dosage forms and doses, and some effective active ingredients of Chinese medications that had not undergone thorough pharmacological mechanisms of action studies. Given this,

#1 "Carotid atherosclerosis" [MeSH Terms]";
#2 ((((Carotid atherosclerosis[MeSH Terms]) OR ("Carotid Artery Diseases"[Mesh])) OR (Carotid Artery Disorder)) OR (Internal Carotid Artery Diseases)) OR (Common Carotid Artery Diseases);
#3 #1 or #2;
#4 "Medicine, Chinese Traditional"[Mesh];
#5 ((("Medicine, Chinese Traditional"[Mesh]) OR (Zhong Yi Xue)) OR (Traditional Chinese Medicine)) OR (Chung I Hsueh);
#6 #4 or #5 ;
#7 (((((Carotid atherosclerosis[MeSH Terms]) OR ("Carotid Artery Diseases"[Mesh])) OR (Carotid Artery Disorder)) OR (Internal Carotid Artery Diseases)) OR (Common Carotid Artery Diseases)) AND ((((("Medicine, Chinese Traditional"[Mesh]) OR (Zhong Yi Xue)) OR (Traditional Chinese Medicine)) OR (Chung I Hsueh));
#8 randomized controlled trial[Publication Type] OR randomized[Title/Abstract] OR placebo[Title/Abstract];
#9 #7 and #8

FIGURE 1
Search strategy.

to aid the development of better clinical judgments, we thoroughly assessed the efficacy and safety of the YQHXZT treatment for CAS in this work.

2 Methods

2.1 Protocol and registration

The International Prospective Register of Systematic Reviews has received the protocol for this study (PROSPERO, CRD42022360529). The Preferred Reporting Items for Systematic Reviews and Meta-Analyses (PRISMA) (Moher et al., 2009) served as the foundation for this meta-analysis (Supplementary Table S1).

2.2 Search strategy

We looked through PubMed, Embase, Cochrane Library, Web of Science, Medline, CNKI, VIP, Wan Fang, and CBM. The period of retrieval, which was only applicable to Chinese and English literature, ran from 1 January 2012, through 1 September 2022. The search was conducted using a combination of subject terms and free words. The Chinese search terms included "carotid artery atherosclerosis," "qi deficiency and phlegm stasis," "benefit qi and resolve phlegm," "activate blood circulation and resolve blood stasis," etc. English search terms included "carotid atherosclerosis," "carotid artery disease," "traditional Chinese medicine," "randomized controlled trial," "RCT," etc., For unified management, the retrieved papers were loaded into Endnote X9. Figure 1 illustrated the precise search approach using PubMed as an example.

3 Eligibility criteria

3.1 Types of studies

A clinical randomized controlled trial (RCT), whether blinded or with allocation concealment.

3.2 Types of participants

Participants who met the Western diagnostic criteria for CAS as well as the Chinese medical evidence of Qi deficiency and phlegm stasis were tested. Gender, race, and disease duration were not limited, and the underlying disease was stable. The Diagnostic Criteria for Neurological Disorders served as the foundation for western medical diagnosis (Bai, 2009). The carotid ultrasound findings were consistent with the Vascular Ultrasound Guidelines' relevant diagnostic criteria. Intima-media thickening was defined as IMT 1.0 mm; limited IMT 1.5 mm, projecting into the lumen, or limited IMT thickening above 50% of the peripheral IMT was defined as AS plaque formation. TCM diagnosis was based on "Guidelines for Clinical Research on New Chinese Medicines" and "National Standard of the People's Republic of China-Chinese Medicine Clinical Diagnosis and Treatment Terminology, Evidence and Marks Part," which were related to Qi deficiency and phlegm stasis. Headache, weakness, dizziness, chest tightness, shortness of breath, dullness, heaviness, and limb numbness are the most common symptoms. Palpitations, insomnia, pale mouth, fatigue, distention, poor appetite, localized tingling, pale or purplish face, pale or cyanotic lips, and cold limbs are secondary symptoms. Pale tongue with tooth marks or purple with petechiae, a thin, white, or slippery coating. The pulse can be slick or tight. If more than two of the primary symptoms listed above are present, or if one primary symptom coexists with two secondary symptoms, the diagnosis may be made by consulting the tongue and pulse signs.

3.3 Types of interventions

Both groups received standard basic therapies like hypotension and glucose reduction. Chinese medicine compound preparations (water decoction and granules only) were used in the test group, whereas lipid-regulating medications like atorvastatin and rosuvastatin were given to the control group.

3.4 Types of outcome measures

Carotid plaque morphological changes [carotid intima-media thickness (CIMT), plaque area], serum hypersensitive C-reactive protein (hs-CRP), and low-density lipoprotein (LDL-C) were the primary outcome indicators.

The effectiveness of TCM symptoms, the effectiveness of plaque area reduction, carotid hemodynamic parameters (peak systolic flow velocity, PSV), and the incidence of adverse events were all secondary outcome indicators.

3.5 Efficacy determination criteria

The book "Diagnostic and efficacy criteria for common diseases" should be read (Sun, 2010). Apparently effective: a 50% reduction in the size of the AS plaque. Effective: 20%–50% reduction in the size of the AS plaque. Ineffective: The area of the AS plaque was reduced by 20%.

According to the Guidelines for Clinical Research on New Chinese Medicines, clinical efficacy was classified into four levels of clinical control, apparently effective, effective, and ineffective, and symptoms were graded and scored as three for severe, two for moderate, one for mild, and 0 for asymptomatic. The total effective rate was determined by adding clinical control + apparently effective + effective. Clinical control: complete or partial disappearance of clinical symptoms and signs, as well as a 95% reduction in symptom score; apparently effective: significant improvement in clinical symptoms and signs, and a 70% reduction in symptom score; effective: improvement in clinical symptoms and signs, and a 30% reduction in symptom score; ineffective: no significant improvement in clinical symptoms and signs, or even aggravation, and a symptom score reduction of less than 30%. (pre-treatment points—post-treatment points)/pre-treatment points x 100% is the calculation formula.

3.6 Exclusion criteria

However, we excluded studies that had the following characteristics: non-clinical studies (animal cell experiments, systematic reviews, reviews, and empirical and medical cases); other therapies such as acupuncture and acupressure were also present in the intervention; outcome indicators did not include the outcome indicators observed in this study; inconsistent evidence patterns; inconsistent dosage forms; duplicate publications; lack of full text available; and tiny sample size.

3.7 Study selection

Two authors worked independently to screen the literature (Jia Li and Yuying Du). First, remove any duplicates. After scanning the study titles and abstracts to eliminate those that did not meet the criteria, a secondary screening was conducted using the inclusion and exclusion criteria after reading the full text of any studies whose status was unclear during the initial screening. In the event of a disagreement, a third assessor (Fuming Liu) joined the conversation and assisted with the decision.

3.8 Data extraction

The data extraction included broad details about the included studies, like the authors and the year of publication, as well as fundamental details of the studies, such as sample size and mean age; interventions and course; components of the risk of bias evaluation; and outcome indicators.

3.9 Quality assessment

Selection bias (random sequence generation and allocation concealment), implementation bias (blinding of the researchers and subjects), measurement bias (blinded evaluation of the study results), follow-up bias (completeness of outcome data), reporting bias (selective reporting of research results), and other biases. Each of the aforementioned entries can be categorized as either "low risk," "unclear," or "high risk," with any discrepancies resolved by consulting with a third assessor.

3.10 Data synthesis and statistical analysis

A meta-analysis was performed using Review Manager 5.3 and Stata 12.1 software. Heterogeneity was analyzed using the $\chi 2$ test (test level $\alpha = 0.10$), and if the heterogeneity between studies was more acceptable ($p > 0.10$ and I $2 \leq 50\%$), a fixed effects model was selected for calculation; otherwise, a random-effects model was chosen. Standardized mean difference (SMD) for continuous variables and the risk ratio (RR) for dichotomous data with 95% confidence intervals (Cl) were used. The level of the meta-analysis was set at $\alpha = 0.05$. When significant heterogeneity existed, subgroup analysis or sensitivity analysis was performed to find the source of heterogeneity, or only descriptive analysis was performed, depending on the data available. The publication bias was checked by funnel plots and Begg's test if the number of trials was sufficient. When heterogeneity was detected, a sensitivity analysis was conducted to assess the stability of the results by excluding individual studies one by one. Subgroup analysis was performed to explore the sources of heterogeneity.

Quality of evidence grade evaluation

The GRADE profiler 3.6 was applied to evaluate the outcome indicators, and the evidence levels were provided as high, moderate, low, and very low.

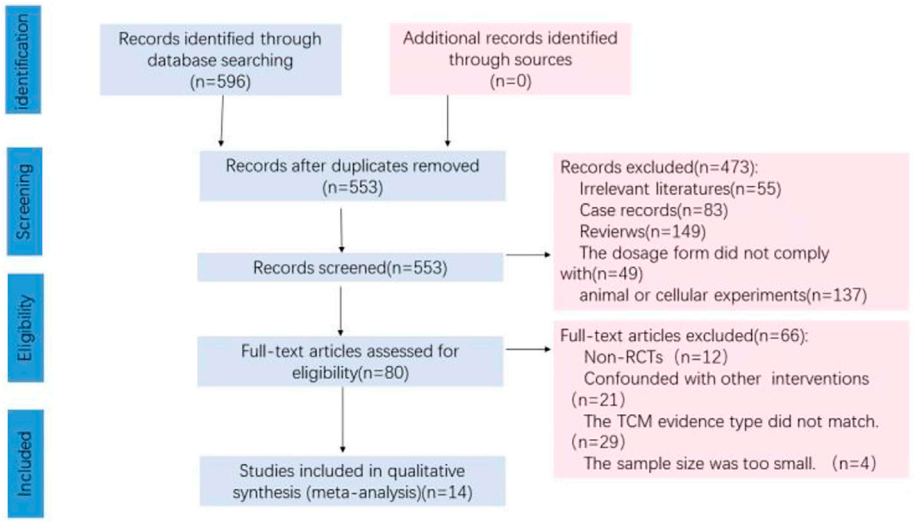

FIGURE 2
Flow diagram of the studies selection process.

TABLE 1 Basic characteristics of the included studies.

Study	Sample size (T/C)	Mean age (years, $\bar{x} \pm s$)		Interventions		Treatment (weeks)	Ending indicators
		T	C	T	C		
Wu et al. (2018)	121 (62/59)	62.4 ± 3.7	61.9 ± 3.5	con + Yiqi huatan huoxue formula	Atorvastatin	24 weeks	①②③⑤⑧
Zhu (2018)	110 (55/55)	58.24 ± 2.96	59.52 ± 2.08	con + Yiqi huatan tongluo decoction	Rosuvastatin	24 weeks	②③⑤⑥⑧
Wang et al. (2019)	61 (31/30)	87.81 ± 4.34	89.10 ± 2.63	con + Yiqi huoxue huatan tongluo formula	Atorvastatin	12 weeks	④⑥⑧
Zhang and Guo (2015)	87 (44/43)	53.43 ± 8.17	52.45 ± 7.69	con + Yiqi huatan huoxue formula	Simvastatin	24 weeks	①②③⑥⑧
Cao and Wang. (2013)	120 (60/60)	57.5	55.6	con + Yiqi huatan huoxue formula	Rosuvastatin	24 weeks	②③⑤⑥⑧
Jiang (2019)	72 (36/36)	59.45 ± 9.879	57.97 ± 8.765	con + Xuemai shutong formula	Atorvastatin	12 weeks	②④⑥⑦⑧
Huang et al. (2012)	124 (64/60)	59.32 ± 7.77	57.27 ± 9.93	con + Liujun danshen granules	Atorvastatin	12 weeks	②⑥
Dong (2013)	60 (30/30)	83.93 ± 5.48	82.03 ± 6.74	con + Yiqi huatan huoxue formula	Simvastatin	24 weeks	②④⑥⑧
Zhang and Ye (2020)	60 (30/30)	49.74 ± 6.81	49.16 ± 6.37	con + Jiawei ditan formula	Atorvastatin	2 weeks	①②⑥⑦⑧
Hai (2017)	60 (30/30)	63.25 ± 9.15	62.15 ± 10.80	con + Jingling granules	Atorvastatin	8 weeks	②③④⑥⑧
Zhao et al. (2012)	76 (38/38)	66.4 ± 11.8	66.4 ± 11.8	con + Yiqi huoxue huatan tongluo decoction	Fluvastatin	16 weeks	②③④⑥⑦⑧
Zheng (2019)	80 (40/40)	74.96 ± 5.45	75.24 ± 5.63	con + Yiqi huoxue huatan tongluo formula	Simvastatin	12 weeks	②
Niu (2017)	80 (40/40)	52.49 ± 7.65	53.45 ± 8.15	con + Yiqi huatan huoxue formula	Simvastatin	24 weeks	①②③⑥
Chen (2020)	80 (40/40)	61.58 ± 8.86	59.68 ± 9.32	con + Buyang huanwu decoction	Atorvastatin	8 weeks	②④⑥⑦

Notes: T, intervention groups; C, control groups; con, control groups; ①PSV; ②CIMT; ③Carotid plaque area; ④Clinical efficacy of Chinese medicine; ⑤Plaque size efficacy; ⑥LDL-C; ⑦hs-CRP; ⑧Incidence of adverse reactions.

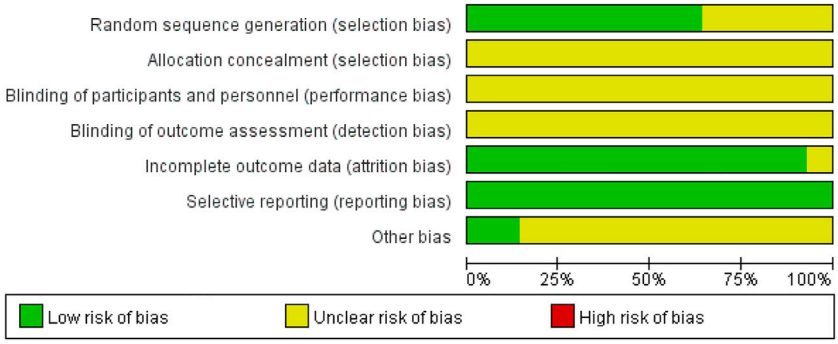

FIGURE 3
Risk-of-bias graph.

4 Results

4.1 Literature search

A total of 596 studies were retrieved in the original screening. Forty-three duplicates were excluded, 473 of which were excluded after scanning the titles and abstracts. Moreover, sixty-six studies were further excluded after intensive full-text rescreening, and fourteen studies finally remained, all of which were in Chinese. The screening flow chart is shown in Figure 2.

4.2 Study characteristics and quality assessment

Fourteen studies were included in this study, involving 1,191 patients, 600 in the treatment group and 591 in the control group, with a sample size of 30–64 cases in the individual studies. The treatment group was the control group with the addition of the YQHXZT formula. The control group was Western medicine for lipid regulation. The duration of treatment lasted from 2 to 24 weeks. The basic characteristics of the 14 studies are detailed in Table 1.

4.3 Literature bias and quality assessment

The quality of the included RCTs is shown in Figure 3. For the 14 included studies, all mentioned a randomized method of grouping, among which nine studies (Huang et al., 2012; Cao and Wang, 2013; Dong, 2013; Zhang and Guo, 2015; Zhu, 2018; Jiang, 2019; Wang et al., 2019; Chen, 2020; Zhang et al., 2020) described randomization methods in detail, such as the use of random number tables and the use of software randomized grouping, which was considered "low risk"; the rest of the studies only covered "randomization" without specifying the scheme. None of the studies mentioned assignment sequence hiding and blinding. There was no explicit description of blinding outcome raters. All studies included a balanced population at baseline with good data completeness. Pre-designed outcomes were reported in all studies, perceiving a low risk of selective reporting bias. Other biases were not found in all included studies. Two studies (Huang et al., 2012; Dong, 2013)were supported by government funding programs, had no conflicts of interest, and were otherwise assessed as "low risk" of bias; the source of the other bias for the remaining trials was unclear. The risk of bias for each study is shown in Figure 3.

5 Results of meta-analysis

5.1 Primary outcomes

5.1.1 Morphological changes of carotid artery plaques

5.1.1.1The thickness of the middle lining of the carotid artery (CIMT)

Pooled data from the thirteen studies (Huang et al., 2012; Zhao et al., 2012; Cao and Wang, 2013; Dong, 2013; Zhang and Guo, 2015; Hai, 2017; Niu, 2017; Wu et al., 2018; Zhu, 2018; Jiang, 2019; Zheng, 2019; Chen, 2020; Zhang et al., 2020) reporting the CIMT showed that YQHXZT formula clearly decreased the thickness of carotid medial intima as an adjuvant or monotherapy for CAS compared with the contrast group [SMD = -0.97, 95%CI (−1.30, −0.65), $p < 0.00001$; p for heterogeneity = 0.00001, I^2 = 85% > 50%; Figure 4]. The heterogeneity between studies was high, and the random effect model was selected for analysis. The Stata software was used for sensitivity analysis of the study, and no significant studies affecting the stability of the results were found (Figure 5).

The high heterogeneity was possibly related to the duration of treatment between studies. A meta-regression analysis of the

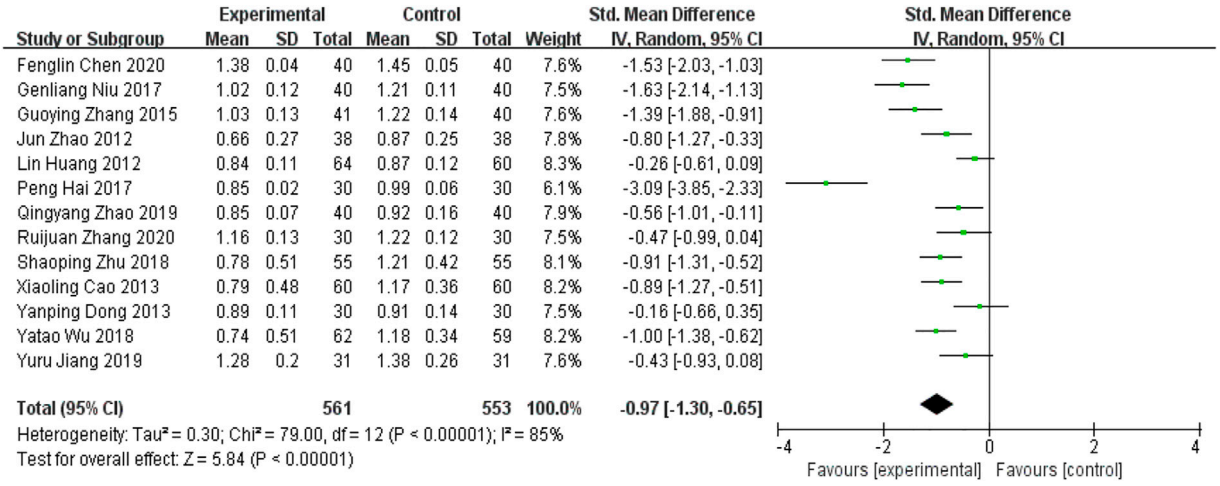

FIGURE 4
Forest plot for CIMT.

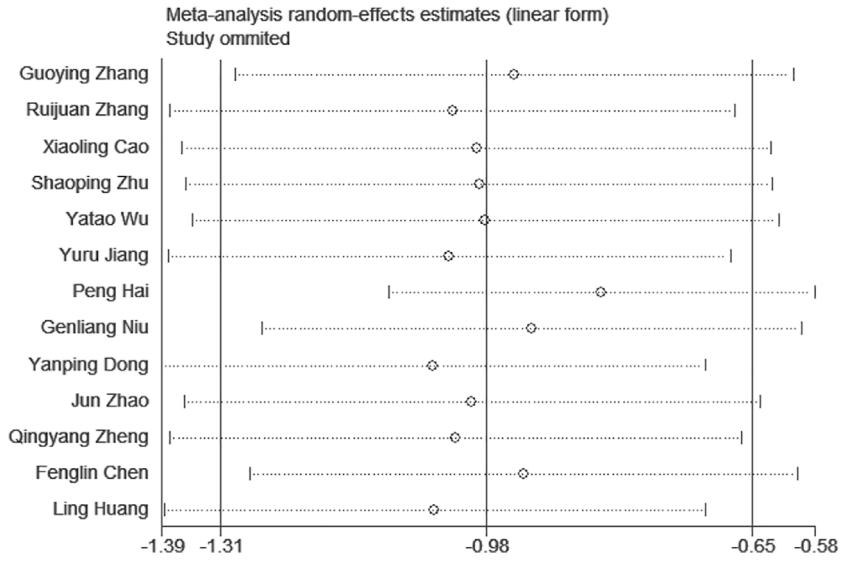

FIGURE 5
CIMT sensitivity analysis.

duration of treatment was performed using Stata 12.1 software to find sources of heterogeneity. Three of the included studies had a treatment duration of <12 weeks and the remaining trials had a treatment duration of 12–24 weeks. The studies were divided into two groups according to treatment duration, and meta-regression was performed with the group (treatment duration) variable as a covariate, resulting in $p = 0.101 > 0.05$ and Adj R-squared = 17.43%, suggesting that the effect of treatment duration on heterogeneity was less likely and considered to be possibly related to the instrument used for measurement, the measurement researcher's manipulation, measurement error, and other factors.

5.1.1.2 Carotid plaque area

Seven RCTs (Zhao et al., 2012; Cao and Wang, 2013; Zhang and Guo, 2015; Niu, 2017; Hai, 2017; Wu et al., 2018; Zhu, 2018) in the included studies reported carotid plaque area as an outcome indicator. Meta-analysis indicated that the addition of YQHXZT

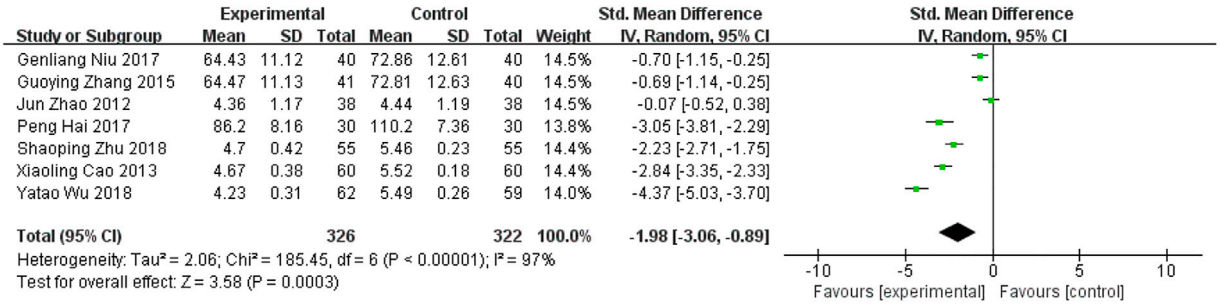

FIGURE 6
Forest plot for carotid plaque area.

TABLE 2 Meta-regression analysis.

Factors	Regression coefficient	Coefficient standard error	t-value	*p*-value
Duration of treatment	−0.62	1.41	−0.44	0.68
Sample size	−2.04	0.94	−2.17	0.08

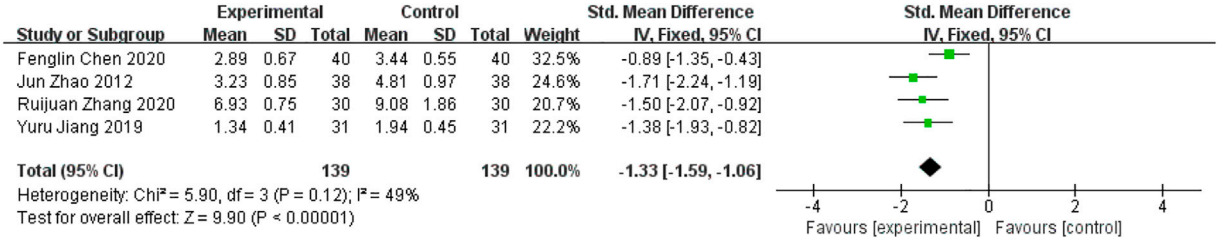

FIGURE 7
Forest plot for hs-CRP.

formula could significant further reduce the carotid plaque area [SMD = -1.98, 95%CI (−3.06, −0.89), $p = 0.0003$; p for heterogeneity $p < 0.00001$, $I^2 = 97\% > 50\%$; Figure 6]. Excluding each of the included studies one by one, no studies were found that significantly affected the stability of the results.

The reasons for the high heterogeneity were possibly related to factors such as duration of treatment and sample size across studies. A meta-regression analysis was performed using Stata 12.1 software to find sources of heterogeneity in terms of duration of treatment and sample size. A meta-regression was performed with the variables of group (duration of treatment (>12 weeks, <12 weeks) and sample size (>100 cases, <100 cases)) as covariates, and the results suggested that the factors of duration of treatment and sample size did not have a significant effect on heterogeneity (Table 2), and it was considered that they might be related to factors such as the instrument used to measure it, the operation of the researcher who measured it, and measurement error.

5.1.1.3 Inflammatory factors— hs-CRP

Four RCTs (Zhao et al., 2012; Jiang, 2019; Chen, 2020; Zhang et al., 2020) conducted hs-CRP as an inflammatory factor outcome. Meta-analysis revealed that the addition of YQHXZT formula was more likely to reduce hs-CRP levels [SMD = −1.33.95% CI (−1.59, −1.06), $p < 0.00001$, P for heterogeneity = 0.12, $I^2 = 49\% < 50\%$, Figure 7).

5.1.1.4 Lipid levels— LDL-C

Twelve RCTs (Huang et al., 2012; Zhao et al., 2012; Cao and Wang, 2013; Dong, 2013; Zhang and Guo, 2015; Hai, 2017; Niu,

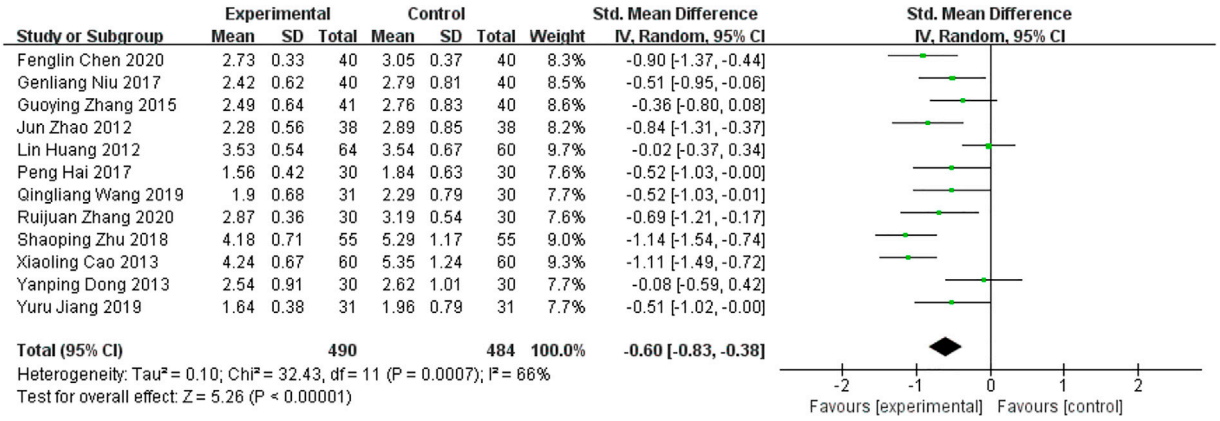

FIGURE 8
Forest plot for LDL-C.

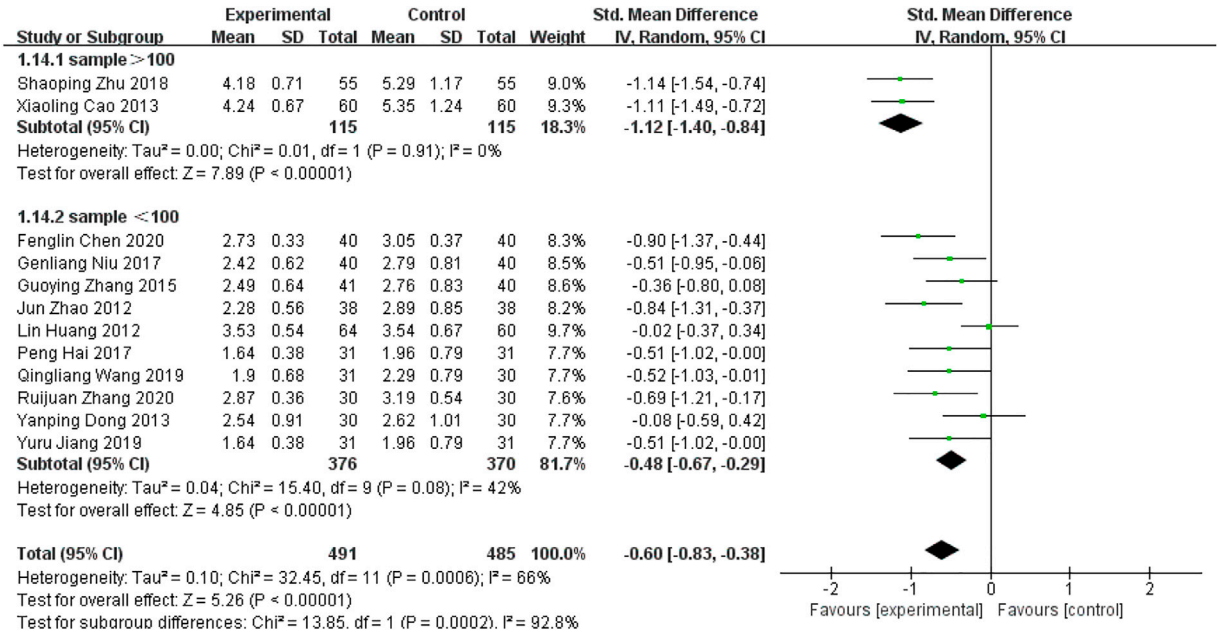

FIGURE 9
Forest plot for LDL-C subgroup analysis.

2017; Zhu, 2018; Jiang, 2019; Wang et al., 2019; Chen, 2020; Zhang et al., 2020) compared LDL-C levels before and after treatment in the two groups. From the data in Figure 8, it is apparent that the addition of the YQHXZT formula was clearly more effective in reducing LDL-C levels [SMD = -0.60.95%CI(−0.83,−0.38),$p < 0.00001$; P for heterogeneity = 0.0007, $I^2 = 66\% > 50\%$]. The results were analyzed by excluding each included study one by one, and no studies were found that significantly affected the stability of the results. The source of heterogeneity was possibly related to the sample size and a subgroup analysis was performed. Sample size >100, subgroup results showed that P for heterogeneity = 0.91, $I^2 = 0\% < 50\%$, $p < 0.00001$; sample size<100, subgroup results showed that P for heterogeneity = 0.08, $I^2 = 42\% < 50\%$, $p < 0.00001$, Figure 9. The heterogeneity of both subgroups was acceptable.

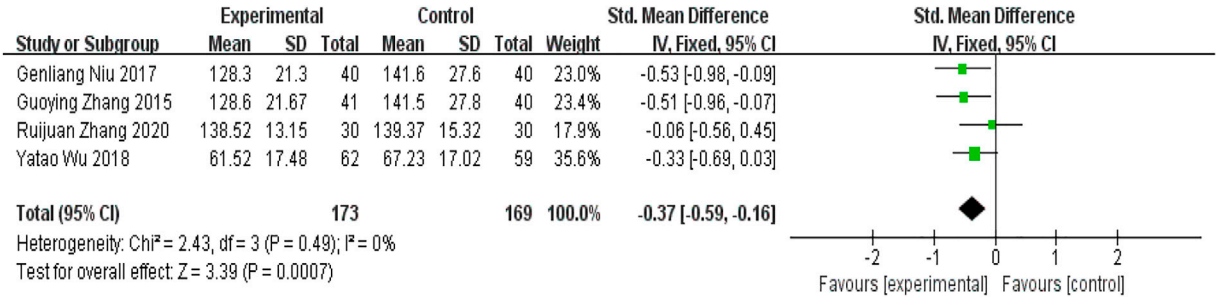

FIGURE 10
Forest plot for peak systolic blood flow velocity.

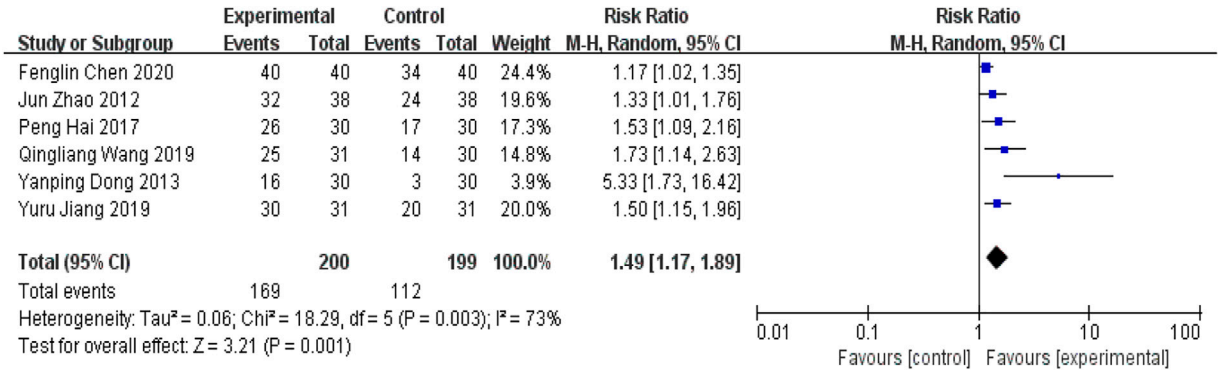

FIGURE 11
Forest plot for clinical efficacy of Chinese medicine.

5.2 Secondary outcome indicators

5.2.1 Carotid flow indicators——Peak systolic blood flow velocity

Four RCTs (Zhang and Guo, 2015; Niu, 2017; Wu et al., 2018; Zhang et al., 2020)used PSV as an outcome indicator. As Figure 10 showed, there was a significant difference between the two groups [SMD = −0.37, 95%CI(−0.59,−0.16),p = 0.0007; p for heterogeneity = 0.49 > 0.1; I^2 = 0% < 50%]. The experimental group was better at improving PSV.

5.2.2 Efficacy indicators

5.2.2.1 Clinical efficacy of Chinese medicine

Six RCTs (Zhao et al., 2012; Dong, 2013; Hai, 2017; Jiang, 2019; Wang et al., 2019; Chen, 2020) in the included studies used the clinical efficacy of TCM as an outcome indicator. Meta-analysis showed that the addition of YQHXZT formula was significantly more effective in improving the clinical outcome of TCM [RR = 1.49, 95%CI(1.17.1.89), p = 0.001,P for heterogeneity = 0.003, I^2 = 73% > 50%, Figure 11]. Excluding each included study one by one, the heterogeneity was found to be reduced after removing the study by Fenglin Chen (Chen, 2020), I^2 = 43%, RR = 1.64, 95%CI (1.39, 1.94), p < 0.00001, the difference between the two groups was statistically significant (Figure 12).

5.2.2.2 Plaque area efficacy

Three RCTs (Cao and Wang, 2013; Wu et al., 2018; Zhu, 2018) reported plaque area efficacy. The results of the meta-analysis were shown in Figure 13. The addition of the YQHXZT formula was superior to the control group in improving plaque size [RR = 1.36, 95%CI(1.22.1.52), p < 0.0001, P for heterogeneity = 1.00, I^2 = 0%].

5.2.2.3 Safety indicators—Incidence of adverse reactions

There were ten RCTs (Zhao et al., 2012; Cao and Wang, 2013; Dong, 2013; Zhang and Guo, 2015; Hai, 2017; Wu et al., 2018; Zhu, 2018; Jiang, 2019; Wang et al., 2019; Zhang et al., 2020) reporting incidence of adverse reactions as a safety indicator. Ruijuan Zhang (Zhang et al., 2020) reported adverse reactions dominated by nausea, rash, and liver function impairment in both groups, eight

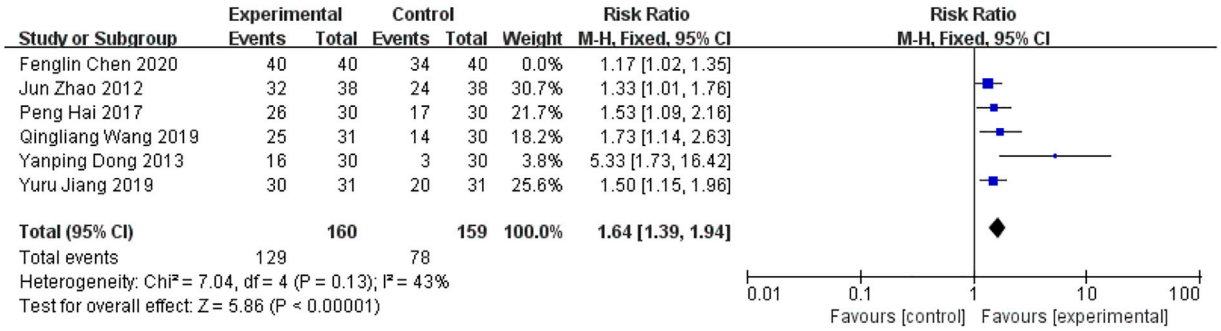

FIGURE 12
Forest plot of clinical efficacy for Chinese medicine excluding Chen.

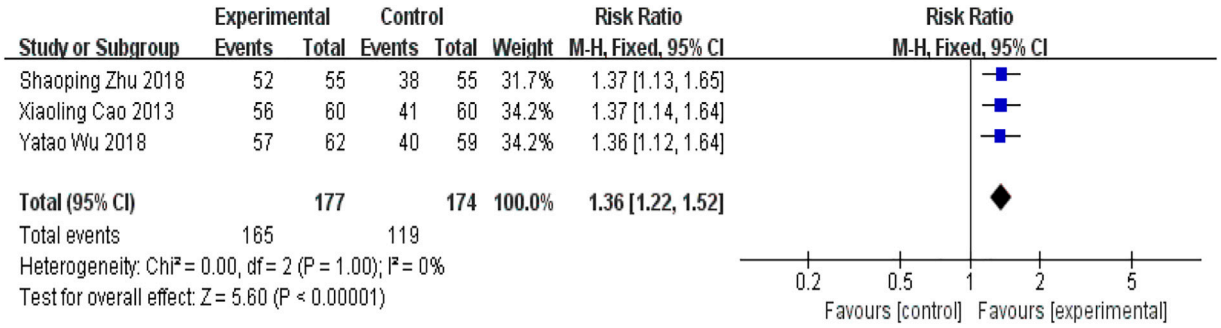

FIGURE 13
Forest plot for plaque area efficacy.

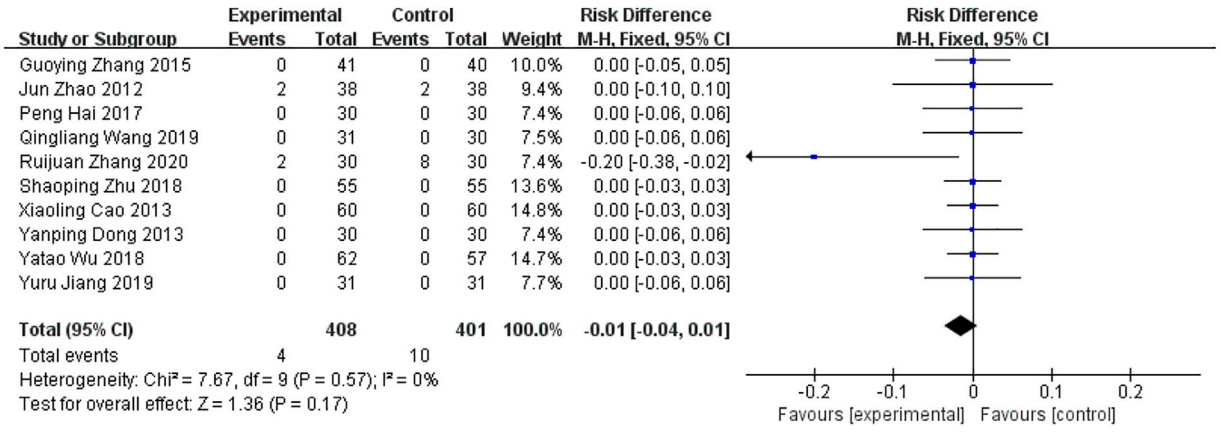

FIGURE 14
Forest plot of incidence for adverse reactions.

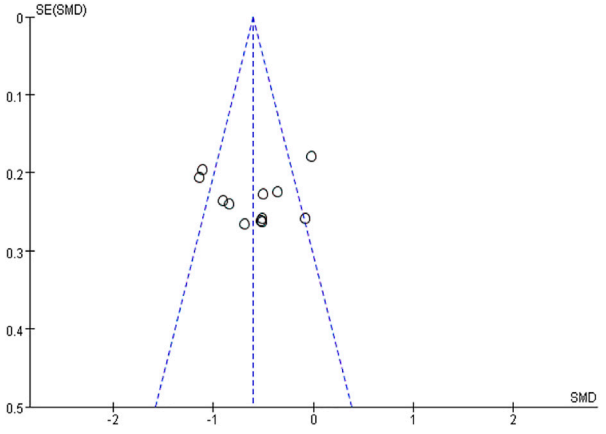

FIGURE 15
Publication risk of bias funnel plot.

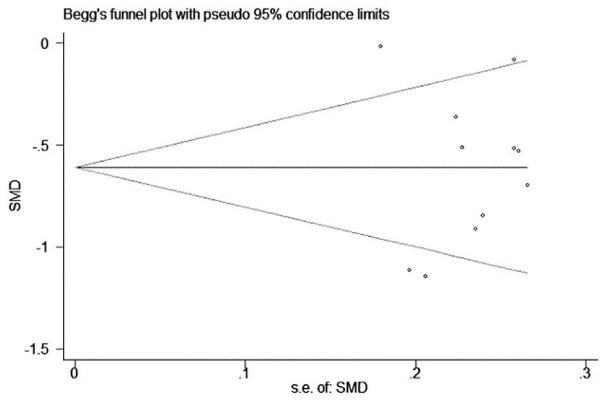

FIGURE 16
Graph of Begg's test results.

cases in the western medicine group and two cases in the trial group. Jun Zhao (Zhao et al., 2012) reported two cases of increased glutathione transaminase in each of the two groups, which returned to normal after discontinuation of the drug. There was no heterogeneity between the study results (I^2 = 0%) and a fixed effects model was used to calculate the combined statistic, which showed that the difference in the rate of adverse reactions between the experimental and control groups was not statistically significant [RD = −0.01, 95% CI (−0.04.0.01), p = 0.17, Figure 14].

5.2.2.4 Publication bias

The funnel plot showed a symmetric distribution of trials on either side of the funnel, and Begg's test (p = 0.990 > 0.05) was consistent with the funnel plot, indicating that the results were reliable in this meta-analysis (Figures 15, 16).

5.3 Grade assessment

The evidence quality of outcomes was graded by using the GRADE system. The table below demonstrated that the outcome indicators PSV, LDL-C, plaque area efficacy, hs-CRP, and incidence of adverse events were moderate-quality evidence. The outcome indicators for CIMT, plaque area reduction, and clinical efficacy of TCM were of low-quality evidence. Relegation factors were mainly the absence of allocation protocol concealment and blinding and the high heterogeneity between studies (Table 3).

6 Discussion

The pathogenesis of AS is very complex. Inflammatory reactions not only run through all stages of the development of AS but also are closely related to the occurrence of various complications. The theory of immune inflammation has become a new breakthrough in the prevention and treatment of AS. The prevention and treatment of AS based on anti-inflammation and immune regulation have broad prospects and great potential. As one of the main blood supply vessels to the brain, the carotid artery plays an important role during AS. One study reported that the incidence of cerebral infarction in patients with greater than 70% carotid stenosis was approximately 13% (Zhang et al., 2020). There is no record of CAS in the Chinese medical literature. Based on its pathological nature, location, and clinical symptoms, it can be classified under the categories of "pulse paralysis", "vertigo", and "stroke." Chinese medicine has recognized for thousands of years that the "veins" are the channels through which blood flows, and their physiological characteristics are similar to those of the "blood vessels" in Western medicine. In TCM, a qi deficiency is the root cause of the disease, and qi and blood are mutually beneficial. If qi is deficient, the blood is unable to move, and the blood is easily blocked and becomes stagnant. In addition, since the blood and fluid are of the same origin, when the arteries are blocked, the fluid stops, and the phlegm grows, the phlegm stagnates and adheres to the arteries, which turns into plaques over time and aggravates the progress of AS. In view of pathological factors such as phlegm, stasis, and turbidity, TCM clinically uses methods such as resolving phlegm, invigorating blood, and eliminating stasis to treat AS-related diseases (Jin et al., 2020). Statins are common clinical lipid-regulating drugs that can effectively improve lipid levels and plaque thickness and number in patients with CAS and reduce the incidence of adverse cardiovascular and cerebrovascular events (Liu et al., 2018). However, recently, investigators have examined the effects of western medicine alone are limited (Li, 2018), with shortcomings such as long duration, easy drug resistance, and side effects. In recent decades, TCM has received increasing attention due to its therapeutic effect and prospective future (Zhang et al., 2022).

TABLE 3 Evaluation of GRADE evidence quality.

Outcome indicators	95%CI	Risk of bias	Inconsistency	Indirectness	Imprecision	Publication bias	Upgrade quality	Quality
CIMT	SMD −0.97 (−1.30, −0.65)	serious①	serious②	No	No	Undetected	None	Low
Carotid plaque area	SMD -1.98 (−3.06, −0.89)	serious①	serious②	No	No	Undetected	None	Low
hs-CRP	SMD −1.33 (−1.59, −1.06)	serious①	No	No	No	Undetected	None	Moderate
LDL-C	SMD −0.60 (−0.83, −0.38)	serious①	No	No	No	Undetected	None	Moderate
PSV	SMD −0.37 (−0.59, −0.16)	serious①	No	No	No	Undetected	None	Moderate
Clinical efficacy of Chinese medicine	RR 1.49 (1.17, 1.89)	serious①	serious②	No	No	Undetected	None	Low
Plaque area efficacy	RR 1.36 (1.22, 1.52)	serious①	No	No	No	Undetected	None	Moderate
Incidence of adverse reactions	RD −0.01 (−0.04.0.01)	serious①	No	No	No	Undetected	None	Moderate

SMD, is the standardized mean difference; RR, is the relative risk; ① absence of allocation concealment and blinding; ② the p value of the heterogeneity test was <0.1, and I^2 >50%.

Previous research has established that the treatment of CAS using the YQHXZT method can effectively reduce intima-media thickness and plaque area, improve arterial stenosis, and enhance blood flow velocity (Chen and Zhang, 2017).

This study was based on Cochrane systematic evaluation principles to systematically evaluate the efficacy and safety of the combination of the YQHXZT method with western medicine in the treatment of CAS, and to evaluate the quality of evidence for the outcome indicators of the included studies by Grade profiler 3.6. As can be seen from above, the experimental group was more effective in improving CIMT [SMD = −0.97, 95%CI (−1.30, −0.65), $p < 0.00001$], reducing carotid plaque area [SMD = −1.98, 95% CI(−3.06,−0.89),$p = 0.0003$], lowering hs-CRP levels [SMD = −1.33, 95%CI(−1.59,−1.06),$p < 0.00001$] and LDL-C levels [SMD = −0.60, 95%CI(−0.83,−0.38), $p < 0.00001$]than the control group. Moreover, the experimental group was superior to PSV [SMD = -0.37, 95%CI(-0.59,-0.16), $p = 0.0007$]. In terms of clinical efficacy, the Chinese medicine clinical efficacy [RR = 1.64, 95%CI(1.39.1.94), $p < 0.00001$] and improvement of plaque area efficacy [RR = 1.36, 95% CI (1.22, 1.52), $p < 0.0001$] were both better in the experimental group. The incidence of adverse reactions was not statistically significant in the two groups [RD = −0.01, 95% CI (−0.04.0.01), $p = 0.17$]. The results of this review, combined with the grade evaluation, suggested that the outcome indicators LDL-C, hs-CRP, plaque area efficacy, PSV, and incidence of adverse events were moderate evidence, and the outcome indicators CIMT, plaque reduction area, and TCM clinical efficacy were low-quality evidence.

AS is a chronic vascular inflammatory response caused by the accumulation of LDL-C and is higher in patients with CAS. Within a certain range, the risk of AS increases logarithmically with higher LDL-C (Chen, 2020). The protein components of LDL particles in the body stimulate T lymphocytes to produce pro-inflammatory cytokines, which aggregate inflammatory factors such as CRP, IL-6, and monocyte chemoattractant protein-1, causing macrophages to phagocytose oxidized LDL and convert it into foam cells, which accumulate and eventually lead to the formation of AS (Beverly and Budoff, 2020). The vascular inflammatory response plays a key role in the pathogenesis of AS (Nie et al., 2020), influencing plaque formation, progression, and stability. Hs-CRP is a sensitive inflammatory factor reflecting vascular inflammatory mechanisms, which can be involved in related gene regulation and is closely related to the formation and breakdown of AS (Chen et al., 2021a). Hs-CRP can induce inflammatory and adhesion factors and make them accumulate under the vascular endo cortex, promote the formation of foam cells, and promote interstitial degradation and vascular smooth muscle cell apoptosis by activating the inflammatory pathway. This increases the risk of AS and plaque rupture. Tigkiropoulos et al. (Tigkiropoulos et al., 2019)demonstrated that PSV could be used to assess the degree of arterial stenosis. Studies suggested that every 0.1 mm thickening of the IMT increased the risk of infarction by 10%–15% and stroke by 13%–18%, especially in unstable plaques, which were more likely to dislodge and lead to stroke (Liu et al., 2020). Research has confirmed Chinese medicine's effectiveness as an effective means of treating cardiovascular diseases (Hao et al., 2017). For example, Huangjing can play a role by regulating lipid metabolism, reducing inflammation, and improving oxidative stress (Chen et al., 2021b). Data from several studies suggest that increasingly Chinese medicine prescriptions, including

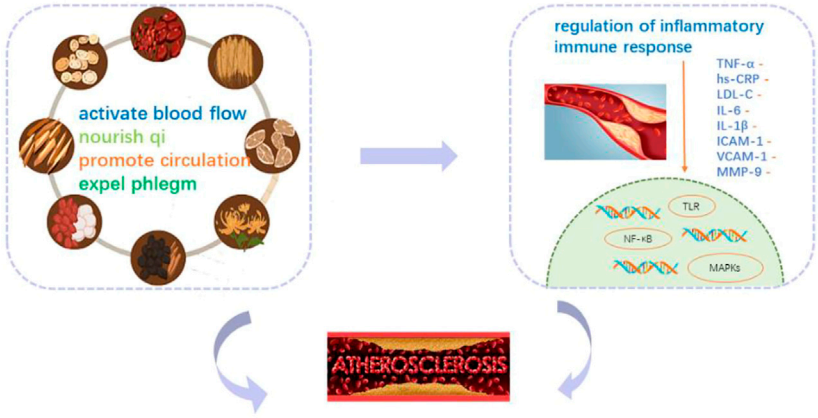

FIGURE 17
Mechanism of YQHXZY in improving CAS.

Chinese patent medicine, classical prescription decoction, self-made prescription, etc., have been confirmed to regulate immune inflammation and antioxidant in a variety of ways (Tang et al., 2022). According to the composition and compatibility effect of the prescription, the most common is to benefit qi, promote blood circulation, and eliminate phlegm. The main pathways involved include Nf-κB pathway, the MAPKs pathway, the Toll-like receptor pathway, the inflammatory body pathway, etc (Figure 17). More attention has been paid to the first two pathways, whose mechanisms may be mainly by inhibiting NF-κB protein phosphorylation or NF-κB p65 gene expression and can also be combined with the MAPKs pathway to regulate the expression of related inflammatory cytokines to play an anti-inflammatory role. For example, berberine, the main compound of Huanglian, can lower blood lipid, antioxidation, anti-inflammation, and protect vascular endothelium (Xu et al., 2019) by downregulating the serum inflammatory factor levels, inhibiting MAPK phosphorylation, inhibiting NF-κBp65 mRNA expression (Feng et al., 2017).

In terms of publication bias, the funnel plot and Begg's test were used to prove that there was no obvious publication bias in this study, and that the study results were reliable. In clinical work, it was found that AS was often combined with other diseases at the same time. According to the existing literature reports, TCM could also improve some symptoms and indicators of concomitant diseases, but its efficacy still needs further standardized study. This study, combined with grade evaluation, provides an evidence-based basis for clinical treatment direction. Compared with the control group, the YQHXZT formula was more comprehensive and safer, which was worthy of further clinical promotion.

7 Conclusion

This study has shown that the combination of the YQHXZT method could inhibit carotid intimal thickening, reduce plaque area, lower LDL-C and hs-CRP levels, and improve clinical efficacy. At the same time, the combination of YQHXZT methods has not found a significant increase in the risk of adverse reactions. Overall, this study probably strengthens the idea that the combination of Chinese medicine and western medicine can slow down the CAS process and improve the prognosis of the disease by inhibiting the inflammatory response and regulating lipid metabolism. That provides new attempts for the treatment of CAS in the future.

8 Limitation

However, this study also had some limitations: ① Some of the included studies did not describe the stochastic method in detail. No trial mentioned allocation concealment and blinding, and selection bias may have occurred. The included studies were Chinese studies with insufficient research dimensions. ② Mostly limited to the observation and analysis of a prescription, should focus on some good curative effects of YQHXZT by TCM fixed prescription or Chinese patent medicine. Therefore, in the future, we should pay attention to the improvement of methodology and carry out multicenter, large sample, high-quality, long-course double-blind RCT with Chinese medicine characteristics for verification. At the same time, the basic research on the treatment of CAS with TCM was relatively weak, and the research on the mechanism of action of drugs needed to be more in-depth and clearer (Yang et al., 2020).

Data availability statement

The raw data supporting the conclusion of this article will be made available by the authors, without undue reservation.

Author contributions

JL and YD designed the study and conducted the data analysis. CC checked the final data. JL and YD screened the articles. JL drafted the manuscript and performed data interpretation. FL suggested changes to the data analysis. YD revised the manuscript. FL conceived and designed the study and acted as the supervisor. All authors significantly contributed to the paper and read and approved the final manuscript.

Funding

This work was financially supported by the Jiangsu Province Key R&D Program—Social Development General Project (BE2020683), the Innovative Talent Team Project of "Six Talent Peaks" of Jiangsu Province (TD-SWYY-069), the Key Planning Project for the Science and Technology Development of Traditional Chinese Medicine of Jiangsu Province (ZD201906), and the Innovation Development Fund Project of Traditional Chinese Medicine of Jiangsu Province (Y2019CX20).

Conflict of Interest

The authors declare that the research was conducted in the absence of any commercial or financial relationships that could be construed as a potential conflict of interest.

Publisher's note

All claims expressed in this article are solely those of the authors and do not necessarily represent those of their affiliated organizations, or those of the publisher, the editors and the reviewers. Any product that may be evaluated in this article, or claim that may be made by its manufacturer, is not guaranteed, or endorsed by the publisher.

Supplementary material

The Supplementary Material for this article can be found online at: https://www.frontiersin.org/articles/10.3389/fphar.2022.1059737/full#supplementary-material

References

Backes, J. M., Ruisinger, J. F., Gibson, C. A., and Moriarty, P. M. (2017). Statin-associated muscle symptoms-Managing the highly intolerant. *J. Clin. Lipidol.* 11 (1), 24–33. doi:10.1016/j.jacl.2017.01.006

Bai, S. P. (2009). *Diagnostic criteria for neurology disorders*. Beijing: Science and Technology Literature Press.

Beverly, J. K., and Budoff, M. J. (2020). Atherosclerosis: Pathophysiology of insulin resistance, hyperglycemia, hyperlipidemia, and inflammation. *J. Diabetes* 12 (2), 102–104. doi:10.1111/1753-0407.12970

Cao, X. L., and Wang, Y. (2013). Clinical observation of qi-replenishing, blood-activating and phlegm-removing therapy in the treatment of 60 cases of carotid atherosclerotic plaques. *Sichuan J. Tradit. Chin. Med.* 31 (12), 69–72.

Chen, F. L. (2020). *Clinical study of buyang huanwu decoction in the treatment of patients with essential hypertension and carotid atherosclerosis (qi deficiency, phlegm and stasis type)*. Nanchang, Jiangxi province, China: Jiangxi University of Traditional Chinese Medicine.

Chen, J. D., and Zhang, Q. (2017). Effect of removing phlegm and blood stasis on carotid atherosclerosis. *Chin J Integr Med Cardio/Cerebrovas Dis.* 15 (11), 1383–1385. doi:10.3969/j.issn.1672-1349.2017.11.029

Chen, J. J., Jiang, W. W., Chen, J., Jiang, X. Z., Zhou, J., Wu, W. J., et al. (2019). Effects of risuvastatin calcium on endothelial diastolic function and carotid arteriosclerosis and hypersensitive C-reactive protein levels in elderly patients with cerebral infarction and carotid atherosclerosis. *Chin. Hosp. Pharm. J.* 39 (12), 1278–1281. doi:10.13286/j.cnki.chinhosppharmacyj.2019.12.13

Chen, Y., Zhou, Y. M., Li, D., and Peng, C. (2021a). Advances in modern pharmacological effects of rhizoma polygonati. *J. Chin. Med. Mate* 44 (1), 240–244. doi:10.13863/j.issn1001-4454.2021.01.046

Chen, Y., Kang, Y., Zhang, Y., Zhang, X., Liu, S. Q., Sha, X. X., et al. (2021b). Transcranial Doppler ultrasonography combined with carotid ultrasonography in elderly patients with cerebral infarction Application in Evaluation. *Chin. J. Gerontol.* 41 (4), 705–708. doi:10.3969/j.issn.1005-9202.2021.04.011

Dong, Y. P. (2013). A randomized controlled trial of the effect of Yiqi Huoxue Huatan Decoction Combined with simvastatin tables in treatment of elderly Patients with carotid atherosclerosis. *J. Pra Tradit. Chin. Inter Med.* 27 (7), 56–58. doi:10.3969/j.issn.1671-7813.2013.07(s).28

Feng, M., Kong, S. Z., Wang, Z. X., He, K., Zou, Z. Y., Hu, Y. R., et al. (2017). The protective effect of coptisine on experimental atherosclerosis ApoE-/- mice is mediated by MAPK/NF-κB-dependent pathway. *Biomed. Pharmacother.* 93, 721–729. doi:10.1016/j.biopha.2017.07.002

Geovanini, G. R., and Libby, P. (2018). Atherosclerosis and inflammation: Overview and updates. *Clin. Sci.* 132 (12), 1243–1252. doi:10.1042/CS20180306

Hai, P. (2017). *The clinical study of Jingling granule in the treatment on atherosclerosis with qi-yin deficiency and phlegm-heat stasis*. Nanjing, China: Nanjing University of Chinese Medicine.

Hao, P., Jiang, F., Cheng, J., Ma, L., Zhang, Y., and Zhao, Y. (2017). Traditional Chinese medicine for cardiovascular disease: Evidence and potential mechanisms. *J. Am. Coll. Cardiol.* 69 (24), 2952–2966. doi:10.1016/j.jacc.2017.04.041

Huang, L., Wu, Y. G., Li, B., Zhang, Z. Z., and Huang, H. C. (2012). Clinical study of liujun danshen granules in treating hypertension combined with carotid atherosclerosis of qi-deficiency and phlegm-blood stasis syndrome. *Inf. Tradit. Chin. Med.* 19 (10), 5–8. doi:10.3969/j.issn.1005-5304.2012.10.003

Humphries, S. E., Cooper, J. A., Seed, M., Capps, N., Durrington, P. N., Jones, B., et al. (2018). Coronary heart disease mortality in treated familial hypercholesterolaemia: Update of the UK Simon Broome FH register. *Atherosclerosis* 274, 41–46. doi:10.1016/j.atherosclerosis.2018.04.040

Jiang, Y. R. (2019). Effect of Xue mai shu tong recipe on patients with carotid arteriosclerosis and plaques of qi dificiency and phlegm stasis type. *Guangzhou Tradit. Chin. Med*, 41. Master's thesis.

Jin, H. G., Zhu, X. X., Zhao, P. P., Zhao, D., and Wang, T. (2020). A review on treating atherosclerosis from Tan and Yu. *CJCM* 12 (4), 145–148. doi:10.3969/j.issn.1674-7860.2020.04.055

Karataş, M. B., İpek, G., Onuk, T., Güngör, B., Durmuş, G., Çanga, Y., et al. (2016). Assessment of prognostic value of neutrophil to lymphocyte ratio and platelet to lymphocyte ratio in patients with pulmonary embolism. *Acta Cardiol. Sin.* 32 (3), 313–320. doi:10.6515/acs20151013a

Li, D., Dong, K. X., Liu, Y. H., Xu, J., and Li, M. D. (2020). Research progress on lipid-lowering components and mechanism of lipid-lowering traditional Chinese medicines. *Jiangxi Med. J.* 55 (11), 1736–1740. doi:10.3969/j.issn.1006-2238.2020.11.063

Li, Y. (2018). Application value of rosuvastatin in the treatment of hyperlipidemia with carotid atherosclerosis. *Med. Equip.* 31 (22), 81–82.

Libby, P. (2021). The changing landscape of atherosclerosis. *Nature* 592 (7855), 524–533. doi:10.1038/s41586-021-03392-8

Liu, D. Q., Du, R. X., Wang, Q. J., Cai, J., Wu, H., and Ye, P. (2018). Role of dynamic contrast enhanced MRI in assessing early curative effect of rosuvastatin on carotid atherosclerotic plaques. *Chin. J. Geriatr. Heart Brain Vessel Dis.* 20 (2), 126–129. doi:10.3969/j.issn.1009-0216.2018.02.004

Liu, J. K., Li, J., Liu, R. M., Liu, B. H., and Xu, K. (2020). Application of cervical vascular ultrasound index in the screening of high risk population of stroke Value and risk factors analysis. *Chin. J. Clin.* 48 (11), 1373–1375. doi:10.3969/j.issn.2095-8552.2020.11.035

Moher, D., Liberati, A., Tetzlaff, J., and Altman, D. G.PRISMA Group (2009). Preferred reporting items for systematic reviews and meta-analyses: The PRISMA statement. *PLoS Med.* 6 (7), e1000097. doi:10.1371/journal.pmed.1000097

Nie, H. J., Li, F. H., Hu, J., Li, J., Luo, X. Y., Zhang, M., et al. (2020). The relationship between carotid plaque contrast-enhanced ultrasound and hs-CRP and the volume of acute cerebral infarction. *Chin. J. Ultrasound Med.* 36 (8), 687–690.

Niu, G. L. (2017). Effect of Yiqi Huatan Huoxue therapy on hypertension complicated with carotid atherosclerosis. *Henan Med. Res.* 26 (15), 2802–2803. doi:10.3969/j.issn.1004-437X.2017.15.077

Pang, S. C., Zhang, J. P., Chen, M. L., and Lv, S. C. (2017). New advances in Chinese medicine for the treatment of atherosclerosis. *CJTCMP* 32 (1), 214–217.

Prandoni, P., Ciammaichella, M., Mumoli, N., Zanatta, N., Visonà, A., Avruscio, G., et al. (2017). An association between residual vein thrombosis and subclinical atherosclerosis: Cross-sectional study. *Thromb. Res.* 157, 16–19. doi:10.1016/j.thromres.2017.06.036

Sun, M. (2010). *Criteria for diagnosis and efficacy of clinical diseases*. Beijing: Science and Technology Literature Press.

Sun, H., Qu, W., Chen, G., Sun, X., Zhang, D., and Shao, S. (2021). Efficacy and safety of traditional Chinese patent medicine on carotid artery atherosclerosis in adults: A network meta-analysis protocol. *Med. Baltim.* 100 (3), e24406. doi:10.1097/MD.0000000000024406

Tang, Z. W., Gu, Y. M., and Xue, M. (2022). Study on prevention and treatment of atherosclerosis with Chinese medicine based on immune inflammation theory. *J. Basic Chin. Med.* 28 (7), 1192–1198. doi:10.19945/j.cnki.issn.1006-3250.2022.07.021

Tigkiropoulos, K., Karamanos, D., Stavridis, K., Zacharopoulos, N., Tympanidou, M., Mantelas, M., et al. (2019). Endovascular stent-graft repair of combined renal artery aneurysm and arteriovenous fistula. *Ann. Vasc. Surg.* 55, e9–e310. e9–e13. doi:10.1016/j.avsg.2018.07.054

Valanti, E. K., Dalakoura-Karagkouni, K., Siasos, G., Kardassis, D., Eliopoulos, A. G., and Sanoudou, D. (2021). Advances in biological therapies for dyslipidemias and atherosclerosis. *Metabolism.* 116, 154461. doi:10.1016/j.metabol.2020.154461

Wang, Q. L., Lu, W. J., and Chen, X. C. (2019). Effect of Yiqi Huoxue Huatan Tongluo formula on T-cells subset in patients with carotid atherosclerosis. *Shanxi Tradit. Chin. Med.* 40 (30), 307–310. doi:10.3969/j.issn.1000-7369.2019.03.010

Wu, Y., Li, X. M., Zhuo, J. F., Cai, Q., and Chen, J. K. (2017). Analysis on medicine related factors and syndrome differentiation of TCM in 192 patients with carotid atherosclerosis. *guid j tradit chin med pharm* 23 (14), 83–85. doi:10.13862/j.cnki.cn43-1446/r.2017.14.028

Wu, Y. T., Wang, L. L., Chen, X. J., et al. (2018). Clinical efficacy and safety of Yiqi Huatan Huoxue in the treatment of carotid atherosclerotic plaque. *Chin J Clin. Ration. Drug Use* 11 (2C), 73–74. doi:10.15887/j.cnki.13-1389/r.2018.06.037

Xu, S., Kamato, D., Little, P. J., Nakagawa, S., Pelisek, J., and Jin, Z. G. (2019). Targeting epigenetics and non-coding RNAs in atherosclerosis: From mechanisms to therapeutics. *Pharmacol. Ther.* 196, 15–43. doi:10.1016/j.pharmthera.2018.11.003

Yang, J., Lei, Y., Xiu, C. K., Wang, X., Hu, Y. H., Yu, B. W., et al. (2020). Research progress of traditional Chinese medicine for yiqi huoxue huatan in treatment of atherosclerosis. *Chin. J. Exp. Tradit. Med. Formulae.* 26 (22), 220–227. doi:10.13422/j.cnki.syfjx.20202222

Zhang, R. J., Ren, S. H., Shi, Y. F., Liu, J. B., Guo, Y., Wu, Y., et al. (2020). Clinical study of Jiawei Diitan Decoction in the treatment of hyperlipidemia of carotid atherosclerosis combined with phlegm and blood stasis. *Chin J Integr Med cardio/cerebrovas Dis.* 18 (11), 1752–1756. doi:10.12102/j.issn,1672-1349.2020.11.020

Zhang, B. L., Li, W. Q., Yang, L. J., and Zhao, G. (2022). Effects of self-made Yishen Yanggan Huatan Tongyu Decoction combined with rosuvastatin on carotid blood flow parameters and blood lipid levels in patients with carotid atherosclerosis. *Liaoning J. Tradit. Chin. Med.*, 14. Available at: https://kns.cnki.net/kcms/detail/21.1128.R.20220815.1612.039.html.

Zhang, B., and Ye, C. (2020). Effect of clopidogrel combined with ginkgo diterpene lactone meglumine on carotid atherosclerosis in patients with cerebral infarction. *Chin. J. Gerontol.* 40 (17), 3611–3614. doi:10.3969/j.issn.1005-9202.2020.17.009

Zhang, G. Y., and Guo, X. (2015). Effect of Yiqi Huatan Huoxue method on carotid atherosclerosis in hypertensive patients with Qi deficiency and phlegm stasis syndrome. *Chin J Integr Med cardio/cerebrovas Dis.* 13 (6), 714–717. doi:10.3969/j.issn.1672-1349.2015.06.00

Zhao, J., Zhang, J., Han, M., Liu, Z. W., and Zhen, F. P. (2012). Therapeutic effect of yiqi, huoxue, huatan and collaterals on carotid atherosclerosis. *Chin J Integr Med cardio/cerebrovas Dis.* 10 (2), 180–181.

Zheng, Q. Y. (2019). Clinical study on the treatment of senile hypertension complicated with carotid atherosclerosis by Invigorating Qi, activating blood, Huatan and dredging collaterals. *Electro J. Clin. Med.* 6 (35), 31–34. doi:10.16281/j.cnki.jocml.2019.35.020

Zhu, S. P. (2018). Yiqi huoxue huatan tongluo decoction combined with aspirin and rosuvastatin treatment of carotid atherosclerosis (qi phlegm and blood stasis network) randomized controlled study. *J. Pra Tradit. Chin. Int. Med.* 32 (3), 27–30. doi:10.13729/j.issn.1671-7813.Z20180013

Zhu, Y. H., Xian, X. M., Wang, Z. Z., Bi, Y. C., Chen, Q. G., Han, X. F., et al. (2018). Research progress on the relationship between atherosclerosis and inflammation. *Biomolecules* 8 (3), 80. doi:10.3390/biom8030080

frontiers | Frontiers in Pharmacology

TYPE Original Research
PUBLISHED 14 November 2022
DOI 10.3389/fphar.2022.956402

OPEN ACCESS

EDITED BY
Qiuwang Zhang,
St Michael's Hospital, Canada

REVIEWED BY
Samuel X. Shi,
Tulane University, United States
Bonnie Dittel,
Versiti Blood Research Institute,
United States

*CORRESPONDENCE
Dongming Wu,
547426170@qq.com
Ying Xu,
yingxu825@126.com

†These authors have contributed equally to this work

SPECIALTY SECTION
This article was submitted to Inflammation Pharmacology, a section of the journal Frontiers in Pharmacology

RECEIVED 30 May 2022
ACCEPTED 17 October 2022
PUBLISHED 14 November 2022

CITATION
Li L, Deng S, Liu M, Yang M, Li J, Liu T, Zhang T, Zhao Y, He M, Wu D and Xu Y (2022), Novel recombinant protein flagellin A N/C attenuates experimental autoimmune encephalomyelitis by suppressing the ROS/NF-κB/NLRP3 signaling pathway. *Front. Pharmacol.* 13:956402. doi: 10.3389/fphar.2022.956402

Novel recombinant protein flagellin A N/C attenuates experimental autoimmune encephalomyelitis by suppressing the ROS/NF-κB/NLRP3 signaling pathway

Li Li[1,2†], Shihua Deng[1,2†], Mingquan Liu[1,2†], Min Yang[1,2†], Jin Li[1,2], Teng Liu[1,2], Ting Zhang[1,2], Yangyang Zhao[1,2], Miao He[1,2], Dongming Wu[1,2*] and Ying Xu[1,2*]

[1]Clinical Medical College and the First Affiliated Hospital of Chengdu Medical College, Chengdu, China, [2]Sichuan Clinical Research Center for Geriatrics, The First Affiliated Hospital, Chengdu Medical College, Chengdu, China

Multiple sclerosis (MS) is a chronic inflammatory autoimmune disease characterized by demyelination and neurodegeneration, for which traditional treatment offers limited relief. Microglial/macrophage modulation plays a critical role in the pathogenesis of MS. Oxygen free radical accumulation can induce axonal and nerve cell damage, and further promote MS development. We created a new recombinant protein based on flagellin from *Legionella pneumophila* named flagellin A with linked *C*- and *N*-terminal ends (FLaAN/C), which is an independent intellectual property of our team. We previously showed that FLaAN/C might mitigate radiation-induced damage by inhibiting inflammatory responses and oxidative stress. However, whether FLaAN/C protects against MS remains unknown. Here, we investigated the anti-inflammatory effects of FLaAN/C on mice with experimental autoimmune encephalomyelitis (EAE) induced by oligodendrocyte glycoprotein peptide 35–55 (MOG35-55). The mice were injected intraperitoneally with FLaAN/C after the onset of clinical symptoms, then clinical behavior scores and changes in body weight were recorded daily. The spinal lumbar spine in model mice was enlarged and accompanied by inflammatory cell infiltration and demyelination that were reversed by FLaAN/C.

Abbreviations: ASC, anti-apoptosis-associated speck-like protein containing a CARD; CASP1, caspase-1 CAT; catalase CD, cluster of differentiation; CNS, central nervous system; COX2, cyclooxygenase 2; DHE, dihydroethidium; EAE, experimental autoimmune encephalomyelitis; GAPDH, glyceraldehyde-3-phosphate dehydrogenase; GSDMD, gasdermin D; IBA1, ionized calcium-binding adapter molecule 1; IFN, interferon; Ig, immunoglobulin; IL, interleukin; iNOS, inducible nitric oxide synthase; LDH, lactate dehydrogenase; LFB, Luxol fast blue stain; MBP, myelin basic protein; MDA, malondialdehyde; MS, multiple sclerosis; MOG, myelin oligodendrocyte glycoprotein; NLRP3, NLR family pyrin domain containing 3; NF, nuclear factor; p, phosphorylated; PBS, phosphate-buffered saline; ROS, reactive oxygen species; SOD, superoxide dismutase; Th, T helper; TNF, tumor necrosis factor; WT, wild-type.

FLaAN/C also induced microglia/macrophages to generate less pro-inflammatory (CD86, iNOS, and TNF-α), and more anti-inflammatory (CD206, IL-10, and Arginase-1) cytokines. These findings suggesting that FLaAN/C promoted microglial/macrophages polarization from the inflammatory M1 to the anti-inflammatory M2 phenotype. Moreover, FLaAN/C inhibited release of the inflammatory cytokines, TNF-α, IL-8, IL-6, IL-17, and IFN-γ. These results indicated that the anti-inflammatory effect of FLaAN/C was associated with the inhibited generation of reactive oxygen species. FLaAN/C downregulated the expression of phosphorylated NF-κB-p65 and prevented downstream NLRP3 inflammasome-mediated pyroptosis. Collectively, these results indicated that FLaAN/C prevents pyroptosis by inhibiting the ROS/NF-κB/NLRP3 signaling pathway, and promotes the microglial/macrophage M1/M2 polarization that significantly alleviated inflammation in mouse models of EAE. Our findings suggested that FLaAN/C could be a promising candidate for MS therapy.

KEYWORDS

FlaAN/C, experimental autoimmune encephalomyelitis, reactive oxygen species, ROS/NF-κB/NLRP3 pathway, pyroptosis

Introduction

Multiple sclerosis (MS) is a chronic inflammatory autoimmune disease of the central nervous system (CNS) that is characterized by multiple lesions, remission, recurrence, and other features (Yong, 2022). The main pathologies are inflammatory cell infiltration, axon loss or damage, white matter demyelination, and chronic neuroinflammation (Correale et al., 2017). Multiple sclerosis is more prevalent in younger individuals, but often continues to progress to advanced stages, leading to severe neurological deficits and loss of the ability to work (Dobson and Giovannoni, 2019). The most prevalent drugs to treat MS comprise glucocorticoids, corticosteroids, intravenous immunoglobulins, interferons, and immunosuppressants such as natalizumab and azathioprine. However, their effects are limited, and long-term use is associated with serious side effects and complications that confer an additional burden on patients (Luna et al., 2020). Therefore, innovative drugs that could delay the onset, or halt the progression of MS are essential.

The pathological mechanisms and treatment of MS have been investigated using mature mouse models of experimental autoimmune encephalomyelitis (EAE) that simulates the key features of human MS (Bolton and Smith, 2018). Lymphocytes, macrophages and dendritic cells, are involved in the pathogenesis of MS, and are thought to form lesions *via* different and interacting mechanisms (Jolivel et al., 2013; Wang et al., 2019; Schafflick et al., 2020). Among these immunocytes, infiltrating microglia/macrophages are major effectors of inflammation and demyelination in MS and EAE (Hao et al., 2021; Lyu et al., 2021). In response to various stimuli, activated microglia/macrophages undergo significant morphological and functional changes and exhibit two phenotypes, i.e., inflammatory M1 and anti-inflammatory M2 that respectively release pro- and anti-inflammatory cytokines (Lyu et al., 2021). The upregulated M1-like phenotype secretes classic inflammatory mediators, such as tumor necrosis factor-alpha (TNF-α) and interleukin-12 (IL-12), and also inducible nitric oxide synthase (iNOS) during the early stages of disease development. These pro-inflammatory factors damage the integrity of myelin and promote its destruction. The M2-like phenotype notably upregulates anti-inflammatory mediators such as arginase-1 (Arg-1), interleukin-10 (IL-10), and CD206 (Leuti et al., 2021). Considering the different role of M1and M2 phenotype of microglia/macrophages in inflammatory response, regulating the transformation of M1 phenotype to M2 phenotype might be helpful for MS. Therefore, new drugs are needed that could promote the polarization of microglia/macrophages from pro-to the anti-inflammatory phenotype and thus be an effective strategy for treating EAE. Activated microglia and infiltrated macrophages are particularly enriched around white matter lesions in the central nervous system. These macrophages can produce a large amount of reactive oxygen (ROS) and nitrogen (RNS) species that damage the numerous axons and oligodendrocytes associated with the clinical course of MS (Pegoretti et al., 2020; Yin et al., 2022). Activated microglia/macrophages can activate the complement pathway, produce pro-inflammatory cytokines, release excitatory amino acids, and produce free radicals (Zhang J. et al., 2022).

Excessive ROS production exerts deleterious effects on lipids, proteins, and nucleic acids, leading to impaired cell function (Chen Y. et al., 2022). Under physiological conditions, ROS/RNS are cleared by antioxidant defense enzymes such as superoxide dismutase (SOD), catalase (CAT) and peroxidase and non-enzymatic compounds. Under pathological conditions, levels of ROS/RNS are elevated during inflammatory processes.

These cause mitochondrial respiratory chain dysfunction and overstimulated glutamate NMDA receptors, which lead to low activities of oxidative scavengers such as cytosolic SOD and CAT, and significantly increased levels of lipid peroxide products, such as malondialdehyde (MDA) and 4-hydroxynonenal (4HNE) (Chen X. et al., 2022; Xue et al., 2022). Lipid peroxidation might be the main factor in free radical-mediated central nervous system damage. When excessive ROS cannot be neutralized by the antioxidant defense system, ROS metabolites can lead to protein and lipid peroxidation and DNA alkylation, which are also closely related to the occurrence of MS (Devanney et al., 2020)

The nuclear factor kappa B (NF-κB) is a family of transcription factors that regulate the expression many genes involved in cell death, inflammation, proliferation, and differentiation (Wang et al., 2022). Activation of NF-κB correlates with immune-associated genes that are upregulated in the serum, brain, and spinal cord of patients who have MS compared with healthy individuals (Soltanmoradi et al., 2021). Moreover, increased levels of NF-κB are associated with the course of MS (Jie et al., 2021). After organismal injury, excessive ROS accumulation results in binding to pattern recognition receptors, which might act as initiating signals to regulate NF-κB translocation to the nucleus and activate the NOD-like receptor family pyrin domain containing 3 (NLRP3) inflammasome, thus inducing IL-1β and IL-18 secretion, and inflammation (Peng et al., 2020). The NLRP3 inflammasomes are large protein complexes consisting of NLRP3, ASC, and caspase-1 (He et al., 2022). It is the most extensively studied type of inflammasome in the CNS and has been assessed in microglia (Chu et al., 2019). Moreover, NLRP3-associated pyroptosis protein is expressed in astrocytes, microglia, and neurons in EAE models (Hou et al., 2020; Zhang Q. et al., 2022; Song et al., 2022). Studies have shown that the activation NLRP3 inflammasomes induces the production of inflammatory cytokines and thus promotes the migration of immunocyte to the CNS in the EAE model of MS (Braga et al., 2019; Zhang Q. et al., 2022). These findings suggested that NLRP3 inflammasomes are associated with MS progress. Therefore, blocking the NLRP3 signaling pathway and pyroptosis can reduce neuroinflammation and thus alleviate disease progression.

We developed a novel recombinant globular protein flagellin A from *Legionella pneumophila* flagella (FLaAN/C). This biological agent is now an independent intellectual property owned by our team. It was designed by linking the C- and N-terminal ends of the flagellin to facilitate the reduction of flagellin's side effects. In our previous studies, FLaAN/C regulates cell functions important for radiation protection by regulating the expression of multiple cytokines, and regulates the inflammatory response by inhibiting NF-κB signaling pathway. For example, FLaAN/C inhibits caspase-1-dependent pyroptosis by reducing NLRP3 inflammasome activity, and thus effectively mitigate radiation-induced intestinal injury (Wu et al., 2018). It significantly reduces radiation-induced pathology and improves the survival of mice after whole-body irradiation compared with controls. In addition, FLaAN/C upregulates miR-142a-3p, inhibits IRAK1/NF-κB signaling pathway in intestinal cells, thereby alleviating radiation-induced pyroptosis (Liu et al., 2022). Therefore, FLaAN/C inhibits inflammatory responses and oxidative stress. However, the role of FLaAN/C in the regulation of inflammasome-associated neuroimmunity remained unknown.

We aimed to determine the anti-demyelinating and anti-neuroinflammatory effects of FLaAN/C and its effects in an EAE mouse model. We also investigated the effects of FLaAN/C on microglial/macrophage polarization and NF-κB/NLRP3 signaling pathway. Our findings provided evidence for FLaAN/C as a new candidate therapeutic for MS.

Materials and methods

Establishment of the EAE model

The Animal Policy and Welfare Committee of Chengdu Medical College approved all animal experiments (Approval ID: 2,021,711). Seven-week-old female C57/BL6 mice (weight, 18–21 g) (GemPharmatech Co., Ltd., Chengdu, China) and *Nlrp3*$^{-/-}$ mice on a C57BL/6 (Weishanglide Biotechnology Co., Ltd., Beijing, China) were raised at the Animal Experimental Center of Chengdu Medical College. We established the EAE model as described (Yu et al., 2020). Briefly, 100 μl of Complete Freund's Adjuvant (CFA; Chondrex, Woodinville, WA, United States) was ultrasonically emulsified with 400 μg of Mycobacterium tuberculosis H37Ra (BD Biosciences, San Jose, CA, United States). Thereafter, 200 μg of myelin oligodendrocyte glycoprotein 35–55 (MOG35-55) peptide (Hooke Laboratories, Lawrence, MA, United States) mixed with 100 μl of PBS and the emulsion, was subcutaneously injected into the mice (immunization day 1). On that day and on post-immunization day 3, 300 ng of pertussis toxin (PTX; List Biological Laboratories Inc., Campbell, CA, United States) was injected i.p. (Figure 1A).

FLaAN/C treatment

The preparation of the FLaAN/C recombinant protein was carried out by BGI Genomics (Shenzhen, China). Detailed preparation process for the FLaAN/C recombinant protein is provided in the supplementary material.The mice were randomly assigned to receive phosphate buffered saline (PBS; control n = 6), MOG + PBS (n = 6), or MOG + FLaAN/C (0.5, 1.0 and 1.5 mg/kg injected intraperitoneally

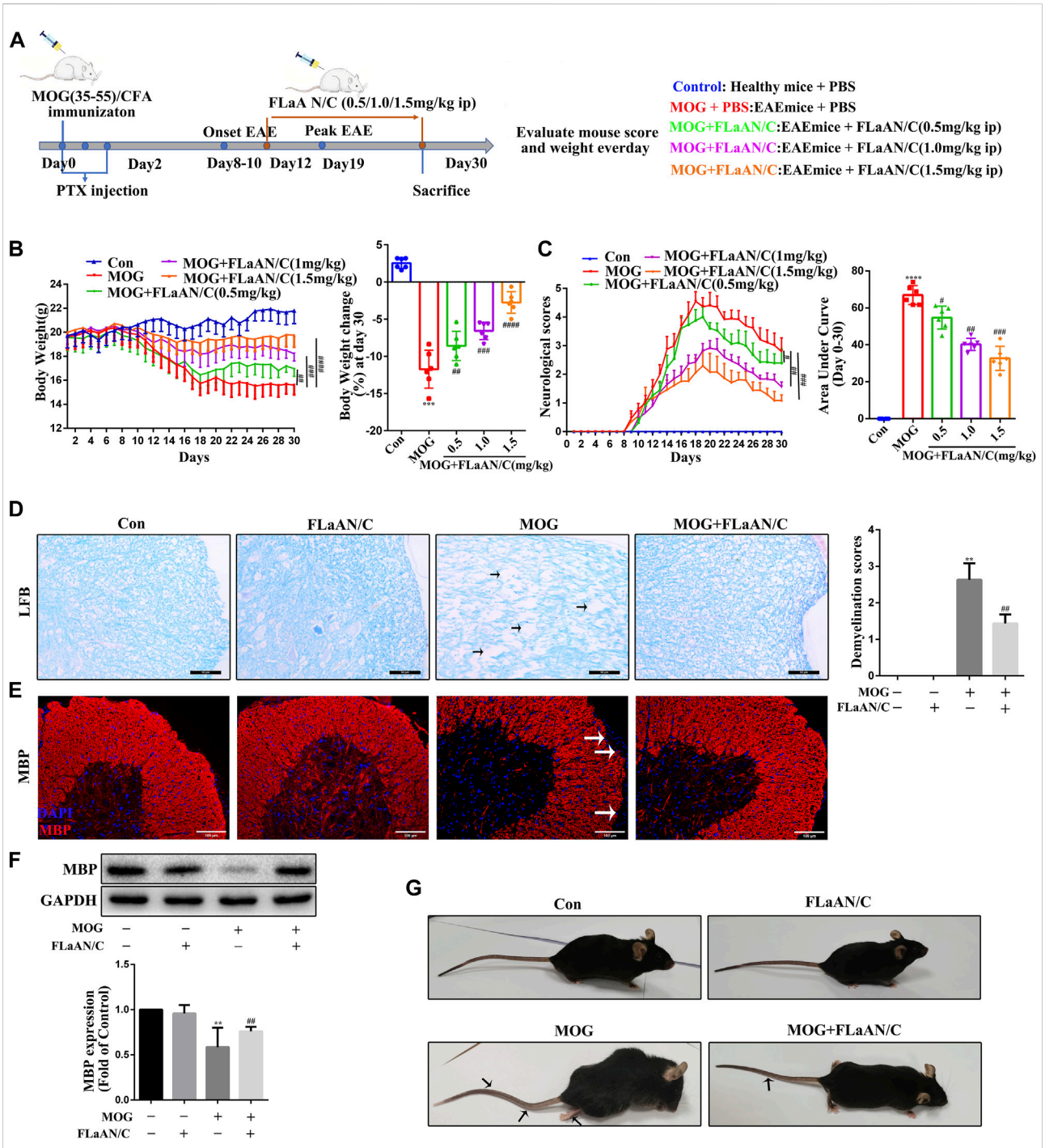

FIGURE 1
FLaAN/C reduces symptoms in EAE mice. **(A)** Study procedure. **(B)** Weight-versus-time curves of all experimental groups. **(C)** Clinical behavior scores for typical symptoms of EAE. **(D)** LFB staining showing demyelination in the spinal cord and the demyelination scores (The arrows present myelin injury and loss, scale bars:50 μm). **(E)** Immunofluorescence staining of MBP in the spinal cord (The arrows present myelin injury and loss, scale bars:100 μm). **(F)**Western bloting of MBP protein expression of the spinal cord. **(G)** Representative images show behavioral symptoms of EAE mice in each group (Black arrows present limp tail or hind limb paralysis). Paraffin sections of spinal cord tissue used for immunofluorescence staining. Data are shown as means ± SD (n = 6 per group). *$p < 0.05$, **$p < 0.01$, ***$p < 0.001$, ****$p < 0.0001$, $^{\#}p < 0.05$, $^{\#\#}p < 0.01$, $^{\#\#\#}p < 0.001$, $^{\#\#\#\#}p < 0.0001$. * vs. Control group; $^{\#}$ vs. MOG group.

(i.p.) daily from post-immunization day (p.i.d) 12 until p.i.d. 30; n = 6 each). On p.i.d. 30, all mice from each group were euthanized and spinal cord and blood were collected. The FLaAN/C treatment concentration was based on our pre-experiment: high-dose (10 mg/kg) single administration and low-dose (0.25 mg/kg) multiple administration. The pre-experiment results showed that the high dose (10 mg/kg) single administration exceeded the tolerance range of mice, and the mice died. Low-dose multiple administrations (0.25 mg/kg) had no significant therapeutic effect on EAE mice. In addition, clinical dosing regimens usually choose low-dose multiple administration. In this study, to better simulate clinical medication, we first determined the concentration gradient of FLaAN/C (0.5, 1.0, 1.5 mg/kg), and then screened the optimal treatment concentration of FLaAN/C (1.5 mg/kg). Therefore, we finally chose FLaAN/C (1.5 mg/kg) for subsequent experiments.

Body weight and behavioral assessment

We weighed the mice daily and scored their clinical behavior from 0-5 according to the respective criteria for EAE: 0, no clinical symptoms; 1, the tail tension disappeared or the gait was awkward; 2, weakness in hind limbs; 3, paralysis of hind limbs; 4, paralysis of hind limbs and weakness in anterior limbs; 5, near-death state (Yu et al., 2020; Zilkha-Falb et al., 2020; Kim et al., 2021; Cai et al., 2022).

Measurement of anti-oxidant activity

We measured SOD (S0101S), MDA (S0131S), and CAT (S0051) activities in mouse serum using the respective kits (Beyotime Biotechnology, Shanghai, China) as described by the manufacturer.

Cytokine quantitation

Serum levels of the inflammatory cytokines TNF-α, IL-10, IL-8, IL-17, IFN-γ, IL-6, IL-1β, and IL-18 in mice were determined using enzyme-linked immunoassay (ELISA) kits (MIBIO Biotechnology, shanghai, China) as described by the manufacturer.

Assays of caspase-1 activity

We evaluated caspase-1 activity in mouse spinal cord tissue using caspase-1 activity assay kit (C1102; Beyotime Biotechnology).

Western bloting

Proteins were extracted from crushed spinal cord tissue by whole-cell lysis or using a nucleocytoplasmic protein extraction kit (KeyGEN BioTECH, Nanjing, China), and then centrifuged at 4°C (13,000 × *g*) for 15 min. Protein concentrations were determined in supernatants using BCA protein assay kits (Beyotime Biotechnology). The proteins (40 μg) were resolved by sodium dodecyl sulfate-polyacrylamide gel electrophoresis (SDS-PAGE), then transferred to PVDF membranes. Nonspecific antigen binding on the membranes was blocked by incubation 1 h at room temperature with 5% skimmed milk. Thereafter, the membranes were incubated overnight at 4°C with the following primary antibodies diluted 1:1000: GAPDH (10494-1-AP), TNF-α (17590-1-AP), CD86 (13395-1-AP), CD206 (18704-1-AP), Arginase-1 (16001-1-AP), IL-10 (D13A11), MBP (10458-1-AP), iNOS (22226-1-AP), nuclear factor of kappa light polypeptide gene enhancer in B-cells inhibitor, alpha IκBα (10268-1-AP), ASC 67494-1-Ig), IL-18 (10663-1-AP), lamin B1 (12987-1-AP), and NF-κB-p65 (10745-1-AP) all from Proteintech Group Inc., Rosemont, IL, United States), NLRP3 (ab270449), caspase-1 p20 (ab179515), IL-1β (ab216995), gasdermin D -N (GSDMD-N; ab219800), phosphorylated p-IκBα (ab133462), and NF-κB-p-p65 (ab194726) (all from Abcam, Cambridge, UK). The membranes were incubated in 1:8000-diluted horseradish peroxidase-conjugated secondary antibodies (SA00001-2; Proteintech) at 37°C for 1.5 h. Bands were visualized using a chemiluminescence horseradish peroxidase substrate (Merck Millipore, Burlington, MA, United States) and quantified using Quantity 5.2 (Bio-Rad Laboratories Inc., Hercules, CA, United States). Relative immunoreactivity was calculated according to gray values and normalized to that of the reference protein (GAPDH) using ImageJ (National Institutes of Health [NIH], Bethesda, MD, United States).

Staining with hematoxylin and eosin (HE) and luxol fast blue (LFB)

We detected inflammatory cell infiltration of spinal cord tissue by staining with HE. Formalin-fixed, paraffin-embedded samples were stained with LFB using a kit (Solebo Biotech, Beijing, China). Six mice in each group were scored for inflammation and demyelination according to the following criteria. For inflammation: 0 = non-inflammatory cells; 1 = a small amount of scattered inflammatory cells; 2 = organization of inflammatory infiltrates around blood vessels; 3 = extensive perivascular cuffing with extension into parenchyma. For demyelination: 0 = none; 1 = rare foci; 2 = several

TABLE 1 Primer sequence information.

Gene	Forward primer (5′F0223′)	Reverse primer (5′F0223′)
Casp1	CATCCTGTCAGGGGCTCACTTTTC	CTATCAGCAGTGGGCATCTGTAGC
Gsdmd	CGATGGGAACATTCAGGGCAGAG	ACACATTCATGGAGGCACTGGAAC
Il1β	CAAGAGCTTCAGGCAGGCAGTATC	AGGTCCACGGGAAAGACACAGG
Il18	GGCTGCCATGTCAGAAGACTCTTG	AGTGAAGTCGGCCAAAGTTGTCTG
Il10	CACTGCTATGCTGCCTGCTCTTAC	TGGGAAGTGGGTGCAGTTATTGTC
Il8	CATGGGTGAAGGCTACTGTTGGC	GCTTCATTGCCGGTGGAAATTCC
Tnfα	TCTACTGAACTTCGGGGTGATCGG	GTGGTTTGTGAGTGTGAGGGTCTG
Ifnγ	AGGAACTGGCAAAAGGATGGTGAC	GTTGTTGCTGATGGCCTGATTGTC
Il17	GCCAAGGACTTCCTCCAGAATGTG	TGGAACGGTTGAGGTAGTCTGAGG
Il6	CTTGGGACTGATGCTGGTGACAAC	AGGTCTGTTGGGAGTGGTATCCTC

demyelination areas; 3 = large areas of demyelination (Yu et al., 2020; Kim et al., 2021; Cai et al., 2022).

Immunofluorescence staining

Paraffin blocks of spinal cord and brain tissue were cut into 5-μm thick sections, dewaxed with a graded ethanol series, and sealed with 5% fetal bovine serum for 30 min. The sections were incubated overnight at 4°C with the following primary antibodies (1:300): MBP (10458-1-AP), CD11b (ab1211), 4HNE (ab48506), 3NT (5411, Millipore), NLRP3 (ab270449), ASC (67494-1-Ig), and NF-κB (10745-1-AP). The sections were washed with PBS, then incubated with anti-Cy3 goat anti-rabbit IgG (H + L, A0516) or FITC goat anti-mouse IgG (H + L, A0568; Beyotime Biotechnology) secondary antibodies (1:200) at room temperature for 2 h. Then, the nuclei were stained with DAPI (1:10,000) for 8 min. Random images were photographed with a fluorescence microscope at ×40 magnification.

Nuclear and cytoplasmic protein extraction

Nuclear and cytoplasmic proteins were extracted using a kit (P0027; Beyotime Biotechnology), then analyzed by western blotting.

Co-immunoprecipitation

Lysed spinal cord tissue were shaken slowly with primary antibody overnight at 4°C, then complexes were immunoprecipitated using protein A + G agarose (P2055-10 ml; Beyotime Biotechnology) as described by the manufacturer.

Quantitation of oxidative stress

Levels of ROS were detected by staining spinal cord and brain tissue with dihydroethidium (DHE) (S0063, Molecular Probe; Solarbio, Beijing, China). Paraffin slices were dewaxed and dehydrated in a graded ethanol series and washed with PBS (pH 7.4). Nonspecific antigen binding was blocked with 5% fetal bovine serum for 40 min, then stained with 5 mmol/L DHE in PBS for 30 min. Random images of brain or spinal cord sections were acquired using an XI 71 fluorescence microscope (Olympus, Tokyo, Japan) at ×20 magnification. The intensity of emitted fluorescence was analyzed using Image.

Reverse transcription-quantitative polymerase chain reaction (RT-qPCR)

Total RNA extracted from mouse spinal cord tissue using a kit (Solarbio) was reverse transcribed into cDNA using iScript cDNA synthesis kit (BioRad Laboratories Inc., Hercules, CA, United States). The mRNA levels of *Il-8, TNF-α, Il-6, Il-10, Il-1β, Il-18, Il-17, IFN-γ, caspase-1,* and *GSDMD* were determined by qPCR using SYBR Green SuperMix (Bio-Rad Laboratories Inc). Expression relative to that of the internal reference β-actin (*Actb*) was calculated using the $2^{-\Delta\Delta CT}$ method. Table 1 shows the synthesized primers (Shenggong, Shanghai, China) and the sequences are shown in Table 1.

Statistical analysis

All experiments were repeated independently three times. All data were statistically analyzed using Prism7.0 (GraphPad Software Inc., San Diego, CA, United States). Pairs of groups were compared using two-tailed Student t-tests, and three or more groups were compared using a one-way ANOVA. Data are expressed as means ± SD, and values with $p < 0.05$ were considered statistically significant.

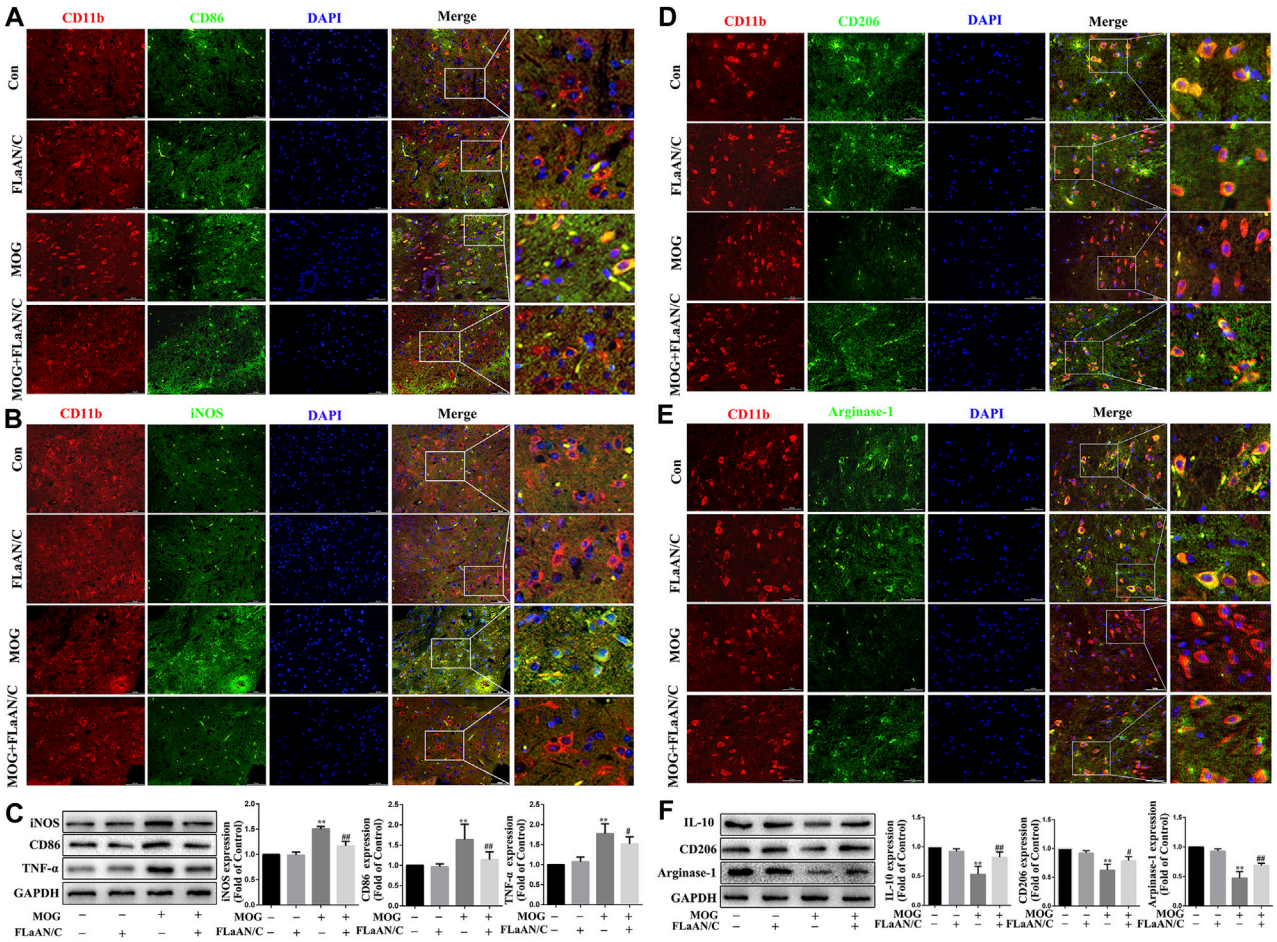

FIGURE 2
FLaAN/C shifted M1 to M2 phenotype in spinal cord of mice with EAE. The mice were euthanized on post-immunization day 30. The spinal cord tissue of each group of mice were isolated and embedded in paraffin.Immunofluorescence was used to detect the colocalization of CD11b with M1 markers (iNOS and CD86) and M2 markers (Arginase-1 and CD206) in spinal cord tissue.The representative images show the expression levels of $CD86^+$ **(A)**, $iNOS^+$ **(B)**, CD206+**(D)** and Arginase-1^+ **(E)** in $CD11b^+$ cells (scale bars: 50 μm). **(C)** The protein expression levels of iNOS, CD86 and TNF-α in the spinal cord of each group was detected by western bloting. **(F)** The protein expression levels of Arginase-1, CD206 and IL-10 in the spinal cord of each group were detected by western bloting. Data are shown as means ± SD (n = 6 per group). $^*p < 0.05$, $^{**}p < 0.01$, $^{***}p < 0.001$; $^{\#}p < 0.05$, $^{\#\#}p < 0.01$, $^{\#\#\#}p < 0.001$. * vs. Control group; # vs. MOG group.

Results

FLaAN/C delayed EAE peak and relieved symptoms

To assess the therapeutic effects of FLaAN/C on EAE severity, mice were injected daily with PBS or with FLaAN/C at doses of 0.5,1.0, or 1.5 mg/kg/day/i.p, from day 12 post first immunization until the end of the study at day 30 (Figure 1A). Daily weight changes and clinical behavioral scores were recorded. More body weight was lost by the MOG-treated, than control mice, but FLaAN/C dose-dependently improved this. The results showed that FLaAN/C treatment significantly delayed the detrimental effects of EAE on body weight (Figure 1B). Furthermore, clinical scores were assessed as the area under the curve (AUC). The clinical scores were higher in the MOG-treated mice than the control mice and FLaAN/C (0.5, 1.0, and 1.5 mg/kg/day) significantly reduced clinical score in a dose-dependent manner (Figure 1C). These data indicated that the best concentration for FLaAN/C was 1.5 mg/kg and we selected this concentration in subsequent experiments. Spinal cord demyelination was more severe in mice with MOG, than that in mice given PBS (Figure 1D), and FLaAN/C (1.5 mg/kg) treatment significantly attenuated this phenomenon. Similarly, IF staining and western bloting showed that FLaAN/C significantly increased MBP expression in MOG mice (Figure 1 E and F). At the same time, we also found that MOG mice showed severe clinical symptoms with loose tails

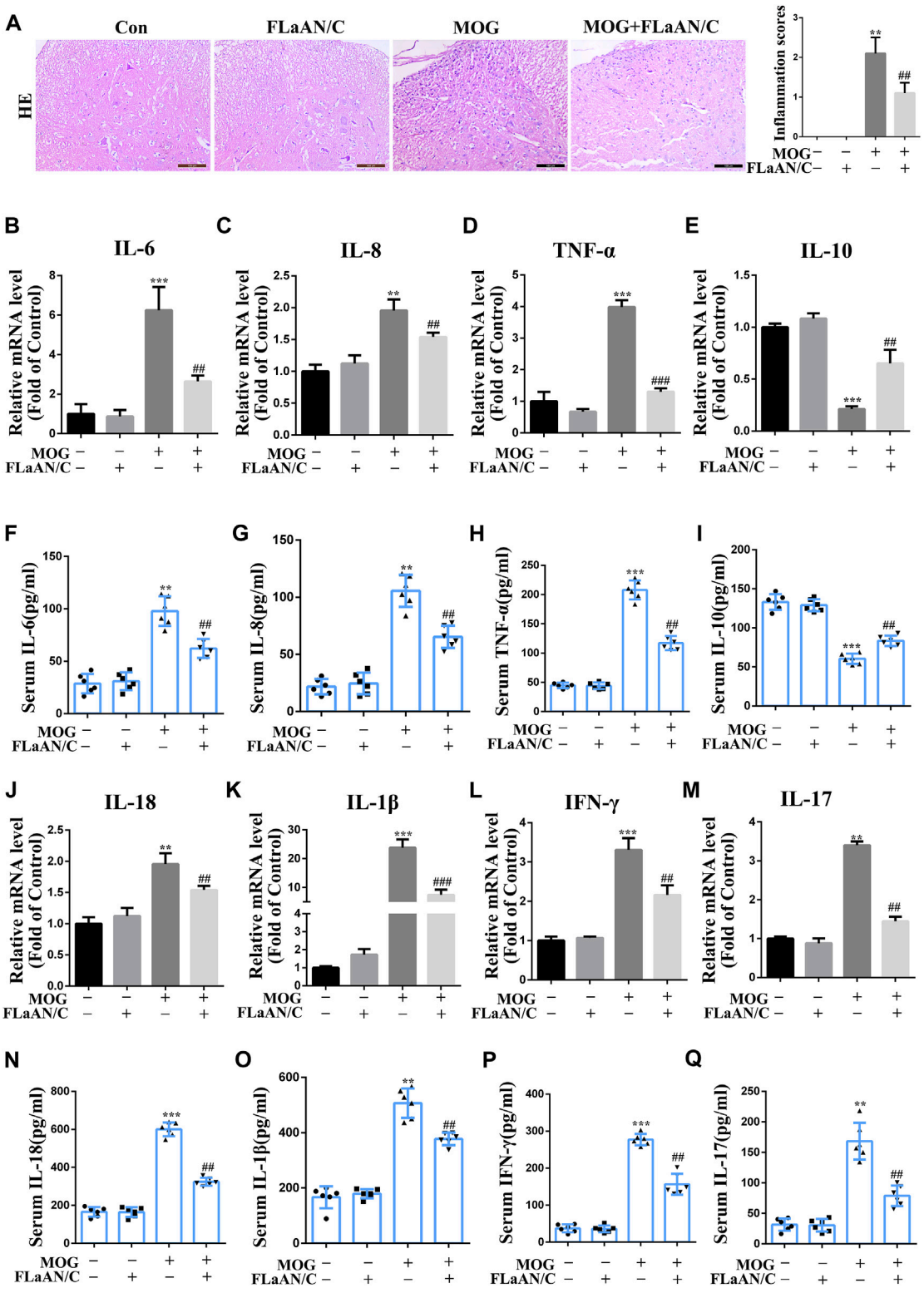

FIGURE 3
Effects of FLaAN/C on inflammation in mice with EAE. **(A)** H&E staining was performed on paraffin-embedded mouse spinal cord sections (scale bars: 100 μm). **(B–E)** The mRNA expression of IL-6 **(B)**, IL-8 **(C)**, TNF-α **(D)**, and IL-10 **(E)** were quantitated by qRT-PCR. **(F–I)** Serum levels of IL-6 **(F)**, IL-8 **(G)**, TNF-α **(H)**, IL-10 **(I)** were measured by ELISA. (J–M) The mRNA expression of IL-18 **(J)**, IL-1β **(K)**, IFN-γ **(L)**, and IL-17 **(M)** were quantitated by qRT-PCR. **(N–Q)** Serum levels of IL-18 **(N)**, IL-1β **(O)**, IFN-γ **(P)**, and IL-17 **(Q)** were measured by ELISA. Data are shown as means ± SD (n = 6 per group). $^{*}p < 0.05$, $^{**}p < 0.01$, $^{***}p < 0.001$; $^{\#}p < 0.05$, $^{\#\#}p < 0.01$, $^{\#\#\#}p < 0.001$. * vs. Control group; # vs. MOG group.

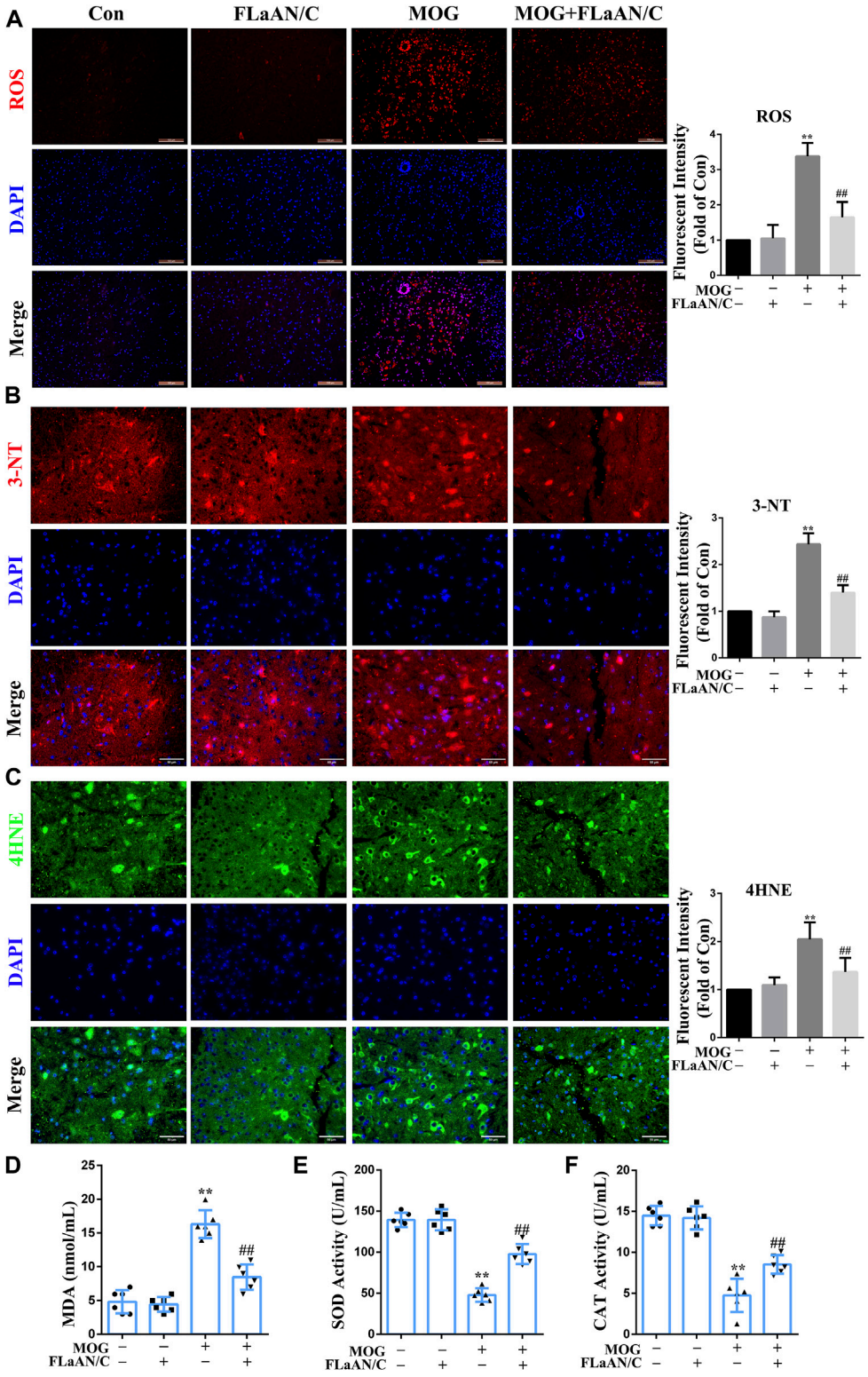

FIGURE 4
FLaAN/C alleviated MOG-induced oxidative stress in the spinal cord of EAE mice. **(A)** Abundance of reactive oxygen species (ROS) in spinal cord detected by DHE staining (scale bars: 100 μm). **(B–C)** Representative immunofluorescent images of 3-NT **(B)** and 4HNE **(C)** in the spinal cord of all experimental mice (scale bars:50 μm). **(D–F)** The activity levels of MDA **(D)**, SOD **(E)** and CAT **(F)** in the serum of each group of mice. Paraffin sections of spinal cord tissue used for immunofluorescence staining. Data are shown as means ± SD (n = 6 per group). $^{*}p < 0.05$, $^{**}p < 0.01$, $^{***}p < 0.001$; $^{\#}p < 0.05$, $^{\#\#}p < 0.01$, $^{\#\#\#}p < 0.001$. * vs. Control group; # vs. MOG group.

and completely paralyzed hind limbs, while EAE mice treated with FLaAN/C showed only weak and drooping tails (Figure 1G). These results indicated that FLaAN/C prevented myelin loss associated with EAE progression.

FLaAN/C shifted the M1 to the M2 phenotype in spinal cord of mice with EAE

The polarization of microglia/macrophages play key roles in the response to inflammation. To evaluate the effect of FLaAN/C on the polarization of microglia/macrophages in spinal cord of mice with EAE, we used immunofluorescence to detect the colocalization of CD11b with M1 markers (iNOS and CD86) and M2 markers (Arginase-1 and CD206) in spinal cord tissue to analyze the microglia/macrophages phenotype. The results showed that the coexpression of CD86 and CD11b was dramatically lower in FLaAN/C-treated mice with EAE than in the PBS-treated EAE mice (Figure 2A), and FLaAN/C treatment markedly decreased the foci of $iNOS^+CD11b^+$ in the EAE mouse spinal cord compared to those of PBS-treated mice with EAE (Figure 2B). Consistent with the immunofluorescence staining results, the western bloting datas showed that the protein levels of M1 phenotypic markers (iNOS, TNF-α, and CD86) were significantly increased in the MOG group compared with the control group, whereas the protein expression levels of iNOS, TNF-α, and CD86 were significantly decreased in the MOG + FLaAN/C group (Figure 2C). In addition, the foci of $CD206^+CD11b^+$ and $Arginase\text{-}1^+CD11b^+$ were significantly increased in spinal cord of FLaAN/C-treated MOG mice compared with the MOG mice treated with PBS (Figures 2D,E). Besides, protein levels of the M2 phenotype markers (IL-10, Arginase-1, and CD206) were substantially increased in the FLaAN/C-treated MOG mice compared with PBS-treated MOG mice (Figure 2F). These results indicated that the anti-inflammatory effect of FLaAN/C in the spinal cord may be related to its regulation of microglia/macrophage phenotype.

FLaAN/C suppressed immune cell infiltration and proinflammatory cytokine production in spinal cord of EAE mice

Considering the important role of inflammatory cytokines in the development of EAE, we evaluated the anti-inflammatory effect of FLaAN/C. Our results showed that MOG significantly increased the number of inflammatory cells and inflammation scores in the spinal cord, however, FLaAN/C noticeably reduced both of these effects (Figure 1A). We also evaluated the levels of several cytokines by qRT-PCR in the spinal cord and found that the mRNA levels of pro-inflammatory cytokines IL-6, IL-8 and TNF-α were markedly increased in the spinal cord of MOG mice, while that of the anti-inflammatory cytokine IL-10 was decreased. Meanwhile, FLaAN/C reduced the mRNA levels of IL-6, IL-8 and TNF-α, and increased that of IL-10 (Figures 3B–E). In addition, we quantified the IL-6, IL-8, TNF-α and IL-10 levels in serum by ELISA assay and found that IL-6, IL-8 and TNF-α levels in serum were increased in MOG mice, and FLaAN/C reduced their upregulation. However, the expression level of IL-10 showed the opposite trend (Figures 3F–I). Furthermore, we quantified the IL-18, IL-1β, IFN-γ and IL-17 levels by qRT-PCR and ELISA assay, and found that MOG significantly upregulated the levels of IL-18, IL-1β, IFN-γ and IL-17, while FLaAN/C remarkably reduced the expression of them (Figure 3J-Q). These results convincingly demonstrated the anti-inflammatory effect of FLaAN/C.

FLaAN/C significantly inhibited oxidative stress in EAE mice

To clarify whether FLaAN/C exerts its anti-inflammatory effect through an antioxidant effect, we used DHE staining to evaluate the levels of ROS in the spinal cord. The results showed that ROS levels were significantly increased in MOG mice compared with the mice in control group, while FLaAN/C effectively inhibited ROS production (Figure 4A). Expression levels of superoxide dismutase (SOD) and catalase (CAT) antioxidant enzyme system mainly reflect the ability to physiologically remove oxygen free radicals. In addition, 3-nitrotyrosine(3-NT), 4-hydroxynonenal (4HNE), and malondialdehyde (MDA) are metabolites of oxidative stress and their expression levels mainly reflect the state of oxidative stress. In this study, we found that the levels of 3-NT, 4HNE, and MDA in MOG mice were reduced by FLaAN/C treatment (Figures 4B–D). Additionally, FLaAN/C can effectively increase the expression of SOD and CAT in MOG mice (Figures 4E,F).

FLaAN/C inhibited NF-κB activation and prevented IκBα degradation and phosphorylation in EAE mice

The transcription factor NF-κB is associated with the development of several neuroinflammatory diseases and its activation is the initiation signal for NLRP3 inflammasome (Cai et al., 2022). Thus, we detected the expression levels of NF-κB-related proteins in spinal cord tissue. Western bloting showed that the expression of p-IκBα, p-NF-κB, and NF-κB were significantly upregulated in the spinal cord of MOG mice, while IκBα expression was downregulated. Furthermore, FLaAN/C reversed these effects. Similarly, in the FLaAN/C-treated MOG group, the expression level of IκBα was significantly improved, while the expression of p-IκBα was significantly reduced (Figure 5A). Immunofluorescence staining revealed that the number of cells with activated p65 also increased in the MOG group. However,

10.3389/fphar.2022.956402

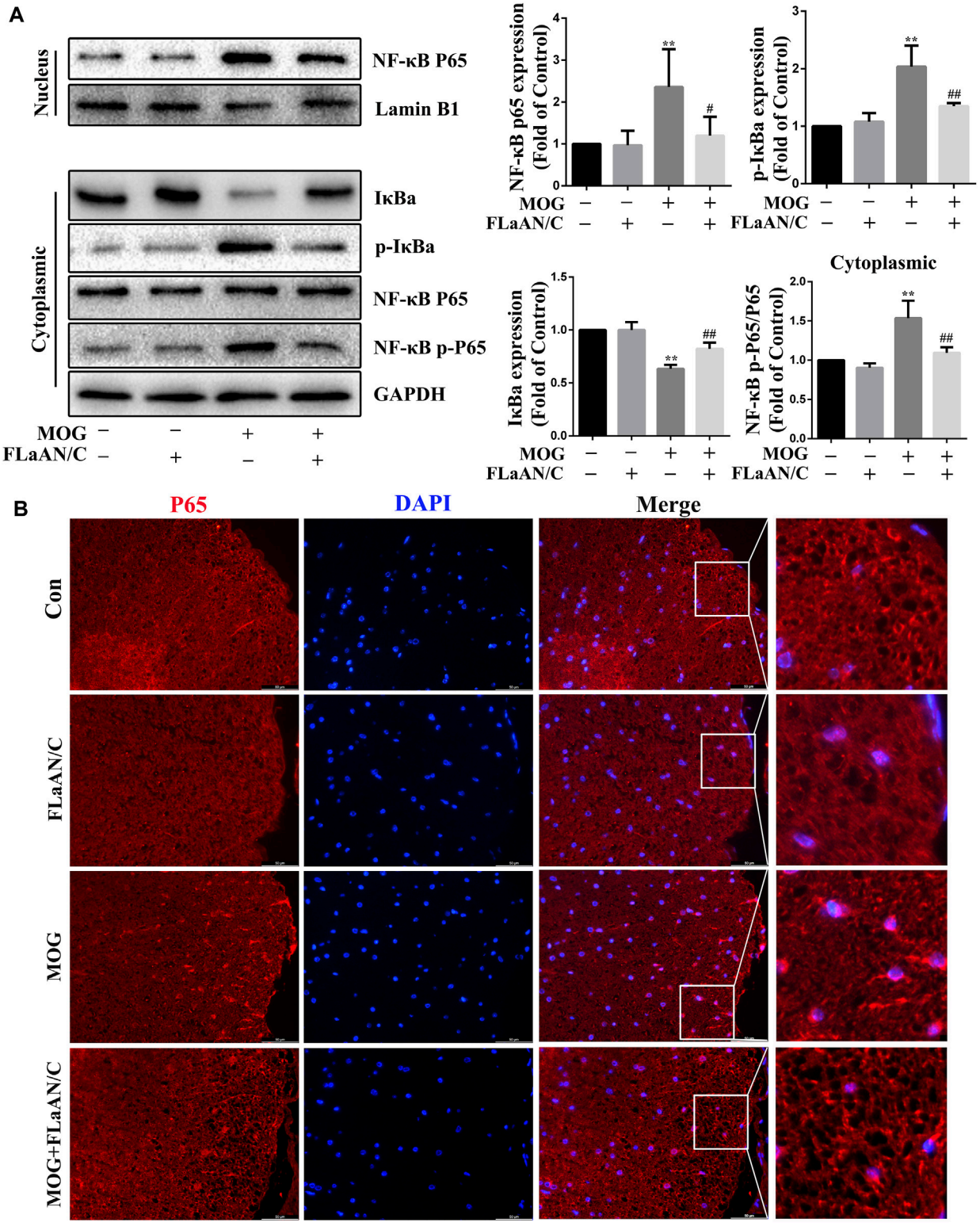

FIGURE 5
FLaAN/C inhibited NF-κB activation in mice with EAE. **(A)** Proteins levels of p-IκBα, IκBα, NF-κB-p65, and NF-κB-p-p65 in mouse spinal cord. **(B)** Representative immunofluorescence images of p65 in paraffin section of spinal cord tissue (scale bars:50 μm). Data are shown as means ± SD (n = 6 per group). *$p < 0.05$, **$p < 0.01$, ***$p < 0.001$; $^{\#}p < 0.05$, $^{\#\#}p < 0.01$, $^{\#\#\#}p < 0.001$. * vs. Control group; $^{\#}$ vs. MOG group.

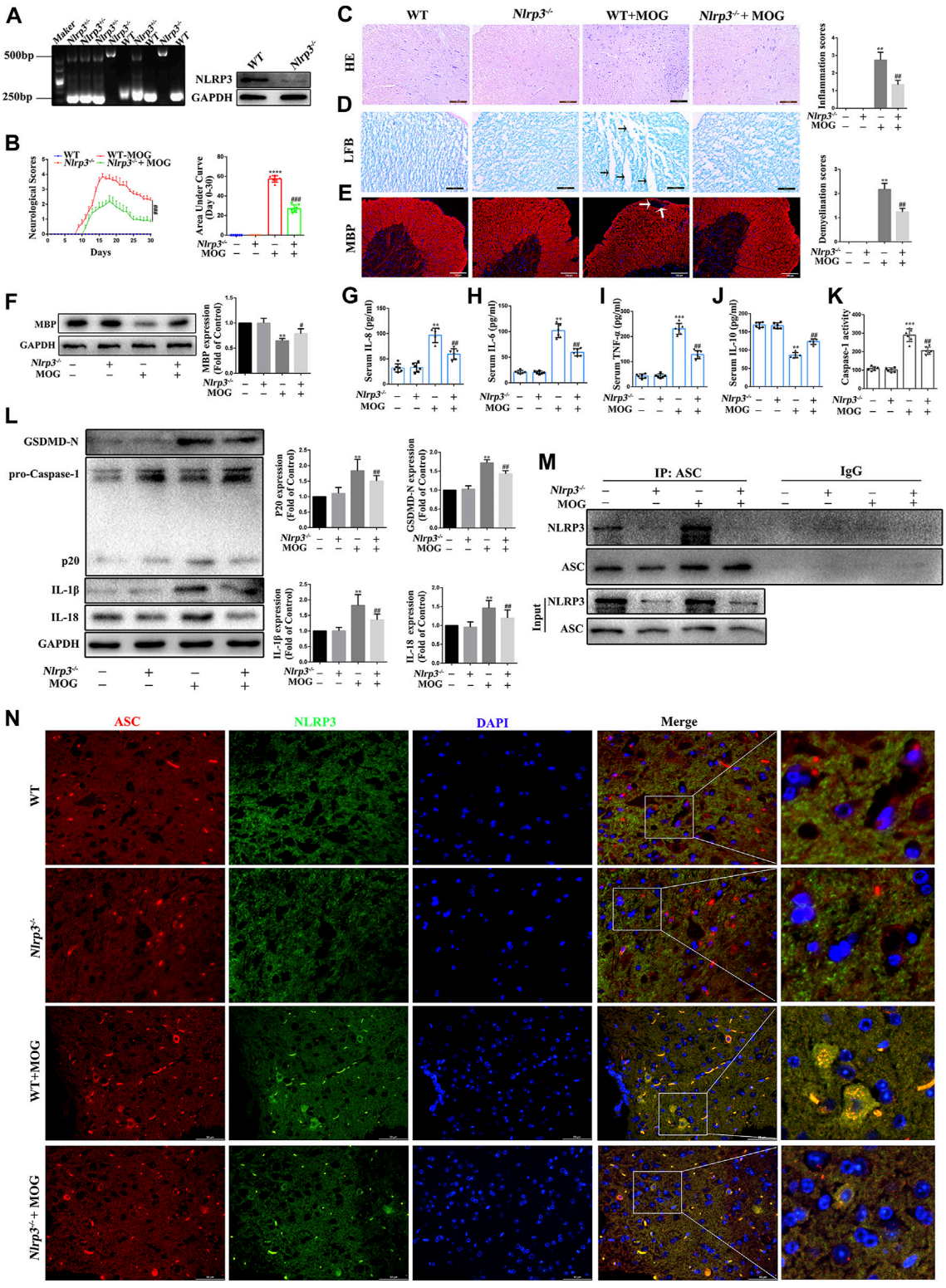

FIGURE 6
NLRP3 inflammasome mediated pyroptosis plays an important role in the pathogenesis of EAE **(A)** Identification of *Nlrp3* knockout (KO) mice. **(B)** Clinical behavioral scores and the area under the curve (AUC). **(C)** H&E staining was performed on paraffin-embedded mouse spinal cord sections (scale bars: 100 μm). **(D)** LFB staining was performed on paraffin-embedded mouse spinal cord sections (The arrows present myelin injury and loss, scale bars:50 μm). **(E)** Immunofluorescence staining of MBP in the spinal cord (The arrows present myelin injury and loss, scale bars:100 μm). **(F)**
(*Continued*)

FIGURE 6 (Continued)
Evaluation of MBP protein expression in spinal cord by western blotting. **(G–J)** Serum inflammatory factor levels of IL-8 **(G)**, IL-6 **(H)**, TNF-α **(I)**, and IL-10 **(J)** are detected using ELISA. **(K)** Caspase-1 activity in mouse spinal cord was detected using the kit. **(L)** The protein levels of pyroptosis markers assessed using western blotting in spinal cord tissue. **(M)** Detection of NLRP3 and ASC complex formation in spinal cord by co-immunoprecipitation. **(N)** Representative image of co-localized NLRP3 and ASC with immunofluorescence staining in spinal cord tissue (scale bars: 50 μm). Paraffin sections of spinal cord tissue used for immunofluorescence staining. Data are shown as means ± SD (n = 6 per group). "-" for "Nlrp3$^{-/-}$" represents wild type mice and "+" for "Nlrp3$^{-/-}$" represents Nlrp3 knockout mice. *$p < 0.05$, **$p < 0.01$, ***$p < 0.001$; $^{\#}p < 0.05$, $^{\#\#}p < 0.01$, $^{\#\#\#}p < 0.001$.* vs. WT group; $^{\#}$ vs. WT + MOG group.

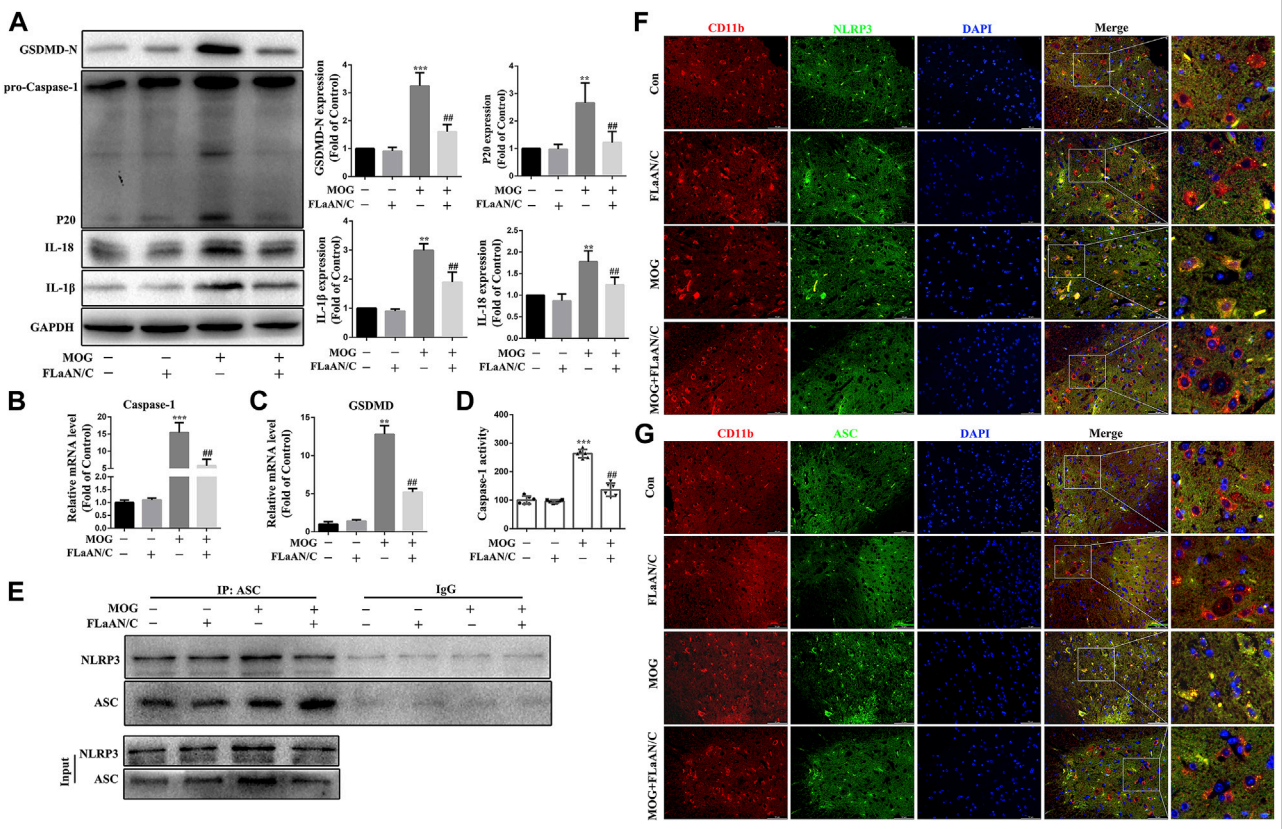

FIGURE 7
FLaAN/C attenuated NLRP3-mediated pyroptosis in EAE mice. **(A)** Abundance of caspase-1 p20, GSDMD-N, and IL-18 and IL-1β proteins in mouse spinal cord. **(B–C)** The mRNA expression of Caspase-1 **(B)** and GSDMD **(C)** were quantitated by qRT-PCR. **(D)** Caspase-1 activity in mouse spinal cord was detected using the kit. **(E)** Detection of NLRP3 and ASC complex formation in spinal cord by co-immunoprecipitation. **(F–G)** Representative images of NLRP3^{+} **(F)** and ASC^{+} **(G)** in CD11b^{+} cells in sections of paraffin-embedded spinal cord tissue (scale bars: 50 μm). Data are shown as means ± SD (n = 6 per group). *$p < 0.05$, **$p < 0.01$, ***$p < 0.001$; $^{\#}p < 0.05$, $^{\#\#}p < 0.01$, $^{\#\#\#}p < 0.001$. * vs. Control group; $^{\#}$ vs. MOG group.

this phenomenon was reversed by FLaAN/C treatment (Figure 5B). These results indicates that FLaAN/C suppresses the NF-κB pathway.

NLRP3-mediated pyroptosis promoted EAE development and progression

The NLRP3 inflammasome plays a key role in innate immunity responses and inflammatory events, and is involved in the occurrence and progression of MS. In this study, we evaluated the role of NLRP3-mediated pyroptosis in the progression of EAE. First, we genetically identified *Nlrp3*-KO mice and screened for *Nlrp3*$^{-/-}$ homozygotes for subsequent experiments (Figure 6A). Then, we found that *Nlrp3*$^{-/-}$-MOG mice had significantly fewer signs of disease and correspondingly lower clinical scores than WT-MOG mice (Figure 6B). At the same time, the results of HE staining showed that MOG significantly increased the number of inflammatory cells in

the spinal cord and the inflammation score, while *Nlrp3*$^{-/-}$-MOG mice were significantly reduced both effects (Figure 6C). Furthermore, LFB staining revealed a lower level of spinal cord demyelination in *Nlrp3*$^{-/-}$-MOG mice compared with WT-MOG mice (Figure 6D). Similarly, IF staining and western bloting showed that the protein levels of MBP were significantly lower in WT-MOG mice than in *Nlrp3*$^{-/-}$-MOG mice (Figures 6E,F). Furthermore, we detected the levels of inflammatory cytokines in the serum of mice by ELISA assay and found that the levels of pro-inflammatory cytokines TNF-α, IL-6, and IL-8 were significantly increased in WT-MOG mice, while the level of anti-inflammatory cytokine IL-10 was decreased (Figures 6G–J). Next, we detected the activity of caspase-1. The activity of caspase-1 in *Nlrp3*$^{-/-}$-MOG mice was lower than that in WT-MOG mice (Figure 6 K). Western bloting results showed that the protein levels of caspase-1 p20, GSDMD-N, IL-18 and IL-1β were increased in WT-MOG mice, but the expression levels of these proteins were significantly decreased in *Nlrp3*$^{-/-}$-MOG mice (Figure 6L). Additionally, co-immunoprecipitation analysis revealed more abundant NLRP3-ASC complexes in the spinal cord of WT-MOG mice (Figure 6M). This finding was confirmed by immunofluorescence staining, which showed that more cells were positive for both NLRP3 and ASC in the WT-MOG group (Figure 6N). Overall, these results showed that NLRP3-mediated pyroptosis plays an important role in the occurrence and development of EAE.

FLaAN/C attenuated NLRP3-mediated pyroptosis in EAE mice

Considering the important role of NLRP3-mediated pyroptosis in EAE, we further explored whether FLaAN/C suppresses inflammatory responses in EAE mice by inhibiting NLRP3-mediated pyroptosis. We evaluated the protein levels of the NLRP3 inflammasome complex in the spinal cord by western blotting. And the results showed that the protein expression levels of caspase-1 p20, GSDMD-N, IL-18 and IL-1β in FLaAN/C-treated MOG mice were significantly lower than those in MOG mice (Figure 7A). The same trend was observed for the mRNA levels of caspase-1 and GSDMD detected by RT-qPCR (Figures 7B,C). Furthermore, FLaAN/C significantly decreased the activity of Caspase-1 in the spinal cord of MOG mice (Figure 7D). Next, co-immunoprecipitation assays revealed that the NLRP3-ASC complex was decreased in FLaAN/C-treated MOG mice (Figure 7E). Since NLRP3 and ASC are closely associated with the activation of NLRP3 signaling pathway, we further detected the expression levels of ASC and NLRP3 in the spinal cord. Immunofluorescence staining confirmed that FLaAN/C markedly decreased the foci of CD11b+NLRP3^{+} and CD11b^{+}ASC^{+} in the MOG mice (Figures 7F,G). Altogether, these findings showed that FLaAN/C inhibited NLRP3 mediated pyroptosis.

Discussion

Multiple sclerosis is a prevalent autoimmune inflammatory demyelinating disease of the CNS that significantly affects the quality of life of patients (Zilkha-Falb et al., 2020). Although there are many drugs available to treat MS, they are not entirely effective. Therefore, the pathogenesis of MS needs to be understood from several perspectives to generate more useful and comprehensive information that will help to improve and optimize of treatment options. Cascade neuroinflammation is a cause of MS, and once the CNS inflammatory response spreads, it can lead to severe and permanent neuronal damage (Zilkha-Falb et al., 2020). Therefore, inflammation control is the main goal of early disease treatment.

Extensive activation of microglia/macrophages is a crucial factor in mediating neuroinflammatory damage to the CNS. Microglia/macrophages comprise M1 and M2 phenotypes. Surface markers of microglia/macrophages recognized by antibodies that assess their activation, comprise CD11b, ionized calcium-binding adaptor molecule 1 (IBA1), CD68, and glycoprotein F4/80. M1 macrophages/microglia secrete the proinflammatory cytokines, IL-1β, IL-6, TNF-α, as well as CD16/32 (Fc gamma III and II receptors, respectively), and inducible nitric oxide synthase (iNOS), whereas the M2 phenotype is generally characterized by upregulated Arginase-1, IL-10, CD206, and CD163 (Cutolo et al., 2019). The phenotypes of microglia/macrophages include M1 phenotype and M2 phenotype. M1 and M2 can play different roles in MS through their secreted cytokines (Jäckle et al., 2020). Accordingly, regulating the polarization of microglia/macrophages from the pro-to the anti-inflammatory phenotype might help to treat inflammatory diseases of the CNS. For example, interleukin one receptor associated kinase M (IRAK-M) significantly improves EAE onset by downregulating the TLR4-MyD88 signaling pathway, which finally leads to differentiation to the M2 phenotype in microglia (Liu et al., 2019; Jäckle et al., 2020). Homeobox protein MSX-3 (MSX3) drives microglia polarization to the M2 phenotype and promotes oligodendrocyte precursor maturation and remyelination, thus preventing experimental EAE progression (Yu et al., 2015). We found that FLaAN/C promoted the shift of microglia/macrophages to an anti-inflammatory phenotype, as indicated by a lower abundance of the M1 marker CD86 and a higher abundance of the M2 marker CD206, accompanied by decreased iNOS and TNF-α secretion, and enhanced IL-10 and Arginase-1 release. Our results indicated that FLaAN/C treatment promoted the polarization of microglia/macrophages from M1 to

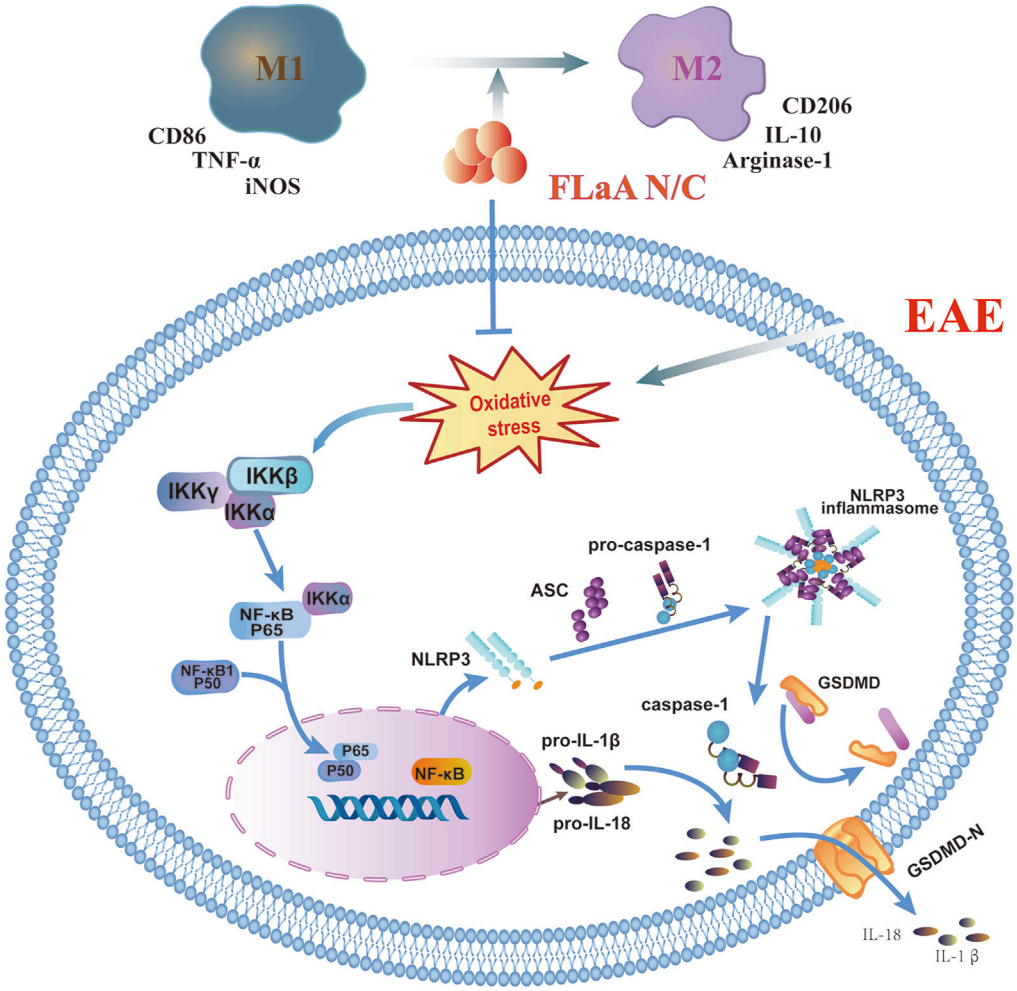

FIGURE 8
FLaAN/C attenuated inflammatory response by facilitating macrophages/microglia polarization from the M1 phenotype to the M2 phenotype and inhibiting the ROS/NF-κB/NLRP3 signaling pathway, and thus alleviated EAE.

M2 phenotype, thereby attenuating the inflammatory response in the spinal cord of EAE mice.

The CNS is highly vulnerable to oxidative stress due to high energy demand, mitochondrial activity, and polyunsaturated fatty acids. Hence, these features increase CNS susceptibility to typical neurodegenerative hallmarks linked with oxidative stress, which might cause CNS dysfunction in patients with MS (Steudler et al., 2022). Novel fatty acid-binding protein five and seven inhibitors ameliorate glial cell injury in EAE by decreasing oxidative stress levels (Cheng et al., 2021). Consistent with these findings, the present study showed that FLaAN/C might prevent ROS accumulation by downregulating 3NT, 4HNE, and MDA levels in EAE mice, while increasing SOD and CAT expression levels. Reactive oxygen species not only mediate oxidative stress but also promote the NF-κB signaling pathway which is widely involved in the occurrence of MS (Gutiérrez-Miranda et al., 2020; Lei et al., 2020). Furthermore, paricalcitol inhibits neuroinflammation and moderates MOG35-55-induced EAE progression by modulating NF-κB signaling both *in vitro* and *in vivo* (Zhang et al., 2020). Current approaches to treating MS, such as IFN-β and glatiramer acetate, significantly inhibit NF-κB activity (Zhao et al., 2018). Our results have consistently showed that FLaAN/C decreases the nuclear expression of NF-κB subunit p65 and the numbers of cells expressing activated NF-κB in mice with EAE.

Pyroptosis is an inflammatory cell death process that is activated by the NLRP3 inflammasome *via* a classical pathway. Emerging evidence suggests that NLRP3-mediated pyroptosis is functioning in the CNS of patients with MS and in mice with EAE (Khan et al., 2018). Moreover, the NLRP3 inflammasome is regulated by upstream components such as NF-κB and ROS

(Yin et al., 2020). Pattern recognition receptors binding to their corresponding ligands, such as ROS, are the first signal to mediate translocation to the nucleus, thus initiating downstream NLRP3, Pro-IL-1β, and Pro-IL-18 transcription, and upregulating the expression of relevant inflammatory factors (Zhang et al., 2018; Li et al., 2021). The NF-κB/NLRP3 signaling pathway plays important roles in inflammatory diseases of the nervous system. For instance, Baicalin exerts neuroprotective effects by inhibiting activation of the GSK3β/NF-κB/NLRP3 signaling pathway in a rat model of depression (Zhang et al., 2018). We found that the NF-κB/NLRP3 signaling pathway is also involved in the occurrence of EAE. Demyelination and inflammatory cell infiltration were alleviated in *Nlrp3*$^{-/-}$-MOG mice. Moreover, *Nlrp3*$^{-/-}$-MOG mice have decreased activation and protein levels of caspase-1 p20 and GSDMD-N, as well as significantly reduced pyroptosis-related indicators, such as caspase-1 activation, and IL-18 and IL-1β levels. Similarly, FLaAN/C significantly decreased caspase-1 activation and inhibited the protein expression of IL-18, IL-1β, pro-caspase-1 p20 and GSDMD-N. Furthermore, FLaAN/C significantly inhibited the colocalization of NLRP3 and ASC and inhibited the activation of NLRP3 inflammasome. These results suggested that the therapeutic effects of FLaAN/C are exerted by inhibiting NLRP3 inflammasome-mediated pyroptosis.

In conclusion, we previously constructed the recombinant FLaAN/C protein to alleviate post-radiation side effects through anti-inflammatory and antioxidant effects. Here, our results showed that FLaAN/C attenuates inflammatory response in mice by facilitating microglia/macrophages polarization from the M1 phenotype to the M2 phenotype and inhibiting the ROS/NF-κB/NLRP3 signaling pathway, and thus alleviates EAE (Figure 8). Our findings provide new evidence of the potential of FLaAN/C as a drug for treating MS.

Data availability statement

The original contributions presented in the study are included in the article/Supplementary Materials, further inquiries can be directed to the corresponding authors.

Ethics statement

The animal study was reviewed and approved by the Animal Policy and Welfare Committee of Chengdu Medical College (Approval No. CDYXY-2021711).

Author contributions

LL, SD, and JL collected the data. LL, MY, ML drafter, reviewed, and edited the manuscript, respectively. JL, TL, TZ, MH, YZ, and MY provided research materials and technical support. DW and YX designed the experiments. All authors read and approved the submission of the final version.

Funding

This study was funded by the National Natural Science Foundation of China (81,972,977), Foundation of Science and Technology Innovation Talent Project of Sichuan Province (2,021,038), Foundation of Health Commission of Sichuan Province (20ZD016), Foundation of Health Commission of Chengdu (2,021,001), Foundation of Chengdu Science and Technology Bureau (2021-YF05-00291-SN), Foundation of Sichuan Science and Technology Agency (2019YJ0589), Foundation of the First Affiliated Hospital of Chengdu Medical College (CYFY202LNZD01, CYFY2020YB05,CYFY2017ZD03, CYFY2018ZD02, and CYFY2019ZD06), and Foundation of Collaborative Innovation Center of Sichuan for Elderly Care and Health, Chengdu Medical College (19Z01), Disciplinary. Construction Innovation Team Foundation of Chengdu Medical College (CMC-XK-2103).

Conflict of interest

The authors declare that the research was conducted in the absence of any commercial or financial relationships that could be construed as a potential conflict of interest.

Publisher's note

Supplementary material

The Supplementary Material for this article can be found online at: https://www.frontiersin.org/articles/10.3389/fphar.2022.956402/full#supplementary-material

References

Bolton, C., and Smith, P. A. (2018). The influence and impact of ageing and immunosenescence (ISC) on adaptive immunity during multiple sclerosis (MS) and the animal counterpart experimental autoimmune encephalomyelitis (EAE). *Ageing Res. Rev.* 41, 64–81. doi:10.1016/j.arr.2017.10.005

Braga, T. T., Brandao, W. N., Azevedo, H., Terra, F. F., Melo, A. C. L., Pereira, F. V., et al. (2019). *NLRP3 gain-of-function in CD4 T lymphocytes ameliorates experiment (Kim et al., 2021) al autoimmune encephalomyelitis*, 133, 1901–1916. doi:10.1042/CS20190506*Clin. Sci. (Lond)*

Cai, L., Gong, Q., Qi, L., Xu, T., Suo, Q., Li, X., et al. (2022). ACT001 attenuates microglia-mediated neuroinflammation after traumatic brain injury via inhibiting AKT/NFκB/NLRP3 pathway. *Cell Commun. Signal.* 20, 56. doi:10.1186/s12964-022-00862-y

Chen, X., Li, C., Cao, X., Jia, X., Chen, X., Wang, Z., et al. (2022). Mitochondria-targeted supramolecular coordination container encapsulated with exogenous itaconate for synergistic therapy of joint inflammation. *Theranostics* 12, 3251–3272. doi:10.7150/thno.70623

Chen, Y., Wu, G., Li, M., Hesse, M., Ma, Y., Chen, W., et al. (2022). LDHA-mediated metabolic reprogramming promoted cardiomyocyte proliferation by alleviating ROS and inducing M2 macrophage polarization. *Redox Biol.* 56, 102446. doi:10.1016/j.redox.2022.102446

Cheng, A., Jia, W., Kawahata, I., and Fukunaga, K. (2021). A novel fatty acid-binding protein 5 and 7 inhibitor ameliorates oligodendrocyte injury in multiple sclerosis mouse models. *EBioMedicine* 72, 103582. doi:10.1016/j.ebiom.2021.103582

Chu, T., Zhang, Y. P., Tian, Z., Ye, C., Zhu, M., Shields, L. B. E., et al. (2019). Dynamic response of microglia/macrophage polarization following demyelination in mice. *J. Neuroinflammation* 16, 188. doi:10.1186/s12974-019-1586-1

Correale, J., Gaitán, M., Ysrraelit, M., and Fiol, M. J. B. a. j. o. n. (2017). Progressive multiple sclerosis: From pathogenic mechanisms to treatment. *Brain* 140, 527–546. doi:10.1093/brain/aww258

Cutolo, M., Trombetta, A. C., and Soldano, S. (2019). Monocyte and macrophage phenotypes: A look beyond systemic sclerosis. Response to: 'M1/M2 polarisation state of M-CSF blood-derived macrophages in systemic sclerosis' by lescoat et al. *Ann. Rheum. Dis.* 78, e128. doi:10.1136/annrheumdis-2018-214371

Devanney, N. A., Stewart, A. N., and Gensel, J. C. (2020). Microglia and macrophage metabolism in CNS injury and disease: The role of immunometabolism in neurodegeneration and neurotrauma. *Exp. Neurol.* 329, 113310. doi:10.1016/j.expneurol.2020.113310

Dobson, R., and Giovannoni, G. (2019). Multiple sclerosis - a review. *Eur. J. Neurol.* 26, 27–40. doi:10.1111/ene.13819

Gutiérrez-Miranda, B., Gallardo, I., Melliou, E., Cabero, I., Álvarez, Y., Magiatis, P., et al. (2020). *Oleacein attenuates the pathogenesis of experimental autoimmune encephalomyelitis through both antioxidant and anti-inflammatory effects*. Basel, Switzerland): Antioxidants. 910.3390/antiox9111161.

Hao, W., Luo, Q., Menger, M. D., Fassbender, K., and Liu, Y. (2021). Treatment with CD52 antibody protects neurons in experimental autoimmune encephalomyelitis mice during the recovering phase. *Front. Immunol.* 12, 792465. doi:10.3389/fimmu.2021.792465

He, Y., Chang, Y., Peng, Y., Zhu, J., Liu, K., Chen, J., et al. (2022). Glibenclamide directly prevents neuroinflammation by targeting SUR1-TRPM4-mediated NLRP3 inflammasome activation in microglia. *Mol. Neurobiol.* 59, 6590–6607. doi:10.1007/s12035-022-02998-x

Hou, B., Zhang, Y., Liang, P., He, Y., Peng, B., Liu, W., et al. (2020). Inhibition of the NLRP3-inflammasome prevents cognitive deficits in experimental autoimmune encephalomyelitis mice via the alteration of astrocyte phenotype. *Cell Death Dis.* 11, 377. doi:10.1038/s41419-020-2565-2

Jäckle, K., Zeis, T., Schaeren-Wiemers, N., Junker, A., van der Meer, F., Kramann, N., et al. (2020). Molecular signature of slowly expanding lesions in progressive multiple sclerosis. *Brain* 143, 2073–2088. doi:10.1093/brain/awaa158

Jie, Z., Ko, C.-J., Wang, H., Xie, X., Li, Y., Gu, M., et al. (2021). Microglia promote autoimmune inflammation via the noncanonical NF-κB pathway. *Sci. Adv.* 7, eabh0609. doi:10.1126/sciadv.abh0609

Jolivel, V., Luessi, F., Masri, J., Kraus, S. H. P., Hubo, M., Poisa-Beiro, L., et al. (2013). Modulation of dendritic cell properties by laquinimod as a mechanism for modulating multiple sclerosis. *Brain* 136, 1048–1066. doi:10.1093/brain/awt023

Khan, N., Kuo, A., Brockman, D. A., Cooper, M. A., and Smith, M. T. (2018). Pharmacological inhibition of the NLRP3 inflammasome as a potential target for multiple sclerosis induced central neuropathic pain. *Inflammopharmacology* 26, 77–86. doi:10.1007/s10787-017-0401-9

Kim, J., Islam, S. M. T., Qiao, F., Singh, A. K., Khan, M., Won, J., et al. (2021). Regulation of B cell functions by S-nitrosoglutathione in the EAE model. *Redox Biol.* 45, 102053. doi:10.1016/j.redox.2021.102053

Lei, Z., Yue, Y., Stone, S., Wu, S., and Lin, W. (2020). NF-κB activation accounts for the cytoprotective effects of PERK activation on oligodendrocytes during EAE. *J. Neurosci.* 40, 6444–6456. doi:10.1523/JNEUROSCI.1156-20.2020

Leuti, A., Talamonti, E., Gentile, A., Tiberi, M., Matteocci, A., Fresegna, D., et al. (2021). Macrophage plasticity and polarization are altered in the experimental model of multiple sclerosis. *Biomolecules* 11, 837. doi:10.3390/biom11060837

Li, H., Yuan, L., Li, X., Luo, Y., Zhang, Z., and Li, J. (2021). Isoorientin attenuated the pyroptotic hepatocyte damage induced by benzo[a]pyrene via ROS/NF-κB/NLRP3/Caspase-1 signaling pathway. *Antioxidants (Basel)* 10, 1275. doi:10.3390/antiox10081275

Liu, B., Gu, Y., Pei, S., Peng, Y., Chen, J., Pham, L. V., et al. (2019). Interleukin-1 receptor associated kinase (IRAK)-M -mediated type 2 microglia polarization ameliorates the severity of experimental autoimmune encephalomyelitis (EAE). *J. Autoimmun.* 102, 77–88. http://dx.doi.org/10.1016/j.jaut.2019.04.020.

Liu, T., Wu, D.-M., Zhang, F., Zhang, T., He, M., Zhao, Y.-Y., et al. (2022). miR-142a-3p enhances FlaA N/C protection against radiation-mediated intestinal injury by modulating the IRAK1/NF-κB signaling pathway. *Int. J. Radiat. Oncol. Biol. Phys.* 112, 1256–1268. doi:10.1016/j.ijrobp.2021.12.003

Luna, G., Alping, P., Burman, J., Fink, K., Fogdell-Hahn, A., Gunnarsson, M., et al. (2020). Infection risks among patients with multiple sclerosis treated with fingolimod, natalizumab, rituximab, and injectable therapies. *JAMA Neurol.* 77, 184–191. doi:10.1001/jamaneurol.2019.3365

Lyu, J., Xie, D., Bhatia, T. N., Leak, R. K., Hu, X., and Jiang, X. (2021). Microglial/Macrophage polarization and function in brain injury and repair after stroke. *CNS Neurosci. Ther.* 27, 515–527. doi:10.1111/cns.13620

Pegoretti, V., Swanson, K. A., Bethea, J. R., Probert, L., Eisel, U. L. M., and Fischer, R. (2020). Inflammation and oxidative stress in multiple sclerosis: Consequences for therapy development. *Oxid. Med. Cell. Longev.* 2020, 7191080. doi:10.1155/2020/7191080

Peng, L., Wen, L., Shi, Q.-F., Gao, F., Huang, B., Meng, J., et al. (2020). Scutellarin ameliorates pulmonary fibrosis through inhibiting NF-κB/NLRP3-mediated epithelial-mesenchymal transition and inflammation. *Cell Death Dis.* 11, 978. doi:10.1038/s41419-020-03178-2

Schafflick, D., Xu, C. A., Hartlehnert, M., Cole, M., Schulte-Mecklenbeck, A., Lautwein, T., et al. (2020). Integrated single cell analysis of blood and cerebrospinal fluid leukocytes in multiple sclerosis. *Nat. Commun.* 11, 247. doi:10.1038/s41467-019-14118-w

Soltanmoradi, S., Tavakolpour, V., Moghadasi, A. N., and Kouhkan, F. (2021). Expression analysis of NF-κB-associated long noncoding RNAs in peripheral blood mononuclear cells from relapsing-remitting multiple sclerosis patients. *J. Neuroimmunol.* 356, 577602. doi:10.1016/j.jneuroim.2021.577602

Song, S., Guo, R., Mehmood, A., Zhang, L., Yin, B., Yuan, C., et al. (2022). Liraglutide attenuate central nervous inflammation and demyelination through AMPK and pyroptosis-related NLRP3 pathway. *CNS Neurosci. Ther.* 28, 422–434. doi:10.1111/cns.13791

Steudler, J., Ecott, T., Ivan, D. C., Bouillet, E., Walthert, S., Berve, K., et al. (2022). Autoimmune neuroinflammation triggers mitochondrial oxidation in oligodendrocytes. *Glia* 70, 2045–2061. doi:10.1002/glia.24235

Wang, J., Wang, J., Wang, J., Yang, B., Weng, Q., and He, Q. (2019). Targeting microglia and macrophages: A potential treatment strategy for multiple sclerosis. *Front. Pharmacol.* 10, 286. doi:10.3389/fphar.2019.00286

Wang, M., Jin, L., Zhang, Q., Zhu, W., He, H., Lou, S., et al. (2022). Curcumin analog JM-2 alleviates diabetic cardiomyopathy inflammation and remodeling by inhibiting the NF-κB pathway. *Biomed. Pharmacother. = Biomedecine Pharmacother.* 154, 113590. doi:10.1016/j.biopha.2022.113590

Wu, D., Han, R., Deng, S., Liu, T., Zhang, T., Xie, H., et al. (2018). Protective effects of flagellin AN/C against radiation-induced NLR pyrin domain containing 3 inflammasome-dependent pyroptosis in intestinal cells. *Int. J. Radiat. Oncol. Biol. Phys.* 101, 107–117. doi:10.1016/j.ijrobp.2018.01.035

Xue, B., Ge, M., Fan, K., Huang, X., Yan, X., Jiang, W., et al. (2022). Mitochondria-targeted nanozymes eliminate oxidative damage in retinal neovascularization disease. *J. Control. Release* 350, 271–283. doi:10.1016/j.jconrel.2022.08.026

Yin, N., Zhao, Y., Liu, C., Yang, Y., Wang, Z.-H., Yu, W., et al. (2022). Engineered nanoerythrocytes alleviate central nervous system inflammation by regulating the polarization of inflammatory microglia. *Adv. Mat.* 34, e2201322. doi:10.1002/adma.202201322

Yin, W., Liu, S., Dong, M., Liu, Q., Shi, C., Bai, H., et al. (2020). A new NLRP3 inflammasome inhibitor, dioscin, promotes osteogenesis. *Small (Weinheim Der Bergstrasse, Ger.* 16, e1905977. doi:10.1002/smll.201905977

Yong, V. J. N. (2022). Microglia in multiple sclerosis: Protectors turn destroyers. *Neuron* S0896-6273 (22), 00602–X. doi:10.1016/j.neuron.2022.06.023

Yu, Y., Wu, D.-M., Li, J., Deng, S.-H., Liu, T., Zhang, T., et al. (2020). Bixin attenuates experimental autoimmune encephalomyelitis by suppressing TXNIP/NLRP3 inflammasome activity and activating NRF2 signaling. *Front. Immunol.* 11, 593368. doi:10.3389/fimmu.2020.593368

Yu, Z., Sun, D., Feng, J., Tan, W., Fang, X., Zhao, M., et al. (2015). MSX3 switches microglia polarization and protects from inflammation-induced demyelination. *J. Neurosci.* 35, 6350–6365. doi:10.1523/JNEUROSCI.2468-14.2015

Zhang, C.-Y.-Y., Zeng, M.-J., Zhou, L.-P., Li, Y.-Q., Zhao, F., Shang, Z.-Y., et al. (2018). Baicalin exerts neuroprotective effects via inhibiting activation of GSK3β/NF-κB/NLRP3 signal pathway in a rat model of depression. *Int. Immunopharmacol.* 64, 175–182. doi:10.1016/j.intimp.2018.09.001

Zhang, D., Qiao, L., and Fu, T. (2020). Paricalcitol improves experimental autoimmune encephalomyelitis (EAE) by suppressing inflammation via NF-κB signaling. *Biomed. Pharmacother. = Biomedecine Pharmacother.* 125, 109528. doi:10.1016/j.biopha.2019.109528

Zhang, J., Su, D., Liu, Q., Yuan, Q., Ouyang, Z., Wei, Y., et al. (2022). Gasdermin D-mediated microglial pyroptosis exacerbates neurotoxicity of aflatoxins B1 and M1 in mouse primary microglia and neuronal cultures. *Neurotoxicology* 91, 305–320. doi:10.1016/j.neuro.2022.06.003

Zhang, Q., Liu, W., Wang, H., Zhou, H., Bulek, K., Chen, X., et al. (2022). TH17 cells promote CNS inflammation by sensing danger signals via Mincle. *Nat. Commun.* 13, 2406. doi:10.1038/s41467-022-30174-1

Zhao, Q., Cheng, W., Xi, Y., Cao, Z., Xu, Y., Wu, T., et al. (2018). IFN-β regulates Th17 differentiation partly through the inhibition of osteopontin in experimental autoimmune encephalomyelitis. *Mol. Immunol.* 93, 20–30. http://dx.doi.org/10.1016/j.molimm.2017.11.002.

Zilkha-Falb, R., Rachutin-Zalogin, T., Cleaver, L., Gurevich, M., and Achiron, A. (2020). RAM-589.555 favors neuroprotective and anti-inflammatory profile of CNS-resident glial cells in acute relapse EAE affected mice. *J. Neuroinflammation* 17, 313. doi:10.1186/s12974-020-01983-2

frontiers | Frontiers in Pharmacology

TYPE Original Research
PUBLISHED 15 November 2022
DOI 10.3389/fphar.2022.1040999

OPEN ACCESS

EDITED BY
Dongdong Sun,
Nanjing University of Chinese Medicine, China

REVIEWED BY
Xiaowei Ma,
Department of Nuclear Medicine, Second Xiangya Hospital, Central South University, China
Fareeha Anwar,
Riphah International University, Pakistan
Weiwei Hu,
Zhejiang University, China

*CORRESPONDENCE
Feiran Zhang,
zhangfr8@mail.sysu.edu.cn
Tingting Zhang,
zhangtt6268@163.com

†These authors have contributed equally to this work and share first authorship

SPECIALTY SECTION
This article was submitted to Inflammation Pharmacology, a section of the journal Frontiers in Pharmacology

RECEIVED 09 September 2022
ACCEPTED 31 October 2022
PUBLISHED 15 November 2022

CITATION
Lin Z, Lin X, Lai Y, Han C, Fan X, Tang J, Mo S, Su J, Liang S, Shang J, Lv X, Guo S, Pang R, Zhou J, Zhang T and Zhang F (2022), Ponatinib modulates the metabolic profile of obese mice by inhibiting adipose tissue macrophage inflammation. *Front. Pharmacol.* 13:1040999. doi: 10.3389/fphar.2022.1040999

Ponatinib modulates the metabolic profile of obese mice by inhibiting adipose tissue macrophage inflammation

Zhuomiao Lin[1†], Xiaochun Lin[1,2†], Ying Lai[1], Congcong Han[1], Xinran Fan[1], Jie Tang[1], Shiqi Mo[1], Jiahui Su[1], Sijia Liang[1,3], Jinyan Shang[1], Xiaofei Lv[1], Siwan Guo[1], Ruiping Pang[4], Jiaguo Zhou[1,3,5,6,7], Tingting Zhang[1,8,5]* and Feiran Zhang[1,3]*

[1]Department of Pharmacology, Cardiac and Cerebral Vascular Research Center, Zhongshan School of Medicine, Sun Yat-Sen University, Guangzhou, China, [2]Department of Clinical Pharmacy, Guangzhou First People's Hospital, School of Medicine, South China University of Technology, Guangzhou, China, [3]Program of Kidney and Cardiovascular Diseases, The Fifth Affiliated Hospital, Zhongshan School of Medicine, Sun Yat-Sen University, Guangzhou, China, [4]Department of Physiology, Pain Research Center, Zhongshan School of Medicine, Sun Yat-Sen University, Guangzhou, China, [5]Department of Cardiology, The Eighth Affiliated Hospital, Sun Yat-sen University, Shenzhen, China, [6]Guangdong Province Key Laboratory of Brain Function and Disease, Zhongshan School of Medicine, Sun Yat-Sen University, Guangzhou, China, [7]Key Laboratory of Cardiovascular Diseases, School of Basic Medical Sciences, Guangzhou Medical University, Guangzhou, China, [8]Program of Cardiovascular Research, The Eighth Affiliated Hospital, Zhongshan School Medicine, Sun Yat-sen University, Guangzhou, China

Obesity-induced metabolic syndrome is a rapidly growing conundrum, reaching epidemic proportions globally. Chronic inflammation in obese adipose tissue plays a key role in metabolic syndrome with a series of local and systemic effects such as inflammatory cell infiltration and inflammatory cytokine secretion. Adipose tissue macrophages (ATM), as one of the main regulators in this process, are particularly crucial for pharmacological studies on obesity-related metabolic syndrome. Ponatinib, a multi-targeted tyrosine kinase inhibitor originally used to treat leukemia, has recently been found to improve dyslipidemia and atherosclerosis, suggesting that it may have profound effect on metabolic syndrome, although the mechanisms underlying have not yet been revealed. Here we discovered that ponatinib significantly improved insulin sensitivity in leptin deficient obese mice. In addition to that, ponatinib treatment remarkably ameliorated high fat diet-induced hyperlipidemia and inhibited ectopic lipid deposition in the liver. Interestingly, although ponatinib did not reduce but increase the weight of white adipose tissue (WAT), it remarkably suppressed the inflammatory response in WAT and preserved its function. Mechanistically, we showed that ponatinib had no direct effect on hepatocyte or adipocyte but attenuated free fatty acid (FFA) induced macrophage transformation from pro-inflammatory to anti-inflammatory phenotype. Moreover, adipocytes co-cultured with FFA-treated macrophages exhibited insulin resistance, while pre-treat these macrophages with ponatinib can ameliorate this process. These results suggested that the beneficial effects of ponatinib on metabolic disorders are achieved by inhibiting the inflammatory phenotypic transformation of ATMs, thereby maintaining the physiological function of adipose tissue under

excessive obesity. The data here not only revealed the novel therapeutic function of ponatinib, but also provided a theoretical basis for the application of multi-target tyrosine kinase inhibitors in metabolic diseases.

KEYWORDS

ponatinib, adipose tissue macrophages, obesity, metabolic dysfunction, tyrosine kinase inhibitors

Introduction

Obesity, especially visceral obesity, can lead to a series of systemic disorders such as hyperlipidemia, hyperglycemia and hypertension which are classified as metabolic syndromes (MS). Obesity-induced MS acts as one of the primary risk factors of coronary artery disease (CAD), stroke, cancer, non-alcoholic fatty liver disease (NAFLD) and type 2 diabetes mellitus (T2DM) and is therefore considered to be one of the major health problems in the modern world (Van Gaal et al., 2006). In dealing with obesity and the metabolic disorders, exercise and diet changes could bring great benefits, but it is difficult to persist in the long run. At present, a variety of pharmacological interventions are used in MS by increasing insulin sensitivity/secretion, regulating blood lipids and suppressing appetite. Although these drugs have proved to be beneficial for MS, there is still an urgent unmet need for more effective pharmacological intervention with less side-effect for obesity-related metabolic disorders (Kusminski et al., 2016).

Growing evidence has suggested that the dysfunction of white adipose tissue (WAT) is one of the earliest and most profound pathological changes in visceral obesity (Kahn et al., 2019). In the physiological state, adipose tissue plays a central role in regulating metabolic homeostasis by severing as a nutrient depository as well as an endocrine organ of multiple adipokines and cytokines. During obesity, dysfunctional WAT is accompanied by a shift in adipokines secretion profile, which typically shows a reduction in anti-inflammatory factors such as adiponectin and interleukin-10 (IL-10), while an elevation in pro-inflammatory cytokines such as TNFα, interleukin- 1β (IL-1β), IL-6 and IL-18. The impaired lipid storage function and abnormal inflammatory cytokine secretion of obese WAT together promote metabolic dysfunction (Tilg and Moschen, 2006; Burhans et al., 2018). In this process, adipose tissue macrophages (ATMs) play an indispensable role due to their high plasticity in response to the microenvironment changes (Kratz et al., 2014; McNelis and Olefsky, 2014). In the context of hypoxia and chronic inflammation, cytokines, chemokines and damage-associated molecular pattern (DAMP) such as free fatty acids (FFAs) released by adipocyte necrosis together promote the monocyte infiltration and pro-inflammatory M1 macrophages polarization. M1 macrophages surround apoptotic adipocytes to form a 'crown-like' structure (CLS) (Cinti et al., 2005), which will lead to the overproduction of pro-inflammatory mediators and ultimately destroy the metabolic function of adipose tissue and the systematic insulin sensitivity. Therefore, the methods to block the obesity-related WAT inflammation and ATM activation would be beneficial for obesity and MS (Kusminski et al., 2016).

Ponatinib (Iclusig™; ARIAD Pharmaceuticals) is a multi-targeted tyrosine-kinase inhibitor approved by the US Food and Drug Administration (FDA) for patients with chronic myeloid leukemia and Philadelphia chromosome-positive acute lymphoblastic leukemia (O'Hare et al., 2009; Frankfurt and Licht, 2013). Interestingly, recent studies revealed that ponatinib can improve dyslipidemia and atherosclerotic plaque formation in apolipoprotein E-deficient ($ApoE^{-/-}$) mice (Pouwer et al., 2018), suggesting that ponatinib may play a pivotal role in the regulation of metabolic disorders. However, the mechanisms to explain the effects of ponatinib on MS are not clear. Here, we observed that ponatinib is effective to ameliorate high-fat diet (HFD)-induced hyperlipidemia and NAFLD in leptin-deficient obesity mice model. Moreover, we provided evidence that inhibition of ATMs transformation from anti-inflammatory to pro-inflammatory phenotype underlies the beneficial effects of ponatinib on MS.

Materials and methods

Reagents

Ponatinib was purchased from Selleck (Houston, TX, United States). Antibodies against insulin receptor-beta; phospho-insulin receptor-beta (Tyr1150/1151); insulin receptor substrate-1; phospho-insulin receptor substrate-1 (Ser636/639); Akt; phosphor-Akt (Ser 473) were purchased from Cell Signaling Technology (Danvers, MA, United States). Antibody against F4/80 was obtained from Servicebio Biotechnology (Wuhan, China). Alexa Fluor®-700 anti-mouse CD38 antibody was obtained from eBioscience (San Diego, CA, United States). Isobutyl-methyl-xanthine (IBMX), dexamethasone, palmitic acid, oleic acid and Oil Red-O were obtained from Sigma-Aldrich (St. Louis, MO, United States). Culture medium, and fetal bovine serum (FBS) were obtained from Gibco (Carlsbad, CA, United States). Insulin was purchased from Novo Nordisk (Copenhagen, Denmark). Macrophage colony-stimulating factor 1 (M-CSF1) was purchased from Novoprotein Scientific (Shanghai, China). Sodium Oleate, Sodium palmitate were purchased from Sigma-Aldrich (St. Louis, MO, United States). DNA ladder, Nucleic Acid Dye and agarose were purchased from Genstar (Beijing, China).

Animal study

All animal experimental procedures were performed in accordance with the policy of the Sun Yat-Sen University Animal Care and Use Committee and conformed to the Guidelines for the ethical review of laboratory animal welfare People's Republic of China National Standard GB/T 35,892-2018. Mice were housed under specific pathogen-free conditions with 12/12 h light/dark cycle and had *ad libitum* access to water and food. Different groups were allocated in a randomized manner and investigators were blinded to the allocation of different groups when doing outcome evaluations. Sample size was determined by pilot experiments and exact n-numbers were shown in the respective figure legend. All mouse tissue samples used in this study were collected after euthanasia by intraperitoneal injection of an overdose of sodium pentobarbital (200 mg/kg).

6-week-old male ob/ob mice and its lean littermates with a genetic background of C57BL/6J were procured from Cyagen Biosciences (Santa Clara, CA, United States). After 2 weeks of adaptation, the ob/ob mice and lean mice were divided into four groups randomly with five animals per group. The drug intervention groups (lean + ponatinib and ob/ob + ponatinib) were treated with ponatinib (5 mg/kg made in 25 mM citrate buffer (pH 2.75)] *via* intragastric administration for 8 weeks, while the control groups were treated with vehicle (citrate buffer). Body weight was measured weekly. After treatment for 8 weeks, fasting blood glucose levels, random blood glucose levels, oral glucose tolerance test (GTT) and insulin tolerance test (ITT) were measured with glucometer. At the end of the experiment, the mice after an overnight fast were euthanized and the blood, liver and adipose tissue samples were collected for subsequent testing.

Glucose and insulin tolerance test

GTT and ITT were performed as previously described (Guo et al., 2020). In brief, GTT and ITT were examined in mice fasted for 12 and 6 h, respectively. Mice were intraperitoneal administration with 1 g/kg glucose (made in 0.9% NaCl) for GTT, while 0.75 U/kg human insulin (made in 0.9% NaCl) was intraperitoneally injected into mice for ITT. Blood glucose were monitored with a glucometer at 0, 15, 30, 60, 120 min. The blood glucose change over time curve was drawn and calculate the area (AUC) under the curve using the GraphPad Prism 8.0 (GraphPad Software, La Jolla, CA, United States).

Histology and immunohistochemistry staining

Four% paraformaldehyde-fixed paraffin-embedded murine tissues were subjected to hematoxylin and eosin (H&E) staining to observe the histological changes in the tissues. Liver sections were embedded in OTC, sliced (7 μm) under freezing conditions and applied for Oil Red-O staining for assessment of lipid deposition.

For immunohistochemistry staining, paraffin sections were deparaffinized, rehydrated, antigen retrieved by immersed in 0.01 M citrate buffer, blocked and then incubated with anti-F4/80 at 1:1000 overnight at 4°C. After washed three times by PBS, sections were tested using Real Envision Detection kit (Dako, Glostrup, Denmark) according to the manufacturer's instructions.

Biochemistry analysis and hepatic lipid analyses

Blood was collected from the Retro-orbital bleeding under terminal anesthesia. Samples were centrifuged at 1000 x *g* for 20 min and then supernatants were collected. Insulin in serum was performed by enzyme-linked immunosorbent assay (ELISA) (RayBiotech, Norcross, GA, United States). Serum lipids, including serum total cholesterol (TC), triglyceride (TG), high-density lipoprotein cholesterol (HDL-C) and low-density lipoprotein cholesterol (LDL-C), were detected by analytical auto analyzer (Mindray, Shenzhen, China). Commercial kits (Applygen, Beijing, China) were used to measure liver tissue triglyceride (TG) and total cholesterol (TC) according to the manufacturer's protocol.

Cell culture and cell differentiation

Human normal hepatocyte LO2 and mouse embryonic fibroblast 3T3-L1 were purchased from Procell Life Science and Technology Co. Ltd. All cell lines were maintained in standard medium containing Dulbecco's modified Eagle's medium (DMEM), 10% fetal bovine serum (FBS),1% penicillin–streptomycin at 37°C in 5% CO2.

3T3-L1 adipocytes was differentiated as previously described (Qi et al., 2019). 3T3-L1 preadipocytes were cultured to confluence (day 0) and disposed in differentiating medium containing Isobutyl-methyl-xanthine (IBMX) (0.5 mmol/L), dexamethasone (1 μmol/L) and insulin (10 μg/ml) for 2 days. The medium was renewed to differentiation-maintenance medium comprising 10 μg/ml insulin for 2 days. Thereafter, the medium was changed to a standard medium and replaced every 2 days. At day 8–12, mature adipocytes can be identified by 60% Oil Red-O solution or used in subsequent experiments.

For lipid droplet deposition experiment in LO2, cells were treated with FFA mixture for 24 h. Afterward, lipid droplet located in these cells were stained with Oil Red-O solution as previously described (Guo et al., 2020).

BMDMs isolation and differentiation were performed as previously described (Pineda-Torra et al., 2015). In short, 8-

week-old mice were anesthetized and sacrificed. The abdomen and hind legs of mice were sterilized with 75% ethanol. The mice were cut an incision in the middle line of the abdomen, exposed the hind legs, and removed all muscle tissue from the bone using scissors. The femur and tibia were separated at the knee joint of the mouse. Bone marrow was then flushed by the medium (RPMI1640). The bone marrow cells were pipetted up and down to become single—cell suspension. The cells were centrifuged at 500 x *g* for 5 min and then supernatants were removed. The sediment was resuspended using a complete medium containing macrophage colony stimulating factor-1 (M-CSF1) (20 ng/ml) and the cells were plated as needed and cultured at 37°C in 5% CO_2. Fresh complete medium was replaced every 3 days and non-adherent cells were removed. After 7 days, fully differentiated macrophages were obtained.

Co-culture of 3T3 and bone marrow-derived macrophages cells

3T3-L1 adipocytes and BMDMs were seeded into 6-well plates respectively and differentiated according to the method in the previous section. On the eighth day, the matured BMDMs was digested and transferred into polycarbonate membrane inserts (Corning, NY, United States), and treated with corresponding reagents such as ponatinib and FFA for 48 h. On the 10th day, the polycarbonate membrane inserts with treated BMDMs were transferred into 6-well plates and co-cultured with mature 3T3 adipocytes. After 24 h, the lysate of 3T3 adipocytes was collected and proceeded.

Preparation of free fatty acid mixture solution

A mixture solution of FFA was prepared as previously described (Lim et al., 2017). Firstly, Sodium Oleate and Sodium Palmitate were prepared as 10 mM stock solutions separately. Subsequently, to prepare the working solution of the FFA mixture, the Palmitate, Oleate and fatty-acid-free bovine serum albumin (BSA) solutions were mixed and diluted with cell culture medium, and then the pH value was adjusted to 7.1 with hydrochloric acid. The final concentration of each component in the FFA solution was 0.66 mM Oleate, 0.33 mM Palmitate and 1% BSA. Accordingly, 1% BSA solution was used as blank control.

Quantitative real time-PCR analysis

To determine mRNA levels, total RNA was isolated from liver tissue, adipose tissue, 3T3-L1 or BMDM cells by using TRIzol reagent according to manufacturer's instructions. RNA (2 μg) was reverse transcribed into cDNA using the QuantiTect Reverse Transcription Kit (Qiagen, Hilden, Germany). Real-time PCR was performed using SYBR Green PCR Master Mix (Invitrogen, Carlsbad, CA, United States) on a CFX96 Real-Time PCR Detection System (Bio-Rad, Hercules, CA, United States) or a LightCycle480 II Real-Time PCR Detection System (Roche, Basel, Switzerland). The sequence-specific primers for the genes are listed in Supplementary Table S1. The fold change in expression of each gene was calculated using the $2^{-\Delta\Delta CT}$ method, with glyceraldehyde-3-phosphate dehydrogenase as an internal control.

Agarose gel electrophoresis

The PCR-amplified products were electrophoretically separated on 3% agarose gel in Tris–acetate–EDTA (TAE) buffer (1×). Agarose gels were stained with Nucleic Acid Dye and visualized under UV light from the Gel Record System (ChemiDoc XRS+, Bio-Rad, Hercules, CA, United States).

Flow cytometry analysis

Flow cytometry analysis was performed as previously described (Jablonski et al., 2015). We use FFA mixture to stimulate differentiated and mature macrophages for 24 h, and then use trypsin to prepare a single cell suspension for fluorescence-activated cell sorting (FACS) staining. After centrifuged at 500x *g* for 5 min the supernatants were removed, then the cells were resuspended with 50 μL of Fc receptor blocker and incubate at room temperature for 20 min. Afterward, cells were incubated with anti-mouse CD38 antibody at room temperature for 20 min. After the antibody incubation, the cells were diluted with 400 μL PBS and analyzed on a flow cytometer (CytoFLEX-S, Beckman Coulter, Inc., CA, United States) according to the manufacturer's instructions.

Western blot

Western blotting was performed as previously described (Huang et al., 2014). Briefly, cells were lysed in lysis buffer which were added with phosphatase inhibitors and protease. Proteins were quantified by the Bradford assay (Thermo Fisher Scientific, Waltham, MA, United States). The proteins were fractionated on a 10%SDS-PAGE gel and then transferred onto polyvinylidene difluoride membranes. The membranes were incubated with different primary antibodies overnight at 4°C and subsequently incubated with Peroxidase-conjugated secondary antibodies. Enhanced chemiluminescence reagents (Merck Millipore, Darmstadt, Germany) were used to visualize the blots according to manufacturer's protocol. ImageJ4.1 software was used to quantify the immunoreactive bands.

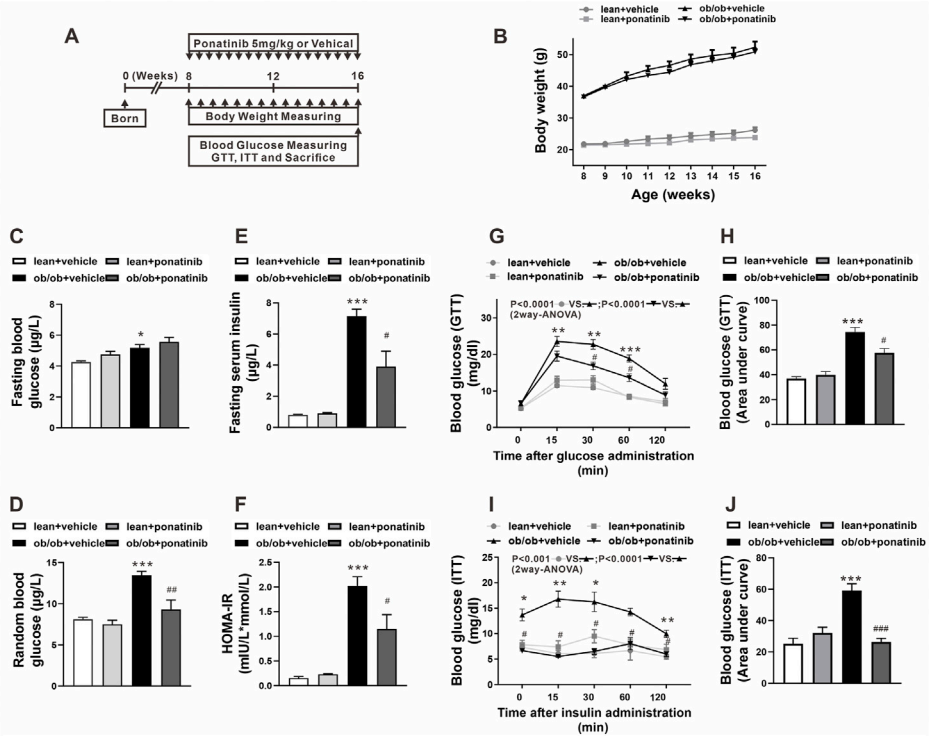

FIGURE 1
Ponatinib improved insulin resistance in ob/ob mice **(A)** Schematic diagram of experimental protocol for studying the effect of ponatinib in ob/ob mice and lean mice. **(B)** Body weight of ob/ob mice and the lean mice after administration with or without ponatinib. $n = 5$. **(C–F)** Fasting blood glucose **(C)**, random blood glucose **(D)**, fasting serum insulin **(E)** and HOMA-IR index **(F)** of ob/ob and lean mice with or without ponatinib. $n = 5$. **(G–J)** GTT **(G)** and ITT **(I)** performed on ob/ob mice and lean mice after 8-week administration with or without ponatinib. Blood glucose area under the curve **(H–J)** measured from G and I. $n = 5$. Statistical comparisons were performed with RM two-way ANOVA with Bonferroni's multiple comparisons test. **(G–I)** and one-way ANOVA **(B–J)** followed by Bonferroni's multiple comparisons post hoc test. Data represent mean ± SEM. $^{*}p < 0.05$, $^{**}p < 0.01$, $^{***}p < 0.001$ *vs.* lean + vehicle. $\#p < 0.05$, $\#\#p < 0.01$, $\#\#\#p < 0.001$ vs. ob/ob + vehicle.

Statistical analyses

All data are expressed as the mean ± standard error of the mean (SEM). Statistical analysis was performed using SPSS 16.0 software (SPSS Inc., Chicago, IL, United States) and unpaired two-tailed Student's t-test or one-way analysis of variance (ANOVA) followed by Bonferroni's multiple comparisons post hoc test with a 95% confidence interval. Correlation analyses were performed using the Pearson correlation test. $p < 0.05$ was considered statistically significant.

Results

Ponatinib improved insulin sensitivity in obese mice

To clarify the potential effect of ponatinib on metabolic disorders during obesity, ponatinib was orally administered to leptin-deficient (ob/ob) mice and the control mice (lean) once-daily for 8 weeks (Figure 1A). As expected, body weight and weight gain of ob/ob mice were significantly higher than those of lean mice, but ponatinib treatment had no effect on body weight in both two groups (Figure 1B). Both the fasting and the random blood glucose levels in ob/ob mice were increased compared with the lean mice at 16 weeks (Figures 1C,D). Ponatinib did not affect the fasting glucose level in ob/ob mice and control mice (Figure 1C). However, the random blood glucose level of ob/ob mice was significantly reduced after ponatinib administration (Figure 1D). Evidently, ob/ob mice at 16 weeks have higher fasting serum insulin level and homeostasis model assessment of insulin resistance (HOMA-IR) value compared with lean mice, ponatinib treatment partially restored these abnormal increases. (Figures 1E,F). Moreover, ponatinib ameliorated glucose tolerance and insulin sensitivity in ob/ob mice as determined by intraperitoneal glucose tolerance test (GTT) and insulin tolerance test (ITT) (Figures 1G–J).

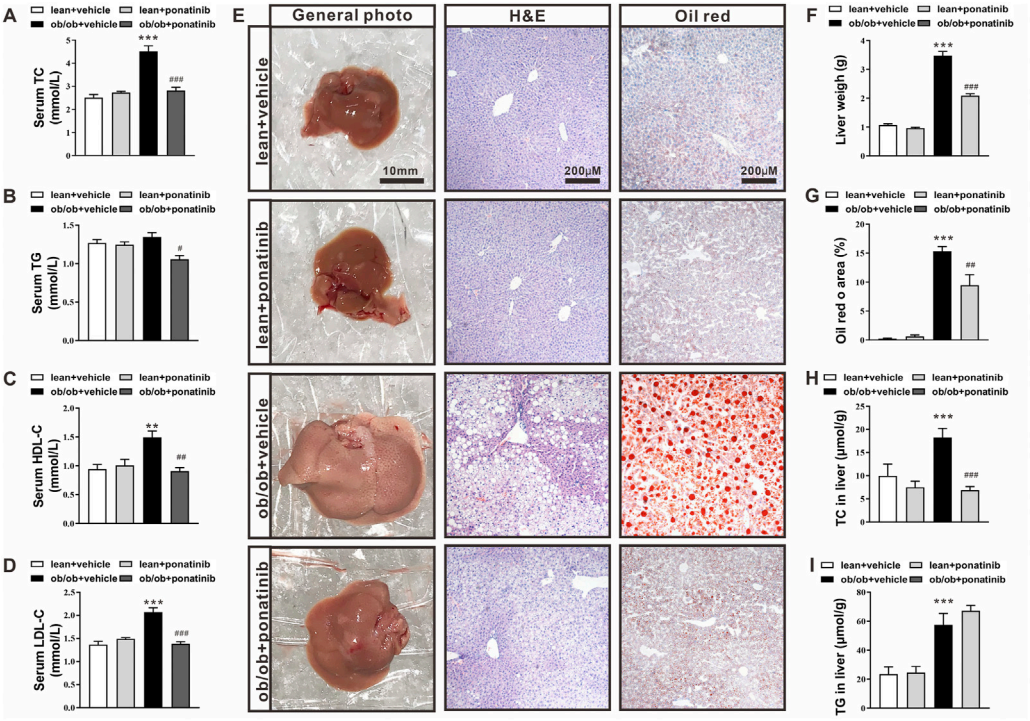

FIGURE 2
Ponatinib improved lipid ectopic deposition in ob/ob mice **(A–D)** Serum TC **(A)**, TG **(B)**, HDL **(C)**, LDL **(D)** of ob/ob mice and lean mice treated with or without ponatinib. $n = 5$. **(E)** Representative images of liver, HE and Oil Red O staining of livers tissues from ob/ob mice and lean mice with or without ponatinib. $n = 5$. Scale bar,10 mm, 200 μm. **(F)** Liver weight in ob/ob mice and control mice treated with ponatinib or vehicle. $n = 5$. **(G)** Quantification of oil red area from **(E) (H–I)** Liver TC **(H)**, TG **(I)** levels in ob/ob mice or lean mice administrated with ponatinib or vehicle. $n = 5$. Statistical comparisons were performed with one-way ANOVA **(A–D) (F–I)** followed by Bonferroni's multiple comparisons post hoc test. Data represent mean ± SEM. $^{**}p < 0.01$, $^{***}p < 0.001$ vs. lean + vehicle. $\#p < 0.05$, $\#\#p < 0.01$, $\#\#\#p < 0.001$ vs. ob/ob + vehicle.

Ponatinib reduced serum lipid levels and hepatic lipid deposition in ob/ob mice

At 16 weeks of age, ob/ob mice exhibited higher levels of serum total cholesterol (TC), high density lipid cholesterol (HDL-C), and low density lipid cholesterol (LDL-C) compared with lean mice. Ponatinib intervention significantly reduced serum TG, TC, HDL-C, and LDL-C in ob/ob mice (Figures 2A–D). Histological analysis using HE and Oil Red-O staining revealed greater lipid accumulation in livers of ob/ob mice than lean mice (Figure 2E). Consistently, ob/ob mice exhibited increased liver weight (Figure 2F) and elevated TG and TC levels in the liver (Figures 2F–I). Ponatinib treatment obviously reduced liver lipid accumulation, liver weight, and lowered liver TC levels of ob/ob mice (Figures 2E–H) However, ponatinib had no effect on liver TG levels of ob/ob mice (Figure 2I).

Ponatinib protects the function of obese adipose tissue and suppresses inflammation

Although the liver weight of ob/ob mice in ponatinib group was significantly lower than that in vehicle group, we surprisingly found that the visceral white adipose tissue (WAT) weight of ob/ob mice after ponatinib treatment was not reduced but increased compared to the vehicle group (Figures 3A,B). Thus, we assessed the morphology of these WAT by HE staining (Figure 3C). We found that the size of adipocytes in ponatinib treated group tended to be larger than that in the vehicle group (Figure 3D). Studies have shown that the size distribution of adipocytes in obese individuals, especially the increase of small adipocytes, is not only highly correlated with type 2 diabetes, but also reflects the dysfunctions in adipose storage and inflammation (McLaughlin et al., 2007; McLaughlin

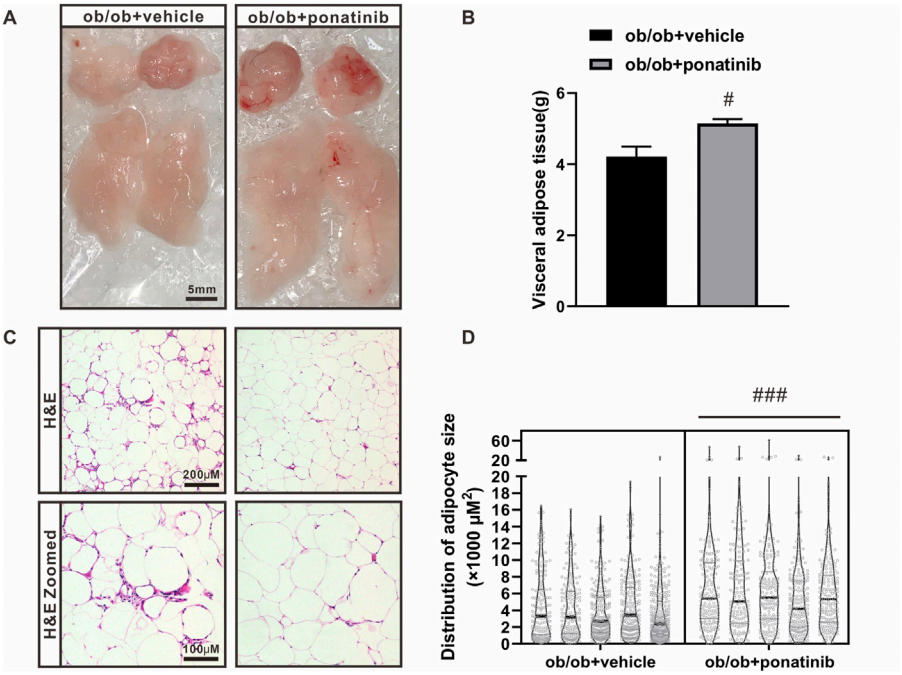

FIGURE 3
The lipid storage function of adipose tissue in ob/ob mice was retained by ponatinib **(A)** The visceral white adipose tissue of ob/ob mice in ponatinib group or vehicle group. *n* = 5. Scale bar, 5 mm. **(B)** Weight of visceral white adipose tissue of ob/ob mice treated with or without ponatinib. *n* = 5. **(C)** Representative images of HE staining of visceral white adipose tissue of ob/ob mice in ponatinib group or vehicle group. *n* = 5. Scale bar, 100 μm and 200 μm. **(D)** Analyzation of adipocyte size in **(C)** *n* = 5. Statistical comparisons were performed with unpaired two-tailed Student's t-test **(B–D)**. Data represent mean ± SEM. $^{\#}p < 0.05$, $^{\#\#\#}p < 0.001$*vs.* ob/ob + vehicle.

et al., 2010; Fang et al., 2015). To this end, we investigated the infiltration of macrophages and the severity of inflammation in obese WAT of this model. We observed that the intervention of ponatinib could not only significantly reduce the infiltration of macrophages in obese WAT, but also reduce the amount of "crown like" structure (Figures 4A–C). Consistently, several pro-inflammatory cytokines such as IL-1β, TNF-α, IL-18, IL-6, and resistin were remarkably decreased after ponatinib treatment (Figures 4D–H). Moreover, ponatinib also significantly increased the level of adiponectin in obese WAT (Figure 4I), but there were no significant differences in other anti-inflammatory cytokines such as IL-10 and IL-1RA (Figures 4J,K). There was no change in macrophage infiltration and inflammatory cytokine levels in the liver of ob/ob mice after ponatinib treatment (Figures 5A–E).

Ponatinib had no effect on the metabolic phenotype of hepatocytes and adipocytes

In order to further study the specific regulation of ponatinib on obesity-related metabolic disorders, we conducted a series of *in vitro* experiments. Firstly, we exposed human fetal hepatocyte line, LO2 (Hu et al., 2013), to a mixture of free fatty acids (palmitic acid, oleic acid and BSA) for 24 h to induce lipid drop disposition. By Oil Red-O staining, we observed that there is a higher degree of lipid droplet deposition under culturing with FFA compared to BSA, but ponatinib had no significant effect on the lipid deposition in these cells (Figures 6A,B). Secondly, we used the classic IBMX-Dex-insulin triple induction method to drive the differentiation of preadipocyte line, 3T3-L1, into adipocytes. However, we did not observe any significant change in the differentiation ratio of adipocytes by ponatinib (Figures 6C,D). Finally, we examined the effect of ponatinib on insulin sensitivity of 3T3-L1 adipocytes. Western blot results showed that ponatinib did not change the phosphorylation levels of insulin receptor-beta (p-IRβ, Tyr1150/1151), insulin receptor substrate-1 (IRS1, Ser636/639) and Akt (Ser473) in adipocytes under the stimulation of insulin (Figures 6E–H).

These results showed that the effects of ponatinib on the metabolic properties of ob/ob mice cannot be reproduced in the individual hepatocyte or adipocyte cell lines *in vitro*. We then analyzed the expression profile from the Genotype-Tissue Expression Project (GTEx, version8) to check the

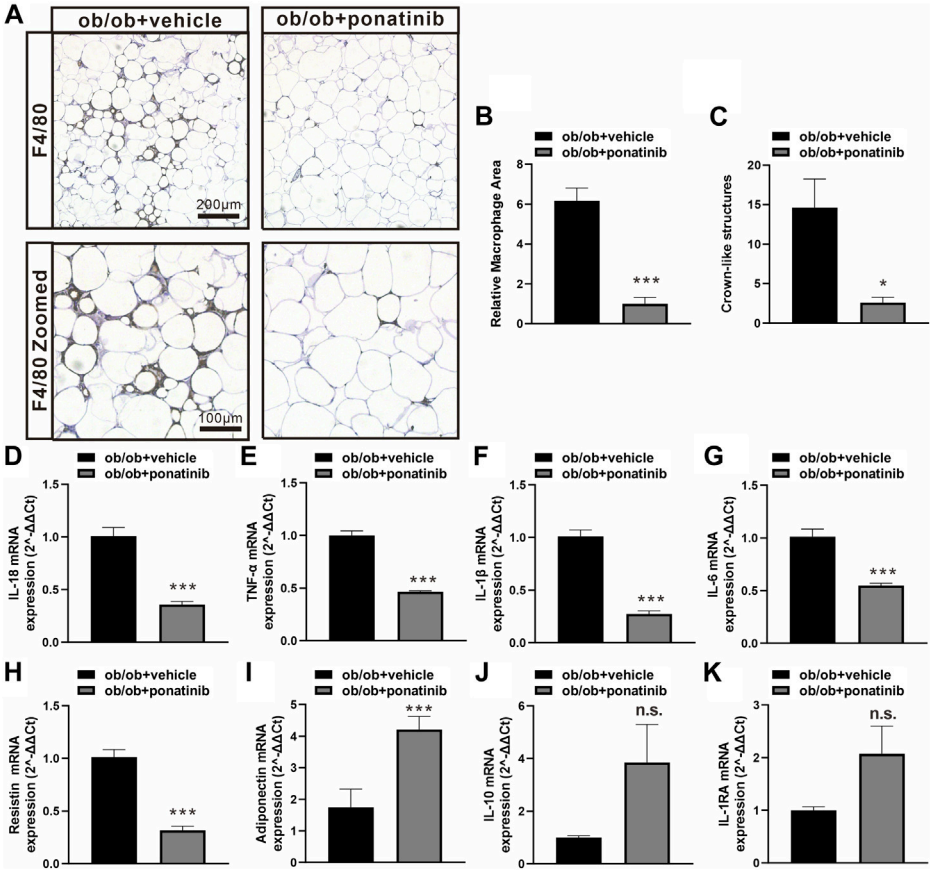

FIGURE 4
Ponatinib inhibited macrophage infiltration and cytokine expression in adipose tissue **(A)** Representative image of F4/80 immunostaining of visceral adipose sections of ob/ob mice in ponatinib group and control group. $n = 5$. Scale bar, 100 μm and 200 μm **(B)** Quantification of relative macrophage from **(A)** $n = 5$ **(C)** Quantitative analysis of crown-like structures from **(A)** $n = 5$. **(D–K)** mRNA levels of gene associated with inflammatory response in visceral adipose tissue of ob/ob mice treated with ponatinib or vehicle. $n = 4$. Statistical comparisons were performed with unpaired two-tailed Student's t-test **(B–K)**. Data represent mean ± SEM. n.s. $p > 0.05$, $^{*}p < 0.05$, $^{***}p < 0.001$ vs. ob/ob + vehicle.

expression profile of ponatinib targets in WAT, liver and skeletal muscle (Lonsdale et al., 2013). As the data showed, about one-third of the 30 major targets of ponatinib were expressed in adipose tissue, but not in liver or skeletal muscle (Figure 6I). Given that there is a range of ponatinib targets expressed in adipose tissue, we were wondering why does ponatinib have no effect on insulin sensitivity in adipocytes cultured *in vitro*? Considering that macrophage is a crucial type of cell in regulating adipose tissue function, we next isolated mouse bone marrow-derived macrophages (BMDM) and compared its expression of ponatinib targets with adipose, liver and skeletal muscle tissue by RT-PCR. Consistent with the previous study (Lowell, 2004), we confirmed the expression of Abl1, Fgr, Hck, Lyn, and Csf1r gene in BMDM; Furthermore, except of Fgfr1, which was expressed in adipose tissue, the rest of these targets could hardly be detect in adipose, liver or skeletal muscle tissues by RT-PCR, i.e., CT value ≥ 35. (Figure 6J; Supplementary Table S2).

Ponatinib blocked free fatty acid-induced inflammatory activation of macrophages

In view of the expression pattern of ponatinib's high affinity targets in macrophages, we speculated whether the inflammatory activation of ATMs in obesity would be regulated by ponatinib. FFA, one of the major damages associated molecular patterns (DAMP) released by apoptotic adipocytes in obese adipose tissue, acts as a crucial stimulus in the inflammatory phenotype transformation of ATMs. Therefore, we analyzed the distribution of CD38, a murine M1 macrophage marker (Jablonski et al., 2015), in BMDM cultured with FFA. As showed by flow cytometry analysis, most of the naive BMDMs transformed into CD38 positive M1 macrophages under FFA stimulation, while the expression intensity of CD38 and the proportion of M1 macrophages decreased significantly under the intervention of ponatinib (Figures 7A–C). Furthermore, we analyzed the expression of inflammatory factors in FFA treated BMDMs. QPCR results showed that the expression levels of IL-1β, TNF-α, IL-

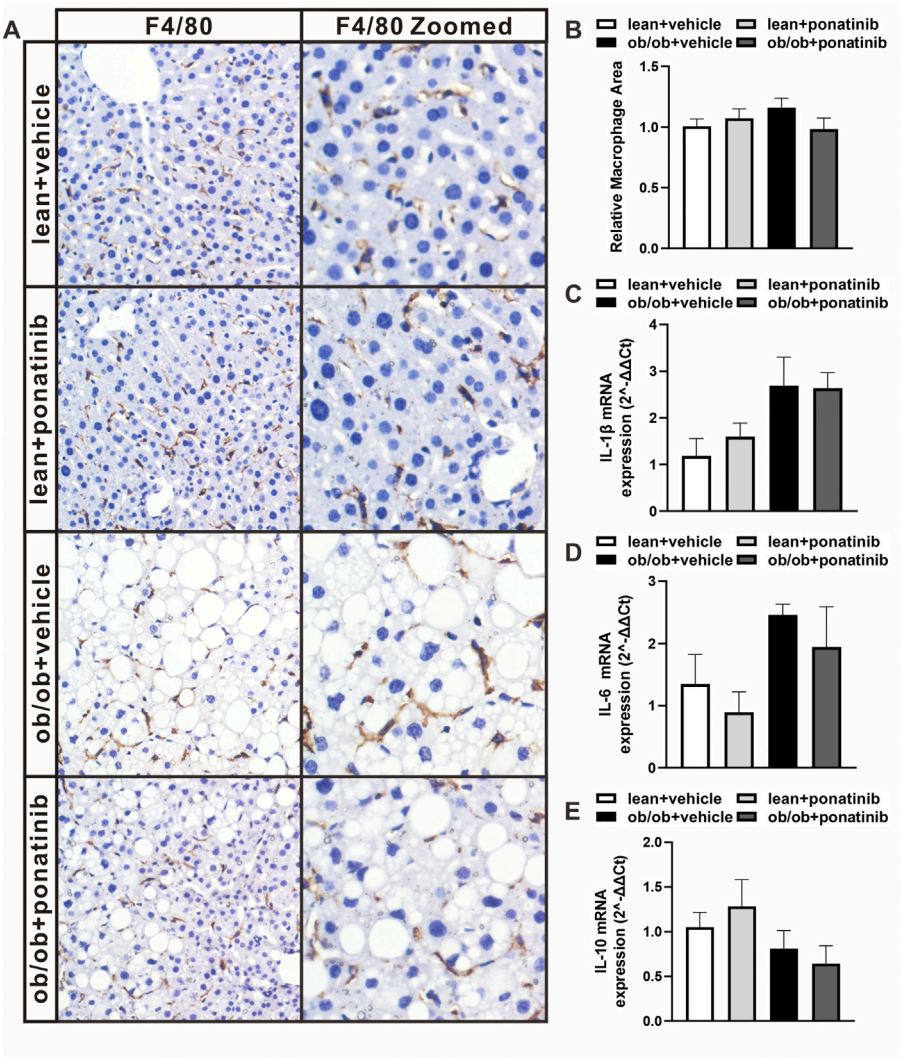

FIGURE 5
Ob/ob mice and lean mice had similar macrophage infiltration and inflammatory factor levels in liver with or without ponatinib. **(A)** Representative image of F4/80 immunostaining of liver sections of ob/ob mice and lean mice administrated with ponatinib or vehicle. *n* = 5. **(B)** Relative macrophage area of each group from **(A)** n = 5. **(C–E)** IL-1β, IL-6, and IL-10 mRNA transcription from liver of ob/ob mice and lean mice treated with or without ponatinib measured by qPCR. *n* = 5. Statistical comparisons were performed with one-way ANOVA **(B–D)** followed by Bonferroni's multiple comparisons post hoc test. Data represent mean ± SEM.

18, IL-6 and resistin in FFA treated group were significantly higher than those in BSA group, ponatinib treatment significantly blocked the effects of FFA (Figures 7D–H). In addition, ponatinib also reversed the inhibition of IL-10 by FFA (Figure 7I).

Ponatinib protected insulin sensitivity of adipocytes co-cultured with macrophages

As ponatinib hinders the FFA-induced inflammatory phenotype transformation of macrophages, we are curious whether ponatinib can improve the insulin sensitivity of adipose tissue through this function. So we then designed the following co-culture experiments of BMDMs and 3T3-L1 cells (Figure 8A). On one hand, we used FFA to induce the inflammatory phenotype of BMDMs on the eighth day of differentiation, with or without ponatinib. On the other, 3T3-L1 cells were used to differentiate into adipocyte. These two types of cells were then co-cultured at the 10th day for 24 h, and the insulin sensitivity of 3T3-L1 adipocytes was assessed by western blot. Results showed that FFA activated BMDMs co-culture impaired adipocyte insulin sensitivity, in which the phosphorylation levels of IRβ(Tyr1150/1151), IRS1(Ser636/639) and Akt (Ser473) under the stimulation of insulin were significantly

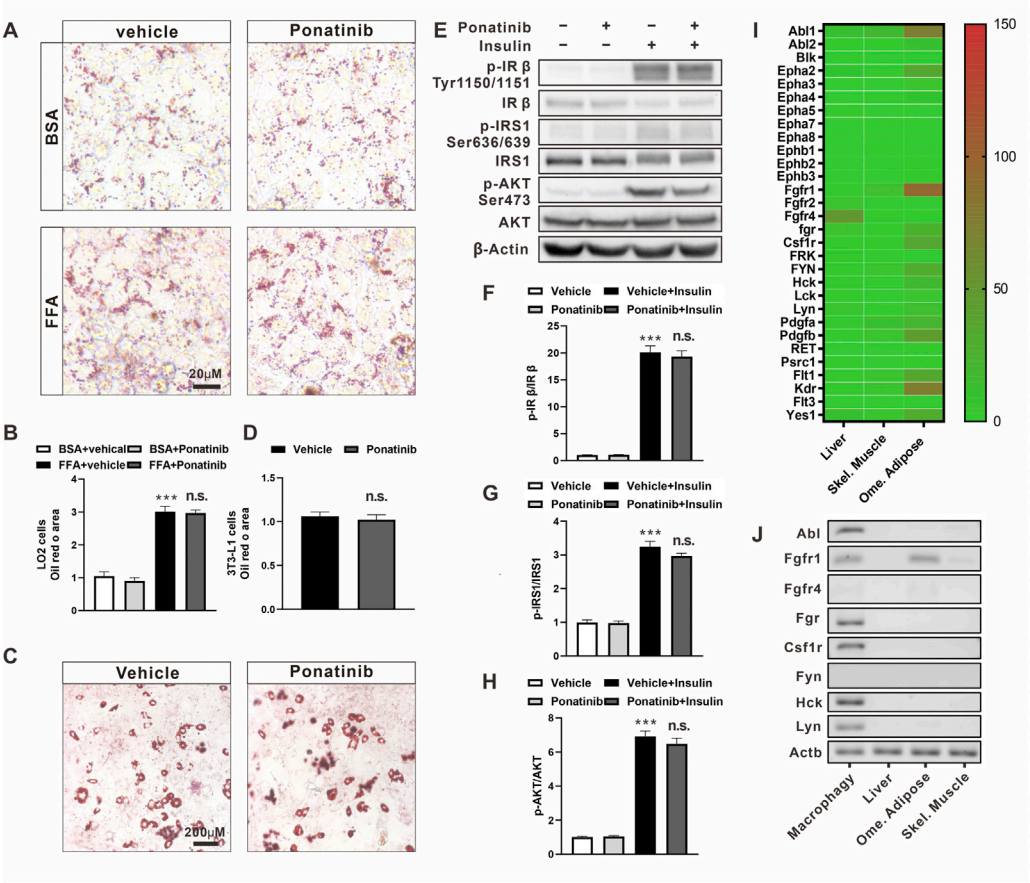

FIGURE 6
The metabolic profile of hepatocytes and adipocytes was not directly affected by ponatinib. **(A)** Representative Oil Red O staining of LO2 cells administrated with ponatinib or vehicle after FFA or BSA stimulation for 24 h $n = 6$. Scale bar, 20 μm **(B)** Quantitative analysis of oil red area of LO2 cells in **(A)**. Statistical comparisons were performed with one-way ANOVA followed by Bonferroni's multiple comparisons post hoc test. Data represent mean ± SEM, ***$p < 0.001$ vs. BSA + vehical; n. s. $p > 0.05$ *vs.* FFA + Vehicle. **(C)** Representative Oil Red O staining of 3T3-L1 adipocytes treated with ponatinib or vehicle. $n = 6$. Scale bar, 200 μm **(D)** Quantitative analysis of oil red area of 3T3-L1 adipocytes in **(C)**. $n = 6$. Statistical comparisons were performed with unpaired two-tailed Student's t-test, Data represent mean ± SEM, n. s. $p > 0.05$ vs. Vehicle. **(E)** Representative western blot showing levels of total and phosphorylation of IR-β (Tyr1150/1151), IRS1(Ser636/639), AKT (Ser473) of 3T3-L1 adipocytes in response to insulin stimulation for 30 min with or without ponatinib treatment. $n = 4$. **(F–H)** Quantification of phosphorylation of IR-β (Tyr1150/1151), IRS1 (Ser636/639), AKT (Ser473) expression level in **(E)**. $n = 4$. Statistical comparisons were performed with one-way ANOVA followed by Bonferroni's multiple comparisons post hoc test. Data represent mean ± SEM, ***$p < 0.001$ vs. Vehical; n. s. $p > 0.05$ vs. Vehicle + Insulin. **(I)** The expression profile of ponatinib's high-affinity targets in liver, skeletal muscle and omentum adipose from Genotype-Tissue Expression (GTEx) Project. Color scale indicates mean TPM (transcripts per million) value. **(J)** Representative electropherogram of one of six mice qPCR products to verify FGR, HCK, Lyn, CSFR, Fyn, FGFR, and ABL mRNA expression levels in BMDM, visceral fat, liver, and skeletal muscle.

lower than those cultured alone. In contrast, ponatinib weakened the activation of BMDM by FFA, thereby preserving the response of adipocytes to insulin signals under co-culture, which is reflected in the restored phosphorylation level of IRβ, IRS1 and Akt (Figures 8B–E).

Discussion

Although the association between obesity and impaired insulin sensitivity has long been recognized, there are still subgroups of obese individuals whose insulin sensitivity is preserved (Appleton et al., 2013). These insulin-sensitive and insulin-resistant obese individuals have no significant difference in BMI, but WAT of the latter one has undergone severe adipose tissue remodeling. Adipose tissue remodeling refers to the dramatic changes in the cellular composition and microenvironment of adipose tissue triggered by excess calories, including hypoxia, fibrosis, and accumulation of pro-inflammatory macrophages (Vishvanath and Gupta, 2019). Similarly, A series of animal studies also showed that the expansion of "healthy" adipose tissue does not impair

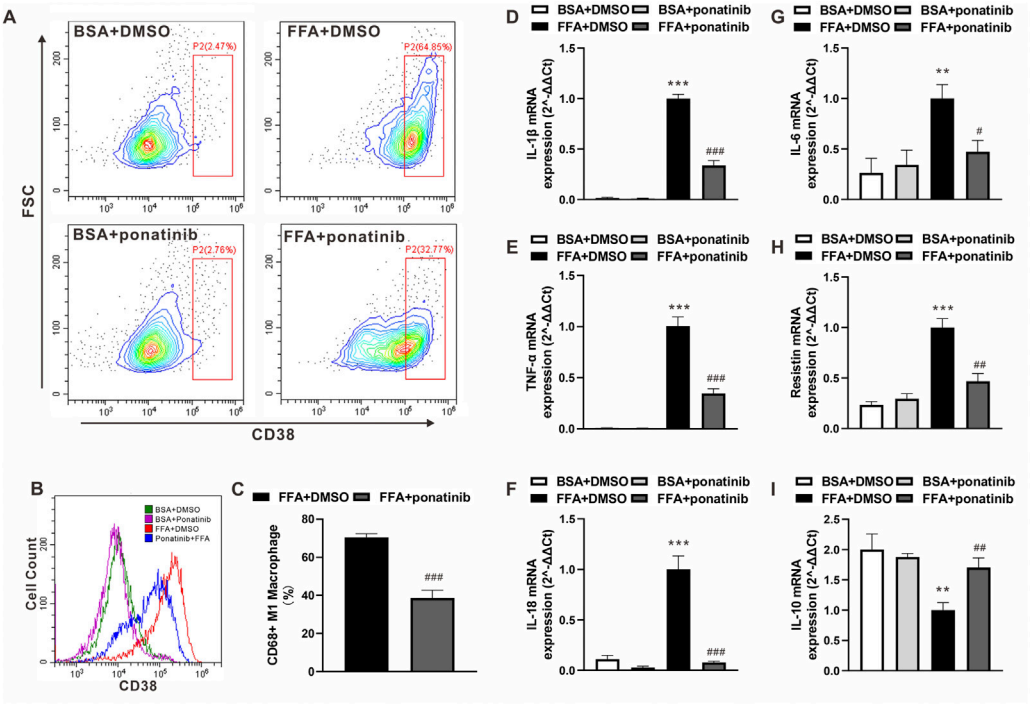

FIGURE 7
Ponatinib attenuated FFA induced Inflammatory phenotypic transformation of macrophages. **(A)** Flow cytometry analysis of the distribution of CD38 in BMDM cultured with FFA or BSA after treated with ponatinib or vehicle. **(B)** Representative overlayed histogram in **(A)** **(C)** Analysis of CD38 positive M1 macrophage ratio after FFA treatment in **(A)** $n = 6$. **(D–I)** mRNA levels of gene associated with inflammatory response in FFA treated BMDMs with or without ponatinib. $n = 4$. Statistical comparisons were performed with unpaired two-tailed Student's t-test **(C)** or one-way ANOVA **(D–I)** followed by Bonferroni's multiple comparisons post hoc test. Data represent mean ± SEM, $^{**}p < 0.01$, $^{***}p < 0.001$ *vs.* BSA + DMSO. $^{\#}p < 0.05$, $^{\#\#}p < 0.01$, $^{\#\#\#}p < 0.001$ vs.FFA + DMSO.

systemic insulin sensitivity. Slc2a4, Adipoq, mitoNEET, and Tnmd transgenic mice had an equal or even higher degree of obesity than their littermates, but their metabolic profile is healthier (Shepherd et al., 1993; Kim et al., 2007; Kusminski et al., 2012; Senol-Cosar et al., 2016). In our study, even if it failed to reduce the weight of obese mice or the mass of visceral adipose, ponatinib significantly attenuated the infiltration of macrophages and reduced pro-inflammatory cytokines in obese adipose tissue, and improved hepatic steatosis, hyperlipidemia and insulin resistance.

Leptin-deficient ob/ob mice are widely used in metabolic studies as a classic obese model. However, leptin seems to play a dual role in non-alcoholic fatty liver disease (NAFLD). It can prevent liver steatosis in the initial stage of NAFLD, but when the NAFLD progresses, it acts as a pro-inflammatory factor to promote non-alcoholic hepatitis (NASH) (Polyzos et al., 2015). In addition, although ob/ob mice can spontaneously form NAFLD under normal diet, the data showed that it is failed to further develop into typical hepatitis or hepatic fibrosis (Trak-Smayra et al., 2011). Unfortunately, this study could not further explore the effect of ponatinib on NASH due to the limitations of the ob/ob mouse model. For further study, high-fat diet (HFD) or methionine choline deficiency (MCD) models could be appropriate options (Soret et al., 2020).

Ponatinib is an orally active tyrosine kinase inhibitor that was originally designed to conquer the resistance mutations of BCR-ABL leukemia (O'Hare et al., 2009), but subsequent studies have shown that it has at least 30 high affinity targets (IC50 < 10 nm) (O'Hare et al., 2009). Due to these additional targets, recent growing evidence have indicated that ponatinib could exert benefits in the intervention of non-cancer diseases such as pulmonary hypertension, pulmonary fibrosis and cerebral cavernous malformations (Qu et al., 2015; Kang et al., 2016; Choi et al., 2018).

Here, ponatinib shows an inhibitory function in M1 macrophage polarization and adipose inflammation, however, the individual effects of each target of ponatinib are intriguing. In the high-affinity target spectrum of ponatinib, Csf1r undoubtedly plays a crucial role in the survival, proliferation and differentiation of myeloid cells, in addition, Fgr, Hck, Abl, and Lyn are also highly expressed in macrophages (Figure 6J) (Lowell, 2004; Tan et al., 2019). A recent study has shown that Fgr expression is up-regulated in macrophages of obese adipose tissue, and bone marrow Fgr deletion can inhibit

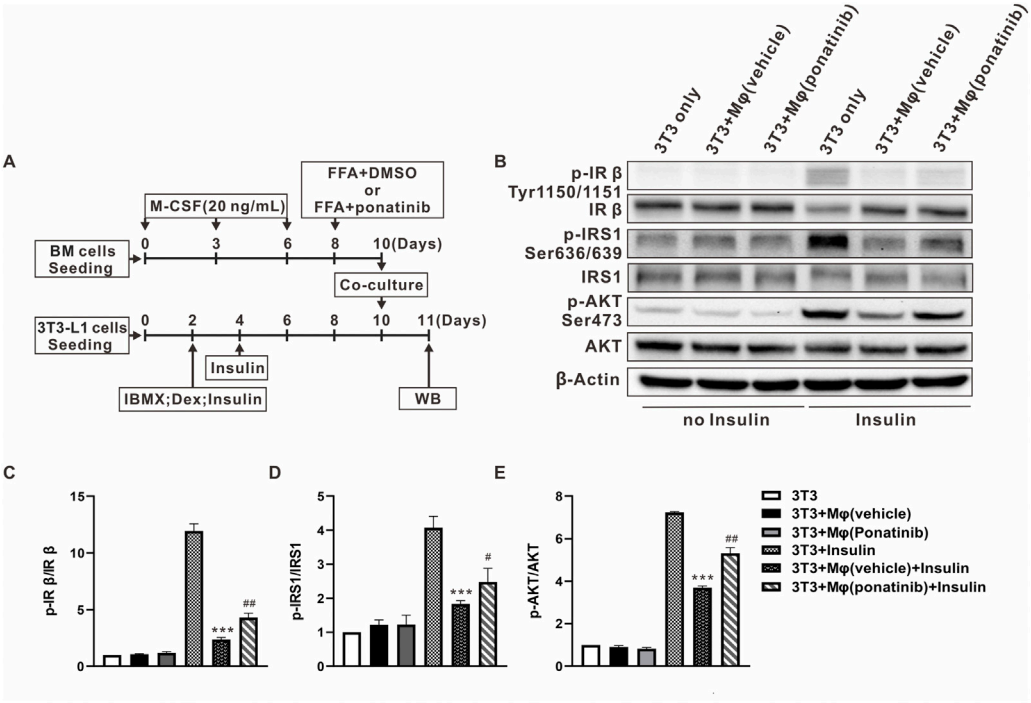

FIGURE 8
Insulin sensitivity of adipocytes co-cultured with macrophages was protected by ponatinib. **(A)** Schematic diagram of experimental design for studying the effect of ponatinib in insulin sensitivity of adipocytes co-cultured with macrophages. **(B)** Representative western blot showing levels of total and phosphorylation of IR-β (Tyr1150/1151), IRS1(Ser636/639), AKT (Ser473) of adipocytes co-cultured with macrophages in response to insulin for 30 min with or without ponatinib treatment. $n = 4$. **(C–E)** Quantification of phosphorylation of IR-β (Tyr1150/1151), IRS1(Ser636/639), AKT (Ser473) expression level in **(B)** $n = 4$. Statistical comparisons were carried out with one-way ANOVA **(C–E)** followed by Bonferroni's multiple comparisons post hoc test. Data represent mean ± SEM, $^{***}p < 0.001$ vs. 3T3+Insulin. $^{\#}p < 0.05$, $^{\#\#}p < 0.01$ vs. 3T3+Mφ(vehicle)+Insulin.

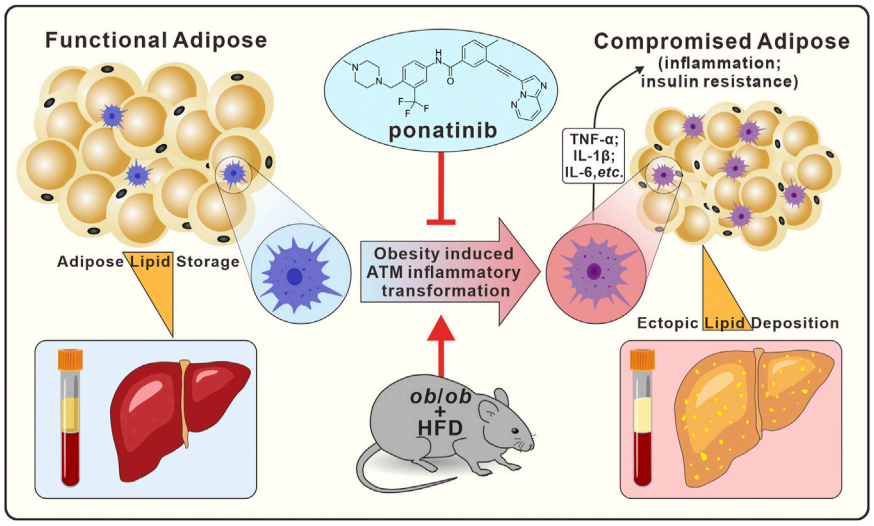

FIGURE 9
Graphical abstract. In ob/ob mice model, ponatinib inhibits obesity-induced adipose tissue macrophage inflammatory transformation, thereby inhibiting obesity adipose tissue inflammation and insulin resistance, accompanied by amelioration of ectopic lipid deposition in peripheral blood and liver.

adipose inflammation and metabolic dysfunction caused by M1 polarization of adipocyte macrophages in diet induced obesity (Acín-Pérez et al., 2020). In addition, although Hck and Abl is crucial for the activation and migration of macrophages (English et al., 1993; Cougoule et al., 2010; Zhou et al., 2020), the function of Hck and Abl in ATMs has not been investigated. In contrast to Fgr, Hck and Abl, Lyn is a unique member of the Src kinase family that negatively regulates innate immune response (Harder et al., 2001). Lyn agonist MLR-1023 has been reported to improve glucose tolerance in type 2 diabetic mice (Ochman et al., 2012). Taking together, the overall effect of ponatinib showed an improvement in the metabolic function of obese mice, but there are still some counterproductive targets in the target list of ponatinib. With the application of machine learning in drug design and optimization (Ekins et al., 2019; Kaiser et al., 2020; Walters and Barzilay, 2021), identifying a series of new compounds that were simultaneously optimized for on-target potency (e.g., Fgr, Hck, Abl) and off-target safety (e.g., Lyn) will provide more promising solutions for the pharmacological intervention of obesity-related metabolic disorders.

In conclusion, our present results indicated that ponatinib had a therapeutic effect on metabolic dysfunction such as insulin resistance, dyslipidemia, NAFLD and adipose tissue inflammation. Ponatinib exerted these effects through inhibiting the inflammatory phenotypic transformation of ATM in the context of obesity. These data provided unequivocally evidence to support the therapeutic effect of ponatinib in obesity-related metabolic disorders, and provide a theoretical basis for the future application of multi-target tyrosine kinase inhibitors in the metabolic disorders (Figure 9, Graphical abstract).

Data availability statement

The raw data supporting the conclusions of this article will be made available by the authors, without undue reservation.

Ethics statement

The animal study was reviewed and approved by Sun Yat-Sen University Animal Care and Use Committee.

Author contributions

FZ, JZ, and TZ conceived and designed the experiments; ZL, FZ, XL, YL, CH, FR, and JT performed the experiments, especially ZL, FZ, and XL carried out most of the experiments; SM, JHS, SL, JYS, XL, and SG analyzed the data; RP, FZ, and JZ wrote the manuscript. All authors participated in the reviewed the manuscript.

Funding

This work was supported by National Key R&D Program of China (2021YFA0805100), National Natural Science Foundation of China (81930106, U21A20342, 82003744, 82170545, 81903598, 82073839, 91739104, and 82204384), National Natural Science Foundation of Guangdong (2019A1515011295), GuangDong Basic and Applied Basic Research Foundation (2019A1515110872), High-level Health Team Foundation of Zhuhai (2018) and High Talents Scientific Research Foundation of Zhongshan School Medicine.

Acknowledgments

The Genotype-Tissue Expression (GTEx) Project was supported by the Common Fund of the Office of the Director of the National Institutes of Health, and by NCI, NHGRI, NHLBI, NIDA, NIMH, and NINDS. The data used for the analyses described in this manuscript were obtained from the GTEx Portal on 06/Feb/2021.

Conflict of interest

The authors declare that the research was conducted in the absence of any commercial or financial relationships that could be construed as a potential conflict of interest.

Publisher's note

Supplementary material

The Supplementary Material for this article can be found online at: https://www.frontiersin.org/articles/10.3389/fphar.2022.1040999/full#supplementary-material

References

Acín-Pérez, R., Iborra, S., Martí-Mateos, Y., Cook, E. C. L., Conde-Garrosa, R., Petcherski, A., et al. (2020). Fgr kinase is required for proinflammatory macrophage activation during diet-induced obesity. *Nat. Metab.* 2 (9), 974–988. doi:10.1038/s42255-020-00273-8

Appleton, S. L., Seaborn, C. J., Visvanathan, R., Hill, C. L., Gill, T. K., Taylor, A. W., et al. (2013). Diabetes and cardiovascular disease outcomes in the metabolically healthy obese phenotype: A cohort study. *Diabetes Care* 36 (8), 2388–2394. doi:10.2337/dc12-1971

Burhans, M. S., Hagman, D. K., Kuzma, J. N., Schmidt, K. A., and Kratz, M. (2018). Contribution of adipose tissue inflammation to the development of type 2 diabetes mellitus. *Compr. Physiol.* 9 (1), 1–58. doi:10.1002/cphy.c170040

Choi, J. P., Wang, R., Yang, X., Wang, X., Wang, L., Ting, K. K., et al. (2018). Ponatinib (AP24534) inhibits MEKK3-KLF signaling and prevents formation and progression of cerebral cavernous malformations. *Sci. Adv.* 4 (11), eaau0731. doi:10.1126/sciadv.aau0731

Cinti, S., Mitchell, G., Barbatelli, G., Murano, I., Ceresi, E., Faloia, E., et al. (2005). Adipocyte death defines macrophage localization and function in adipose tissue of obese mice and humans. *J. Lipid Res.* 46 (11), 2347–2355. doi:10.1194/jlr.M500294-JLR200

Cougoule, C., Le Cabec, V., Poincloux, R., Al Saati, T., Mège, J. L., Tabouret, G., et al. (2010). Three-dimensional migration of macrophages requires Hck for podosome organization and extracellular matrix proteolysis. *Blood* 115 (7), 1444–1452. doi:10.1182/blood-2009-04-218735

Ekins, S., Puhl, A. C., Zorn, K. M., Lane, T. R., Russo, D. P., Klein, J. J., et al. (2019). Exploiting machine learning for end-to-end drug discovery and development. *Nat. Mat.* 18 (5), 435–441. doi:10.1038/s41563-019-0338-z

English, B. K., Ihle, J. N., Myracle, A., and Yi, T. (1993). Hck tyrosine kinase activity modulates tumor necrosis factor production by murine macrophages. *J. Exp. Med.* 178 (3), 1017–1022. doi:10.1084/jem.178.3.1017

Fang, L., Guo, F., Zhou, L., Stahl, R., and Grams, J. (2015). The cell size and distribution of adipocytes from subcutaneous and visceral fat is associated with type 2 diabetes mellitus in humans. *Adipocyte* 4 (4), 273–279. doi:10.1080/21623945.2015.1034920

Frankfurt, O., and Licht, J. D. (2013). Ponatinib--a step forward in overcoming resistance in chronic myeloid leukemia. *Clin. Cancer Res.* 19 (21), 5828–5834. doi:10.1158/1078-0432.Ccr-13-0258

Guo, J. W., Liu, X., Zhang, T. T., Lin, X. C., Hong, Y., Yu, J., et al. (2020). Hepatocyte TMEM16A deletion retards NAFLD progression by ameliorating hepatic glucose metabolic disorder. *Adv. Sci.* 7 (10), 1903657. doi:10.1002/advs.201903657

Harder, K. W., Parsons, L. M., Armes, J., Evans, N., Kountouri, N., Clark, R., et al. (2001). Gain- and loss-of-function Lyn mutant mice define a critical inhibitory role for Lyn in the myeloid lineage. *Immunity* 15 (4), 603–615. doi:10.1016/s1074-7613(01)00208-4

Hu, X., Yang, T., Li, C., Zhang, L., Li, M., Huang, W., et al. (2013). Human fetal hepatocyte line, L-02, exhibits good liver function *in vitro* and in an acute liver failure model. *Transpl. Proc.* 45 (2), 695–700. doi:10.1016/j.transproceed.2012.09.121

Huang, L. Y., He, Q., Liang, S. J., Su, Y. X., Xiong, L. X., Wu, Q. Q., et al. (2014). ClC-3 chloride channel/antiporter defect contributes to inflammatory bowel disease in humans and mice. *Gut* 63 (10), 1587–1595. doi:10.1136/gutjnl-2013-305168

Jablonski, K. A., Amici, S. A., Webb, L. M., Ruiz-Rosado Jde, D., Popovich, P. G., Partida-Sanchez, S., et al. (2015). Novel markers to delineate murine M1 and M2 macrophages. *PLoS One* 10 (12), e0145342. doi:10.1371/journal.pone.0145342

Kahn, C. R., Wang, G., and Lee, K. Y. (2019). Altered adipose tissue and adipocyte function in the pathogenesis of metabolic syndrome. *J. Clin. Invest.* 129 (10), 3990–4000. doi:10.1172/JCI129187

Kaiser, T. M., Dentmon, Z. W., Dalloul, C. E., Sharma, S. K., and Liotta, D. C. (2020). Accelerated discovery of novel ponatinib analogs with improved properties for the treatment of Parkinson's disease. *ACS Med. Chem. Lett.* 11 (4), 491–496. doi:10.1021/acsmedchemlett.9b00612

Kang, Z., Ji, Y., Zhang, G., Qu, Y., Zhang, L., and Jiang, W. (2016). Ponatinib attenuates experimental pulmonary arterial hypertension by modulating Wnt signaling and vasohibin-2/vasohibin-1. *Life Sci.* 148, 1–8. doi:10.1016/j.lfs.2016.02.017

Kim, J. Y., van de Wall, E., Laplante, M., Azzara, A., Trujillo, M. E., Hofmann, S. M., et al. (2007). Obesity-associated improvements in metabolic profile through expansion of adipose tissue. *J. Clin. Invest.* 117 (9), 2621–2637. doi:10.1172/jci31021

Kratz, M., Coats, B. R., Hisert, K. B., Hagman, D., Mutskov, V., Peris, E., et al. (2014). Metabolic dysfunction drives a mechanistically distinct proinflammatory phenotype in adipose tissue macrophages. *Cell Metab.* 20 (4), 614–625. doi:10.1016/j.cmet.2014.08.010

Kusminski, C. M., Bickel, P. E., and Scherer, P. E. (2016). Targeting adipose tissue in the treatment of obesity-associated diabetes. *Nat. Rev. Drug Discov.* 15 (9), 639–660. doi:10.1038/nrd.2016.75

Kusminski, C. M., Holland, W. L., Sun, K., Park, J., Spurgin, S. B., Lin, Y., et al. (2012). MitoNEET-driven alterations in adipocyte mitochondrial activity reveal a crucial adaptive process that preserves insulin sensitivity in obesity. *Nat. Med.* 18 (10), 1539–1549. doi:10.1038/nm.2899

Lim, D. W., Bose, S., Wang, J. H., Choi, H. S., Kim, Y. M., Chin, Y. W., et al. (2017). Modified SJH alleviates FFAs-induced hepatic steatosis through leptin signaling pathways. *Sci. Rep.* 7, 45425. doi:10.1038/srep45425

Lonsdale, J., Thomas, J., Salvatore, M., Phillips, R., Lo, E., Shad, S., et al. (2013). The genotype-tissue expression (GTEx) project. *Nat. Genet.* 45 (6), 580–585. doi:10.1038/ng.2653

Lowell, C. A. (2004). Src-family kinases: Rheostats of immune cell signaling. *Mol. Immunol.* 41 (6-7), 631–643. doi:10.1016/j.molimm.2004.04.010

McLaughlin, T., Deng, A., Yee, G., Lamendola, C., Reaven, G., Tsao, P. S., et al. (2010). Inflammation in subcutaneous adipose tissue: Relationship to adipose cell size. *Diabetologia* 53 (2), 369–377. doi:10.1007/s00125-009-1496-3

McLaughlin, T., Sherman, A., Tsao, P., Gonzalez, O., Yee, G., Lamendola, C., et al. (2007). Enhanced proportion of small adipose cells in insulin-resistant vs insulin-sensitive obese individuals implicates impaired adipogenesis. *Diabetologia* 50 (8), 1707–1715. doi:10.1007/s00125-007-0708-y

McNelis, J. C., and Olefsky, J. M. (2014). Macrophages, immunity, and metabolic disease. *Immunity* 41 (1), 36–48. doi:10.1016/j.immuni.2014.05.010

O'Hare, T., Shakespeare, W. C., Zhu, X., Eide, C. A., Rivera, V. M., Wang, F., et al. (2009). AP24534, a pan-BCR-ABL inhibitor for chronic myeloid leukemia, potently inhibits the T315I mutant and overcomes mutation-based resistance. *Cancer Cell* 16 (5), 401–412. doi:10.1016/j.ccr.2009.09.028

Ochman, A. R., Lipinski, C. A., Handler, J. A., Reaume, A. G., and Saporito, M. S. (2012). The Lyn kinase activator MLR-1023 is a novel insulin receptor potentiator that elicits a rapid-onset and durable improvement in glucose homeostasis in animal models of type 2 diabetes. *J. Pharmacol. Exp. Ther.* 342 (1), 23–32. doi:10.1124/jpet.112.192187

Pineda-Torra, I., Gage, M., de Juan, A., and Pello, O. M. (2015). Isolation, culture, and polarization of murine bone marrow-derived and peritoneal macrophages. *Methods Mol. Biol.* 1339, 101–109. doi:10.1007/978-1-4939-2929-0_6

Polyzos, S. A., Kountouras, J., and Mantzoros, C. S. (2015). Leptin in nonalcoholic fatty liver disease: A narrative review. *Metabolism.* 64 (1), 60–78. doi:10.1016/j.metabol.2014.10.012

Pouwer, M. G., Pieterman, E. J., Verschuren, L., Caspers, M. P. M., Kluft, C., Garcia, R. A., et al. (2018). The BCR-ABL1 inhibitors imatinib and ponatinib decrease plasma cholesterol and atherosclerosis, and nilotinib and ponatinib activate coagulation in a translational mouse model. *Front. Cardiovasc. Med.* 5, 55. doi:10.3389/fcvm.2018.00055

Qi, G., Zhou, Y., Zhang, X., Yu, J., Li, X., Cao, X., et al. (2019). Cordycepin promotes browning of white adipose tissue through an AMP-activated protein kinase (AMPK)-dependent pathway. *Acta Pharm. Sin. B* 9 (1), 135–143. doi:10.1016/j.apsb.2018.10.004

Qu, Y., Zhang, L., Kang, Z., Jiang, W., and Lv, C. (2015). Ponatinib ameliorates pulmonary fibrosis by suppressing TGF-β1/Smad3 pathway. *Pulm. Pharmacol. Ther.* 34, 1–7. doi:10.1016/j.pupt.2015.07.004

Senol-Cosar, O., Flach, R. J., DiStefano, M., Chawla, A., Nicoloro, S., Straubhaar, J., et al. (2016). Tenomodulin promotes human adipocyte differentiation and beneficial visceral adipose tissue expansion. *Nat. Commun.* 7, 10686. doi:10.1038/ncomms10686

Shepherd, P. R., Gnudi, L., Tozzo, E., Yang, H., Leach, F., and Kahn, B. B. (1993). Adipose cell hyperplasia and enhanced glucose disposal in transgenic mice overexpressing GLUT4 selectively in adipose tissue. *J. Biol. Chem.* 268 (30), 22243–22246. doi:10.1016/s0021-9258(18)41516-5

Soret, P. A., Magusto, J., Housset, C., and Gautheron, J. (2020). *In vitro* and *in vivo* models of non-alcoholic fatty liver disease: A critical appraisal. *J. Clin. Med.* 10 (1), E36. doi:10.3390/jcm10010036

Tan, F. H., Putoczki, T. L., Stylli, S. S., and Luwor, R. B. (2019). Ponatinib: A novel multi-tyrosine kinase inhibitor against human malignancies. *Onco. Targets. Ther.* 12, 635–645. doi:10.2147/ott.S189391

Tilg, H., and Moschen, A. R. (2006). Adipocytokines: Mediators linking adipose tissue, inflammation and immunity. *Nat. Rev. Immunol.* 6 (10), 772–783. doi:10.1038/nri1937

Trak-Smayra, V., Paradis, V., Massart, J., Nasser, S., Jebara, V., and Fromenty, B. (2011). Pathology of the liver in obese and diabetic ob/ob and db/db mice fed a standard or high-calorie diet. *Int. J. Exp. Pathol.* 92 (6), 413–421. doi:10.1111/j.1365-2613.2011.00793.x

Van Gaal, L. F., Mertens, I. L., and De Block, C. E. (2006). Mechanisms linking obesity with cardiovascular disease. *Nature* 444 (7121), 875–880. doi:10.1038/nature05487

Vishvanath, L., and Gupta, R. K. (2019). Contribution of adipogenesis to healthy adipose tissue expansion in obesity. *J. Clin. Invest.* 129 (10), 4022–4031. doi:10.1172/jci129191

Walters, W. P., and Barzilay, R. (2021). Applications of deep learning in molecule generation and molecular property prediction. *Acc. Chem. Res.* 54 (2), 263–270. doi:10.1021/acs.accounts.0c00699

Zhou, Y., Feng, Z., Cao, F., Liu, X., Xia, X., and Yu, C. H. (2020). Abl-mediated PI3K activation regulates macrophage podosome formation. *J. Cell Sci.* 133 (11), jcs234385. doi:10.1242/jcs.234385

frontiers | Frontiers in Pharmacology

TYPE Review
PUBLISHED 16 January 2023
DOI 10.3389/fphar.2022.1046687

OPEN ACCESS

EDITED BY
Peixiang Zhang,
University of California, Los Angeles, United States

REVIEWED BY
Huaxun Wu,
Anhui Medical University, China
Merry Gunawan,
Santen Pharmaceutical Co., Ltd., Singapore

*CORRESPONDENCE
Sandeep K. Agarwal,
skagarwa@bcm.edu

†These authors have contributed equally to this work

SPECIALTY SECTION
This article was submitted to Inflammation Pharmacology, a section of the journal Frontiers in Pharmacology

RECEIVED 16 September 2022
ACCEPTED 05 December 2022
PUBLISHED 16 January 2023

CITATION
Bruera S, Chavula T, Madan R and Agarwal SK (2023), Targeting type I interferons in systemic lupus erythematous.
Front. Pharmacol. 13:1046687.
doi: 10.3389/fphar.2022.1046687

Targeting type I interferons in systemic lupus erythematous

Sebastian Bruera[1‡], Thandiwe Chavula[1‡], Riya Madan[2] and Sandeep K. Agarwal [1*]

[1]Section of Immunology, Allergy and Rheumatology, Department of Medicine, Baylor College of Medicine, Houston, TX, United States, [2]Section of General Internal Medicine, Department of Medicine, Baylor College of Medicine, Houston, TX, United States

Systemic lupus erythematosus (SLE) is a complex autoimmune disease with systemic clinical manifestations including, but not limited to, rash, inflammatory arthritis, serositis, glomerulonephritis, and cerebritis. Treatment options for SLE are expanding and the increase in our understanding of the immune pathogenesis is leading to the development of new therapeutics. Autoantibody formation and immune complex formation are important mediators in lupus pathogenesis, but an important role of the type I interferon (IFN) pathway has been identified in SLE patients and mouse models of lupus. These studies have led to the development of therapeutics targeting type I IFN and related pathways for the treatment of certain manifestations of SLE. In the current narrative review, we will discuss the role of type I IFN in SLE pathogenesis and the potential translation of these data into strategies using type I IFN as a biomarker and therapeutic target for patients with SLE.

KEYWORDS

lupus (SLE), interferons, rheumatology, dendritic cell, treatment

Introduction

Systemic Lupus Erythematosus (SLE) is a complex autoimmune disease clinically characterized by inflammation of tissues clinically manifesting as rashes, inflammatory arthritis, serositis, glomerulonephritis, central nervous system involvement and hematological abnormalities. SLE predominates in women of childbearing age with a 9:1 female to male prevalence and higher incidence in black and Hispanic women (McCarty et al., 1995; Izmirly et al., 2017; Izmirly et al., 2021). Genome Wide Association Studies (GWAS) have been key in identifying SLE susceptibility genes in different ancestral populations (Hom et al., 2008; International Consortium for Systemic Lupus Erythematosus et al., 2008; Sánchez et al., 2011; Sanchez et al., 2011; Bentham et al., 2015; Wang et al., 2021). Other factors including environmental, hormonal, and infections also promote risk of disease development (James et al., 2001; Costenbader et al., 2007; Cooper et al., 2010).

Therapeutic approaches to SLE patients depend on the disease manifestations and activity, but ultimately seek to achieve remission or low disease activity using a variety of immunomodulatory and immunosuppressive therapies. Commonly used therapeutics

include hydroxychloroquine, methotrexate, azathioprine, mycophenolate mofetil, and cyclophosphamide. Treatment paradigms in SLE is now entering the age of biologics targeting specific cellular targets and cytokines. Belimumab, a monoclonal antibody that targets B Lymphocyte stimulator (BLys) and inhibits the survival of autoreactive B cells, is approved for use in a variety of manifestations of SLE including lupus nephritis (Baker et al., 2003; Furie et al., 2011; Navarra et al., 2011). Based on extensive preclinical and clinical studies further detailed in this review, the type I interferon (IFN) pathway has now become a new therapeutic target (Fure et al., 2019; Morand et al., 2020).

Immunologically, SLE is characterized by activation of aberrant autoreactive T and B cell activation, autoantibody production against nuclear antigens and immune complex formation. In addition, innate immunity is central to the immunopathogenesis of SLE. Much attention has focused on type I IFN production by plasmacytoid dendritic cells (pDCs) which activates multiple immune cells and is central in B cell activation and autoantibody production (Choi et al., 2012; Pan et al., 2020). There is growing interest in the therapeutic targeting of type I IFNs in SLE. In this review, we will discuss the role of type I IFNs in SLE immunopathogenesis starting with a basic overview of type I interferons and murine models of lupus. We will also discuss translational studies in SLE patients that demonstrate the importance of type I interferons in SLE and finally discuss the more recent clinical trials that led to the use of therapeutics targeting type I interferons being used in the clinics for the management of SLE.

Biology and function of type I interferons

Type I IFNs are a family of cytokines that mediate responses to antiviral infection. Discovered in 1957 as the initial defense to viral infections (Isaacs and Lindenmann, 1957), our understanding has expanded with numerous studies implicating their involvement in cell growth regulation, immune cell activation, bacterial responses, and autoimmunity. Type I IFNs also possess anti-tumor properties including immune-editing, inhibition of cell growth, and angiogenesis (Yano et al., 1999; Dunn et al., 2005; Swann et al., 2007). The IFN-I locus in humans codes for IFN-α

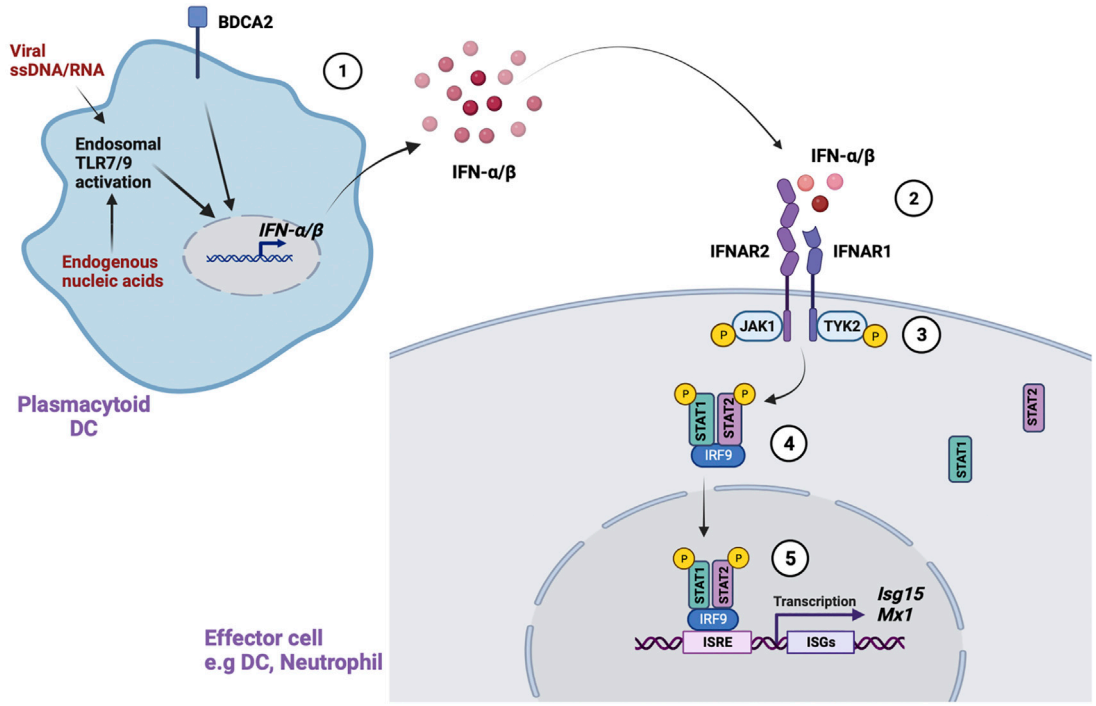

FIGURE 1
Type 1 IFN signaling. Type 1 IFN signaling is mediated through several steps. (McCarty et al., 1995). Activation of endosomal TLR7/9 by viral ssDNA/RNA or endogenous nucleic acids in pDCs leads to IFN-α/β production. Activation of an important receptor, BDCA2, also promotes IFN-α/β production (Izmirly et al., 2017). In the canonical pathway, IFN-α/β binds to the IFN-α receptor (IFNAR) in IFN responsive cells (Izmirly et al., 2021). This leads to phosphorylation and activation of IFNAR associated JAKs (JAK1, Tyk2) (International Consortium for Systemic Lupus Erythematosus et al., 2008). The activated JAKs phosphorylate STAT1/STAT2, which form a heterodimer that further complexes with IRF9 in the cytoplasm (Hom et al., 2008). Finally, the STAT1-STAT2-IRF9 complex translocates to the nucleus, binds to conserved IFN-stimulated response elements (ISREs), and leads to transcription of IFN stimulated genes (ISGs).

(13 subtypes), IFN-β, IFN-ε, IFN-ω, and IFN-κ. This review focuses on IFN-α and IFN-β. The production of IFN-α is predominant in dendritic cells (DCs), with pDCs being the most potent producers (Cella et al., 1999; Siegal et al., 1999). Myeloid DCs, monocytes and macrophages also produce IFN-α albeit at lower levels (Izaguirre et al., 2003). IFN-β is encoded by a single *IFNβ* gene and is mostly produced by fibroblasts and epithelial cells (Reis et al., 1989; Erlandsson et al., 1998).

Type I IFN signaling

All type I IFNs bind a common receptor called IFN-α receptor (IFNAR) (Figure 1). IFNAR is a transmembrane receptor consisting of two subunits, IFNAR1 (Uzé et al., 1990) and IFNAR2 (Novick et al., 1994) that interact with a group of kinases called Janus activated kinases (JAKs) in the cytoplasm. IFNAR1 constitutively associates with tyrosine kinase 2 (TYK2) whereas IFNAR2 associates with JAK1 (Velazquez et al., 1992; Domanski et al., 1995). These JAKs activate a group of transcription factors called signal transducer and activator of transcription (STAT). Extensive complementary work by James Darnell, Ian Kerr and George Stark established the JAK-STAT signaling as the major pathway through which type 1 IFNs mediate their effects (Darnell et al., 1994). Binding of IFN-α/β to the IFNAR results in auto-phosphorylation and activation of the IFNAR-associated JAKs, which in turn phosphorylate and activate STATs. The phosphorylated STATs form heterodimers or homodimers that translocate to the nucleus to induce transcription of IFN stimulated genes (ISGs).

In the canonical pathway, the phosphorylated STAT1-STAT2 heterodimer forms an important complex with IFN-regulatory factor 9 (IRF9) called IFN-stimulated gene factor 3 (ISGF3) in the cytosol (Fu et al., 1992). The ISGF3 complex translocates to the nucleus and binds conserved elements called IFN-stimulated response elements (ISREs) in ISGs to initiate transcription of antiviral and antibacterial genes. IFN-α/β can also signal through non-canonical pathways involving STAT1 homo dimers that directly translocate to the nucleus and bind to γ-activated sequences (GAS) in gene promoters. GAS sequences are commonly used by IFN-γ signaling. IFN-α/β can also signal through other STATs, including STAT3, STAT4 and STAT5, which associate with cytokine signaling pathways. The non-canonical IFN signaling pathways and their effects have been extensively detailed in other reviews (Saleiro and Platanias, 2019; Mazewski et al., 2020).

The effects of type I IFN signaling are broad. At the transcription level, hundreds of ISGs induced by IFN-α/β have been identified through microarrays and more recently, RNA sequencing assays. Early work by Der et al identified 122 ISGs using oligonucleotide microarrays. The human fibrosarcoma cell line HT1080 was induced by IFN-α, IFN-β and IFN-γ. Of the 122 ISGs, 40 were known and 82 were novel genes that regulated apoptosis, angiogenesis, protein kinase receptors, and synthetases, among others (Der et al., 1998). De Veer et al extended these findings in a subsequent review of different microarray analysis data. Their analysis detailed over 300 genes that regulate cellular functions including adhesion, apoptosis, immune modulation, and cell growth (de Veer et al., 2001).

The number of ISGs discovered has grown exponentially over time with studies expanding to different primary cells and cell lines. These include PBMCs, human and murine epithelial cells, fibroblasts, T cells, and DCs (Hilkens et al., 19502003) (Indraccolo et al., 2007) (Rani et al., 2007). Recently, 617 ISGS with 137 novel genes were identified in three human immune cell lines, $CD4^+$ T cell-derived CEM, monocyte-derived U937 and B cell-derived Daudi cells after stimulation with IFN-α (Zhang et al., 2018).

At cellular level, IFN-α/β signaling affects both innate and adaptive immune cells, with cell specific functions. DCs are a key source and effector of type I IFNs. IFN-α has autocrine effects on pDCs, with increased IFN-α secretion in response to type I IFN signaling (Montoya et al., 2002). Further, IFN-α promotes DC maturation, expression of costimulatory MHCII molecules and antigen presentation (Simmons et al., 2012). In macrophages, IFN-α enhances LPS-induced activation, cell survival, and Mtb-induced cell death in murine bone marrow derived macrophages *in vitro* (Vadiveloo et al., 2000; Zhang et al., 2020). In Natural Killer (NK) cells, IFN-α/β promotes NK cell cytotoxicity (Orange and Biron, 1996; Nguyen et al., 2002). In T-cells, IFN-α/β promotes survival of activated $CD4^+$ and $CD8^+$ T cells *in vitro* (Marrack et al., 1999), $CD8^+$ T cells differentiation and expansion (Curtsinger et al., 2005), and clonal expansion of $CD4^+$ and $CD8^+$ T cells in response to viral infection *in vivo* (Kolumam et al., 2005). Finally, B cells have enhanced activation, antibody production, and class switching *in vivo* in response to IFN-α (Coro et al., 19502006).

Type I IFNs in SLE pathogenesis

Although type I IFNs have a central role in anti-viral responses, their effects in regulating the immune system are crucial in autoimmune disease. A pivotal study by Steinberg et al was the first to establish a link between type I IFNs and SLE in 1969. NZB/W F1 mice, which spontaneously develop lupus, were treated with polyinosinic: polycytidylic acid (Poly I: C), a synthetic double stranded RNA with antiviral properties, to ameliorate disease. However, the mice produced significant amounts of IFN which contributed to worsening disease (Steinberg et al., 1969). Further work in different genetic models has extended these observations. In MRL/lpr mice, a

different spontaneous lupus model, injection of Poly I:C led to accelerated glomerulonephritis and autoantibody production (Braun et al., 2003). Conversely, type I IFN receptor deficiency attenuated disease in both spontaneous (Braun et al., 2003; Santiago-Raber et al., 2003; Keller et al., 2021) and induced models of lupus (Nacionales et al., 2007). Thus, a pathogenic role of type I IFNs in murine lupus *in vivo* was established.

Alterations in DCs have been linked to IFN-α production in pediatric SLE patients (Blanco et al., 2001). IFN-α mediated differentiation of monocytes to DCs and the induction of DCs correlated with increased serum IFN-α production in SLE (Blanco et al., 2001). Further evidence demonstrated that type 1 IFN production in SLE is mainly driven by pDCs. In support of this, depletion, or genetic impairment of pDCs *in vivo* has been shown to ameliorate disease and IFN-α/β driven inflammation in murine models (Rowland et al., 2014; Sisirak et al., 2014). In humans, targeting of pDCs with a monoclonal antibody to blood dendritic cell antigen 2 (BDCA2) receptor reported decreased expression of IFN-regulated genes and reduced immune infiltrates in skin lesions of SLE patients with cutaneous disease (Furie et al., 2019).

Several factors can activate pDCs in SLE. Endogenous nucleic acids released from apoptotic or necrotic cells can form immune complexes (ICs) with IgG autoantibodies (Båve et al., 2000; Lövgren et al., 2004). Uptake of these ICs by pDCs leads to activation of endosomal toll-like receptors TLR7 and TLR9, which triggers IFN-α production. Another important trigger is Neutrophil Extracellular Traps (NETs) where neutrophils extrude their nucleic material in an extracellular web-like structure. SLE patients have increased formation of NETs coupled with dysfunctional clearance of these NETs, resulting in their exposure to autoreactive B cells and autoantibodies (Lande et al., 2011). Indeed, studies have shown that NETs are important in driving pDC activation and IFN-α production *in vitro* (Garcia-Romo et al., 2011). Finally, pDCs can also be activated by viral or bacterial infections in a TLR7-MYD88 dependent pathway (Abbas et al., 2020). In addition to pDCs, other cells including monocytes and neutrophils have been shown to produce IFN-α in SLE (Stone et al., 2012; Palanichamy et al., 2014). However, the extent of their contribution in the clinical setting has not been fully established and more work still needs to be done.

SLE patients have high levels of IFN-α (Niewold et al., 2007). However the large number of type I IFN, the complexity of IFN signaling and the myriad of upregulated ISGs in SLE presents a unique challenge in pinpointing suitable targets. Discovery of the "IFN signature", a cluster of upregulated ISGs, has overcome this challenge in part and enabled better assessment of IFN expression in the clinical setting (Baechler et al., 2003). It is now established that 50–70% of adult and pediatric SLE patients have an IFN signature that correlates with disease activity and severity (Wahadat et al., 2018) as will be further discussed in later sections.

Type I IFN in murine models of lupus

The bulk of our knowledge on type I IFN dysregulation in SLE is driven by *in vivo* work. In NZB/W F1 mice susceptible to lupus, continuous *in vivo* administration of adenovector-derived murine IFN-α resulted in enhanced clinical disease and IFN signaling (Mathian et al., 2005; Liu et al., 2011). In comparison, other spontaneous lupus models including MRL/lpr, MRL$^{+/+}$, and B6/lpr have a weak or absent IFN signature (Zhuang et al., 2015). A possible explanation for these differences is the different genetic background of these models and the spontaneous *lpr* mutation they carry which accelerates lymphoproliferation but could also influence type 1 IFN signaling. More work still needs to be done to parse this out.

The pristane induced lupus model is an established model with strong type 1 IFN signaling and clinical features that mimic human disease in non-autoimmune-prone mice (Reeves et al., 2009). Interestingly, IFN production appears to be largely driven by Ly6C + inflammatory monocytes in a TLR7-dependent manner, and less so by pDCs (Lee et al., 2008). Utility of pristane induction has also allowed for the identification of individual factors that regulate IFN signaling in SLE pathogenesis. In a novel humanized lupus mouse model, injection of pristane into mice reconstituted with human immune system mimics human disease with autoantibody production, inflammatory cytokines and enhanced ISGs in hepatocytes (Gunawan et al., 2017). Similar to the pristine induced lupus model, cutaneous administration of the TLR7 agonist Imiquimod in different strains of wild-type mice induced pDC-driven lupus-like disease with glomerulonephritis, autoantibodies, and increased expression of the IFN regulated genes *Mx1* and *IFna* (Yokogawa et al., 2014). Expanding on this, Liu et al demonstrated enhanced clinical disease that was TLR9 mediated (Liu et al., 2018).

Genetic association between type1 IFN pathway and SLE susceptibility

The development of SLE is strongly influenced by genetic factors. The human leukocyte antigen region (HLA) is the strongest predictor, but the genetic component of disease susceptibility in autoimmune disease, in particular SLE is complex involving large number of variants and loci across the genome (Ortíz-Fernández et al., 2022). While monogenic causes of SLE (e.g., complement deficiencies) exist, the genetic architecture of SLE is far more complex but have provided insight into the immunopathogensis of SLE, especially with regards to type I IFN. Genome wide association studies in SLE patients has demonstrated single nucleotide polymorphisms (SNPs) in loci near IFN related genes, in particular interferon regulatory factor 5 (IRF5), IRF7, IRF8, STAT4 and Tyk2, that are associated with the risk of developing SLE in adults (Sigurdsson et al., 2005;

TABLE 1 Selected studies with clinical correlations of interferon signature and SLE.

Author	Country	Type of Study, N	IFN measured	Clinical outcomes	Summary of findings
Adel 2020 (Adel and Sadeq, 2020)	Egypt	Prospective (n = 82)	IFN-α	SLAM, SLEDAI	High IFN is correlated with increased disease activity, refractory to therapy, and lupus nephritis
Fu 2008 (Fu et al., 2008)	China	Cross-sectional (n = 67)	IFN signature	SLEDAI, SLICC, lupus nephritis	Increased gene signature is associated with worse SLEDAI, SLICC, and prevalence of lupus nephritis
Guthridge 2020 (Guthridge et al., 2020)	United States	Cross-sectional (n = 198)	IFN Signature	SLEDAI, lupus nephritis	Increased IFN signature is associated with increased SLEDAI and renal activity
Han 2020 (Han et al., 2020)	United States	Cross-sectional (n = 141)	IFN signature	Leukopenia	Increased interferon signature is associated with leukopenia
Iwamoto 2022 (Iwamoto et al., 2022)	United States	Cross-sectional (n = 221)	IFN signature	Lupus Nephritis	Type I IFN is a strong predictor of class III/IV lupus nephritis
Jakiela 2018 (Jakiela et al., 2018)	Poland	Cross-sectional (n = 35)	Urinary IFN signature	Lupus Nephritis	Patients with active lupus nephritis had increased urinary cytokines
Landolt-Marticorena 2009 (Landolt-Marticorena et al., 2009)	Canada	Prospective (3 months to 1 year) (n = 94)	IFN signature	SLEDAI	Baseline increased interferon signature is associated with increased disease activity—however, changes in interferon signature are not associated with clinical outcomes
Mai 2021 (Mai et al., 2021)	Canada	Prospective (n = 137)	IFN Signature	SLEDAI, SLE Flare Index	High baseline interferon index is associated with more severe disease activity and flares
Merrill 2017 (Merrill et al., 2017)	United States	Prospective (6 months) (n = 41)	IFN Signature	SLEDAI, BILAG	Patients with high IFN signature had improvement in IFN after treatment with HCQ. Unclear if this clinically correlated
Munroe 2017 (Munroe et al., 2017)	United States	Prospective (3 months) (n = 31)	IFN signature	Disease flare	Increased baseline IFN signature is associated with an increased risk of disease flare
Northcott 2022 (Northcott et al., 2022)	United States	Prospective (n = 205)	IFN signature	SLEDAI	Baseline high IFN status is associate with more severe disease but does not change over time
Petri 2019 (Petri et al., 2019)	United States	Prospective (2 years) (n = 243)	IFN signature	SLEDAI, serologic markers	Increased baseline IFN signatures were associated with increased skin and arthritis—however, changes in IFN signatures were not associated with changes in disease activities
Rose 2013 (Rose et al., 2013)	Germany	Prospective (6 months) (n = 79)	IFN Signature	SLEDIA, BILAG	Increased levels of IFN- α are associated with increased disease activity
Schneider 2015 (Schneider et al., 2015)	Brazil	Cross-sectional (n = 172)	IFN signature	SLEDAI	Increased baseline IFN is associated with increased SLEDAI.
Wilkinson 2020 (Wilkinson et al., 2020)	International Multicenter	Post hoc meta-analysis from Phase 3 Belimumab RCTs (n = 554)	IFN-1 signature	SRI-4 response rate	Patients with increased baseline IFN signatures had improves response rates compared to their counterparts
Willis 2012 (Willis et al., 2012)	United States	Prospective (1 year) (n = 35)	IFN signature	SLAM-R	Patients with increased IFN signatures had increased disease activity. Patients with improved disease activity after hydroxychloroquine therapy had decreased IFN-a

Abbreviations: SLE, systemic lupus erythematosus; IFN, interferon; SLAM, systemic lupus activity measure; SLEDAI, SLE disease activity index; SLICC, SLE international collaborating clinics damage index; BILAG, british isles lupus assessment group; SLE response index (SRI-4) response rate.

Graham et al., 2007). Consistent with these observations, using a candidate gene approach of type I IFN related genes, the T allele of rs3747517 in the IFIH1 gene was associated with a reduced risk of SLE while the T allele of rs7574865 in STAT4 was associated with an increased risk of developing SLE in children and adolescents (Zedan et al., 2021). In conjunction with our understanding of type I IFN in mouse models with SLE and translational studies demonstrating increased expression of type I IFN and related pathways in SLE, these genetic studies strongly support an important role for type I IFN related pathways in SLE pathogenesis and the potential for translation of these findings to the care of patients with SLE.

In summary, extensive research has established the role of type1 IFNs in SLE at genetic, molecular, and cellular level. Type I interferons in pDCs are an important driver of disease. Given the complexity of type 1 IFN signaling and the challenges with elucidating mechanisms in human SLE patients, it not surprising that a significant amount of the supportive evidence is derived from both spontaneous and induced murine models of SLE. Later in this review, we will discuss the evidence for type I interferon activation in SLE patients and review the clinical trails that have led to type I interferon directed therapies in SLE.

Clinical correlations between type I IFN and SLE

IFN therapy and lupus-like illnesses

The use of IFN therapy for cancer and viral infections, such as hepatitis B and C, contributed to the earliest clinical evidence that IFN may play a role in the development of SLE. In the 1990s and early 2000s, multiple cases of autoimmune diseases arising shortly after administration of IFN therapy were reported (the most common of which was thyroid disease). Multiple cases of new diagnoses of SLE after IFN therapy have been reported (García-Porrúa et al., 1998; Wilson et al., 2002; Khalil and Khokhar, 2016). It is unclear whether these patients may have had "pre-clinical" SLE that was exacerbated by IFN therapy *versus* new formulation of antibodies. One study showed that 61% of patients that were initially antinuclear antibody (ANA) negative developed positive ANA tests after IFN therapy for hepatitis C (Noda et al., 1996). Although this study did not show causality, it highlighted a potential association between IFN therapy and development of autoimmunity.

Association of baseline type I IFN activity with disease activity and clinical manifestations

After the discovery that dysregulation of the type I IFN pathways may contribute to the pathogenesis of SLE, there have been multiple cross-sectional and prospective studies seeking to determine if increased type I IFN levels and/or the type I IFN signature correlates with disease activity. There is a strong correlation between baseline increased IFN levels and SLE disease activity. Table 1 summaries a large number of published studies demonstrating an association of increased baseline type I IFNs or type I IFN signature levels with increased SLE disease activity in patients with new or established SLE (Al-Mutairi et al., 2007; Fu et al., 2008; Landolt-Marticorena et al., 2009; Willis et al., 2012; Rose et al., 2013; Schneider et al., 2015; Munroe et al., 2017; Liu et al., 2018; Petri et al., 2019; Adel and Sadeq, 2020; Guthridge et al., 2020; Mai et al., 2021). One notable study followed 137 SLE patients for 5 years after initial IFN signatures were obtained (Mai et al., 2021). The type I IFN signature was determined based on the expression of five IFN related genes, *EPSTI1, IFI44L, LY6E, OAS3,* and *RSAD2*. Patients with high type I IFN signatures were more likely to have more severe disease activity as defined by the SLE disease activity-2000 index (SLEDAI-2K) at study entry and over time, including an increase in disease flares and a need for treatment with additional immunosuppressive agents and corticosteroids. In contrast, patients with lower type I IFN signatures were more likely to achieve low lupus disease activity. Northcott et al analyzed 729 serum samples from 205 SLE patients, including 142 patients with multiple samples (Northcott et al., 2022). High baseline type I IFN signatures were observed in 63% of patients and predicted future high disease activity in multiple organ domains but the type I IFN signature itself was stable and did not change with disease activity (Northcott et al., 2022). Finally, prospective studies have also shown that an increased baseline IFN is associated with an increased risk of disease flare in the future (Merrill et al., 2017). These studies show that baseline increases in type I IFN signatures may have potential prognostic value and predict severe disease activity.

There has also been interest in determining if IFN levels may help predict the response to treatments in SLE patients. Adel et al reported that serum levels of IFN-α were associated with the presence of lupus nephritis and a poor response to immunosuppressive treatments (Adel and Sadeq, 2020). However, a meta-analysis of randomized controlled phase 3 trials of belimumab in the treatment of SLE, including 554 SLE patients found that patients with increased baseline levels of IFN were more likely to respond to therapy with belimumab than those with lower baseline IFN levels (Wilkinson et al., 2020). In a pooled post-hoc analysis of both the TULIP-1 and TULIP-2 randomized controlled trials testing the clinical effectiveness of the anti-IFNAR monoclonal antibody anifrolumab (discussed below), SLE patients with higher baseline interferon levels had better response rates to anifrolumab treatment (Vital et al., 2022). This was also noted in the phase 2 trials with anifrolumab (Furie et al., 2017). However, this data should be interpreted with caution as it remains unclear whether the improved responses to therapy in these trials are because patients at baseline had an increased disease activity, and therefore more likely to improve. Furthermore, the difference in the ability of type I IFN

TABLE 2 Randomized Controlled Clinical Trials of anti-interferon therapy.

Study	Trial phase	Number of participants	Clinical efficacy (primary endpoints)	Serious adverse events
Anifrolumab				
Furie 2017 (Furie et al., 2017)	2	305	Patients with anifrolumab had improved SRI and BICLA scores *versus* placebo	Anifrolumab patients had more infections with Herpes zoster
Tanaka 2020 (Tanaka et al., 2020)	2	20	This study was not powered for clinical efficacy	Adverse events were similar between anifrolumab and placebo
Jayne 2022 (Jayne et al., 2022)	2	147	Similar clinical outcomes for lupus nephritis between anifrolumab and placebo	Increased Herpes Zoster in anifrolumab *versus* placebo
Furie 2019 (Fure et al., 2019)	3	457	There was no difference in SRI-4 response rates between Placebo and Anifrolumab. However, patients had improved CLASI scores and BICLA responses	There were similar serious adverse events between anifrolumab and placebo
Morand 2020 (Morand et al., 2020)	3	362	Anifrolumab had improved BICLA and SRI scores than placebo	Anifrolumab patients had increased infections with Herpes zoster
Sifalimumab				
Merrill 2011 (Merrill et al., 2011)	1	33	Less disease flares as measured by SLEDAI	Similar between placebo and Sifalimumab
Petri 2012 (Petri et al., 2013)	1	161	No differences in clinical outcomes between placebo and Sifalimumab	Similar between placebo and Sifalimumab
Khamashta 2016 (Khamashta et al., 2016)	2	431	Patients with Sifalimumab had improved SRI scores than placebo	There was increased Herpes zoster infections with Sifalimumab *versus* placebo
Takeuchi 2020 (Takeuchi et al., 2020)	2	30	Not powered for clinical efficacy	There was no placebo group, but Sifalimumab was well tolerated
Rontalizumab				
McBride 2012 (McBride et al., 2012)	1	60	Not powered to detect clinical efficacy between both groups	Similar adverse events between placebo and rontalizumab
Kalunian 2016 (Kalunian et al., 2016)	2	238	No difference between placebo and rontalizumab	Similar adverse events between placebo and rontalizumab
IFN-α Kinoid				
Houssiau 2019 (Houssiau et al., 2020)	2	185	No differences noted between placebo or IFN-k in the primary endpoints	Similar adverse events between IFN-k and placebo

Abbreviations: SRI-4, SLE response index-4; BICLA, BILAG-based composite lupus assessment; CLASI, cutaneous lupus erythematosus disease area and severity index; SLEDAI, SLE disease activity index.

activity to predict treatment responses might also depend on the mechanism of action of the intervention. Therefore additional prospective studies are needed to better understand the predictive capacity of baseline type I IFN activity with treatment responses.

The increased expression of type I IFNs also associated with specific disease manifestations including lung disease, lupus nephritis, skin disease, arthritis, and leukopenia (Al-Mutairi et al., 2007; Fu et al., 2008; Petri et al., 2019; Adel and Sadeq, 2020; Han et al., 2020). A recent study found the presence of class III or IV lupus nephritis was increased in patients with higher expression of the type I IFN, assessed using an IFN bioassay (OR 5.4, $p < .01$) (Iwamoto et al., 2022). Furthermore, the IFN signature was more predictive for lupus nephritis than low complement C3 levels and anti-double stranded DNA antibodies. Increased urinary excretion of type IFNs has also been associated with lupus nephritis (Jakiela et al., 2018). However, these sample sizes have been small and have not been adequately controlled to draw further recommendations for clinical practice. Finally, cerebrospinal levels from patients with neuropsychiatric lupus had elevated levels of IFN-α compared to patients with other neurological diseases such as multiple sclerosis (Santer et al., 2009).

Together these studies highlight that type I IFN are associated with active lupus manifestations and suggest a potential use of the IFN signature to stratify patients into those with higher and lower risk of developing future severe disease activity and manifestations, and possible predict treatment responses. However more studies are needed to validate these data and to determine how precisely this may be utilized by practitioners.

Trending type I IFN levels with SLE disease activity

The use of the IFN levels or gene expression has also generated interest if levels can be followed over time and used as a biomarker of

disease activity. For example, two studies compared the levels of IFN in SLE patients with a high baseline level that initiated treatment with hydroxychloroquine (Willis et al., 2012; Merrill et al., 2017). After initiating treatment, patients had a significant decrease in IFN levels, and improvement in disease activity. Interestingly, this was not seen with other immunosuppressants such as azathioprine. However, a treatment effect on type I IFN levels was not observed in a larger study (Petri et al., 2019). In this cohort, while patients with a high baseline IFN level had increased disease activity, the type I interferon scores were stable over a 2 year period including, after treatment there. Therefore, there was no correlation between IFN levels and improvement in disease activity (Petri et al., 2019). Finally, other studies have confirmed that IFN signature is stable across time and does not correlate with changes in disease activity, except for high doses of glucocorticoids (Northcott et al., 2022). It is not currently known why interferon expression is stable and does not correlate with SLE activity in patients who have an inherently high type I IFN expression. It has been suggested that genetic factors may drive the increase in type I interferons as opposed to disease activity, but additional research is needed better understand these questions. Together these studies suggest that while baseline type I IFN activity might predict future disease activity, their role in tracking disease activity and response to treatment is likely limited.

Finally, our understanding of the relationship of long-term outcomes in SLE patients and type 1 IFN gene signatures remains poor. Fortunately, there is an ongoing 3 year observational study following patients with low and high IFN gene signatures with plans to enroll 900 patients. The estimated study completion is 2022 and will hopefully provide substantial additional insight in the application of type I IFN activity as a SLE biomarker (Hammond et al., 2020).

Therapeutic targeting of type I interferons in SLE

Anti-IFN therapy and SLE

The critical role of type1 IFNs in SLE immunopathogenesis makes it an intriguing therapeutic target in SLE. Multiple biologics have been developed targeting the type1 IFN pathway as well as a unique anti-IFNα vaccine strategy. These studies have produced conflicting results, perhaps due to the large number of type1 IFN with potentially redundant functions. These studies are summarized in Table 2.

Sifalimumab

Sifalimumab is a monoclonal antibody that directly targets multiple subtypes of IFN-α. This drug was studied in phase 1 and 2 trials (Merrill et al., 2011; Petri et al., 2013; Khamashta et al., 2016; Takeuchi et al., 2020). There has been one published successful phase 2 trial for the use of sifalimumab in patients with SLE (111). This trial enrolled 431 patients with SLE and randomized these patients into varying doses of sifalimumab (200 mg, 600 mg, or 1200 mg) and placebo. The primary endpoint for this study was SLE Responder Index 4 (SRI-4) response rate and found that patients on sifalimumab had improved disease activities (59.8% 1200 mg, 56.5% 600 mg, 58.3% 200 mg, 45.4% placebo). Despite the promise this drug showed in phase 2 trials (Khamashta et al., 2016), its development was discontinued in favor of anifrolumab, which showed greater efficacy in pre-phase 3 trial data as discussed below.

Rontalizumab

Rontalizumab is a monoclonal antibody that directly binds to multiple subtypes of IFN-α. Trials for this agent also did not show clinical efficacy including a phase 2 trial with 238 patients that were randomized to either 750 mg or 300 mg of rontalizumab *versus* placebo (Kalunian et al., 2016). This study showed that there were no differences in responses in the primary outcomes (SRI-4 or BILAG-based Composite Lupus Assessment (BICLA) responses). Due to this negative study, drug development was discontinued.

Interferon- α kinoid

IFN-α kinoid (IFN-k) is an interesting immunotherapeutic vaccine agent in which patients are injected with IFN-k and subsequently develop neutralizing anti-IFN antibodies. There has been one phase IIb trial conducted for IFN-k (Houssiau et al., 2020). This study enrolled 185 patients who were randomized into either IFN-k *versus* placebo. This study did not meet the primary endpoint of BICLA response rate but did show improvements in SRI-4 response rates and attainment of lupus low disease activity states. There have been no phase 3 trials registered for this therapy.

Anifrolumab

Anifrolumab is a monoclonal antibody that binds to IFNAR, therefore blocking the activity of all type I IFN. Anifrolumab is the only anti-IFN therapy to undergo Phase 3 randomized controlled trials (RCTs). The RCTs for Anifrolumab are summarized in Table 2. There have been three large double-blinded RCTs published for anifrolumab–the MUSE, TULIP-1, and TULIP-2 trials (Furie et al., 2017; Fure et al., 2019; Morand et al., 2020).

The MUSE was a multicenter phase 2b trial that randomized patients into varying doses of anifrolumab (300 mg or 1000 mg) and placebo. A total of 307 patients were enrolled. The primary outcome for this trial was the SRI-4 at 6 months with sustained reduction in corticosteroids. This study met its primary end point of improved SRI-4 response rates (36% anifrolumab 300 mg, 28% anifrolumab 1000 mg, 13% placebo). Furthermore, this trial demonstrated that SLE patients with a baseline high IFN signature had the largest treatment response. There were also improvements in BICLA responses, tender joints, and Cutaneous Lupus Erythematosus Disease Area and Severity Index (CLASI) scores.

The TULIP-1 was a phase 3 double-blinded RCT that randomized patients to anifrolumab (300 mg or 150 mg) or placebo. A total of 457 patients were enrolled in this trial. The primary endpoint was SRI-4 responses. This trial failed to meet its primary outcome at 1 year (36% response in anifrolumab *versus* 40% response in placebo, 95% CI -14.2 to 5.8). However, secondary outcomes such as BICLA response, CLASI scores, joint tenderness, and corticosteroid reduction were observed with anifrolumab. The authors of this study hypothesized that the BICLA response rate but not the SRI-4 met the primary outcomes because the BICLA response rate can capture partial improvements in disease activity. Furthermore, they attributed the failure of reaching the primary outcome due to strict outcomes, such as considering the use of non-steroids anti-inflammatory drugs (NSAIDs) as a treatment failure for SLE.

The TULIP-2 trial was a phase 3 double-blinded RCT that randomized patients to anifrolumab 300 mg and placebo. There were 365 patients enrolled. Due to the failure of the TULIP-1 not meeting its primary endpoint of SRI-4 response, the endpoint of TULIP-2 was modified to the BICLA response to capture partial improvements. This study showed an increased BICLA response for the anifrolumab *versus* placebo groups (48% *versus* 32%, $p < .05$). Furthermore, the anifrolumab patients had improvements in the SRI-4, CLASI scores, and corticosteroid reduction. Interestingly, there were no differences noted in swollen and tender joints.

These studies overall indicate that anifrolumab is an agent that has efficacy for cutaneous and musculoskeletal activity for patients with SLE. Furthermore, it has been shown in these studies to be a useful agent to specifically help patients titrate down glucocorticoids. Accordingly, anifrolumab was granted FDA approval for the treatment of SLE on 30 July 2021. However, to date, the use of anifrolumab has not been adequately studied in severe organ manifestations such as lupus nephritis but these studies are currently being performed. There has been a recently published phase 2 trial for the use of anifrolumab in patients with lupus nephritis (Jayne et al., 2022). Unfortunately, this study did not meet its primary endpoint. However, it was hypothesized that patients with lupus nephritis have increased excretion of anifrolumab related to their proteinuria and therefore at "baseline dosing" may have inadequate serum levels to achieve a therapeutic effect. In the patient population that was treated with higher doses of anifrolumab, there were improvement in surrogate markers suggesting a potential therapeutic role for high doses of anifrolumab. Currently anifrolumab is being tested in an ongoing phase 3 clinical trial in lupus nephritis (AstraZeneca, 2022).

Adverse reactions from anifrolumab in phase 3 trials were primarily from herpes zoster infections and upper respiratory tract infections (including bronchitis and pneumonias). These are hypothesized to be due to decreased antiviral responses that require interferon to be activated. There were also severe hypersensitivity reactions noted. Currently, there is insufficient data to determine if anti-IFN therapies have an increased risk of malignancy.

Alternative therapeutic strategies targeting type I IFN in SLE

As noted above, there are multiple steps in the type I IFN pathway that are activated and play a role in SLE. Accordingly, the type I IFN pathway may be therapeutically targeted in multiple ways, aside from directly targeting IFN-α or IFNAR. For example, as noted in Figure 1, type I IFN signal through JAK proteins. Targeting JAK proteins has been successful in the treatment of rheumatoid arthritis (Burmester et al., 2013; Genovese et al., 2016; Genovese et al., 2018). Baracitinib, a JAK1 and JAK2 inhibitor, has been tested in a phase 3 trial, demonstrating improvements of SRI-4 (BRAVE 1) but a separate phase 3 trial did not show similar improvements (BRAVE II) (Updates, 2022). As such, this drug's investigation in SLE has been suspended. Upadacitinib, a selective JAK1 inhibitor, is currently being investigated in a phase 2 clinical trial in combination with Elsubrutinib–a Bruton tyrosine kinase inhibitor. The phase 2 trial has been completed and results are currently pending.

Finally, as noted above, pDCs are critical producers of type I IFN. As such, directing therapies against pDCs is a potential strategy to target type I IFN in SLE. Litifilimab is a humanized IgG1 targeting BDCA2 receptor on pDCs, which subsequently decreases type I IFN levels. A recent phase 2 clinical trial with 334 patients showed improvements in tender and swollen joints *versus* placebo (Furie et al., 2022). However, secondary endpoints including disease activity markers and skin disease showed no differences (Furie et al., 2022). Interestingly, a separate phase 2 trial investigating litifilimab for cutaneous SLE found improvements in CLASI scores *versus* placebo (Werth et al., 2022). Both these trials showed an increase in herpes zoster infections. Additional studies are needed to determine the efficacy of litifilimab in SLE.

Future directions

Although anti-interferon therapies, especially anifrolumab, have shown promise in SLE, there are still many unanswered questions. More studies are needed to determine if anifrolumab will be efficacious in more severe manifestations of SLE such as nephritis and there are on going trials testing anifrolumab in the treatment of lupus nephritis. More evidence is also needed to determine the role of anifrolumab in subsets of patients (ex: males *versus* females, younger *versus* older, different racial groups). Current evidence shows that type 1 interferons may be expressed higher in females *versus* males (Ziegler et al., 2017; Webb et al., 2018). This suggests that anti-interferon therapy may also have a stronger effect in males *versus* females, though this is not currently known. Another important consideration is understanding when anifrolumab should be used in SLE patients, as opposed to other therapeutics, especially biologics. There is no evidence as to how anifrolumab may directly compare to belimumab (another FDA approved biologic for the treatment of SLE) as there have been to head-to-head trials. However, anifrolumab showed marked improvement in cutaneous manifestation of SLE in the TULIP-1 and TULIP-2 trials (Fure et al., 2019; Morand et al., 2020). However, the role of belimumab in cutaneous SLE has not been as extensively tested in trials. In the future, it may be that the decision of anifrolumab *versus* belimumab may be decided through disease manifestations (i.e., anifrolumab for cutaneous SLE and belimumab with mycophenolate for lupus nephritis), but these treatment decisions will require future studies to better inform the clinicians and patients.

Lastly, it is also of interest to see if type I interferon therapeutics will be beneficial in the treatment of other autoimmune diseases with activation of the type I interferon pathways. Type I interferons have been shown to be elevated in patients with Sjögren's syndrome (Wildenberg et al., 2008; Vakaloglou and Mavragani, 2011; Bodewes and Versnel, 2018), systemic sclerosis (Assassi et al., 2010), mixed connective tissue disease (Paradowska-Gorycka et al., 2021) and dermatomyositis (Baechler et al., 2007; Pinal-Fernandez et al., 2019). A phase 1 b study in dermatomyositis patients was conducted with sifalimumab, which suggested a small benefit (Higgs et al., 2014). Non-controlled, pilot clinical studies a have suggested that JAK inhibitors, which can block type I interferon signaling, might be beneficial in adult and pediatric cases of dermatomyositis (Ladislau et al., 2018; Le Voyer et al., 2021; Paik et al., 2021). Finally, anifrolumab is also currently being investigated in a phase II trial for the treatment of Sjögren's Syndrome (NCT05383677, ANISE-II). While these studies are of interest, larger, randomized controlled clinical trials are needed to determine if targeting type I interferons is a viable strategy in these autoimmune diseases as it has been shown to be in SLE.

Conclusion

The IFN pathways are highly involved in the pathogenesis in SLE and have provided excitement in the diagnosis, prognosis, and treatment of patients with SLE. However, more research is currently needed to understand the extent to which IFN gene signatures can be used in clinical practice. The emergence of anifrolumab highlights the potential for targeting type I IFN in the treatment of SLE, but continued studies of anifrolumab and other therapeutics targeting type I IFN are important to determine the extent to which targeting type I IFN will be used in the treatment of SLE.

Author contributions

All authors listed have made a substantial, direct, and intellectual contribution to the work and approved it for publication.

Conflict of interest

The authors declare that the research was conducted in the absence of any commercial or financial relationships that could be construed as a potential conflict of interest.

Publisher's note

References

Abbas, A., Vu Manh, T. P., Valente, M., Collinet, N., Attaf, N., Dong, C., et al. (2020). The activation trajectory of plasmacytoid dendritic cells *in vivo* during a viral infection. *Nat. Immunol.* 21 (9), 983–997. doi:10.1038/s41590-020-0731-4

Adel, Y., and Sadeq, Y. (2020). Impact of IL-34, IFN-α and IFN-λ1 on activity of systemic lupus erythematosus in Egyptian patients. *Reumatologia* 58 (4), 221–230. doi:10.5114/reum.2020.98434

Al-Mutairi, S., Al-Awadhi, A., Raghupathy, R., Al-Khawari, H., Sada, P., Al-Herz, A., et al. (2007). Lupus patients with pulmonary involvement have a pro-inflammatory cytokines profile. *Rheumatol. Int.* 27 (7), 621–630. doi:10.1007/s00296-006-0268-3

Assassi, S., Mayes, M. D., Arnett, F. C., Gourh, P., Agarwal, S. K., McNearney, T. A., et al. (2010). Systemic sclerosis and lupus: Points in an interferon-mediated continuum. *Arthritis Rheum.* 62 (2), 589–598. doi:10.1002/art.27224

AstraZeneca (2022). Phase 3 study of anifrolumab in adult patients with active proliferative lupus nephritis (IRIS). *clinicaltrialsgov.*, NCT05138133.

Baechler, E. C., Batliwalla, F. M., Karypis, G., Gaffney, P. M., Ortmann, W. A., Espe, K. J., et al. (2003). Interferon-inducible gene expression signature in peripheral blood cells of patients with severe lupus. *Proc. Natl. Acad. Sci. U. S. A.* 100 (5), 2610–2615. doi:10.1073/pnas.0337679100

Baechler, E. C., Bauer, J. W., Slattery, C. A., Ortmann, W. A., Espe, K. J., Novitzke, J., et al. (2007). An interferon signature in the peripheral blood of dermatomyositis patients is associated with disease activity. *Mol. Med.* 13 (1-2), 59–68. doi:10.2119/2006-00085.Baechler

Baker, K. P., Edwards, B. M., Main, S. H., Choi, G. H., Wager, R. E., Halpern, W. G., et al. (2003). Generation and characterization of LymphoStat-B, a human monoclonal antibody that antagonizes the bioactivities of B lymphocyte stimulator. *Arthritis Rheum.* 48 (11), 3253–3265. doi:10.1002/art.11299

Båve, U., Alm, G. V., Rönnblom, L., and Bave, U. (2000). The combination of apoptotic U937 cells and lupus IgG is a potent IFN-α inducer. *J. Immunol.* 165 (6), 3519–3526. doi:10.4049/jimmunol.165.6.3519

Bentham, J., Morris, D. L., Graham, D. S. C., Pinder, C. L., Tombleson, P., Behrens, T. W., et al. (2015). Genetic association analyses implicate aberrant regulation of innate and adaptive immunity genes in the pathogenesis of systemic lupus erythematosus. *Nat. Genet.* 47 (12), 1457–1464. doi:10.1038/ng.3434

Blanco, P., Palucka, A. K., Gill, M., Pascual, V., and Banchereau, J. (2001). Induction of dendritic cell differentiation by IFN-alpha in systemic lupus erythematosus. *Science* 294 (5546), 1540–1543. doi:10.1126/science.1064890

Bodewes, I. L. A., and Versnel, M. A. (2018). Interferon activation in primary sjögren's syndrome: Recent insights and future perspective as novel treatment target. *Expert Rev. Clin. Immunol.* 14 (10), 817–829. doi:10.1080/1744666X.2018.1519396

Braun, D., Geraldes, P., and Demengeot, J. (2003). Type I Interferon controls the onset and severity of autoimmune manifestations in lpr mice. *J. Autoimmun.* 20 (1), 15–25. doi:10.1016/s0896-8411(02)00109-9

Burmester, G. R., Blanco, R., Charles-Schoeman, C., Wollenhaupt, J., Zerbini, C., Benda, B., et al. (2013). Tofacitinib (CP-690, 550) in combination with methotrexate in patients with active rheumatoid arthritis with an inadequate response to tumour necrosis factor inhibitors: A randomised phase 3 trial. *Lancet* 381 (9865), 451–460. doi:10.1016/S0140-6736(12)61424-X

Cella, M., Jarrossay, D., Facchetti, F., Alebardi, O., Nakajima, H., Lanzavecchia, A., et al. (1999). Plasmacytoid monocytes migrate to inflamed lymph nodes and produce large amounts of type I interferon. *Nat. Med.* 5 (8), 919–923. doi:10.1038/11360

Choi, J., Kim, S. T., and Craft, J. (2012). The pathogenesis of systemic lupus erythematosus-an update. *Curr. Opin. Immunol.* 24 (6), 651–657. doi:10.1016/j.coi.2012.10.004

Cooper, G. S., Wither, J., Bernatsky, S., Claudio, J. O., Clarke, A., Rioux, J. D., et al. (2010). Occupational and environmental exposures and risk of systemic lupus erythematosus: Silica, sunlight, solvents. *Rheumatology* 49 (11), 2172–2180. doi:10.1093/rheumatology/keq214

Coro, E. S., Chang, W. L., and Baumgarth, N. (1950). Type I IFN receptor signals directly stimulate local B cells early following influenza virus infection. *J. Immunol.* 176 (7), 4343–4351. doi:10.4049/jimmunol.176.7.4343

Costenbader, K. H., Feskanich, D., Stampfer, M. J., and Karlson, E. W. (2007). Reproductive and menopausal factors and risk of systemic lupus erythematosus in women. *Arthritis Rheum.* 56 (4), 1251–1262. doi:10.1002/art.22510

Curtsinger, J. M., Valenzuela, J. O., Agarwal, P., Lins, D., and Mescher, M. F. (2005). Cutting edge: Type I IFNs provide a third signal to CD8 T cells to stimulate clonal expansion and differentiation. *J. Immunol.* 174 (8), 4465–4469. doi:10.4049/jimmunol.174.8.4465

Darnell, J. E., Jr., Kerr, I. M., and Stark, G. R. (1994). Jak-STAT pathways and transcriptional activation in response to IFNs and other extracellular signaling proteins. *Sci. (New York, NY)* 264 (5164), 1415–1421. doi:10.1126/science.8197455

de Veer, M. J., Holko, M., Frevel, M., Walker, E., Der, S., Paranjape, J. M., et al. (2001). Functional classification of interferon-stimulated genes identified using microarrays. *J. Leukoc. Bio.* 69 (6), 912–920. doi:10.1189/jlb.69.6.912

Der, S. D., Zhou, A., Williams, B. R. G., and Silverman, R. H. (1998). Identification of genes differentially regulated by interferon alpha, beta, or gamma using oligonucleotide arrays. *Proc. Natl. Acad. Sci. U. S. A.* 95 (26), 15623–15628. doi:10.1073/pnas.95.26.15623

Domanski, P., Witte, M., Kellum, M., Rubinstein, M., Hackett, R., Pitha, P., et al. (1995). Cloning and expression of a long form of the beta subunit of the interferon alpha beta receptor that is required for signaling. *J. Biol. Chem.* 270 (37), 21606–21611. doi:10.1074/jbc.270.37.21606

Dunn, G. P., Bruce, A. T., Sheehan, K. C., Shankaran, V., Uppaluri, R., Bui, J. D., et al. (2005). A critical function for type I interferons in cancer immunoediting. *Nat. Immunol.* 6 (7), 722–729. doi:10.1038/ni1213

Erlandsson, L., Blumenthal, R., Eloranta, M-L., Engel, H., Alm, G., Weiss, S., et al. (1998). Interferon-β is required for interferon-α production in mouse fibroblasts. *Curr. Biol.* 8 (4), 223–226. doi:10.1016/s0960-9822(98)70086-7

Fu, Q., Chen, X., Cui, H., Guo, Y., Chen, J., Shen, N., et al. (2008). Association of elevated transcript levels of interferon-inducible chemokines with disease activity and organ damage in systemic lupus erythematosus patients. *Arthritis Res. Ther.* 10 (5), R112. doi:10.1186/ar2510

Fu, X. Y., Schindler, C., Improta, T., Aebersold, R., and Darnell, J. E. (1992). The proteins of ISGF-3, the interferon alpha-induced transcriptional activator, define a gene family involved in signal transduction. *Proc. Natl. Acad. Sci. U. S. A.* 89 (16), 7840–7843. doi:10.1073/pnas.89.16.7840

Fure, R., Morand, E. F., Bruce, I. N., Manzi, S., Kalunian, K. C., Vital, E. M., et al. (2019). Type I interferon inhibitor anifrolumab in active systemic lupus erythematosus (TULIP-1): A randomised, controlled, phase 3 trial. *Lancet Rheumatology* 1 (4), E208–e219. doi:10.1016/s2665-9913(19)30076-1

Furie, R., Khamashta, M., Merrill, J. T., Werth, V. P., Kalunian, K., Brohawn, P., et al. (2017). Anifrolumab, an anti-interferon-α receptor monoclonal antibody, in moderate-to-severe systemic lupus erythematosus. *Arthritis Rheumatol.* 69 (2), 376–386. doi:10.1002/art.39962

Furie, R., Petri, M., Zamani, O., Cervera, R., Wallace, D. J., Tegzová, D., et al. (2011). A phase III, randomized, placebo-controlled study of belimumab, a monoclonal antibody that inhibits B lymphocyte stimulator, in patients with systemic lupus erythematosus. *Arthritis Rheum.* 63 (12), 3918–3930. doi:10.1002/art.30613

Furie, R., Werth, V. P., Merola, J. F., Stevenson, L., Reynolds, T. L., Naik, H., et al. (2019). Monoclonal antibody targeting BDCA2 ameliorates skin lesions in systemic lupus erythematosus. *J. Clin. Invest.* 129 (3), 1359–1371. doi:10.1172/JCI124466

Furie, R. A., van Vollenhoven, R. F., Kalunian, K., Navarra, S., Romero-Diaz, J., Werth, V. P., et al. (2022). Trial of anti-BDCA2 antibody litifilimab for systemic lupus erythematosus. *N. Engl. J. Med.* 387 (10), 894–904. doi:10.1056/NEJMoa2118025

García-Porrúa, C., González-Gay, M. A., Fernández-Lamelo, F., Paz-Carreira, J. M., Lavilla, E., and González-López, M. A. (1998). Simultaneous development of SLE-like syndrome and autoimmune thyroiditis following alpha-interferon treatment. *Clin. Exp. Rheumatol.* 16 (1), 107–108.

Garcia-Romo, G. S., Caielli, S., Vega, B., Connolly, J., Allantaz, F., Xu, Z., et al. (2011). Netting neutrophils are major inducers of type I IFN production in pediatric systemic lupus erythematosus. *Sci. Transl. Med.* 3, 73ra20. doi:10.1126/scitranslmed.3001201

Genovese, M. C., Fleischmann, R., Combe, B., Hall, S., Rubbert-Roth, A., Zhang, Y., et al. (2018). Safety and efficacy of upadacitinib in patients with active rheumatoid arthritis refractory to biologic disease-modifying anti-rheumatic drugs (SELECT-BEYOND): A double-blind, randomised controlled phase 3 trial. *Lancet* 391 (10139), 2513–2524. doi:10.1016/S0140-6736(18)31116-4

Genovese, M. C., Kremer, J., Zamani, O., Ludivico, C., Krogulec, M., Xie, L., et al. (2016). Baricitinib in patients with refractory rheumatoid arthritis. *N. Engl. J. Med.* 374 (13), 1243–1252. doi:10.1056/NEJMoa1507247

Graham, R. R., Kyogoku, C., Sigurdsson, S., Vlasova, I. A., Davies, L. R., Baechler, E. C., et al. (2007). Three functional variants of IFN regulatory factor 5 (IRF5) define risk and protective haplotypes for human lupus. *Proc. Natl. Acad. Sci. U. S. A.* 104 (16), 6758–6763. doi:10.1073/pnas.0701266104

Gunawan, M., Her, Z., Liu, M., Tan, S. Y., Chan, X. Y., Tan, W. W. S., et al. (2017). A novel human systemic lupus erythematosus model in humanised mice. *Sci. Rep.* 7 (1), 16642. doi:10.1038/s41598-017-16999-7

Guthridge, J. M., Lu, R., Tran, L. T., Arriens, C., Aberle, T., Kamp, S., et al. (2020). Adults with systemic lupus exhibit distinct molecular phenotypes in a cross-sectional study. *EClinicalMedicine* 20, 100291. doi:10.1016/j.eclinm.2020.100291

Hammond, E. R., Tummala, R., Berglind, A., Syed, F., Wang, X., Desta, B., et al. (2020). Study protocol for the international systemic lupus erythematosus prospective observational cohort study (SPOCS): Understanding lupus and the role of type I interferon gene signature. *BMJ Open* 10 (9), e036563. doi:10.1136/bmjopen-2019-036563

Han, B. K., Wysham, K. D., Cain, K. C., Tyden, H., Bengtsson, A. A., and Lood, C. (2020). Neutrophil and lymphocyte counts are associated with different immunopathological mechanisms in systemic lupus erythematosus. *Lupus Sci. Med.* 7 (1), e000382. doi:10.1136/lupus-2020-000382

Higgs, B. W., Zhu, W., Morehouse, C., White, W. I., Brohawn, P., Guo, X., et al. (2014). A phase 1b clinical trial evaluating sifalimumab, an anti-IFN-α monoclonal antibody, shows target neutralisation of a type I IFN signature in blood of dermatomyositis and polymyositis patients. *Ann. Rheum. Dis.* 73 (1), 256–262. doi:10.1136/annrheumdis-2012-202794

Hilkens, C. M., Schlaak, J. F., and Kerr, I. M. (1950)., 171. Baltimore, Md, 5255–5263. doi:10.4049/jimmunol.171.10.5255 Differential responses to IFN-alpha subtypes in human T cells and dendritic cells. *J. Immunol.*10.

Hom, G., Graham, R. R., Modrek, B., Taylor, K. E., Ortmann, W., Garnier, S., et al. (2008). Association of systemic lupus erythematosus with C8orf13-BLK and ITGAM-ITGAX. *N. Engl. J. Med.* 358 (9), 900–909. doi:10.1056/NEJMoa0707865

Houssiau, F. A., Thanou, A., Mazur, M., Ramiterre, E., Gomez Mora, D. A., Misterska-Skora, M., et al. (2020). IFN-A kinoid in systemic lupus erythematosus: Results from a phase IIb, randomised, placebo-controlled study. *Ann. Rheum. Dis.* 79 (3), 347–355. doi:10.1136/annrheumdis-2019-216379

Indraccolo, S., Pfeffer, U., Minuzzo, S., Esposito, G., Roni, V., Mandruzzato, S., et al. (2007). Identification of genes selectively regulated by IFNs in endothelial cells. *J. Immunol.* 178 (2), 1122–1135. doi:10.4049/jimmunol.178.2.1122

International Consortium for Systemic Lupus Erythematosus, G., Harley, J. B., Alarcón-Riquelme, M. E., Criswell, L. A., Jacob, C. O., Kimberly, R. P., et al. (2008). Genome-wide association scan in women with systemic lupus erythematosus identifies susceptibility variants in ITGAM, PXK, KIAA1542 and other loci. *Nat. Genet.* 40 (2), 204–210. doi:10.1038/ng.81

Isaacs, A., and Lindenmann, J. (1957). Virus interference. I. The interferon. *Proc. R. Soc. Lond. B Biol. Sci.* 147 (927), 258–267. doi:10.1098/rspb.1957.0048

Iwamoto, T., Dorschner, J. M., Selvaraj, S., Mezzano, V., Jensen, M. A., Vsetecka, D., et al. (2022). High systemic type I interferon activity is associated with active class III/IV lupus nephritis. *J. Rheumatol.* 49 (4), 388–397. doi:10.3899/jrheum.210391

Izaguirre, A., Barnes, B. J., Amrute, S., Yeow, W-S., Megjugorac, N., Dai, J., et al. (2003). Comparative analysis of IRF and IFN-alpha expression in human plasmacytoid and monocyte-derived dendritic cells. *J. Leukoc. Biol.* 74 (6), 1125–1138. doi:10.1189/jlb.0603255

Izmirly, P. M., Parton, H., Wang, L., McCune, W. J., Lim, S. S., Drenkard, C., et al. (2021). Prevalence of systemic lupus erythematosus in the United States: Estimates from a meta-analysis of the centers for disease control and prevention national lupus registries. *Arthritis Rheumatol.* 73 (6), 991–996. doi:10.1002/art.41632

Izmirly, P. M., Wan, I., Sahl, S., Buyon, J. P., Belmont, H. M., Salmon, J. E., et al. (2017). The incidence and prevalence of systemic lupus erythematosus in New York county (manhattan), New York: The manhattan lupus surveillance program. *Arthritis Rheumatol.* 69 (10), 2006–2017. doi:10.1002/art.40192

Jakiela, B., Kosałka, J., Plutecka, H., Węgrzyn, A. S., Bazan-Socha, S., Sanak, M., et al. (2018). Urinary cytokines and mRNA expression as biomarkers of disease activity in lupus nephritis. *Lupus* 27 (8), 1259–1270. doi:10.1177/0961203318770006

James, J. A., Neas, B. R., Moser, K. L., Hall, T., Bruner, G. R., Sestak, A. L., et al. (2001). Systemic lupus erythematosus in adults is associated with previous Epstein-Barr virus exposure. *Arthritis Rheum.* 44 (5), 1122–1126. doi:10.1002/1529-0131(200105)44:5<1122::AID-ANR193>3.0.CO;2-D

Jayne, D., Rovin, B., Mysler, E. F., Furie, R. A., Houssiau, F. A., Trasieva, T., et al. (2022). Phase II randomised trial of type I interferon inhibitor anifrolumab in patients with active lupus nephritis. *Ann. Rheum. Dis.* 81 (4), 496–506. doi:10.1136/annrheumdis-2021-221478

Kalunian, K. C., Merrill, J. T., Maciuca, R., McBride, J. M., Townsend, M. J., Wei, X., et al. (2016). A Phase II study of the efficacy and safety of rontalizumab (rhuMAb interferon-α) in patients with systemic lupus erythematosus (ROSE). *Ann. Rheum. Dis.* 75 (1), 196–202. doi:10.1136/annrheumdis-2014-206090

Keller, E. J., Patel, N. B., Patt, M., Nguyen, J. K., and Jørgensen, T. N. (2021). Partial protection from lupus-like disease by B-cell specific type I interferon receptor deficiency. *Front. Immunol.* 11, 11. doi:10.3389/fimmu.2020.616064

Khalil, Ur R., and Khokhar, N. (2016). Development of systemic lupus erythematosus following interferon-α therapy for hepatitis C infection. *J. Coll. Physicians Surg. Pak* 26 (3), 223–224.

Khamashta, M., Merrill, J. T., Werth, V. P., Furie, R., Kalunian, K., Illei, G. G., et al. (2016). Sifalimumab, an anti-interferon-α monoclonal antibody, in moderate to severe systemic lupus erythematosus: A randomised, double-blind, placebo-controlled study. *Ann. Rheum. Dis.* 75 (11), 1909–1916. doi:10.1136/annrheumdis-2015-208562

Kolumam, G. A., Thomas, S., Thompson, L. J., Sprent, J., and Murali-Krishna, K. (2005). Type I interferons act directly on CD8 T cells to allow clonal expansion and memory formation in response to viral infection. *J. Exp. Med.* 202 (5), 637–650. doi:10.1084/jem.20050821

Ladislau, L., Suárez-Calvet, X., Toquet, S., Landon-Cardinal, O., Amelin, D., Depp, M., et al. (2018). JAK inhibitor improves type I interferon induced damage: Proof of concept in dermatomyositis. *Brain* 141 (6), 1609–1621. doi:10.1093/brain/awy105

Lande, R., Ganguly, D., Facchinetti, V., Frasca, L., Conrad, C., Gregorio, J., et al. (2011). Neutrophils activate plasmacytoid dendritic cells by releasing self-DNA-peptide complexes in systemic lupus erythematosus. *Sci. Transl. Med.* 3 (73), 73ra19. doi:10.1126/scitranslmed.3001180

Landolt-Marticorena, C., Bonventi, G., Lubovich, A., Ferguson, C., Unnithan, T., Su, J., et al. (2009). Lack of association between the interferon-alpha signature and longitudinal changes in disease activity in systemic lupus erythematosus. *Ann. Rheum. Dis.* 68 (9), 1440–1446. doi:10.1136/ard.2008.093146

Le Voyer, T., Gitiaux, C., Authier, F. J., Bodemer, C., Melki, I., Quartier, P., et al. (2021). JAK inhibitors are effective in a subset of patients with juvenile dermatomyositis: A monocentric retrospective study. *Rheumatol. Oxf.* 60 (12), 5801–5808. doi:10.1093/rheumatology/keab116

Lee, P. Y., Weinstein, J. S., Nacionales, D. C., Scumpia, P. O., Li, Y., Butfiloski, E., et al. (2008). A novel type I IFN-producing cell subset in murine lupus. *J. Immunol.* 180 (7), 5101–5108. doi:10.4049/jimmunol.180.7.5101

Liu, M., Liu, J., Hao, S., Wu, P., Zhang, X., Xiao, Y., et al. (2018). Higher activation of the interferon-gamma signaling pathway in systemic lupus erythematosus patients with a high type I IFN score: Relation to disease activity. *Clin. Rheumatol.* 37 (10), 2675–2684. doi:10.1007/s10067-018-4138-7

Liu, Z., Bethunaickan, R., Huang, W., Lodhi, U., Solano, I., Madaio, M. P., et al. (2011). Interferon-α accelerates murine systemic lupus erythematosus in a T cell–dependent manner. *Arthritis Rheum.* 63 (1), 219–229. doi:10.1002/art.30087

Lövgren, T., Eloranta, M-L., Båve, U., Alm, G. V., and Rönnblom, L. (2004). Induction of interferon-α production in plasmacytoid dendritic cells by immune complexes containing nucleic acid released by necrotic or late apoptotic cells and lupus IgG. *Arthritis Rheum.* 50 (6), 1861–1872. doi:10.1002/art.20254

Mai, L., Asaduzzaman, A., Noamani, B., Fortin, P. R., Gladman, D. D., Touma, Z., et al. (2021). The baseline interferon signature predicts disease severity over the subsequent 5 years in systemic lupus erythematosus. *Arthritis Res. Ther.* 23 (1), 29. doi:10.1186/s13075-021-02414-0

Marrack, P., Kappler, J., and Mitchell, T. (1999). Type I interferons keep activated T cells alive. *J. Exp. Med.* 189 (3), 521–530. doi:10.1084/jem.189.3.521

Mathian, A., Weinberg, A., Gallegos, M., Banchereau, J., and Koutouzov, S. (2005). IFN-alpha induces early lethal lupus in preautoimmune (New Zealand Black x New Zealand White) F1 but not in BALB/c mice. *J. Immunol.* 174 (5), 2499–2506. doi:10.4049/jimmunol.174.5.2499

Mazewski, C., Perez, R. E., Fish, E. N., and Platanias, L. C. (2020). Type I interferon (IFN)-Regulated activation of canonical and non-canonical signaling pathways. *Front. Immunol.* 11, 606456. doi:10.3389/fimmu.2020.606456

McBride, J. M., Jiang, J., Abbas, A. R., Morimoto, A., Li, J., Maciuca, R., et al. (2012). Safety and pharmacodynamics of rontalizumab in patients with systemic lupus erythematosus: Results of a phase I, placebo-controlled, double-blind, dose-escalation study. *Arthritis Rheum.* 64 (11), 3666–3676. doi:10.1002/art.34632

McCarty, D. J., Manzi, S., Medsger, T. A., Ramsey-Goldman, R., Laporte, R. E., and Kwoh, C. K. (1995). Incidence of systemic lupus erythematosus race and gender differences. *Arthritis Rheum.* 38 (9), 1260–1270. doi:10.1002/art.1780380914

Merrill, J. T., Immermann, F., Whitley, M., Zhou, T., Hill, A., O'Toole, M., et al. (2017). The biomarkers of lupus disease study: A bold approach may mitigate interference of background immunosuppressants in clinical trials. *Arthritis Rheumatol.* 69 (6), 1257–1266. doi:10.1002/art.40086

Merrill, J. T., Wallace, D. J., Petri, M., Kirou, K. A., Yao, Y., White, W. I., et al. (2011). Safety profile and clinical activity of sifalimumab, a fully human anti-interferon α monoclonal antibody, in systemic lupus erythematosus: A phase I, multicentre, double-blind randomised study. *Ann. Rheum. Dis.* 70 (11), 1905–1913. doi:10.1136/ard.2010.144485

Montoya, M., Schiavoni, G., Mattei, F., Gresser, I., Belardelli, F., Borrow, P., et al. (2002). Type I interferons produced by dendritic cells promote their phenotypic and functional activation. *Blood* 99 (9), 3263–3271. doi:10.1182/blood.v99.9.3263

Morand, E. F., Furie, R., Tanaka, Y., Bruce, I. N., Askanase, A. D., Richez, C., et al. (2020). Trial of anifrolumab in active systemic lupus erythematosus. *N. Engl. J. Med.* 382 (3), 211–221. doi:10.1056/NEJMoa1912196

Munroe, M. E., Vista, E. S., Merrill, J. T., Guthridge, J. M., Roberts, V. C., and James, J. A. (2017). Pathways of impending disease flare in African-American systemic lupus erythematosus patients. *J. Autoimmun.* 78, 70–78. doi:10.1016/j.jaut.2016.12.005

Nacionales, D. C., Kelly-Scumpia, K., Lee, P. Y., Weinstein, J. S., Lyons, R., Sobel, E., et al. (2007). Deficiency of the type I interferon receptor protects mice from experimental lupus. *Arthritis Rheum.* 56 (11), 3770–3783. doi:10.1002/art.23023

Navarra, S. V., Guzmán, R. M., Gallacher, A. E., Hall, S., Levy, R. A., Jimenez, R. E., et al. (2011). Efficacy and safety of belimumab in patients with active systemic lupus erythematosus: A randomised, placebo-controlled, phase 3 trial. *Lancet* 377 (9767), 721–731. doi:10.1016/S0140-6736(10)61354-2

Nguyen, K. B., Salazar-Mather, T. P., Dalod, M. Y., Van Deusen, J. B., Wei, X-q., Liew, F. Y., et al. (2002). Coordinated and distinct roles for IFN-alpha beta, IL-12, and IL-15 regulation of NK cell responses to viral infection. *J. Immunol.* 169 (8), 4279–4287. doi:10.4049/jimmunol.169.8.4279

Niewold, T. B., Hua, J., Lehman, T. J. A., Harley, J. B., and Crow, M. K. (2007). High serum IFN-α activity is a heritable risk factor for systemic lupus erythematosus. *Genes. Immun.* 8 (6), 492–502. doi:10.1038/sj.gene.6364408

Noda, K., Enomoto, N., Arai, K., Masuda, E., Yamada, Y., Suzuki, K., et al. (1996). Induction of antinuclear antibody after interferon therapy in patients with type-C chronic hepatitis: Its relation to the efficacy of therapy. *Scand. J. Gastroenterol.* 31 (7), 716–722. doi:10.3109/00365529609009156

Northcott, M., Jones, S., Koelmeyer, R., Bonin, J., Vincent, F., Kandane-Rathnayake, R., et al. (2022). Type 1 interferon status in systemic lupus erythematosus: A longitudinal analysis. *Lupus Sci. Med.* 9 (1), e000625. doi:10.1136/lupus-2021-000625

Novick, D., Cohen, B., and Rubinstein, M. (1994). The human interferon alpha/beta receptor: Characterization and molecular cloning. *Cell* 77 (3), 391–400. doi:10.1016/0092-8674(94)90154-6

Orange, J. S., and Biron, C. A. (1996). Characterization of early IL-12, IFN-alphabeta, and TNF effects on antiviral state and NK cell responses during murine cytomegalovirus infection. *J. Immunol.* 156 (12), 4746–4756.

Ortíz-Fernández, L., Martín, J., and Alarcón-Riquelme, M. E. (2022). A summary on the genetics of systemic lupus erythematosus, rheumatoid arthritis, systemic sclerosis, and sjögren's syndrome. *Clin. Rev. Allerg. Immunol.* doi:10.1007/s12016-022-08951-z

Paik, J. J., Casciola-Rosen, L., Shin, J. Y., Albayda, J., Tiniakou, E., Leung, D. G., et al. (2021). Study of tofacitinib in refractory dermatomyositis: An open-label pilot study of ten patients. *Arthritis Rheumatol.* 73 (5), 858–865. doi:10.1002/art.41602

Palanichamy, A., Bauer, J. W., Yalavarthi, S., Meednu, N., Barnard, J., Owen, T., et al. (2014). Neutrophil-mediated IFN activation in the bone marrow alters B cell development in human and murine systemic lupus erythematosus. *J. Immunol.* 192 (3), 906–918. doi:10.4049/jimmunol.1302112

Pan, L., Lu, M. P., Wang, J. H., Xu, M., and Yang, S. R. (2020). Immunological pathogenesis and treatment of systemic lupus erythematosus. *World J. Pediatr.* 16 (1), 19–30. doi:10.1007/s12519-019-00229-3

Paradowska-Gorycka, A., Wajda, A., Stypinska, B., Walczuk, E., Rzeszotarska, E., Walczyk, M., et al. (2021). Variety of endosomal TLRs and Interferons (IFN-α, IFN-β, IFN-γ) expression profiles in patients with SLE, SSc and MCTD. *Clin. Exp. Immunol.* 204 (1), 49–63. doi:10.1111/cei.13566

Petri, M., Fu, W., Ranger, A., Allaire, N., Cullen, P., Magder, L. S., et al. (2019). Association between changes in gene signatures expression and disease activity among patients with systemic lupus erythematosus. *BMC Med. Genomics* 12 (1), 4. doi:10.1186/s12920-018-0468-1

Petri, M., Wallace, D. J., Spindler, A., Chindalore, V., Kalunian, K., Mysler, E., et al. (2013). Sifalimumab, a human anti-interferon-α monoclonal antibody, in systemic lupus erythematosus: a phase I randomized, controlled, dose-escalation study. *Arthritis Rheum.* 65 (4), 1011–1021. doi:10.1002/art.37824

Pinal-Fernandez, I., Casal-Dominguez, M., Derfoul, A., Pak, K., Plotz, P., Miller, F. W., et al. (2019). Identification of distinctive interferon gene signatures in different types of myositis. *Neurology* 93 (12), e1193–e1204. doi:10.1212/WNL.0000000000008128

Rani, M. R. S., Shrock, J., Appachi, S., Rudick, R. A., Williams, B. R. G., and Ransohoff, R. M. (2007). Novel interferon-β-induced gene expression in peripheral blood cells. *J. Leukoc. Biol.* 82 (5), 1353–1360. doi:10.1189/jlb.0507273

Reeves, W. H., Lee, P. Y., Weinstein, J. S., Satoh, M., and Lu, L. (2009). Induction of autoimmunity by pristane and other naturally occurring hydrocarbons. *Trends Immunol.* 30 (9), 455–464. doi:10.1016/j.it.2009.06.003

Reis, L. F., Ho Lee, T., and Vilcek, J. (1989). Tumor necrosis factor acts synergistically with autocrine interferon-beta and increases interferon-beta mRNA levels in human fibroblasts. *J. Biol. Chem.* 264 (28), 16351–16354. doi:10.1016/s0021-9258(19)84711-7

Rose, T., Grützkau, A., Hirseland, H., Huscher, D., Dähnrich, C., Dzionek, A., et al. (2013). IFNα and its response proteins, IP-10 and SIGLEC-1, are biomarkers of disease activity in systemic lupus erythematosus. *Ann. Rheum. Dis.* 72 (10), 1639–1645. doi:10.1136/annrheumdis-2012-201586

Rowland, S. L., Riggs, J. M., Gilfillan, S., Bugatti, M., Vermi, W., Kolbeck, R., et al. (2014). Early, transient depletion of plasmacytoid dendritic cells ameliorates autoimmunity in a lupus model. *J. Exp. Med.* 211 (10), 1977–1991. doi:10.1084/jem.20132620

Saleiro, D., and Platanias, L. C. (2019). Interferon signaling in cancer. Non-canonical pathways and control of intracellular immune checkpoints. *Semin. Immunol.* 43, 101299. doi:10.1016/j.smim.2019.101299

Sánchez, E., Comeau, M. E., Freedman, B. I., Kelly, J. A., Kaufman, K. M., Langefeld, C. D., et al. (2011). Identification of novel genetic susceptibility loci in African American lupus patients in a candidate gene association study. *Arthritis Rheum.* 63 (11), 3493–3501. doi:10.1002/art.30563

Sanchez, E., Nadig, A., Richardson, B. C., Freedman, B. I., Kaufman, K. M., Kelly, J. A., et al. (2011). Phenotypic associations of genetic susceptibility loci in systemic lupus erythematosus. *Ann. Rheum. Dis.* 70 (10), 1752–1757. doi:10.1136/ard.2011.154104

Santer, D. M., Yoshio, T., Minota, S., Möller, T., and Elkon, K. B. (2009). Potent induction of IFN-alpha and chemokines by autoantibodies in the cerebrospinal fluid of patients with neuropsychiatric lupus. *J. Immunol.* 182 (2), 1192–1201. doi:10.4049/jimmunol.182.2.1192

Santiago-Raber, M-L., Baccala, R., Haraldsson, K. M., Choubey, D., Stewart, T. A., Kono, D. H., et al. (2003). Type-I interferon receptor deficiency reduces lupus-like disease in NZB mice. *J. Exp. Med.* 197 (6), 777–788. doi:10.1084/jem.20021996

Schneider, L., Colar da Silva, A. C., Werres Junior, L. C., Alegretti, A. P., Pereira dos Santos, A. S., Santos, M., et al. (2015). Vitamin D levels and cytokine profiles in patients with systemic lupus erythematosus. *Lupus* 24 (11), 1191–1197. doi:10.1177/0961203315584811

Siegal, F. P., Kadowaki, N., Shodell, M., Patricia, A. F-B., Shah, K., Ho, S., et al. (1999). The nature of the principal type 1 interferon-producing cells in human blood. *Science* 284 (5421), 1835–1837. doi:10.1126/science.284.5421.1835

Sigurdsson, S., Nordmark, G., Göring, H. H., Lindroos, K., Wiman, A. C., Sturfelt, G., et al. (2005). Polymorphisms in the tyrosine kinase 2 and interferon regulatory factor 5 genes are associated with systemic lupus erythematosus. *Am. J. Hum. Genet.* 76 (3), 528–537. doi:10.1086/428480

Simmons, D. P., Wearsch, P. A., Canaday, D. H., Meyerson, H. J., Liu, Y. C., Wang, Y., et al. (2012). Type I IFN drives a distinctive dendritic cell maturation phenotype that allows continued class II MHC synthesis and antigen processing. *J. Immunol.* 188 (7), 3116–3126. doi:10.4049/jimmunol.1101313

Sisirak, V., Ganguly, D., Lewis, K. L., Couillault, C., Tanaka, L., Bolland, S., et al. (2014). Genetic evidence for the role of plasmacytoid dendritic cells in systemic lupus erythematosus. *J. Exp. Med.* 211 (10), 1969–1976. doi:10.1084/jem.20132522

Steinberg, A. D., Baron, S., and Talal, N. (1969). The pathogenesis of autoimmunity in New Zealand mice, I. Induction of antinucleic acid antibodies by polyinosinic-polycytidylic acid. *Proc. Natl. Acad. Sci. U. S. A.* 63 (4), 1102–1107. doi:10.1073/pnas.63.4.1102

Stone, R. C., Feng, D., Deng, J., Singh, S., Yang, L., Fitzgerald-Bocarsly, P., et al. (2012). Interferon regulatory factor 5 activation in monocytes of systemic lupus erythematosus patients is triggered by circulating autoantigens independent of type I interferons. *Arthritis Rheum.* 64 (3), 788–798. doi:10.1002/art.33395

Swann, J. B., Hayakawa, Y., Zerafa, N., Sheehan, K. C. F., Scott, B., Schreiber, R. D., et al. (2007). Type I IFN contributes to NK cell homeostasis, activation, and antitumor function. *J. Immunol.* 178 (12), 7540–7549. doi:10.4049/jimmunol.178.12.7540

Takeuchi, T., Tanaka, Y., Matsumura, R., Saito, K., Yoshimura, M., Amano, K., et al. (2020). Safety and tolerability of sifalimumab, an anti-interferon-α monoclonal antibody, in Japanese patients with systemic lupus erythematosus: A multicenter, phase 2, open-label study. *Mod. Rheumatol.* 30 (1), 93–100. doi:10.1080/14397595.2019.1583832

Tanaka, Y., Takeuchi, T., Okada, M., Ishii, T., Nakajima, H., Kawai, S., et al. (2020). Safety and tolerability of anifrolumab, a monoclonal antibody targeting type I interferon receptor, in Japanese patients with systemic lupus erythematosus: A multicenter, phase 2, open-label study. *Mod. Rheumatol.* 30 (1), 101–108. doi:10.1080/14397595.2019.1583833

Updates, Lilly. (2022). *OLUMIANT® (baricitinib) phase 3 lupus program and FDA review for atopic dermatitis: Lilly*. [Available from: https://investor.lilly.com/news-releases/news-release-details/updates-olumiantr-baricitinib-phase-3-lupus-program-and-fda.

Uzé, G., Lutfalla, G., and Gresser, I. (1990). Genetic transfer of a functional human interferon α receptor into mouse cells: Cloning and expression of its c-DNA. *Cell* 60 (2), 225–234. doi:10.1016/0092-8674(90)90738-z

Vadiveloo, P. K., Vairo, G., Hertzog, P., Kola, I., and Hamilton, J. A. (2000). Role of type I interferons during macrophage activation by lipopolysaccharide. *Cytokine* 12 (11), 1639–1646. doi:10.1006/cyto.2000.0766

Vakaloglou, K. M., and Mavragani, C. P. (2011). Activation of the type I interferon pathway in primary sjögren's syndrome: An update. *Curr. Opin. Rheumatol.* 23 (5), 459–464. doi:10.1097/BOR.0b013e328349fd30

Velazquez, L., Fellous, M., Stark, G. R., and Pellegrini, S. (1992). A protein tyrosine kinase in the interferon alpha/beta signaling pathway. *Cell* 70 (2), 313–322. doi:10.1016/0092-8674(92)90105-l

Vital, E. M., Merrill, J. T., Morand, E. F., Furie, R. A., Bruce, I. N., Tanaka, Y., et al. (2022). Anifrolumab efficacy and safety by type I interferon gene signature and clinical subgroups in patients with SLE: Post hoc analysis of pooled data from two phase III trials. *Ann. Rheum. Dis.* 81 (7), 951–961. doi:10.1136/annrheumdis-2021-221425

Wahadat, M. J., Bodewes, I. L. A., Maria, N. I., van Helden-Meeuwsen, C. G., van Dijk-Hummelman, A., Steenwijk, E. C., et al. (2018). Type I IFN signature in

childhood-onset systemic lupus erythematosus: A conspiracy of DNA- and RNA-sensing receptors? *Arthritis Res. Ther.* 20 (1), 4. doi:10.1186/s13075-017-1501-z

Wang, Y. F., Zhang, Y., Lin, Z., Zhang, H., Wang, T. Y., Cao, Y., et al. (2021). Identification of 38 novel loci for systemic lupus erythematosus and genetic heterogeneity between ancestral groups. *Nat. Commun.* 12 (1), 772–y. doi:10.1038/s41467-021-21049-y

Webb, K., Peckham, H., Radziszewska, A., Menon, M., Oliveri, P., Simpson, F., et al. (2018). Sex and pubertal differences in the type 1 interferon pathway associate with both X chromosome number and serum sex hormone concentration. *Front. Immunol.* 9, 3167. doi:10.3389/fimmu.2018.03167

Werth, V. P., Furie, R. A., Romero-Diaz, J., Navarra, S., Kalunian, K., van Vollenhoven, R. F., et al. (2022). Trial of anti-BDCA2 antibody litifilimab for cutaneous lupus erythematosus. *N. Engl. J. Med.* 387 (4), 321–331. doi:10.1056/NEJMoa2118024

Wildenberg, M. E., van Helden-Meeuwsen, C. G., van de Merwe, J. P., Drexhage, H. A., and Versnel, M. A. (2008). Systemic increase in type I interferon activity in sjögren's syndrome: A putative role for plasmacytoid dendritic cells. *Eur. J. Immunol.* 38 (7), 2024–2033. doi:10.1002/eji.200738008

Wilkinson, C., Henderson, R. B., Jones-Leone, A. R., Flint, S. M., Lennon, M., Levy, R. A., et al. (2020). The role of baseline BLyS levels and type 1 interferon-inducible gene signature status in determining belimumab response in systemic lupus erythematosus: A post hoc meta-analysis. *Arthritis Res. Ther.* 22 (1), 102. doi:10.1186/s13075-020-02177-0

Willis, R., Seif, A. M., McGwin, G., Martinez-Martinez, L. A., González, E. B., Dang, N., et al. (2012). Effect of hydroxychloroquine treatment on pro-inflammatory cytokines and disease activity in SLE patients: Data from LUMINA (LXXV), a multiethnic US cohort. *Lupus* 21 (8), 830–835. doi:10.1177/0961203312437270

Wilson, L. E., Widman, D., Dikman, S. H., and Gorevic, P. D. (2002). Autoimmune disease complicating antiviral therapy for hepatitis C virus infection. *Semin. Arthritis Rheum.* 32 (3), 163–173. doi:10.1053/sarh.2002.37277

Yano, H., Iemura, A., Haramaki, M., Ogasawara, S., Takayama, A., Akiba, J., et al. (1999). Interferon alfa receptor expression and growth inhibition by interferon alfa in human liver cancer cell lines. *Hepatology* 29 (6), 1708–1717. doi:10.1002/hep.510290624

Yokogawa, M., Takaishi, M., Nakajima, K., Kamijima, R., Fujimoto, C., Kataoka, S., et al. (2014). Epicutaneous application of toll-like receptor 7 agonists leads to systemic autoimmunity in wild-type mice: A new model of systemic lupus erythematosus. *Arthritis Rheumatol.* 66 (3), 694–706. doi:10.1002/art.38298

Zedan, M. M., Attia, Z. R., Abd El Azeem, R. A., Mutawi, T. M., El Shehawy, A. S., and Bakr, A. (2021). Genetic polymorphisms in genes involved in the type I interferon system (IFIH1/MDA-5, TNFAIP3/A20, and STAT4): Association with SLE risk in Egyptian children and adolescents. *J. Inflamm. Res.* 14, 3349–3358. doi:10.2147/JIR.S309008

Zhang, L., Jiang, X., Pfau, D., Ling, Y., and Nathan, C. F. (2020). Type I interferon signaling mediates Mycobacterium tuberculosis–induced macrophage death. *J. Exp. Med.* 218 (2), e20200887. doi:10.1084/jem.20200887

Zhang, X., Yang, W., Wang, X., Tian, H., Deng, H., Zhang, L., et al. (2018). Identification of new type I interferon-stimulated genes and investigation of their involvement in IFN-β activation. *Protein Cell* 9 (9), 799–807. doi:10.1007/s13238-018-0511-1

Zhuang, H., Szeto, C., Han, S., Yang, L., and Reeves, W. H. (2015). Animal models of interferon signature positive lupus. *Front. Immunol.* 6, 291. doi:10.3389/fimmu.2015.00291

Ziegler, S. M., Beisel, C., Sutter, K., Griesbeck, M., Hildebrandt, H., Hagen, S. H., et al. (2017). Human pDCs display sex-specific differences in type I interferon subtypes and interferon α/β receptor expression. *Eur. J. Immunol.* 47 (2), 251–256. doi:10.1002/eji.201646725

Frontiers in Pharmacology

Explores the interactions between chemicals and living beings

The most cited journal in its field, which advances access to pharmacological discoveries to prevent and treat human disease.

Discover the latest Research Topics

See more →

Frontiers

Avenue du Tribunal-Fédéral 34
1005 Lausanne, Switzerland
frontiersin.org

Contact us

+41 (0)21 510 17 00
frontiersin.org/about/contact